

*Synthesis and Characterization of
Biodegradable Thermoplastic Elastomers for
Medical Applications:
Novel copolyesters as an alternative to
polylactide and poly(ϵ -caprolactone)*

Jorge Fernández Hernández

Supervisor

Jose Ramon Sarasua

2016

The Thesis has been performed at:

ZIBIO Group

Department of Mining-Metallurgy Engineering
and Materials Science

School of Engineering, Bilbao

Spain



*“Now is the law of the jungle,
as old and true as the sky;
And the wolf that shall keep it may prosper,
but the wolf that shall break it must die.

As the creeper that girdles the tree trunk,
the Law runneth forward and back;
For the strength of the pack is the wolf.
And the strength of the wolf is the pack.”*

Rudyard Kipling

Acknowledgments/Agradecimientos

Tras cuatro años de trabajo en el laboratorio, el camino llega a su fin. Puedo decir que durante este periodo he convivido con muchos fracasos y unos pocos éxitos, pero siempre con algo que aprender. Y aunque muchos no lo crean, he de reconocer que me he divertido. Ahora, echando la vista atrás, ha llegado el momento de acordarse de todos aquellos que me han ayudado a alcanzar la meta.

En primer lugar, he de agradecer a la Universidad del País Vasco (UPV-EHU) por la beca de investigación que me fue concedida. Sin ella, no hubiera sido posible la realización de este trabajo.

También quería dar las gracias a mis compañeros de laboratorio y profesores del departamento de Ingeniería Minero-Metalúrgica y Ciencia de los materiales, que me sufrieron y toleraron día si, día también: Ainhoa, Emilio, Erlantz, Ester, Eva, Hegoi, Inger, Jone, Natalia, Naroa, Nerea, Nuria y Susana. Sin embargo, hay algunas personas concretas que fueron muy importantes y a las que haré una mención especial. A Joserra, mi director de tesis, que confió en mí y me dió un primer empujón. A Agustín, que me fue de gran ayuda con el RMN y me dio divertidas charlas sobre ciclismo. Y a Aitor, por ser un ejemplo como investigador. Además de ser un amigo, fue una valiosísima fuente de ideas.

Además, me gustaría reconocer la labor de SGiker en lo que respecta al microscopio electrónico, difracción de rayos X y espectroscopia de emisión atómica. Así como a los grupos de Ana Alonso y Abhay Pandit por mis pequeñas incursiones en el trabajo con células vivas. Tampoco me quiero olvidar del equipo de guardas de la Escuela de Ingenieros de Bilbao, que no obstaculizaron mi trabajo en días festivos, ni de Luisa y Ander, nuestros técnicos de laboratorio.

Para terminar, doy las gracias a mi familia por su continuado apoyo. En particular, a mis padres, Fernando y Raquel, y a mi hermanita Eva. Y gracias también a mis amig@s y compañeros de baloncesto, que evitaron que me transformase en una auténtica rata de laboratorio.

Table of Contents

Acknowledgments/Agradecimientos	1
Table of Contents	5
Scope and objectives.....	9
Introduction	13
Section 1 - Copolymers of high glass transition temperature	69
Chapter 1. Lactide-co- ϵ -Caprolactone Copolymers	75
Chapter 1.1 Synthesis and Characterization of Statistical L-lactide-co- ϵ -caprolactone Copolymers with Well-Resolved Chain Microstructures	77
Chapter 1.2 Effects of Chain Microstructures and Derived Crystallization Capability on Hydrolytic Degradation of L-Lactide-co- ϵ -Caprolactone Copolymers	109
Chapter 1.3 A New Generation of Lactide-co- ϵ -Caprolactone Copolymers for Application in the Medical Field	133
Chapter 2. Lactide-co- δ -Valerolactone Copolymers	161
Chapter 2.1 Tensile Behaviour and Dynamic Mechanical Analysis of Novel Lactide-co- δ -Valerolactone Statistical Copolymers.....	163
Chapter 2.2 <i>In Vitro</i> Degradation Study of Biopolyesters Using Lactide-co- δ -Valerolactone Copolymers.....	191
Section 2- Copolymers of low glass transition temperature	227
Chapter 3. ϵ -Caprolactone Copolymers with L-Lactide and δ -Valerolactone	233
Chapter 3.1 Crystallization and Melting Behaviour of Poly(ϵ -Caprolactone-co- δ -Valerolactone) and Poly(ϵ -Caprolactone-co-L-Lactide) with Novel Chain Microstructures.	235

Table of Contents

Chapter 3.2 In Vitro Degradation Studies and Mechanical Behaviour of Poly(ϵ -Caprolactone-co- δ -Valerolactone) and Poly(ϵ -Caprolactone-co-L-Lactide) with Random and Semi-alternating Chain Microstructures	271
Chapter 4. Synthesis and Characterization of ω -Pentadecalactone-co- ϵ -Decalactone Copolymers: Evaluation of Thermal, Mechanical and Biodegradation Properties	295
Chapter 5. Synthesis and Properties of ω -Pentadecalactone-co- δ -Hexalactone copolymers: A Biodegradable thermoplastic elastomer as an Alternative to Poly(ϵ -Caprolactone).....	327
Chapter 6. Ethylene brassylate-co- δ -Hexalactone Biobased Polymers for Application in the Medical Field: Synthesis, Characterization and Cell Culture Studies	363
General Conclusions	401
Appendix	405
A1. Symbols and Abbreviations	407
A2. List of Publications and Congresses	413
A3. Curriculum Vitae	417

Scope and objectives

Scope and Objectives

The main objective of this thesis is to synthesize and characterize novel biodegradable copolyester elastomers which can be employed in several applications in the medical field. To achieve this, the drawbacks of polylactide and poly(ϵ -caprolactone), two polymer models, have to be overcome. Therefore, our materials must satisfy the following characteristics prior to carrying out tests on animals and clinical trials:

- ✓ Reliability. Predictable degradability and mechanical behaviour during the use of the material. Do not undergo significant supramolecular rearrangements during either the storage time before use or/and for long-term applications (physical aging).
- ✓ Efficient processing with thermoplastic techniques. Good thermal stability and do not present excessively high melting temperatures.
- ✓ Proper mechanical performance at room temperature (21 °C) and at body temperature (37 °C), the temperatures at which the biomaterials are intended to be employed. Exhibit stable mechanical properties at both temperatures and cover a wide range of stress-related properties (elastic modulus and tensile strength).
- ✓ Flexibility and ductility. They have to display high elongation at break values and avoid the inherent brittleness of polylactides.
- ✓ Not to be cytotoxic. Allow the adhesion and proliferation of cells on the biopolymers.
- ✓ High hydrolytic degradation rates. Improve the degradability of poly(ϵ -caprolactone). The degradation of the biomaterials should meet the requirements of the medical device or match the tissue regeneration rate (in the case of tissue engineering scaffolds).
- ✓ Do not generate highly crystalline resistant remnants in advanced stages of degradation. These residues can trigger foreign body reactions and remain in the human body for years once the biomaterial has lost its properties and has fulfilled its function.

For this purpose, in this work it will be necessary to:

- Develop a synthesis procedure for the ring-opening polymerization of several cyclic esters and establish the mechanisms of the reactions. Work at different synthesis conditions and check several catalysts in order to obtain efficient yields and polymers with large enough molecular weights.
- Determine accurate values of the copolymer compositions and study their chain microstructure distribution of sequences.
- Study the thermal properties and the crystallization of the different polymers.
- Test the mechanical properties at room temperature and body temperature and after different times of degradation in an aqueous medium.
- Carry out *in vitro* degradation studies at 37 °C. The changes in water absorption, weight loss, macroscopic morphology, crystallinity, phase structure, molecular weight and mechanical properties of the copolymers must be monitored.
- Evaluate the thermal stability of the materials by means of thermogravimetric analysis.
- Study the cytotoxicity of the materials by means of cell adhesion and proliferation studies.

Introduction

1. Thermoplastic Elastomers

This group of polymers [1-2] consists of materials that can be melted and reshaped by processing techniques (i.e., injection, compression molding or extrusion) and that they also exhibit elastic behaviour similar to that of vulcanized (chemically crosslinked) conventional elastomers. The principal difference between thermoplastic and thermosetting polymers is the type of cross-linking bond in their structures. Thermosets form irreversible covalent chemical bonds during the curing process and do not melt, but decompose while thermoplastic become pliable or mouldable above a specific temperature and solidifies upon cooling.

1.1. Morphology

Crosslinking is a critical structural factor which contributes to impart high elastic properties. Rubber-like materials consists of relatively long polymeric chains having a high degree of flexibility and mobility, which are joined into a network structure. This linkage may be either chemical or physical. Physical linking can be obtained by [3]

- (1) absorption of chains onto the surface of finely divided particulate fillers;
- (2) formation of small crystallites;
- (3) coalescence of ionic centers; and
- (4) coalescence of glassy blocks.

These physical crosslinks are, in general, not permanent and may disappear on swelling or increase in temperature. Physical, thermoreversible networks are present in most thermoplastic elastomers (TPEs).

Most TPEs are essentially phase-separated systems. Usually, one phase is hard and solid at ambient temperature whereas the other is an elastomer. Often, the phases are bonded chemically by block or multiblock polymerization. In other cases a fine dispersion of the phases is apparently sufficient [4]. The hard phase gives these TPEs their strength and represents the physical crosslinks. Without it, the elastomer phase would be free to

flow under stress and the polymer would be practically unusable. On the other hand, the elastomer phase provides flexibility and elasticity to the system. The glass transition temperature (T_g) and the crystalline melting temperature (T_m) determine the points at which the particular elastomer goes through transitions in its physical properties. As an illustration, Figure I represents the measurements of flexural modulus over a wide range of temperatures. There are three distinct regions:

- (1) At very low temperatures, that is, below the glass transition of the elastomeric phase, both the hard and elastomer phases are hard, so the material is stiff and brittle.
- (2) Above the T_g temperature, the elastomeric phase softens and the material is elastic, resembling a conventional vulcanized rubber.
- (3) As the temperature increases, the modulus stays relatively constant (a region referred to as “rubbery plateau”) until the point where the hard phase softens or melts. At this point the material becomes a viscous fluid.

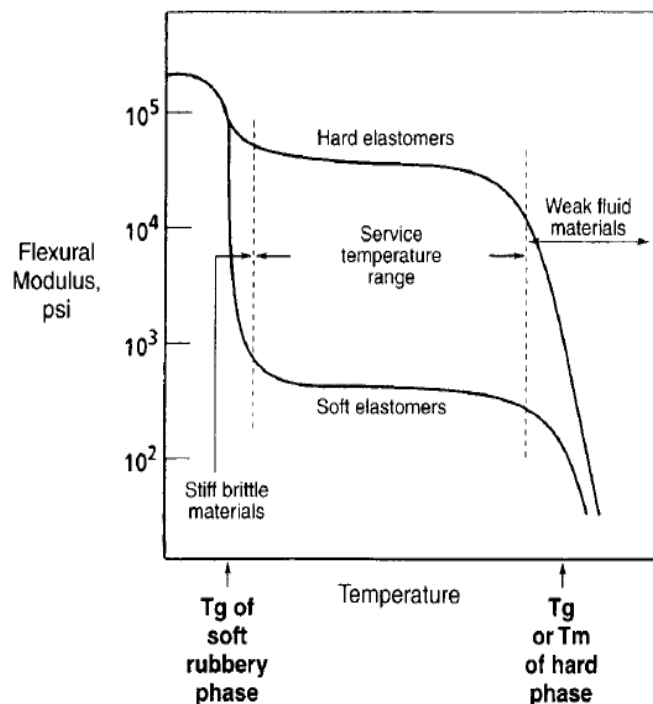


Figure I. Stiffness of typical thermoplastic elastomers in dependence on temperature (Courtesy Hanser Publishers).

The service temperature range lies between the T_g of the elastomeric phase (lower service temperature) and the T_g or T_m of the hard phase (upper service temperature). The exact values depend on the service conditions of the final product and, often, the actual lower service temperature will be higher than T_g of the elastomer and the actual upper service temperature will be lower than the T_g or T_m of the hard phase.

1.2. Types and History

The development of thermoplastic materials having more or less elastic properties started in the early 1930s with the invention of plasticization of PVC at the B.F. Goodrich Company [5]. This invention led to further interest in flexible plastics and eventually to the development of blends of PVC and NBR (butadiene-acrylonitrile rubber) [6-7]. The PVC/NBR blends, when properly formulated, have a rubber-like look and feel and bridge the gap between liquid plasticized PVC and conventional cured elastomers. Thus, they can be considered as the precursors of thermoplastics elastomers, as we know them today.

A major breakthrough occurred with the discovery of the basic diisocyanate polyaddition reaction in 1937 [8], which was first applied to produce polyurethane fibers and then to the development of some elastomeric polyurethanes by DuPont and ICI [9-11]. The work at DuPont focused on elastic fibers and eventually led to the invention of elastic linear copolyesters, prepared by melt-ester interchange between two melt copolymerized polymers [12]. This synthetic elastomer had higher strength than vulcanized natural rubber and exhibited a rapid elastic recovery. It was used to make fibers by extrusion or spinning from solutions and can be considered to be the first thermoplastic elastomer. The DuPont patent dated 1954 [13] describes it as a segmented polyurethane fiber with excellent elastic properties.

Further development of *thermoplastic polyurethanes* continued through the 1950s and 1960s. In 1962 a group from the B.F. Goodrich Company presented an article on “Virtually cross-linked polymer, Polyurethane VC” which was soluble, had high tensile strength, good elasticity, high abrasion resistance, and could be processed as a thermoplastic [14-15]. Commercial polyurethane thermoplastic elastomers were

introduced in the 1960s by B.F. Goodrich, Mobay and Upjohn in the United States and by Bayer A.G. and Elastogran in Europe.

Styrene-diene block copolymers were first developed by Shell utilizing anionic block copolymerization of styrene with butadiene (S-B-S) and styrene with isoprene (S-I-S) and were introduced commercially in 1966 as Kraton[®]. Phillips Petroleum Co. Entered this field in 1968 with radial styrenic block copolymers. In 1972 Shell added the S-EB-S copolymer, where, EB is the ethylene-butylene copolymer segment. S-EB-S copolymer is prepared by hydrogenation of the polybutadiene center block thus eliminating the double bonds and improving resistance of the product to oxidative scission and ozone attack [16]. The product was introduced as Kraton G[®].

Copolyetherester thermoplastic elastomers were developed during the 1960s and were commercialized by DuPont in 1972 as Hytrel[®]. The randomly segmented copolymer contains poly(tetramethylene oxide) terephthalate soft segments and multiple tetramethylene terephthalate hard segments. The attributes of this material were high strength, high elasticity, excellent dynamic properties, and creep resistance. Similar products were commercialized by the GAF Corporation in the late 1970 (Pelprene[®]), by Eastman Chemical Co. in 1983 (Ecdel[®]), and by the General Electric Corporation in 1985 (Lomod[®]).

Thermoplastic polyolefin blends (TPOs) were developed throughout the 1960s. The first patent on record is that of Hercules Inc. covering blends of crystalline polypropylene and ethylene-propylene copolymers (EPM), in which the propylene content was more than 50 % [17]. Dynamically vulcanized blends of polypropylene and chlorinated butyl rubber were patented in 1962 [18]. Partially dynamically cured blends of EPM or ethylene-propylene monomer with polypropylene using peroxide curing were the subject of two Unroyal patents issued in 1974 [19-20]. Uniroyal Inc. introduced TPR thermoplastic rubber materials consisting of blends of partially dynamically cured EPDM with polypropylene in 1972.

Thermoplastic vulcanizates (TPVs) are materials based on an extensive research done at the Monsanto Company during the 1970s and 1980s. These are mechanically mixed

blends with a thermoplastic [21]. The first commercial product was Santoprene[®] based on a blend (or alloy) of EPDM and polypropylene introduced in 1981. A similar product based on a blend of butadiene-acrylonitrile rubber (ASTM designation NBR) and polypropylene, Geolast[®] was introduced in 1985 [22].

Polyamide thermoplastic elastomers were introduced in 1982 by ATO Chemie followed by Grilamid[®] and Grilon produced by Emser Industries and by Dow Chemical Company's Estamid[®] [23-25]. The properties of polyamide TPEs depend upon the chemical composition of the hard (polyamide) block and the soft (polyether, polyester, or polyetherester) block.

Single-phase melt-processable rubber (MPR) is based on work done at DuPont in the early 1980s and led to the commercialization of proprietary products under the name Alcryn[®] in 1985.

During the last two decades of the 20th century many new developments have taken place, such as functionalized styrenic TPEs [26-27], new and improved TPVs, softer MPRs, and MPRs with improved physical properties, TPEs based on blends of natural rubber and polypropylene [28], thermoplastic fluoroelastomers [29], etc.

1.3. Thermoplastic Polyether Ester Elastomers

Thermoplastic polyether ester elastomers (COPEs) are multi-block copolymers, which can be represented by a generalized formula $(-A-B-)_n$ [30]. They are essentially copolyether esters with alternating, random-length sequences of either long-chain or short chain oxyalkylene glycols connected by ester linkages [31]. Structurally, they are related to polyurethanes and polyamide elastomers in that they also contain repeating high-melting blocks that are capable of crystallization (hard segments) and amorphous blocks with a relatively low glass transition temperature (soft segments). The elastomeric behaviour of these materials is due to the presence of a physical network between the hard blocks (formed by rigid chains or crystalline domains), which act as physical cross-links, and the soft amorphous phase which surrounds them. Figure II shows a model of microstructure of chain conformation in the COPs materials. The ratio of hard to soft segments, the length of the sequences and the chain microstructure

distribution determine the properties of the polymers, which can range from soft elastomers to hard elastoplastics slightly flexible.



Figure II. Model of microstructure of chain conformation in the COPs materials with large amorphous, rubbery regions between crystalline or rigid domains.

2. Properties of the (Co)polyesters

In the last decade, the synthesis of biodegradable polymers has been stimulated to fill the needs of new materials in the regenerative medical science. Polyesters synthesized from ring-opening polymerization (ROP) of cyclic ester monomers [32,33] (lactones and cyclic carbonates) have found wide applications in temporary implants used in surgical procedures of osteosynthesis, surgical threads and fibers, controlled-release drug carriers, scaffolds in tissue engineering and medical devices like catheters in urology and stents in cardiology. In addition to tin (II) octoate, extensively used in the synthesis on a large scale of resorbable polymers [34], other metal-containing catalysts have been studied for the ROP of ring-strained lactones and cyclic carbonates. These include zinc or aluminium alkoxides [35-39], rare earth metal compounds [36, 39-42] and bismuth catalysts [43]. Some of these catalysts also raise health safety concerns. Hence, enzymatic ROP has also been studied to address attention about possible toxicity of heavy metal catalyst and initiators [44].

2.1. Structural Units

A great number of monomers are commercially available for the synthesis of (co)polyesters. Figure III shows the chemical structure of some of them, including lactide, glycolide and ϵ -caprolactone, three of the best known cyclic esters. The racemic stereochemistry, the length of straight methylenes and the ratio of ester groups will determine the properties of the copolymers obtained from them.

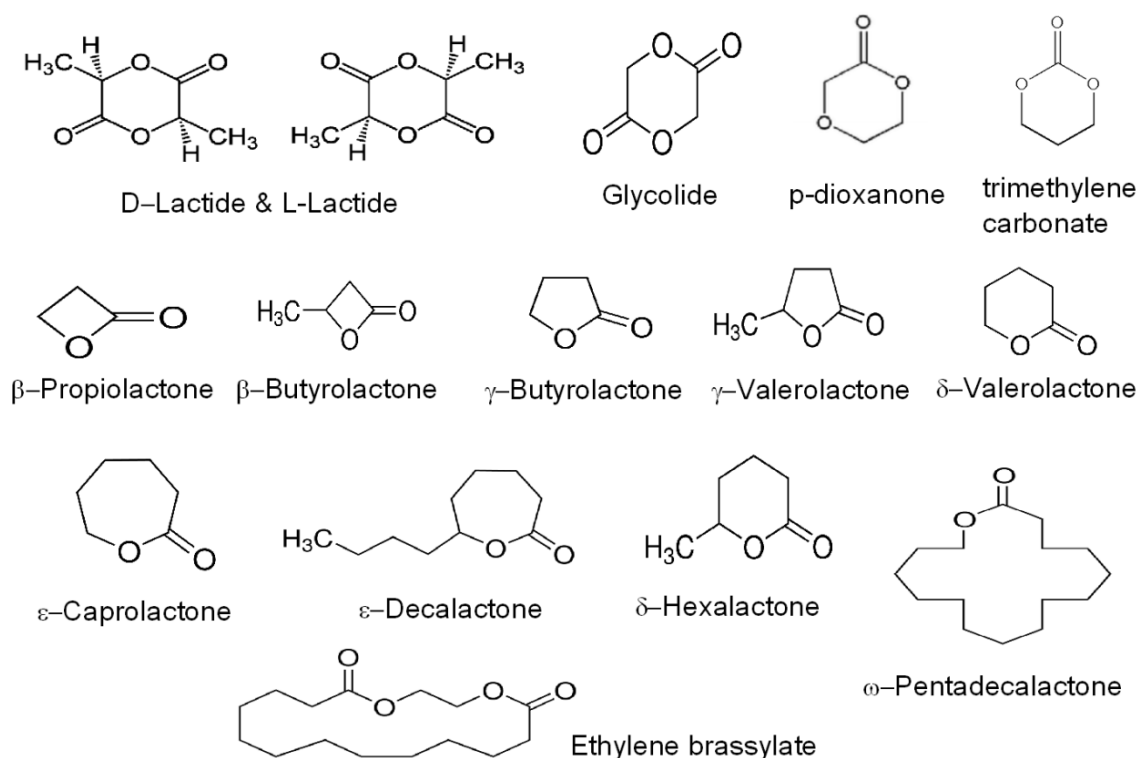


Figure III. Scheme of the chemical structures of several cyclic esters.

2.2. Chain Microstructure

Statistical copolymers, synthesized by simultaneous polymerization of two comonomers, can show different chain microstructures ranging from blocky to random depending on synthesis conditions, relative rates of incorporation of each comonomer [45-47] and catalysts used to control the tacticity and monomer alternation [48-50]. If copolymer distribution obeys Bernoullian statistics, random copolymers are formed and their number average sequence lengths are given by the molar content of the repeat units

with the following expressions: $l_A = 1/(B)$ and $l_B = 1/(A)$ [51]. However, polymerization may follow other types of statistics (e.g. Markovian), resulting in a variety of statistical copolymers that show longer sequences than Bernoullian random structures [52]. These copolymers, known as tapered or gradient, are intermediate structures showing block lengths between those of random and diblock copolymers, as shown in Figure IV. The values of number average sequence lengths, estimated by means of Nuclear Magnetic Resonance (NMR) spectroscopy, are usually compared to the Bernoullian random lengths obtaining the randomness character value (R), which is commonly used as a comparative parameter in the chain microstructure discussion. Thus, R tends to 0 for a block copolymer while in a random one R tends to 1.

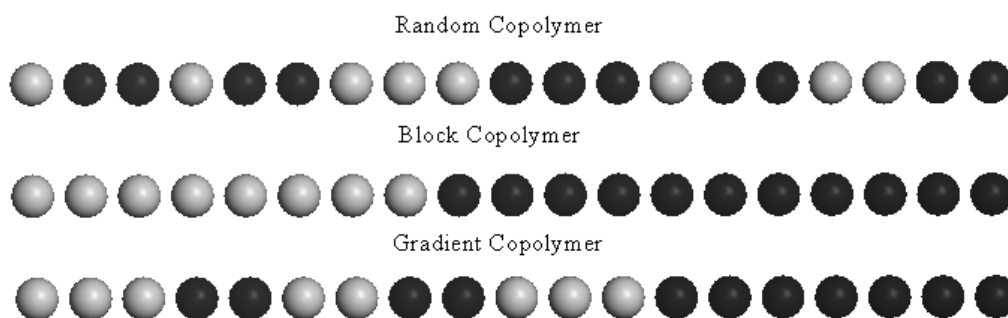


Figure IV. Illustration of random, block and tapered (gradient) copolymers.

Repeat unit sequence is a useful but underutilized tool for the control of copolymer properties. Properties of many naturally occurring macromolecules and biological macromolecules such as enzymes, transport proteins, cytochromes, polypeptides, DNA or polysaccharides, are vitally dependent on their repeat unit sequence distribution. In contrast, the sequence control to tune properties has not been fully exploited in synthetic copolymers [53-55]. Different distribution of sequences affects the copolymer properties and, as a consequence, copolymers having similar comonomer composition may differ dramatically in their behaviour. It has been reported that final properties of statistical copolymers, including solubility, thermal and mechanical properties and biodegradability, are strongly dependent on chain microstructure [56-57].

As an example, three statistical poly(L-lactide-co- ϵ -caprolactone) (PLCL) copolymers of 70 % L-lactide content with different chain microstructure ranging from moderate blocky to random ($R = 0.47, 0.69$ and 0.92 , respectively) were studied in a previous work of our group [58]. The results demonstrate that higher randomness character ($R \rightarrow 1$) limits the capability of crystallization of L-LA-unit sequence shifting the melting temperature of the copolymers to lower values and reducing the crystallinity fraction substantially (see Figure V). On the other hand, the PLCL showing a random character closest to Bernoullian distribution of sequences was found to exhibit higher strain capability and strain recovery values (see Table I) and also was less prone to supramolecular arrangements during storage.

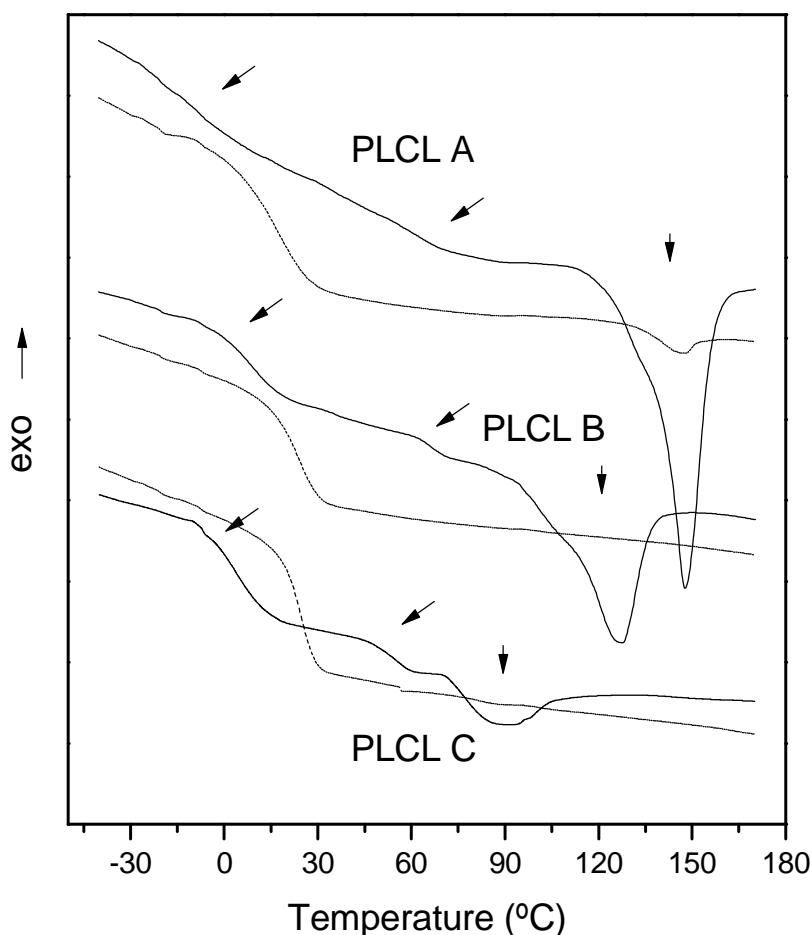


Figure V. DSC first scans (straight) and second scans (dash) of the nascent copolymers of PLCL A ($R = 0.47$), PLCL B ($R = 0.69$) and PLCL C ($R = 0.92$).

Table I. Mechanical properties at room temperature (21 °C) of the PLCLs of different randomness character.

Sample	Secant Modulus at 2 %	Ultimate Tensile Strength	Elongation at Break	Strain Recovery
	(MPa)	(MPa)	(%)	(%)
PLCL A ($R = 0.47$ and $l_{LA} = 6.50$)	12.0 ± 1.2	17.2 ± 0.7	486	93.5 ± 2
PLCL B ($R = 0.69$ and $l_{LA} = 4.35$)	17.1 ± 0.2	29.0 ± 1.7	514	99.3 ± 1
PLCL C ($R = 0.92$ and $l_{LA} = 3.45$)	17.1 ± 1.2	22.7 ± 2.6	531	99.8 ± 1

2.3. Thermal Properties and Crystal Structure

Polyesters can be either semicrystalline or amorphous [59]. Semicrystalline polymers have regular repeating units that allow the chains to fold into dense regions called crystallites. These act as crosslinks giving the polymer higher tensile strengths and higher modulus (stiffness) as compared to an amorphous analog. No polymer can completely organize into a fully crystalline material so there are still amorphous areas in semicrystalline polymers. When a semicrystalline polymer is raised above its melting point (T_m) it may be shaped into rods or molded parts. Amorphous polymers and the amorphous regions of semicrystalline polymers exhibit a glass transition temperature (T_g). At temperatures above T_g , a polymer acts more like a rubber and at temperatures below T_g , a polymer acts more like a glass. A polymer that has a T_g around body temperature may be much more ductile when implanted than it appears to be at room temperature. These properties can affect both the mechanical properties as well as other properties such as biodegradability.

As well as the chain microstructure features, the polymer composition also affects the thermal properties of the copolyesters. By increasing the content of one of the structural units, the T_g and the melting temperature approached to that of its homopolymer. Polyglycolide ($T_g \sim 35-40$ and $T_m \sim 225-230$), poly(L-lactide) ($T_g \sim 60-65$ and $T_m \sim 170-180$) and poly(D,L-lactide) ($T_g \sim 55-60$) are the polyesters that exhibit higher melting points and glass transitions temperatures. On the contrary, poly(ϵ -caprolactone) (PCL), with a T_m at ~ 60 °C, is the one that shows the lowest T_g (at -65 °C) while other

homopolymers such as poly(γ -butirolactone) or poly(δ -valerolactone) have lower T_{ms} (at 53-60 °C and at 57 °C).

Differential scanning calorimetry (DSC), a thermoanalytical technique developed by Watson and O'Neill in 1962 [60], allows to study the thermal transitions of a polymer. As the polymer sample undergoes exothermic processes (such as crystallization) less heat is required to raise the sample temperature. By observing the difference in heat flow between the sample and reference, differential scanning calorimeters are able to measure the amount of heat absorbed or released during such transitions. DSC is also employed to observe other physical changes, such as glass transitions and it is widely used in industrial settings owing to its applicability in evaluating sample purity and for studying polymer curing or crystallization

The degree of crystallinity, crystalline thickness, lattice dimensions, spherulitic size and morphology and the molecular orientation are parameters of great importance to characterize the crystalline phase. In addition to the microscopic techniques, wide angle X-ray diffraction (WAXRD) [61] is often used to determine the crystalline structure of the semicrystalline polymers. When X-rays are directed in solids they scatter in predictable patterns based upon the internal structure of the solid. A crystalline solid consists of regularly spaced atoms (electrons) that can be described by imaginary planes. The distance between these planes is called the d-spacing. Every crystalline solid will have a unique pattern of d-spacings (known as the powder pattern), which is a “finger print” for that solid. In fact solids with the same chemical composition but different phases can be identified by their pattern of d-spacings.

On the other hand, Dynamic Mechanical Analysis (DMA) is becoming more and more popular in the laboratory as a tool to investigate the thermal transitions and the relaxation processes of polymers, including biodegradable (co)polyesters. These properties can be described in terms of either free volume changes or relaxation times and are closely related to the dynamic properties [62].

2.4. Thermal Stability

Thermoplastic polyesters are thought to be transformed into implants or scaffolds by processing techniques such as injection moulding, blow moulding, thermoforming or extrusion [63-65]. The understanding of the thermal stability of biopolymers is particularly important when considering this kind of processes at high processing temperatures, especially where the final product is intended for use in the biomedical field [66]. Hence, at high temperatures, as a consequence of thermal decomposition reactions, biomaterials can undergo a reduction in their properties (e.g. mechanical properties) not maintaining their performance and reliability during their use. Moreover, special care has to be taken when processing these polymers because some thermal degradation byproducts may be toxic to the human body [67].

Thermal degradation studies on poly(ϵ -caprolactone) (PCL) [68-70] and polylactides (PLA) [71-72] have already received special attention. PCL is believed to degrade by a two step mechanism, in which random chain scission dominates at lower temperatures and as the temperature increases specific chain end scission (from the hydroxyl chain end of the polymer chain) becomes more significant [73]. On the other hand, PLA has been reported to degrade by a multi step process [74]. The dominant reaction pathway is an intramolecular transesterification, giving rise to the formation of cyclic oligomers; in addition, acrylic acid from cis-elimination as well as carbon oxides and acetaldehyde from fragmentation reactions were also observed.

With regard to L-lactide-co- ϵ -caprolactone copolymers (PLCL), they show intermediate properties of thermal stability between PCL and poly(L-lactide) [45, 66-67] improving the features of the latter owing to the presence of highly resistant ϵ -CL units. However, due to the different sequence distributions of LA and ϵ -CL units, the copolymers undergo a more complex degradation mechanism. Thus, the PLCLs with higher randomness character ($R \rightarrow 1$) degraded almost entirely in a single stage, and were more resistant to heat. In contrast, the blockier PLCLs were found more sensitive to thermal degradation and degraded heterogeneously presenting two different peaks in the differential thermogravimetric (DTG) curve (see Figure VI). LA-rich sequences degrade at lower temperatures; the mechanism of this first stage of decomposition is highly

influenced by the lactide average sequence length (l_{LA}), and, at a later stage, those of CL.

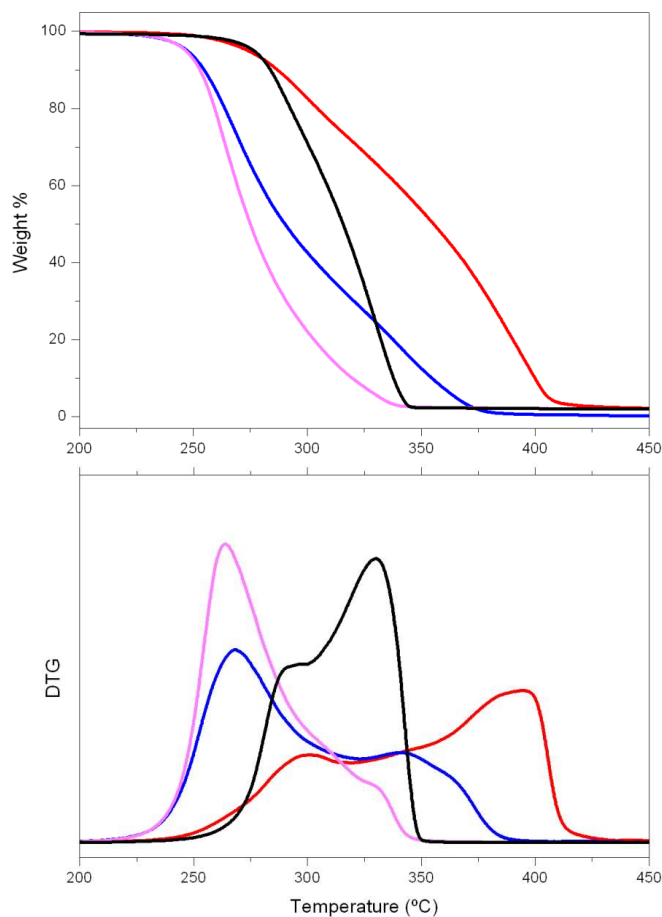


Figure VI. Thermogravimetric (TG) and differential thermogravimetric (DTG) curves of PLCLs synthesized with SnOct_2 ($R \sim 0.5$) having different LA-unit average sequence length: PLLA (black —); PLCL 9010 (pink —); PLCL 6634 (blue —); PLCL 4654 (red —).

The factors that influence the thermal degradation of copolyesters, apart from the thermal resistance of their building units (and their chain microstructural features), include molecular weight and the presence of moisture, residual and hydrolyzed monomers, oligomers and residual metals. In particular, the effect of residual metal compounds is very important. Many authors [75-79] have evidenced the accelerating effect of SnOct_2 on PLA pyrolysis and the results of our group also demonstrated a large influence of metal-catalyzed depolymerisation in PCL, PLLA and their copolymers, yet more significant for tin than for bismuth [80]. Figure VII presents the curves of percent

weight loss and first derivative of weight loss against temperature of three PCLs having approximately 6000 ppm of residual bismuth content, 4500 ppm of residual tin content and 50 ppm of residual tin content.

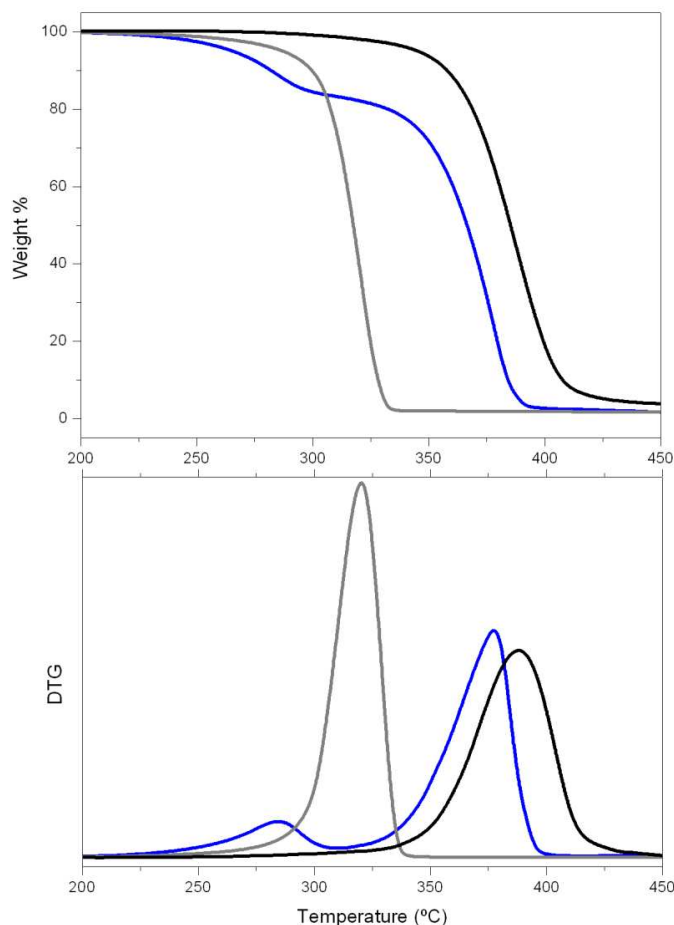


Figure VII. TG and DTG curves of PCLs with different metal content: PCL 6000 ppm of Bi (blue —); PCL 4500 ppm of Sn (grey —); PCL 50 ppm of Sn (black —).

2.5. Mechanical Properties

Most of the homopolyesters employed today display a very similar mechanical behaviour. On the one hand, polyglycolide, polylactides and their copolymers are rather brittle materials that display high elastic modulus and low elongation at break values (< 15 %) due to their high glass transition temperatures. Polyglycolide and poly(L-lactide) show modulus of around 7000 MPa and 2700 MPa, respectively and the latter has a modulus about 25 % higher than amorphous poly(DL,lactide) [59]. These materials are,

therefore, clearly inappropriate for numerous clinical uses, where highly flexible biodegradable materials are required. On the contrary, poly(ϵ -caprolactone) (PCL) and other polyethylene-like polylactones, i.e. poly(ω -pentadecalactone) [81] exhibit modulus from 300 to 400 MPa and deformation at break values > 750 %) but biodegrade at a very slow rate.

This unsuitability shown by the mentioned polyesters might be overcome by blending or copolymerization, which can be appropriate methods for the control of mechanical properties, thermal stability and degradation rates, and thereby to achieve copolyesters with an elastomeric behaviour. The flexibility, high elongation at break values and elevated recovery ratios of the elastomers are highly valued features requested for some medical applications.

2.6. Physical Aging

For creation of reliable medical devices the manufacturers require a deep confidence on the material supply that must present stability, durability and predictability of the macroscopic and microscopic properties. Therefore, it is necessary to understand the changes that biopolymers can undergo in their phase structure and mechanical properties during either the storage time before use or/and for long-term applications depending on temperature. This process by which a polymer tends to reach the equilibrium through slow rearrangement of its chains from a nonequilibrium glassy state is often referred to as physical aging. Many (co)polyesters resulting from melt solidification are metastable, i.e. prone to changes in supramolecular organization in function of time and temperature, and can suffer significant physical aging, particularly when stored at temperatures close to the T_g [82].

Tsuji et al. [83-84], after studying the behaviour of poly(L-lactide-co- ϵ -caprolactone) (PLCLs) of 50 % and 82 % L-lactide (LA) content, demonstrated that these copolymers changed their physical properties during storage at 37°C. In an earlier paper [45], in an attempt to study in more detail the aging effect on the thermal properties of these copolyesters, films of PLCL with different composition (from 66 % to 90 % LA molar content) and similar randomness character ($R \sim 0.5$) were stored at room temperature

(21 °C) for 5 weeks. The mobility of crystallisable LA unit sequences was found to be favoured in the case of the ϵ -CL-rich copolymers, making possible the formation of polylactide crystallites which act as points of reinforcement. As a result, PLCLs in excess of ϵ -CL (above 23 % ϵ -CL molar content) underwent dramatic changes in their mechanical properties. On the contrary, at higher LA contents the mobility of chains was impeded and the crystallization process during storage was limited. Nevertheless, enthalpy relaxations associated to the chain arrangements in the amorphous regions were found in the LA-rich copolymers as a result of aging. In this context, it is worth mentioning that a comparison of homopolylactides of L-LA-isomer with various polylactides with several contents of D-LA-isomer, aged at a similar degree of undercooling, showed that the enthalpy relaxation value was somewhat higher for the PLA samples with lower D-isomer content [85], in agreement with the results observed for the PLCL copolymers.

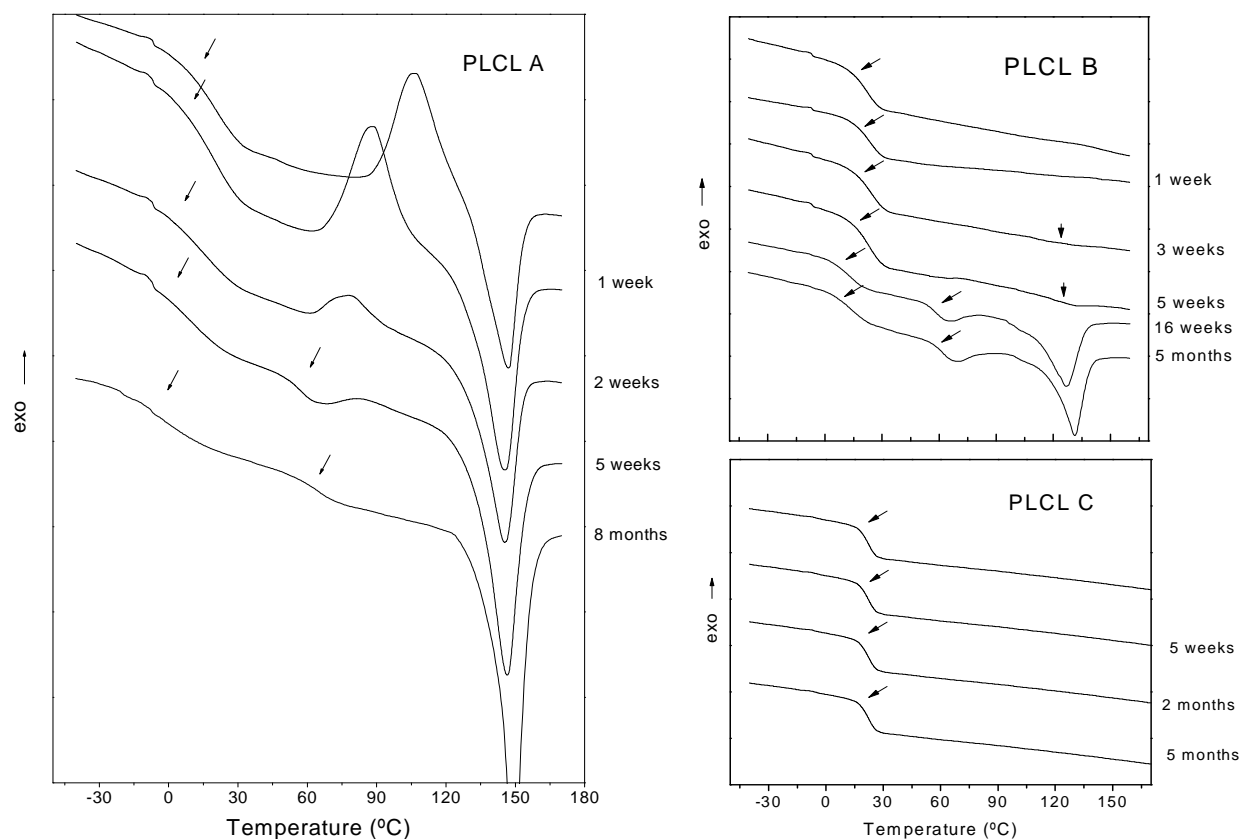


Figure VIII. DSC scans of the film of PLCL A ($R = 0.47$), PLCL B ($R = 0.69$) and PLCL C ($R = 0.92$) at different times of storage.

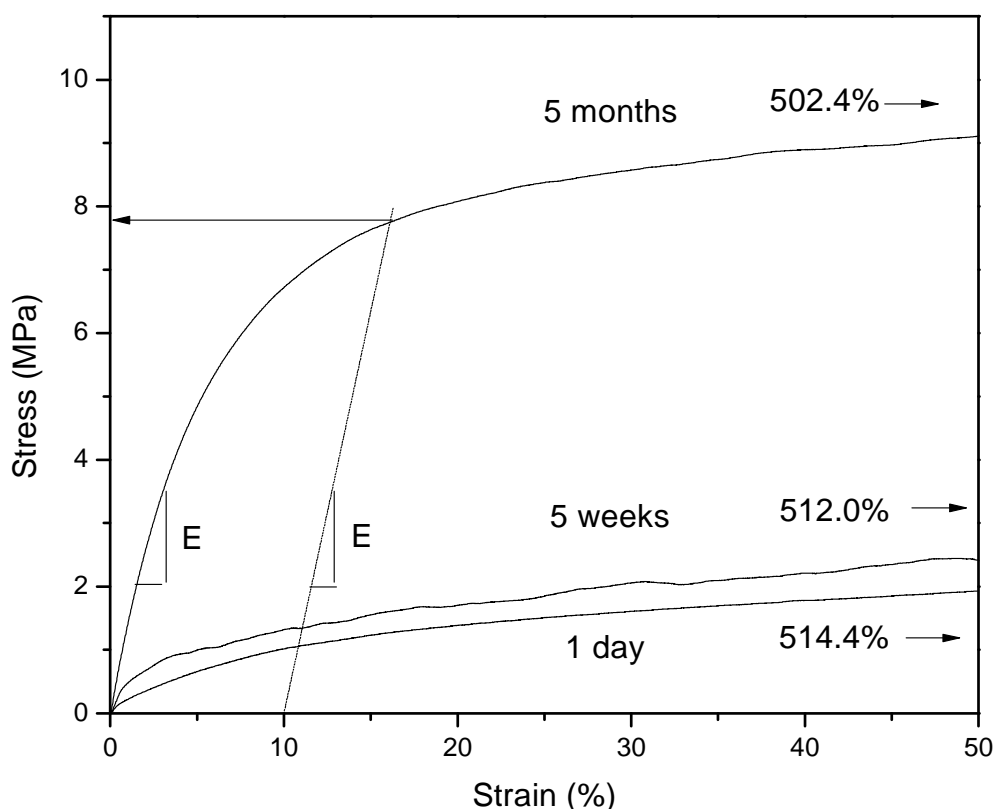


Figure IX. Tensile stress-strain curve of the films of PLCL B ($R = 0.69$) at different times of storage.

In a later work [58], the aging effect on initially amorphous films of three PLCL with equal L-LA content and differing chain microstructure (the previously seen PLCL A, PLCL B and PLCL C) was also investigated. It was proved that the copolymer with higher random character ($R = 0.92$) was less prone to rearrangements during its storage in comparison to the copolymers with larger L-LA average sequence lengths. In contrast, the moderate blocky copolymers (with lower R) underwent changes in supramolecular organization in function of time during storage at room temperature (21°C) and presented a double T_g behaviour indicative of the existence of phase separation into two compositionally different amorphous phases (see Figure VIII). These structural changes, associated to the crystallization of LA building blocks during aging, led to significant variations in their mechanical properties. The moderate blocky PLCLs evolved from being an elastomeric to be partly a glassy semicrystalline thermoplastic, and, thus, can eventually condition its potential uses for medical devices. On the contrary, the most random copolymer among them did not undergo any change in its physical and mechanical properties during the 5 months of the study. Figure IX

shows the tensile stress-strain curve of the PLCL with $R = 0.69$ at different times of storage. At short aging times, the polymer behaved more like an elastomer thermoplastic but after 5 months the elastic modulus increased from 17 to 123 MPa, the offset yield strength rose from 1.3 to 7.6 MPa, its strain at break decreased and its strain recovery was slightly reduced.

2.7. Biodegradability

Once implanted in the body, the biodegradable device should maintain mechanical properties until it is no longer needed and then be degraded, absorbed and excreted by the body, leaving no trace. In the case of the scaffolds applied in tissue engineering, their degradation should match the tissue regeneration rate and completely disappear once the tissue has fully regenerated.

Simple chemical hydrolysis of the hydrolytically unstable backbone is the prevailing mechanism for the polymer degradation. This occurs in two phases. In the first, water penetrates the bulk of the device, preferentially attacking the chemical bonds in the amorphous phase and converting long polymer chains into shorter, ultimately water-soluble fragments. The reduction in molecular weight is soon followed by a decrease in physical properties as water begins to deteriorate the device. In the second phase, the fragments are metabolized or released to the outside medium resulting in a rapid loss of polymer mass [59].

The diffusion of water and the degradation of the polymer compete during the erosion process of the device. If the water uptake mechanism is dominant, the splitting of chemical bonds has a smaller effect and the erosion is homogeneous. This is known as “bulk erosion”. In the opposite case “surface erosion” occurs and degradation proceeds at the interfacial areas between polymeric specimens and the aqueous environment [86]. Bio(co)polyesters are known to degrade by bulk erosion [87-88]. The diffusion of water inside the polymer is dominant and so the degradation occurs throughout the whole material equally and does not proceed from the exterior surface. In the hydrolytic degradation, a combination of two mechanisms, random and chain-end scission (also known as backbiting), are identified [89-90]. The chain scission of a polymer is called

random if the bonds at any position along the polymer chain have the same probability of being cleaved. In contrast, in chain-end scission, the number of chains ends and the rate constant for the cleavage of the terminal bond are the essential kinetic parameters. It is known that random scission controls the molecular weight reduction whereas the mass loss is due to end scission [90].

Hydrolytic degradation of (co)polyesters is affected by a large number of factors. The mentioned auto-catalysis effect is reported to be a very important factor [91-93]. Thicker devices are degraded more quickly because all the leachable oligomeric compounds formed within the matrix are not able to escape from it as soon as they become soluble [94]. The geometry of the shaped bodies, the surface properties (contact angle, roughness and surface tension), the pH changes, which can be due to the degradation products, or the stresses applied during degradation, could also affect the degradation rate. Chemical composition, the type of chemical bond, sequence structure [46-47 57] and the morphology (crystalline or amorphous domains) are among other factors that have an impact on the degradation process. As has been demonstrated, amorphous regions are preferentially degraded because they are more accessible to water molecules [95], whereas the presence of crystalline domains slows hydrolytic degradation down dramatically.

2.8. Biocompatibility and Toxicity

Materials that are biocompatible are those that are not toxic to the body on implantation and can be classified as being bioinert or biodegradable. There are many factors that may influence the reaction of the body to the presence of a biodegradable implant. The response may be related to the size, the processing method that produces it and the composition of the implant. Not only should implanted materials avoid eliciting inflammatory and immunogenic responses, but also degraded materials and related chemicals (monomers, initiators and residual solvents) should be biocompatible in terms of both the local and the systemic response [96-97]. The degradation rate of the polymer and the implant site's ability to eliminate the acidic degradants play an important role in the local tissue's reaction to the implant. If the surrounding tissue cannot eliminate the acid by-products of a rapidly degrading implant then an inflammatory or toxic response

may result [98]. Toxicity can also occur with normally biocompatible polymers due to leaching of low molecular weight plasticisers and additives. Therefore, it is important to characterise the grade of polymer in use. What is sold as polymer X by one manufacturer may be very different from polymer X sold by another, due to purity and additives present. Surface reactions and absorption of proteins at the polymer surface can also provoke problems. Thus, the surface texture and the shape of the implant are also important.

There have been numerous studies on the biocompatibility of implants since the early 1960s mostly focusing on polyesters of lactide and glycolide. The majority of results from studies in humans with this kind of polymers are favourable making the future of biodegradable implants bright.

2.9. Processing, Storage and Sterilization

Biopolyesters may be processed similar to any engineering thermoplastic in that they can be melted and formed into fibers, rods and molded parts. Final parts can be extruded, injection molded, compression molded, or solvent spun or cast. High temperatures are often needed to reduce the melt viscosity or high pressures needed to enable the polymer to flow through small orifices to create fiber or fill a mold. However, excessively high processing temperatures can decrease the molecular weight depending on the thermal stability of the polymer chains. Moreover, the presence of moisture during processing can also reduce the molecular weight and alter the final polymer properties. There are also strong interactions among temperature, moisture content, shear rate and residence time in the machine. Residence time is defined as time at temperature the material is in the barrel of a molding machine. Higher shear rates and longer residence times resulted in increasing polymer degradation even at lower temperatures. In general, processing at the mildest conditions possible and the rigorous exclusion of moisture are the recommended [99-100].

Due to the fact that the polyesters are in general hydrolytically unstable, the presence of moisture can degrade them during storage, processing (as already discussed) and after device fabrication. Therefore, polymers should be packed after manufacture and if

possible, double bagged under an inert atmosphere or vacuum. In addition, they must be stored in a freezer to minimize the effects of moisture. The final devices should not be sterilized by autoclaving or dry heat because this could degrade the device. The polyester devices are typically sterilized by γ -radiation, ethylene oxide, plasma of hydrogen peroxide or electron beam irradiation.

2.10. Other Properties

For some specific applications, other properties could play an important role. Therefore, the electric and optical properties, the permeability, swelling and solubility, the surface properties or the viscosity of the (co)polyesters also have to be investigated.

3. Potential Medical Applications of Copolyester Elastomers

The applications in the medical science of the copolyester elastomers include cell therapy for the regeneration of soft tissues and some implants and devices employed in surgical procedures in several branches of medicine. Biodegradable materials with an elastomeric behaviour are greatly valued in cardiology (heart, valves, arteries and veins) and urology (urinary track and male genitalia), and for applications in the respiratory system (larynx, trachea, bronchus, diaphragm and lungs), the digestive track (esophagus, bile ducts and liver) and the nervous and muscular systems.

If the scaffold or the medical device is to be mass produced, so that surgeons can use it in the clinic, they must be made from a processing technique that can be up-scaled for mass production and that can form a variety of shapes and sizes to match that of the defect of the patient. The products must also have the potential to fill the required International Standards Organization (ISO) or Food and Drug Administration (FDA) standards and be easily sterilised.

3.1. Medical Devices

3.1.1. Occlusion devices for cardiac defects

There are several defects inside the chambers of the heart, if left untreated, may result in severe health consequences, including heart failure. Earlier interventions were predominantly surgical, but following the success of transcatheter techniques in the 1970s, most occlusion devices are currently inserted percutaneously. The first occlusion device to obtain approval for commercialization was the AMPLATZER™ septal occluder (ASO) for the treatment of septal defects. The approved device consists of two Nitinol discs connected by a waist, and each disc has polyester fabric woven around it. Since 2001, several new designs have been introduced and many approved for treatment of defects. All such devices are permanent, and non-retrievable except by surgery. In general, the devices consist of two components: the frame (support material) and the fabric (occluding material). The support frames are made from stainless steel, Nitinol and cobalt-based alloys and must show the ability to “self-expand” with the myocardium contractions. The purpose of the occluding material for the fabric is to prevent blood flow, and to provide the platform for cell growth, but it also should be able to stretch with the frame during deployment [101].

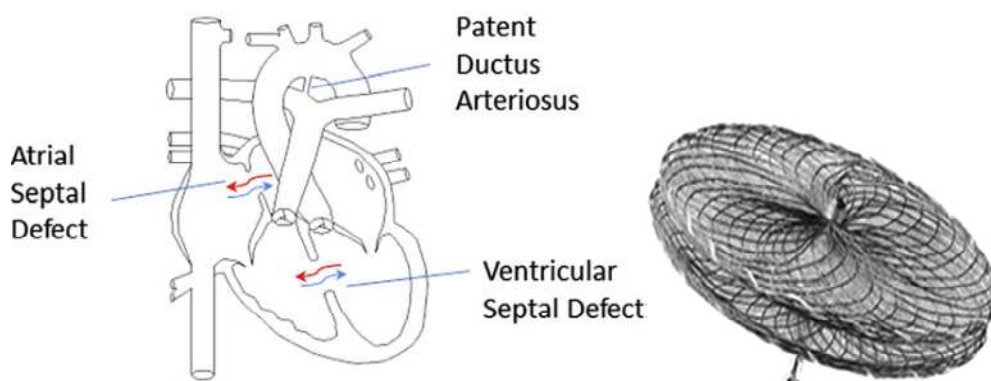


Figure X. Schematics of ASD, VSD and PDA defects and an ASO septal occluder.

The complications associated with occlusion device are malposition/ embolization [102-103], erosion [104-105] and thrombus formation associated with atrial septal defects (ASDs) [106-107]; a similar incidence rate is seen with patent ductus arteriosus (PDA) devices and a slightly higher incidence rate is associated with ventricular septal defect

(VSD) devices [108-109]. Although the incidence rates are low, the complication is usually serious enough to warrant immediate surgical retrieval [102,103,110–113]. The complications are of particular concern, because they may occur in the more vulnerable pediatric population; the prediction of the adverse event is not possible because a clear cause has not been consistently identified; and the severity of an event is with rare exception an urgent life threatening event.

Most of these long-term complications can be alleviated by the use of fully degradable devices which eliminate concerns regarding the use of metals inside the heart, and if fully endothelialized, also minimize migration concerns. The sooner the material becomes covered with endothelial cells, the better the chances for the long-term survival of the implant. However, the cellular ingrowth has to be balanced against the primary need of preventing blood flow through the fabric. Early attempts focused on synthetic Dacron (poly(ethelene terephthalate), poly(tetrafluoroethylene) or polyurethanes as occluders fabric materials, but in recent years biodegradable polyesters are being employed, such as the based on lactide, ϵ -caprolactone and glycolide from the patent of Venkatraman et al. [114]. The concept of a fully degradable occlusion device is that it acts as a temporary template for the ingrowing host tissue from the defect edge to cover the device and thus the defect underneath. The biodegradable occlude should promote the complete healing response and eventually disappear, because once the defect is closed and covered, a permanent implant is unnecessary and has potential disadvantages. Fully biodegradable occluders made of polydioxanone [115], poly(ϵ -caprolactone) [116] and poly(ϵ -caprolactone) with BaSO₄ radiopacity filler [117] have been recently developed. However, biodegradable frames present lower stiffness than the permanent occlusion devices and the use of nano- or micro-sized fillers could be necessary to improve the stiffness required for deployment.

3.1.2. Stents

Cardiovascular stents

The coronary arteries supply blood to the heart muscle. Cholesterol and calcium can deposit plaques on the walls of these vessels, reducing the amount of blood that can

flow through them. This is known as atherosclerosis. Lack of enough blood to the heart muscle may cause chest pain and when there is a severe shortage of blood supply to the heart, some of its muscle may die, causing a heart attack (myocardial infarction). A coronary stent is a tube-shaped device placed in the coronary arteries that supply blood to the heart, to keep the arteries open in the treatment of coronary heart disease. It is used in a procedure called percutaneous coronary intervention. Similar stents and procedures are used in non-coronary vessels e.g. in the legs in peripheral artery disease.

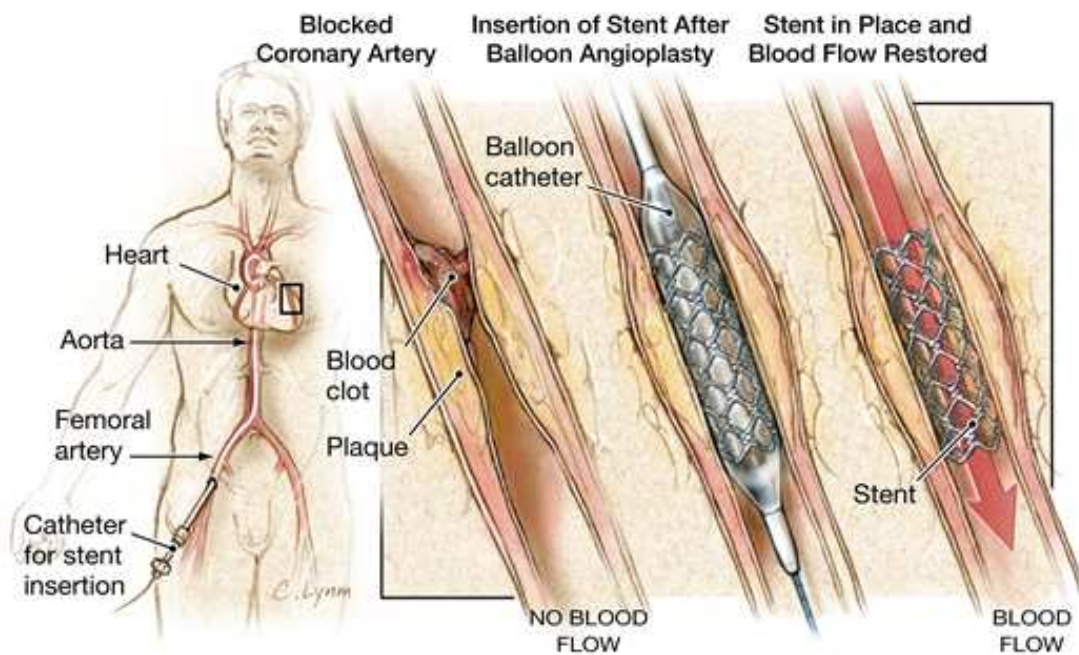


Figure XI. Schematic of stent placement [118]

An ideal stent should control restenosis by limiting negative remodelling and by controlling excessive healing by delivery of an antiproliferative drug. It also must have an optimal lumen size and allow vessel growth (for potential pediatric applications) [119-122]. Beyond 6 months, a permanent implant is unnecessary (the artery does not need the mechanical support of a stent) and has potential disadvantages including changes in vessel area or late thrombosis. Although multiple factors predispose to late thrombosis, it is unusual if the stent is completely absorbed because there would not be a permanent foreign body exposed to blood even if endothelialisation were functionally abnormal, delayed or incomplete [123-126]. A number of different materials ranging from magnesium to a variety of polymers have been used to construct biodegradable

stents of different designs. However, there are challenges in making a stent that has sufficient radial strength for an appropriate duration, that does not have unduly thick struts, that can be a drug delivery vehicle, and in which degradation does not generate an unacceptable inflammatory response.

The Igaki-Tamai [127-128], constructed from poly(L-lactide) (PLLA), and the magnesium stents [129] were the first absorbable stents implanted in humans. REVA stent is made from a tyrosine-derived polycarbonate polymer that metabolizes to amino acids, ethanol and carbon dioxide, but the best outcomes to date have been with the BVS stent [130-133]. This stent has a biodegradable polymer backbone of PLLA with a polymer coating of poly(D,L-lactide) that contains and controls the release of the antiproliferative drug, everolimus.

Stents for the gastrointestinal tract

Obstruction of the gastrointestinal tract in patients with cancer occurs frequently and may be mechanical or functional, partial or complete, and may occur at one or at many sites [134-136]. Tumours can impair bowel function in several ways: occlusion of the lumen, impairment of peristalsis due to tumour ingrowth, masses in the mesentery or omentum or adhesions creating an extra-luminal obstruction, and finally infiltration of the enteric nervous system causing dysmotility [137]. Obstruction due to intraor extra-luminal obstruction can be treated by endoscopic placement of metallic self-expandable stents. These prostheses have made it possible to reestablish luminal continuity in patients with malignant obstruction of esophagus, gastric outlet, small bowel, or colon who are at high risk of surgical intervention [138-139].

Use of metal and plastic stents for treatment of benign stenoses of the gastrointestinal tract is associated with several problems [140]. They induce early mucosal hyperplastic reaction (tissue ingrowth) and are associated with a higher risk of migration. The rigidity of the metallic stents has also brought some complications. When the stents directly contact with the tract wall it could become encrusted with body tissue. Stents made of biodegradable materials could overcome the above mentioned drawbacks and, furthermore, a surgical removal from body after disease it is not required. Polylactide,

poly(ϵ -caprolactone-D,L-lactide) or poly(p-dioxanone) biodegradable stents [141-145] are being investigated for treatment of esophageal strictures and achalasia and benign intestinal, colonic and biliary strictures.

3.1.3. Urological catheters

Urological catheters are hollow, partially flexible tubes that are used for diagnosing pathology in the lower urinary tract, to monitor urine output and to relieve urinary retention. The term catheter comes from the Greek and means to let or send down. The first catheters were created by the ancient Syrians from reeds and then were developed in the beginning of the 11th century [146]. Rubber catheters were produced in the 18th century but initially were weak and friable at body temperature, resulting in intravesical fragmentation. Vulcanization improved the firmness, flexibility and durability of rubber, and popularized catheter use with the availability of later rubber in the 1930s [147]. Nowadays urinary catheters are made of rubber, polyurethane and other thermoplastic elastomers, silicone or latex and come in many sizes and types including both external (condom) as well as indwelling catheters, which may be either a urethral or a suprapubic catheter.

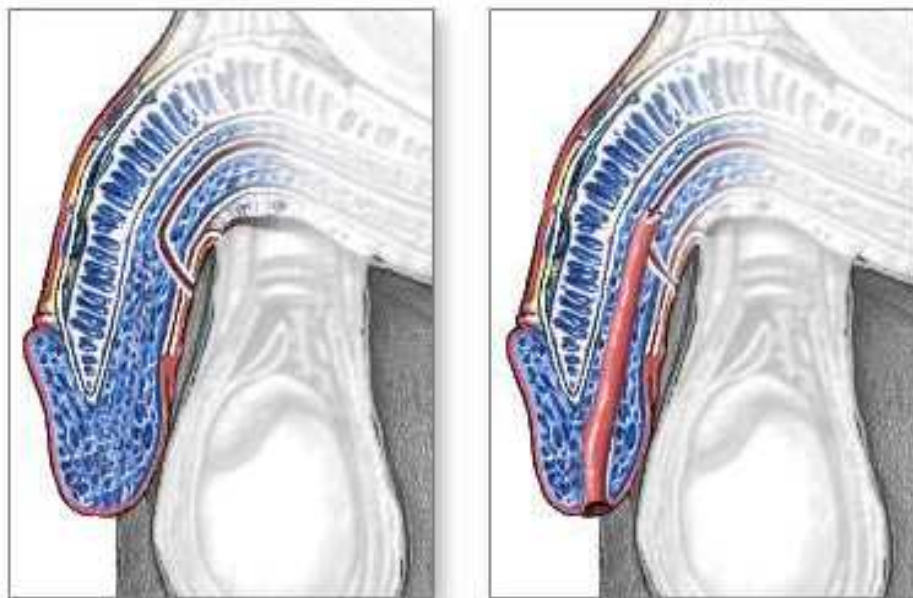


Figure XII. Schematic from ADAM of the hypospadias defect and the urethra reconstruction.

Biodegradable devices could be of interest for urethral and ureteral diseases since they do not need eventual surgery removal. Copolyester elastomers could be an alternative to the silicone tubes that are currently employed in the surgery of urethral strictures or hypospadias. After surgery, the catheter holds the new shape of the urethra which is reconstructed using foreskin or buccal mucosa grafts [148-149]. 2 weeks later this tube is removed and so may result in healing problems.

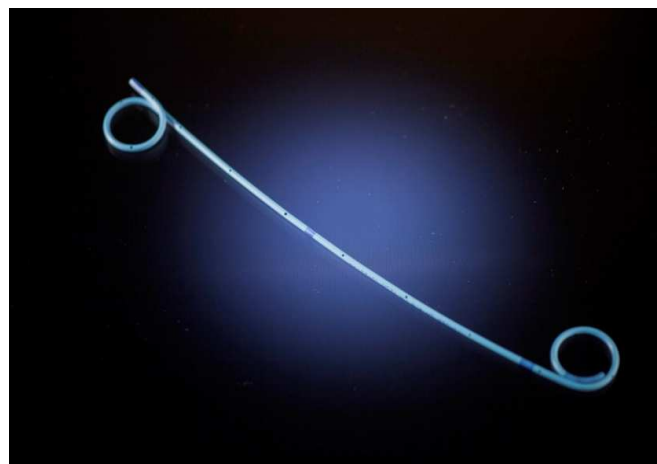
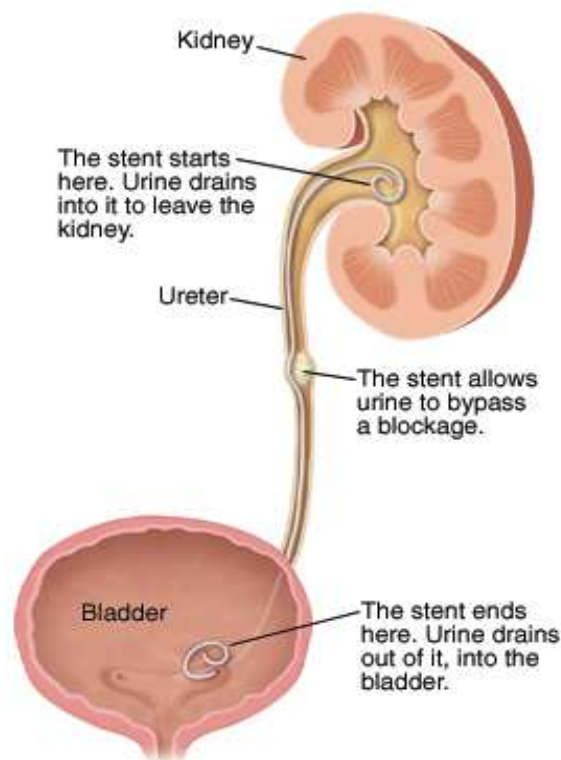


Figure XIII. Suprapubic ureteral catheter.

With regard to ureteral catheters, they find wide application in urology when obstruction of the ureter occurs (most commonly from kidney stones which affect 10 % of population, tumour, stenosis or blood clots), for extrinsic obstructions (fibrosis, adenopathy or tumours) or to maintain the integrity of the conduct after surgery or during the treatment of urinary fistulas [150]. Figure XIII show a typical double J catheter. The pigtail curl on either end help maintain its position in the bladder and kidney so that the catheter will not migrate. However, as no ideal device has been developed, the majority of patients with indwelling ureteral stents are at an increased risk of urinary tract infection and suffer problems of encrustation, bacterial colonization, dislocation or fragmentation [151]. A perfect ureteral catheter should be biocompatible to avoid swelling, erosions or hyperplasia and biodurable, displaying an adjusted degradation rate and showing proper elastomeric behaviour during its use. It also should be easy to insert, has good internal flow and resists encrustation [152-157].

3.1.4. Nerve guidance conduits

Peripheral nerve injury is often a very serious, debilitating condition that affects 1 in 1000 patients [158-160]. There are a number of established techniques for the treatment of peripheral nerve repair [161]. For small nerve injury gaps, the coaptation of the two severed nerve ends via direct suturing is common. For larger gaps this technique is frequently not possible or results in increased tension along the re-joined nerve, decreasing blood flow to the injury site, diminishing the regenerative capacity and overall surgical outcome [162]. In these cases autologous nerve grafts are commonly used [163], but are associated with a number of major disadvantages, including donor site morbidity and increased surgical complications.

An alternative approach to peripheral nerve repair of short injury gap is to utilise an implantable entubulation device known as a nerve guidance conduit (NGC). These devices are usually designed not only to act as a guide for the regenerating nerve end, but also to modulate the internal environment and to promote host regeneration [164-165]. A small range of commercially available devices exists (i.e. Neurolac or Neurotube), fabricated from FDA approved materials. While these devices show similar efficacy to autograft surgery for short injury gap repair, their efficacy for gaps beyond ~

20 mm is limited [166]. Synthetic NGC materials typically include polymers such as poly(lactide-co-glycolide) [167], poly(ϵ -caprolactone-co-glycolide) [168] or poly(lactide-co- ϵ -caprolactone [169]. The only naturally derived material used commercially to date is collagen [158], although spider silk is being investigated experimentally [170], as are polymers produced by bacterial fermentation e.g. polyhydroxyalkanoates [171].

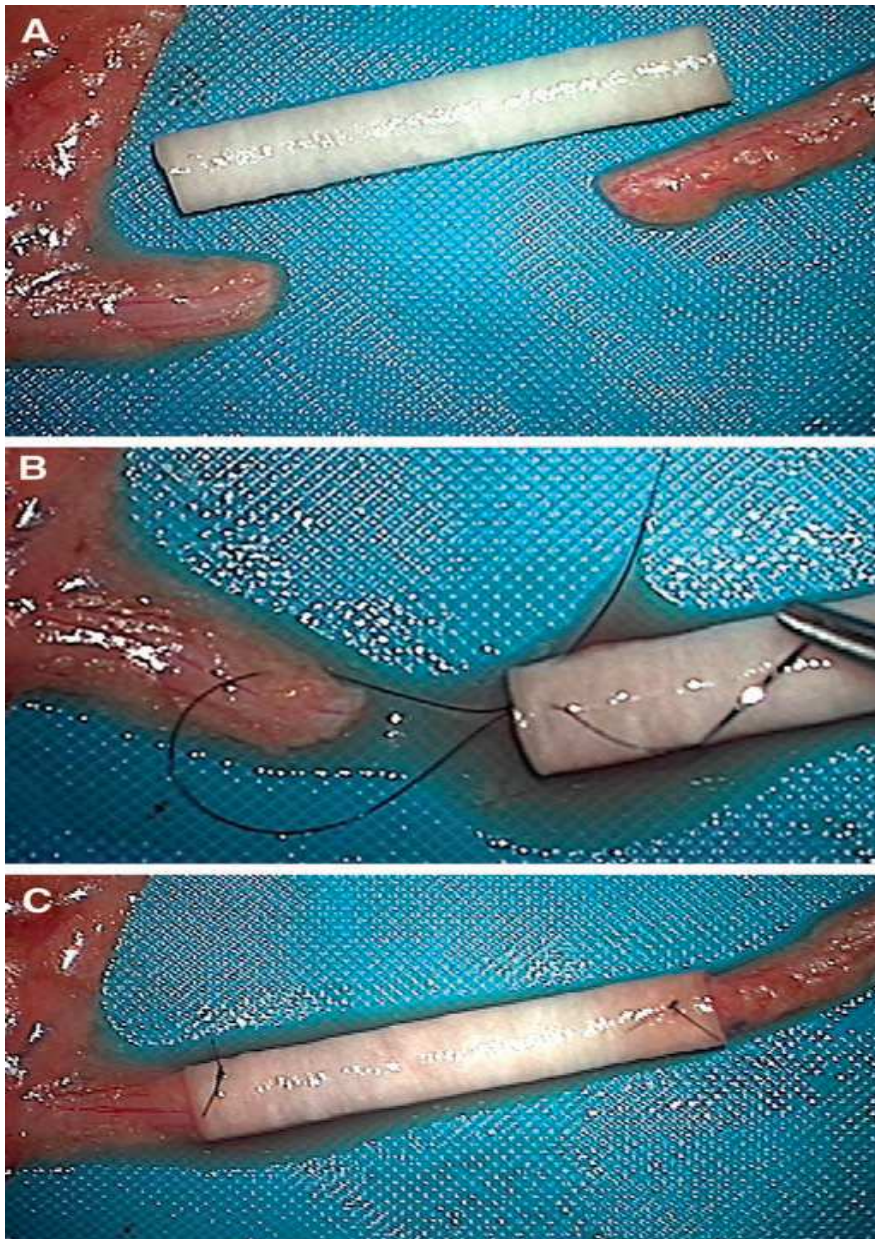


Figure XIV. A nerve tube repair of a nerve injury gap (using NeuraGen, Integra Life Sciences) [172].

3.2. Regeneration of Soft Tissues

Implants lack three of the most critical characteristics of living tissues: (1) the ability to self-repair; (2) the ability to maintain a blood supply; and (3) the ability to modify their structure and properties in response to environmental factors such as mechanical load. All implants have a limited lifespan and, as life expectancy is continually increasing, it is proposed that a shift in emphasis from *replacement* of tissues to *regeneration* of tissues is required to satisfy this growing need for very long-term repair [173].

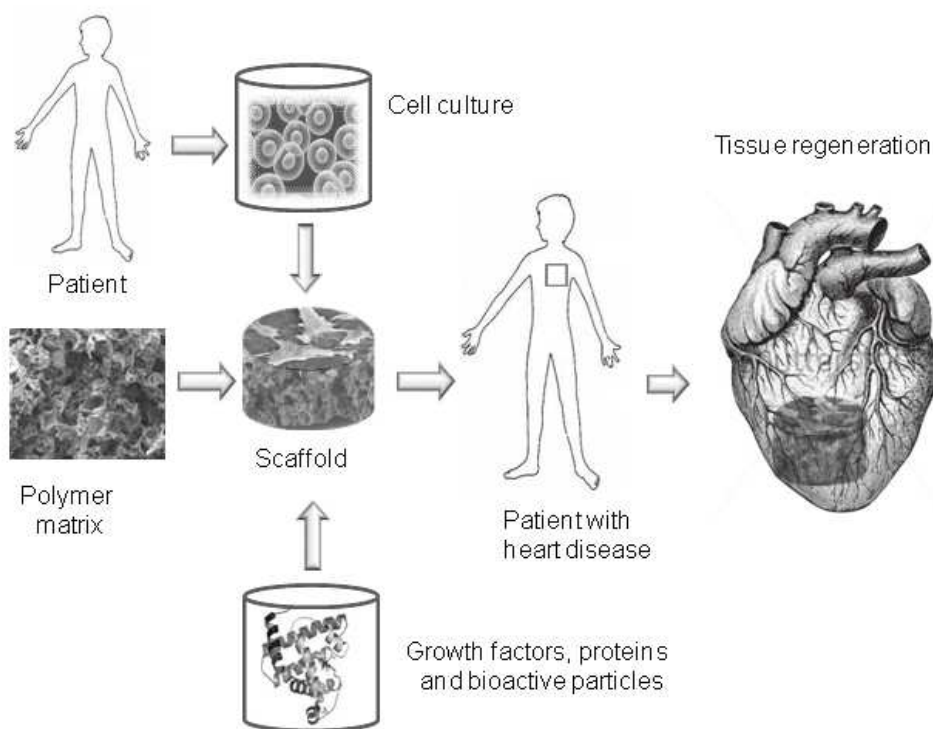


Figure XVI. Schematic illustration of tissue engineering strategy for the regeneration of a damaged tissue.

Tissue engineering can be defined as an interdisciplinary field that applies the principles of engineering and life sciences toward the development of biological substitutes that restore, maintain or improve tissue function [174-176]. There are three strategies in tissue engineering: the use of isolated cells or cell substitutes, the delivery of tissue-inducing substances such as growth and differentiation factors to targeted locations, and that we are interested in, the cell culture in three dimensional scaffolds.

There are many criteria that must be fulfilled to create an ideal scaffold. To be able to regenerate a tissue, the matrix should have a structure that acts as a template for tissue growth in three dimensions and stimulates new growth in the shape dictated by the scaffold. To allow a tissue to grow in 3-D, the matrix must be a network of interconnected pores (see Figure XV) that let cells to migrate through the scaffold and promote tissue growth throughout the template. The pore network must allow the culture media to reach all cells, providing them with essential nutrients. Once the tissue engineered construct has been implanted, the pores must be connected sufficiently such that blood can penetrate to provide those nutrients. An ideal scaffold would stimulate blood vessels to grow inside the pore network (angiogenesis) and not only act as a template for tissue growth, but it should also activate the cells of the tissue for self-regeneration. It has to be considered that cells seeded on the scaffolds receive and process a multiple combination of physicochemical and biological cues that will define their attachment, proliferation and differentiation and, in consequence, the cell cycle [177]. Therefore, the most critical aspects of the native extracellular matrix should be mimicked to control the processes regulating cell fate and function. The scaffolds should act as a delivery system for the controlled release of cell- and gene-stimulating agents. Common synthetic polymers lack in signals on their surface that promote the appropriate biological functions of the seeded cells. Growth factors can be incorporated into biodegradable polymer to immobilise proteins of specific binding sites [178-179]. Alternatively, the incorporation of inorganic bioactive particles [180-183] such as hydroxyapatite or bioactive glasses has been found to stimulate the cell proliferation.

The scaffold must also be biodegradable or bioresorbable leaving eventually no trace of its presence. The material by-products should be ones that can be excreted or metabolised by the body. The degradation and resorption rates must be controllable so that it can be tailored to match the cell/tissue growth *in vitro* and/or once it has been implanted, transfer gradually the mechanical loads from the scaffold to the regenerated host tissue. Importantly, the mechanical properties of the tissue engineered construct should also match that of the host tissue and the structure and strength must be maintained until enough tissue has been regenerated.

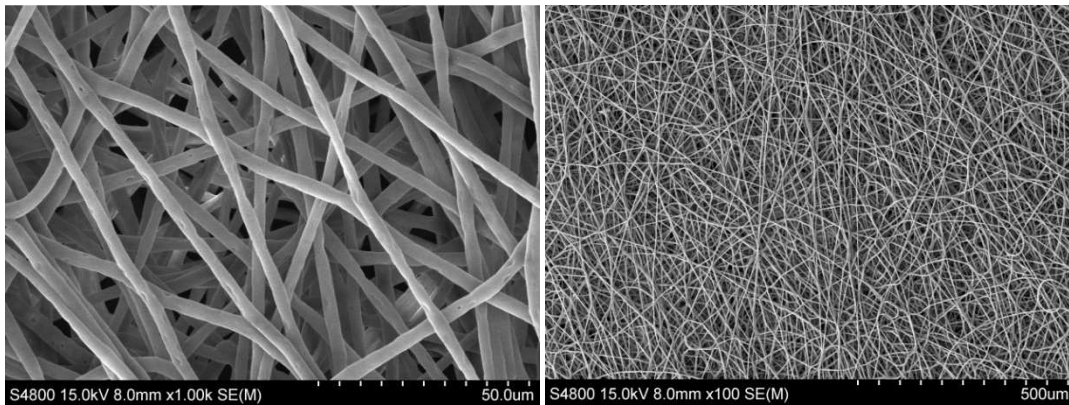


Figure XV. Scanning Electron Microscope (SEM) images of a 3-D polymer matrix made by electrospinning with a 90:10 DL,lactide- ϵ -caprolactone copolymer from this thesis.

(Co)polyesters are a popular choice of material for tissue-engineered scaffolds and are suited for the regeneration of soft tissues such as the described below. However, most tissue-engineered applications are still experimental with limited human trials and several technological barriers must be overcome in order for clinical use of tissue-engineered constructs to become routine [184].

Musculoskeletal system

Tendons connect bones and muscles, while ligaments joint one bone to another. Both show thick, closely packed collagenous bundles oriented parallel to the longitudinal axis of each structure with regular sinusoidal waves in the fibrillar matrix [185]. These dense fibrous connective tissues are considered as viscoelastic materials, transmitting load with minimal energy loss and deformation [186].

Several approaches are proposed to produce bioengineered tissues for the reconstruction of anterior cruciate ligament, Achilles tendon or patellar tendon, which are often the target of traumatic injuries. However, there is still much research required to achieve the ultrastructural characteristics of the cell-extracellular matrix of these natural tissues. The poor mechanical properties of the tissue-engineered constructs are a consequence, in part, of the difficulty of applying proper mechanical-chemical stimuli to the cells as they proliferate *in vitro* in their tissue-engineered scaffolds. Current research into the use of bioreactors that can apply such stimuli in a controlled manner may solve this problem.

(Co)polyester elastomers are gaining interest in the regeneration of muscles, tendons, or ligaments thanks to their shape recovery capacity. This property permits a dynamic cell culture with mechanical stimulation which promotes cell proliferation, extracellular matrix production, gene expression, etc [187]. By contrast, in non-elastomeric materials (poly(L-lactide), poly(DL-lactide/glycolide), etc.), this mechanical stimulus could cause an undesired permanent deformation of the construct.

Cardiovascular system

Cardiovascular disease is by far the most common reason for morbidity and mortality in the Western world. It comprises malfunction of heart valves, blood vessels, and myocardium, all of which are subject to tissue-engineering programs [188].

The development of tissue-engineered heart valves is fuelled by the idea of creating a growing valve for children with congenital cardiac malformations and a totally autologous biological valve for adults with acquired valve defects. Commercially available tissue valves include heterograft (porcine and bovine, cross-linked with gluteraldehyde) and autograft. The disadvantage of these tissue valves is limited durability (10-15 years). Use of autologous tissue, such as the pericardium, for valve repair or replacement is a step towards but the goal of several laboratories is to create heart valves *in vitro* using stem cell technology.

Vascular replacement or bypass is used to prolong the life of thousands of patients annually. Blood vessel engineering aims predominantly at generating small-diameter (< 6 mm; e.g., coronary arteries) rather than large-diameter vessels (e.g., aorta, large mesenteric or femoral arteries), due to the fact that Dacron and other polymers are already being used in the latter with satisfying results. The supports used as vascular grafts must be biocompatible (non-thrombogenic, non-inflammatory, non-immunogenic), be compliant and elastic; they must closely mimic the unique viscoelastic nature of the artery (elongation at break of ~ 125 % and ultimate tensile strength of 1 MPa), accommodate pressure changes (and be non-disruptive to blood flow) and should also be able to “remodel” efficiently: i.e., to allow for growth of a layer of endothelium in a reasonable period of time [189].

Finally, myocardial-tissue engineering aims at creating force-developing cardiac tissue patches to correct cardiac congenital malformations in children (“the growing patch”) and replace or support heart muscle function after myocardial infarction or in patients with cardiomyopathies. An alternative to stem cell-mediated cardiac repair is to associate cells and biomaterials providing an adequate 3D support for transplanted cells, thereby increasing cell survival and even guiding cell differentiation and fate *in vivo*. Biomaterials not only must provide support for the cells but may also mimic the structural architecture of the heart. The constructs should have enough flexibility to respond synchronically with the myocardium contraction and to effectively transfer the mechanical stimulus from the myocardial microenvironment to the incorporated cells [190].

Digestive system

Since the mid-1980s, reconstructing the alimentary tract based on the principles of tissue engineering has emerged as an alternative treatment to transplantation or the attempts of substituting native tissue with autogenous tissue derived from another anatomic location. Recently, tissue engineering has made significant progress in terms of successfully recapitulating all major structures within the alimentary tract. To date, esophagus, stomach, small intestine, and large intestine have all been created experimentally using the methods of tissue engineering and, more importantly, preliminary studies of these tissue-engineered constructs are beginning to show evidence for physiological function in a number of animal models. Despite significant challenges unique to the fabrication of the alimentary tract, ongoing work suggests enormous therapeutic potential in the years to come [191].

Genitourinary system

Tissue-engineering techniques are currently being investigated for the replacement of lost or deficient genitourinary structures, including urethra, bladder, male and female genital tissues, ureter, and renal structures [192]. Kidney is possibly the most challenging organ in the genitourinary system to reconstruct using tissue-engineering techniques due to its complex structure and function. Some investigators are pursuing

the replacement of isolated kidney function parameters with the use of extracorporeal units, while others are working toward the replacement of total renal function by tissue-engineered bioartificial structures. Gastrointestinal segments are commonly used as tissues for bladder replacement or repair. However, these tissues present multiple complications and investigators have attempted alternative reconstructive procedures, such as the use of tissue expansion, seromuscular grafts, matrices for tissue regeneration, and tissue engineering with cell transplantation.

Urothelial defects are fairly common, mainly caused by congenital malformation, trauma or stricture. Nowadays, they are repaired by traditional reconstructive surgery using the patient's own genital tissue or buccal mucosal grafts. However, these operations are prone to complications, such as fistula formation of urethral strictures, and alternative methods are needed. Native urethra has a tubular structure; therefore an ideal biomaterial for urothelial tissue engineering should be elastic to form the tube-like structure; further, the basement membrane of urothelium is elastic and, therefore, the elastic biomaterial would mimic the natural growth surface of human urothelial cells. Additionally, the ideal tissue-engineered urothelium should have a urothelial-specific surface structure: the cells in the superficial cell layer of native urothelium are large and frequently binucleated umbrella cells characterized by compact tight junctions and the presence of defined plaques of asymmetric unit membrane. The native urothelium expresses intermediate filament proteins, cytokeratins and uroplakins and these proteins should also be present in the ideal tissue-engineered urothelium. Various natural biomaterials, such as collagen, small intestinal submucosa or human amniotic membrane and different synthetic polymers, such as polyglycolide or polylactide have been studied for urothelial tissue-engineering applications. The problems concerning the natural biomaterials (poor mechanical properties, xenograft origin and fabrication difficulties) and the synthetic biomaterials mentioned (hardness and inelasticity) may be avoided using copolyester elastomers such as poly(L-lactide-co- ϵ -caprolactone) [193].

Respiratory system

Acute and chronic pulmonary disorders are common causes of morbidity and mortality throughout life. Since respiration is solely dependent on lung structure and function,

failure to form adequate lung tissue during morphogenesis and loss of lung tissue related to acquired or inherited pulmonary disorders are common clinical occurrences that are often life threatening. While no single system has been developed for regeneration of functional lung tissue capable of engraftment into the lung, a number of model systems have been developed that allow the study of various aspects of the processes that will be required for lung regeneration. The remarkable complexity of the lung and its requirement for bronchial pulmonary arterial and lymphatic circulations as well as its connection to the conducting airways and the cardiovascular system present a considerable engineering hurdle. Various pulmonary cell types can be isolated and grown under conditions that retain their capacity to reorganize into lung-like structures *in vitro*. However, pulmonary cells cannot be readily infused or explanted into airways or into the pulmonary circulation to induce formation of functional tissue. The study of lung formation, repair, and tissue engineering will likely provide knowledge regarding the cellular and molecular processes that allow for future cell- and tissue-based therapies for the treatment of lung disease [194].

Nervous system

The peripheral nervous system has the potential for self-repair following injury but clinical success is variable. As previously seen, nerve guidance tubes are the most promising approach to nerve repair. However, the use of a new generation of nerve guidance scaffolds that provide controlled release of neurotrophic factors that are specific to nerve outgrowth, neuronal survival, and nerve sprouting appear to be the key to achieving a tissue-engineered solution.

Cartilage

Articulating cartilage does not have a blood supply so has little capacity for self-repair. Tissue-engineered repair of defective cartilage caused by arthritis or trauma could potentially benefit an estimated 1 million patients per year. Three tissue-engineered options are available clinically after harvesting chondrocytes from a patient: expand the cells to a population of millions per cm^2 *in vitro* followed by injection into the site of damage; harvest chondrocytes as small plugs and transplant them into the defect

creating a “mosaicplasty”; or grow an expanding cell population on a porous resorbable fibrous scaffold, followed by implantation into the defect site.

Skin

Many patients need a supply of replacement skin to treat severe burns, loss of skin in accidents, chronic ulcerations, especially in legs and feet, and for repair of sites where tumours have been removed. The clinical “gold standard” is use of the patient’s own skin in the form of a split-thickness autograft. The advantage is the absence of immunorejection but the disadvantages are limited availability of normal skin, morbidity of the site of the autograft and final cosmetic outcome. Tissue engineering of skin substitutes offer a much needed solution to these problems. The objective is to produce a “ready to use” skin substitute that performs as well as the patient’s own skin.

References

- [1] Drobny, J.G. Handbook of Thermoplastic Elastomers. A volume in Plastics Design Library. William Andrew Inc. Elsevier 2007.
- [2] Holden, G.; Kricheldorf, H.R.; Quirk, R.P. Thermoplastic Elastomers, 3rd edition. Hanser Publishers, Munich 2004.
- [3] Erman, B.; Mark, J.E. in Science and Technology of Rubber, 2nd edition. Eds. Mark, J.E.; Erman, B.; Eirich, F.R. Academic Press, San Diego 1994, 190.
- [4] Holden, G. Understanding Thermoplastic Elastomers, Hanser Publishers, Munich 2000, 9.
- [5] Semon, W.L. U.S. Patent 1,929,453 (1933, to B.F. Goodrich Co.).
- [6] Henderson, D.E.. U.S. Patent 2,330,353 (1943, to B.F. Goodrich Co.).
- [7] Wolfe Jr., J.R. in Thermoplastic Elastomers—A Comprehensive Review, chapter 6. Eds. Legge, N.R., Holden, G.; Schroeder, H.E. Hanser Publishers, Munich, 1987.
- [8] Bayer, O.; et al. German Patent 738,981 (1937, to I.G. Farben, A.G.).
- [9] Christ, A.E.; Hanford, W.E. U.S. Patent 2,333,639 (1940, to DuPont).
- [10] British Patents 580,524 (1941) and 574,134 (1942) (both to ICI Ltd.).
- [11] Hanford, W.E; Holmes, D.F. U.S. Patent 2,284,896 (1942, to DuPont).
- [12] Snyder, M.D. U.S. Patent 2,632,031 (1952, to DuPont).
- [13] U.S. Patent 2,629,873 (1954, to DuPont).
- [14] Schollenberger, C.S.; Scott, H.; Moore, G.R. Paper at the Rubber Division Meeting, September 13, 1957. *Rubber Chemistry and Technology* 1962, 35, 742.
- [15] Schollenberger, C.S. U.S. Patent 2,871,218 (1959, to B.F. Goodrich Co.).
- [16] Gergen, W.P. in Thermoplastic Elastomers—A Comprehensive Review, chapter 14. Eds. Legge, N.R.; Holden, G.; Schroeder, H.E. Hanser Publishers, Munich 1987, p. 507.
- [17] Holzer, R., et al. U.S. Patent 3,262,992 (1967, to Hercules Inc.).

- [18] Gessler, A.M.; Haslett, W.H. U.S. Patent 3,307,954 (1962, to Esso).
- [19] Fisher, W.K. U.S. Patent 3,806,558.
- [20] Fisher, W.K.. U.S. Patent 3,835,201.
- [21] Coran, A.Y. in *Thermoplastic Elastomers. A Comprehensive Review*, chapter 14. Eds. Legge, N.R.; Holden, G.; Schroeder, H.E. Hanser Publishers, Munich 1987, p. 132.
- [22] Rader, C. P. in *Handbook of Thermoplastic Elastomers*, 2nd edition, chapter 7. Eds. Walker, B.M.; Rader, C.P. Van Nostrand Reinhold, New York 1988, p. 85.
- [23] Nelb, R.G., et al. in *Thermoplastic Elastomers— A Comprehensive Review*, chapter 9A. Eds. Legge, N.R.; Holden, G.; Schroeder, H.E. Hanser Publishers, Munich 1987, p. 197.
- [24] Deleens, G. in *Thermoplastic Elastomers—A Comprehensive Review*, chapter 9B. Eds. Legge, N.R.; Holden, G.; Schroeder, H.E. Hanser Publishers, Munich 1987, p. 215.
- [25] Farrisey, W.J.; Shah, T.M. in *Thermoplastic Elastomers—A Comprehensive Review*, chapter 8. Eds. Legge, N.R.; Holden, G.; Schroeder, H.E. Hanser Publishers, Munich 1987, p. 258.
- [26] Modification of thermoplastics with Kraton® polymers, Shell Chemical Publ. 5C:165-87, 11/87.
- [27] Kirkpatrick, J.P.; Preston, D.T. *Elastomerics* 1988, 120, 30.
- [28] Tinker, A.J.; Icenogle, R.D.; Whittle, I. Paper No. 48, presented at the Rubber Division of ACS Meeting, Cincinnati, OH, October 1988.
- [29] Daikin America, Inc., DAI-EL Thermoplastic.
- [30] Adams, R.K.; Hoeschelle, G.K.; Witsiepe, W.K. in *Thermoplastic Elastomers, A Comprehensive Review*. Eds. Legge, N.R.; Holden, G.; Schroeder, H.E. Hanser Publishers, Munich 1987, p. 164.
- [31] Adams, R.K.; Hoeschelle, G.K.; Witsiepe, W.K. in *Thermoplastic Elastomers*, 3rd edition. Eds. Holden, G.; Kricheldorf, H.R.; Quirk, R.P. Hanser Publishers, Munich 2004, p. 183.
- [32] Jerome, C.; Lecomte, P. Recent advances in the synthesis of aliphatic polyesters by ring-opening polymerization. *Advanced Drug Delivery Reviews* 2008, 60, 1056-1076.
- [33] Albertsson, A.C.; Varma, I.K. Recent developments in ring opening polymerization of lactones for biomedical applications. *Biomacromolecules* 2003, 4, 1466-1486.

- [34] Stjernthal, A.; Wistrand, A.F.; Albertsson, A.C. Industrial utilization of tin-initiated resorbable polymers: synthesis on a large scale with a low amount of initiator. *Biomacromolecules* 2007, 8, 937-940.
- [35] Dechy-Cabaret, O.; Martin-Vaca, B.; Bourissou, D. Controlled ring-opening polymerization of lactide and glycolide. *Chemical Reviews* 2004, 104, 6147-6176.
- [36] O'Keefe, B.J.; Hillmyer, M.A.; Tolman, W.B. Polymerization of lactide and related cyclic esters by discrete metal complexes. *Journal of the Chemical Society, Dalton Transactions* 2001, 2215-2224.
- [37] Barakat, L.; Dubois, P.; Jerome, R.; Teyssié, P. Living polymerization and selective end functionalization of ϵ -caprolactone using zinc alkoxides as initiators. *Macromolecules* 1991, 24, 6542-6545.
- [38] Baran, J.; Duda, A.; Kowalski, A.; Szymanski, R.; Penczek, S. Quantitative comparison of selectivities in the polymerization of cyclic esters. *Macromolecular Symposia* 1997, 123, 93-101.
- [39] Ovitt, T.M.; Coates, G.W. Stereochemistry of lactide polymerization with chiral catalysts: new opportunities for stereocontrol using polymer exchange mechanisms. *Journal of the American Chemical Society* 2002, 124, 1316-1326.
- [40] Shen, Y.; Shen, J.; Zhang, Y.; Yao, K. Characteristics and mechanism of ϵ -caprolactone polymerization with rare earth halide systems. *Macromolecules* 1996, 29, 3441-3446.
- [41] Ravi, P.; Gröv, T.; Dehnicke, K.; Greiner, A. Novel $[\text{Sm}_2\text{I}(\text{NPPH}_3)_5(\text{DME})]$ initiator for the living ring-opening polymerization of ϵ -caprolactone and δ -caprolactone. *Macromolecules* 2001, 34, 8649-8653.
- [42] Chamberlin, B.M.; Jazdzewski, B.A.; Pink, M.; Hillmyer, M.A. Controlled polymerization of DL-lactide and ϵ -caprolactone by structurally well-defined alkoxo-bridged di- and tritytrium (III) complexes. *Macromolecules* 2000, 33, 3970-3977.
- [43] Kricheldorf, H.R. Syntheses of Biodegradable and Biocompatible Polymers by Means of Bismuth Catalysts. *Chemical Reviews* 2009, 109, 5579-5594.
- [44] Albertsson, A.C.; Srivastava, R.K. Recent developments in enzyme-catalyzed ring-opening polymerization. *Advanced Drug Delivery Reviews* 2008, 60, 1077-1093.
- [45] Fernández, J.; Etxeberria, A.; Sarasua, J.R. Synthesis, structure and properties of poly(L-lactide-co- ϵ -caprolactone) statistical copolymers. *Journal of Mechanical Behavior of Biomedical Materials* 2012, 9, 100-112.

- [46] Dobrzynski, P.; Li, S.; Kasperczyk, J.; Bero, M.; Gasc, F.; Vert, M. Structure-property relationships of copolymers obtained by ringopening polymerization of glycolide and ϵ -caprolactone. Part 1. Synthesis and characterization. *Biomacromolecules* 2005, 6, 483-488.
- [47] Jelonek, K.; Kasperczyk, J.; Dobrzynski, P.; Jarzabek, B. Controlled poly(1-lactide-co-trimethylene carbonate) delivery system of cyclosporine A and rapamycin- the effect of copolymer chain microstructure on drug release rate. *International Journal of Pharmaceutics* 2011, 414, 203-209.
- [48] Stanford, M.J.; Dove, A.P. Stereocontrolled ring-opening polymerisation of lactide. *Chemical Society Reviews* 2010, 39, 486-494.
- [49] Kramer, J.W.; Treitler, D.S.; Dunn, E.W.; Castro, P.M.; Roisnel, T.; Thomas, C.M.; Coates, G.W. Polymerization of enantiopure monomers using syndiospecific catalysts: a new approach to sequence control in polymer synthesis. *Journal of the American Chemical Society* 2009, 131, 16042-16044.
- [50] Coates, G.W. Precise control of polyolefin stereochemistry using single-site metal catalysts. *Chemical Reviews* 2000, 100, 1223-1252.
- [51] Herbert, I.R. Statistical analysis of copolymer sequence distribution, in: Ibbet, R.N. (Ed.), In *NMR Spectroscopy of Polymers*. Blackie Academic & Professional, London 1993., pp. 50-79. (Chapter 2).
- [52] Sarasua, J.R.; Prud'homme, R.E.; Wisniewski, M.; Le Borgne, A.; Spassky, N. Crystallization and melting behaviour of polylactides. *Macromolecules* 1998, 31, 3895-3905.
- [53] Li, J.; Stayshich, R.M.; Meyer, T.Y. Exploiting sequence to control the hydrolysis behaviour of biodegradable PLGA copolymers. *Journal of the American Chemical Society* 2011, 133, 6910-6913.
- [54] Badi, N.; Lutz, J-F. Sequence control in polymer synthesis. *Chemical Society Reviews* 2009, 38, 3383-3390.
- [55] Stayshich, R.M.; Meyer, T.Y. New insights into poly(lactic-co-glycolic acid) microstructure: Using repeating sequence copolymers to decipher complex NMR and thermal behaviour. *Journal of the American Chemical Society* 2010, 132, 10920-10934.
- [56] Lee, S.Ch.; Kim, K.J.; Kang, S.W.; Kim, Ch. Microstructural analysis and structure-property relationship of poly(glycolide-co-1,3-trimethylene carbonate). *Polymer* 2005, 46, 7953-7960.
- [57] Hua, J.; Gebarowska, K.; Dobrzynski, P.; Kasperczyk, J.; Wei, J.; Li, S. Influence of chain microstructure on the hydrolytic degradation of copolymers from 1,3-trimethylene carbonate and 1-lactide. *Journal of Polymer Science: Part A: Polymer Chemistry* 2009, 47, 3869-3879.

- [58] Fernández, J.; Etxeberria, A.; Ugartemendia, J.M.; Petisco, S.; Sarasua, J.R. Effects of chain microstructures on mechanical behaviour and aging of poly(L-lactide-co- ϵ -caprolactone) biomedical thermoplastic elastomer. *Journal of Mechanical Behavior of Biomedical Materials* 2012, 12, 29-38.
- [59] Middleton, J.C.; Tipton, A. Synthetic biodegradable polymers as orthopaedic devices. *Biomaterials* 2000, 21, 2335-2346.
- [60] O'neill, M.J.; Watson, E.S. U.S. Patent 3,263,484.
- [61] Podorov, S.G.; Faleev, N.N.; Pavlov, K.M.; Paganin, D.M.; Stepanov, S.A.; Forster, E. A new approach to wide-angle dynamical X-ray diffraction by deformed crystals. *Journal of Applied Crystallography* 2006, 39, 652-655.
- [62] Menard, K.P. Dynamic mechanical analysis: a practical introduction. CRC Press LLC, Boca Raton (Florida), 1999.
- [63] Gupta, A.P.; Kumar, V. New emergin trends in synthetic biodegradable polymers-Polylactide: A critique. *European Polymer Journal* 2007, 43, 4053-4074.
- [64] Auras, R.; Harte, B.; Selke, S. An overview of polylactides as packaging materials. *Macromolecular Bioscience* 2004, 4, 835-864.
- [65] Pielichowski, K.; Njuguna, J. Thermal degradation of polymeric materials. Rapra Technology Limited, Shawbury, 2005. ISBN: 1-85957-498-X
- [66] Larrañaga, A.; Sarasua, J.R. Effect bioactive glass particles on the thermal degradation behavior of medical polyesters. *Polymer Degradation and Stability* 2013, 98, 751-758.
- [67] Nalampang, K.; Molloy, R.; Punyodom, W. Synthesis and characterization of poly(L-lactide-co- ϵ -caprolactone) copolymers: influence of sequential monomer addition on chain microstructure. *Polymers for advanced technologies* 2007, 18, 240-248.
- [68] Persenaire, O.; Alexandre, M.; Degée, P.; Dubois, P. Mechanisms and kinetics of Thermal Degradation of Poly(ϵ -caprolactone). *Biomacromolecules* 2001, 2, 288-294.
- [69] Draye, A.; Persenaire, O.; Brozek, O.; Roda, J.; Kosek, T.; Dubois P. Thermogravimetric analysis of poly(ϵ -caprolactam) and poly[(ϵ -caprolactam)-co-(ϵ -caprolactone)] polymers. *Polymer* 2001, 42, 8325-8332.
- [70] Aoyagi, Y.; Yamashita, K.; Doi, Y. Thermal degradation of poly[(R)-3-hydroxybutyrate], poly[ϵ -caprolactone] and poly[(S)-lactide]. *Polymer Degradation and Stability* 2002, 76, 53-59.

- [71] Kopinke, F.D.; Mackenzie, K. Mechanistic aspects of the thermal degradation of poly(lactic acid) and poly(β -hydroxybutyric acid). *Journal of Analytical and Applied Pyrolysis* 1997, 40, 43-53
- [72] Wachsen, O.; Platkowski, K.; Reichert, K-H. Thermal degradation of poly-L-lactide: studies on kinetics, modeling and melt stabilization. *Polymer Degradation and Stability* 1997, 57, 87-94.
- [73] Sivalingam, G.; Madras, G. Thermal degradation of binary physical mixtures and copolymers of poly(ϵ -caprolactone), poly(D,L-lactide), poly(glycolide). *Polymer Degradation and Stability* 2004, 84, 393-398.
- [74] Kopinke, F.D.; Remmler, M.; Mackenzie, K.; Möder, M.; Wachsen, O. Thermal decomposition of biodegradable polyesters-II. Poly(lactic acid). *Polymer Degradation and Stability* 1996, 53, 329-342.
- [75] Södergard, A.; Näsman, J.H. Melt stability study of various types of poly(L-lactide). *Industrial and Engineering Chemical Research* 1996, 35, 732-735.
- [76] Nishida, H.; Mori, T.; Hoshihara, S.; Fan, Y.; Shirai, Y.; Endo, T. Effect of tin on poly(L-lactic acid) pyrolysis. *Polymer Degradation and Stability* 2003, 81, 515-523.
- [77] Kopinke, F.D.; Remmler, M.; Mackenzie, K.; Moder, M.; Wachsen, O. Thermal decomposition of biodegradable polyesters-II. Poly(lactic acid). *Polymer Degradation and Stability* 1996, 53, 329-542.
- [78] Kricheldorf, H.R.; Kreiser-Saunders, I.; Boettcher, C. Poly lactones:31. Sn(II) octoate-initiated polymerization of L-lactide: a mechanistic study. *Polymer* 1995, 36, 1253-1259.
- [79] Mori, T.; Nishida, H.; Shirai, Y.; Endo, T. Effects of chain end structures on pyrolysis of poly(L-lactic acid) containing tin atoms. *Polymer Degradation and Stability* 2004, 84, 243-251.
- [80] Fernandez, J.; Etxeberria, A.; Sarasua, J.R. Effects of repeat unit sequence distribution and residual catalyst on thermal degradation of poly(L-lactide/ ϵ -caprolactone) statistical copolymers. *Polymer Degradation and Stability* 2013, 98, 1293-1299.
- [81] Pepels, M.P.F.; Hanse, M.R.; Goossens, H.; Duchateau, R. From Polyethylene to Polyester: Influence of Ester Groups on the Physical Properties. *Macromolecules* 2013, 46, 7668-7677.
- [82] Ugartemendia, J.M.; Sarasua, J.R. ANTEC Proceedings 2011, 1, 230-235.
- [83] Tsuji, H.; Mizuno, A.; Ikada, Y. Enhanced Crystallization of Poly(L-lactide-co- ϵ -caprolactone) During Storage at Room Temperature. *Journal of Applied Polymer Science* 2000, 76, 947-953.
- [84] Saha, S.K.; Tsuji, H. Effects of rapid crystallization on hydrolytic degradation and mechanical properties of poly(L-lactide-co- ϵ -caprolactone. *Reactive & Functional Polymers* 2006, 66, 1362-1372.

- [85] Kwon, M.; Lee, S.C.; Jeong, Y.G. Influences of physical aging on enthalpy relaxation behavior, gas permeability, and dynamic mechanical property of polylactide films with various D-isomer contents. *Macromolecular research* 2010, 4, 346-351.
- [86] Hofmann, D.; Entrialgo-Castaño, M.; Kratz, K.; Lendlein, A. Knowledge-Based Approach towards Hydrolytic Degradation of Polymer-Based Biomaterials. *Advanced Materials* 2009, 21, 3237-3245
- [87] Göpferich, A. Mechanism of polymer degradation and erosion. *Biomaterials* 1996, 17, 103-114.
- [88] von Burkersroda, F.; Schedl, L.; Göpferich, A. Why degradable polymers undergo surface erosion or bulk erosion. *Biomaterials* 2002, 23, 4221-4231.
- [89]. Kulkarni, A.; Reiche, J.; Lendlein A. Hydrolytic degradation of poly(rac-lactide) and poly[(rac-lactide)-co-glycolide] at the air water interface. *Surface and Interface Analysis* 2007, 39, 740-746.
- [90] Gleadall, A.; Pan, J.; Kruff, M-A.; Kellomaki, M. Degradation mechanisms of bioresorbable polyesters. Part 1. Effects of random scission, end scission and autocatalysis. *Acta Biomaterialia* 2014, 10, 2223-2232.
- [91] Suping J.S.; Loy, B.; Lind, D.; Hobot, C.; Sparer, R.; Untereker, D. Kinetics and time-temperature equivalence of polymer degradation. *Biomacromolecules* 2007, 8, 2301-10.
- [92] Tsuji, H. Autocatalytic hydrolysis of amorphous-made polylactides: effects of L-lactide content, tacticity, and enantiomeric polymer blending. *Polymer* 2002, 43, 1789-1796.
- [93] Siparsky, G.L.; Voorhees, K.J.; Miao, F. Hydrolysis of polylactic acid (PLA) and polycaprolactone (PCL) in aqueous acetonitrile solutions: autocatalysis. *Journal of Environmental Polymer Degradation* 1998, 6, 31-41.
- [94] Grizzi, I.; Garreau, H.; Li, S.; Vert, M. Hydrolytic degradation of devices based on poly(DL-lactic acid) size-dependence. *Biomaterials* 1995, 16, 305-311.
- [95] Albertsson, A.C.; Eklund, M. Influence of molecular structure on the degradation mechanism of degradable polymers: In vitro degradation of poly(trimethylene carbonate), poly(trimethylene carbonate-co-caprolactone) and poly(adipic anhydride). *Journal of Applied Polymer Science* 1995, 57, 87-103.
- [96] Bostman, O.; Pihlajamaki, H. Clinical Biocompatibility of Biodegradable Orthopaedic Implants for Internal Fixation: A Review. *Biomaterials* 2000, 21, 2615-2621.
- [97] Fleming, J.; Muschler, G.; Boehm, C.; Lieberman, I.; McLain, R. Intraoperative harvest and concentration of human bone marrow osteoprogenitors for enhancement of spinal fusion. In *Orthopedic*

Tissue Engineering: Basic Science and Practice.; Goldberg, V. and Caplan, A., Eds.; Marcel Decker: New York, 2004, pp. 51–65.

[98] Suganuma, J.; Alexandar, H. Biological response of intramedullary bone to poly(L-lactic acid). *Journal of Applied Biomaterials* 1993, 4, 13-27.

[99] Michaeli, W.; Von Oepen, R. Processing of degradable polymers. ANTEC 1994, 796-804.

[100] Von Oepen, R.; Michaeli, W. Injection moulding of biodegradable implants. *Clinical Materials* 1992, 10, 21-28.

[101] Huang, Y.; Kong, J.F.; Venkatraman, S.S. Biomaterials and design in occlusion devices for cardiac defects: A review. *Acta Biomaterialia* 2014, 10, 1088-1101.

[102] Chessa, M.; Carminati, M.; Butera, G.; Bini, R.M.; Drago, M.; Rosti, L.; Giamberti, A.; Pomé, G.; Bossone, E.; Frigiola, A. Early and late complications associated with transcatheter occlusion of secundum atrial septal defect. *Journal of the American College of Cardiology* 2002, 39, 1061–1065.

[103] Cotts, T.; Strouse, P.J.; Graziano, J.N. Late migration of a Sideris buttoned device for occlusion of atrial septal defect. *Catheterization and Cardiovascular Interventions* 2006, 68, 754–757.

[104] Delaney, J.W.; Li, J.S.; Rhodes, J.F. Major complications associated with transcatheter atrial septal occluder implantation: a review of the medical literature and the manufacturer and user facility device experience (MAUDE) database. *Congenital Heart Disease* 2007, 2, 256–264.

[105] Crawford, G.B.; Brindis, R.G.; Krucoff, M.W.; Mansalis, B.P.; Carroll, J.D. Percutaneous atrial septal occluder devices and cardiac erosion: a review of the literature. *Catheterization and Cardiovascular Interventions* 2012, 80, 157–67.

[106] Vogt, M.O.; Kuhn, A.; Horer, J.; Schreiber, C.; Schneider, H.; Foth, R.; Eicken, A.; Hess, J.; Sigler, M. Clinical, echocardiographic and histopathologic findings in nine patients with surgically explanted ASD/PFO devices: do we know enough about the healing process in humans? *International Journal of Cardiology* 2011, 147, 398–404.

[107] Raghu, A.; Kawalsky, D.; Feldman, M. Embolic stroke due to a left atrial thrombus two years after placement of an atrial septal defect closure device. *American Journal of Cardiology* 2006, 98, 1294–1296.

[108] Krumsdorf, U.; Ostermayer, S.; Billinger, K.; Trepels, T., Zadan, E.; Horvath, K.; Sievert, H. Incidence and clinical course of thrombus formation on atrial septal defect and patient foramen ovale

closure devices in 1,000 consecutive patients. *Journal of the American College of Cardiology* 2004, 43, 302–309.

[109] Spies, C.; Cao, Q-L.; Hijazi, Z.M. Transcatheter closure of congenital and acquired septal defects. *European Heart Journal Supplements* 2010, 12, 24–34.

[110] Harahsheh, B. A complication of the Amplatzer PDA occluder requiring surgical correction. *Pakistan Journal of Medical Sciences* 2007, 23, 130–131.

[111] Amanullah, M.M.; Siddiqui, M.T.; Khan, M.Z.; Atiq, M.A. Surgical rescue of embolized amplatzer devices. *Journal of Cardiac Surgery* 2011, 26, 254–258.

[112] Tripathi, R.; Agarwal, R.; Premsekar, R. Late surgical removal of an embolized patent ductus arteriosus device causing erosion of the aortic wall. *Pediatric Cardiology* 2012, 33, 1453–1455.

[113] Gupta, P.; Szczeklik, M.; Selvaraj, A.; Lall, K.S. Emergency surgical retrieval of a migrated left atrial appendage occlusion device. *Journal of Cardiac Surgery* 2013, 28, 26–28.

[114] Venkatraman, S.S.; Boey, Y.C.F.; Wu, W.; Tang, Y.; Yip, W.L.J.; Duong, H.C. Occlusion device for closing anatomical defects. U.S. Patent 2013/0046254 A1.

[115] Zhu, Y.F.; Huang, X.M.; Cao, J.; Hu, J.Q.; Bai, Y.; Jiang, H.B.; Li, Z-F.; Chen, Y.; Wang, W.; Qin, Y-W.; Zhao, X-X. Animal experimental study of the fully biodegradable atrial septal defect (ASD) occluder. *Journal of Biomedicine and Biotechnology* 2012, 735989.

[116] Liu, S-J.; Peng, K-M.; Hsiao, C-Y.; Liu, K-S.; Chung, H-T.; Chen, J-K. Novel biodegradable polycaprolactone occlusion device combining nanofibrous PLGA/Collagen membrane for closure of atrial septal defect (ASD). *Annals of Biomedical Engineering* 2011, 39, 2759–2766.

[117] Duong-Hong, D.; Tang, Y-D.; Wu, W.; Venkatraman, S.S.; Boey, F.; Lim, J.; Yip, J. Fully biodegradable septal defect occluder—A double umbrella design. *Catheterization and Cardiovascular Interventions* 2010, 76, 711–718.

[118] Livingston, E.H.; Lynn, C. Stents to treat coronary artery blockages. *The Journal of the American Medical Association* 2012, 308, 1824.

[119] Ormiston, J.A.; Serruys, P.W.S. Bioabsorbable coronary stents. *Journal of the American Heart Association: Circulation Cardiovascular Interventions* 2009, 2, 255-260.

- [120] Mintz, G.; Popma, J.; Pichard, A.; Kent, K.; Satler, L.; Wong, C.; Hong, M.; Kovach, J.; Leon, M. Arterial remodelling after coronary angioplasty: a serial intravascular ultrasound study. *Circulation* 1996, 94, 35-43.
- [121] Zartner, P.; Cesjnevcar, R.; Singer, H.; Weyand, M. First successful implantation of a biodegradable metal stent into the left pulmonary artery of a preterm baby. *Catheterization and Cardiovascular Interventions* 2005, 66, 590–594.
- [122] Kimura, T.; Abe, K.; Shizuta, S.; Odashiro, K.; Yoshida, Y.; Sakai, K.; Kaitani, K.; Inoue, K.; Nakagawa, Y.; Yokoi, H.; Iwabuchi, M.; Hamasaki, N.; Nosaka, H.; Nobuyoshi, M. Long-term clinical and angiographic followup after coronary stent placement in native coronary arteries. *Circulation* 2002, 105, 2986–2991.
- [123] Joner, M.; Finn, A.; Farb, A.; Mont, E.; Kologie, F.; Ladich, E.; Kutys, R.; Skorija, K.; Gold, H.; Virmani, R. Pathology of drug-eluting stents in man: delayed healing and late thrombotic risk. *Journal of the American College of Cardiology* 2006, 48, 193–202.
- [124] Kotani, J.; Awata, M.; Nanto, S.; Uematsu, M.; Oshima, F.; Minamiguchi, H.; Mintz, G.; Nagata, S. Incomplete neointimal coverage of sirolimus-eluting stents: angioscopic findings. *Journal of the American College of Cardiology* 2006, 47, 2108–2111.
- [125] Hofma, S.; Van der Giessen, W.; van Dalen, B.; Lemos, P.; McFadden, E.; Sianos, G.; Lighthart, J.; van Essen, D.; de Feyter, P.J.; Serruys, P.W. Indication of long-term endothelial dysfunction after sirolimus-eluting stent implantation. *European Heart Journal* 2006, 27, 166–170.
- [126] Togni, M.; Windecker, S.; Cocchia, R.; Wenaweser, P.; Cook, S.; Billinger, M.; Meier, B.; Hess, O. Sirolimus-eluting stents associated with paradoxical coronary vasoconstriction. *Journal of the American College of Cardiology* 2005, 46, 231–236.
- [127] Nishio, S.; Kosuga, K.; Igaki, K.; Okada, M.; Kyo, E.; Tsuji, T.; Takeuchi, E.; Inuzuka, Y.; Takeda, S.; Hata, T.; Takeuchi, Y.; Kawada, Y.; Harita, T.; Seki, J.; Akamatsu, S.; Hasegawa, S.; Bruining, N.; Brugaletta, S.; de Winter, S.; Muramatsu, T.; Onuma, Y.; Serruys P.W.; Ikeguchi, S. Long-Term (>10 years) clinical outcomes of first-in-man biodegradable poly-L-lactid acid coronary stents: Igaki-Tamai stents. *Journal of the American Heart Association: Circulation* 2012, 125, 2343-2353.
- [128] Tamai, H.; Igaki, K.; Kyo, E.; Kosuga, K.; Kawashima, A.; Matsui, S.; Komori, H.; Tsuji, T.; Motohara, S.; Uehata, H. Initial and 6-month results of biodegradable poly-L-lactic acid coronary stents in humans. *Circulation* 2000, 102, 399–404.
- [129] Erbel, R.; Di Mario, C.; Bartunek, J.; Bonnier, J.; de Bruyne, B.; Erbeli, F.R.; Erne, P.; Haude, M.; Heublein, B.; Horrigan, M.; Ilesley, C.; Bose, D.; Koolen, J.; Luscher, T.F.; Weissman, N.; Waksman, R.

Temporary scaffolding of coronary arteries with bioabsorbable magnesium stents: a prospective, non-randomized multicentre trial. *Lancet* 2007, 369, 1869–1875.

[130] Ormiston, J.; Serruys, P.W.; Regar, E.; Dudek, D.; Thuesen, L.; Webster, M.; Onuma, Y.; Garcia-Garcia, H.; McGreevy, R.; Veldhof, S. A bioabsorbable everolimus-eluting coronary stent system for patients with single de-novo coronary artery lesions (ABSORB): a prospective open-label trial. *Lancet* 2008, 371, 899–907.

[131] Ormiston, J.; Webster, M.; Armstrong, G. First-in-human implantation of a fully bioabsorbable drug-eluting stent: the BVS poly-L-lactic acid everolimus-eluting coronary stent. *Catheterization and Cardiovascular Interventions* 2007, 69, 128–131.

[132] Serruys, P.W.; Ormiston, J.; Onuma, Y.; Regar, E.; Gonzalo, N.; Garcia-Garcia, H.; Nieman, K.; Bruining, N.; Dorange, C.; Miquel-Herbert, K.; Veldhof, S.; Webster, M.; Thuesen, L.; Dudek, D. Absorbent trial first-in-man evaluation of a bioabsorbable everolimus-eluting coronary stent system: two-year outcomes and results from multiple imaging methods. *Lancet* 2009, 373, 897.

[133] Uurto, I.; Mikkonen, J.; Parkkinen, J.; Kesti-Nisula, L.; Nevalainen, T.; Kellomäki, M.; Törmälä, P.; Salenius, J-P. Drug-eluting biodegradable poly-d/l-lactic acid vascular stents: an experimental pilot study. *Journal of Endovascular Therapy* 2005, 12, 371-379

[134] Loffeld, R.J.L.F.; Dekkers, P.E.P. Palliative stenting of the digestive tract: a case series of a single centre. *Journal of Gastrointestinal Oncology* 2013, 4, 14-19.

[135] Pameijer, C.R.; Mahvi, D.M.; Stewart, J.A. Weber, S.M. Bowel obstruction in patients with metastatic cancer: does intervention influence outcome? *International Journal of Gastrointestinal Cancer* 2005, 35, 127-33.

[136] Laval, G.; Arvieux, C.; Stefani, L.; Villard, M.L.; Mestrallet, J.P.; Cardin, N. Protocol for the treatment of malignant inoperable bowel obstruction: a prospective study of 80 cases at Grenoble University Hospital Center. *Journal of Pain and Symptom Manage* 2006, 31, 502-512.

[137] Rousseau, P. Management of malignant bowel obstruction in advanced cancer: a brief review. *Journal of Palliative Medicine* 1998, 1, 65-72.

[138] Mergener, K.; Kozarek, R.A. Stenting of the Gastrointestinal tract. *Digestive Diseases* 2002, 20, 173-181.

[139] Singh, S.; Gagneja, H.K. Stents in the small intestine. *Current Gastroenterology Reports* 2002, 4, 383-391.

- [140] Lorenzo-Zuñiga, V.; Moreno-de-Vega, V.; Marín, I.; Boix, J. Biodegradable stents in gastrointestinal endoscopy. *World Journal of Gastroenterology* 2014, 20, 2212-2217.
- [141] Goldin, E.; Fiorini, A.; Ratan, Y.; Keter, D.; Loshakove, A.; Globerman, O.; Beyar, M. A new biodegradable and self-expandable stent for benign esophageal strictures. *Gastrointestinal Endoscopy* 1996, 43, 294.
- [142] Fry, S.W.; Fleischer, D.E. Management of a refractory benign esophageal stricture with a new biodegradable stent. *Gastrointestinal Endoscopy* 1997, 45, 179-182.
- [143] Rejchrt, S.; Kopacova, M.; Bartova, J.; Vacek, Z.; Bures, J. Intestinal biodegradable stents. *Folia Gastroenterology and Hepatology* 2009, 1, 7-11.
- [144] Bhasin, D.K.; Rana, S.S. Biodegradable pancreatic stents: are they a disappearing wonder?. *Gastrointestinal Endoscopy* 2008, 67, 1113-1116.
- [145] Yu, X.; Wang, L.; Huang, M.; Gong, T.; Li, W.; Cao, Y.; Ji, D.; Wang, P.; Wang, J.; Zhou, S. A shape memory stent of poly (ϵ -caprolactone-co-DL-lactide) copolymer for potential treatment of esophageal stenosis. *Journal of Materials Science: Materials in Medicine* 2012, 23, 581-589.
- [146] Mattelaer, H.; Billier, I. Catheters and sounds: the history of bladder catheterization. *Paraplegia* 1995, 33, 429-33.
- [147] Ramakrishnan, K.; Mold, J. Urinary Catheters: A review. *The Internet Journal of Family Practice* 2004, 3, 2.
- [148] Lozano-Ortega, J.L.; Pertusa-Peña, C. Cirugía de la estenosis de uretra. Actualización. *Archivos Españoles de Urología* 2007, 60, 633-637.
- [149] Lozano-Ortega, J.L.; Pertusa-Peña, C. Tratamiento quirúrgico de la estenosis uretral. Resultados de 100 uretroplastias. *Archivos Españoles de Urología* 2009, 62, 109-114
- [150] Venkatesan, M.; Jayachandran, K. Polymers as ureteral stents. *Journal of Endourology* 2010, 24, 1-8
- [151] Dyer, R.B.; Chen, M.Y.; Zagoria, R.J.; Regan, J.D.; Hood, C.G.; Kavanagh, P.V. Complications of ureteral stent placements. *RadioGraphics* 2002, 22, 1005-1022.
- [152] Siegel, J.F.; Smith, A.D. The ideal ureteral stent for antegrade and retrograde endopyelotomy: What would it be like? *Journal of Endourology* 1993, 7, 151-154

- [153] Van Arsdalen, K.N.; Pollack, H.M.; Wein, A.J. Ureteral stenting. *Seminars in Urology* 1984, 2, 180–186.
- [154] Chen, A.S.C.; Saltzman, B. Stent use with extracor-poreal shock wave lithotripsy. *Journal of Endourology* 1993, 7, 155–162.
- [155] Denstedt, J.D.; Reid, G.; Sofer, M. Advances in ureteral stent technology. *World Journal of Urology* 2000, 18, 237–242.
- [156] Watson, G. Problems with double-J stents and nephrostomy tubes. *Journal of Endourology* 1997, 11, 413–417.
- [157] Hood, C.G.; Dyer, R.B.; Zagoria, R.J. Complications of ureteral stenting. *Applied Radiology* 1990, 19, 35–42.
- [158] Bell, J.H.; Haycock, J.W. Next generation nerve guides: materials, fabrication, growth factors and cell delivery. *Tissue Engineering Part B Reviews* 2011, 18, 116-128.
- [159] Daly, W.; Yao, L.; Zeugolis, D.; Windebank, A.; Pandit, A. A biomaterials approach to peripheral nerve regeneration: bridging the peripheral nerve gap and enhancing functional recovery. *Journal of the Royal Society Interface* 2012, 9, 202-221.
- [160] Taylor, C.A.; Braza, D.; Rice, J.B.; Dillingham, T. The incidence of peripheral nerve injury in extremity trauma. *American Journal of Physical Medicine and Rehabilitation* 2008, 87, 381-385.
- [161] Pateman, C.J.; Harding, A.J.; Glen, A.; Taylor, C.S.; Christmas, C.R.; Robinson, P.P.; Rimmer, S.; Boissonade, F.M.; Claeysens, F.; Haycock, J.W. Nerve guides manufactured from photocurable polymers to aid peripheral nerve repair. *Biomaterials* 2015, 49, 77-89.
- [162] Clark, W.L.; Trumble, T.E.; Swiontkowski, M.F.; Tencer, A.F. Nerve tension and blood flow in a rat model of immediate and delayed repairs. *Journal of Hand Surgery American Volume* 1992, 17, 677-687.
- [163] Haftek, J. Autogenous cable nerve grafting instead of end to end anastomosis in secondary nerve suture. *Acta Neurochirurgica* 1976, 34, 217-221.
- [164] Jiang, X.; Lim, S.H.; Mao, H-Q, Chew, S.Y. Current applications and future perspectives of artificial nerve conduits. *Experimental Neurology* 2010, 223, 86-101.

- [165] Ichihara, S.; Inada, Y.; Nakada, A.; Endo, K.; Azuma, T.; Nakai, R.; Tsutsumi, S.; Kurosawa, H.; Nakamura, T. Development of new nerve guide tube for repair of long nerve defects. *Tissue Engineering Part C Methods* 2009, 15, 387-402.
- [166] Kehoe, S.; Zhang, X.F.; Boyd, D. FDA approved guidance conduits and wraps for peripheral nerve injury: a review of materials and efficacy. *Injury* 2012, 43, 553-572.
- [167] Sundback, C.A.; Shyu, J.Y.; Wang, Y.; Faquin, W.C.; Langer, R.S.; Vacanti, J.P.; Hadlock, T.A. Biocompatibility analysis of poly(glycerol sebacate) as a nerve guide material. *Biomaterials* 2005, 26, 5454-5464.
- [168] Bockelmann, J.; Klinkhammer, K.; von Holst, A.; Seiler, N.; Faissner, A.; Brook, G.A.; Klee, D.; Mey, J. Functionalization of electrospun poly(ϵ -caprolactone) fibers with the extracellular matrix-derived peptide GRGDS improves guidance of Schwann cell migration and axonal growth. *Tissue Engineering Part A* 2011, 17, 475-486.
- [169] Chiriac, S.; Facca, S.; Diaconu, M.; Gouzou, S.; Liverneaux, P. Experience of using the bioresorbable copolyester poly(DL-lactide- ϵ -caprolactone) nerve conduit guide Neurolac for nerve repair in peripheral nerve defects: report on a series of 28 lesions. *Journal of Hand Surgery European Volume* 2012, 37, 342-249.
- [170] Radtke, C.; Allmeling, C.; Waldmann, K.H.; Reimers, K.; Thies, K.; Schenk, H.C.; Hilmer, A.; Guggenheim, M.; Brandes, G.; Vogt, P.M. Spider silk constructs enhance axonal regeneration and remyelination in long nerve defects in sheep. *Plos One* 2011, 6, 16990.
- [171] Bian, Y.Z.; Wang, Y.; Aibaidoula, G.; Chen, G.Q.; Wu, Q. Evaluation of poly(3-hydroxybutyrate-co-3-hydroxyhexanoate) conduits for peripheral nerve regeneration. *Biomaterials* 2009, 30, 217-225.
- [172] Midha, R. Emerging techniques for nerve repair: Nerve transfers and nerve guidance tubes. *Clinical Neurosurgery* 2006. Vol 53: Chapter 18.
- [173] Hench, L.L.; Jones, J.R. et. al. Biomaterials, artificial organs and tissue engineering. Ed. Hench, L.L.; Jones, J.R. Woodhead Publishing and Maney Publishing on behalf of the Institute of Materials, Minerals & Mining. Boca Raton (USA) 2005.
- [174] Langer, R.; Vacanti, J.P. Tissue Engineering. *Science* 1993, 260, 920-926.
- [175] Langer, R. Perspectives and Challenges in Tissue Engineering and Regenerative Medicine. *Advanced Materials* 2009, 21, 3235-3236.
- [176] Ma, P.X. Scaffolds for Tissue Fabrication. *Materials Today* 2004, 7, 30-40.

- [177] Santos, E.; Hernández, R.M.; Pedraz, J.L.; Orive, G. Novel Advances in the Design of Three-Dimensional Bio-Scaffolds to Control Cell Fate: Translation from 2D to 3D. *Trends in Biotechnology* 2012, 30, 331-341.
- [178] Desmet, T.; Morent, R.; De Geyter, N.; Leys, C.; Schacht, E.; Dubruel, P. Nonthermal Plasma Technology as a Versatile Strategy for Polymeric Biomaterials Surface Modification: A Review. *Biomacromolecules* 2009, 10, 2351-2378.
- [179] Lee, K.; Silva, E.A.; Mooney, D.J. Growth factor delivery-based tissue engineering: general approaches and a review of recent developments. *Journal of the Royal Society Interface* 2011, 8, 153-170.
- [180] Boccaccini, A.R.; Erol, M.; Stark, W.J.; Mohn, D.; Hong, Z.; Mano, J.F. Polymer/Bioactive Glass Nanocomposites for Biomedical Applications: A Review. *Composites Science and Technology* 2010, 70, 1764-1776.
- [181] Larrañaga, A.; Petisco, S.; Sarasua, J.R. Improvement of Thermal Stability and Mechanical Properties of Medical Polyesters Composites by Plasma Surface Modification of the Bioactive Glass Particles. *Polymer Degradation and Stability* 2013, 98, 1717-1723.
- [182] Larrañaga, A.; Ramos, D.; Amestoy, H.; Zuza, E.; Sarasua, J.R. Coating of bioactive glass particles with mussel inspired polydopamine as a strategy to improve the thermal stability of poly(L-lactide)/bioactive glass composites. *RSC Advances* 2015, 5, 65618-65626.
- [183] Larrañaga, A.; Alonso-Varona, A.; Palomares, T.; Rubio-Azpeitia, E.; Aldazabal, P.; Martin, F.J. Sarasua, J.R. Effect of Bioactive Glass Particles on Osteogenic Differentiation of Adipose-Derived Mesenchymal Stem Cells Seeded on Lactide and Caprolactone Based Scaffolds. *Journal of Biomedical Materials Research Part A*, 2015, 35525.
- [184] Lanza, R.P.; Langer, R.; Vacanti, J. Principles of Tissue Engineering. in Tissue Engineering Intelligence Unit. Elsevier, San Diego, California 2007.
- [185] Amiel, D.; Frank, C.; Harwood, F.; Fronek, J.; Akeson, W. Tendons and ligaments: a morphological and biochemical comparison. *Journal of Orthopaedic Research* 1984, 1, 257.
- [186] Iannace, S.; Sabatini, G.; Ambrosio, L.; Nicolais, L. Mechanical behaviour of composite artificial tendons and ligaments. *Biomaterials* 1995, 16, 675.
- [187] Lee, J.; Guarino, V.; Gloria, A.; Ambrosio, L.; Tae, G.; Kim, Y.H.; Jung, Y.; Kim, S-H.; Kim, S.H. Regeneration of achilles tendon: The role of dynamic stimulation for enhanced cell proliferation and mechanical properties. *Journal of Biomaterials Science* 2010, 21, 1173-1190.

- [188] Eschenhagen, T.; Reichenspurner, H.; Zimmermann, W.H. Principles of Tissue Engineering. in Tissue Engineering Intelligence Unit. Eds. Lanza, R.P.; Langer, R.; Vacanti, J. Elsevier, San Diego, California 2007, Chapter 82.
- [189] Venkatraman, S.; Boey, F.; Lao, L.L. Implanted cardiovascular polymers: Natural, synthetic and bio-inspired. *Progress in Polymer Science* 2008, 33, 853–874.
- [190] Karam, J-P.; Muscari, C.; Montero-Menei, C.N. Combining adult stem cells and polymeric devices for tissue engineering in infarcted myocardium. *Biomaterials* 2012, 33, 5683–5695.
- [191] Kunisaki, S.M.; Vacanti, J. Principles of Tissue Engineering. in Tissue Engineering Intelligence Unit. Eds. Lanza, R.P.; Langer, R.; Vacanti, J. Elsevier, San Diego, California 2007, Chapter 46.
- [192] Atala, A. Principles of Tissue Engineering. in Tissue Engineering Intelligence Unit. Eds. Lanza, R.P.; Langer, R.; Vacanti, J. Elsevier, San Diego, California 2007, Chapter 54.
- [193] Sartoneva, R.; Haimi, S.; Miettinen, S.; Mannerström, B.; Haaparanta, A.M.; Sándor, G.K.; Kellomäki, M.; Suuronen, R.; Lahdes-Vasama, T. Comparison of a poly(L-lactic-co-e-caprolactone) and human amniotic membrane for urothelium tissue engineering applications. *Journal of the Royal Society Interface* 2011, 8, 671–677.
- [194] Besnard, V.; Whitsett, J.A. Principles of Tissue Engineering. in Tissue Engineering Intelligence Unit. Eds. Lanza, R.P.; Langer, R.; Vacanti, J. Elsevier, San Diego, California 2007, Chapter 73.

**Section 1 - Copolymers of high glass
transition temperature**

Summary

In this section several copolyesters with a glass transition temperature over 20 °C were synthesized by ring-opening polymerization and then characterized using different techniques. They are composed mainly of lactide (L-lactide or D,L-lactide), whose homopolymer shows a T_g at 55-65 °C, while ϵ -caprolactone (**Chapter 1**) or δ -valerolactone (**Chapter 2**) monomers were added to bring flexibility to the polymer chain and disrupt the arrangement of the lactide blocks. Both lactide-co- ϵ -caprolactone and lactide-co- δ -valerolactone copolymers present a random distribution of sequences and an adjusted crystallization capability, and degrade at a very fast rate (far above the values documented in the literature for the poly(L-lactide)). In view of their mechanical behaviour these polymeric materials can be employed in the medical field primarily for the regeneration of soft tissues and for various clinical implants of devices in which an elastomeric character is desirable.

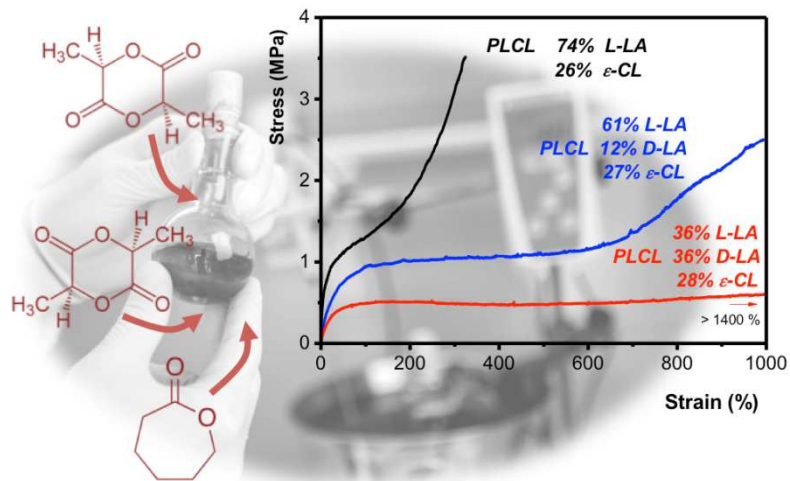
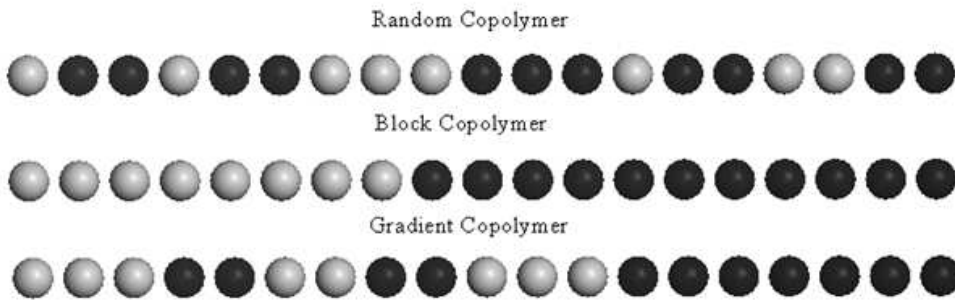
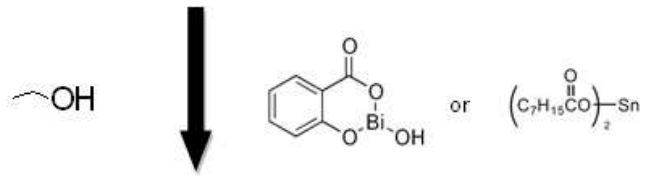
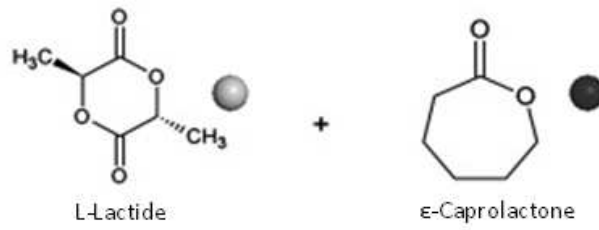
- Microstructural control has been demonstrated to be a really interesting way to tailor the properties of the copolyesters. In **Chapter 1.1**. (*Synthesis and Characterization of Statistical l-lactide-co- ϵ -caprolactone Copolymers with Well-Resolved Chain Microstructures*) several syntheses of statistical poly(L-lactide-co- ϵ -caprolactone) were conducted at a 75:25 mass feed ratio evaluating the polymerization conditions (temperatures, times of reaction and comonomer/catalyst molar ratios) in order to find under which conditions random copolymers are obtained. The mechanisms of reaction of both catalyst employed, SnOct₂ and BiSS, differed in the coordination and activation of the monomers leading to different chain microstructures. BiSS was found to be less prone to react with lactide, the monomer with higher reactivity, than SnOct₂, and consequently, the desired random copolymers ($R \rightarrow 1$) were obtained. In contrast, the stannous catalyst exhibits a tendency to favor the formation of blocky sequences ($R < 0.6$) that provide more capability to crystallize. As a result, the latter copolymers present a T_m higher than the corresponding to the random BiSS-copolymers. Finally, in this study the attachment and proliferation of ADSCs on some of the obtained copolyemrs were also assessed demonstrating that these biomaterials are not cytotoxic despite their residual catalyst content.

-
- In **Chapter 1.2.** (*Effects of Chain Microstructures and Derived Crystallization Capability on Hydrolytic Degradation of L-Lactide co- ϵ -Caprolactone Copolymers*) the influence on the hydrolytic degradation of the chain microstructure features and the crystallization capabilities of various statistical L-lactide-co- ϵ -Caprolactone were studied. Two of the employed PLCLs, despite having similar composition, displayed completely different performance during the course of degradation owing to their different randomness character ($R = 0.46$ vs. 0.96). The blocky copolymer was very prone to crystallize and undergo more significant supramolecular rearrangements of their chains. The development of lactide crystalline domains was demonstrated to be an undesired factor during the degradation process because it dramatically slows down the degradation rate, inhibits the homogeneous degradation of the biomaterial and causes greater deterioration in its mechanical properties. In addition, highly resistant crystalline remnants of low molecular weight are formed which can trigger foreign body reactions and remain in the human body for years.
- In **Chapter 1.3.** (*A New Generation of Lactide-co- ϵ -Caprolactone Copolymers for Application in the Medical Field*) L-lactide and rac-lactide (50:50 mix of L-LA and D-LA) were copolymerized with ϵ -caprolactone using a catalyst that allows the random distribution of sequences. D-LA was added, on the one hand, to replace ϵ -CL, increasing the stress related properties (elastic modulus and strength) and, on the other hand, substituting L-LA decreases its crystallization capability and enlarges the amorphous character of the polymer. As a result, the terpolymers of L-LA, D-LA and ϵ -CL display proper and tunable mechanical behavior, show very little or no crystallization capability and degrade at a very fast rate while do not generate resistant crystalline remnants during hydrolytic degradation. This is achieved because of their controlled D-LA and ϵ -CL average sequence lengths and the inability to arrange into highly crystalline organized structure of their L-lactide unit chains.
- The mechanical performance of several lactide-co- δ -valerolactone copolymers (poly(L-LA-co- δ -VL) and L-LA-D-LA- δ -VL terpolymers) was studied in **Chapter**

2.1. (Tensile Behaviour and Dynamic Mechanical Analysis of Novel Lactide-co- δ -Valerolactone Copolymers) by means of mechanical testing at 21 and 37 °C and dynamic mechanical analysis (DMA). Noteworthy improvements in stiffness and strength were achieved by adding δ -VL to the reaction mix instead of ϵ -CL, although both monomers have analogous chemical properties. Poly(lactide-co- δ -valerolactone)s, having higher T_g s than the poly(lactide-co- ϵ -caprolactone)s of equal composition, may be more attractive in some medical applications, when highly flexible and deformable materials with adequate mechanical strength are both required.

- When a biodegradable material is implanted in the human body, medical staff have to know how it is actually going to behave. Therefore, several parameters should be taken into consideration when designing and producing a medical device. For a better understanding of the mechanism of hydrolytic degradation of the copolyesters, in **Chapter 2.2. (In Vitro Degradation Study of Biopolyesters Using Lactide-co- δ -Valerolactone Copolymers)** the most important factors were evaluated in a study carried out on poly(lactide-co- δ -valerolactone). The results probed that water absorption is the key factor in the degradation process and it was favoured by the resistance of polymers to crystallize, the presence of large amorphous domains and the decrease in microstructural stereoregularity of the polymer chains. Therefore, the copolymers that displayed higher levels of water uptake also presented the fastest degradation rates.

Chapter 1. Lactide-co- ϵ -Caprolactone Copolymers



**Chapter 1.1 Synthesis and Characterization
of Statistical L-lactide-co- ϵ -caprolactone
Copolymers with Well-Resolved Chain
Microstructures**

Polymer 2013, 54, 2621-2631.

Abstract

In view of the improved properties of elastomeric copolymers with a random distribution of sequences (randomness coefficient (R) $\rightarrow 1$), several synthesis of statistical poly(L-lactide/ ϵ -caprolactone) (PLCL) at a 75:25 mass feed ratio were conducted evaluating the polymerization conditions (temperatures, times of reaction and comonomer/catalyst (M/C) molar ratios). The mechanisms of reaction of both catalyst employed, SnOct₂ and BiSS, differed in the coordination and activation of the monomers leading to different chain microstructures. BiSS was found to be less prone to react with the monomer with higher reactivity, i. e., lactide (LA), than SnOct₂, and consequently, the desired random PLCLs ($R > 0.85$) were obtained. In contrast, the more reactive SnOct₂ exhibits a tendency to favour blocky sequences ($R < 0.6$) that provide more capability to crystallize. The random BiSS-PLCLs showed crystallinity with lower melting temperature (T_m) than moderately blocky SnOct₂-copolymers, being both influenced by the average lactide block length (l_{LA}) obtained, a parameter affected by the LA content and R . The T_m values increase from 82 to 125 °C when l_{LA} only rises from 3.3 to 5.4, whereas the corresponding T_m of the SnOct₂-PLCLs is in the range of 148-163 °C despite the wide range of l_{LA} (5.4-23.5). Also indicative of the high sensitivity to microstructural chain aspects of the copolymers, the crystallinity degree (X_c) of the PLCLs grows in a logarithmic manner shifting quickly from 2.0 % to around 20.0 % when l_{LA} increases from 3.3 to 5.0. Finally, the adhesion and proliferation of adipose derived mesenchymal stem cells (ADSCs) on some representative PLCLs were successfully performed with no signs of cytotoxicity despite in some cases of the presence of a slight residual amount of toxic tin.

1.1.1. Introduction

Stannous octoate (SnOct_2) is the most commonly used initiator/catalyst for ring-opening polymerization (ROP) of cyclic esters (including cyclic carbonates and cyclic oligoesters). Several factors are responsible for this fact starting by an excellent performance that provides high conversion and reaction rates and makes high molar masses accessible. In addition, SnOct_2 is easy to handle, displays good thermostability and is soluble in common organic solvents and monomers [1-3]. SnOct_2 has been approved by the Food and Drug Administration (FDA) as a food additive, yet it is slightly toxic [4].

The ROP of cyclic esters induced by SnOct_2 is carried out in the presence of active hydrogen compounds [5-6] and several mechanisms have been proposed. Some authors consider SnOct_2 to be merely a catalyst [6-9]. In every propagation step, a hydroxyl-group-containing compound (eg. H_2O , alcohol or a macromolecule with an $-\text{OH}$ at its end) reacts with one monomer unit in presence of the catalyst. It is important to stress that, according to this group of mechanisms, SnOct_2 , either “free” or complexed, survives during polymerization and is not converted into any other species chemically different. There is a second group of authors that assume that SnOct_2 must be converted into tin alkoxides in order to initiate polymerization [10-11]. Evidence in support of this mechanism was provided by Kowalski and co-workers [12] by both a direct observation of Sn atoms in the polyester chains and kinetics studies. Admitting this mechanism of reaction, the possible toxicity of the residual amount of tin in the material is an important issue in SnOct_2 initiated polymerizations.

When an absorbable polymer is used as a material for a medical implant application, the metal catalyst is exposed to the body during its degradation and, above threshold concentrations, may have harmful effects. Therefore the metal catalyst residual content must be reduced as much as possible. Regarding SnOct_2 , the FDA has set a threshold

limit of 20 ppm maximum residual tin in commercially used medical polymers, being thus essential not to exceed the said threshold [3].

A number of different purification procedures for SnOct₂-containing materials have been reported [13-16], however, the final properties of the biomaterial can be affected by acid/organic solutions used during the extraction techniques. Decreasing the initial amount of catalyst is another strategy to reduce the residual amount of tin, however in this case the impact on the final conversion, reaction control, molecular weights etc. have to be evaluated.

Using less toxic catalyst/initiators with a performance similar to that of tin compounds is the alternative that is explored in this work. Among the potential catalysts, bismuth salts or complexes, such as the bismuth subsalicylate (BiSS), are outstanding for their low toxicity [3]. In this context, some studies concerning toxicity [17] have demonstrated that bismuth compounds belong to the least toxic heavy metal compounds. Bi³⁺ performs even better than Zn²⁺, although small amounts of zinc are needed in the human metabolism.

Bismuth subsalicylate, under the U.S. trademark Pepto-Bismol, has been used for at least one hundred years as drug against gastro-intestinal complaints, such as diarrhea, nausea, heart burn, indigestion, etc [18-20]. This bismuth salt has been also demonstrated to be useful as catalyst/initiator for homo- and copolymerizations of lactones and lactides [21-23]. An interesting result was the finding that BiSS favored the presence of less blocky sequences than those copoly lactones prepared with SnOct₂ under identical conditions [23].

The microstructural control is particularly relevant to tailor the properties of copolymers, yet it is usually a forgotten parameter when developing new biomaterials and when judging their behaviour for medical uses. Depending on the synthesis conditions, the relative rates of incorporation of each comonomer and the catalyst nature, different distribution of the sequences of the comonomers building blocks can be obtained [24-29]. The randomness character value (R), which relates the number average sequence length values (l_i) determined by NMR to the Bernoullian random

number-average sequence lengths $(l_i)_{\text{random}}$, can be used as a comparative parameter in the chain microstructure discussion. In this way, the R coefficient is equal to 1 for completely random chains and 0 for diblock copolymers while values above 1 indicate increased concentration of alternating sequences.

Higher degree of randomness improves the solubility in organic solvents and allows a more homogeneous hydrolytic degradation [25-27]. At equal comonomers content, random copolymers are more amorphous than others with higher block unit's distribution, exhibiting fastest degradation rates, and even, at certain copolymer compositions, maintaining their amorphous structure during degradation [26]. In addition, other properties of statistical copolymers, including thermal and mechanical properties and resistance to physical aging, are strongly dependent on chain microstructure [30-31]. In a previous work [30], we studied three statistical poly(L-lactide-co- ϵ -caprolactone) (PLCL) of 70 % L-lactide content having different chain microstructures ranging from moderate blocky to random ($R = 0.47, 0.69$ and 0.92 , respectively). The results demonstrated that higher randomness character ($R \rightarrow 1$) limits the capability of crystallization of LA-unit sequence shifting the melting temperature of the copolymers to lower values and reducing the crystallinity fraction substantially. As a consequence, the PLCL with a shorter average length of lactide unit sequences was found to exhibit higher strain capability and strain recovery values and was less prone to supramolecular arrangements during its storage at room temperature ($21 \pm 2^\circ\text{C}$). On the basis of the above, improving the randomness of copolyesters may be an issue of great interest [32-34].

In this work several statistical poly(L-lactide/- ϵ -caprolactone) at a 75:25 mass feed ratio were synthesized in bulk by ROP. Either SnOct₂ or BiSS were added as catalyst/initiator under different polymerization conditions, that is, varying the temperatures, the times of reaction and the comonomer/catalyst molar ratios. The aim is to evaluate the different synthesis in order to find under which conditions random copolymers are obtained. In addition, in this study the attachment and proliferation of adipose derived mesenchymal stem cells (ADSCs) on some of the obtained materials were also investigated to evaluate the cytotoxicity.

Copolymer composition and chain microstructure of the PLCLs were investigated by means of proton and carbon nuclear magnetic resonance spectroscopy (^1H NMR and ^{13}C NMR), their molecular weight distribution was determined using gel permeation chromatography (GPC) measurements and the phase structure was studied by analysis of thermal transitions determined by differential scanning calorimetry (DSC). Finally, the cytotoxic evaluation of the materials was studied by means of a colorimetric MTT assay of ADSCs, whereas the adhesion was investigated on films by scanning electron microscopy (SEM).

1.1.1. Materials and methods

Materials

L-lactide monomer (assay > 99.5 %) with < 0.02 % of water content was supplied by Purac Biochem (The Netherlands). ϵ -caprolactone monomer (assay > 98 %) was provided by Merck. Stannous octoate (assay 95 %) and bismuth (III) subsalicylate (99.9 % metals basis) were obtained from Sigma Aldrich. The methanol and chloroform were utilized as received. Sulfuric acid (98 % assay) and nitric acid (67 % assay) were employed in the digestion of the samples previous to their introduction to ICP-AES (Inductively Coupled Plasma with Atomic Emission Spectroscopy).

Synthesis Procedure

The synthesis reactions were carried out in a flask, immersed in a controlled temperature oil bath. In each polymerization, predetermined amounts of LA and ϵ -CL at a 75:25 mass feed ratio were simultaneously added and melted. The flask was purged for 30 minutes with a nitrogen stream under the surface of the melt. Then, the catalyst (either stannous octoate or bismuth subsalicylate) was added using the chosen comonomers:catalyst feed molar ratio. The magnetic stirrer was maintained at 100 rpm. After the corresponding time of reaction, the product was dissolved in chloroform and precipitated pouring the polymer solution into excess of methanol in order to remove

the catalyst impurities and the monomers that did not react. Finally, the product was dried at 45°C under vacuum until it reached constant weight.

Methods

The thermal properties were determined on a DSC Q200 (TA Instruments) calibrated with pure indium and sapphire standards. Samples of 5-9 mg were cooled at -85°C and heated to 185°C at 20°C min⁻¹ in a first scan. This was used to determine the melting temperature (T_m) and the heat of fusion (ΔH_m) of the copolymers. The degree of crystallinity (X_c) in % was calculated from eq. (1), having proven previously by X ray diffraction that only lactide units in those PLCLs are able to crystallize [35].

$$x_c(\%) = \frac{100 \Delta H_m}{\Delta H_m^0 \cdot (LA^*)} \quad (1)$$

where $\Delta H_m^0 = 106$ (J g⁻¹ of PLLA) is the enthalpy of fusion of PLLA crystals having the infinite crystal thickness [36] and (LA*) is the actual (experimental) lactide mass fraction in the copolymer obtained by NMR.

Then, samples were quenched in the DSC and a second scan was made from -85 to 185°C at 20°C min⁻¹ to determine the glass transition temperatures (T_g) from the inflection point of the heat flow curve.

Gel permeation chromatography (GPC) measurements were performed with a Waters 1515 chromatograph apparatus equipped with a Waters 2414 refractive index (RI) detector. The Styragel columns were calibrated with polystyrene standards at 50 mV of signal. The samples were prepared at a concentration of 10 mg in 1 mL. Chloroform was used as the mobile phase at a flow rate of 1.0 mL min⁻¹. Since polystyrene standards were used, it should be taken into account that the real molar masses of the polyesters of this work are lower than those determined with polystyrene calibration [37-38].

Proton and carbon nuclear magnetic resonance (¹H NMR and ¹³C NMR) spectra were recorded in a Bruker Avance DPX 300 at 300.16 MHz and at 75.5 MHz of resonance

frequency, respectively, using 5 mm O.D. sample tubes. All spectra were obtained at room temperature from solutions of 0.7 mL of deuterated chloroform (CDCl_3). Experimental conditions were as follows: a) for ^1H NMR: 10 mg of sample; 3 s acquisition time; 1 s delay time; 8.5 μs pulse; spectral width 5000 Hz and 32 scans; b) for ^{13}C NMR: 40 mg, inverse gated decoupled sequence; 3 s acquisition time; 4 s delay time; 5.5 μs pulse; spectral width 18800 Hz and more than 10000 scans.

The signals of the lactide methine, centered at 5.15 ppm, and the signals of the α and ϵ methylenes of the ϵ -caprolactone, around 2.35 and 4.1 ppm, from the ^1H NMR spectrum can be assigned to the different dyads [24]. The copolymer composition and the microstructural magnitudes of the copolymers were obtained from the average dyad relative molar fractions. Equations 2-5 [39] were employed to obtain the number-average sequence lengths (l_i) of LA and CL building blocks, the Bernoullian random number-average sequence lengths (l_i)_{random} and the randomness character (R):

$$l_{\text{LA}} = \frac{2(\text{LA})}{(\text{LA} - \text{CL})} ; \quad l_{\text{CL}} = \frac{2(\text{CL})}{(\text{LA} - \text{CL})} \quad (2)$$

$$(l_{\text{LA}})_{\text{random}} = \frac{1}{(\text{CL})} ; \quad (l_{\text{CL}})_{\text{random}} = \frac{1}{(\text{LA})} \quad (3)$$

$$R = \frac{(l_{\text{LA}})_{\text{random}}}{l_{\text{LA}}} = \frac{(l_{\text{CL}})_{\text{random}}}{l_{\text{CL}}} = \frac{(\text{LA} - \text{CL})}{2(\text{LA})(\text{CL})} \quad (4)$$

where (LA) and (CL) are the two comonomer molar fractions, obtained from the integration of the lactide methine signals and the ϵ -caprolactone methylene signals, and (LA-CL) is the LA-CL average dyad relative molar fraction.

The composition of the PLCL copolymers was also calculated from the integral areas of bands of the carbon signals present in ^{13}C NMR spectra [40]. The region of β and γ methylene carbon atoms [31] was employed for obtaining the randomness character from eq. (5).

$$R = \frac{(l_{\text{CL}})_{\text{random}}}{l_{\text{CL}}} \quad \text{where} \quad l_{\text{CL}} = \frac{I_{\text{CL-CL-CL}} + I_{\text{LA-CL-CL}}}{I_{\text{CL-CL-LA}} + I_{\text{LA-CL-LA}}} + 1 \quad (5)$$

Two types of transesterification reactions were introduced, i.e., the first and second modes [40-41]. Lactide (LA or LL) undergo bond cleavage, which leads to the formation of -CL-L-CL- and -CL-L-L-L-CL- sequences, both with an odd number of lactydil (L) units. This phenomenon is named second mode of transesterification with the coefficient defined as follows:

$$T_{II} = \frac{(CL-L-CL)}{(CL-L-CL)_R}$$

where (CL-L-CL) is the experimentally determined concentration of the CL-L-CL sequences from the ^{13}C NMR spectrum at 170.9 ppm and $(CL-L-CL)_R$ is the calculated concentration for completely random chains:

$$(CL-L-CL)_R = \frac{k^2}{(k+1)^3} \quad \text{where } k = (CL)/(LA)$$

The tin content analysis was performed using ICP-AES (Inductively Coupled Plasma with Atomic Emission Spectroscopy). Previous to the introduction to the ICP-AES, samples of 1g of copolymer were degraded by 5mL of a hot 50:50 (volume ratio) HNO_3 : H_2SO_4 solution, microfiltered through 0.45 μm pore size filters and dissolved in distilled water. A commercially available tin standard solution (1000 $\mu\text{g}/\text{mL}$ Tin in 2 % HNO_3 and 0.5 % HF, produced by High-Purity Standards) was used as standard in the calibration of the instrument. Experimental conditions in the measurements were as follows: 1200W of power; 12 L/min of Ar plasma flow; 0.2 L/min of Ar sheath flow; 1.0 L/min of nebulizer flow; Ar as humidifier. The results are the average of the measurements collected at three different wavelength of emission of Sn (at 235.484 nm, 242.949 nm and 283.999 nm).

Cell Culture studies

Human Mesenchymal Stem Cells

Primary cultures of human adipose-derived stem cells (ADSCs) were kindly supplied by Histocell S.L. Cells were cultured in Dulbecco's modified Eagle's medium with high-glucose (DMEM+GlutaMAX; Gibco BRL, USA) containing 10 % Fetal Calf Serum

(Biochrom, Cambridge, UK), 2mM glutamine and 1 % antibiotic-antimycotic (Bio Whittaker, Cambrex) and maintained in a humidified atmosphere (5 % CO₂, 95 % relative humidity) at 37 °C. Medium changes were made every 3 days. ADSCs were used for the experiments at passages 2 – 5. Exponentially growing cell cultures were used in all experiments. Subconfluent cell monolayers were dissociated by a brief exposure to ethylenediaminetetraacetic acid (EDTA 0.5 mM)-Trypsin (0.02 mM) in phosphate-buffered saline (PBS) and centrifuging; the pellet was resuspended in Hank's solution and cells were enumerated with a Coulter counter. Viability, as determined by Trypan blue exclusion, ranged from 95 to 98 %.

In vitro cytotoxicity test

For *in vitro* cytotoxicity tests, films of thickness 175-225 µm, previously prepared by solvent casting using chloroform, were sterilized by ethanol. The ratio of material surface to extract fluid was constant and equal to 6 cm²/ml, according to ISO 10993-12 [42], and the time of extraction was 24 h at 37 °C in a humidified atmosphere containing 5 % CO₂. To provide the basis for a comparison of the effects of the test material, we used standard culture medium (DMEM+GlutaMAX), a negative control (High-Density PolyEthylene, USP Rockville, USA) and a positive control (Polyvinyl chloride, Portex Ltd, UK).

To assess the short-term cytotoxicity of the developed polymers, ISO/EN 10993 part 5 guidelines were used: medium extraction with a 24 h extraction period and MTT assay to establish the possible toxic effects of leachables released from polymers during extraction [43]. ADSCs (4×10³ cells/well) were plated in 96-well clusters, which were used for cytotoxicity assays. All cultures were incubated in corresponding medium for 24, 48, and 72 h. Toxicity was determined by a colorimetric assay (Cell Proliferation Kit I MTT, Roche, Basel, Switzerland). Briefly, viable cells are able to reduce the MTT to formazan pigment, which was dissolved by 100 µl dimethyl sulphoxide (DMSO) after removal of the culture medium. The cell number per well was proportional to the absorbance recorded at 540 nm using an ELISA plate reader. Experiments were performed by triplicate and each assay was repeated three times. Mean values and their standard deviations were estimated.

Cell Adhesion and Morphology by Scanning Electron Microscopy (SEM)

The adhesion and morphology of ADSCs was assessed by SEM. Before cell seeding, the PLCL films (175-225 μm of thickness) were sterilized by ethanol and pre-wetted with standard culture medium containing 10 % PBS during 24h in ultra-low cluster flat-bottom 24 well tissue culture plates. ADSCs (5×10^4 cells) were thereafter suspended in 30 μl of culture medium, seeded onto each sample, and incubated for 2 h to allow cell attachment (37 $^\circ\text{C}$, 5 % CO_2 , 95 % relative humidity). When cells were attached, an additional 1 ml of culture medium was added into each well. After 72 h of incubation, the samples were washed twice with pre-warmed PBS, fixed with 2 % glutaraldehyde in cacodylate buffer (0.1 M pH = 7.4) for 2 h at room temperature and post-fixed in 1 % OsO_4 for 1 h, washed in PBS and subjected to a graded ethanol series and dried through the CO_2 critical point. Finally, samples were sputter-coated with a thin layer of gold and observed in a Hitachi SEM (Hitachi S-3400N). The voltage used was 15.0 kV. The working distance was ranging from 28.0 to 30.0 mm, depending on the sample. Relating to magnification selected for SEM images, we used a range from 250 to 1000 \times .

1.1.3. Results and Discussion

Influence of the synthesis conditions

Using SnOct_2 as catalyst/initiator

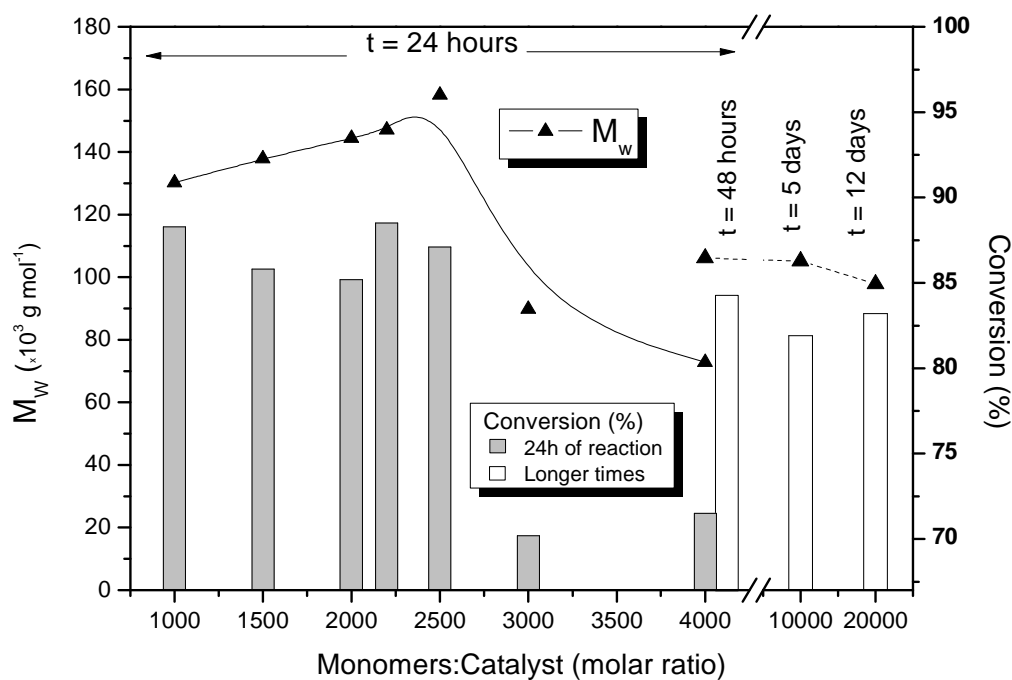
Several poly(L-lactide-co- ϵ -caprolactone) (PLCL) were synthesized with stannous octoate (SnOct_2) in order to evaluate the influence of the monomers/ SnOct_2 molar ratio (M/C). The polymerizations were carried out for 24 hours, however, at the highest M/C ratios longer times of reaction were necessary to obtain substantial yields. The copolymerization results are summarized in Table 1. Figure 1 represents graphically the dependence of molecular weights and conversions on M/C molar ratio.

Table 1. NMR characterization, thermal properties and GPC measurements of the statistical PLCL copolymers synthesized at 140 °C with different Monomers/SnOct₂ molar ratios.

Sample	Composition ¹ (% molar)		Yield (%)	M _w kg mol ⁻¹	D	1 st DSC scan			2 nd DSC scan	Microstructural Magnitudes ²				
	M/C	%LA				%CL	T _m (°C)	ΔH _m (J g ⁻¹)	X _c (%)	T _g (°C)	I _{LA}	I _{CL}	R _H	R _C
1000 24h	73.0	27.0	88.3	130.2	1.90	156.3	24.4	29.8	28.9	8.62	3.15	0.43	0.47	0.45
1500 24h	72.3	27.7	85.8	137.8	1.97	160.3	24.5	30.1	31.6	9.17	3.38	0.41	0.39	0.40
2000 24h	74.1	25.9	85.2	144.4	1.82	156.7	24.2	29.1	29.8	7.94	2.73	0.49	0.52	0.50
2200 24h	73.0	27.0	88.5	147.1	2.08	157.7	22.9	27.9	30.3	7.30	2.70	0.51	0.50	0.50
2500 24h	74.2	25.8	87.1	158.2	1.95	157.7	24.3	29.2	31.4	8.55	2.94	0.46	0.45	0.46
3000 24h	74.9	25.1	70.2	89.8	1.62	149.6	17.2	20.5	24.9	5.75	1.88	0.71	0.73	0.72
4000 24h	81.9	28.1	71.5	72.8	1.43	129.9	19.6	21.7	32.0	6.35	1.37	0.89	0.91	0.90
4000 48h	72.2	27.8	83.6	106.1	1.75	148.7	15.0	18.5	24.9	5.35	2.05	0.68	0.68	0.68
10000 5d	77.8	22.2	81.9	105.2	1.70	128.3	18.9	21.9	28.9	6.31	1.85	0.70	0.71	0.70
20000 12d	73.5	26.5	83.2	97.9	1.72	131.0	18.2	22.1	29.4	6.43	2.23	0.60	0.67	0.64

¹ Calculated averaging the copolymer composition obtained by ¹H NMR and ¹³C NMR

² I_{LA} and I_{CL} were calculated from ¹H NMR spectra and R is the average value of the randomness character obtained by ¹H NMR (R_H) and ¹³C NMR (R_C)

**Figure 1.** Dependence of molecular weights and conversions on M/C molar ratio.

As can be seen, the highest weight average molecular weights ($M_w = 144.4\text{-}158.2 \text{ kg mol}^{-1}$) and yields of reaction ($\sim 87 \%$) were obtained at 2000-2500 of M/C ratio. When more SnOct_2 was added (at lower M/C ratios), the rate of reaction was increased and the copolymer composition was closer to the feed composition (70.4 % molar content of LA) at the cost of losing molecular weight. At M/C ratios higher than 4000, low amounts of catalyst were employed requiring long times of reaction to obtain optimum results. As an illustration, 12 days of reaction were needed to get, at an overall conversion of 83.2 %, a PLCL having around 50 ppm of Sn (M/C = 20000) and 97.9 kg mol^{-1} of M_w .

With regard to the chain microstructure parameters, it is noted that the randomness character (R) approached to 1 increasing the M/C ratio. Therefore, the value of R is 0.4-0.5 for M/C = 1000-1500, 0.5 for M/C = 2000-2500, 0.7 for M/C = 3000 and 0.9 for M/C = 4000. Nevertheless, the time of polymerization might also have influence on the repeat unit distribution of sequences and, for this reason, random copolymers ($R \rightarrow 1$) were not obtained at advanced states of reaction.

Table 2. Tin content measured by ICP-AES compared with the calculated values on the assumption that all the tin becomes part of the copolymers.

Sample (M:C)	Expected Sn content (ppm)	Measured Sn content (ppm)
1000 24h	1055	1018
2000 24h	498	535
3000 24h	417	360
4000 24h	307	305

The tin content was measured by ICP-AES for some of the PLCLs of Table 1 proving that all the tin is held within the polymer structure, refuting the mechanisms of reaction [6-9] that assumes that the SnOct_2 survives during polymerizations as such. As can be seen in Table 2, the measured values are very similar to the calculated on the assumption that all the tin becomes part of the copolymers.

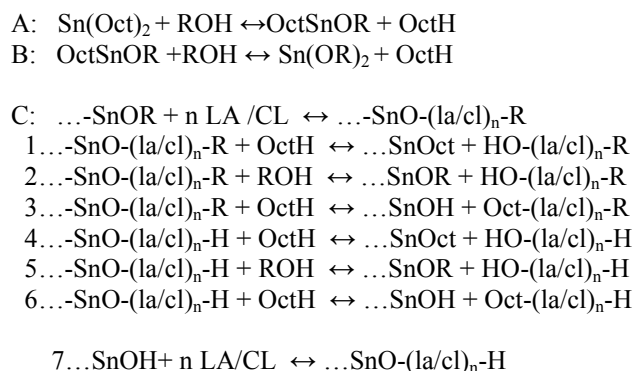


Figure 2. General scheme of reactions in LA/CL/SnOct₂/ROH system.

Figure 2 presents a scheme of reactions for the LA/CL/SnOct₂/ROH system based on the reactions proposed by Kowalski et al. [10] for a LA/SnOct₂/ROH system. The reactions “A” and “B” involve the formation of the initiating species (OctSnOR, Sn(OR)₂ and their derivatives) by means of the reaction of SnOct₂ with ROH (H₂O or impurities provided by the monomers or the catalyst). Afterwards, these alkoxides initiate the reaction “C” with the comonomers. The polymerizations proceed on the –Sn-O- bonds of the growing species, presumably by a coordination-insertion mechanism. If excess of SnOct₂ is added, more octanoic acid (OctH) is formed and the termination reactions “1”, “3”, “4” and “6” occur, inhibiting the growing of the copolymer chains. Conversely, if a low amount of catalyst is employed, the concentration of the initiating species is too small and the polymerization proceeds at a very slow rate. On the other hand, if there is ROH in excess in the medium, the termination reactions “2” and “5” take place to a larger extent competing with the growing of the copolymer chains (–SnO-(la/cl)_n-R) while more OctH is also produced in the initiation. In view of the above, it can be concluded that there is an optimal M/C ratio to synthesize polymers with high molecular weights and, in this case, it is in the range of 2000-2500 mol/mol of monomers/SnOct₂ ratio.

A second series of SnOct₂-initiated copolymerizations were also conducted with variation of the temperature and the time of reaction. The synthesis results are summarized in Table 3. Comparing these results of the copolymerizations performed for

8 hours of reaction using a M/C ratio of 2500 at 130, 140, 150 and 160 °C (the top four synthesis of the Table), it can be seen that higher rates of reaction were obtained rising the temperature of reaction. The copolymerization of LA at lower temperatures was much faster than that of CL, so that LA monomers polymerized first whereas the CL units reacted later. On the contrary, at higher temperatures the reactivities of the two comonomers were more similar due to the increased reactivity of CL. Therefore, after 8 hours of reaction the PLCL synthesized at 130 °C only had a 4.7 % of CL content, 98.5 kg mol⁻¹ of M_w and 1.26 of dispersity (D), while the overall conversion was only 48.2 %. On the contrary, the incorporation of CL units into polymer chains was almost complete when polymerizing at 160 °C and the values of M_w and D were 177.2 kg mol⁻¹ and 2.27, respectively. The yield of reaction was almost 88 %.

Table 3. NMR characterization, thermal properties and GPC measurements of the statistical PLCL copolymers synthesized with SnOct₂ at different temperatures and times of reaction.

Sample	Composition ¹ (% molar)		Yield (%)	M _w kg mol ⁻¹	D	1 st DSC scan			2 nd DSC scan	Microstructural Magnitudes ²				
	%LA	%CL				T _m (°C)	ΔH _m (J g ⁻¹)	X _c (%)	T _g (°C)	I _{LA}	I _{CL}	R _H	R _C	R
2500 130°C 8h	95.3	4.7	48.2	98.5	1.26	162.7	33.2	32.5	50.2	23.53	1.20	0.88	0.88	0.88
2500 140°C 8h	86.3	13.7	76.7	144.9	1.79	160.2	30.2	32.0	45.5	12.42	2.06	0.57	0.56	0.57
2500 150°C 8h	77.3	22.7	84.8	189.7	2.18	152.5	24.5	28.5	31.3	8.00	2.35	0.55	0.51	0.53
2500 160°C 8h	73.8	26.2	87.5	177.2	2.27	148.8	21.1	25.5	24.1	7.07	2.58	0.53	0.50	0.52
2500 130°C 24h	77.0	23.0	84.0	139.3	1.73	160.3	25.9	30.2	35.0	9.48	2.76	0.47	0.46	0.46
2500 140°C 24h	74.2	25.8	87.1	158.2	1.95	157.7	24.3	29.2	31.4	8.55	2.94	0.46	0.45	0.46
2500 150°C 24h	71.6	28.4	88.2	175.6	2.36	150.0	17.1	21.2	29.3	6.45	2.49	0.56	0.54	0.55
2500 130°C 48h	73.1	26.9	88.1	194.9	2.20	157.7	22.5	27.4	34.9	7.22	2.73	0.50	0.48	0.49
5000 150°C 24h	74.0	26.0	86.9	129.8	1.90	153.2	21.6	26.1	24.1	7.30	2.50	0.54	0.55	0.54
5000 150°C 48h	72.3	27.7	82.5	110.7	1.96	156.6	26.4	32.5	24.9	8.70	3.25	0.42	0.43	0.42
10000 150°C 3d	71.8	28.2	81.7	129.2	1.85	148.2	16.5	20.4	25.6	5.65	2.15	0.64	0.66	0.65

¹ Calculated averaging the copolymer composition obtained by ¹H NMR and ¹³C NMR.

² I_{LA} and I_{CL} were calculated from ¹H NMR spectra and R is the average value of the randomness character obtained by ¹H NMR (R_H) and ¹³C NMR (R_C).

As well as the M/C ratio, the time of reaction also affects the chain microstructure parameters. As the polymerization progresses and more CL reacts, the randomness coefficient (R) decreases. As an illustration, R is 0.88 after 8 hours of reaction at 130 °C and 0.46 after 24 hours of reaction. These PLCLs synthesized with SnOct₂ seem to be built by hard LA-rich domains and soft CL-rich chains formed later, which at short times of reaction were not formed yet. In the case of the copolymers synthesized at higher temperatures, the LA-rich domains might have a larger CL content whereas the CL building blocks might have more LA units, shortening the number average sequence lengths (l_{LA} and l_{CL}) of the copolymers. That is why in a previous work [24] we found a predominant formation of copolymers with less blocky character at higher temperatures.

Reactions of depolymerization may appear at high temperatures (> 150 °C) or at long times of reaction and, in consequence, the M_w and D grew only with the time of reaction up to a certain limit. Due to this fact, the PLCL synthesized at 150 °C and M/C = 2500 for 8 hours has larger M_w than the corresponding to 24 hours whereas the copolymerized at 150 °C with M/C = 5000 for 24 hours has larger M_w than the corresponding to 48 hours. On the other hand, it is also noted that transesterification reactions were negligible during the entire study with SnOct₂.

Polymerizing with a M/C molar ratio of 2500, synthesis conditions of 160 °C and 8 hours of reaction / 150 °C and 24 hours of reaction / 140 °C and 24 hours of reaction or 130 °C and 48 hours of reaction were established as optimal to obtain highest yields and molecular weights as well as a copolymer composition closer to the feed composition. SnOct₂ shows a marked tendency to favor blocky sequences ($R < 0.6$). However, depending on time, temperature and M/C molar ratio, some random copolymers can be achieved, e.g. R was 0.90 when polymerizing with a synthesis conditions of M/C = 4000, 140 °C for 24 hours of reaction. It is nevertheless worth mentioning that the yields of reaction are not really ideal and the feed composition has to be adjusted to fulfill the requirements. Moreover, an extra purification stage may be needed to reduce the residual content of metal catalyst not to exceed the limit set by the FDA.

Using BiSS as catalyst/initiator

Two series of copolymerizations using bismuth subsalicylate (BiSS) were performed with variation of M/C molar ratio, temperature and time of reaction. While SnOct₂ imparted a yellow colour to the transparent molten mass, the bismuth salts imparted a greyish colour of decreasing intensity at lower reaction temperatures or at lower concentration of Bi-salts. Table 4 summarizes the characterization results of the PLCL copolymers synthesized at 140 °C with different Monomers/BiSS molar ratios. Figure 3 represents graphically the dependence of molecular weights and conversions on M/C molar ratio.

Table 4. NMR characterization, thermal properties and GPC measurements of the statistical PLCL copolymers synthesized at 140 °C with different Monomers/BiSS molar ratios.

Sample	Composition ¹		Yield	M _w	D	1 st DSC scan					2 nd DSC scan	Microstructural Magnitudes ²				
	%LA	%CL				(%)	kg mol ⁻¹	T _{g1} /T _{g2} (°C)	T _m (°C)	ΔH _m (Jg ⁻¹)		X _c (%)	T _g (°C)	I _{LA}	I _{CL}	R _H
500 140°C 48h	70.8	29.2	77.4	69.0	2.22	4.9 / 57.9	82.6	1.6	2.0	16.6	3.33	1.33	1.05	1.08	1.07	0.63
1000 140°C 48h	72.1	27.9	76.0	82.5	1.89	9.2 / 55.9	101.9	7.1	8.7	22.5	3.59	1.36	1.01	1.02	1.02	0.39
1500 140°C 48h	74.2	25.8	83.8	85.9	1.86	19.8 / 55.2	115.7	14.0	16.8	24.6	4.01	1.41	0.96	0.97	0.97	0.22
1500 140°C 3d	73.2	26.8	92.3	79.3	1.81	6.6 / 57.7	111.6	7.3	8.9	18.8	3.69	1.37	1.00	1.01	1.00	0.40
2000 140°C 48h	77.7	22.3	66.9	79.9	1.83	21.8 / 52.0	122.0	17.1	19.8	28.2	4.85	1.38	0.93	0.94	0.94	0.14
2000 140°C 3d	74.1	25.9	81.1	84.0	2.00	17.6 / 52.3	117.8	13.5	16.3	26.8	4.00	1.40	0.96	0.94	0.95	0.21
2500 140°C 48h	78.4	21.6	68.8	64.0	1.75	23.8 / 52.7	124.7	17.6	20.2	31.9	5.29	1.41	0.90	0.89	0.89	0.16
5000 140°C 6d	75.9	24.1	75.5	80.8	1.84	18.0 / 55.2	122.5	16.9	20.0	26.1	5.00	1.56	0.84	0.88	0.86	0.10

¹ Calculated averaging the copolymer composition obtained by ¹H NMR and ¹³C NMR

² I_{LA} and I_{CL} were calculated from ¹H NMR spectra and R is the average value of the randomness character obtained by ¹H NMR (R_H) and ¹³C NMR (R_C)

Compared to SnOct₂, BiSS is slightly less reactive so that longer reaction times were needed to achieve similar conversions. Furthermore, copolymers having a lower weight

average molecular weight ($M_w < 90 \text{ kg mol}^{-1}$) were synthesized. An interesting point was to see that BiSS favored the formation of alternating dyads LA-CL and alternating triads LA-CL-LA. Their predominance brings about the shortening of the number average sequence lengths (l_{LA} and l_{CL}) of the copolymers and, as a result, the randomization of their morphology. The randomness coefficient (R) was in every copolymer higher than 0.85 proving a low level of blocky character.

As can be seen in Figure 3, the highest weight average molecular weights were obtained at a M/C ratio of 1500. At higher or lower M/C ratios the yields of reaction dropped and lower molar mass copolymers were prepared. According to previous studies [23] and in view of these results the BiSS polymerization pathway involves the same mechanism established for SnOct_2 in Figure 2. This mechanism consists of an activation of the catalyst/initiator by a reversible exchange with the ROH. Nevertheless, the polymerization mechanisms of SnOct_2 and BiSS entail characteristic differences in the coordination and activation of different monomers. Kricheldorf et al [23] discussed a hypothetical reaction mechanism for the predominant formation of alternating triads, however, a reaction mechanism providing a satisfactory explanation does not exist at this time [3].

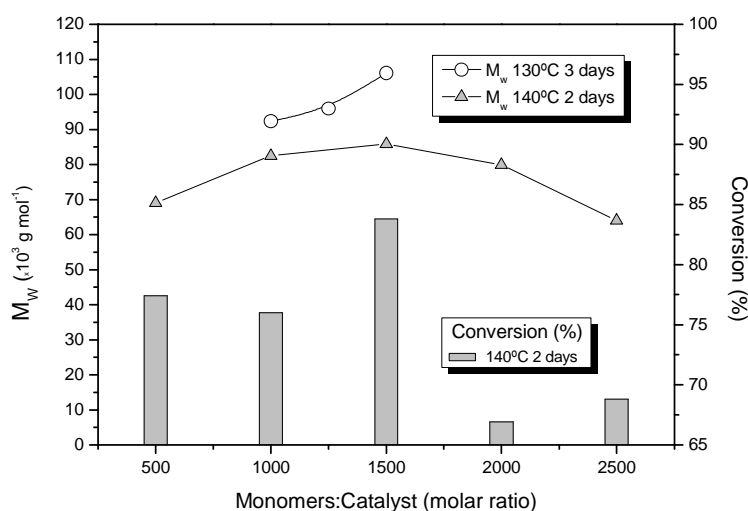


Figure 3. Dependence of molecular weights and conversions on M/C molar ratio. Characterization results of these copolymers are given in Table 4 and 5.

The second mode of transesterification (T_{II}), which represents the -CL-L-CL- sequences with an odd number of lactydil units, was detected in all the ^{13}C spectrum of the synthesized PLCLs demonstrating the higher transesterification activity of BiSS in contrast to SnOct_2 . This T_{II} coefficient was found to shift to higher values, either increasing the amount of catalyst, that is, decreasing the M/C ratio, or extending the reaction time. However, this finding might be related to the increased CL content in the composition of those copolymers. It should be stated that these transesterification reactions do not affect the rate of polymerization, but yet may reduce the molecular weights of the copolymers obtained.

Regarding the chain microstructure distribution of sequences, higher M/C molar ratios resulted in higher R values and, consequently, shorter repeat unit length values of LA and CL. In some cases, R was even higher than 1, e.g. PLCLs using M/C ratios lower than 1000. This fact can be explained by the transesterification reactions occurring during the synthesis or also could be an evidence of the presence of alternating sequences (-LA-CL-LA-CL-LA-CL-) in the copolymer chains.

A second series of BiSS-initiated copolymerizations were also conducted varying the temperature and the time of reaction and the results are summarized in Table 5. According to these results, the PLCLs synthesized at 130 °C exhibit higher molecular weights ($M_w \sim 90\text{-}115 \text{ kg mol}^{-1}$) than those prepared at 140 °C (Table 4). 3 days of reaction were necessary to obtain conversions higher than 80 % and CL contents in the copolymer similar to those achieved when synthesizing at 140 °C for 2 days or at 150 °C for 24 hours, at the same M/C ratio (M/C = 1500). At 130 °C, the polymerization progressed very quickly in the first 24 hours of reaction incorporating the LA first, the LA content is 82.6 % at this point of polymerization, and later on, more slowly, the remaining CL. As a result, the LA content in the copolymer shifted to 76 % after 48 hours and reached a final value of 74.9 % after 3 days of reaction. In any case, BiSS was found to be less prone to react with the LA monomer than SnOct_2 , favoring the random copolymerization.

Table 5. NMR characterization, thermal properties and GPC measurements of the statistical PLCL copolymers synthesized with BiSS at different temperatures and times of reaction.

Sample	Composition ¹ (% molar)		Yield (%)	M _w kg mol ⁻¹	D	1 st DSC scan				2 nd DSC scan T _g (°C)	Microstructural Magnitudes ²					
	%LA	%CL				T _{g1} / T _{g2} (°C)	T _m (°C)	ΔH _m (J g ⁻¹)	X _c (%)		I _{LA}	I _{CL}	R _H	R _C	R	T _H
1500 150°C 24h	74.4	25.6	95.5	90.4	2.41	6.7 / 58.9	105.6	7.5	9.0	22.8	3.72	1.32	1.03	1.04	1.03	0.48
1500 150°C 48h	72.5	27.5	95.4	75.8	2.09	5.3 / 59.1	88.1	3.0	3.7	21.4	3.47	1.31	1.05	1.06	1.06	0.42
1000 130°C 3d	72.1	27.9	97.5	92.3	1.96	5.4 / 66.1	113.7	3.5	4.3	18.9	3.49	1.36	1.02	1.02	1.02	0.53
1250 130°C 3d	73.1	26.9	88.4	95.9	1.97	11.9 / 52.1	118.5	7.5	9.1	21.5	3.80	1.39	0.98	0.99	0.99	0.40
1500 130°C 3d	74.9	25.1	83.1	106.1	2.02	19.4 / 51.1	116.1	14.3	17.1	25.8	4.13	1.39	0.96	0.97	0.96	0.22
1500 130°C 48h	76.0	24.0	85.7	110.7	2.08	22.6 / 51.8	116.3	14.8	17.5	29.6	4.28	1.37	0.96	0.96	0.96	0.27
1500 130°C 24h	82.6	17.4	77.8	138.8	1.99	28.9 / 65.0	124.8	19.0	21.1	38.7	5.36	1.19	1.03	1.00	1.01	0.12
1500 120°C 4d	77.0	23.0	83.1	113.4	2.01	22.3 / 65.3	117.8	16.0	18.7	32.8	4.78	1.43	0.91	0.92	0.91	0.14

¹ Calculated averaging the copolymer composition obtained by ¹H NMR and ¹³C NMR.

² I_{LA} and I_{CL} were calculated from ¹H NMR spectra and R is the average value of the randomness character obtained by ¹H NMR (R_H) and ¹³C NMR (R_C).

At elevated temperatures, such as 150 °C, copolyesters having broader molar mass distributions were obtained because of the fact that those temperatures may allow depolymerizing reactions to take place. At temperatures lower than 130°C long times of reaction were required. The incorporation of CL units into polymer chains was incomplete because of the low reactivity of CL, thus at 120°C the copolymer composition was 77:23 % of LA:CL after 4 days of reaction.

As has been seen, BiSS demonstrates to be a suitable catalyst to synthesize statistical copolymers having a more random morphology. The polymerization at 130 °C using a M/C molar ratio of 1000-1500 was established as an appropriate way to achieve random copolyesters ($R \rightarrow 1$) with a M_w of 90-110 kg mol⁻¹, having the possibility of reducing their molecular weight by controlling the concentration of ROH. The differences in the chain microstructure existing between these PLCLs with a random distribution of

sequences and the copolymers synthesized with SnOct₂ will be reflected in their physical properties. The discussion of the thermal properties of the different PLCLs will be treated in the next section.

Thermal properties discussion

In the precipitation of a polymer, an ordered, oriented, metastable structure, that does not suffer changes in its physical properties after being dried, is formed [31, 44]. The analysis of the thermal properties of the copolymers is going to be conducted on the basis of the discussion of the DSC thermograms of those nascent polymers. The glass transition temperatures (T_g) of the first and second scans, the heat of fusion (ΔH_m) and the correlated melting temperature (T_m) and degree of crystallinity (X_c) estimated from the first DSC scans are all summarized in Tables 1,3, 4, 5, previously provided.

Figure 4 shows the influence of the average block length of LA (l_{LA}) on the melting temperature (T_m) and the crystallinity (X_c) of the copolymers. It can be observed that both T_m and X_c shift to lower values decreasing the l_{LA} , a parameter affected by the LA content and the randomness character (R) of the PLCLs. The copolymers synthesized with BiSS, all of them having distribution of sequences close to the Bernoullian ($R \sim 1$), present a T_m greatly influenced by the l_{LA} and lower than the corresponding to the SnOct₂-copolymers. Their T_m values increase from 82 to 125 °C when l_{LA} only rises from 3.3 to 5.4. On the contrary, the melting temperature of the moderate blocky PLCLs catalyzed by SnOct₂ is in the range of 148-163 °C, despite the wide range of their respective number-average sequence length values of LA ($l_{LA} = 5.4-23.5$). It is worth mentioning that the T_m of some PLCLs, which have low Sn content and higher randomness character, is around 130 °C as a result of their more amorphous homogeneous phase structure (i.e. see the PLCL D of the Figure 5). The LA-unit sequences of those copolymers may form crystallites that have a lower melting point due to their more imperfect crystals grown under less favourable supramolecular chain arrangements.

In regard to the evolution of the crystallinity degree (X_c) with the average sequence length of LA (l_{LA}), the X_c grows in a logarithmic manner and has a maximum value of

32.5 % when l_{LA} is 23.5 (% LA = 95.3 and $R = 0.88$). The crystallinity degree rises quickly from 2.0 % to around 20.0 % increasing the average sequence length from 3.3 to 5.0, grows moderately when l_{LA} is in the range of 5.0-9.0 and then, at higher values of l_{LA} , stabilizes, because of the LA-unit sequences capability of crystallization is close to its limit.

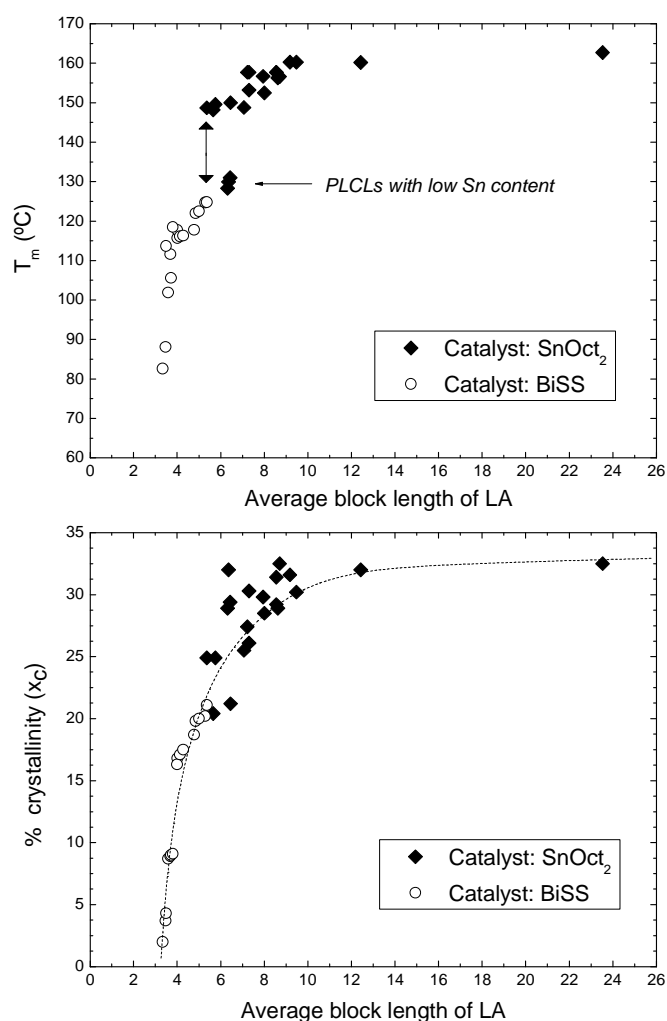


Figure 4. Melting temperature (T_m) and crystallinity degree (X_c) of the PLCLs synthesized using either SnOct₂ or BiSS as catalyst/initiator as a function of their average block sequence length of LA.

Figure 5 presents the DSC curves of the first and second scan of some of the most representative copolymers of this study. The DSC traces show a double glass transition temperature (T_g) behaviour. The T_g signals are more clearly defined (larger ΔC_p change at the glass transitions) in the PLCLs with a larger amorphous character and are almost

indistinguishable in the copolymers with more capability to crystallize. The lower T_g is associated to the hybrid amorphous miscible LA-CL phase, composed of mainly CL units, whereas the higher T_g observed in the range of 50 to 65 °C suggests the presence of phase separated amorphous polylactide domains. Increasing the l_{LA} of the PLCLs the capability to crystallize of the LA building blocks rises due to the incorporation of LA repeat units of the amorphous LA fraction to the crystalline domains and, as a consequence, the ΔC_p associated to this second T_g drops as well as the melting peak is increased. It is also remarkable that, in the copolymers having a higher random character (the BiSS-catalyzed PLCLs), the LA content of the LA/CL mixed phase drops leading to a displacement of the first T_g to lower values.

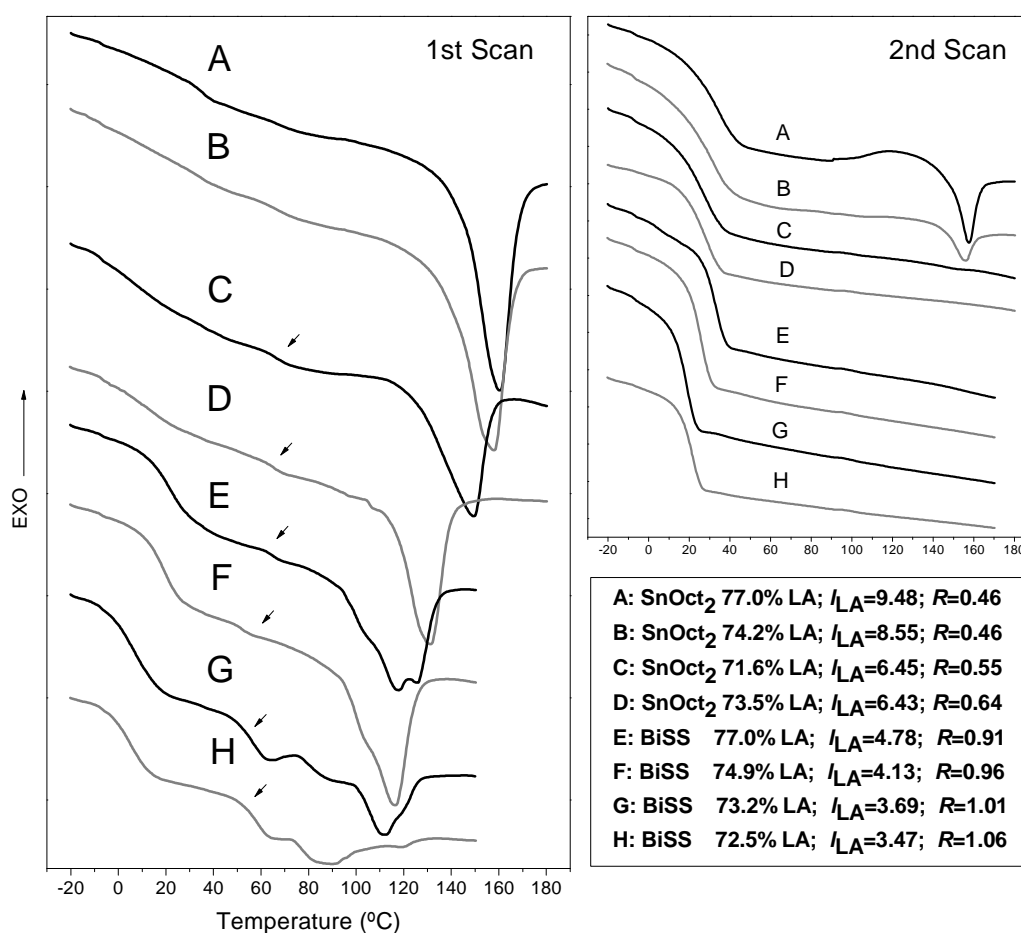


Figure 5. DSC curves of the first and second scan of some of the most representative copolymers: A: SnOct₂ M/C = 2500 130 °C 24 h; B: SnOct₂ M/C = 2500 140 °C 24 h; C: SnOct₂ M/C = 2500 150 °C 24

h; D: SnOct₂ M/C = 20000 140 °C 12 d; E: BiSS M/C = 1500 120 °C 4 d; F: BiSS M/C = 1500 130 °C 3 d; G: BiSS M/C = 1500 140 °C 3 d; H: BiSS M/C = 1500 150 °C 48 h.

A second scan was made for all the PLCLs and the corresponding DSC curves revealed a homogeneous amorphous phase structure for all the copolymers studied. As can be seen, a single T_g appeared in each copolymer showing lower T_g values when the l_{LA} was decreased, that is, reducing the LA content or enhancing the amorphous character of the copolymers by increasing their randomness. It is worth mentioning that at higher values of the average sequence lengths of LA, the PLCLs presented a cold crystallization peak as a result of crystallization of LA building blocks during the DSC scan, however the neat heat enthalpy of fusion obtained was negligible demonstrating their amorphous phase structure.

Cell adhesion and proliferation

Cell adhesion and proliferation studies were conducted using films of three representative copolymers of this work, the PLCL synthesized at 130 °C for 2 days with a 2500 M/C molar ratio (73.1 % LA, $R = 0.49$, aprox. 400 ppm of residual Sn), the PLCL synthesized at 140 °C for 12 days with a 20000 M/C molar ratio (73.5 % LA, $R = 0.64$, aprox. 50 ppm of residual Sn) and the PLCL synthesized at 130 °C for 3 days with a 1000 M/C molar ratio (72.1 % LA, $R = 1.02$, aprox. 1600 ppm of residual Bi).

Proliferation values of adipose derived mesenchymal stem cells (ADSCs) were obtained by the colorimetric MTT assay method. Figure 6 shows cell viability values expressed in relation to the control, a standard culture medium that represents 100 % cell viability. As can be observed, cell proliferation trends of all the materials tested, including the negative control, are very similar during the 72 hours of incubation. In addition, the measured values of cell viability are above the 70 % of the control, which is the threshold level required by the ISO 10993-5:2009 to guarantee that the materials are not cytotoxic.

In view of these results, it can be concluded that the three materials selected have no cytotoxic effects on the proliferation of human mesenchymal stem cells despite their high metal content (~ 400 ppm of Sn and ~ 1600 ppm of BiSS) proving that the rest of

PLCLs synthesized in this study will not have signs of cytotoxicity. Regardless of the inappropriate residual Sn content of these materials, that it is not sufficiently low for biomedical application, the cell proliferation study showed that cells could grow on the biomaterials with an efficiency equal to or better than on the negative control culture plastic used (high-density polyethylene).

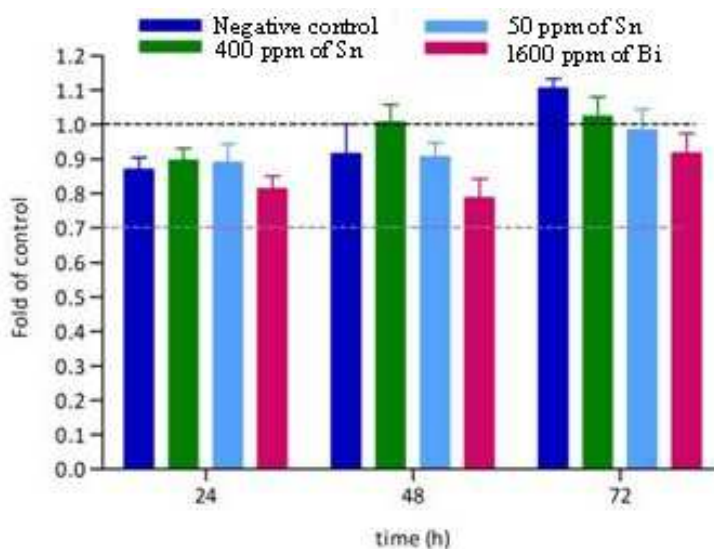


Figure 6. Cell viability values, relative to those for the control, of the selected PLCLs and the negative control, a material that allows the cell survival.

SEM analysis was conducted to determine the cell morphology, spreading and adhesion of ADSCs on films of the three selected PLCLs having different residual catalyst content (~ 1600 ppm of Bi, ~ 400 ppm of Sn and ~ 50 ppm of Sn). Figure 7 shows scanning electron micrographs before and after cell seeding with a magnification of 1000 \times .

Before cell seeding all materials exhibited similar surface characteristics when viewed under SEM. Afterwards, their ability to support ADSCs growth in vitro was examined in further detail. The adhesion and growth of ADSCs was assessed after 3 days cultured on materials. ADSCs were well spread on all supports and revealed somewhat uniform morphological features such a random orientation, without differences among them. Cells were able to proliferate during the subsequent periods in culture. It is observed that the cells were able to form a continuous layer of cells well attached and fully

covering the surface of materials. These results are in good agreement with the growth rate obtained with cells cultured in extracted medium from materials.

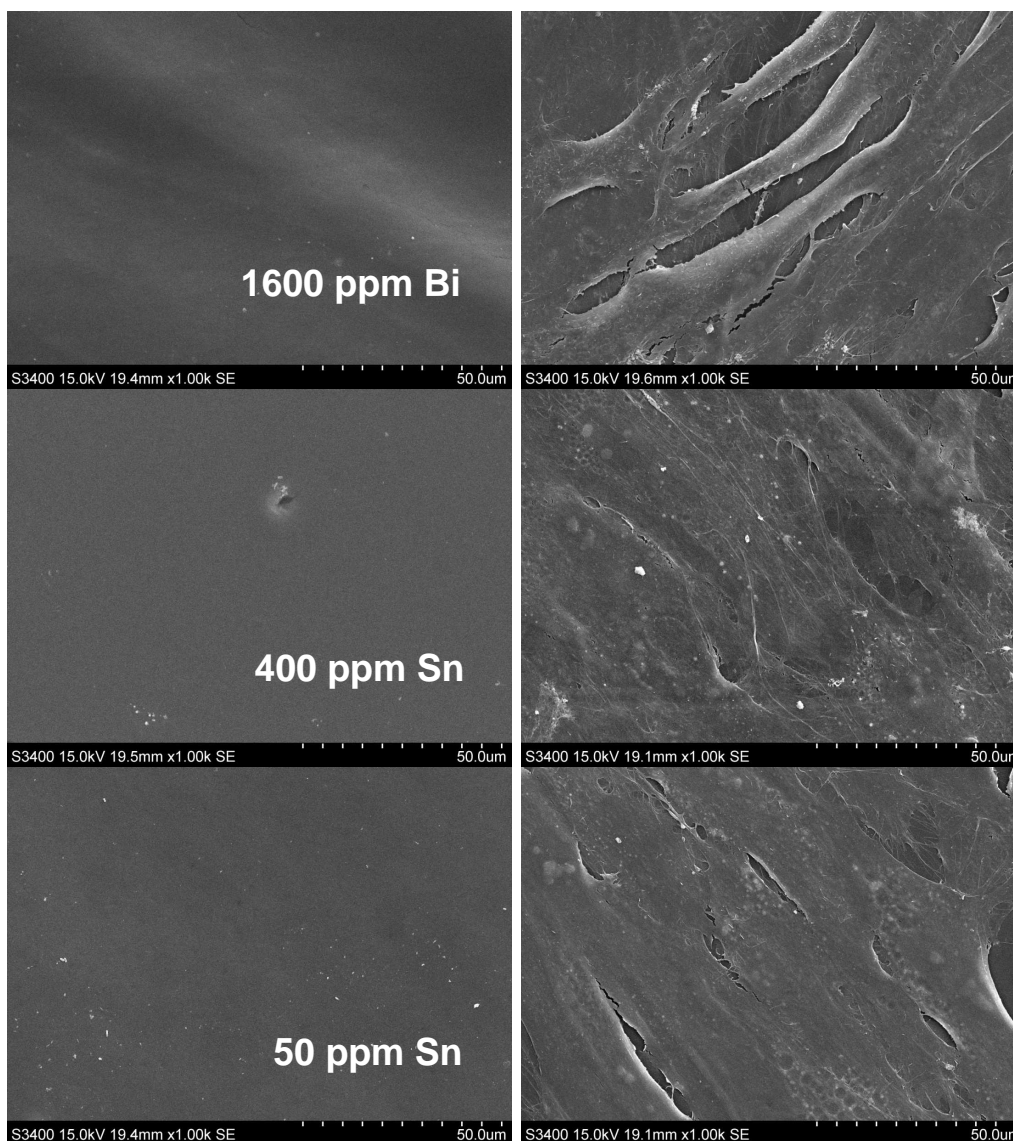


Figure 7. Scanning electron micrographs (SEM) before (left) and after cell seeding (right) of the three PLCLs having different catalyst content.

1.1.4. Conclusions

Increasing the randomness character has been demonstrated to be a really interesting way to improve the biodegradation rates, the elastomeric character and the resistance to

physical aging of copolyesters of equal comonomer composition. In view of the above, several statistical poly(L-lactide-co- ϵ -caprolactone) (PLCL) at a 75:25 mass feed ratio were synthesized in bulk by ROP with the goal of achieving copolyesters of a marked random distribution of sequences ($R > 0.8$). Either SnOct₂ or BiSS were added as catalyst/initiator varying the synthesis conditions (temperatures, times of reaction and comonomer/catalyst molar ratios). The mechanisms of reaction of both SnOct₂ and BiSS involve an activation of the catalyst/initiator by a reversible exchange with the ROH (H₂O, impurities provided by the monomers or the catalyst or alcohols added intentionally). In both cases, there is an optimal M/C ratio to synthesize polymers with high molecular weights at high yields of reaction. Nevertheless, the polymerization mechanisms entail differences in the coordination and activation of the monomers leading to different chain microstructure distributions of sequences.

BiSS was probed to be a suitable catalyst to obtain statistical copolymers presenting a random morphology. Compared to SnOct₂, it was slightly less reactive (longer reaction times were needed to get similar conversions) and, in addition, copolymers of a lower weight average molecular weight were synthesized. BiSS was found to be less prone to react with the monomer with higher reactivity (LA) than SnOct₂ and, consequently, the randomness coefficient (R) was in every PLCL higher than 0.85. Copolymerization at 130 °C during three days with a M/C molar ratio of 1000-1500 was established as an appropriate manner to obtain random copolyesters ($R \rightarrow 1$) with a M_w of 90-110 kg mol⁻¹, having the possibility of reducing their molecular weight by controlling the concentration of ROH.

On the contrary, SnOct₂ shows a tendency to favor the formation of blocky sequences ($R < 0.6$). Nevertheless, depending on time, temperature and M/C molar ratio, some random copolymers can be achieved, e.g. R was 0.90 when polymerizing with a synthesis conditions of M/C = 4000, 140 °C for 24 hours of reaction. However, in these cases it is worth mentioning that the yields of reaction are not really good and the feed composition has to be adjusted to fulfill the requirements. In addition, an extra purification stage may be needed to reduce the residual content of metal catalyst not to exceed the limit set by the FDA.

The differences in the chain microstructure existing between the PLCLs with a random distribution of sequences and the copolymers with a blockier character are reflected in their thermal properties. Both melting point (T_m) and crystallinity degree (X_c) of the PLCLs shift to lower values decreasing l_{LA} , a parameter affected by the LA content and the randomness character (R). The random BiSS-copolymers, present a T_m lower than the corresponding to the moderate blocky SnOct₂-copolymers. Their T_m values increase from 82 to 125 °C when the l_{LA} only rises from 3.3 to 5.4. On the contrary, the T_m of the SnOct₂-PLCLs is in the range of 148-163 °C, despite the wide range of their respective l_{LA} (5.4-23.5). The LA-unit sequences of the more amorphous copolymers may form crystallites that have a lower melting point due to their more imperfect morphology. In regard to the crystallinity of the PLCLs it should be stated that X_c grows in a logarithmic manner and rises quickly from 2.0 % to around 20.0 % increasing the average sequence length from 3.3 to 5.0, grows moderately when l_{LA} is in the range of 5.0-9.0 and then, at higher values of l_{LA} , stabilizes, because of the LA-unit sequences capability of crystallization is close to its limit.

The first DSC scans show also a double glass transition temperature (T_g) behaviour, which is indicative of the existence of phase separation. The T_g signals are more clearly defined (larger ΔC_p change at the glass transitions) in the PLCLs with a larger amorphous fraction and are almost indistinguishable in the copolymers with more capability to crystallize. A second scan was also made for all the PLCLs and the corresponding DSC curves revealed a homogeneous amorphous phase structure for all the copolymers studied.

Finally, in this study the attachment and proliferation of adipose derived mesenchymal stem cells (ADSCs) on some of the obtained PLCLs were also investigated demonstrating that the biomaterials are not cytotoxic despite their residual catalyst content (~ 1600 ppm of Bi, ~ 400 ppm of Sn and ~ 50 ppm of Sn). The cells were well spread on all supports and were able to form a continuous layer of cells well attached. These results are in good agreement with the proliferation rate obtained by the colorimetric MTT assay method with cells cultured in extracted medium from materials.

References

- [1] Albertsson, A.C; Varma, I.K. Recent Developments in Ring Opening Polymerization of Lactones for Biomedical Applications. *Biomacromolecules* 2003, 4, 1466-1486.
- [2] Stjern Dahl, A; Wistrand, A.F; Albertsson, A.C. Industrial Utilization of Tin-initiated Resorbable Polymers: Synthesis on a Large Scale with a Low Amount of Initiator Residue. *Biomacromolecules* 2007, 8, 937-940.
- [3] Kricheldorf, H.R. Syntheses of Biodegradable and Biocompatible Polymers by means of Bismuth Catalysts. *Chemical Reviews* 2009, 109, 5579-5594.
- [4] Tanzi, M.C; Verderio, P.; Lampugnani, M.G, Resnati, M; Dejana, E; Sturani, E. Cytotoxicity of some catalysts commonly used in the synthesis of copolymers for biomedical use. *Journal of Materials Science, Materials in Medicine* 1994,5,393-396.
- [5] Kafrawy, A; Shalaby, S.W. A new synthesis of 1,5-dioxepan-2-one. *Journal of Polymer Science, Polymer Chemistry*. 1987, 25, 2629-2630.
- [6] Neijenhuis, A.J; Grijpma, D.W; Pennings, A.J. Lewis acid catalyzed polymerization of L-lactide. Kinetics and mechanism of the bulk polymerization. *Macromolecules* 1992, 25, 6419-6424.
- [7] Du, Y.J; Lemstra, P.J; Neijenhuis, A.J; van Aert, H.A.M; Bastiaansen, C. ABA type copolymers of Lactide with Poly(ethylene glycol). Kinetic, Mechanistic and Model Studies. *Macromolecules* 1995, 28, 2124-2132.
- [8] Kricheldorf, H.R; Kreiser-Saunders, I; Boettcher, C. Polylactones. 31. Sn(II)octoate-initiated polymerization of L-lactide: a mechanistic study. *Polymer* 1995, 36, 1253-1259.
- [9] In't Veld, P.J; Velner, E.M; van de Witte, P.; Hamhuis, J.; Dijkstra, P.J.; Feijen, J. Melt block copolymerization of ϵ -caprolactone and L-lactide. *Journal of Polymer Science Part A: Polymer Chemistry*, 1997, 35, 219-226.
- [10] Leenslag, J.W; Pennings, A.J. Synthesis of high-molecular-weight poly(L-lactide) initiated with tin-2 ethylhexanoate. *Makromolekulare Chemie* 1987, 188, 1809-1814.
- [11] Zhang, X.; MacDonald, D.A.; Goosen, M.F.A.; McAuley, K.B. Mechanism of lactide polymerization in the presence of stannous octoate: the effect of hydroxyl and carboxylic acid substances. *Journal of Polymer Science Part A: Polymer Chemistry* 1994, 32, 2965-2970.

- [12] Kowalski, A.; Duda, A.; Penczek, S. Kinetics and Mechanism of Cyclic Esters Polymerization Initiated with Tin(II) Octoate. 3. Polymerization of L,L-dilactide. *Macromolecules* 2000, 33, 7359-7370.
- [13] Stjern Dahl, A.; Wistrand, A.F.; Albertsson, A.C.; Bäckesjö, C.M.; Lindgren, U. Minimization of residual tin in the controlled Sn(II) octoate-catalyzed polymerization of ϵ -caprolactone. *Journal of Biomedical Materials Research Part A* 2008, 87, 1086-1091.
- [14] Tamaya, H.; Ajioka, M.; Yamaguchi, T. Japanese Patent Kokai Tokkyo Koho Jp 06256492 A2, 1994.
- [15] Arimura, H.; Takahashi, Y.; Yamauchi, K. Patent US 2009/0171064 A1, July 2009.
- [16] Mori, T.; Nishida, H.; Shirai, Y.; Endo, T. Effects of chain end structures on pyrolysis of poly(L-Lactic acid) containing tin atoms. *Polymer Degradation and Stability* 2004, 84, 243-251.
- [17] Kricheldorf, H.R.; Behnken, G. Copolymerization of Glycolide and L-lactide initiated with Bismuth(III) n Hexanoate or Bismuth Subsalicylate. *Journal of Macromolecular Science, Part A: Pure and Applied Chemistry* 2007, 44, 795-800.
- [18] Gordon, M.F.; Abrams, R.I.; Rubin, D.R.; Barr, W.B.; Correa, D.D. Bismuth subsalicylate toxicity as a cause of prolonged encephalopathy with myoclonus. *Movement Disorders* 1995, 10, 220-222.
- [19] Gill, H.H.; Desai, H.G.; Mehta, P.R.; Ranganathan, S.; Kalro, R.H.; Musti, P.K.; Prabhu, S.R. Mono and dual therapy for Helicobacter pylori associated gastritis. *The Journal of the Association of Physicians of India* 1991, 39, 743-745.
- [20] Suarez, M.S.; Gonzales-Cansino, J.; Velasco-Ilizalde, C.; Sabatier, C.A.; Castillo-Hernandez, J. Three treatments schemes with colloidal bismuth subcitrate (Q-Ulcer) in peptic ulcer with helicobacter pylori. *Archives of Medical Research* 1999, 30, 55-59.
- [21] Kricheldorf, H.R.; Hachmann-Thiessen, H. Di-, Tri- and Tetrafunctional Poly(ϵ -caprolactone)s by Bi(OAc)₃. Catalyzed Ring-Opening Polymerizations of ϵ -caprolactone. *Macromolecules* 2004, 37, 6340-6345.
- [22] Kricheldorf, H.R.; Hachmann-Thiessen, H.; Schwarz, G. Telechelic and Star-Shaped Poly(L-lactide)s by Means of Bismuth(III) Acetate as Initiator. *Biomacromolecules* 2004, 8, 492-496.
- [23] Kricheldorf, H.R.; Rost, S. Copolymerization of ϵ -caprolactone and glycolide- A comparison of Tin(II)Octanoate and Bismuth(III) Subsalicylate as Initiators. *Biomacromolecules* 2005, 6, 1345-1352.

- [24] Fernández, J.; Etxeberria, A.; Sarasua, J.R. Synthesis, structure and properties of poly(L-lactide-co- ϵ -caprolactone) statistical copolymers. *Journal of the Mechanical Behaviour of Biomedical Materials* 2012, 9, 100-112.
- [25] Dobrzynski, P.; Li, S.; Kasperczyk, J.; Bero, M.; Gasc, F.; Vert, M. Structure property relationships of copolymers obtained by ring-opening polymerization of glycolide and ϵ -caprolactone. Part 1. Synthesis and characterization. *Biomacromolecules* 2005, 6, 483-488.
- [26] Jelonek, K.; Kasperczyk, J.; Dobrzynski, P.; Jarzabek, B. Controlled poly(l-lactide-co-trimethylene carbonate) delivery system of cyclosporine A and rapamycin- the effect of copolymer chain microstructure on drug release rate. *International Journal of Pharmaceutics* 2011, 414, 203-209.
- [27] Florczak, M.; Duda, A. Effect of the Configuration of the Active Center on Comonomer Reactivities: The case of ϵ -caprolactone/ L,L-lactide copolymerization. *Angewandte Chemie International Edition* 2008, 47, 9088-9091.
- [28] Florczak, M.; Libiszowski, J.; Mosnacek, J.; Duda, A.; Penczek, S. L,L-Lactide and ϵ -caprolactone Block Copolymers by a Poly(L,L-lactide) Block First Route. *Macromolecular Rapid Communications* 2007, 28, 1385-1391.
- [29] Hua, J.; Gebarowska, K.; Dobrzynski, P.; Kasperczyk, J.; Wei, J.; Li, S. Influence of chain microstructure on the hydrolytic degradation of copolymers from 1,3-trimethylene carbonate and l-lactide. *Journal of Polymer Science: Part A: Polymer Chemistry* 2009, 47, 3869-3879.
- [30] Lee, S.C.; Kim, K.J.; Kang, S.W.; Kim, C. Microstructural analysis and structure-property relationship of poly(glycolide-co-1,3-trimethylene carbonate). *Polymer* 2005, 46, 7953-7960.
- [31] Fernández, J.; Etxeberria, A.; Ugartemendia, J.M.; Petisco, S.; Sarasua, J.R. Effects of chain microstructures on mechanical behaviour and aging of poly(L-lactide-co- ϵ -caprolactone) biomedical thermoplastic elastomer. *Journal of Mechanical Behavior of Biomedical Materials* 2012, 12, 29-38.
- [32] Nomura, N.; Akita, A.; Ishii, R.; Mizuno, M. Random Copolymerization of ϵ -Caprolactone with Lactide using a Homosalen-Al Complex. *Journal of the American Chemistry Society* 2010, 132, 1750-1751.
- [33] Dakshinamoorthy, D.; Peruch, F. Block and Random copolymerization of ϵ -Caprolactone, L- and rac-lactide using titanium complex derived from aminodiols ligand. *Journal of Polymer Science: Part A: Polymer Chemistry* 2012, 50, 2161-2171.

-
- [34] Li, G.; Lamberti, M.; Pappalardo, D.; Pellicchia, C. Random Copolymerization of ϵ -Caprolactone and Lactides Promoted by Pyrrolylpyridylamido Aluminium Complexes. *Macromolecules* 2012, 45, 8614-8620.
- [35] Ugartemendia, J.M.; Sarasua, J.R. ANTEC Proceedings 2011, 1, 230-235.
- [36] Sarasua, J.; Prud'homme, R.E.; Wisniewski, M.; Le Borgne, A.; Spassky, N. Crystallization and Melting Behaviour of Poly lactides. *Macromolecules* 1998, 31, 3895-3905.
- [37] Biela, T.; Duda, A.; Penczek, S. Control of Mn, Mw/Mn, end-groups and kinetics in living polymerization of cyclic esters. *Macromolecular Symposia* 2002, 183, 1-10.
- [38] Save, M.; Schappacher, M.; Soum, A. Controlled Ring-Opening Polymerization of Lactones and Lactides Initiated by Lanthanum Isopropoxide, 1. General Aspects and Kinetics. *Macromolecular Chemistry and Physics* 2002, 203, 889-899.
- [39] Herbert, I.R. Statistical analysis of copolymer sequence distribution, in: Ibbett RN. (Ed.), In *NMR Spectroscopy of Polymers*. Blackie Academic & Professional, London, 1993; p 50-79. (Chapter 2).
- [40] Kasperczyk, J.; Bero, M. Coordination polymerization of lactides, 2. Microstructure determination of poly[(L,L-lactide)-co-(ϵ -caprolactone)] with ^{13}C nuclear magnetic resonance spectroscopy. *Makromolekulare Chemie* 1991, 192, 1777-1787.
- [41] Kasperczyk, J.; Bero, M. Coordination polymerization of lactides, 4. The role of transesterification in the copolymerization of L-L-lactide and ϵ -caprolactone. *Makromolekulare Chemie* 1993, 194, 913-925.
- [42]. ISO 10993-12: Biological Evaluation of Medical Devices -- Part 12: Sample Preparation and Reference Materials, 2002.
- [43]. ISO 10993-5: Biological Evaluation of Medical Devices -- Part 5: Tests for in Vitro Cytotoxicity, 2009.
- [44] Serkov, A.T.; Khanchich, O.A. Formation of Oriented structures in the precipitation of polymers from concentrated solutions. *Fibre Chemistry* 1977, Vol 9. 4, 327-332.

**Chapter 1.2 Effects of Chain
Microstructures and Derived
Crystallization Capability on
Hydrolytic Degradation of L-Lactide-
co- ϵ -Caprolactone Copolymers**

Polymer Degradation and Stability 2013, 98, 481-489

Abstract

Hydrolytic degradation of bioabsorbable (co)polyesters is affected by a great number of factors, such as chemical composition, hydrophilicity, pH of the medium, morphology of the sample, initial distribution of molecular weights, etc. In this study it is demonstrated the importance of the amorphous/crystalline character, controlled by the repeat unit sequence distribution in chain microstructure of crystallizable lactide building block copolymers. Three statistical poly(L-lactide/ ϵ -caprolactone) were degraded in phosphate buffered saline (PBS) at 37 °C for a period up to 14 weeks. PLCL74b and PLCL74r, presenting similar copolymer composition (~ 74 % of lactide) but a different randomness character ($R = 0.46$ vs. 0.96) reflected in their lactide sequence length distribution (l_{LA}) (8.16 vs. 4.01), displayed a completely dissimilar behaviour during the course of degradation. The blocky PLCL74b showed a high crystallization capability, reaching a value of 51.0 J g^{-1} of melting enthalpy (ΔH_m) at the end of the study, whereas random PLCL74r presented a $\Delta H_m = 33.7 \text{ J g}^{-1}$. On the contrary, PLCL62r, having a similar randomness character to PLCL74r, a ~ 62 % of lactide content and the lowest l_{LA} (2.55), showed a $\Delta H_m = 10.9 \text{ J g}^{-1}$. As a consequence, PLCL74b exhibited the slowest degradation rate (half degradation time ($t_{1/2}$) = 31.5 days), while PLCL62r was the less resistant to hydrolytic degradation with a $t_{1/2} = 18.2$ days. This is due to the larger hindrance the water finds to penetrate the crystalline domains and consequently, to the higher resistance of crystalline domains to hydrolytic degradation. Apart from slowing down the degradation, the development of crystalline domains caused deterioration in the mechanical properties of the studied copolymers, which make them unworkable as the degradation process progressed.

1.2.1. Introduction

Better understanding of the mechanisms and kinetics of biodegradation of absorbable homo- and co-polyesters permits the prediction and the adjustment of their degradation rate, enabling the adaptation of the polymers to the requirements of a specific biomedical application. Following the definitions given by Goepferich [1,2], polymers can suffer two processes of decomposition: degradation and erosion. Degradation involves the chain scission of the polymer chains by means of the bond cleavage on a molecular level, to form oligomers and finally to form monomers. Erosion designates the macroscopic loss of material related to monomers, oligomers or not biodegraded fragments of polymer leaving the biomaterial. Therefore, the process of degradation is, in the above context, part of the erosion, which encompasses, in addition to degradation, physical phenomena, such as swelling, dissolution and diffusion, and morphological changes [3].

The diffusion of water and the degradation of the polymer compete during the erosion process. If the water uptake mechanism is dominant, the splitting of chemical bonds has a smaller effect and the erosion is homogeneous. This is known as “bulk erosion”. In the opposite case “surface erosion” occurs and degradation proceeds at the interfacial areas between polymeric specimens and the aqueous environment [4]. Von Burkersroda et al. [2] explained the occurrence of bulk degradation or surface erosion in a polymer on the basis of the diffusivity of water inside the polymer, the degradation rate and the dimensions of the degrading object. Most hydrolytically degradable polymeric materials, such as (co)poly(α -hydroxy esters) of glycolide or lactide, show predominantly bulk erosion. On the contrary, some polymers as polyanhydrides or polyorthoesters are considered surface eroding systems, in which the erosion progresses at constant velocity and the mass loss is linear.

In hydrolytic degradation, two mechanisms can be distinguished: random and chain-end scission (also known as backbiting) [5]. The chain scission of a polymer is called random, if the bonds at any position along the polymer chain have the same probability

to be cleaved. As a consequence, the main chain breaks down randomly via cascades of irreversible scission steps following a first-order kinetic, irrespective of the chain length of the polymer molecules involved. In this case, the number of chain increases gradually leading to a higher molecular weight decrease than in backbiting dominated mechanism. By contrast, in the chain-end scission, the number of chain ends and the rate constant for the cleavage of the terminal bond are the essential kinetic parameters. The contribution of chain-end scission raises with decreasing the molecular weight of the polymer since the fraction of chain ends increases as a consequence of the degradation process. Several factors, such as the proximity of a polar group to the chain end, can enhance the hydrophilicity of the polymer chain and attract water molecules leading to a preferred hydrolysis of the terminal ester bonds. Van Nostrum et al. [6] studied the influence of different terminal groups on the hydrolytic degradation of oligolactides concluding that the mechanism and kinetics of degradation of these materials are strongly dependent on the nature of the chain end. Van Nostrum anticipated that, for high molecular weight polyesters, random chain scission initially dominates because of the small number of chain ends. However, once an ester bond is hydrolyzed via random chain scission, a shorter chain with a free hydroxyl end group is formed, which can be rapidly degraded via chain-end scission. Backbiting is reported to be more than 100 times faster than the random chain scission of hydroxyl terminated oligomers of polylactide.

As have been seen, the variation of the molecular weight is one of the most important factors influencing both the chain-scission kinetics and the diffusivity of water in the polymer, however, other parameters have to be taken into account. The auto-catalysis due to the accumulation of acidic degradation products is reported to be an important factor for the erosion of polylactide (PLA) and poly(lactide-co-glycolide) (PLGA). The devices of larger thickness are degraded more quickly because all the leachable oligomeric compounds formed within the matrix are not able to escape from it as soon as they become soluble [7]. The geometry of shaped bodies, the type of the chemical bond within the polymer backbone, the pH changes, that can be due to the degradation products, or the stresses applied during degradation could also affect the degradation rate. On the other hand, surface modifications, such as plasma treatment [8,9], are

gaining attention to modify the hydrophilic properties of the polymers altering the superficial properties (contact angle, wettability, roughness and surface tension) to accelerate or to slow down the degradation.

In the (co)polyesters, chemical composition, sequence structure and morphology (crystalline or amorphous domains in the copolymer), among other factors, have an impact on the degradation process. The glycolyl units are more hydrophilic than other units such as the caproyl and lactyl ones. However, all of the copolymers of glycolide display higher degradation rates than the corresponding homopolymers thanks to their higher amorphous character [10]. Amorphous regions are preferentially degraded because they are more accessible to water molecules [11]. This effect is more important than the hydrophilic character of the structural units and, for this reason, copolymers of lactide/glycolide, lactide/ ϵ -caprolactone or glycolide/ ϵ -caprolactone at 50:50 comonomer composition present the highest velocities of degradation [10,12]. The crystallinity fraction can be reduced to accelerate the degradation by means of adjusting the composition during the synthesis procedure or by shortening the crystallizable blocks with the increase of the randomness of the copolymers, that is, controlling their chain microstructure distribution.

Different distribution of sequences affects the copolymer properties and, as a consequence, copolymers having similar comonomer composition may differ dramatically in their behaviour. It has been reported that final properties of statistical copolymers, including solubility, resistance to physical aging, thermal and mechanical properties and biodegradability, are strongly dependent on chain microstructure [13,14]. Great efforts have been directed toward the study of the influence of chain microstructures on hydrolytic degradation; Dobrzynski et al. [15] and Hua et al. [16] worked with poly(glycolide-co- ϵ -caprolactone) and poly(L-lactide-co-trimethylene carbonate) copolymers, respectively, demonstrating that chain microstructure dramatically affects the hydrolysis degradation profile. In this context, it is remarkable that a regular drug release process is mainly obtained from highly randomized copolymers which undergo homogeneous degradation without rapid changes of randomness or composition. Degradation occurs preferentially in the amorphous zones whereas crystalline parts degraded much more slowly. Hence, random copolymers at

equal comonomers content are more amorphous than others with higher block unit's distribution, exhibiting the fastest degradation rate, and even, at certain copolymer compositions, maintaining the amorphous structure during degradation [17].

The objectives of this study were to elucidate the effects of the crystallization and the chain microstructure distribution on the biodegradation. For this purpose, three statistical poly(L-lactide-co- ϵ -caprolactone) having different capability to crystallize were selected. The hydrolytic degradation in phosphate-buffered saline was carried out at 37 °C for a period up to 14 weeks and the changes in water absorption, weight loss, crystallinity, phase structure, molecular weight, composition, randomness character and mechanical properties of the PLCL films were studied using differential scanning calorimetry (DSC), gel permeation chromatography (GPC), proton nuclear magnetic resonance spectroscopy (^1H NMR) and mechanical testing.

1.2.2. Materials and methods

Materials

In vitro degradation studies were done in phosphate buffer saline (PBS) (pH 7.2) supplied from Fluka Analytical (Sigma Aldrich). The statistical poly(L-lactide-co- ϵ -caprolactone), PLCL74b, PLCL74r and PLCL62r, were synthesized using L-lactide monomer (assay > 99.5 %), obtained from Purac Biochem (The Netherlands), and ϵ -caprolactone monomer (assay > 98 %), provided by Merck. Stannous octoate (assay 95 %) was the catalyst employed for the synthesis of the copolymer showing higher blocky character ($R \rightarrow 0$), PLCL74b. Bismuth (III) subsalicylate (99.9 % metals basis) was added to carry out the polymerization of the random ($R \rightarrow 1$) PLCLs, PLCL74r and PLCL62r. Both catalysts were supplied by Sigma Aldrich.

Table 1 summarizes the characterization data of the three PLCLs. The molecular weights (M_w) of each of the copolymers are ranging from 50.3 to 78.7 kg mol $^{-1}$ (and dispersity index (D) from 1.79 to 1.95) in such a way that the impact on their properties will be considered negligible in comparison to the effect of sequence length distribution

or copolymer composition. According to those results of Table 1, PLCL74b presents a slightly lower LA content (73.5 %) than PLCL74r (74.0 %). These are not considered large differences in composition so as to conduct the study in terms of LA block length distribution since l_{LA} is larger for PLCL74b ($l_{LA} = 8.16$) than PLCL74r ($l_{LA} = 4.01$). Finally, PLCL62r ($l_{LA} = 2.55$) exhibits similar randomness character to PLCL74r, both of them closest to the Bernoullian random distribution ($R \sim 1$), however PLCL62r has a different copolymer composition (62.2 % of lactide content) than PLCL74r.

Table 1. NMR characterization and GPC measurements of the three statistical PLCL copolymers studied in this work.

Sample	Composition ¹ (% molar)		M_w kg mol ⁻¹	D	Microstructural Magnitudes ¹		
	%LA	%CL			l_{LA}	l_{CL}	R
PLCL74b	73.5	26.5	50.3	1.95	8.16	2.95	0.46
PLCL74r	74.0	26.0	68.9	1.88	4.01	1.41	0.96
PLCL62r	62.2	37.8	78.7	1.79	2.55	1.55	1.04

¹ Calculated from ¹H NMR. l_{LA} and l_{CL} are the LA and CL number average sequence lengths. These values are compared to the Bernoullian random number-average sequence lengths ($l_A=1/B$), obtaining the randomness character value (R).

Methods

150-200 μm films were prepared by solvent-casting using chloroform (Panreac, Spain) as solvent. The solutions were transferred to square (10x10 cm^2) Teflon molds and dried for 48 h at room temperature and another 48 h at vacuum. In the case of PLCL74b, an additional treatment was employed to reduce the crystallinity of the sample. For this purpose, PLCL74b films obtained from solvent-casting were pressure melted at 175 $^\circ\text{C}$ for 2 minutes followed by water quenching. From these films samples for mechanical characterization (10cmx1cm) and for the *in vitro* degradation study (1x1 cm^2) were obtained.

For the *in vitro* degradation study, square samples of ~ 20 mg (W_0) ($n = 3$) were placed in Falcon tubes containing phosphate buffered saline (PBS) (pH = 7.2) and maintaining a surface area to volume ratio equal to 0.1 cm^{-1} . The samples were stored in an oven at

37 °C. At different periods of time, 3 samples of each polymer were removed from the PBS and weighed wet (W_w) immediately, after wiping the surface with a filter paper to adsorb the surface water. These samples were air-dried overnight and vacuum-dried for another 24 h. Then, they were weighed again to obtain the dry weight (W_d). Water absorption (% WA) and remaining weight (% RW) were calculated according to Eqs. (1) and (2):

$$\% \text{WA} = \frac{W_w - W_d}{W_d} \cdot 100 \quad (1)$$

$$\% \text{RW} = \frac{W_d}{W_0} \cdot 100 \quad (2)$$

In order to compare the degradation rate of the different PLCLs, the exponential relationship between molecular weight and degradation time for biodegradable polyesters degrading under bulk degradation was used [18]:

$$\ln M_w = \ln M_{w0} - K_{Mw} \cdot t \quad (3)$$

$$t_{1/2} = 1/K_{Mw} * \ln 2 \quad (4)$$

where M_w is the weight-averaged molecular weight, M_{w0} is the initial weight-averaged molecular weight, K_{Mw} is the apparent degradation rate and $t_{1/2}$ is the half degradation time (the amount of time required to fall to half the initial value of molecular weight).

The molecular weight of the samples was determined by GPC using a Waters 1515 GPC apparatus equipped with two Styragel columns ($10^2 - 10^4 \text{ \AA}$). Chloroform was used as an eluent at a flow rate of 1 mL min^{-1} and polystyrene standards (Shodex Standards, SM-105) were used to obtain a primary calibration curve. The samples were prepared at a concentration of 10 mg in 1 mL.

Proton nuclear magnetic resonance ($^1\text{H NMR}$) spectra were recorded in a Bruker Avance DPX 300 at 300.16 MHz of resonance frequency, using 5 mm O.D. sample tubes and following the experimental conditions described in previous works [14]. The signals of the lactide methine, centered at 5.15 ppm, and the signals of the α and ϵ

methylens of the ϵ -caprolactone, around 2.35 and 4.1 ppm, from the ^1H NMR spectrum (see Figure 4 below) can be assigned to the different dyads [19]. The copolymer composition and the microstructural magnitudes of the copolymers were obtained from the average dyad relative molar fractions. Equations 5-7 [20] were employed to obtain the number-average sequence lengths (l_i) of LA and CL building blocks, the Bernoullian random number-average sequence lengths (l_i) and the randomness character (R):

$$l_{\text{LA}} = \frac{2(\text{LA})}{(\text{LA} - \text{CL})} ; \quad l_{\text{CL}} = \frac{2(\text{CL})}{(\text{LA} - \text{CL})} \quad (5)$$

$$(l_{\text{LA}})_{\text{random}} = \frac{1}{(\text{CL})} ; \quad (l_{\text{CL}})_{\text{random}} = \frac{1}{(\text{LA})} \quad (6)$$

$$R = \frac{(l_{\text{LA}})_{\text{random}}}{l_{\text{LA}}} = \frac{(l_{\text{CL}})_{\text{random}}}{l_{\text{CL}}} = \frac{(\text{LA} - \text{CL})}{2(\text{LA})(\text{CL})} \quad (7)$$

where (LA) and (CL) are the two comonomer molar fractions, obtained from the integration of the lactide methine signals and the ϵ -caprolactone methylene signals, and (LA-CL) is the LA-CL average dyad relative molar fraction.

The thermal properties of the samples were determined on a DSC 2920 (TA Instruments) after being vacuum-dried. Samples of 5-10 mg were heated from $-85\text{ }^\circ\text{C}$ to $185\text{ }^\circ\text{C}$ at $20\text{ }^\circ\text{C min}^{-1}$. This first scan was used to determine the melting temperature (T_m) and the heat of fusion (ΔH_m) of the samples. The melting peaks are associated only to lactide crystals since the caprolactone segments are not large enough to crystallize. After this first scan, the samples were quenched in the DSC and a second scan was made from $-85\text{ }^\circ\text{C}$ to $185\text{ }^\circ\text{C}$ at $20\text{ }^\circ\text{C min}^{-1}$. In this second scan the glass transition temperatures (T_g) were determined from the inflection point of the heat flow curve.

The mechanical properties of the non-degraded samples and the samples submerged in PBS during 14 and 21 days were determined by tensile tests with an Instron 5565 testing machine at a crosshead displacement rate of 10 mm min^{-1} . These tests were performed at $21 \pm 2\text{ }^\circ\text{C}$ and $50 \pm 5\%$ relative humidity following ISO 527-3/1995. The mechanical properties reported correspond to average values of at least 5 determinations.

1.2.3. Results and discussion

Thermal analysis

Figure 1 shows the DSC curves of the first scans of samples of PLCL74b, PLCL74r and PLCL62r at different degradation times. The values of these thermograms are detailed in Table 2.

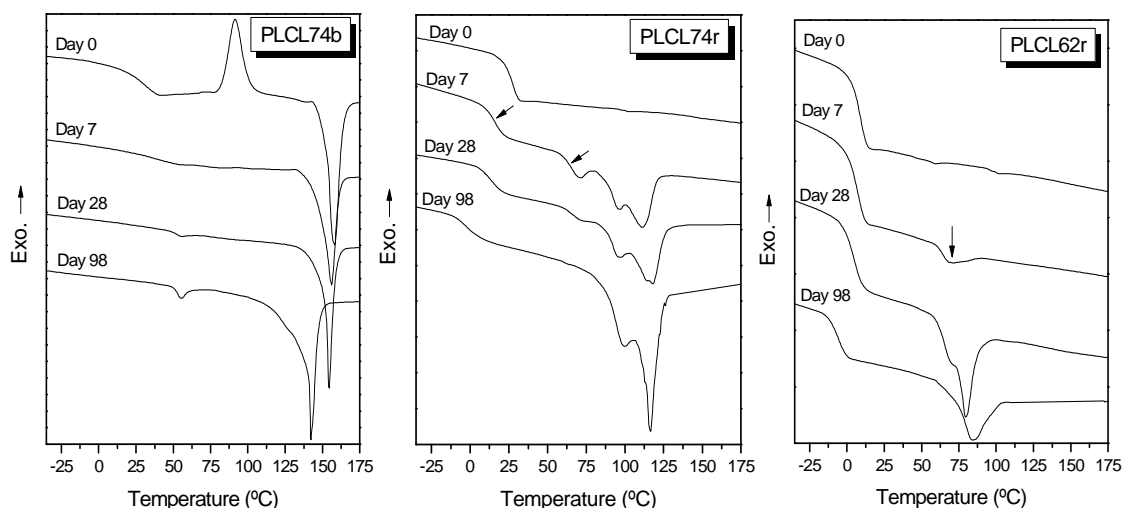


Figure 1. DSC curves of the first scans of PLCL74b, PLCL74r and PLCL62r at different degradation times.

Initially, PLCL74b displayed a heat of fusion of 11.6 J g^{-1} which is obtained by the difference between the melting (at $\sim 157 \text{ }^\circ\text{C}$) and cold crystallization (at $\sim 90 \text{ }^\circ\text{C}$) enthalpies. During the *in vitro* degradation process, PLCL74b tended to crystallize and the cold crystallization peak disappeared after just 3 days submerged in PBS. As a result, the melting enthalpy (ΔH_m) increased from the initial value of 11.6 to 51.0 J g^{-1} at the end of the experiment (day 98). The corresponding melting temperature (T_m) moved toward lower temperatures as the time submerged in PBS increased. As an illustration, T_m moved from $157.2 \text{ }^\circ\text{C}$ on day 0 to $142.1 \text{ }^\circ\text{C}$ on day 98. As the degradation occurs and the polymer chains become shorter, the chain mobility is favoured and, although the crystallinity rose, the created crystallites may become more disordered and imperfect, leading to a lower T_m . Regarding T_g behaviour, PLCL74b exhibited a single T_g which shifted to higher temperatures and became less defined (lower ΔC_p change at the glass transition because of the lower amorphous character) as

the degradation time increased. In this sense, the glass transition temperature shifted monotonously from 32.7 °C on day 0 to 53.1 °C on day 98. This can be attributed to the growing hindrance the polymer chains find to relax due to the presence of crystalline domains [21- 22]. In the last weeks of the experiments, a small enthalpy of relaxation appeared ($\sim 1 \text{ J g}^{-1}$) which reflected the presence of the glass transition more clearly.

PLCL74r was initially completely amorphous, showing a single T_g at 27.9 °C. However, a double T_g behaviour was clearly visible on day 7 and a melting peak appeared around 113 °C. As for PLCL74b, ΔH_m increased during the degradation process from 9.3 J g^{-1} , on day 3 to 33.7 J g^{-1} on day 98. This double T_g behaviour has been previously reported by our group [14]. The lower T_g should be associated to the hybrid amorphous miscible LA-CL phase, whereas the higher T_g suggests the presence of phase separated amorphous polylactide domains. As the time submerged in PBS increased, the lower T_g shifted to lower temperatures (from 17.1 °C on day 3 to -2.8 °C on day 98) because of the incorporation of some LA content of the LA-CL mixed phase to the polylactide crystalline domains. As this migration occurs, the hybrid amorphous miscible LA-CL became richer in CL and, as a result, the lower T_g took lower values. On the contrary, the higher T_g was maintained almost constant at ~ 65 °C. However, as the degradation time increased, it became less defined and on day 56 it was almost indistinguishable because of the lower amorphous character of the polymer.

PLCL62r presented a single T_g at 8.9 °C and no melting peak on day 0, indicating a completely amorphous character at the beginning of the experiment. However, after 7 days submerged in PBS a small melting peak appeared at 69.1 °C with its associated ΔH_m of 2.2 J g^{-1} . This value increased during the degradation process and it reached 10.9 J g^{-1} on day 98. In this case, a single T_g behaviour was observed during all the degradation process due to the homogenous distribution of LA and CL chains. Again, the T_g shifted to lower temperatures (from 7.1 °C on day 7 to -5.9 °C on day 98) because of the incorporation of LA of the LA-CL phase to the polylactide crystalline domains.

As it has been previously reported [14, 19], the PLCLs suffer a physical aging during its storage and try to reach the equilibrium through the slow rearrangement of the chains from a nonequilibrium glassy state. These rearrangements occur faster in an aqueous

medium thanks to the plastizing effect of water molecules [23] and the higher mobility of shorter chains produced during the hydrolytic scission. In this way, a quick increment in the crystallinity was observed in the studied materials resulting from the migration of lactide from the amorphous phases. Although PLCL74b and PLCL74r had a similar LA content, their physical aging process will be closely related to their LA block length distribution (l_{LA}) and a very different behaviour during the *in vitro* degradation process is expected. In this sense, the larger l_{LA} of PLCL74b (8.16 vs. 4.01) favoured the crystallization of lactide blocks in comparison with PLCL74r. On the contrary, the more amorphous PLCL62r showed the lowest l_{LA} (2.55) and the development of polylactide crystalline domains was inhibited.

Molecular weights evolution and degradation kinetics

Table 2. M_w , D and DSC results of the studied PLCLs at different times of degradation.

Sample	time (days)	M_w (kg mol ⁻¹)	D	1st Scan			2nd Scan
				T_{g1}/T_{g2} (°C)	T_m (°C)	ΔH_m (J g ⁻¹)	T_g (°C)
PLCL74b	0	50.3 ± 0.0	1.95	32.7	157.2	11.6	34.1
	3	44.6 ± 0.5	2.06	36.2	154.6	32.4	34.6
	7	40.6 ± 0.2	2.29	36.5	155.4	33.0	34.5
	14	37.7 ± 0.4	2.68	47.7	156.7	33.9	34.8
	21	32.0 ± 0.5	3.85	53.2	154.7	36.0	32.0
	28	27.8 ± 1.0	9.73	52.5	154.7	34.6	31.9
	42	19.7 ± 0.9	9.72	53.0	152.8	35.0	25.5
	56	14.0 ± 0.5	*	52.2	149.9	37.1	20.9
	77	9.6 ± 0.4	*	52.3	147.2	40.4	19.7
	98	8.1 ± 0.2	*	53.1	142.1	51.0	19.8
PLCL74r	0	68.9 ± 0.0	1.88	27.9	-	-	27.9
	3	63.1 ± 0.2	1.97	17.1/64.6	113.1	9.3	27.3
	7	54.7 ± 0.4	2.06	16.5/65.4	111.5	10.6	26.8
	14	40.4 ± 1.1	2.27	16.7/67.8	115.8	12.6	27.2
	21	32.8 ± 0.5	2.64	15.5/66.3	119.5	15.9	26.6
	28	25.9 ± 0.2	4.04	13.5/64.3	118.9	18.2	24.7
	42	15.3 ± 0.6	12.18	8.6/63.8	117.0	22.5	22.2
	56	11.1 ± 0.5	*	7.1	117.0	25.7	20.7
	77	8.4 ± 0.2	*	3.0	117.1	29.8	20.4
	98	8.1 ± 0.2	*	-2.8	117.9	33.7	18.9
PLCL62r	0	78.7 ± 0.0	1.88	8.9	-	-	8.9
	3	72.1 ± 1.2	2.08	7.9	-	-	9.4
	7	62.6 ± 0.0	2.10	7.1	69.1	2.2	9.5
	14	47.0 ± 0.7	2.72	5.1	69.0	5.1	10.0
	21	35.1 ± 0.8	7.66	4.6	69.1	4.3	8.6
	28	26.0 ± 0.8	16.68	4.7	79.3	10.1	7.6
	42	14.3 ± 0.2	*	2.4	79.6	10.5	6.4
	56	10.6 ± 0.5	*	0.4	78.2	9.7	3.5
	77	8.0 ± 0.5	*	-5.5	83.1	11.3	0.0
	98	7.1 ± 0.2	*	-5.9	83.8	10.9	-1.6

* Not measurable because of the uncertainty in the number-average molecular weight (M_n) measurements.

Table 2 summarizes the evolution of weight-average molecular weight (M_w), dispersity index (D) and DSC results during the *in vitro* degradation study. As the degradation occurs, the M_w of the samples decreased and the D increased, indicating a broader distribution of polymer chain length. In this sense, D increased from 1.95, 1.88 and 1.88 on day 0 for PLCL74b, PLCL74r and PLCL62r, respectively to 9.73, 4.04 and 16.68 on day 28. The reduction in molecular weight leads to a decrease in molecular entanglement and an increase in chain mobility that affected directly the observed glass transition temperature in the second DSC scan [24]. As an illustration, T_g dropped from the initial value of 34.1, 27.9 and 8.9 °C for PLCL74b, PLCL74r and PLCL62r, respectively to 19.8, 18.9 and -1.6 °C at the end of the study (day 98).

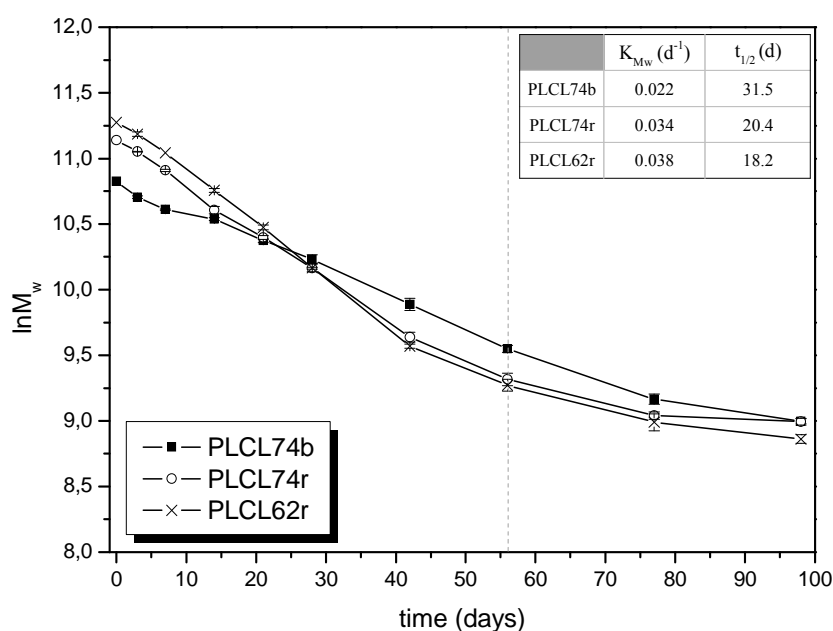


Figure 2. $\ln M_w$ vs. degradation time of the studied PLCLs.

Figure 2 shows the progress of $\ln M_w$ versus degradation time. The values of K_{M_w} and $t_{1/2}$ were calculated from the slope of the fitting curve during the first 56 days of study ($R^2 > 0.99$). Obtained K_{M_w} for PLCL74b, PLCL74r and PLCL62r were respectively, 0.022, 0.034 and 0.038 days⁻¹ with corresponding $t_{1/2}$ of 31.5, 20.4 and 18.2 days. It must be stated that extending the fitting of the curve beyond 56 days, the correlation coefficient gradually decreased and the values of M_w obtained from the fitting curve deviated from the experimental data. This fact indicates that the degradation mechanism

is changing from one dominated by bulk degradation to another controlled by surface erosion [25]. Random chain scission dominates at early stages of degradation leading to a higher molecular weight decrease than in later stages, when backbiting is the dominant mechanism. Finally, the oligomers and byproducts of low molecular weight are transported by diffusion and released to the outside medium

Although PLCL74b and PLCL74r had a similar composition, LA block length distribution (l_{LA}) played a pivotal role in the degradation rate of these two materials. As previously mentioned, PLCL74b presented a larger l_{LA} that favours the crystallization of lactide sequence blocks with regard to PLCL74r. In the crystalline domains, the polymer chains are more packed and water finds more difficulties to penetrate. Thus, the crystalline domains are more resistant to degradation than the amorphous regions and, for this reason, the blocky PLCL74b presented the slowest degradation rate. Although PLCL62r is richer in CL, which displays higher resistance to hydrolysis because of its more hydrophobic character [26], and had a higher initial molecular weight, it presented the fastest degradation rate owing to its more amorphous nature. Thus, this study confirms the importance of chain microstructure and crystallization capability on degradation rates of PLCL copolymers.

Previous studies calculated K_{Mw} values for PLCL copolymers. As an illustration, Larrañaga et al. [27] reported a value of 0.017 days^{-1} for a PLCL film of 70 % LA content, a l_{LA} of 3.45 and a $R = 0.92$. Although the l_{LA} is shorter in this copolymer than in PLCL74b and PLCL74r studied here, its degradation rate is slower. This difference may be due to the higher molecular weight of the copolymer specimen compared with those in the present study ($193.0 \text{ kg mol}^{-1}$ versus 50.3 kg mol^{-1} and 68.9 kg mol^{-1}). As mentioned in the introduction, in high molecular weight polyesters, random chain scission is the dominating degradation mechanism, which is a slower mechanism than chain-end scission one. This is why, higher molecular weight polyesters show slower degradation rates. In another study, Malin et al. [24] reported a K_{Mw} of 0.032 days^{-1} for a PLCL copolymer of 61 % LA molar content and $145.0 \text{ kg mol}^{-1}$ of weight-average molecular weight. In this case, the slower degradation rate of the copolymer specimen compared with PLCL62r may be attributable to the blockier character ($R = 0.68$ and $l_{CL} = 2.40$ vs $R = 1.04$ and $l_{CL} = 1.55$ of PLCL62r) and the higher molecular weight of the

PLCL used in their study. These two examples manifest the difficulty in comparing different *in vitro* degradation studies because of the high number of factors that affect the degradation rate of the same material (initial molecular weight, sample size, etc.).

Weight loss and water absorption

Figure 3 shows remaining weight and water absorption curves of PLCL74b, PLCL74r and PLCL62r during *in vitro* degradation study. Obtained results are in accordance with the trend observed above in the molecular weight discussion, presenting the following order in degradation rate from the fastest to the slowest: PLCL62r > PLCL74r > PLCL74b. The degradation of crystalline domains proceeds much more slowly and, as consequence, in highly crystalline polymers the mass loss is impeded. PLCL74b displays the greatest crystallization capacity and its weight loss was almost negligible during the first 77 days of the study. Then, it suffered a very slight loss of material and its remaining weight on day 98 was 81.5 %. PLCL74r maintained its initial weight until day 42, when it started to drop taking a value of 68.7 % at the end of the study. Remaining weight of PLCL62r was maintained constant (~ 99 %) during the first 14 days and then it began to decrease, reaching a value of 19.4 % on day 98. It has to be pointed out that, as the degradation occurred, PLCL62r became sticky and difficult to manipulate. As a consequence, the calculated remaining weights for the last days of the experiment presented high standard deviations and thus, these data has to be interpreted prudently. According to the literature, the molecular weight of the polyesters has to be reduced substantially to permit mass loss through solubilisation of the oligomers. That is why, the weight of the samples remained constant during the first weeks of the study and, once the molecular weight reached a critical value, they started to loss mass.

Water absorption of both PLCL74b and PLCL74r showed a similar tendency. It was maintained almost constant (being slightly higher in the case of PLCL74r) until day 28, when it suffered a sharp increase reaching a value of ~ 25 % at the end of the study. On the contrary, PLCL62r presented a continuous rise and reached a value of 24 % in just 28 days. From this point, the water absorption was not measurable for PLCL62r because the samples were viscous and difficult to manipulate. It is remarkable to take into

account that PLCL62r exhibits the highest water absorption capacity, despite being richest in CL, which is known to have a more hydrophobic character than LA [26]. However, thanks to its shorter l_{LA} , PLCL62r presents a more amorphous nature than PLCL74r and PLCL74b. The chains are less packed in the amorphous regions than in crystalline domains and, in consequence, the water has the ability to penetrate these regions more easily.

Finally, it is also noteworthy to mention that in crystallisable polymers at advanced stages of degradation, highly resistant crystalline remnants are formed. The presence of these remnants, more abundant in PLCL74b, apart from hindering the weight loss process and the water uptake, could cause foreign body reactions and limit the application of these biopolymers for some medical applications.

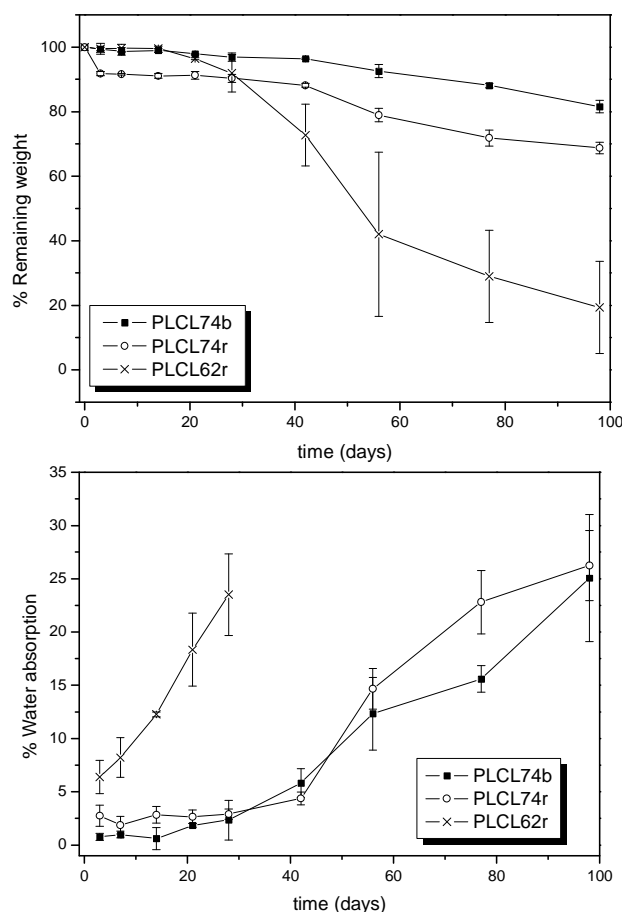


Figure 3. Evolution of the remaining weight and water absorption of the PLCLs during the *in vitro* degradation.

NMR analysis of the copolymers at different times

Table 3 presents the evolution during degradation of LA content, LA average sequence block and randomness character of the three PLCL copolymers. As can be seen, all these parameters were slightly altered during the course of the degradation process. PLCL74b, the most significantly affected material, and PLCL74r suffered minor changes in their composition and microstructural parameters from day 77 of degradation, which are associated to the beginning of weight loss in these materials. PLCL74b registered an increase in LA content from 73.5 to 78.7 % and a drop of its randomness character from 0.46 to 0.43 during the 98 days of the study and, as a result, its LA unit's average sequence block rose from 8.16 to 11.05. This faster degradation of CL than LA can be explained by the fact that amorphous regions composed of mainly CL moieties degrade earlier than hard domains where most of LA units are located [28]. PLCL74b exhibits the blockiest distribution of sequences, so that LA-rich hard domains and soft CL-rich building blocks were larger than in the other copolymers and, when it starts to lose weight, amorphous CL-rich fragments of polymer are released. On the contrary, the highly amorphous randomized PLCL62r did not undergo changes during the time submerged in PBS and the degradation was more homogeneous in such a way that the chain distribution of sequences was unaltered.

Table 3. Molar composition and microstructural parameters of the PLCLs at different times of degradation.

Sample	time (days)	% LA	l_{LA}	R
PLCL74b	0	73.5	8.16	0.46
	7	74.2	8.70	0.45
	14	74.4	8.66	0.45
	28	74.7	8.81	0.45
	42	74.7	8.66	0.46
	77	75.2	9.52	0.42
	98	78.7	11.05	0.43
PLCL74r	0	74.0	4.01	0.96
	7	75.8	4.30	0.96
	14	74.8	4.08	0.97
	28	75.2	4.18	0.96
	42	75.1	4.18	0.96
	77	76.7	4.47	0.96
	98	76.8	4.44	0.97
PLCL62r	0	62.2	2.55	1.04
	7	62.2	2.53	1.05
	14	62.1	2.51	1.05
	28	62.1	2.48	1.06
	42	61.9	2.49	1.05
	56	60.3	2.38	1.06

As the degradation progresses, new signals appeared at the ^1H NMR spectra of the PLCLs. In addition to the lactide methine and the caprolactone methylenes signals, small peaks, linked to the terminal groups of the degradation byproducts, are found. As an illustration, Figure 4 shows the spectrum of the PLCL74b on day 77, where the quadruplet at 4.35 ppm and the triplet at 3.65 ppm could be assigned to $-\text{CHOH}$ and $-\text{CH}_2\text{OH}$ terminal groups.

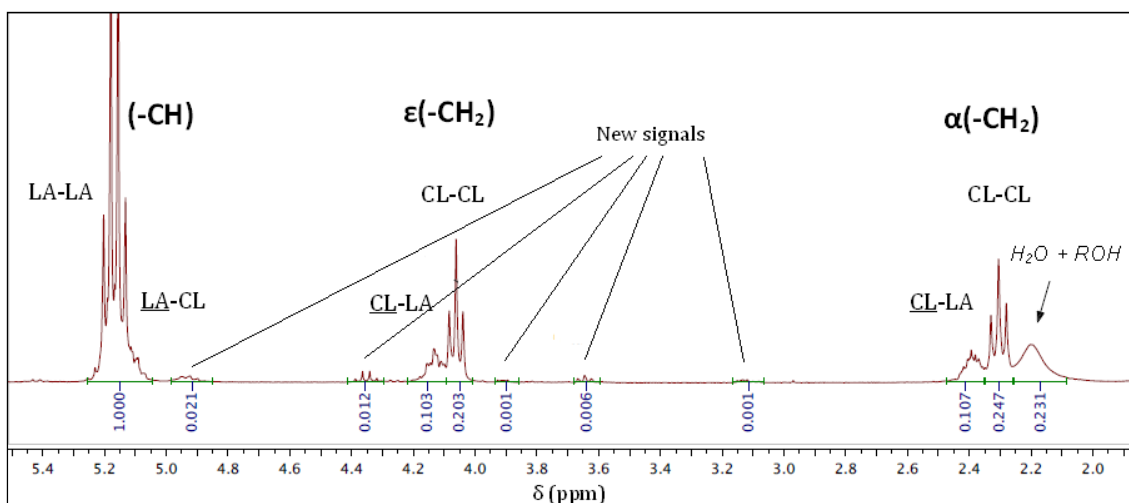


Figure 4. ^1H NMR spectrum of PLCL74b on day 77 of degradation.

Mechanical properties

In the present study mechanical testing of PLCL samples submerged in PBS during different times (14 and 21 days) were intended to perform. Nevertheless, as a consequence of the degradation process, PLCL74b and PLCL74r were too brittle due to the elevated crystallization of polylactide domains, whereas PLCL62r became sticky and impossible to manipulate. Table 4 summarizes the mechanical properties of the non-degraded copolymer films and the PLCL74r on day 14, the only tests that could be completed. Figure 5 shows some typical strain-stress curves of these assays.

As it can be observed, the three materials displayed a completely different mechanical performance. Blocky PLCL74b ($l_{\text{LA}} = 8.16$ and $R = 0.46$), regardless its equal copolymer composition to PLCL74r, showed a partly glassy semicrystalline behaviour having a secant modulus of 310.1MPa and presenting a yield point at 4.9 %, that did not

appear in the other two PLCLs. In contrast, random PLCL74r ($l_{LA} = 4.01$ and $R = 0.96$) and PLCL62r ($l_{LA} = 2.55$ and $R = 1.04$), were elastomeric or highly elastomeric thermoplastics, with secant modulus values of 19.3MPa and 2.7MPa, offset yield strengths of 0.80 MPa and 0.25MPa, ultimate stress values of 3.2 MPa and 0.37 MPa and elongation at break of 325 % and > 1400 %, respectively. It is noteworthy the great effect of CL content, which is 26 % for PLCL74r and 38 % for PLCL62r, on the deformation at break, when both copolymers have similar randomness character. This fact could be explicated by the higher amorphous structure of the CL-richest PLCL. At a critical average sequence LA unit's block, the contribution of these hard domains on the stiffness of the material decreases substantially.

Table 4. Mechanical properties data of the PLCL74b, PLCL74r and PLCL62r.

Sample		Secant Modulus at 2 %	Yield Strength or Offset Yield Strength at 10 % ¹	Tensile Strength ²	Elongation at Break
		(MPa)	(MPa)	(MPa)	(%)
PLCL74b	Non-degraded	310.1 ± 6.1	7.9 ± 0.3	9.0 ± 0.8	163
PLCL74r	Non-degraded	19.4 ± 1.3	0.80 ± 0.02	3.2 ± 0.6	325
	After 2 weeks	134.9 ± 16.0	9.9 ± 0.1	10.3 ± 0.1	121
PLCL62r	Non-degraded	2.73 ± 0.2	0.25 ± 0.02	0.37 ± 0.02	> 1400

¹Yield Strength was calculated for PLCL74b. Offset Yield Strength was calculated for PLCL74r and PLCL62r at a 10 % of strain using the secant modulus at 2 % as elastic modulus (E).

²The tensile strength was determined as ultimate stress value (σ_u).

In the first two weeks of the study, a melting peak of 12.6 J g⁻¹, related to LA crystallizable blocks, become visible in the initially fully amorphous PLCL74r. This crystallization process was reflected on its mechanical properties and its elastomeric behaviour shifted to a slightly glassy one; 133.9 MPa of secant modulus, 9.9 MPa of offset yield strength, 10.3 MPa of tensile strength and 121 % of elongation at break. The strength related values are considerably higher than the corresponding values of the non-degraded PLCL74r and even higher than the PLCL74b ones. One week later, on day 21, the test samples of PLCL74r were unworkable owing to its brittleness. This phenomenon, very typical of semicrystalline polymers such as poly(L-lactide) or

polyglycolide at advanced states of decomposition, was magnified in the PLCL74b and, in consequence, it was not able to carry out mechanical testing neither on day 14. The deterioration of the mechanical properties during degradation causes the fragmentation of the samples in crystallites that are unwanted and limit the uses of these biomaterials in some applications. On the other hand, a material based on PLCL62r will require more consistency for devices with the necessity of mechanical support.

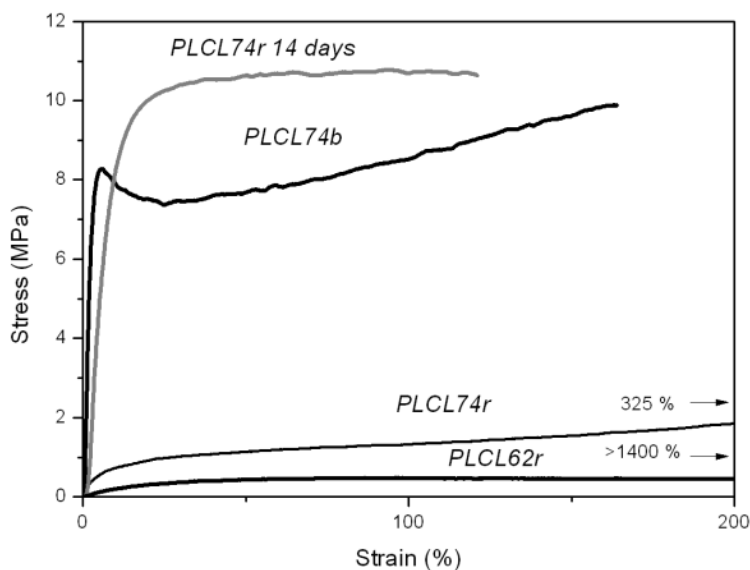


Figure 5. Strain-stress typical curves of the PLCL74b, PLCL74r and PLCL62r.

1.2.4. Conclusions

In this study the influence on the degradation behaviour of the chain microstructure features and the crystallization capability of various statistical PLCLs has been highlighted. Two of the studied PLCLs (PLCL74b and PLCL74r), despite having similar composition, displayed completely different performance during the course of degradation due to their different randomness character ($R = 0.46$ vs 0.96). Blocky PLCL74b with a lactide unit average sequence length (l_{LA}) of 8.16 was very prone to crystallize and reached a value of $\Delta H_m = 51.0 \text{ J g}^{-1}$ on day 98, whereas random PLCL74r with $l_{LA} = 4.01$ presented a $\Delta H_m = 33.7 \text{ J g}^{-1}$ at the same day. This fact had a direct effect in the degradation rate of the polymers. PLCL74b exhibited the slowest degradation rate, which is attributable to the higher resistance of crystalline domains,

with a $K_{Mw} = 0.022 \text{ d}^{-1}$ and a remaining weight of 81.5 % at the end of the experiment. This demonstrates that, although PLCL74b had a higher initial molecular weight, the randomness character has a greater effect on the degradation of the studied PLCLs. On the other hand, random PLCL62r ($I_{LA} = 2.55$), despite being richer in ϵ -CL (more hydrophobic character than LA), presented the fastest degradation rate with a $K_{Mw} = 0.038 \text{ d}^{-1}$ and a remaining weight of 19.4 %, proving that the amorphous character is a decisive factor in the degradation of the statistical copolyesters.

The LA content and I_{LA} and R parameters of the three PLCL copolymers were slightly modified during the course of the degradation process. PLCL74b was the most significantly affected material and suffered minor changes in their composition and microstructural parameters from day 77 of degradation. These changes are associated to the beginning of weight loss in these materials, when amorphous CL-rich fragments of polymer are released. In contrast, the highly amorphous randomized PLCL62r did not undergo changes during the time submerged in PBS and the degradation was more homogeneous in such a way that the chain distribution of sequences was unaltered.

Regarding the mechanical properties, PLCL74b showed initially a partly glassy semicrystalline behaviour having a secant modulus of 310.1MPa and presenting a yield point at 4.9 %. However, it became very brittle as a consequence of the high crystallinity and, on day 14, was not able to manipulate. Random PLCL74r shifted from an initial elastomeric behaviour to a slightly glassy one on day 14, with an increase in the strength related properties and a sharp decrease in the elongation at break (from 325 to 121 %). Finally, PLCL62r presented a highly elastomeric behaviour but became too sticky and its properties were not measurable during the course of degradation.

From this study it can be concluded that the development of crystalline domains is an unwanted factor during the degradation process of these statistical copolyesters. As it has been demonstrated, the presence of crystalline domains slows down dramatically the hydrolytic degradation of the polymers and causes a deterioration of the mechanical properties. Moreover, the presence of highly crystalline remnants could cause foreign body reactions and limit the application of these biopolymers for some medical applications.

References

- [1] Göpferich, A. Mechanism of polymer degradation and erosion. *Biomaterials* 1996, 17, 103-114.
- [2] von Burkersroda, F.; Schedl, L.; Göpferich, A. Why degradable polymers undergo surface erosion or bulk erosion. *Biomaterials* 2002, 23, 4221-4231.
- [3] Engineer, C.; Parikh, J.; Raval, A. Review on Hydrolytic Degradation Behavior of Biodegradable Polymers from Controlled Drug Delivery System. *Trends in Biomaterials and Artificial Organs* 2011, 25, 79-85.
- [4] Hofmann, D.; Entrialgo-Castaño, M.; Kratz, K.; Lendlein, A. Knowledge-Based Approach towards Hydrolytic Degradation of Polymer-Based Biomaterials. *Advanced Materials* 2009, 21, 3237-3245
- [5] Kulkarni, A.; Reiche, J.; Lendlein, A. Hydrolytic degradation of poly(rac-lactide) and poly[(rac-lactide)-co-glycolide] at the air water interface. *Surface and Interface Analysis* 2007, 39, 740-746.
- [6] van Nostrum, C.F.; Veldhuis, T.F.J.; Bos, G.W.; Hennink, W.E. Hydrolytic degradation of oligo(lactid acid): a kinetic and mechanistic study. *Polymer* 2004, 45, 6779-6787.
- [7] Grizzi, I.; Garreau, H.; Li, S.; Vert, M. Hydrolytic degradation of devices based on poly(DL-lactic acid) size-dependence. *Biomaterials* 1995, 16, 305-311.
- [8] Żenkiewicz, M.; Rytlewski, P.; Malinowski, R. Compositional, physical and chemical modification of polylactide. *Journal of Achievements in Materials and Manufacturing Engineering* 2010, 43, 192-199.
- [9] Wang, S.; Cui, W.; Bei, J. Bulk and surface modifications of polylactide. *Analytical and Bioanalytical chemistry* 2005, 381, 547-556.
- [10] Vert, M.; Li, S.; Garreau, H. More about the degradation of LA/GA derived matrices in aqueous media. *Journal of Controlled Release* 1991, 16, 15-26
- [11] Albertsson, A.C.; Eklund, M. Influence of molecular structure on the degradation mechanism of degradable polymers: In vitro degradation of poly(trimethylene carbonate), poly(trimethylene carbonate-co-caprolactone) and poly(adipic anhydride). *Journal of Applied Polymer Science* 1995, 57, 87-103.
- [12] Karperczyk, J.; Li, S.; Jaworskam, J.; Dobrynski, P.; Vert, M. Degradation of copolymers obtained by ring-opening polymerization of glycolide and ϵ -caprolactone: A high resolution NMR and ESI-MS study. *Polymer Degradation and Stability* 2008, 93, 990-999.
- [13] Lee, S.C.; Kim, K.J.; Kang, S.W.; Kim, C. Microstructural analysis and structure-property relationship of poly(glycolide-co-1,3-trimethylene carbonate). *Polymer* 2005, 46, 7953-7960.

- [14] Fernández, J.; Etxeberria, A.; Ugartemendia, J.M.; Petisco, S.; Sarasua, J.R. Effects of chain microstructures on mechanical behaviour and aging of poly(L-lactide-co- ϵ -caprolactone) biomedical thermoplastic elastomer. *Journal of Mechanical Behavior of Biomedical Materials* 2012, 12, 29-38.
- [15] Dobrzynski, P.; Li, S.; Kasperczyk, J.; Bero, M.; Gasc, F., Vert, M. Structure-property relationships of copolymers obtained by ringopening polymerization of glycolide and ϵ -caprolactone. Part 1. Synthesis and characterization. *Biomacromolecules* 2005, 6, 483-488.
- [16] Hua, J.; Gebarowska, K.; Dobrzynski, P.; Kasperczyk, J.; Wei, J.; Li, S. Influence of chain microstructure on the hydrolytic degradation of copolymers from 1,3-trimethylene carbonate and L-lactide. *Journal of Polymer Science: Part A: Polymer Chemistry* 2009, 47, 3869-3879.
- [17] Jelonek, K.; Kasperczyk, J.; Dobrzynski, P.; Jarzabek, B. Controlled poly(L-lactide-co-trimethylene carbonate) delivery system of cyclosporine A and rapamycine- the effect of copolymer chain microstructure on drug release rate. *International Journal of Pharmaceutics* 2011, 414, 203-209.
- [18] Wu, L.; Ding, J. Effects of porosity and pore size on in vitro degradation of three-dimensional porous poly(D,L-lactide-co-glycolide) scaffolds for tissue engineering. *Journal of Biomedical Materials Research* 2005, 75, 767-777.
- [19] Fernández, J.; Etxeberria, A.; Sarasua, J.R. Synthesis, structure and properties of poly(L-lactide-co- ϵ -caprolactone) statistical copolymers. *Journal of the Mechanical Behavior of Biomedical Materials* 2012, 9, 100-112.
- [20] Herbert, I.R. Statistical analysis of copolymer sequence distribution. In *NMR Spectroscopy of Polymers*. Ibbet, R.N. Ed.: Blackie Academic & Professional, London, 1993:50-79. (Chapter 2).
- [21] del Río, J.; Etxeberria, A.; López-Rodríguez, N.; Lizundia, E.; Sarasua, J.R. A PALS Contribution to the Supramolecular Structure of Poly(L-lactide). *Macromolecules* 2010, 43, 4698-4707.
- [22] Sarasua, J.R.; Zuza, E.; Imaz, N.; Meaurio, E. Crystallinity and Crystalline Confinement of the Amorphous Phase in Poly lactides. *Macromolecular Symposia* 2008, 272, 81-86.
- [23] Saha, S.K.; Tsuji, H. Enhanced crystallization of poly(L-lactide-co- ϵ -caprolactone) in the presence of water. *Journal of Applied Polymer Science* 2009, 112, 715-720.
- [24] Malin, M.; Hiljanen-Vainio, M.; Karjalainen, T.; Seppälä, J. Biodegradable Lactone Copolymers. II. Hydrolytic Study of ϵ -caprolactone and Lactide Copolymers. *Journal of Applied polymer science* 1996, 59, 1289-1298.

- [25] Yoshioka, T.; Kawazoe, N.; Tateishi, T.; Chen, G. In vitro evaluation of biodegradation of poly(lactic-co-glycolic acid) sponges. *Biomaterials* 2008, 29, 3438-3443.
- [26] Qian, H.; Bei, J.; Wang, S. Synthesis, characterization and degradation of ABA block copolymer of L-lactide and ϵ -caprolactone. *Polymer degradation and Stability* 2000, 68, 423-429.
- [27] Larrañaga, A.; Sarasua, J.R. In vitro degradation of lactide based polymers and copolymers. *Annual Technical Conference-Society of Plastics Engineers* 2011, 3, 1989-1993.
- [28] Jeong, S.I.; Kim, B.S.; Kang, S.W.; Kwon, J.H.; Lee, Y.M.; Kim, S.H.; Kim, Y.H. In vivo biocompatibility and degradation behavior of elastic poly(l-lactide-co- ϵ -caprolactone) scaffolds. *Biomaterials* 2004, 25, 5939-5946.

**Chapter 1.3 A New Generation of
Lactide-co- ϵ -Caprolactone
Copolymers for Application in the
Medical Field**

Journal of Biomedical Materials Research A 2014, 102A, 3573-3584.

Abstract

Thermoplastic biodegradable polymers displaying an elastomeric behaviour are greatly valued for the regeneration of soft tissues and for various medical devices. In this work, terpolymers composed of ϵ -caprolactone (CL), D-lactide (D-LA) and L-lactide (L-LA) were synthesized. These poly(lactide- ϵ -caprolactone) (PLCLs) presented an elevated randomness character ($R \sim 1$), glass transition temperatures (T_g) higher than 20 °C and adjusted L-LA content. In this way, the L-LA average sequence length (l_{L-LA}) was reduced to below 3.62 and showed little or no crystallization capability during *in vitro* degradation. As a result, the obtained materials underwent homogenous degradation exhibiting K_{Mw} ranging from 0.030 to 0.066 d⁻¹ and without generation of crystalline remnants in advanced stages of degradation. Mechanical performance was maintained over a period of 21 days for a rac-lactide- ϵ -caprolactone copolymer composed of ~ 85 % D,L-LA and ~ 15 % CL and also for a terpolymer composed of ~ 72 % L-LA, ~ 12 % D-LA and ~ 16 % CL. Terpolymers having L-LA content from ~ 60 to 70 % and CL content from ~ 10 to 27 % were also studied. In view of the results, those materials having CL and D-LA units disrupting the microstructural arrangement of the L-LA crystallizable chains, an L-LA content < 72 % and a random distribution of sequences, may display proper and tunable mechanical behaviour and degradation performance for a large number of medical applications. Those with a CL content from 15 to 30 % will fulfill the demand of elastomeric materials of T_g higher than 20 °C whereas those with a CL content from 5 to 15 % might be applied as ductile stiff materials.

1.3.1. Introduction

There is a growing demand, in the biomedical field particularly, for the regeneration of soft tissues and for various clinical implants and devices, of highly flexible and deformable materials having degradability and mechanical behaviour that, during their use, are predictable. Some applications in which an elastomeric character is desirable include cardiac tissue engineering applications, where the biomaterials should have enough flexibility to respond synchronically with the myocardium contraction and to effectively transfer the mechanical stimulus from the myocardial microenvironment to the incorporated cells [1]. Also in the cardiovascular system, the supports used as vascular grafts must present similar mechanical behaviour to that of the damaged artery to be replaced (elongation at break of $\sim 125\%$ and ultimate tensile strength of ~ 1 MPa [2]). Biodegradable thermoplastic elastomers (TPEs) are also gaining interest in the regeneration of muscles, tendons or ligaments thanks to their shape recovery capacity. This property permits a dynamic cell culture with mechanical stimulation which promotes cell proliferation, extracellular matrix production, gene expression, etc. [3]. By contrast, in non-elastomeric materials (poly(L-lactide), poly(DL-lactide/glycolide), etc.), this mechanical stimulus could cause an undesired permanent deformation. Additionally, in urothelium tissue engineering applications, the use of TPEs for the restoration of damaged urethra is also being considered as an alternative to the more traditional possibilities such as the use of the patient's own genital tissue or the use of the buccal mucosal grafts [4]. Finally, other potential applications of these biodegradable polymers found in the literature include stents for the treatment of esophageal stenosis [5] and nerve conduct guides for the repair of nerve defects [6,7].

Although the initial properties of poly(lactide- ϵ -caprolactone) polymers (PLCLs) can be appropriate for the above mentioned medical applications, these polymers present several problems that could be overcome by proper macromolecular design. The crystallization capability of the commonly used PLCLs can be found to be higher than expected when there is a miscalculation of the crystallizable L-lactide(L-LA) or D-lactide (D-LA) content, or also because of an underestimation of the impact that

microstructural chain features can have on supramolecular arrangements. Hence, most of the poly(L-lactide/ ϵ -caprolactone) (L-PLCL) [8] or poly(D-lactide- ϵ -caprolactone) (D-PLCL) copolymers are prone to undergo supramolecular rearrangements of their chains associated to the development of lactide crystalline domains, leading to unwanted changes in their properties [9-11]. These rearrangements occur faster in an aqueous medium due to the plasticizing effect of water molecules and the higher mobility of shorter chains produced during the hydrolytic scission [9, 12]. Therefore, a quick increase in the crystallinity resulting from the migration of lactide chains from the amorphous phases was observed in a previous work, where some statistical poly(L-lactide- ϵ -caprolactone) of different chain microstructure distribution and different capability to crystallize were degraded *in vitro* at 37 °C [13]. The presence of crystalline domains was demonstrated to be an undesired factor during the degradation process because it dramatically slows down the hydrolytic degradation rate which inhibits the homogeneous degradation of the biomaterial and causes greater deterioration in the mechanical properties. In addition, highly resistant crystalline remnants of low molecular weight are formed. These residues can trigger foreign body reactions and remain in the human body for years [14] once the biomaterial has lost its properties and has fulfilled its function.

Shortening the crystallizable L-LA or D-LA average sequence length, by means of reducing the LA content or by synthesizing polymers with a more random distribution of sequences [15-18], might be an appealing solution. However, decreasing the LA content too much in the L-PLCL or D-PLCL copolymers considerably reduces their mechanical performance. Thus, the random ($R \sim 1$) L-PLCL of 62 % L-LA molar content ($I_{L-LA} = 2.55$) of our previous study [13], while presenting a faster degradation rate than that of the 74 % L-LA random copolymer, nevertheless shows a glass transition temperature (T_g) at 8.9 °C which turns it into a sticky material difficult to handle.

Poly(D,L-lactide) (PDLLA), an amorphous polymer obtained from rac-lactide (50:50 mix of L-LA and D-LA), displays high elastic modulus (1.9 GPa) and rather low strain at break values (3-10 %) despite presenting lower tensile strength than poly(L-lactide) (PLLA) [19]. Nevertheless, the T_g (55-60 °C) is lower than that of the PLLA (60-65 °C)

and its degradation time is much shorter. Consequently, poly(D,L-lactide-co- ϵ -caprolactone) (D,L-PLCL or rac-PLCL) copolymers are an attractive alternative to L- and D-PLCLs because of the inability to arrange into a crystalline organized structure of both enantiomeric forms of LA. However, because this strategy will result in a copolymer having lower stereoregularity, it is necessary to raise the D,L-LA content in order to achieve PLCL copolymers that display similar thermal properties and mechanical strength as those of the L and D-PLCLs counterparts. On the other hand, it should be pointed out that controlling the repeat unit sequence distribution in chain microstructure, and developing random copolymers ($R \rightarrow 1$) with improved properties, is as yet an underutilized tool to tailor the copolymer properties [11, 20-25].

In this work, with the goal of forming reliable and stable medical polymeric biomaterials, several PLCLs exhibiting a better performance than the commercial ones and those reported in other papers [10, 26-28] were synthesized. They are statistical PLCLs with a high randomness character ($R \sim 1$) (Bernoullian copolymers) composed of L-LA and CL, in which D-LA is added, on the one hand, to replace CL, increasing the consistency and the stress related properties (elastic modulus and strength) and, on the other hand, substituting L-LA decreases its crystallization capability and enlarges the amorphous character of the polymer. These terpolymers, presenting very little or no crystallization capability, were characterized by proton nuclear magnetic resonance spectroscopy (^1H NMR) and gel permeation chromatography (GPC) measurements. Films of the PLCL polymers were prepared for mechanical testing at room temperature (21 ± 2 °C) and a hydrolytic degradation study in phosphate-buffered saline at 37 °C was carried out over 14 weeks. The changes in water absorption, weight loss, crystallinity, phase structure, molecular weight and mechanical properties of the PLCL films were studied using differential scanning calorimetry (DSC), gel permeation chromatography (GPC) and mechanical testing.

1.3.2. Materials and methods

Materials

Statistical poly(lactide-co- ϵ -caprolactone) (PLCL) terpolymers of different L-lactide, D-lactide and ϵ -caprolactone content were synthesized following the procedure described in a previous work [15]. L-lactide and D,L-lactide monomers (assay > 99.5 %) were supplied from Purac Biochem (The Netherlands) while ϵ -caprolactone monomer (assay > 98 %) was provided by Merck. Bismuth (III) subsalicylate (BiSS) (99.9 % metals basis) catalyst was supplied by Sigma Aldrich. *In vitro* degradation studies were carried out in phosphate buffer saline (PBS) (pH 7.2) obtained from Fluka Analytical (Sigma Aldrich).

Methods

Ring-opening polymerizations (ROP) were conducted in bulk by a one pot-one-step procedure. The synthesis reactions using BiSS as catalyst (1500:1 comonomers: catalyst molar ratio) were conducted for 48 hours (at 140 °C) or for 72 hours (at 130 °C). The products were dissolved in chloroform and precipitated pouring the polymer solution into excess of methanol in order to remove the catalyst impurities and those monomers that did not react.

150-200 μm films were prepared by solvent-casting using chloroform (Panreac, Spain) as solvent. The solutions were transferred to square (10x10 cm^2) Teflon molds and dried for 2 weeks at room temperature. Then, the PLCL films were heated to 180 °C for 1.5 minutes followed by ice-water quenching in order to remove the chloroform traces and to erase the previous processing history. From these films, repetitive samples for mechanical characterization (10cmx1cm) and for the *in vitro* degradation study (1x1 cm^2) were obtained.

Proton nuclear magnetic resonance (^1H NMR) spectra were recorded in a Bruker Avance DPX 300 at 300.16 MHz of resonance frequency, respectively, using 5 mm O.D. sample tubes and following the experimental conditions described in previous works [11]. The signals of the lactide methine, centered at 5.15 ppm and the signals of

the α and ϵ methylenes of the ϵ -caprolactone, around 2.35 and 4.1 ppm, from the ^1H NMR spectrum can be assigned to the different dyads [10]. The lactide and ϵ -caprolactone molar content and the microstructural magnitudes of the copolymers were obtained from the average dyad relative molar fractions. L-LA and D-LA are indistinguishable in the NMR spectrum so their contents and average sequence lengths are approximate values calculated on the assumption that the reactivities of both L-LA and D-LA are the same (having taken into account the L-LA:D-LA feed ratios). Equations 1-4 [29] were employed to obtain the number-average sequence lengths (l_i), the Bernoullian random number-average sequence lengths ($(l_i)_{random}$) and the randomness character (R):

$$l_{\text{LA}} = \frac{2(\text{LA})}{(\text{LA} - \text{CL})} ; \quad l_{\text{CL}} = \frac{2(\text{CL})}{(\text{LA} - \text{CL})} \quad (1)$$

$$(l_{\text{LA}})_{\text{random}} = \frac{1}{(\text{CL})} ; \quad (l_{\text{CL}})_{\text{random}} = \frac{1}{(\text{LA})} \quad (2)$$

$$R = \frac{(l_{\text{LA}})_{\text{random}}}{l_{\text{LA}}} = \frac{(l_{\text{CL}})_{\text{random}}}{l_{\text{CL}}} \quad (3)$$

For the terpolymers:

$$l_{\text{L-LA}} = \frac{1}{((\text{D} - \text{LA}) + (\text{CL})) R} ; \quad l_{\text{D-LA}} = \frac{1}{((\text{L} - \text{LA}) + (\text{CL})) R} \quad (4)$$

where (LA) and (CL) are the lactide and ϵ -caprolactone molar fractions, obtained from the integration of the lactide methine signals and the ϵ -caprolactone methylene signals, (L-LA) and (D-LA) are the L-lactide and D-lactide approximate molar fractions and (LA-CL) is the LA-CL average dyad relative molar fraction.

For the *in vitro* degradation study, square samples (~ 20 mg (W_0) ($n = 3$)) of PLCL 008515, PLCL 502525, PLCL 504010 and PLCL 602515 were placed in Falcon tubes containing phosphate buffered saline (PBS) (pH = 7.2) and maintaining a surface area to volume ratio equal to 0.1 cm^{-1} . The samples were stored in an oven at 37°C . Three samples of each polymer were removed at different times from the PBS and weighed wet (W_w) immediately after wiping the surface with a filter paper to adsorb the surface

water. These samples were air-dried overnight and vacuum-dried for another 24 h. Then, they were weighed again to obtain the dry weight (W_d). Water absorption (% WA) and remaining weight (% RW) were calculated according to Eqs. (5) and (6):

$$\% \text{WA} = \frac{W_w - W_d}{W_d} \cdot 100 \quad (5)$$

$$\% \text{RW} = \frac{W_d}{W_0} \cdot 100 \quad (6)$$

In order to compare the degradation rate of the studied PLCLs, the exponential relationship between molecular weight and degradation time for biodegradable polyesters degrading under bulk degradation was used [30]:

$$\ln M_w = \ln M_{w0} - K_{Mw} \cdot t \quad (7)$$

$$t_{1/2} = 1/K_{Mw} \cdot \ln 2 \quad (8)$$

where M_w is the weight-averaged molecular weight, M_{w0} is the initial weight-averaged molecular weight, K_{Mw} is the apparent degradation rate and $t_{1/2}$ is the half degradation time (the amount of time required to fall to half the initial value of molecular weight).

The molecular weight evolution of the samples during hydrolytic degradation was determined by GPC using a Waters 1515 GPC apparatus equipped with two Styragel columns ($10^2 - 10^4 \text{ \AA}$). Chloroform was used as an eluent at a flow rate of 1 mL min^{-1} and polystyrene standards (Shodex Standards, SM-105) were used to obtain a primary calibration curve. The samples were prepared at a concentration of 10 mg in 1 mL

The thermal properties were determined on a DSC 2920 (TA Instruments). Samples of 5-10 mg were heated from $-85 \text{ }^\circ\text{C}$ to $185 \text{ }^\circ\text{C}$ at $20 \text{ }^\circ\text{C min}^{-1}$. This first scan was used to determine the melting temperature (T_m) and the heat of fusion (ΔH_m) of the samples. After this first scan, the samples were quenched in the DSC and a second scan was made from $-85 \text{ }^\circ\text{C}$ to $185 \text{ }^\circ\text{C}$ at $20 \text{ }^\circ\text{C min}^{-1}$. In this second scan the glass transition temperatures (T_g) were determined from the inflection point of the heat flow curve.

The mechanical properties of the non-degraded samples and the samples submerged in PBS during 7, 14 and 21 days were determined by tensile tests with an Instron 5565 testing machine at a crosshead displacement rate of 10 mm min⁻¹. These tests were performed at 21 ± 2 °C and 50 ± 5 % relative humidity following ISO 527-3/1995. The mechanical properties reported correspond to average values of at least 5 determinations.

1.3.3. Results and discussion

Characterization

Table 1 summarizes the characterization data of the different PLCL films. In each sample name, the first two digits represent the L-LA mass content; the following two the D,L-LA mass content and the last two the CL mass content in the feeding mix. As an example, PLCL 502525 was synthesized adding 50 wt. % of L-LA, 25 wt. % of D,L-LA and 25 wt. % of ε-CL.

Table 1. NMR characterization and GPC measurements of the films from the PLCL polymers studied in this work.

Sample ¹	Terpolymer Composition ² (% molar)			M _w kg mol ⁻¹	D	Microstructural Magnitudes ³					T _g ⁵ °C
	% L-LA	% D-LA	% CL			<i>l</i> _{LA}	<i>l</i> _{L-LA} ⁴	<i>l</i> _{D-LA} ⁴	<i>l</i> _{CL}	<i>R</i>	
PLCL 007525	36.25	36.25	27.5	57.2	1.87	3.77	1.63	1.63	1.43	0.96	11.5
PLCL 008515	41.85	41.85	16.3	82.8	1.88	6.39	1.79	1.79	1.24	0.96	28.7
PLCL 502525	60.8	12.1	27.1	81.3	1.92	3.47	2.39	1.07	1.29	1.06	20.8
PLCL 503020	63.6	14.7	21.7	58.1	1.88	4.58	2.73	1.16	1.27	1.01	24.8
PLCL 504010	69.7	19.9	10.4	68.7	1.95	9.57	3.28	1.24	1.11	1.01	38.0
PLCL 554005	74.4	19.8	5.8	56.0	1.87	18.87	4.29	1.37	1.17	0.91	40.3
PLCL 602515	72.0	12.4	15.6	76.8	1.96	6.49	3.62	1.16	1.20	0.99	36.1
PLCL 600040	62.2	0	37.8	78.7	1.79	2.55	2.55	-	1.55	1.04	8.9
PLCL 750025	74.0	0	26.0	68.9	1.88	4.01	4.01	-	1.41	0.96	27.9

¹ The first two digits of the sample name represent the L-LA mass content in the feeding mix, the following two the D,L-LA mass content in the feeding mix and the last two the CL mass content in the feeding mix.

² Calculated from ¹H NMR spectra. Because of the impossibility of offering the exact L-LA and D-LA molar content (indistinguishable in the NMR spectrum), approximate values are given under the assumption that the reactivity of both L-LA and D-LA are the same.

³ l_{LA} and l_{CL} are the LA and CL number average sequence lengths obtained from ¹H NMR. These values are compared to the Bernoullian random number-average sequence lengths ($l_{LA}=1/CL$ and $l_{CL}=1/LA$), obtaining the randomness character value (R).

⁴ l_{L-LA} and l_{D-LA} are the L-LA and D-LA approximate values of number average sequence lengths under the assumption that the reactivity of both L-LA and D-LA are the same.

⁵ Obtained from the second scan of the DSC curves.

As can be seen, the molecular weights (M_w) of each polymer range from 56.0 to 82.8 kg mol⁻¹ (and dispersity (D) from 1.79 to 1.96) in such a way that the impact on their initial properties can be assumed as negligible in comparison to that corresponding to sequence length distribution or terpolymer composition. As it was expected for all of these BiSS-initiated PLCLs, they exhibit a random distribution of sequences ($R \sim 1$). Two of them, PLCL 600040 and PLCL 750025, are L-lactide-co- ϵ -caprolactone copolymers (L-PLCL), already employed in our earlier hydrolytic degradation study [13], used in this work as comparison polymers. PLCL 600040 (62.2 % of L-LA, $l_{L-LA} = 2.55$ and $l_{CL} = 1.55$) and PLCL 750025 (74.0 % of L-LA, $l_{L-LA} = 4.01$ and $l_{CL} = 1.41$) present glass transition temperatures (T_g s) at 8.9 and 27.9 °C, respectively, and are demonstrated to be able to crystallize during degradation, developing, at those l_{L-LA} , crystalline L-LA domains.

PLCL 007525 (36.25 % of L-LA and 36.25 % of D-LA, $l_{L-LA} = l_{D-LA} = 1.63$ and $l_{CL} = 1.43$) and PLCL 008515 (41.85 % of L-LA and 41.85 % of D-LA, $l_{L-LA} = l_{D-LA} = 1.79$ and $l_{CL} = 1.24$) are rac-lactide-PLCLs with T_g s at 11.5 and 28.7 °C, respectively. PLCL 502525 ($l_{L-LA} = 2.39$, $l_{D-LA} = 1.07$ and $l_{CL} = 1.29$), PLCL 503020 ($l_{L-LA} = 2.73$, $l_{D-LA} = 1.16$ and $l_{CL} = 1.27$) and PLCL 504010 ($l_{L-LA} = 3.28$, $l_{D-LA} = 1.24$ and $l_{CL} = 1.11$) are terpolymers having a L-LA content ranging from ~ 60 to 70 % and T_g s that shift to higher values when decreasing their CL content (in the range of 20.8 to 38.0 °C). Finally, two more terpolymers richer in L-LA were studied, PLCL 554005 ($l_{L-LA} = 4.29$, $l_{D-LA} = 1.37$ and $l_{CL} = 1.17$) and PLCL 602515 ($l_{L-LA} = 3.62$, $l_{D-LA} = 1.16$ and $l_{CL} = 1.20$). They also show single T_g s at 40.3 and 36.1 °C.

In view of the given glass transition temperatures (T_g s) of the PLCLs there is a well-known temperature lowering effect of the CL units since, it is worth remembering, the

poly(ϵ -caprolactone) (PCL) homopolymer presents a glass transition temperature at -60°C . In addition, the L-LA/D-LA ratio has a major impact on the T_g of those polymers increasing their T_g values. This is because at L-LA/D-LA ratios closer to one (this is the case of rac-lactide copolymers), the polymers are more amorphous because of the lower L-LA and D-LA average sequence lengths. However, at compositions richer in L-LA, the L-LA sequence blocks may be large enough to provide stiffness or even form crystalline organized structures. The discussion of this effect will be treated in a more comprehensive way evaluating the mechanical behaviour of the different PLCLs.

Mechanical Properties

Mechanical properties of 150-200 μm thick films from the polymers of the Table 1 were measured with an Instron testing machine at room temperature ($21 \pm 2^{\circ}\text{C}$) and the results are summarized in Table 2.

Table 2. Mechanical properties data of the PLCLs of this work.

Sample	Secant Modulus at 2 %	Yield Strength or Offset Yield Strength at 10 % ¹	Tensile Strength ²	Elongation at break
	(MPa)	(MPa)	(MPa)	(%)
PLCL 007525	4.6 ± 0.3	0.34 ± 0.02	0.67 ± 0.06	> 1400
PLCL 008515	146.5 ± 8.9	3.7 ± 0.4	5.4 ± 0.6	361
PLCL 502525	5.7 ± 0.3	0.44 ± 0.02	2.3 ± 0.2	994
PLCL 503020	10.9 ± 1.0	0.58 ± 0.04	1.7 ± 0.2	697
PLCL 504010	336.7 ± 39.8	7.4 ± 0.8	5.1 ± 0.4	59
PLCL 554005	473.7 ± 39.7	11.0 ± 1.0	6.6 ± 0.5	8.5
PLCL 602515	331.3 ± 41.3	7.9 ± 0.9	9.2 ± 0.6	230
PLCL 600040	2.7 ± 0.2	0.25 ± 0.02	0.37 ± 0.02	> 1400
PLCL 750025	19.4 ± 1.3	0.80 ± 0.02	3.2 ± 0.6	325

¹ The data of the two L-PLCLs, PLCL 600040 and 700025 are extracted from a previous study [13].

² Offset Yield Strength was calculated at a 10 % of strain using the secant modulus at 2 % as elastic modulus (E) for PLCL 007525, PLCL 502525, PLCL 503020, PLCL 600040 and PLCL 750025.

³ The tensile strength was determined as ultimate stress value (σ_u).

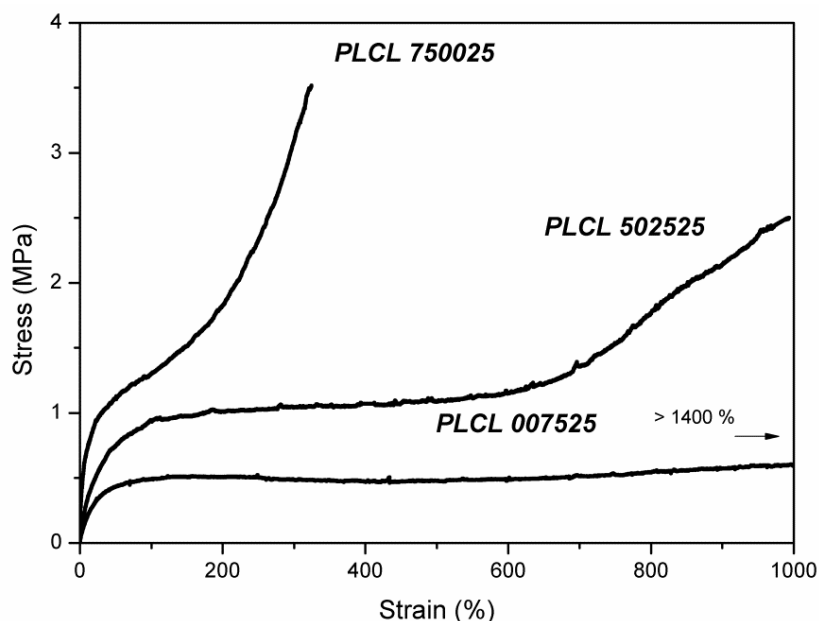


Figure 1. Tensile stress-strain curves of PLCLs that have approx. 75 % of LA content.

Figure 1 shows typical stress-strain curves of the three PLCLs of this study that have approximately a 75 % of lactide content (L-LA+D-LA). The poly(L-lactide/ ϵ -caprolactone) L-PLCL 750025 (74 % of L-LA), exhibits a partly elastomeric behaviour having secant modulus of 19.3 MPa, offset yield strength of 0.80 MPa, ultimate stress value of 3.2 MPa and elongation at break of 325 MPa. In contrast, PLCL 502525 (60.8 % of L-LA and 12.1 % of D-LA) and PLCL 007525 (36.25 % of L-LA and 36.25 % of D-LA) are highly elastomeric polymers with secant modulus values of 5.7 MPa and 4.6 MPa, offset yield strengths of 0.44 MPa and 0.34 MPa, ultimate stress values of 2.3 MPa and 0.67 MPa and elongation at break of 994 % and > 1400 %, respectively. As can be seen, by means of raising the L-LA content, it was possible to increase the stress related properties of these PLCLs. In the case of the PLCL 502525, the addition of D-LA units disrupts the microstructural arrangement of the L-LA crystallizable chains shortening their average sequence length ($l_{L-LA} = 2.39$ for PLCL 502525 vs. $l_{L-LA} = 4.01$ for PLCL 750025). As a consequence, a more disordered structure is achieved presenting a lower T_g (20.8 °C for PLCL 502525 vs. 27.9 °C for PLCL 750025) and a more elastomeric behaviour. The differences between PLCL 502525 and PLCL 007525

($l_{L-LA} = l_{D-LA} = 1.63$), were less significant. However, it must be emphasized that the latter presents higher elongation at break values and does not display a cold-drawing deformation profile that appears in the stress-strain curve of PLCL 502525 over 600 % of strain. The exceptionally high elastomeric response of the PLCL 007525 can be explained by its low T_g value (11.5 °C) and lower stereoregularity.

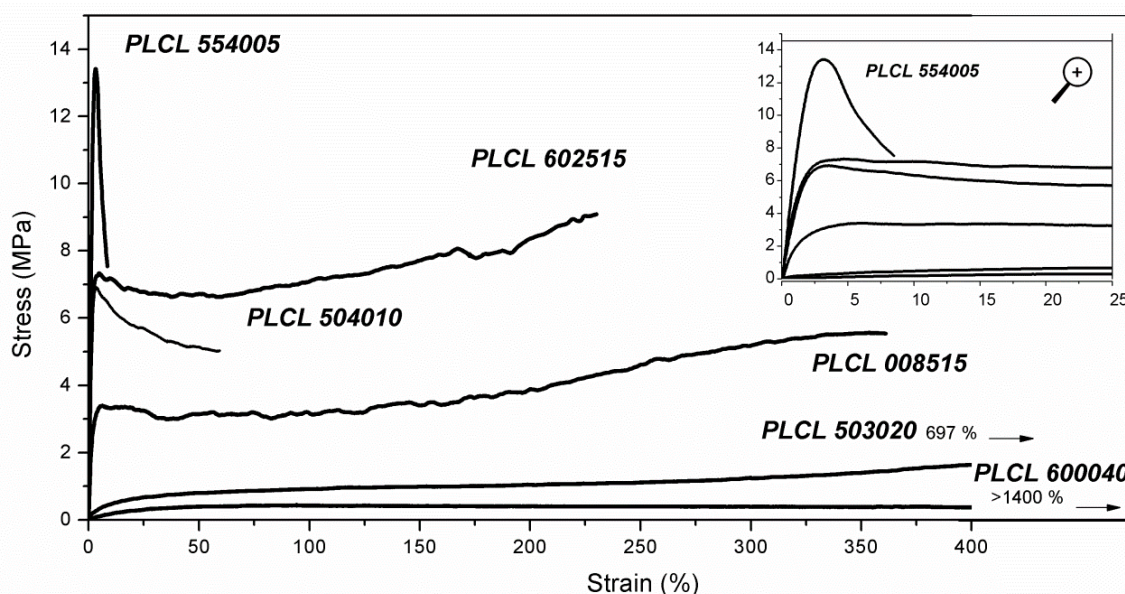


Figure 2. Tensile stress-strain curves of PLCLs.

Figure 2 shows the stress-strain typical curves of the other polyesters of this work: PLCL 554005, PLCL 504010, PLCL 602515, PLCL 008515, PLCL 503020 and PLCL 600040. The influence of the L-LA/D-LA ratio in the mechanical properties of the PLCLs is also reflected when comparing the mechanical data of rac-PLCL 008515 and PLCL 602515, both having similar lactide content (~ 84 % of LA). PLCL 008515 (41.85 % of L-LA, 41.85 % of D-LA and $l_{L-LA} = 1.79$) has 146.5 MPa of secant modulus, 3.7 MPa of yield strength (yield point at 5.4 %), 5.4 MPa of tensile strength and 361 % of elongation at break. By contrast, PLCL 602515 (72.0 % of L-LA and $l_{L-LA} = 3.62$) exhibits a more glassy semicrystalline behaviour presenting a neat yield point at 4.8 % and values of the stress related properties that are nearly twice than those of the rac-PLCL (secant modulus of 331.5 MPa, yield strength of 7.9 MPa and tensile strength of 9.2 MPa). It was again demonstrated that larger average sequence blocks of L-LA are responsible for a stiffer effect on the mechanical behaviour of the PLCLs.

By comparison, as it is featured in Figure 2, the PLCLs with a lower CL content (< 20 %) exhibit glassy responses with clearly defined yield points. PLCL 554005 (74.4 % of L-LA, 19.8 % of D-LA and $l_{L-LA} = 4.29$) shows a typical curve for a glassy semicrystalline plastic with a prompt failure after yield point (3.2 % of elongation) at 8.5 % strain due to its low CL content (5.8 %). However, the presence of D-LA and CL in the polymer chains considerably reduces the stiffness and strength of this terpolymer (473.7 MPa of secant modulus and 6.6 MPa of ultimate stress value) in regard to polylactides (PLAs) or other L- or D-PLCL copolymers with larger l_{L-LA} or l_{D-LA} [10, 31]. Despite this fact, there is little interest in this biomaterial because of its elevated L-LA content. This is about equal to the PLCL 750025 ($l_{L-LA} = 4.01$) which showed high crystallization capability during hydrolytic degradation [13]. PLCL 504010 (69.7 % of L-LA, 19.9 % of D-LA and $l_{L-LA} = 3.28$) and PLCL 602515 (72.0 % of L-LA, 12.4 % of D-LA and $l_{L-LA} = 3.62$), having less L-LA units and being richer in CL, improve the deformability of PLCL 554005, as is proven by their 59 % and 230 % values of elongation at break, and seem to be very promising materials for substitution of rather brittle PLAs or PLCLs of large l_{L-LA} .

Finally, it should also be noticed that the elongation at break measured value of the PLCLs depends greatly on their CL content and the ultimate strain values of the three PLCLs of this study in excess of 25 % CL content (PLCL 007525, PLCL 502525 and PLCL 600040) are higher than 990 %. PLCL 503020 (63.8 % of L-LA, 14.7 % of D-LA and 21.7 % of CL) and PLCL 600040 (62.2 % of L-LA and 37.8 % of CL) present a thermoplastic-elastomer behaviour and no yield point was observed. PLCL 503020 displays mechanical properties between PLCL 504010 (69.7 % of L-LA) and PLCL 502525 (60.8 % of L-LA), e.g. secant modulus of 10.9 MPa, ultimate stress value of 1.7 MPa and strain at break of 697 %, improving the stress related properties and the mechanical performance of PLCL 600040 (secant modulus of 2.7 MPa, tensile strength of 0.37 MPa and strain at break > 1400 %). Both polymers have similar L-LA content (~ 63 % of L-LA and $l_{L-LA} \sim 2.6$), but replacing CL with D-LA-units a higher T_g polymer is achieved (24.8 °C for PLCL 503020 vs 8.9 °C for PLCL 600040), which is more attractive for medical applications at human body temperature (37 °C).

Hydrolytic degradation study

From the random PLCLs of the Table 1, PLCL 008515, PLCL 502525, PLCL 504010 and PLCL 602515 were considered the most representative and were selected to carry out a hydrolytic degradation study.

Thermal properties evolution

Figure 3 shows the first DSC scans of samples of PLCL 008515, PLCL 502525, PLCL 504010 and PLCL 602515 at different degradation times. The thermal properties data of each material obtained from these thermograms are detailed in Table 3.

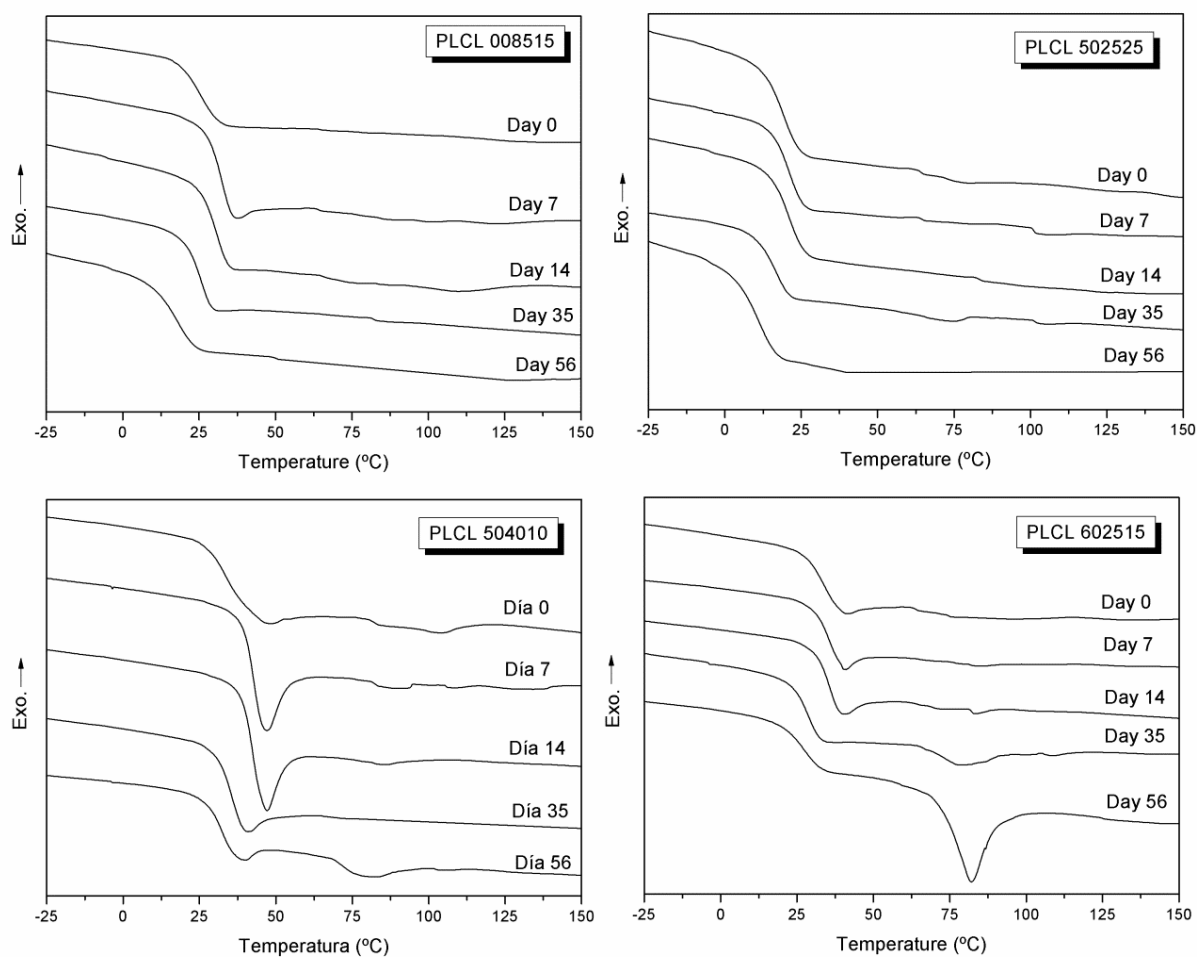


Figure 3. First DSC scans of PLCL 008515, PLCL 502525, PLCL 504010 and PLCL 602515 at different degradation times.

Table 3. M_w , D , and DSC results of the studied PLCLs at different times of degradation.

Sample	time (days)	M_w (kg mol ⁻¹)	D	1st Scan				2nd Scan
				T_{g1} (°C)	δ (J g ⁻¹)	T_m (°C)	ΔH_m (J g ⁻¹)	T_g (°C)
PLCL 008515	0	82.8 ± 0.0	1.88	24.1	-	-	-	28.7
	3	73.7 ± 0.5	1.97	30.3	0.4	-	-	32.7
	7	65.1 ± 1.4	2.04	33.0	0.6	-	-	33.2
	14	40.4 ± 1.0	2.26	31.0	-	-	-	32.2
	21	25.8 ± 1.1	2.99	28.8	-	-	-	27.0
	28	14.7 ± 0.3	14.80	27.3	-	-	-	29.0
	35	8.4 ± 0.8	*	26.6	-	-	-	26.6
	42	6.9 ± 0.2	*	21.3	-	-	-	21.3
	49	6.5 ± 0.02	*	19.2	-	-	-	10.6
	56	6.3 ± 0.02	*	18.4	-	-	-	6.1
	63	5.4 ± 0.3	*	19.5	-	-	-	4.3
77	4.6 ± 0.0	*	14.7	-	-	-	-0.9	
PLCL 502525	0	81.3 ± 0.0	1.92	19.3	-	-	-	20.8
	3	72.8 ± 1.6	1.98	20.5	-	-	-	22.2
	7	63.1 ± 0.9	2.09	21.0	-	-	-	21.3
	14	43.8 ± 0.8	2.28	20.5	-	-	-	20.7
	21	30.1 ± 0.8	3.29	19.3	-	-	-	19.8
	28	18.5 ± 0.1	13.19	18.1	-	-	-	18.1
	35	11.8 ± 0.4	*	17.0	-	-	-	15.2
	42	8.7 ± 0.2	*	10.1	-	-	-	10.1
	49	7.6 ± 0.03	*	11.9	-	-	-	13.0
	56	7.7 ± 0.2	*	11.0	-	-	-	16.0
	63	6.8 ± 0.05	*	7.9	-	-	-	13.7
77	6.0 ± 0.3	*	6.3	-	-	-	-1.6	
PLCL 504010	0	68.7 ± 0.0	1.94	33.7	0.4	-	-	38.0
	3	62.8 ± 0.4	1.99	38.4	0.6	-	-	39.1
	7	59.3 ± 0.2	2.03	42.0	3.4	-	-	41.6
	14	52.6 ± 1.7	2.04	42.0	3.7	-	-	40.0
	21	44.2 ± 0.8	2.21	42.8	4.4	-	-	41.0
	28	33.8 ± 0.6	2.88	38.8	2.3	-	-	38.4
	35	26.9 ± 0.3	3.67	35.4	1.4	-	-	34.1
	49	15.0 ± 0.8	*	35.0	1.7	82.0	1.9	26.5
	56	12.0 ± 0.4	*	33.4	1.3	79.0	3.0	24.7
	70	9.0 ± 0.1	*	35.7	1.1	**	**	22.2
	84	7.4 ± 0.2	*	30.0	-	**	**	17.1
98	6.5 ± 0.0	*	30.1	-	80.2	8.0	17.7	
PLCL 602515	0	76.8 ± 0.0	1.96	34.3	0.3	-	-	36.1
	3	68.3 ± 0.5	2.01	33.1	0.1	-	-	35.4
	7	62.6 ± 0.8	2.05	34.9	0.8	-	-	34.1
	14	52.4 ± 1.6	2.06	34.4	1.2	-	-	34.8
	21	38.8 ± 1.0	2.27	35.7	1.1	-	-	35.4
	28	27.2 ± 0.6	3.17	31.7	0.6	-	-	30.2
	35	19.9 ± 0.3	3.95	29.1	-	77.6	2.4	30.6
	49	11.0 ± 0.05	*	32.6	-	81.8	10.6	26.4
	56	9.4 ± 0.09	*	26.8	-	81.6	11.4	25.9
	70	8.2 ± 0.4	*	23.0	-	81.8	10.5	18.5
	84	6.8 ± 0.2	*	22.7	-	84.7	18.6	14.8
98	6.0 ± 0.0	*	18.0	-	82.7	17.8	10.6	

* Not measurable because of the uncertainty in the number-average molecular weight (M_n) measurements.

** Not measurable because of water traces in the DSC sample.

After being conformed, the rac-PLCL 008515 (41.85 % of L-LA and 41.85 % of D-LA) film presented a T_g of 24.1 °C. Then, on day 3, a small enthalpy of relaxation peak (δ) appeared at the T_g , which slightly increased to about 30 °C as a result of the densification of the polymer chains. However, on day 14 the δ disappeared and the T_g

started to move toward lower temperatures because of the higher mobility of the shorter polymer chains produced during the degradation process. Finally, after 77 days submerged in PBS, when the weight-average molecular weight (M_w) of the polymer was 4.6 kg mol^{-1} , the T_g reached a final value of $14.7 \text{ }^\circ\text{C}$. PLCL 008515 degraded homogeneously and no melting peaks were detected in the DSC analysis thanks to the combination of short L-LA, D-LA and CL sequences.

The DSC curves of PLCL502525 (60.8 % of L-LA and 12.1 % of D-LA) developed in a manner similar to those of rac-PLCL 008515, maintaining its amorphous character, and no phase separation was detected. In this case an enthalpy relaxation peak was not found during degradation process, probably because the storage temperature ($37 \text{ }^\circ\text{C}$) was well above the glass transition temperature for this material. It should also be noticed that, in contrast to a L-lactide/ ϵ -caprolactone copolymer studied in our previous work (PLCL 750025) [13] which has similar lactide content ($\sim 75 \%$), L-lactide segments of PLCL 502525 were not able to crystallize because of the shorter average sequence length of L-lactide ($l_{L-LA} = 2.39$) in comparison to the $l_{L-LA} = 4.01$ of the previously mentioned PLCL750025. Throughout the entire study, PLCL502525 displayed a single T_g , initially at $19.3 \text{ }^\circ\text{C}$, that shifted to $6.3 \text{ }^\circ\text{C}$ on day 77, when M_w took a value of 6.0 kg mol^{-1} .

Regarding PLCL 504010 (69.7 % of L-LA and 19.9 % of D-LA), in the first DSC scan this terpolymer showed a T_g at $33.7 \text{ }^\circ\text{C}$ at the beginning of the experiment accompanied by a small enthalpic relaxation peak. Both T_g and δ increased substantially during the first 21 days submerged in PBS at $37 \text{ }^\circ\text{C}$ reaching a value of $42.8 \text{ }^\circ\text{C}$ and 4.4 J g^{-1} respectively. This indicates that polymer chains were relaxing toward an equilibrium state [32]. From this day (day 21), the values of T_g and δ decreased uniformly and the enthalpic relaxation peak even became negligible on day 84. In this material, a melting peak was found at around $80 \text{ }^\circ\text{C}$ on day 49 (ΔH_m of 1.9 J g^{-1}), demonstrating that the lactide average sequence length ($l_{L-LA} = 3.28$) was large enough to crystallize during the degradation period studied. This value shifted to 8.0 J g^{-1} on day 98.

Finally, the terpolymer richer in L-LA, PLCL 602515 (72.0 % of L-LA, 12.4 of D-LA and $l_{L-LA} = 3.62$), presented an initial T_g of $34.3 \text{ }^\circ\text{C}$ while its associated δ was 0.3 J g^{-1} .

This value shifted to 1.2 J g^{-1} on day 21 and then started to drop until it completely disappeared on day 35. On this same day, a melting peak was observed at $77.6 \text{ }^\circ\text{C}$, presenting a melting enthalpy (ΔH_m) of 2.4 J g^{-1} , which rose to 17.8 J g^{-1} at the end of the study (day 98).

Comparing PLCL 602515 and PLCL 504010 with the previously studied L-lactide/ ϵ -caprolactone PLCL 600040 (62.2 % of LA and $l_{L-LA} = 2.55$) [13] it has to be pointed out that the latter, having shorter l_{L-LA} and lower L-LA content, crystallizes faster than the two terpolymers. In this sense, a melting peak was observed in PLCL600040 after just 7 days submerged in PBS whereas PLCL 504010 and PLCL 602515 maintained their amorphous character until day 49 and day 35, respectively. The low T_g of PLCL 600040 in comparison to PLCL 504010 and PLCL 602515 ($8.9 \text{ }^\circ\text{C}$ vs. $33.7 \text{ }^\circ\text{C}$ and $34.3 \text{ }^\circ\text{C}$) leads to higher mobility of polymer chains promoting an earlier development of crystalline domains during the hydrolytic degradation. On the other hand, it should also be noted that, despite the small variations of L-LA content existing between the crystallisable PLCL 602515 (72.0 % of L-LA and $l_{L-LA} = 3.62$) and PLCL 504010 (69.7 % of L-LA and $l_{L-LA} = 3.28$) with respect to the previously studied PLCL 750025 (74.0 % of L-LA, $l_{L-LA} = 4.01$), large differences were observed in their melting enthalpy values. Thus, PLCL 750025 had a ΔH_m of 33.7 J g^{-1} on day 98, almost twice that the corresponding to the PLCL 602515. This fact can be explained by an earlier work [15] where it was found that the crystallinity degree (X_c) of nascent L-PLCLs grows in a logarithmic manner and rises quickly from 2.0 % to around 20.0 % increasing l_{L-LA} from 3.3 to 5.0, grows moderately when l_{L-LA} is in the range of 5.0-9.0 and then, at higher values of l_{LA} , stabilizes. Therefore, at l_{L-LA} lower than 4.0, major changes in the crystallization capability during degradation will also be usual.

Molecular weights evolution and degradation kinetics

The data of weight-average molecular weight (M_w) and dispersity (D) during the *in vitro* degradation study are summarized in Table 3. As degradation evolves, the M_w of the samples decreases while their D increases as expected. As an illustration, D of PLCL 008515, PLCL 502525, PLCL 504010 and PLCL 602515 raised from 1.88, 1.92, 1.94 and 1.96 on day 0 to 14.80, 13.19, 2.88 and 3.17 on day 28, respectively. The

larger values of dispersity for PLCL 008515 and PLCL 502525 indicate that these two materials were, at this point of the study, in a more advanced state of degradation presenting a broader distribution of polymer chain length.

The loss of M_w resulted in a reduction in molecular entanglement and an increase in chain mobility that directly affected the observed glass transition temperatures in the second DSC scan. As an illustration, T_g dropped from the initial value of 28.7, 20.8, 38.0 and 36.1 °C for PLCL 008515, PLCL 502525, PLCL 504010 and PLCL 602515 respectively, to -0.9, -1.6, 17.7 and 10.6 °C at the end of the study, when M_w were in the range of 4.5 to 6.0 kg mol⁻¹.

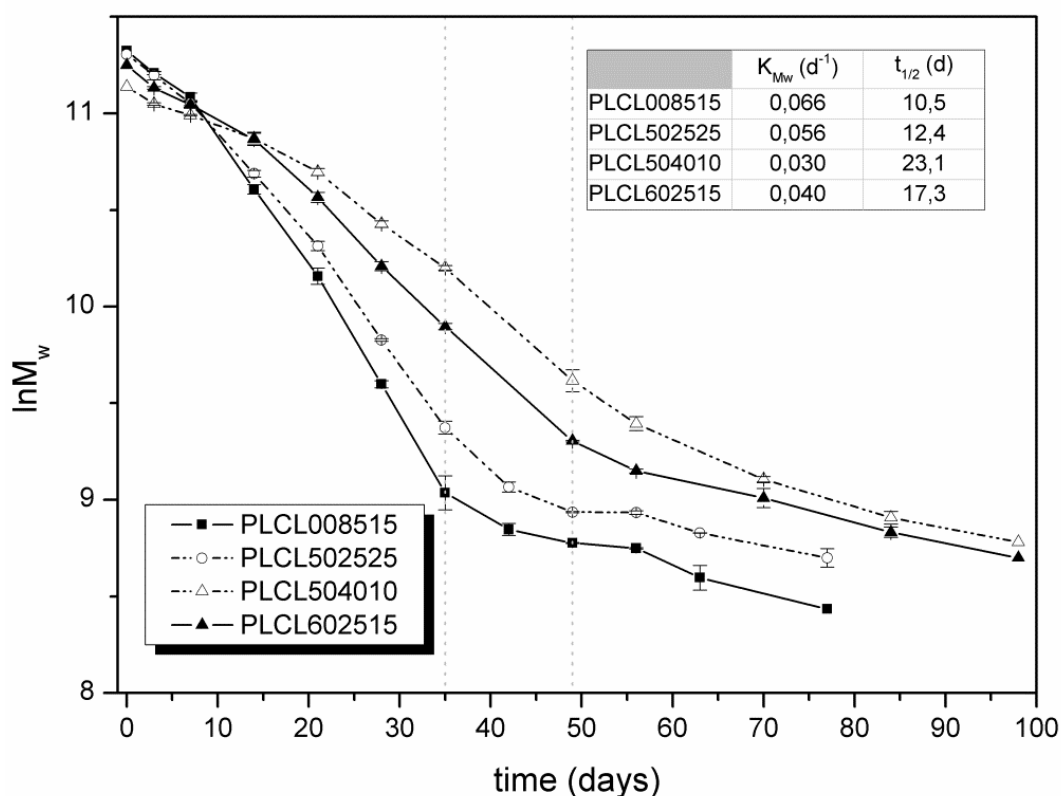


Figure 4. $\ln M_w$ vs. degradation time of the studied PLCLs.

Figure 4 shows the progress of $\ln M_w$ versus degradation time. The values of K_{M_w} and $t_{1/2}$ were calculated from the slope of the fitting curve during the first 35 days of study for PLCL 008515 and PLCL 502525 and during the first 49 days for PLCL 504010 and PLCL 602515 ($R^2 > 0.99$). It must be stated that extending the fitting of the curve

beyond these days (35 or 49 days), the correlation coefficient gradually decreased and the values of M_w obtained from the fitting curve deviated from those of the experimental data. This fact indicates that the degradation mechanism is changing from one dominated by bulk degradation to another controlled by surface erosion [33]. Obtained K_{Mw} for PLCL 008515, PLCL 502525, PLCL504010 and PLCL602515 are, 0.066, 0.0056, 0.030 and 0.040 days⁻¹ respectively, with corresponding $t_{1/2}$ of 10.5, 12.4, 23.1 and 17.3 days. To provide framework for comparison, apart from K_{Mw} values for the PLCL's studied in this work, K_{Mw} values of previously studied [13] PLCL750025 and PLCL600040 are given in Figure 4.

As can be seen, rac-PLCL 008515 (41.85 % of L-LA, 41.85 % of D-LA and $l_{L-LA} = 1.79$) presents the fastest degradation rate ($K_{Mw} = 0.066$ days⁻¹), due to its completely amorphous morphology. Conversely, the introduction of rigid L-lactide blocks, increasing the L-LA/D-LA ratio in the PLCL chains and the l_{L-LA} , leads to polymers with higher resistance to hydrolytic degradation. In this way, PLCL 602515 (72.0 % of L-LA and $l_{L-LA} = 3.62$) shows a slower degradation rate than PLCL 008515, despite having similar lactide content (~ 84 %). The K_{Mw} of PLCL 602515 (0.040 days⁻¹) is almost equal to that of the previously studied [13] L-PLCL 600040 ($K_{Mw} = 0.038$ days⁻¹), which has a 62.2 % of L-LA content. The L-LA average sequence length of the latter copolymer is lower ($l_{L-LA} = 2.55$) but, as a consequence of its low T_g (8.9 °C), the mobility of its polymer chains is favoured and the crystallization of L-lactide sequences begins at shorter times. Hence, the melting peak appeared at 69.1 °C on day 7 of degradation (shifting to 83.8 °C on day 98), while it takes 35 days to be distinguished in the thermograms of the PLCL 602515. Because the crystallinity is the most important factor influencing biodegradability, this should be taken into account when comparing the K_{Mw} that PLCL 600040 is richer in CL unit (37.8 % for PLCL 600040 vs 15.6 % for PLCL 602515), which displays higher resistance to hydrolysis than LA because of its more hydrophobic character.

PLCL 502525 (60.8 % of L-LA and 12.1 % of D-LA) displayed faster degradation than L-PLCL 750025 (74 % of L-LA and 26 % of CL). In this case, the reduction of l_{LA} (from 4.01 for PLCL 750025 to 2.39 for PLCL 502525) played a pivotal role in the degradation kinetics of these two materials. PLCL 750025 presented a peak of fusion of

9.3 J g⁻¹ after just 3 days submerged in PBS (reaching a final value of 33.7 J g⁻¹ on day 98) leading to a biomaterial with much higher resistance to hydrolytic degradation ($K_{Mw} = 0.034 \text{ days}^{-1}$) than the amorphous PLCL 502525.

With regard to PLCL 504010 (69.7 % of L-LA and 19.9 % of D-LA), the elevated T_g (38 °C) and the more packed structure of this material which contains less flexible CL units, seemed to slow down its hydrolytic degradation. The polymer chains are more compacted in the amorphous regions of this terpolymer than in other studied materials, as demonstrated by large enthalpic relaxation peaks observed in DSC results. Thus, water penetration is more difficult in these regions and the polymer displays higher resistance to hydrolytic degradation. Consequently, PLCL 504010 exhibited the lowest degradation rate of the studied PLCLs although this terpolymer was less prone to crystallization than PLCL 602515.

Weight loss and water absorption

Figure 5 shows remaining weight and water absorption curves of PLCL008515, PLCL 502525, PLCL 504010 and PLCL 602515 during *in vitro* degradation study. Obtained results are perfectly in accordance with the change of degradation mechanism on day 35 for PLCL 008515 and PLCL 502525 and on day 49 for the other two studied PLCLs, proposed in the 3.2.2 section. This occurs when erosion is the dominant degradation mechanism and oligomers and degradation byproducts are released from the sample leading to weight losses. In this sense, both PLCL 008515 and PLCL 502525 suffered a sharp decrease in their remaining weight from day 35 accompanied by a significant increment in the water absorption. As an illustration, the weight of PLCL 008515 and PLCL 502525 was maintained almost constant until day 35 and then it dropped to around 55 % on day 49. In the case of PLCL 504010 and PLCL 602515, the remaining weight did not undergo important changes until day 49 when they started to lose weight and reached a value of ~ 60 % and ~ 55 % on day 70 for PLCL 504010 and PLCL 602515, respectively.

As seen in the plot of water absorption, in PLCL 008515 and PLCL 502525 the increase of water uptake started 14 days earlier than in PLCL 504010 and PLCL 602515,

indicating that degradation is in a more advanced state in these two polymers with shorter l_{L-LA} . As previously mentioned, the developed crystalline domains in PLCL 602515 and the more packed amorphous regions in PLCL 504010 may hinder water absorption. Since the degradation of these polyesters is dominated by the attack of water to the ester bonds, the degradation kinetics and the mass loss of these two materials is less pronounced and retarded with respect to PLCL 008515 and PLCL 502525.

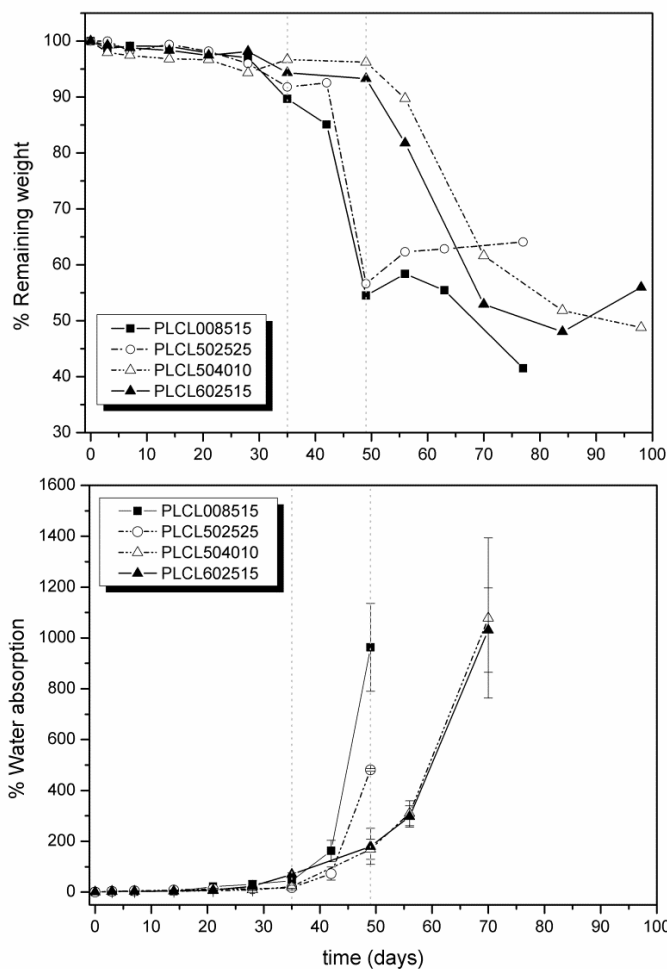


Figure 5. Remaining weight and water absorption of the PLCLs during the *in vitro* degradation study.

It is remarkable that, in contrast to the previously studied PLCL 750025 (74.0 % of L-LA and $l_{L-LA} = 4.01$) [13] or PLAs (poly(L-lactide) and poly(D-lactide) homopolymers), the PLCLs of the current work did not produce highly resistant crystalline fragments during their degradation. Since these remnants can damage surrounding tissues they are highly undesirable in medical applications. However, the PLCLs studied here degraded homogeneously and soft and pasty residues were observed at long degradation times.

Even PLCL 602515 (72.0 % of L-LA and $l_{L-LA} = 3.62$) and PLCL 504010 (69.7 % of L-LA and $l_{L-LA} = 3.28$), which crystallized and underwent a noteworthy enthalpic relaxation at the T_g during degradation, did not generate brittle resistant fragments.

Mechanical properties evolution

Mechanical testing was foreseen to be conducted at room temperature (21 ± 2 °C) on samples of PLCL 008515, PLCL 502525, PLCL 504010 and PLCL 602515 submerged in PBS for different times (7, 14 and 21 days). Some samples were found difficult to handle because they became too brittle or sticky during degradation. For example PLCL504010 was found to be too brittle in weeks 2 and 3 due to its elevated densification (enthalpy relaxation of its amorphous domains). PLCL 502525 became sticky and impossible to handle due to its poor mechanical performance. Table 4 summarizes the mechanical properties of PLCL 008515, PLCL 504010 and PLCL 602515 during degradation from the tests that could be completed.

It can be noticed that PLCL 008515, PLCL 504010 and PLCL 602515 undergo changes in their mechanical performance associated with the loss of molecular weight and to the decrease of specific free volume during degradation. For the PLCL 602515 (72.0 % of L-LA, 12.4 % of D-LA and $l_{L-LA} = 3.62$), as a consequence of the rising of the enthalpy relaxation peak at T_g (δ) from 0.3 J g^{-1} (day 0) to 1.2 J g^{-1} (day 14), an increase of stiffness is observed, reaching a secant modulus of 455.4 MPa and a yield strength of 12.9 MPa on day 14. Then, the δ value starts to decrease and, on day 21, the stress related properties are even lower than the initial ones of the non-degraded samples. On day 21 of the study, M_w takes a value of 38.8 kg mol^{-1} and the elongation at break reaches a value of 38 %, when initially it was 230 %. This is an indicative of severe deterioration of the mechanical properties at longer times.

In the PLCL 008515 (41.85 % of L-LA, 41.85 % of D-LA and $l_{L-LA} = 1.79$) an enthalpy relaxation peak appeared on day 7 ($\delta = 0.6 \text{ J g}^{-1}$), disappearing at longer times when the molecular weight was lower ($M_w = 25.8 \text{ kg mol}^{-1}$ on day 21) and the mobility of the polymer chains was favoured. As a result, the tensile properties of this PLCL undergo small fluctuations towards the increase of stiffness and, thereafter, they begin to drop.

Thus, after 21 days submerged in PBS, the secant modulus evolved from 146.5 to 32.2 MPa and the ultimate stress value from 5.4 to 1.6 MPa. By contrast, the strain at break value constantly fell during the first 14 days, surprisingly rising to 422 % at the end of the study. Both PLCL 602515 and PLCL 008515 provided a suitable mechanical performance during those 3 weeks.

Table 4. Evolution of the mechanical properties during degradation.

Sample		Secant Modulus at 2 %	Yield Strength or Offset Yield Strength at 10 % ¹	Tensile Strength ²	Elongation at break	Strain Recovery
		(MPa)	(MPa)	(MPa)	(%)	(%)
PLCL 008515	Day 0	146.5 ± 8.9	3.7 ± 0.4	5.4 ± 0.6	361	96.4 ± 1
	Day 7	189.6 ± 19.4	8.1 ± 0.3	8.0 ± 1.0	258	95.4 ± 1
	Day 14	169.1 ± 11.2	5.4 ± 0.4	5.0 ± 0.5	167	97.8 ± 1
	Day 21	32.2 ± 4.0	1.3 ± 0.1	1.6 ± 0.2	422	91.0 ± 1
PLCL 504010	Day 0	336.7 ± 39.8	7.4 ± 0.8	5.1 ± 0.4	59	80.9 ± 8
	Day 7	742.8 ± 37.3	-	23.6 ± 1.3	3.8	-
PLCL 602515	Day 0	331.3 ± 41.3	7.9 ± 0.9	9.2 ± 0.6	230	95.1 ± 2
	Day 7	374.1 ± 30.2	12.1 ± 1.4	11.4 ± 0.5	235	86.8 ± 2
	Day 14	455.4 ± 48.5	12.9 ± 1.1	8.2 ± 0.9	134	96.3 ± 1
	Day 21	225.6 ± 11.0	8.0 ± 1.0	5.7 ± 0.6	38	95.3 ± 2

¹ Offset Yield Strength was calculated at a 10 % of strain using the secant modulus at 2 % as elastic modulus (E) for PLCL 008515 on day 21 of degradation.

² The tensile strength was determined as ultimate stress value (σ_u).

With regard to the PLCL 504010, it can be said that this PLCL is the most affected by the PBS degradation process in terms of stiffness increase. Its elevated T_g (38.0 °C) and its low CL content makes it more susceptible to densification changes involving enthalpy relaxations, which are associated with the arrangements of the lactide rich chains in the amorphous regions. On day 7 of the study, the enthalpy relaxation peak dramatically increased from 0.4 (day 0) to 3.4 J g⁻¹. As a result, this PLCL broke at 3.8

% before yielding, reaching an ultimate stress value of 23.6 MPa whereas the secant modulus value shifted from 336.7 to 742.8 MPa. PLCL 504010 became rather brittle during degradation and it was not possible to carry out mechanical testing at other times.

A material based on PLCL 504010 (69.7 % of L-LA, 19.9 % of D-LA and $I_{L-LA}=3.28$) or PLCL 502525 (60.8 % of L-LA, 12.1 % of D-LA and $I_{L-LA}=2.39$) will require more stiffness or greater strength for devices with the necessity of consistency. However, the terpolymers having LA content from ~ 60 to 70 % and CL content from ~ 10 to 27 % will be very valuable for the medical applications discussed in the introduction.

1.3.4. Conclusions

In this work a new generation of poly(lactide/ ϵ -caprolactone) polymers (PLCLs) of molecular weights (M_w) ranging from 56.0 to 82.8 kg mol⁻¹, and composed of ϵ -caprolactone (CL), L-lactide (L-LA) and D-lactide (L-LA) (L-LA content < 72 %), were synthesized using bismuth (III) subsalicylate (BiSS) as catalyst. These polymers, having glass transition temperatures (T_g) higher than 20 °C, present a random distribution of sequences (randomness character: $R \sim 1$), show very little or no crystallization capability and do not generate resistant crystalline remnants during hydrolytic degradation. This is achieved because of their controlled D-LA and CL average sequence lengths and the inability to arrange into highly crystalline organized structure of their L-lactide (L-LA)-unit chains. Apart from the well-known elastomeric effect of CL, the addition of D-LA units allows the formation of more amorphous polymers. In the L-LA/D-LA/CL terpolymers, the D-LA and CL units disrupt the microstructural arrangement of the L-LA crystallizable chains shortening their average block sequence. As a result, a more disordered structure is obtained presenting a lower T_g , less resistance to hydrolytic degradation and a more elastomeric behaviour. Likewise, the presence of D-LA replacing CL units was found to be very useful in order to tune the T_g and the stress related properties (elastic modulus and strength) of the L-LA/CL or rac-LA/CL elastomeric copolymers of low T_g (< 20 °C).

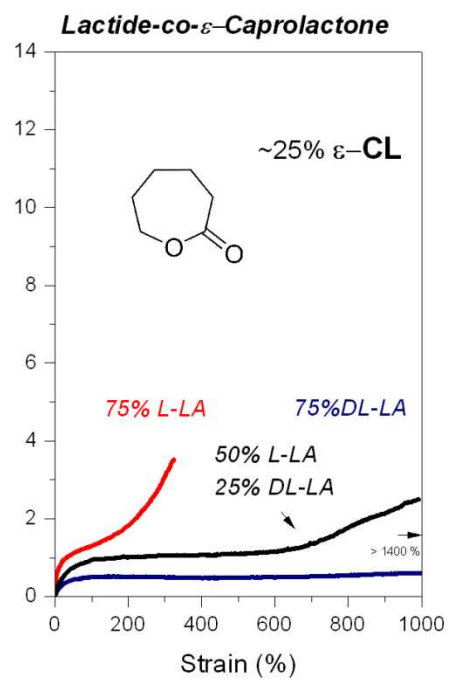
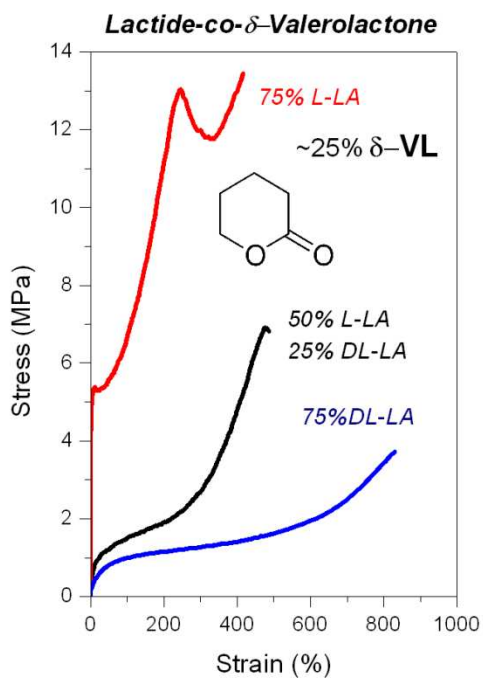
References

- [1] Karam, J-P.; Muscari, C.; Montero-Menei, C.N. Combining adult stem cells and polymeric devices for tissue engineering in infarcted myocardium. *Biomaterials* 2012, 33(23), 5683-5695.
- [2] Venkatraman, S.; Boey, F.; Lao, L.L. Implanted cardiovascular polymers: natural, synthetic and bio-inspired. *Progress in Polymer Science* 2008, 33, 853-874.
- [3] Lee, J.; Guarino, V.; Gloria, A.; Ambrosio, L.; Tae, G.; Kim, Y.H.; Jung, Y.; Kim, S-H.; Kim, S.H. Regeneration of Achilles' Tendon: The Role of Dynamic Stimulation for Enhanced Cell Proliferation and Mechanical Properties. *Journal of Biomaterials Science* 2010, 21, 1173-1190.
- [4] Sartoneva, R.; Haimi, S.; Miettinen, S.; Mannerström, B.; Haaparanta, A.M.; Sándor, G.K.; Kellomäki, M.; Suuronen, R.; Lahdes-Vasama, T. Comparison of a poly(L-lactic-co- ϵ -caprolactone) and human amniotic membrane for urothelium tissue engineering applications. *Journal of the Royal Society Interface* 2011, 8, 671-677.
- [5] Yu, X.; Wang, L.; Huang, M.; Gong, T.; Li, W.; Cao, Y.; Ji, D.; Wang, P.; Wang, J.; Zhou, S. A shape memory stent of poly(ϵ -caprolactone-co-DL-lactide) copolymer for potential treatment of esophageal stenosis. *Journal of Materials Science: Materials in Medicine* 2012, 23(2), 581-589.
- [6] Chiriac, S.; Facca, S.; Diaconu, M.; Gouzou, S.; Liverneaux, P. Experience of using the bioresorbable copolyester poly(DL-lactide- ϵ -caprolactone) nerve conduit guide Neurolac for nerve repair in peripheral nerve defects: report on a series of 28 lesions. *Journal of Hand Surgery, European Volume* 2012, 37(4), 342-249.
- [7] Ichihara, S.; Inada, Y.; Nakada, A.; Endo, K.; Azuma, T.; Nakai, R.; Tsutsumi, S.; Kurosawa, H.; Nakamura, T. Development of new nerve guide tube for repair of long nerve defects. *Tissue Engineering Part C Methods* 2009, 15 (3), 387-402.
- [8] Li, S.; Espartero, J.L.; Foch, P.; Vert, M. Structural characterization and hydrolytic degradation of a Zn metal initiated copolymer of L-lactide and ϵ -caprolactone. *Journal of Biomaterials Science: Polymer Edition* 1996, 8, 165-187.
- [9] Saha, S.K.; Tsuji, H. Enhanced crystallization of poly(L-lactide-co- ϵ -caprolactone) in the presence of water. *Journal of Applied Polymer Science* 2009, 112, 715-720.
- [10] Fernández, J.; Etxeberría, A.; Sarasua, J.R. Synthesis, structure and properties of poly(L-lactide-co- ϵ -caprolactone) statistical copolymers. *Journal of the Mechanical Behavior of Biomedical Materials* 2012, 9, 100-112.

- [11] Fernández, J.; Etxeberria, A.; Ugartemendia, J.M.; Petisco, S.; Sarasua, J.R. Effects of chain microstructures on mechanical behaviour and aging of poly(L-lactide-co- ϵ -caprolactone) biomedical thermoplastic elastomer. *Journal of Mechanical Behavior of Biomedical Materials* 2012, 12, 29-38.
- [12] Li, S. Hydrolytic degradation characteristics of aliphatic polyesters derived from lactic and glycolic acids. *Journal of Biomedical Materials Research, Part B: Applied Biomaterials* 1999, 48B, 342-353.
- [13] Fernández, J.; Larrañaga, A.; Etxeberria, A.; Sarasua, J.R. Effects of chain microstructures and derived crystallization capability on hydrolytic degradation of poly(L-lactide/ ϵ -caprolactone) copolymers. *Polymer Degradation and Stability* 2013, 98, 1293-1299.
- [14] Tsuji, H.; Ikarashi, K. In vitro hydrolysis of poly(L-lactide) crystalline residues as extended-chain crystallites. Part I: long-term hydrolysis in phosphate-buffered solution at 37 °C. *Biomaterials* 2004, 25, 5449-5455.
- [15] Fernández, J.; Meaurio, E.; Chaos, A.; Etxeberria, A.; Alonso-Varona, A.; Sarasua, J.R. Synthesis and characterization of poly(L-lactide/ ϵ -caprolactone) statistical copolymers with well resolved chain microstructures. *Polymer* 2013, 54, 2621-2631.
- [16] Nomura, N.; Akita, A.; Ishii, R.; Mizuno, M. Random Copolymerization of ϵ -Caprolactone with Lactide using a Homosalen-Al Complex. *Journal of the American Chemistry Society* 2010, 132, 1750-1751.
- [17] Dakshinamoorthy, D.; Peruch, F. Block and Random copolymerization of ϵ -Caprolactone, L- and rac-lactide using titanium complex derived from aminodiol ligand. *Journal of Polymer Science: Part A: Polymer Chemistry* 2012, 50, 2161-2171.
- [18] Li, G.; Lamberti, M.; Pappalardo, D.; Pellicchia, C. Random Copolymerization of ϵ -Caprolactone and Lactides Promoted by Pyrrolylpyridylamido Aluminium Complexes. *Macromolecules* 2012, 45, 8614-8620.
- [19] Middleton, J.C.; Tipton, A.J. Synthetic biodegradable polymers as orthopedic devices. *Biomaterials* 2000, 21, 2335-2346.
- [20] Li, J.; Stayshich, R.M.; Meyer, T.Y.. Exploiting sequence to control the hydrolysis behaviour of biodegradable PLGA copolymers. *Journal of American Chemistry Society* 2011, 133, 6910-6913.
- [21] Badi, N.; Lutz, J-F. Sequence control in polymer synthesis. *Chemical Society Review* 2009, 38, 3383-3390.

- [22] Stayshich, R.M.; Meyer, T.Y. New insights into poly(lactic-co-glycolic acid) microstructure: Using repeating sequence copolymers to decipher complex NMR and thermal behaviour. *Journal of American Chemical Society* 2010, 132, 10920-10934.
- [23] Dobrzynski, P.; Li, S.; Kasperczyk, J.; Bero, M.; Gasc, F.; Vert, M. Structure property relationships of copolymers obtained by ring-opening polymerization of glycolide and ϵ -caprolactone. Part 1. Synthesis and characterization. *Biomacromolecules* 2005, 6, 483-488.
- [24] Dobrzynski, P.; Kasperczyk, J.; Jelonek, K.; Ryba, M.; Walski, M.; Bero, M. Application of the lithium and magnesium initiators for the synthesis of glycolide, lactide, and ϵ -caprolactone copolymers biocompatible with brain tissue. *Journal of Biomedical Materials Research Part A* 2006, 44, 98-114.
- [25] Kasperczyk, J.; Li, S.; Jaworska, J.; Dobrzyński, P.; Vert, M. Degradation of copolymers obtained by ring-opening polymerization of glycolide and ϵ -caprolactone: A high resolution NMR and ESI-MS study. *Polymer Degradation and Stability* 2008, 93, 990-999.
- [26] Lu, X.L.; Cai, W.; Gao Z.Y. Shape-memory behaviors of biodegradable poly(L-lactide-co- ϵ -caprolactone) copolymers. *Journal of Applied Polymer Science* 2008, 108, 1109-1115.
- [27] Garkhal, K.; Verma, S.; Jonnalagadda, S.; Kumar, N. Fast Degradable Poly(L-lactide-co- ϵ -caprolactone) Microspheres for Tissue Engineering: Synthesis, Characterization, and Degradation Behavior. *Journal of Polymer Science* 2007, 45, 2755-2764 .
- [28] Jeong, S.I.; Kim, B-S.; Lee, Y.M.; Ihn, K.J.; Kim, S.H.; Kim, Y.H. Morphology of Elastic Poly(L-lactide-co- ϵ -caprolactone) Copolymers and in Vitro and in Vivo Degradation Behavior of Their Scaffolds. *Biomacromolecules* 2004, 5, 1303-1309.
- [29] Herbert, I.R. Statistical analysis of copolymer sequence distribution. In *NMR Spectroscopy of Polymers*. Ibbet, R.N. Ed.: Blackie Academic & Professional, London, 1993:50-79. (Chapter 2).
- [30] Wu, L.; Ding, J. Effects of porosity and pore size on in vitro degradation of three-dimensional porous poly(D,L-lactide-co-glycolide) scaffolds for tissue engineering. *Journal of Biomedical Materials Research Part A* 2005, 75, 767-777.
- [31] Garlotta, D. A literature review of poly(lactic acid). *Journal of Polymers and the Environment* 2001, 9(2), 63-84.
- [32] Hutchinson, J.M. Physical aging of polymers. *Progress in Polymer Science* 1995, 20, 703-760.
- [33] Yoshioka, T.; Kawazoe, N.; Tateishi, T.; Chen, G. In vitro evaluation of biodegradation of poly(lactic-co-glycolic acid) sponges. *Biomaterials* 2008, 29, 3438-3443.

Chapter 2. Lactide-co- δ -Valerolactone Copolymers



**Chapter 2.1 Tensile Behaviour and
Dynamic Mechanical Analysis of
Novel Lactide-co- δ -Valerolactone
Statistical Copolymers**

Journal of Mechanical Behavior of Biomedical Materials 2014, 35, 39-50.

Abstract

Lactide-co- δ -valerolactone copolymers (PLVL) have not attracted as much research interest as the more popular poly(lactide-co- ϵ -caprolactone) (PLCL) elastomeric materials. In this work the study of the mechanical performance is focused on the former with the aim of identifying the potential advantages of these thermoplastic elastomers for their application in the biomedical field. Mechanical testing (at 21 °C and at 37 °C) of at least 5 specimens and dynamic mechanical analysis (DMA) in duplicate were carried out on various PLVL, which include a moderately blocky L-lactide/ δ -valerolactone copolymer (~ 70 % of L-LA and $R = 0.68$) and several that showed a random distribution of sequences ($R \sim 1$): some terpolymers based on L-lactide, D-lactide and δ -valerolactone (with a lactone content of ~ 25 % and ~ 14 %) and a series of copolymers of L-LA and δ -VL having L-LA molar contents ranging from 69 to 74 %. In view of the results, it can be concluded that noteworthy improvements in stiffness and strength were achieved by adding δ -VL to the reaction mix instead of ϵ -CL, although both monomers have analogous chemical properties. For example, a PLVL with a 75:25 molar composition of L-LA/ δ -VL at 21 °C presented a secant modulus of 213.7 ± 36.5 MPa and $\sigma_u = 14.7 \pm 1.4$ MPa whereas a previously studied PLCL of equal composition had a secant modulus and an ultimate stress value of 19.4 ± 1.3 MPa and 3.2 ± 0.6 MPa, respectively. At 37 °C, the differences in the mechanical properties between the different PLVLs of this work were far less relevant, with most of them showing a fully elastomeric behaviour. Referring to the DMA measurements, the reduction in the peak of $\tan \delta$ (from ~ 2.5 to 0.5) through the glass transition was a clear indicator that crystalline domains formed during hydrolytic degradation in some of the polymers. However, the more amorphous PLVLs with short L-LA average sequence lengths ($l_{L-LA} < 2.91$) did not undergo changes in the storage modulus and $\tan \delta$ curves after two weeks submerged in PBS at 37 °C.

2.1.1. Introduction

Attaining a combination of strength and elasticity has been a particular challenge for researchers working on synthetic biodegradable polyesters. Copolymerization with a complementing monomer is the strategy typically employed to tailor the mechanical, thermal and biodegradation properties of a final polymer, thereby allowing the enhancement of the ductility of polylactides and polyglycolides. ϵ -caprolactone (ϵ -CL) and β -butyrolactone (β -BL) are two of the best-known cyclic esters and have been widely employed by many researchers in the past in numerous polymerization routes with lactide or glycolide [1-16]. ϵ -caprolactone is a seven membered ring with five methylene groups, which provides increased flexibility to the main chain of the polymer. Poly(ϵ -caprolactone) (PCL) homopolymer [17-18] presents a glass transition temperature (T_g) in the range of -60 to -65 °C, a melting point at 56-65 °C and biodegrades slowly, from several months to several years, as a result of its high crystallinity and hydrophobicity. The values, reported in literature, for its mechanical properties reflect high elongation at break values (750-1000 %) and Young's modulus between 210 and 444 MPa. On the contrary, β -butyrolactone is a four membered ring with a methyl side-group. Poly(3-hydroxybutyrate) (P3HB) [19-25], which can be synthesized by a fermentation process using bacteria or by the ring-opening polymerization of β -BL, contains a chiral centre (as does lactic acid) and the properties of the polymer depend upon the tacticity. P3HB, or simply polyhydroxybutyrate (PHB), has a T_g value of 1-5 °C, a melting point between 150-180 °C and a stiff and brittle behaviour (Young's modulus of 1688-3670 MPa, tensile strength of 28-36 MPa and elongation at break value of 1-7.5 %).

In the search for new biomaterials, several other lactones have attracted the interest of researchers. These cyclic esters (see Figure 1) include, among others, β -propiolactone (β -PL) [26-27], γ -butyrolactone (γ -BL) [28-29], γ -valerolactone (γ -VL) [30], δ -valerolactone (δ -VL), δ -methyl- ϵ -caprolactone [31], decalactones [32-33] (such as γ -decalactone (γ -DL), δ -decalactone (δ -DL) or ϵ -decalactone (ϵ -DL) with lactone ring

sizes of five, six or seven, respectively) and ω -pentadecalactone (PDL) [34-36]. However, β -PL monomer is a relatively potent carcinogen [37] and for this reason poly(β -propiolactone) has not usually been considered for use in biomedical applications. On the other hand, γ -BL and γ -VL (both lactones with a five-membered ring) do not undergo ring-opening polymerization as easily as other lactones do and are considered practically unpolymerisable [29,38] since they have a very small ring strain with low geometric distortion in the ester group. Likewise, Houk et al. [38], explaining the contrasting thermodynamic polymerizability of these cyclic lactones of different ring size, also demonstrated that the stability of the fully extended conformation is higher for δ -VL (six-membered ring without side-groups) than for γ -BL (five-membered ring).

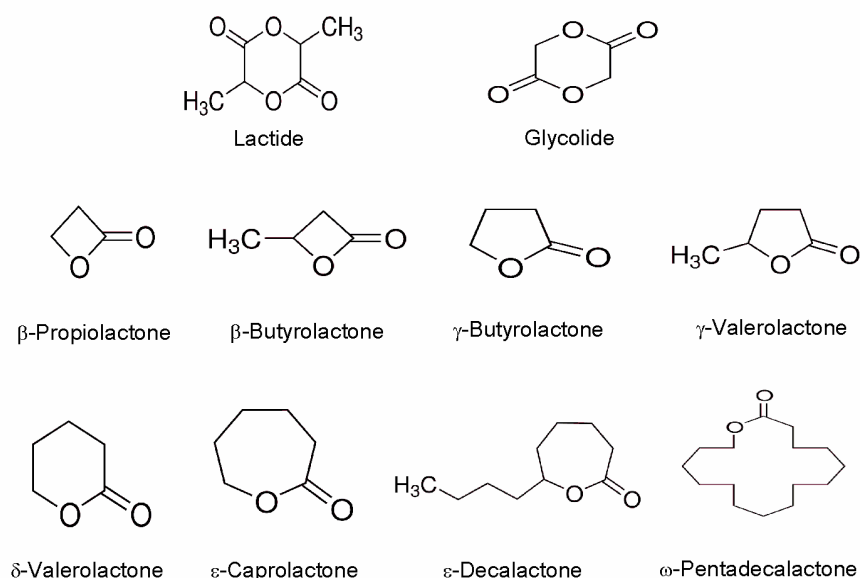


Figure 1. Scheme of some of the cyclic esters mentioned in the text.

δ -valerolactone does not approach the industrial importance of ϵ -caprolactone and has attracted less attention than the latter, above all because of their similar chemical properties (δ -VL has an identical structure to ϵ -CL but has four straight methylenes instead of five). Poly (δ -valerolactone) (PVL) [27, 39-41] is a semicrystalline aliphatic polymer with a low melting point of 57 °C and a glass transition temperature of approximately -55 °C and exhibits a less elastomeric behaviour than PCL (Young's modulus of 570 MPa and a strain at break of 150-200 %).

Both lactide-co- δ -valerolactone and lactide-co- ϵ -caprolactone copolymers can be employed in the biomedical field mainly for the regeneration of soft tissues and for various clinical implants and devices in which an elastomeric character is desirable [6]. The objective of this paper is to focus on the lactide-co- δ -valerolactone copolymers with the aim of identifying the potential advantages of these materials against the more popular poly(lactide- ϵ -caprolactone) polymers and, at the same time, of learning more about the mechanical behaviour of this kind of polyester. Thus, in this work several statistical poly(lactide-co- δ -valerolactone) polymers (PLVL), composed of δ -valerolactone (δ -VL), L-lactide (L-LA) and D-lactide (D-LA), and synthesized using different metal catalysts, were characterized by means of proton nuclear magnetic resonance spectroscopy (^1H NMR) and gel permeation chromatography (GPC) measurements. The mechanical performance of these polymeric materials was studied by testing their mechanical properties at room temperature (21 °C) and at 37 °C, the human body temperature at which these biomaterials are usually applied. Films of the PLVL copolymers were prepared for mechanical testing in order to evaluate the influence of the polymer composition and the chain distribution of sequences, comparing some of the results achieved to those from lactide-co- ϵ -caprolactone copolymers used in a previous study of ours [6]. In addition, the viscoelastic behaviour of the PLVLs was investigated by means of dynamic mechanical analysis (DMA). Dynamic mechanical measurements were carried out on non-degraded samples and on samples which were submerged for 14 days in a phosphate buffer saline (PBS) (pH 7.2) at 37 °C, with the objective of assessing the physical changes during the initial stages of degradation.

2.1.2. Materials and methods

Materials

L-lactide and D,L-lactide (also known as rac-lactide: 50:50 mix of L-LA and D-LA) monomers (assay > 99.5 %) were supplied by Purac Biochem (The Netherlands) while δ -valerolactone monomer was provided by Sigma Aldrich. Triphenyl bismuth (Ph_3Bi)

catalyst was obtained from Gelest. Stannous octoate (SnOct_2) (assay 95 %) and bismuth (III) subsalicylate (BiSS) (99.9 % metals basis) catalysts were supplied by Sigma Aldrich. Phosphate buffer saline (PBS) (pH 7.2) was obtained from Fluka Analytical (Sigma Aldrich).

Synthesis procedure

Statistical poly(lactide-co- δ -valerolactone) (PLVL) polymers of different L-lactide, D-lactide and δ -valerolactone content were synthesized in bulk by one pot-one-step ring-opening polymerizations (ROP). In each polymerization, predetermined amounts of L-LA, D,L-LA (50:50 mix of L-LA and D-LA) and δ -VL at the chosen mass feed ratio were simultaneously added and melted. Then, the catalyst was added. The PLVL polymerizations using BiSS as catalyst (1500:1 comonomers/catalyst molar ratio) and the synthesis reactions employing Ph_3Bi (1000:1 comonomers/catalyst molar ratio) were carried out for 72 hours at 130 °C. The copolymerization of the only PLVL synthesized with SnOct_2 (1665:1 comonomers/catalyst molar ratio) was conducted for 48 hours at 140 °C.

After the corresponding reaction time the products were dissolved in chloroform and precipitated, pouring the polymer solution into an excess of methanol in order to remove the catalyst impurities and those monomers that did not react. Finally the product was dried at room temperature and then given a heat treatment at 100 °C for 1 hour to ensure the complete elimination of solvent.

Methods

200-300 μm films were prepared by pressure melting at 140 °C and followed by water quenching so as to achieve an amorphous state. In the case of the single PLVL synthesized using SnOct_2 , with a melting peak at 135 °C, it was necessary to work at a temperature of 175 °C. From these films, repetitive samples for mechanical characterization (10x1cm²) and for the dynamic mechanical analysis (DMA) (0.4x2 cm²) were obtained. For the DMA study, dynamic mechanical measurements were carried out on non-degraded samples and on samples of PLVL copolymers which were placed in Falcon tubes containing phosphate buffered saline (PBS) (pH = 7.2) and

maintaining a surface area to volume ratio equal to 0.1 cm^{-1} . These samples were stored in an oven at $37 \text{ }^\circ\text{C}$ and were removed after 2 weeks from the PBS. Then they were air-dried overnight and vacuum-dried for another 48 h prior to their DMA characterization.

Proton nuclear magnetic resonance (^1H NMR) spectra were recorded in a Bruker Avance DPX 300 at a resonance frequency of 300.16 MHz, using 5 mm O.D. sample tubes. All spectra were obtained at room temperature from solutions of 0.7 mL of deuterated chloroform (CDCl_3). Experimental conditions were as follows: 10 mg of sample; 3 s acquisition time; 1 s delay time; $8.5 \mu\text{s}$ pulse; spectral width 5000 Hz and 32 scans.

The lactide methine signals, centered at 5.15 ppm and those of the α and ϵ methylenes of the δ -valerolactone, around 2.4 and 4.1 ppm, seen in the ^1H NMR spectrum can be assigned to the different dyads. The lactide and δ -valerolactone molar content and the microstructural magnitudes of the copolymers were obtained from the average dyad relative molar fractions. L-LA and D-LA are indistinguishable in the NMR spectrum so their contents and average sequence lengths are approximate values calculated on the assumption that the reactivities of both L-LA and D-LA are the same (having taken into account the L-LA/D-LA feed ratios). Equations 1-4 [4, 42] were employed to obtain the number-average sequence lengths (l_i), the Bernoullian random number-average sequence lengths (l_i) and the randomness character (R):

$$l_{\text{LA}} = \frac{2(\text{LA})}{(\text{LA} - \text{VL})} ; \quad l_{\text{VL}} = \frac{2(\text{VL})}{(\text{LA} - \text{VL})} \quad (1)$$

$$(l_{\text{LA}})_{\text{random}} = \frac{1}{(\text{VL})} ; \quad (l_{\text{VL}})_{\text{random}} = \frac{1}{(\text{LA})} \quad (2)$$

$$R = \frac{(l_{\text{LA}})_{\text{random}}}{l_{\text{LA}}} = \frac{(l_{\text{VL}})_{\text{random}}}{l_{\text{VL}}} \quad (3)$$

For the terpolymers:

$$l_{\text{L-LA}} = \frac{1}{((\text{D} - \text{LA}) + (\text{VL})) R} ; \quad l_{\text{D-LA}} = \frac{1}{((\text{L} - \text{LA}) + (\text{VL})) R} \quad (4)$$

where (LA) and (VL) are the lactide and δ -valerolactone molar fractions, obtained from the integration of the lactide methine signals and the δ -valerolactone methylene signals, (L-LA) and (D-LA) are the L-lactide and D-lactide approximate molar fractions and (LA-VL) is the LA-VL average dyad relative molar fraction.

The molecular weights of the polymers were determined by GPC using a Waters 1515 GPC device equipped with two Styragel columns (10^2 - 10^4 Å). Chloroform was used as eluent at a flow rate of 1 mL min^{-1} and polystyrene standards (Shodex Standards, SM-105) were used to obtain a primary calibration curve. The samples were prepared at a concentration of 10 mg in 1.25 mL.

The thermal properties were determined on a DSC 2920 (TA Instruments). Samples of 5-9 mg were heated from -50 °C to 175 °C at 20 °C min^{-1} . This first scan was used to determine the melting temperature (T_m), the heat of fusion (ΔH_m) and the glass transition temperatures (T_g) of the samples. After this first scan, the samples were quenched in the DSC and a second scan was made from -50 °C to 175 °C at 20 °C min^{-1} . In this second scan the glass transition temperatures were also determined from the inflection point of the heat flow curve.

The mechanical properties were determined by tensile tests with an Instron 5565 testing machine at a crosshead displacement rate of 10 mm min^{-1} . These tests were performed at room temperature (21 ± 2 °C) and at human body temperature (37 °C) following ISO 527-3/1995. The specimens had the following dimensions: overall length = 100 mm, distance between marks = 50 mm, width = 10mm; and were cut out from films of 200-300 μm thickness. The mechanical properties reported (secant modulus at 2%, yield strength or offset yield strength at 10 %, ultimate tensile strength and elongation at break) correspond to average values of at least 5 determinations. Mechanical testing at 37 °C was conducted in an Instron controlled temperature chamber. The tests were stopped at 300 % of strain due to the size limitations of the temperature chamber.

Dynamic mechanical measurements were carried out in duplicate using a DMA/SDTA861° (Mettler Toledo) in tensile mode. The samples (length = 5.5 mm, width = 4mm, thickness = 0.2-0.3 mm) were heated from -30 to 100 °C at a rate of 3 °C min^{-1} at a frequency of 1 Hz. The displacement and force amplitude were adjusted to 20

μm and 0.3 N, respectively. The evolution of storage modulus, loss modulus and $\tan \delta$ with temperature were recorded during the tests. The storage modulus is shown normalized in the different figures contained in this work so as to avoid errors related to sample dimensions measurements.

Statistical differences were analyzed using one-way analysis of variance (ANOVA) and p values of < 0.05 were considered significant. Tukey means comparison method and Levene's test for equal variance were employed.

2.1.3. Results and discussion

Characterization

Table 1. Characterization data of the different poly(lactide-co- δ -valerolactone) (PLVL).

Sample ¹ and Catalyst	Composition ¹ (% molar)			M_w kg mol ⁻¹	D	Microstructural Magnitudes ²					T_g ⁴ °C
	% L-LA	% D-LA	% VL			l_{LA}	l_{L-LA} ³	l_{D-LA} ³	l_{VL}	R	
PLVL 007525 BiSS	37.4	37.4	25.2	101.1	1.83	3.99	1.61	1.61	1.34	0.99	26.3
PLVL 002525 BiSS	62.3	12.5	25.2	87.7	1.82	4.19	2.80	1.21	1.41	0.95	29.6
PLVL 750025 BiSS	73.6	0	26.4	90.0	1.81	3.82	3.82	-	1.37	0.99	32.7
PLVL 008515 BiSS	42.9	42.9	14.2	110.8	1.83	7.42	1.84	1.84	1.23	0.95	37.2
PLVL 404515 BiSS	62.9	22.7	14.4	116.4	1.83	7.50	2.91	1.39	1.26	0.93	40.0
PLVL 69 Ph ₃ Bi	68.6	0	31.4	87.7	1.81	3.11	3.11	-	1.43	1.02	27.0
PLVL 71 Ph ₃ Bi	70.8	0	29.2	120.7	1.89	3.32	3.32	-	1.37	1.03	30.3
PLVL 74 Ph ₃ Bi	73.6	0	26.4	118.8	1.85	3.73	3.73	-	1.34	1.01	32.3
PLVL 70Sn SnOct ₂	70.1	0	29.9	129.1	1.88	4.94	4.94	-	2.11	0.68	31.0

¹ Calculated from ¹H NMR spectra. Because of the impossibility of offering the exact L-LA and D-LA molar content (indistinguishable in the NMR spectrum), approximate values are given under the assumption that the reactivity of both L-LA and D-LA are the same.

² l_{LA} and l_{VL} are the LA and VL number average sequence lengths obtained from ¹H NMR. These values are compared to the Bernoullian random number-average sequence lengths ($l_{LA}=1/VL$ and $l_{VL}=1/LA$), obtaining the randomness character value (R).

³ l_{L-LA} and l_{D-LA} are the L-LA and D-LA approximate values of number average sequence lengths under the assumption that the reactivity of both L-LA and D-LA are the same.

⁴ Obtained from the second scan of the DSC curves.

Table 1 summarizes the characterization data of the different PLVL films fabricated from the nascent polymers. In each sample name of those polymers from the upper part of the table (achieved using BiSS as catalyst), the first two digits represent the L-LA mass content; the following two the D,L-LA mass content and the last two the δ -VL mass content in the feeding mix. For example, PLVL 502525 was synthesized adding 50 wt. % of L-LA, 25 wt. % of D,L-LA and 25 wt. % of δ -VL. PLVL 69, PLVL 71 and PLVL 74 are L-lactide-co- δ -valerolactone copolymers synthesized with Ph_3Bi and PLVL 70Sn was obtained by copolymerizing L-LA and δ -VL employing SnOct_2 .

As can be seen, the molecular weights (M_w) of the different polymers range from 87 to 130 kg mol^{-1} (and dispersity (D) from 1.81 to 1.89) and are large enough in such a way that the impact on the mechanical properties can be assumed as negligible compared to sequence length distribution or polymer composition. As was expected for all these bismuth initiated PLVLs, they exhibited a random distribution of sequences ($R \sim 1$). In contrast, PLVL 70Sn, obtained using SnOct_2 , was moderately blocky having a randomness character value of 0.68.

PLVL 007525 (37.4 % of L-LA and 37.4 % of D-LA, $l_{\text{L-LA}} = l_{\text{D-LA}} = 1.61$ and $l_{\text{VL}} = 1.34$), PLVL 502525 (62.3 % of L-LA and 12.5 % of D-LA, $l_{\text{L-LA}} = 2.80$, $l_{\text{D-LA}} = 1.21$ and $l_{\text{VL}} = 1.41$) and PLVL 750025 (73.6 % of L-LA, $l_{\text{L-LA}} = 3.82$ and $l_{\text{VL}} = 1.37$) are lactide-co- δ -valerolactone polymers having a similar δ -VL content (~ 25 %), but a different L-LA/D-LA ratio. Their T_g s shifted to higher values (from 26 to 33 $^{\circ}\text{C}$) when the L-LA content was increased. Two more terpolymers richer in lactide (~ 86 %) were analyzed: PLVL 008515 (42.9 % of L-LA and 42.9 % of D-LA, $l_{\text{L-LA}} = l_{\text{D-LA}} = 1.84$ and $l_{\text{VL}} = 1.23$) and PLVL 404515 (62.9 % of L-LA and 22.7 % of D-LA, $l_{\text{L-LA}} = 2.91$, $l_{\text{D-LA}} = 1.39$ and $l_{\text{VL}} = 1.26$). They also show single T_g s, at 37 and 40 $^{\circ}\text{C}$, respectively.

L-lactide-co- δ -valerolactone copolymers of L-LA content ranging from 68.6 to 73.6 % ($l_{\text{L-LA}}$ from 3.11 to 3.73) were also evaluated in this work to assess the stiffening effect of L-LA, within the range of values of $l_{\text{L-LA}}$ in which most changes occurred in terms of capability of crystallization [5]. PLVL 69, PLVL 71 and PLVL 74 present their T_g s at 27, 30 and 32 $^{\circ}\text{C}$, respectively. Finally, the mechanical behaviour of a SnOct_2 - initiated PLVL, presenting an almost equal L-LA content to PLVL 71 (70.1 % vs. 70.8 %), was

also studied. Its moderately blocky character is reflected in its average sequence lengths of L-LA and δ -VL ($l_{L-LA} = 4.94$ and $l_{VL} = 2.11$) compared to the shorter sequence lengths ($l_{L-LA} = 3.32$ and $l_{VL} = 1.37$) of the previously mentioned PLVL 71.

Mechanical properties

The mechanical properties of 200-300 μm thick films obtained from the lactide-co- δ -valerolactone polymers in this work were measured with an Instron testing machine at room temperature (21 °C). The different PLVL polymeric materials displayed a partly elastomeric thermoplastic behaviour with a wide range of mechanical properties.

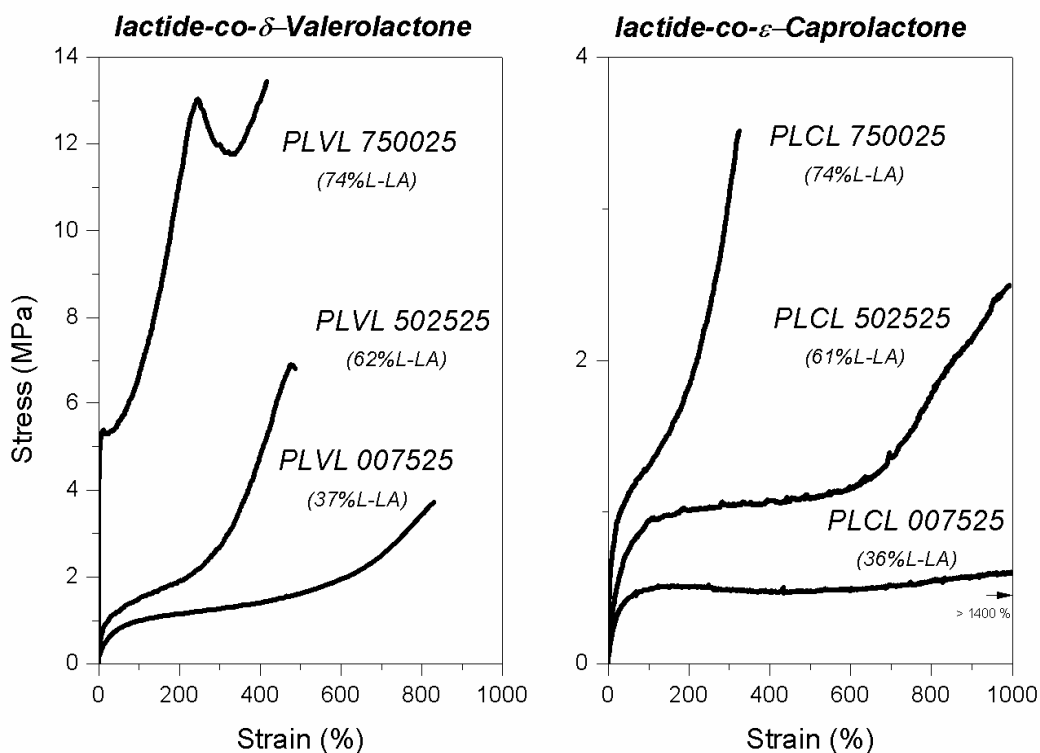


Figure 2. Tensile stress-strain curves of PLVLs and PLCLs that have approx. 75 % LA content.

Figure 2 shows typical stress-strain curves of the three PLVLs in this study, with a lactide content of approximately 75 %, (PLVL 007525, PLVL 502525 and PLVL 750025) and the stress-strain curves corresponding to the lactide-co- ϵ -caprolactone copolymers of a previous work of ours [6] that have intercomparable compositions. As can be seen it is possible to increase the stress related properties (elastic modulus and

strength) of the PLVLs and PLCLs by means of raising the L-LA content while maintaining the ϵ -CL or δ -VL content constant. The increase in L-LA content in the polymers brought about a mechanical behaviour change, from an elastomeric behaviour to that of a glassy plastic, reflecting the fact that the L-LA-unit blocks are responsible for this stiffening effect.

It is worth noting the scale of the two stress-axes of the curves featured in Figure 2, which belong to PLVLs (left) and PLCLs (right). The three PLVLs, thanks to the lower flexibility provided by the δ -VL-units with respect to ϵ -CL (with one less straight methylene sandwiched between the ester groups of the polymer chain) and therefore, due to their higher glass transition temperatures (ranging from 26 to 33 °C for the PLVLs and 12 to 28 °C for the PLCLs) showed a relevant improvement in their stiffness and strength over the PLCLs. As an illustration, the secant modulus of the PLVL 007525 (8.6 MPa) is almost twice than that of the rac-lactide/ ϵ -CL copolymer (PLCL 007525), moreover, PLVL 502525 presents a similar modulus (\sim 20 MPa) to that of the copolymer based on L-LA and ϵ -CL (secant modulus of 19.4 MPa and ultimate tensile strength (σ_u) = 3.2 MPa for PLCL 750025). PLVLs exhibit stress values at break within the range of 3.8 to 14.7 MPa, having an elongation at break of 831 % for PLVL 007525 and 417 % for the less elastomeric PLVL 750025. On the contrary, PLCL 007525, PLCL 502525 and PLCL 750025 present σ_u of 0.67, 2.3 and 3.2 MPa and elongation at break values $>$ 1400, 994 and 325 %, respectively [6]. The exceptionally high elastomeric response of PLCL 007525 and PLCL 502525, explained by their low T_g values and lower stereoregularity, makes them less useful for medical applications that require a suitable mechanical performance, at both room temperature (location of the device) and at human body temperature. In such cases, PLVLs of equal compositions displaying increased mechanical strength may be a more attractive substitute for the PLCLs. However, it should also be taken into consideration that at lower ϵ -CL or δ -VL contents, that is to say in the polymers richer in LA, the differences in the mechanical behaviour between PLVLs and PLCLs will be smaller.

PLVL 008515 and PLVL 404515, both with a lower δ -valerolactone content (\sim 14 % of δ -VL), exhibit a more glassy semicrystalline behaviour than the rest of the materials in this study, presenting neat yield points at 3.9 % and at 4.9 %, respectively. Both

polymers undergo an appreciable drop in the stress after the yield point but then the stress value fluctuates within a very narrow range while the specimens of these polymers continue to deform until they fail. PLVL 404515, with larger average sequence blocks of L-LA ($l_{L-LA} = 2.91$ for PLVL 404515 vs. $l_{L-LA} = 1.84$ for PLVL 008515), shows increased stress related properties with a secant modulus of 910.6 MPa, 29.0 MPa of yield strength and 16.9 MPa of ultimate tensile strength. In contrast, PLVL 008515 shows secant modulus values of 663.2 MPa, 16.3 MPa of yield strength and 10.1 MPa of σ_u . On the other hand, no yield point was observed in a previously studied rac-lactide-co- ϵ -caprolactone based copolymer [6], which had the same approximate lactide content (and ~ 16 % molar content of ϵ -CL) as these two PLVLs. The above mentioned PLCL 008515 displayed secant modulus of 146.5 MPa, σ_u of 5.4 MPa and 361 % of strain at break.

Table 2. Mechanical properties measured at room temperature (21 °C) of the different poly(lactide-co- δ -valerolactone) (PLVL) in this work.

Sample	Secant Modulus at 2 %	Yield Strength or Offset Yield Strength at 10 % ¹	Tensile Strength ²	Elongation at break	Strain Recovery after break ³
	(MPa)	(MPa)	(MPa)	(%)	(%)
PLVL 007525	8.6 ± 1.0	0.51 ± 0.03	3.8 ± 0.3	831	98.2 ± 0.3
PLVL 502525	20.8 ± 2.3	0.84 ± 0.06	6.9 ± 0.3	488	98.5 ± 0.3
PLVL 750025	213.7 ± 36.5	5.4 ± 0.3	14.7 ± 1.4	417	97.3 ± 0.5
PLVL 008515	663.2 ± 19.2	16.3 ± 0.9	10.1 ± 0.9	229	95.2 ± 1.3
PLVL 404515	910.6 ± 49.1	29.0 ± 1.7	16.9 ± 2.3	290	39.4 ± 3.7
PLVL 69	22.4 ± 1.4	0.9 ± 0.1	8.3 ± 0.5	522	98.9 ± 0.2
PLVL 71	29.3 ± 0.7	1.1 ± 0.1	13.8 ± 1.2	573	98.8 ± 0.2
PLVL 74	131.5 ± 7.4	3.3 ± 0.2	16.4 ± 0.8	533	98.2 ± 0.1
PLVL 70Sn	81.3 ± 12.4	2.6 ± 0.2	27.5 ± 2.3	620	98.9 ± 0.2

¹ Offset Yield Strength was calculated at a 10 % of strain using the secant modulus at 2 % as elastic modulus (E).

² The tensile strength was determined as ultimate stress value (σ_u).

³ Measured 24 hours after break.

The mechanical testing results of the featured polymers, together with the results of the L-lactide-co- δ -valerolactone copolymers of this work, are summarized in Table 2. It can be seen that all the PLVLs in the study displayed high elongation at break values, exceeding 229 % in all cases, and large strain recovery rates after break (higher than 95 %), the only exception being PLVL 404515 (39.4 %) the material that showed the highest T_g (40 °C) in the study, in addition to a significantly higher yield strength.

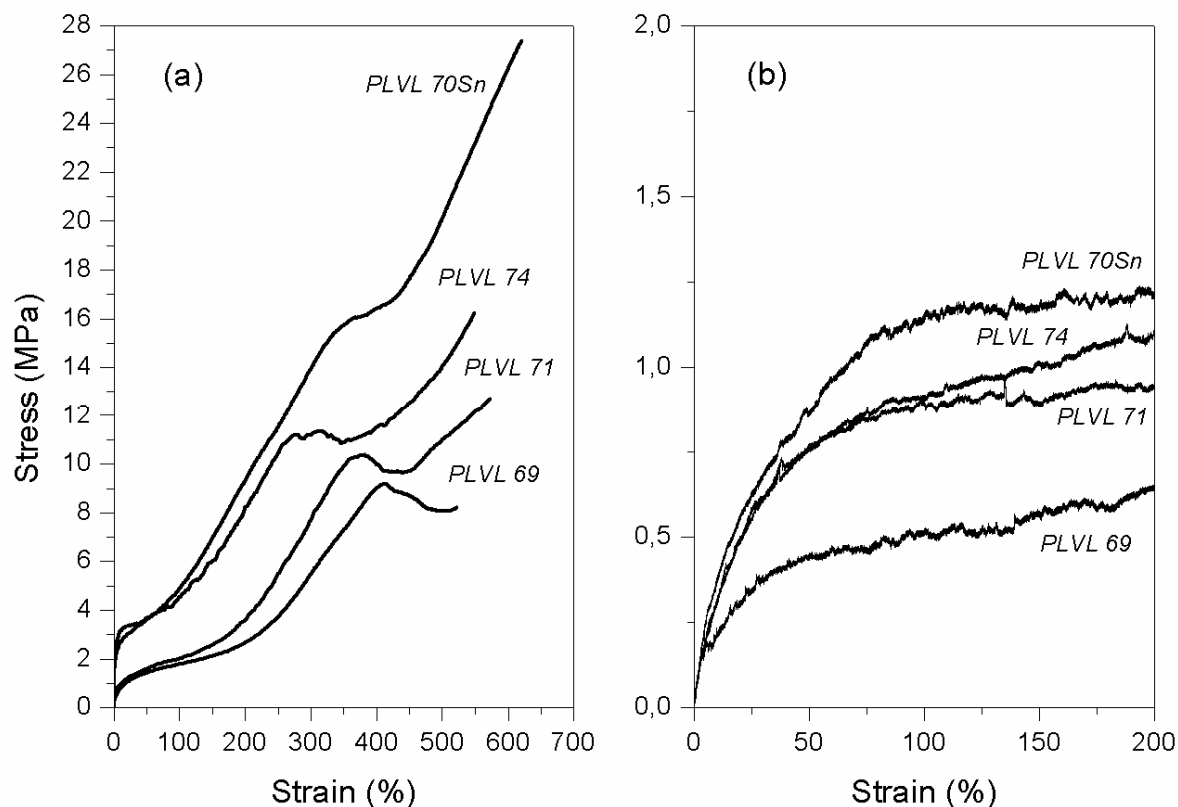


Figure 3. Tensile stress-strain curves of the L-lactide co- δ -valerolactone copolymers: (a) at room temperature (21 °C); (b) at human body temperature (37 °C).

Figure 3a shows the typical stress-strain curves of the copolymers synthesized from L-LA and δ -VL (not containing D-LA). Large differences were found between the mechanical properties of the L-LA-co- δ -VL copolymers within a narrow range of l_{L-LA} values (from 3.11 to 3.73). As the L-LA content and the L-LA average sequence length grow an increase in the stress related properties of the polymers was seen. PLVL 69 (68.6 % of L-LA and $l_{L-LA} = 3.11$) presents a secant modulus of 22.4 MPa, tensile strength of 8.3 MPa and strain at break of 522 %. However, it should be noted that

PLVL 71 (70.8 % of L-LA and $l_{L-LA} = 3.32$) and PLVL 74 (73.6 % of L-LA and $l_{L-LA} = 3.73$) show higher elongation at break values due to a cold-drawing deformation profile that appears in their stress-strain curves over 400 % of strain. These two copolymers exhibit secant modulus of 29.3 MPa and 131.5 MPa and ultimate stress values of 13.8 MPa and 16.4 MPa, respectively. Finally, the elevated tensile strength at break ($\sigma_u = 27.5$ MPa) of PLVL 70Sn, the moderately blocky copolymer ($R = 0.68$) of almost equal L-LA content to PLVL 71 (70.1 % vs 70.8 %) should also be mentioned. Its microstructural arrangement, with a larger average sequence of L-lactide blocks ($l_{L-LA} = 4.94$) in comparison to the $l_{L-LA} = 3.32$ of the previously mentioned PLVL 71, leads to a more glassy semicrystalline behaviour. At a certain point during the tensile test, the polymer chains may be aligned inducing a process of crystallization by orientation.

Table 3. Mechanical properties measured at human body temperature (37 °C) of the different poly(lactide-co- δ -valerolactone) (PLVL) of this work.

Sample	Secant Modulus at 2 %	Yield Strength or Offset Yield Strength at 10 % ¹	Tensile Strength at 300 %
	(MPa)	(MPa)	(MPa)
PLVL 007525	1.4 ± 0.3	0.15 ± 0.04	0.35 ± 0.05
PLVL 502525	4.5 ± 0.3	0.35 ± 0.04	0.59 ± 0.04
PLVL 750025	6.1 ± 0.4	0.57 ± 0.03	0.99 ± 0.03
PLVL 008515	7.4 ± 1.1	0.43 ± 0.03	1.30 ± 0.07
PLVL 404515	45.8 ± 4.8	1.32 ± 0.12	3.33 ± 0.21
PLVL 69	5.4 ± 0.3	0.28 ± 0.05	0.69 ± 0.03
PLVL 71	5.5 ± 0.4	0.48 ± 0.03	1.19 ± 0.02
PLVL 74	6.0 ± 0.9	0.48 ± 0.03	1.24 ± 0.09
PLVL 70Sn	5.8 ± 0.3	0.55 ± 0.03	1.41 ± 0.10

¹ Offset Yield Strength was calculated at a 10 % of strain using the secant modulus at 2 % as elastic modulus (E).

The results of the mechanical testing at 37 °C of the poly(lactide-co- δ -valerolactone) polymers are summarized in Table 3. As can be seen in Figure 3b, and from the evaluation of the data of the Table 3, the changes in the mechanical behaviour between the different polymers are much lower at human body temperature. At this temperature the polymeric materials are several degrees above their glass transition temperature and their mechanical response is quite similar. Only PLVL 404515 (T_g of 40 °C) does not display a fully elastomeric behaviour and had significantly different mechanical properties with respect to the rest of the polymers ($p < 0.05$); with secant modulus of 45.8 MPa, offset yield strength of 1.32 MPa and 3.33 MPa of tensile strength at 300 % of strain. PLVL 007525, PLVL 502525 and PLVL 750025 exhibit a secant modulus that ranges from 1.4 to 6.1 MPa, offset yield strength within 0.15 and 0.57 MPa and tensile strength values at 300 % of strain in the range of 0.35 to 0.99 MPa. PLVL 69, PLVL 71, PLVL 74 and PLVL 70Sn, whose stress-strain curves up to 200 % of strain are shown in Figure 3b, have analogous secant modulus values (approximately 5.5 MPa) and present slight differences in offset yield strength and tensile strength at 300 %.

Dynamic mechanical analysis (DMA)

DMA is becoming more and more popular in the laboratory as a tool to investigate the thermal transitions and the relaxation processes of polymers, including biodegradable polyesters such as polylactides, their blends and their copolymers [43-48]. These properties can be described in terms of either free volume changes or relaxation times and are closely related to the dynamic properties [49].

Figure 4 shows the curves of storage modulus (elastic modulus) and tangent of the phase angle ($\tan \delta$) of PLVL 007525, PLVL 502525 and PLVL 750025. The $\tan \delta$, also called the damping, is an indicator of how efficiently the material loses energy to molecular rearrangements and internal friction, it is also the ratio of the loss (E'') to the storage modulus (E'). Therefore, this factor is independent of geometry effects, and takes a value of zero for an elastic material and infinite for a viscous material. With regard to all the samples of poly(lactide-co- δ -valerolactone) in this work, the $\tan \delta$ is well below 0.1 at low temperatures, leading up to the glass transition (< 20 °C). The polymers are in glassy state and behave like a rigid body. Then, as the glass transition

temperature is approached (determined from the peak of the $\tan \delta$), a rapid decline in the storage modulus occurs and coincides with the rising of the $\tan \delta$ curve. $\tan \delta$ reaches a peak value in the range of 2.0 to 2.8 for all the non-degraded samples which were fully amorphous in their initial state. At this point, the contribution of the loss modulus is higher than that of the storage modulus and PLVLs, thanks to their viscoelastic character, are able to dissipate part of the mechanical energy that they received. Finally, once the glass transition is passed, the $\tan \delta$ declines to a level close to the pre-transition values until the material reaches a viscous liquid state (amorphous polymers) or its melting point (semicrystalline polymers, such as some of the degraded samples). The low storage modulus values above the T_g of these polymers, indicate that only a small load is required to deform the material.

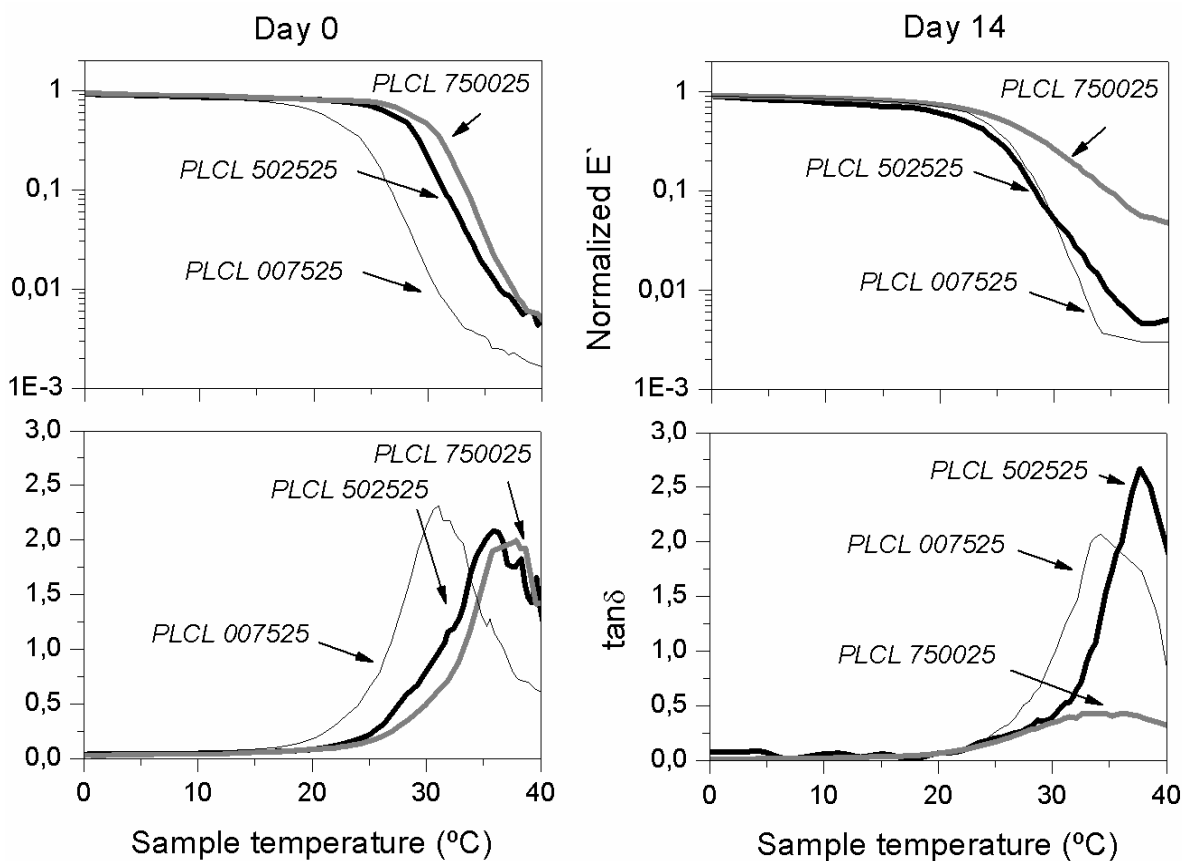


Figure 4. Storage modulus and $\tan \delta$ curves of PLVL 007525, PLVL 502525 and PLVL 750025: (a) non-degraded samples; (b) after 14 days of hydrolytic degradation at 37 °C.

As seen in the plot on the left of the Figure 4 (non-degraded samples of the three PLVLs which have approximately 75 % lactide content), an increase in the L-LA/D-LA ratio at the same content in δ -VL, brings about a growth in the glass-rubber transition of the polymers. This is easily distinguished by looking at the shift in the peak of $\tan \delta$ to higher values and is related to the fact that D-LA units disrupt the microstructural arrangement of the L-LA crystallizable chains, shortening their average sequence length ($l_{L-LA} = 1.61$ for PLVL 007525 and $l_{L-LA} = 2.80$ for PLVL 502525 vs. $l_{L-LA} = 3.82$ for PLVL 750025). As a consequence, more disordered structures are achieved, with lower T_g s (31 and 34 °C for the terpolymers vs. 37 °C for PLVL 750025). After 14 days of hydrolytic degradation, the $\tan \delta$ curves of PLVL 007525 and PLVL 502525 remain almost unchanged, not undergoing any noteworthy variations; the same occurred with the peak temperature and the peak width (in that hypothetical case, it may be associated to enthalpy relaxation changes at the T_g [43]). However, the copolymer composed of L-LA and δ -VL (PLVL 750025), was prone to crystallize and after 14 days of degradation presents a crystalline phase with a melting enthalpy of 19.9 J g⁻¹, measured by Differential Scanning Calorimetry (DSC). As a result, its storage modulus decreases but not as dramatically as those of the other polymers. Thanks to the fact that it is semicrystalline it does not soften too much above glass transition and exhibits certain solid state properties until approaching the melting point. Referring to its $\tan \delta$ curve, the peak height of PLVL 750025 did not exceed a value of 0.5, having a value of 2.0 before the start of the hydrolytic degradation process. This fact is explained by the less efficient process of energy dissipation resulting from the L-LA crystalline domains formed during degradation. Therefore, the reduction in the peak of $\tan \delta$ through the glass transition could serve as a relative indicator of degree of crystallinity [44, 47]. These rearrangements leading to a development of a crystalline phase may be accompanied by a loss of elastomeric character in the polymer [50].

The curves of PLVL 008515 and PLVL 404515 (not shown), like the other L-LA, D-LA and δ -VL based terpolymers in this work, were not affected by the hydrolytic degradation process either. Non-degraded samples as well as the ones degraded show T_g s at ~ 41 and 46 °C, respectively, and a maximum of $\tan \delta$ of ~ 2.8. Accordingly, it could be concluded that the PLVL samples of short average sequence lengths ($l_{L-LA} <$

2.91) did not undergo changes in their dynamic mechanical behaviour after 14 days submerged in PBS.

Figure 5 presents the $\tan \delta$ curves of the L-lactide-co- δ -valerolactone copolymers (containing 69, 71 and 74 % of L-LA) in their initial state (on the left) and after 14 days degraded *in vitro* at 37 °C (on the right). As can be observed, the peak height of $\tan \delta$ from PLVL 69, PLVL 71 and PLVL 74, decreased to an approximate value of 0.5-0.7 as a result of the crystallization process of L-LA. The rapid increase in the crystallinity was demonstrated by DSC analysis; the measured melting enthalpy of these three copolymers on day 14 was 14.2, 14.6 and 19.5 J g⁻¹, respectively, while the featured melting peaks appeared at temperatures within the range of 82 to 104 °C. On the other hand, it is also worth noting that the migration of lactide from the amorphous phases to the crystalline phase leads to a displacement of the T_g to lower values. This point is detected in both the first DSC scans (not shown) and the $\tan \delta$ curves. The T_g of PLVL 69, taken from the peak of $\tan \delta$, shifts from 33 to 28 °C and the T_g s of PLVL 71 and PLVL 74 decreased by about 3 °C.

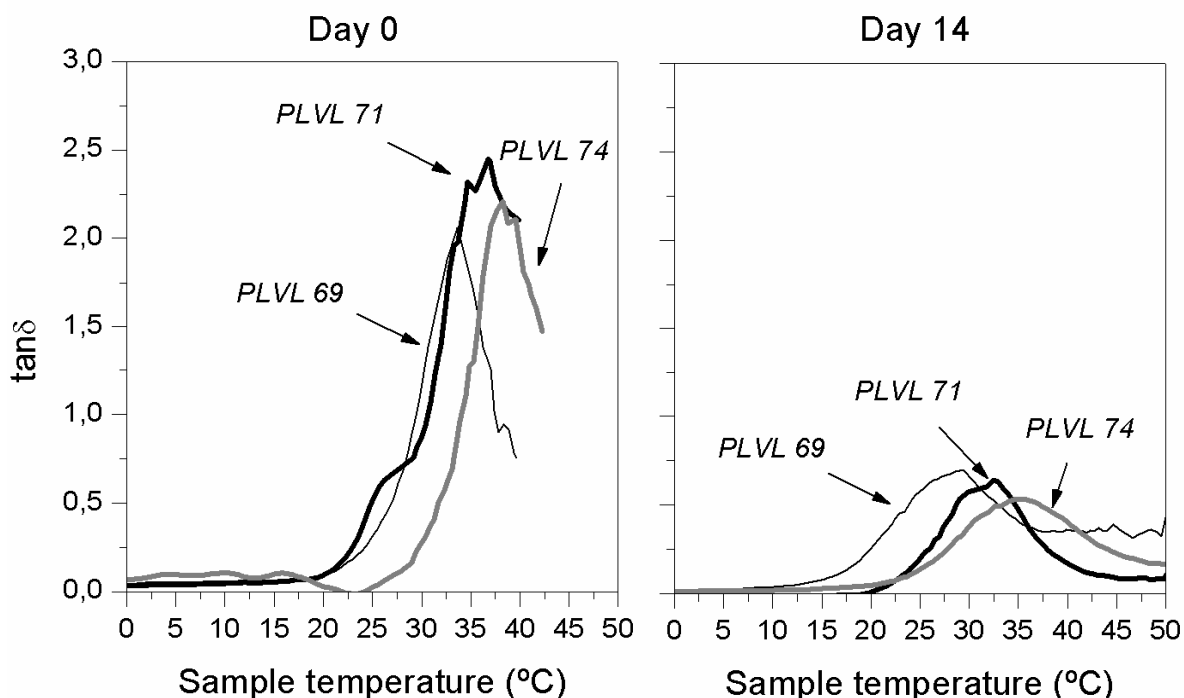


Figure 5. $\tan \delta$ curves on day 0 and after 14 days of hydrolytic degradation of PLVL 69, PLVL 71 and PLVL 74 L-lactide-co- δ -valerolactone copolymers.

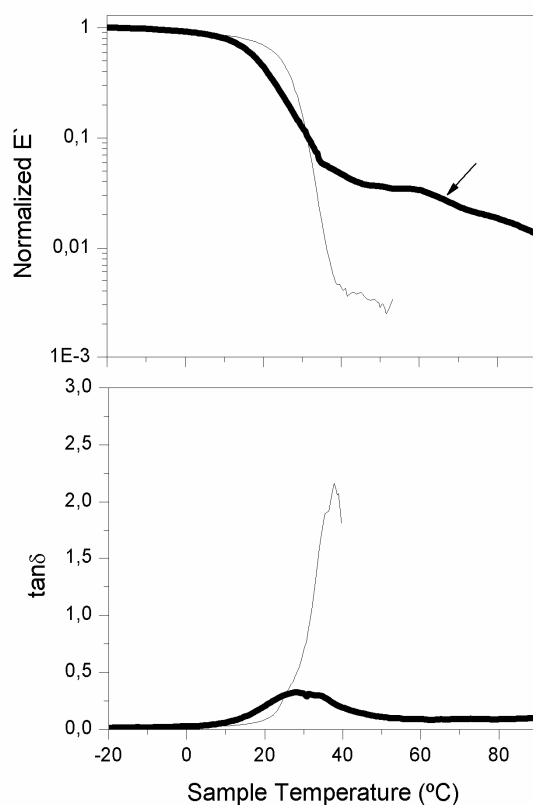


Figure 6. Storage modulus and $\tan \delta$ curves of PLVL 70Sn on day 0 and after 14 days of degradation (in bold).

Figure 6 shows the storage modulus and $\tan \delta$ curves belonging to PLVL 70Sn. This copolymer has almost equal L-LA content to PLVL 71 (70.1 % vs 70.8 %) but presents a moderately blocky character ($R = 0.68$ and $I_{L-LA} = 4.94$) that confer a higher capability to crystallize during degradation. Therefore, on day 14 of degradation a melting peak of 17.6 J g^{-1} at $139 \text{ }^\circ\text{C}$ was found in the DSC scan. This melting temperature is considerably higher than the one corresponding to the random PLVL 71 ($T_m = 89 \text{ }^\circ\text{C}$), mainly due to the formation of more ordered and perfect crystallites of L-LA. In the storage modulus and $\tan \delta$ plots the large differences between the curves of the non-degraded sample and those corresponding to the sample degraded for two weeks can clearly be seen. The storage modulus of the degraded copolymer (in bold type) falls in a more continuous way, not as fast as the non-degraded modulus, because of the presence of a crystalline matrix which provides some stiffness above the T_g . Moreover, the storage modulus curve drops in two steps, both being related to two glass transition temperatures, corresponding well with the DSC results in which two T_g s were

also observed. The $\tan \delta$ curve shows only the first transition. The peak of $\tan \delta$ has a height of 0.3 and is the lowest of all the samples in this work, with a value eight times lower than the peak of $\tan \delta$ on day 0. It is centred at 29 °C when it rises to 37 °C in the non-degraded sample. The second T_g that appears at 73 °C in the DSC curve was not measurable by means of the $\tan \delta$ peak method of determining the glass transition.

Table 4 presents the characteristic thermal values of the different polymers studied in this work (non-degraded and after 14 days of hydrolytic degradation at 37 °C), achieved through DSC, the T_g values determined from the peak of the $\tan \delta$ and the height of the $\tan \delta$ peak, which is used to express the magnitude of the transition. It should be stated that these T_g values obtained by dynamic mechanical measurements were higher (by 5-10 °C) than in the case of those taken from the DSC analysis.

Table 4. DMA and DSC results of the studied PLVLs on day 0 and after 14 days of degradation.

Sample		DMA		1 st DSC SCAN		
		T_g (°C) ¹	$\tan \delta$	T_g (°C)	T_m (°C)	ΔH_m (J g ⁻¹)
PLVL 007525	day 0	31	2.2	24.7	-	-
	day 14	34	2.4	25.8	-	-
PLVL 502525	day 0	35	2.4	27.5	-	-
	day 14	37	2.6	29.4	-	-
PLVL 750025	day 0	37	2.0	30.6	-	-
	day 14	34	0.5	26.0	111.8	19.9
PLVL 008515	day 0	41	2.8	34.6	-	-
	day 14	40	2.8	37.3	-	-
PLVL 404515	day 0	46	2.8	37.2	-	-
	day 14	46	2.7	37.9	-	-
PLVL 69	day 0	33	2.2	26.6	-	-
	day 14	28	0.7	20.0	82.2	14.2
PLVL 71	day 0	35	2.5	28.3	-	-
	day 14	32	0.7	26.3	88.5	14.6
PLVL 74	day 0	38	2.3	30.3	-	-
	day 14	35	0.5	28.1	104.0	19.5
PLVL 70Sn	day 0	37	2.4	31.5	-	-
	day 14	29/ T_g^2	0.3	18.8/72.8	139.2	17.6

¹ T_g value was obtained from the peak of the curve of $\tan \delta$.

² A second T_g was observed in the storage modulus curve but it could not be quantified in the $\tan \delta$ curve.

2.1.4. Conclusions

In this work the mechanical performance of several poly(lactide-co- δ -valerolactone) polymers (PLVL) was studied by means of mechanical testing and dynamic mechanical analysis (DMA). For this purpose, a series of statistical PLVLs composed of δ -valerolactone (δ -VL), L-lactide (L-LA) and D-lactide (D-LA), were synthesized using BiSS, PH_3Bi or SnOct_2 as catalysts and characterized by means of proton nuclear magnetic resonance spectroscopy (^1H NMR) and gel permeation chromatography (GPC) measurements. The similarity between the units of δ -valerolactone and ϵ -caprolactone (four and five straight methylenes in their structure) and the analogous thermal properties of the respective homopolymers suggest that the mechanical behaviour of PLVLs and the polymers based on lactide and ϵ -caprolactone (PLCL) should be similar. However, major differences were found when comparing the mechanical properties at room temperature (21 ± 2 °C) of both kinds of polymeric materials. PLVLs, having higher glass transition temperatures than the PLCLs of equal composition, showed an increase in their stress related properties (secant modulus, yield strength and ultimate tensile stress), which is translated into an important improvement in their stiffness and strength. Therefore, this type of copolymer may be more attractive as a substitute for the PLCLs employed in some medical applications; when highly flexible and deformable materials with adequate mechanical strength are both required.

The changes in the mechanical behaviour between the different PLVLs were much lower at human body temperature (37 °C). At this temperature, the polymers are several degrees above their glass transition temperature (T_g) and their mechanical performance presented small differences, most of them displaying a fully elastomeric behaviour. Dynamic mechanical measurements were also carried out on non-degraded samples and on samples which were degraded for 14 days in phosphate buffer saline (PBS) (pH 7.2) at 37 °C. This technique demonstrated that the rubbery transition of the polymers depends on the L-LA/D-LA ratio. At the same content in δ -VL, an increase in the L-LA/D-LA ratio has an impact on the T_g of the polymers (taken from the peak of $\tan \delta$), and raises their values. The more amorphous PLVLs of short average sequence lengths ($l_{\text{L-LA}} < 2.91$) did not undergo any changes in their storage modulus and $\tan \delta$ curves and

these were almost identical on day 0 and after 14 days of degradation. However, with compositions richer in L-LA, the L-LA sequence blocks are large enough to form crystalline organized structures, proved by thermal analysis, and on day 14 of the study the $\tan \delta$ values were significantly lower than before submerging the samples in PBS. This is because the materials dissipate energy less efficiently, as a result of the supramolecular arrangements that occurred in their polymer chains during degradation.

References

- [1] Grijpma, D.W.; Pennings, A.J. Polymerization temperature effects on the properties of L-lactide and ϵ -caprolactone copolymers. *Polymer Bulletin* 1991, 25, 335-341.
- [2] Vanhoorne, P.; Dubois, P.; Jerome, R.; Teyssie, P. Macromolecular engineering of polylactones and polylactides. 7. Structural analysis of copolyesters of epsilon-caprolactone, L-lactide or D,L-lactide initiated by AL(OIPR)₃. *Macromolecules* 1992, 25, 37-44
- [3] HiljanenVainio, M.; Karjalainen, T.; Seppala, J. Biodegradable lactone copolymers .1. Characterization and mechanical behavior of epsilon-caprolactone and lactide copolymers. *Journal of Applied Polymer Science* 1996, 59, 1281-1288.
- [4] Fernández, J.; Etxeberria, A.; Sarasua, J.R. Synthesis, structure and properties of poly(L-lactide-co- ϵ -caprolactone) statistical copolymers. *Journal of the Mechanical Behavior of Biomedical Materials* 2012, 9, 100-112.
- [5] Fernández, J.; Meaurio, E.; Chaos, A.; Etxeberria, A.; Alonso-Varona, A.; Sarasua J.R. Synthesis and characterization of poly(L-lactide/ ϵ -caprolactone) statistical copolymers with well resolved chain microstructures. *Polymer* 2013, 54, 2621-2631.
- [6] Fernández, J.; Larrañaga, A.; Etxeberria, A.; Wang, W.; Sarasua, J.R. A new generation of poly(lactide/ ϵ -caprolactone) polymeric biomaterials for application in the biomedical field. *Journal of Biomedical Materials Research A* 2014, 102A, 3573–3584.
- [7] Lu, X.L.; Cai, W.; Gao, Z.Y. Shape-memory behaviors of biodegradable poly(L-lactide-co- epsilon-caprolactone) copolymers. *Journal of Applied Polymer Science* 2008, 108, 1109-1115.
- [8] Kricheldorf, H.R.; Mang, T.; Jonte, J.M. Polylactones .1. Copolymerization of glycolide and epsilon-caprolactone. *Macromolecules* 1984, 17, 2173-2181.
- [9] Dobrzynski, P.; Li, S.; Kasperczyk, J.; Bero, M.; Gasc, F.; Vert, M. Structure property relationships of copolymers obtained by ring-opening polymerization of glycolide and ϵ -caprolactone. Part 1. Synthesis and characterization. *Biomacromolecules* 2005, 6, 483-488.
- [10] Li, S.; Dobrzynski, P.; Kasperczyk, J.; Bero, M.; Braud, C.; Vert, M. Structure property relationships of copolymers obtained by ring-opening polymerization of glycolide and ϵ -caprolactone. Part 2. Influence of composition and chain microstructure on the hydrolytic degradation. *Biomacromolecules* 2005, 6, 489-497.

- [11] Kasperczyk, J.; Li, S.; Jaworska, J.; Dobrzyński, P.; Vert, M. Degradation of copolymers obtained by ring-opening polymerization of glycolide and ϵ -caprolactone: A high resolution NMR and ESI-MS study. *Polymer Degradation and Stability* 2008, 93, 990-999.
- [12] Yoo, Y.C.; Kim, H.Y.; Jin, F.L.; Park, S.J. Synthesis of poly(glycolide-caprolactone) copolymers for application as bioabsorbable suture materials. *Macromolecular Research* 2013, 21, 687-692.
- [13] Lee, S.H.; Kim, B.S.; Kim, S.H.; Choi, S.W.; Jeong, S.I.; Kwon, I.K.; Kang, S.W.; Nikolovski, J.; Mooney, D.J.; Han, Y.K.; Kim, Y.H. Elastic biodegradable poly(glycolide-co-caprolactone) scaffold for tissue engineering. *Journal of Biomedical Materials Research Part A*, 2003, 66, 29-37.
- [14] Grunova, E.; Kirillov, E.; Roisnel, T.; Carpentier, J.F. Group 3 Metal Complexes of Salen-like Fluorous Dialkoxy-Diimino Ligands: Synthesis, Structure, and Application in Ring-Opening Polymerization of rac-Lactide and rac-beta-Butyrolactone. *Organometallics* 2008, 27, 5691-5698.
- [15] Jeffery, B.J.; Whitelaw, E.L.; Garcia-Vivo, D.; Stewart, J.A.; Mahon, M.F.; Davidson, M.G.; Jones, M.D. Group 4 initiators for the stereoselective ROP of rac-beta-butyrolactone and its copolymerization with rac-lactide. *Chemical Communications* 2011, 47, 12328-12330.
- [16] Cross, E.D.; Allan, L.E.N.; Decken, A.; Shaver, M.P. Aluminum salen and salan complexes in the ring-opening polymerization of cyclic esters: Controlled immortal and copolymerization of rac-beta-butyrolactone and rac-lactide. *Journal of Polymer Science Part A: Polymer Chemistry* 2013, 51, 1137-1146.
- [17] Labet, M.; Thielemans, W. Synthesis of polycaprolactone: a review. *The Royal Society of Chemistry* 2009, 38, 3484-3504.
- [18] Woodruff, M.A.; Hutmacher, D.W. The Return of a forgotten polymer: Polycaprolactone in the 21st century. *Progress in polymer Science* 2010, 35, 1217-1256.
- [19] Hazer, D.B.; Ebru, K.; Hazer, B. Poly(3-hydroxyalkanoate)s: Diversification and biomedical applications: A state of the art review. *Materials Science and Engineering C* 2012, 32, 637-647.
- [20] Poirier, Y.; Dennis, D.; Klomparens, K.; Somerville, C. Polyhydroxybutyrate, a biodegradable thermoplastic produced in transgenic plants. *Science* 1992, 256, 520-223.
- [21] Hori, Y.; Yamaguchi, A.; Hagiwara, T. Chemical synthesis of high molecular weight poly(3-hydroxybutyrate-co-4-hydroxybutyrate). *Polymer* 1995, 36(24), 4703-4705.
- [22] Pajerski, A.D.; Lenz, R.W. Stereoregular polymerisation of β -butyrolactone by aluminoxane catalysis. *Makromolekulare Chemie. Macromolecular Symposia* 1993, 73, 7-26.

- [23] Nakamura, S.; Doi, Y.; Scandola, M. Microbial synthesis and characterisation of poly(3-hydroxybutyrate-co- 4-hydroxybutyrate). *Macromolecules* 1992, 25(17), 4237–4241.
- [24] Brulé, E.; Gaillard, S.; Rager, M-N.; Roisnel, T.; Guérineau, V.; Nolan, S.P.; Thomas, C.M. Polymerization of Racemic β -Butyrolactone Using Gold Catalysts: A Simple Access to Biodegradable Polymers. *Organometallics* 2011, 30, 2650-2653.
- [25] Freier, T.; Kunze, C.; Nischan, C.; Kramer, S.; Sternberg, K.; SaX, M., Hopt, U.T.; Schmitz, K-P. In vitro and in vivo degradation studies for development of a biodegradable patch based on poly(3-hydroxybutyrate). *Biomaterials* 2002, 23, 2649–2657.
- [26] Crescenzi, V.; Manzini, G.; Calzolari, G.; Borri, C. Thermodynamics of fusion of poly(beta-propiolactone) and poly(epsilon-caprolactone) comparative analysis of melting of aliphatic polylactone and polyester chains. *European Polymer Journal* 1972, 8, 449-463.
- [27] Na, Y-H.; He, Y.; Asakawa, N.; Yoshie, N.; Inoue, Y. Miscibility and phase structure of blends of poly(ethylene oxide) with poly(3-hydroxybutyrate), poly(3-hydroxypropionate), and their copolymers. *Macromolecules* 2002, 35(3), 727–735.
- [28] Martin, D.P.; Williams, S.F. Medical applications of poly-4-hydroxybutyrate: a strong flexible absorbable biomaterial. *Biochemical Engineering Journal* 2003, 16, 97–105.
- [29] Moore, T.; Adhikari, R.; Gunatillake, P. Chemosynthesis of bioresorbable poly(γ -butyrolactone) by ring-opening polymerization: a review. *Biomaterials* 2005, 26, 3771-3782.
- [30] Lee, C.W.; Urakawa, R.; Kimura, Y. Copolymerization of γ -valerolactone and β -butyrolactone. *European Polymer Journal* 1998, 34, 117-122.
- [31] Martello, M.T.; Hillmyer, M.A. Polylactide. Poly(6-methyl- ϵ -caprolactone)-Polylactide thermoplastic elastomers. *Macromolecules* 2011, 44, 8537-8545.
- [32] Martello, M.T.; Hillmyer, M.A. Bulk Ring-Opening Transesterification Polymerization of the Renewable δ -Decalactone Using an Organocatalyst. *ACS Macro Letters* 2012, 1, 131-135.
- [33] Olsén, P.; Borke, T.; Odélius, K.; Albertsson, A.C. ϵ -Decalactone: A thermoresilient and toughening comonomer to poly(L-lactide). *Biomacromolecules* 2013, 14, 2883-2890.
- [34] de Geus, M.; van der Meulen, I.; Goderis, B.; van Hecke, K.; Dorschu, M.; van der Werff, H.; Coning, C.E.; Heise, A. Performance polymers from renewable monomers: high molecular weight poly(pentadecalactone) for fiber applications. *Polymer Chemistry* 2010, 1, 525-533.

- [35] Jiang, Z.; Azim, H.; Gross, R.A. Lipase-Catalyzed Copolymerization of ω -Pentadecalactone with p-Dioxanone and Characterization of Copolymer Thermal and Crystalline Properties. *Biomacromolecules* 2007, 8, 2262-2269.
- [36] Bouyahyi, M.; Duchateau, R. Metal-Based catalysts for Controlled Ring-Opening Polymerization of Macrolactones: High Molecular Weight and Well-Defined Copolymer Architectures. *Macromolecules* 2014, 47, 517-524.
- [37] Cheeseman, M.A.; Machuga, E.J.; Bayley, A.B. A tiered approach to threshold of regulation. *Food and Chemical Toxicology* 1999, 37, 387-412.
- [38] Houk, K.N.; Jabbari, A.; Hall, Jr HK.; Alemán, C. Why δ -valerolactone Polymerizes and γ -butyrolactone Does Not. *The Journal of Organic Chemistry* 2008, 73, 2674-2678.
- [39] Aubin, M. ; Prud'homme, R.E. Preparation and properties of poly(valerolactone). *Polymer* 1981, 22, 1223-1226.
- [40] Cao, H.; Han, H.; Li, G.; Yang, J.; Zhang, L.; Yang, Y.; Fang, X.; Li, Q. Biocatalytic Synthesis of Poly(δ -Valerolactone) Using a Thermophilic Esterase from *Archaeoglobus fulgidus* as Catalyst. *International Journal of Molecular Sciences* 2012, 13, 12232–12241.
- [41] Nakayama, A.; Kawasaki, N.; Maeda, Y.; Arvanitoyannis, I.; Aiba, S.; Yamamoto, N. Study of biodegradability of poly(delta-valerolactone-co-L-lactide)s. *Journal of Applied Polymer Science* 1997, 66, 741-748.
- [42] Herbert, I.R. Statistical analysis of copolymer sequence distribution. In *NMR Spectroscopy of Polymers*. Ibbet, R.N. Ed.: Blackie Academic & Professional, London, 1993:50-79. (Chapter 2).
- [43] Pan, P.; Zhu, B.; Inoue, Y. Enthalpy relaxation and Embrittlement of Poly(L-lactide) during Physical Aging. *Macromolecules* 2007, 40, 9664-9671.
- [44] López-Rodríguez, N.; López-Arraiza, A.; Meaurio, E.; Sarasua, J.R. Crystallization, Morphology, and Mechanical Behavior of Polylactide/Poly(ϵ -caprolactone) blends. *Polymer Engineering and Science* 2006, 46, 1299-1308.
- [45] Helminen, A.O.; Korhonen, H.; Seppala, J.V. Cross-linked Poly(ϵ -caprolactone/D,L-lactide) copolymers with elastic properties. *Macromolecular Chemistry and Physics* 2002; 203, 2630-2639.
- [46] Zuza, E.; Ugartemendia, J.M.; López, A.; Meaurio, E.; Lejardi, A.; Sarasua, J.R. Glass transition behavior and dynamics fragility in polylactides containing mobile and rigid amorphous fractions. *Polymer* 2008, 49, 4427-4432.

[47] Lizundia, E.; Petisco, S.; Sarasua, J.R. Phase-structure and mechanical properties of isothermally melt- and cold-crystallized poly(L-lactide). *Journal of Mechanical Behavior of Biomedical Materials* 2013, 17, 242:251.

[48] Urayama, H.; Kanamori, T.; Kimura, Y. Microstructure and Thermomechanical Properties of Glassy Polylactides with Different Optical Purity of the Lactate Units. *Macromolecular Materials and Engineering* 2001, 286, 705-713.

[49] Menard, K.P. Dynamic mechanical analysis: a practical introduction. CRC Press LLC, Boca Raton (Florida), 1999.

[50] Fernández, J.; Larrañaga, A.; Etxeberria, A.; Sarasua, J.R. Effects of chain microstructures and derived crystallization capability on hydrolytic degradation of poly(L-lactide/ ϵ -caprolactone) copolymers. *Polymer Degradation and Stability* 2013, 98, 481-489.

**Chapter 2.2 *In Vitro* Degradation Study
of Biopolyesters Using Lactide-co- δ -
Valerolactone Copolymers**

Polymer Degradation and Stability 2015, 112, 104-116.

Abstract

The *in vitro* hydrolytic degradation study was carried out at 37 °C on lactide-co- δ -valerolactone (PLVL) biopolyesters and demonstrated that water uptake was favoured by the resistance of polymers to crystallize, the presence of large amorphous domains and the decrease in microstructural stereoregularity of the polymer chains. Those copolymers that displayed higher levels of water absorption (WA > 30 % on day 42) experienced the fastest degradation rates. Thus, two amorphous rac-lactide-co- δ -VL, with a δ -VL content of 25 % and 15 % and short L-lactide and D-lactide segments, showed degradation rates (K_{Mw}) of 0.060 and 0.047 days⁻¹, respectively, the highest of the study. On the other hand, high T_g s (> 37 °C) and a greater capacity to crystallize (with L-LA-unit average sequence lengths > 3.82), hinder water diffusion inside the polymer. For example, an 82:18 L-LA-co- δ -VL copolymer (K_{Mw} = 0.017 days⁻¹) did not lose weight until day 98 when it began to absorb water. Conversely, amorphous PLVL 53 (53.4 % of L-LA and 46.6 % of δ -VL) exhibited a K_{Mw} (0.030 days⁻¹) that was slightly lower than those of the crystallisable copolymers with L-LA contents between 69 and 74 %. WA started at shorter times due to its low T_g (at 6 °C), however, its more hydrophobic character and lower amount of ester groups slowed its hydrolysis rate down. It is also worth stating that the PLVLs degraded at a slower rate than the lactide-co- ϵ -caprolactone (PLCLs) of the same composition. This can be explained by the fact that PLVLs, despite presenting a higher proportion of hydrolyzable esters than PLCLs, have more packed amorphous regions related to higher T_g s. To illustrate this, rac-LA-co-CL 85:15 used in a previous work of ours presented a K_{Mw} of 0.066 days⁻¹ and a T_g value of 29 °C whereas the equivalent PLVL of this study has a K_{Mw} of 0.047 days⁻¹ and a T_g of 37 °C.

2.2.1. Introduction

When a biodegradable material is implanted in the human body, medical staff have to know how it is actually going to behave [1, 2]. Therefore, several parameters should be taken into consideration when designing and producing a medical device. The degradation rate should be predicted and adjusted and at the same time the period during which the biomaterial will support actual mechanical performance must be determined. In addition, the changes in the thermal and mechanical properties and the morphological modifications that the biomaterial may undergo during degradation have to be assessed in detail and, in order to avoid undesirable body reactions [3], the remnants and polymer fragments leaving the biomaterial must also be studied. Finally, another important aspect to consider is the part of the body where the device will be inserted. If the biomaterial is in direct contact with a human fluid, such as blood or urine, the degradation residues can be easily transported or excreted. However, if the polymer is implanted for example, as a bone fixation, the material can only be resorbed and eliminated via metabolic pathways. In the case of the scaffolds applied in tissue engineering [4, 5], their degradation should match the tissue regeneration rate and completely disappear once the tissue has fully regenerated. It is worth stating that these porous samples degrade slower than their non-porous counterparts [6-9]. Porous structures enable the diffusion of degradation by-products to the outside medium and therefore, the autocatalytic effect, which is the acceleration of the hydrolysis rate due to entrapped acidic short chains, is clearly limited.

Bio(co)polyesters are known to degrade by bulk erosion [10,11]. The diffusion of water inside the polymer is dominant over the splitting of the chemical bonds, and so the material loses volume homogenously. Therefore, degradation occurs throughout the whole material equally and does not proceed from the exterior surface, that is at the interfacial areas between polymeric specimens and the aqueous environment (surface erosion). In the hydrolytic degradation, a combination of two mechanisms, random and chain-end scission (also known as backbiting), are identified [12, 13]. The chain scission of a polymer is called random if the bonds at any position along the polymer

chain have the same probability of being cleaved. As a consequence, the main chain breaks down randomly via cascades of irreversible scission steps following a first-order kinetic, irrespective of the chain length of the polymer molecules involved. In contrast, in chain-end scission, the number of chains ends and the rate constant for the cleavage of the terminal bond are the essential kinetic parameters. The contribution of chain-end scission rises with a decrease in the molecular weight of the polymer since the fraction of chain ends increases as a result of the degradation process. Shih et al. suggested that end scission dominates, being approximately 10 times the rate of random scission. Ester bonds towards the end of polymer chains are more susceptible to hydrolysis than those in the middle, however, for a high molecular weight sample, a single random scission has a greater impact on molecular weight than 1000 end scissions [14]. Therefore, it can be concluded that random scission controls the molecular weight reduction whereas the mass loss is due to end scission [13].

Hydrolytic degradation of (co)polyesters is affected by a large number of factors [15]. The mentioned auto-catalysis effect is reported to be a very important factor [16-18]. Thicker devices are degraded more quickly because all the leachable oligomeric compounds formed within the matrix are not able to escape from it as soon as they become soluble [19]. The geometry of the shaped bodies, the surface properties (contact angle, roughness and surface tension), the pH changes, which can be due to the degradation products, or the stresses applied during degradation, could also affect the degradation rate. Chemical composition, the type of chemical bond, sequence structure [20-23] and the morphology (crystalline or amorphous domains) are among other factors that have an impact on the degradation process. As has been demonstrated, amorphous regions are preferentially degraded because they are more accessible to water molecules [24], whereas the presence of crystalline domains slows hydrolytic degradation down dramatically [23].

The high number of factors influencing hydrolytic degradation and the inconsistency between different experiments found in the bibliography hampers the understanding of (co)polyester degradation behaviour. The aim of this work is to evaluate in depth the most important factors affecting the hydrolytic degradation of poly(lactide-co- δ -valerolactone) (PLVL) polymers [25]. The resulting conclusions will be useful for

better understanding of the mechanism of biodegradation of other lactide-co-lactone copolymers and (co)polyesters. In this paper an *in vitro* hydrolytic degradation study was carried out in phosphate buffered solution (PBS) at 37 °C for a period up to 98 days. The changes in water absorption, weight loss, macroscopic morphology, crystallinity, phase structure, molecular weight, composition and randomness character of the PLVLs were studied using different techniques, such as differential scanning calorimetry (DSC), gel permeation chromatography (GPC) and proton nuclear magnetic resonance spectroscopy (^1H NMR). For the study, repetitive square samples were obtained from films of several previously synthesized PLVLs: some terpolymers based on L-lactide, D-lactide and δ -valerolactone and a series of copolymers of L-LA and δ -VL having L-LA molar contents ranging from 53 to 82 %.

2.2.2. Materials and methods

Materials

L-lactide and D,L-lactide monomers (assay > 99.5 %) were supplied from Purac Biochem (The Netherlands) while δ -valerolactone monomer was provided by Sigma Aldrich. Triphenyl bismuth (Ph_3Bi) catalyst was obtained from Gelest. Stannous octoate (SnOct_2) (assay 95 %) and bismuth (III) subsalicylate (BiSS) (99.9 % metals basis) catalysts were supplied by Sigma Aldrich. Phosphate buffer saline (PBS) (pH 7.2) was obtained from Fluka Analytical (Sigma Aldrich).

Methods

200-300 μm films were prepared by pressure melting at 140 °C and followed by water quenching so as to achieve an amorphous state. In the cases of the single PLVL synthesized using SnOct_2 and the PLVL of 82 % lactide content, with melting peaks at ~ 130 °C and 135 °C, it was necessary to work at a temperature of 175 °C to ensure the complete melting of the crystalline phase. From these films, repetitive square samples for the *in vitro* degradation study (1x1 cm^2) were obtained.

For the *in vitro* degradation study, square samples (25-35 mg (W_0) ($n = 3$)) of the different copolymers were placed in Falcon tubes containing phosphate buffered saline (PBS) (pH = 7.2) maintaining a surface area to volume ratio equal to 0.1 cm^{-1} . The samples were stored in an oven at $37 \text{ }^\circ\text{C}$. Three samples of each polymer were removed at different times from the PBS and weighed wet (W_w) immediately after wiping the surface with a filter paper to absorb the surface water. These samples were air-dried overnight and vacuum-dried for another 48 h. Then, they were weighed again to obtain the dry weight (W_d). Water absorption (% WA) and remaining weight (% RW) were calculated according to Eqs. (1) and (2):

$$\% \text{ WA} = \frac{W_w - W_d}{W_d} \cdot 100 \quad (1)$$

$$\% \text{ RW} = \frac{W_d}{W_0} \cdot 100 \quad (2)$$

In order to compare the degradation rate of the studied PLVLs, the exponential relationship between molecular weight and degradation time for biodegradable polyesters degrading under bulk degradation was used [26]:

$$\ln M_w = \ln M_{w0} - K_{Mw} \cdot t \quad (3)$$

$$t_{1/2} = 1/K_{Mw} * \ln 2 \quad (4)$$

where M_w is the weight-averaged molecular weight, M_{w0} is the initial weight-averaged molecular weight, K_{Mw} is the apparent degradation rate and $t_{1/2}$ is the half degradation time (the amount of time required to fall to half the initial value of molecular weight).

The molecular weights of the polymers were determined by GPC using a Waters 1515 GPC device equipped with two Styragel columns ($10^2 - 10^4 \text{ \AA}$). Chloroform was used as eluent at a flow rate of 1 mL min^{-1} and polystyrene standards (Shodex Standards, SM-105) were used to obtain a primary calibration curve. The samples were prepared at a concentration of 10 mg in 1.25 mL.

The thermal properties were determined on a DSC 2920 (TA Instruments). Samples of 5-9 mg were heated from -50 °C to 175 °C at 20 °C min⁻¹. This first scan was used to determine the melting temperature (T_m), the heat of fusion (ΔH_m) and the glass transition temperatures (T_g) of the samples. After this first scan, the samples were quenched in the DSC and a second scan was made from -50 °C to 175 °C at 20 °C min⁻¹. In this second scan the glass transition temperatures were also determined from the inflection point of the heat flow curve.

Proton and carbon nuclear magnetic resonance (¹H NMR and ¹³C NMR) spectra were recorded in a Bruker Avance DPX 300 at 300.16 MHz and at 75.5 MHz of resonance frequency, respectively, using 5 mm O.D. sample tubes. All spectra were obtained at room temperature from solutions of 0.7 mL of deuterated chloroform (CDCl₃). Experimental conditions were as follows: a) for ¹H NMR: 10 mg of sample; 3 s acquisition time; 1 s delay time; 8.5 μs pulse; spectral width 5000 Hz and 32 scans; b) for ¹³C NMR: 40 mg, inverse gated decoupled sequence; 3 s acquisition time; 4 s delay time; 5.5 μs pulse; spectral width 18800 Hz and more than 25000 scans.

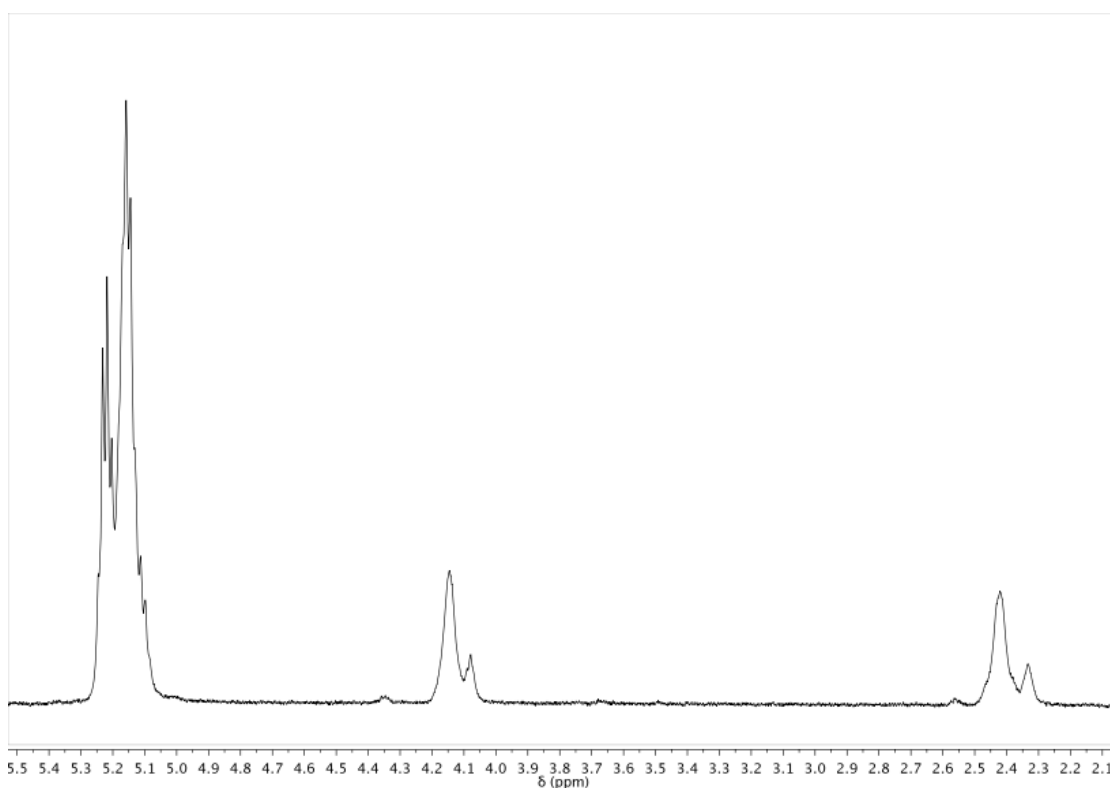


Figure 1. ¹H NMR spectrum of PLVL 008515.

The different signals of the ^1H NMR spectrum, shown in Figure 1, can be easily assigned. The lactide methine gives the signal centered at 5.15 ppm, the signals around 4.1 and 2.4 ppm correspond to the δ and α methylenes of the δ -valerolactone (see the scheme of the units in Figure 2), respectively, and the rest of H are included in the signal between 1.7 and 1.3 ppm (not shown). These signals can be assigned to the different dyads of δ -valerolactone and lactide in the same way as before, as with the lactide-co- ϵ -caprolactone statistical copolymers [27, 28].

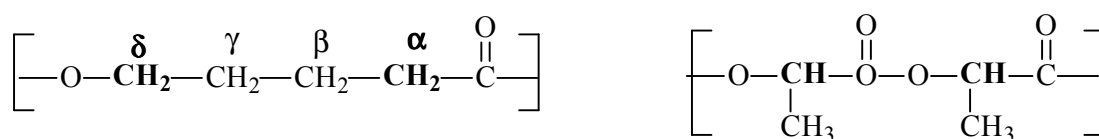


Figure 2. Scheme of the units of δ -valerolactone (left) and lactide (right).

It can be observed that both α and δ methylenes give two signals (two triplets). The signals of the α and δ methylenes at the lowest chemical shift, at 2.34 and 4.08 respectively, correspond to the VL-VL dyad, while the ones at lowest field (at 2.43 and 4.15) can be assigned to the VL-LA dyad (from now on underlining will be used to emphasize that the analysed nuclei belongs to that unit). In the case of LA unit signals, the H-H coupling hinders this type of analysis significantly and the signals corresponding to LA-LA and LA-VL are overlapped in the LA methine signal at 5.15 ppm, even though the quartet at highest field, at ≈ 5.07 ppm, could be assigned to sequence LA-VL. Taking into account the fact that the LA-VL dyad contribution to the LA methine signal will take the same relative molar fraction obtained for the VL-LA dyad, the experimental integration of the α and δ methylenes provides a way of calculating the total relative molar fraction of the VL-LA dyad. In this way, all the average dyad relative molar fractions could be calculated and, therefore, the copolymer composition and the microstructural magnitudes of the copolymers could be obtained from them. L-LA and D-LA are indistinguishable in the NMR spectrum so their contents and average sequence lengths are approximate values calculated on the assumption that the reactivities of both L-LA and D-LA are the same (having taken into account the L-LA:D-LA feed ratios), that is, the reaction with the employed bismuth based catalysts is not stereoselective. Equations 5-8 [29] were employed to obtain the

number-average sequence lengths (l_i), the Bernoullian random number-average sequence lengths (l_i) and the randomness character (R):

$$l_{LA} = \frac{(LA - LA) + \frac{1}{2}(LA - VL)}{\frac{1}{2}(LA - VL)} = \frac{2(LA)}{(LA - VL)} ; \quad (5)$$

$$l_{VL} = \frac{(VL - VL) + \frac{1}{2}(LA - VL)}{\frac{1}{2}(LA - VL)} = \frac{2(VL)}{(LA - VL)}$$

$$(l_{LA})_{random} = \frac{1}{(VL)} ; \quad (l_{VL})_{random} = \frac{1}{(LA)} \quad (6)$$

$$R = \frac{(l_{LA})_{random}}{l_{LA}} = \frac{(l_{VL})_{random}}{l_{VL}} \quad (7)$$

For the terpolymers:

$$l_{L-LA} = \frac{1}{((D - LA) + (VL)) R} ; \quad l_{D-LA} = \frac{1}{((L - LA) + (VL)) R} \quad (8)$$

where (LA) and (VL) are the lactide and δ -valerolactone molar fractions, obtained from the integration of the lactide methine signals and the δ -valerolactone methylene signals, (L-LA) and (D-LA) are the L-lactide and D-lactide approximate molar fractions and (LA-VL) is the LA-VL average dyad relative molar fraction.

Synthesis procedure

For the hydrolytic degradation study, statistical poly(lactide-co- δ -valerolactone) (PLVL) polymers of different L-lactide, D-lactide and δ -valerolactone content were synthesized by ring-opening polymerizations (ROP). The synthesis reactions were carried out in a flask, immersed in a controlled temperature oil bath. In each polymerization, predetermined amounts of L-LA, D,L-LA and δ -VL at the chosen mass feed ratio were simultaneously added and melted. The flask was purged for 30 minutes with a nitrogen stream under the surface of the melt. Then, the catalyst was added and the magnetic stirrer was maintained at 100 rpm. The PLVL polymerizations using BiSS as catalyst (1500:1 comonomers:catalyst molar ratio) and the synthesis reactions

employing Ph_3Bi (1000:1 comonomers:catalyst molar ratio) were carried out for 72 hours at 130 °C. The copolymerization of the only PLVL synthesized with SnOct_2 (1665:1 comonomers:catalyst molar ratio) was conducted for 48 hours at 140 °C.

After the corresponding reaction time, the products were dissolved in chloroform and precipitated by pouring the polymer solution into abundant methanol in order to remove the catalyst impurities and those monomers that did not react. Finally the product was dried at room temperature and then, a heat treatment at 100 °C for 1 hour was performed to ensure the complete elimination of solvent.

2.2.3. Results and discussion

Characterization

Table 1 and Table 2 summarize the characterization data of the several PLVL films studied in this work. As can be seen, the initial molecular weights (M_w) of each polymer, measured after film conformation, range from 87 to 130 kg mol^{-1} (and dispersity (D) from 1.78 to 1.89). As was expected for all these bismuth initiated PLVLs, they exhibited a random distribution of sequences ($R \sim 1$). In contrast, the copolymer achieved using SnOct_2 , PLVL 70Sn, was moderately blocky having a randomness character value of 0.68.

Several poly(L-lactide-co- δ -valerolactone) of L-LA molar content ranging from 53.4 to 81.9 % ($l_{\text{L-LA}}$ from 1.79 to 5.55) were evaluated in this work to assess the effect of the crystalline domains of L-LA formed during the hydrolytic degradation. The characterization data of these PLVLs, synthesized using Ph_3Bi as catalyst, are gathered in Table 1. This set of copolymers show glass transition temperatures (T_g s) within the range of 6 °C to 42 °C, in ascending order as the δ -VL content decreased. In addition, a SnOct_2 - initiated PLVL, presenting an almost equal L-LA content to PLVL 71 (70.1 % vs. 70.8 %), was also studied. Its moderately blocky character is reflected in its average sequence lengths of L-LA and δ -VL ($l_{\text{L-LA}} = 4.94$ and $l_{\text{VL}} = 2.11$) compared to the shorter sequence lengths ($l_{\text{L-LA}} = 3.32$ and $l_{\text{VL}} = 1.37$) of the previously mentioned

PLVL 71. Its blocky character could give it a higher capability of crystallization during the time submerged in PBS.

Table 1. Characterization data of the different poly(L-lactide-co- δ -valerolactone).

Sample	Catalyst	Composition ¹ (% molar)		M_w kg mol ⁻¹	D	Microstructural Magnitudes ²				T_g^3 °C
		% L-LA	% VL			l_{LA}	l_{L-LA}	l_{VL}	R	
PLVL 53	Ph ₃ Bi	53.4	46.6	88.1	1.79	1.79	1.79	1.56	1.20	5.9
PLVL 69	Ph ₃ Bi	68.6	31.4	87.7	1.81	3.11	3.11	1.43	1.02	27.0
PLVL 71	Ph ₃ Bi	70.8	29.2	120.7	1.89	3.32	3.32	1.37	1.03	30.3
PLVL 74	Ph ₃ Bi	73.6	26.4	118.8	1.85	3.73	3.73	1.34	1.01	32.3
PLVL 82	Ph ₃ Bi	81.9	18.1	117.7	1.78	5.55	5.55	1.23	1.00	42.5
PLVL 70 Sn	SnOct ₂	70.1	29.9	129.1	1.88	4.94	4.94	2.11	0.68	31.0

¹ Calculated from ¹H NMR spectra.

² l_{LA} and l_{VL} are the LA and VL number average sequence lengths obtained from ¹H NMR. These values are compared to the Bernoullian random number-average sequence lengths ($l_{LA}=1/VL$ and $l_{VL}=1/LA$), obtaining the randomness character value (R).

³ Obtained from the second scan of the DSC curves.

Table 2. Characterization data of the different poly(lactide-co- δ -valerolactone) (PLVL) synthesized using BiSS.

Sample	Catalyst	Composition ¹ (% molar)			M_w kg mol ⁻¹	D	Microstructural Magnitudes ²					T_g^4 °C
		% L-LA	% D-LA	% VL			l_{LA}	l_{L-LA}^3	l_{D-LA}^3	l_{VL}	R	
PLVL 007525	BiSS	37.4	37.4	25.2	101.1	1.83	3.99	1.61	1.61	1.34	0.99	26.3
PLVL 502525	BiSS	62.3	12.5	25.2	87.7	1.82	4.19	2.80	1.21	1.41	0.95	29.6
PLVL 750025	BiSS	73.6	0	26.4	90.0	1.81	3.82	3.82	-	1.37	0.99	32.7
PLVL 008515	BiSS	42.9	42.9	14.2	110.8	1.83	7.42	1.84	1.84	1.23	0.95	37.2
PLVL 404515	BiSS	62.9	22.7	14.4	116.4	1.83	7.50	2.91	1.39	1.26	0.93	40.0

¹ Calculated from ¹H NMR spectra. Because of the impossibility of offering the exact L-LA and D-LA molar content (indistinguishable in the NMR spectrum), approximate values are given under the assumption that the reactivity of both L-LA and D-LA are the same.

² l_{LA} and l_{VL} are the LA and VL number average sequence lengths obtained from ¹H NMR. These values are compared to the Bernoullian random number-average sequence lengths ($l_{LA}=1/VL$ and $l_{VL}=1/LA$), obtaining the randomness character value (R).

³ l_{L-LA} and l_{D-LA} are the L-LA and D-LA approximate values of number average sequence lengths under the assumption that the reactivity of both L-LA and D-LA are the same.

⁴ Obtained from the second scan of the DSC curves.

A second series of polymerizations were also conducted with BiSS, in which D-LA was added. In Table 2, the first two digits represent the L-LA mass content in each sample

name of these polymers; the next two the D,L-LA mass content and the last two the δ -VL mass content in the feeding mix. For example, PLVL 502525 was synthesized adding 50 wt. % of L-LA, 25 wt. % of D,L-LA and 25 wt. % of δ -VL. With these series of polymers we sought to study the effect of the stereoregularity and the disruption of the microstructural arrangement of the L-LA crystallizable chains by means of D-LA units on the hydrolytic degradation mechanisms. PLVL 007525, PLVL 502525 and PLVL 750025 are lactide-co- δ -valerolactone polymers having a similar δ -VL content ($\sim 25\%$), but a different L-LA/D-LA ratio. Their T_g s shifted to higher values (from 26 to 33 °C) when the L-LA content was increased. Two more terpolymers richer in lactide ($\sim 86\%$) were analyzed: PLVL 008515 and PLVL 404515. They also show single T_g s, at 37 and 40 °C, respectively.

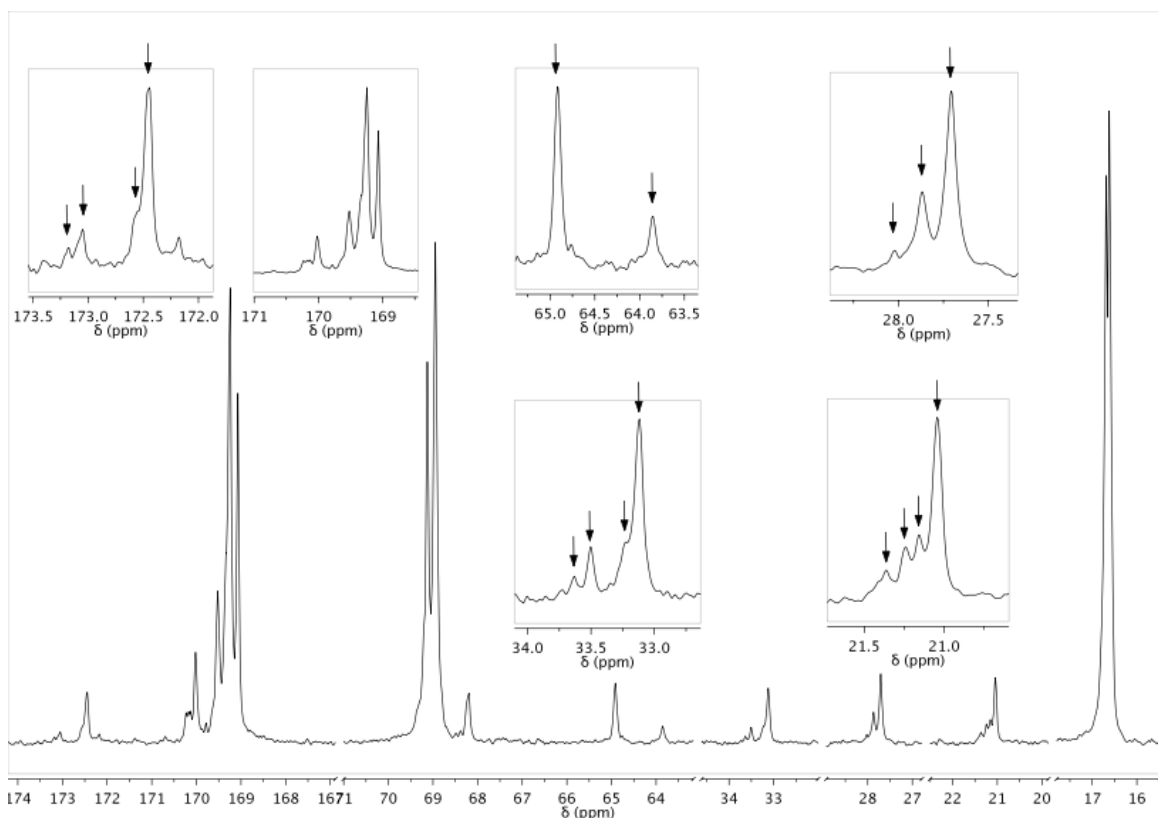


Figure 3. ^{13}C NMR spectrum of PLVL 008515 with some regions enlarged; the peaks assigned in the text to dyads and triads are marked with arrows.

In order to confirm the random character ($R \rightarrow 1$) of these series of copolymers, as well as the absence of the second mode transesterification, that is, the formation of δ -VL-

lactyl- δ -VL sequences during copolymerization, ^{13}C NMR spectrum was recorded for PLVL 008515. This copolymer of rac-lactide and δ -valerolactone showed a R value of 0.95 in the proton nuclear magnetic resonance with a δ -VL molar content of 14.2 % and a δ -VL average sequence length (l_{VL}) of 1.23. Figure 3 shows the ^{13}C NMR spectrum of this copolymer with some regions of interest enlarged.

Reactions of second mode transesterification, a phenomenon which lead to the bond cleavage of lactide (LA or LL), might occur during the copolymerizations. In the lactide-co- ϵ -caprolactone copolymers, the concentration of ϵ -CL-L- ϵ -CL sequences are experimentally determined from the signal of the ^{13}C NMR spectrum at 170.9 ppm [28]. It is noted that the lactide signals of the carbonyl carbon atom are located at the same chemical shift in the spectra of both lactide-co- ϵ -caprolactone and lactide-co- δ -valerolactone copolymers (within the range of 169.0 to 170.5 ppm), so it is expected that the peak assigned to the VL-L-VL sequences appears also around 171 ppm. However, as can be seen in the figure, it was not found any peak at this shift, demonstrating that in these polymerizations the second mode transesterification reactions were negligible.

The composition of PLVL 008515 was also calculated from the integral areas of bands of the carbon signals present in ^{13}C NMR and was 86.5 % of lactide and 13.5 % of δ -VAL, equivalent to the previously obtained by ^1H NMR. With regard to the calculus of its randomness coefficient, it can be employed equation 9 [30-31], in which l_{VL} is determined from the triad peak intensities (I_i) identified in the ^{13}C NMR spectrum, while the Bernoullian random number-average sequence length for this copolymer is 1.16 ($l_{\text{VLrandom}} = 1/(\text{LA}) = 1/0.865$),

$$R = \frac{(l_{\text{VL}})_{\text{random}}}{l_{\text{VL}}} \quad \text{where} \quad l_{\text{VL}} = \frac{I_{\text{VL-VL-VL}} + I_{\text{LA-VL-VL}}}{I_{\text{VL-VL-LA}} + I_{\text{LA-VL-LA}}} + 1 \quad (9)$$

The region of the carbonyl carbon atom (at 172.5 ppm) and the signals of the α , β and γ methylene carbon atoms, located at ~ 33.5 , 21.0 and 28.0 ppm respectively, present triad sensitivity. Based on the LA-co- ϵ -CL spectrum [32], VL-VL-VL, LA-VL-VL, VL-VL-LA and LA-VL-LA triads of the LA-co- δ -VL can be assigned from left to right in

the carbonyl and the α and γ methylene carbons while in the γ region the intermediate sequences change their relative order. It can be observed that the signal of the last one is significantly more intense than the rest of triads. These four triads are easily distinguished in the β methylene region. On the other hand, VL-VL-LA and LA-VL-LA triad peaks appear overlapped in both the carbonyl region and the α methylene region, but still allows us to calculate the δ -VL average sequence length through the integration of the area of the two triads. Its integral gives directly a value of the VL-LA dyad area $[(\underline{\text{VL}}\text{-LA}) = (\text{LA-VL-LA}) + 1/2 (\text{LA-VL-VL}) + 1/2 (\text{VL-VL-LA})]$ under the assumption that $(\text{LA-VL-VL}) = (\text{VL-VL-LA})$. On the contrary, in the γ methylene signal the two intermediate triads (LA-VL-LA and VL-VL-LA) are overlapped, but an approximate calculation can also be made taking into account the relation given above between the areas of these triads. The average value of l_{VL} obtained from the four mentioned estimates is 1.25 which means that the associated R coefficient calculated is 0.93.

The study of the chain microstructure can also be carried out through the δ carbon atom signal of the δ -VAL, in which the peaks of the δ -valerolactone dyads are well resolved. The peak at the highest chemical shift, at 65.0 ppm, corresponds to the VL-LA dyad, while the signal at 63.9 ppm is assigned to the VL-VL dyad. Therefore, the average dyad relative molar fractions can be calculated in the same way as before in the ^1H NMR, employing equations 5-7, though the integration of the signals from the LA-LA and LA-VL dyads, which are overlapped in the LA methine signal centered at 69.0 ppm. Values of $l_{\text{VL}} = 1.28$ and $R = 0.90$ were achieved, in agreement with the rest of results and proving again the random character of PLVL 008515.

Hydrolytic degradation study

Thermal properties evolution

Figure 4 shows typical DSC thermograms of PLVL 007525, PLVL 71, PLVL 82 and PLVL 70Sn at different times of degradation. The terpolymers based on L-lactide, D-lactide and δ -valerolactone (PLVL 007525, PLVL 502525, PLVL 008515 and PLVL 404515), follow the trend shown in Figure 4a. Owing to the presence of D-LA disrupting their chain microstructure and having an estimated value of $l_{\text{L-LA}}$ lower than

2.91, they maintained their amorphous character during the degradation process and no phase separation or melting peaks were detected. Throughout the entire study, these PLVLs presented a single glass transition temperature (T_g) which, as hydrolytic degradation progresses, moved toward lower temperatures because of the higher mobility of the shorter polymer chains that had been created. Hence, as an illustration, the T_g of PLVL 007525 shifted from 26 °C to a value of 15 °C on day 98 and the T_g s of PLVL 502515, PLVL 008515 and PLVL 404515 reached final values of 20, 28 and 29 °C, respectively.

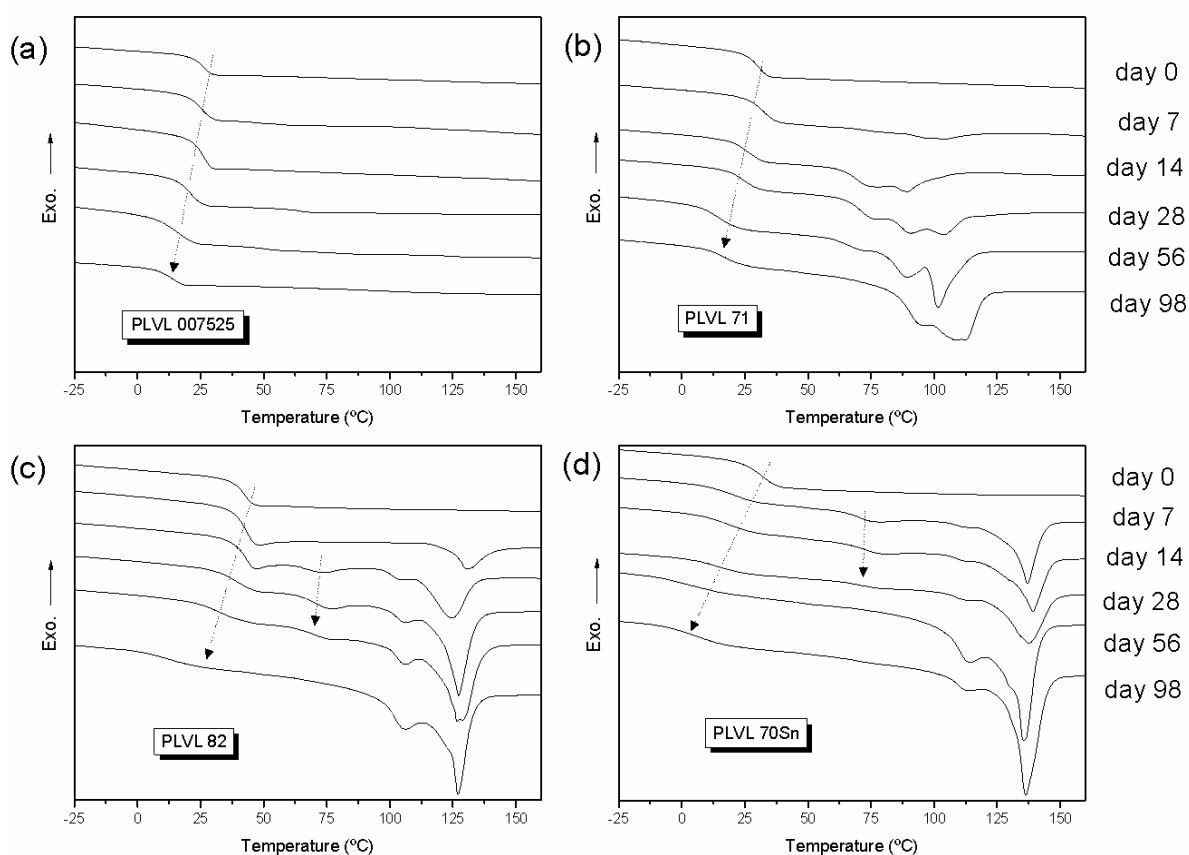


Figure 4. DSC evolution during degradation of PLVL 007525 (a), PLVL 71 (b), PLVL 82 (c) and PLVL 70Sn (d).

The DSC first scan curves of PLVL 53 (containing 53 % of L-LA and 47 % of δ -VL) developed in a manner similar to those of terpolymers. With a short average sequence length, $l_{L-LA} = 1.79$, this material was not able to crystallize during the 98 days it was submerged in PBS. Its single T_g , initially at 6 °C, shifted, from day 56, to values lower

than 0 °C. At this stage of the degradation process, the weight-average molecular weight (M_w) of the polymer was lower than 17 kg mol^{-1} .

The rest of the polymers in this study, that is, the copolymers of L-LA and δ -VL of L-LA molar content ranging from 69 to 82 %, were prone to crystallization and their L-lactide (L-LA)-unit chains arranged into crystalline organized structures. At l_{L-LA} values higher than 3.11, the L-LA sequences were large enough to crystallize during the degradation period studied. In order to discuss the supramolecular rearrangements of these materials, the thermal properties data obtained from their thermograms are detailed in Table 3.

The evolution of the DSC curves of PLVL 69 ($l_{L-LA} = 3.11$), PLVL 71 ($l_{L-LA} = 3.32$), PLVL 74 ($l_{L-LA} = 3.73$) and PLVL 750025 ($l_{L-LA} = 3.82$) followed the trend shown in Figure 4b, which belongs to PLVL 71. Initially, they were completely amorphous showing single T_g s at 27, 28, 30 and 31 °C, respectively. However, after 7 days submerged in PBS, a small melting peak appeared in all of them ($T_m = 82$ °C for PLVL 69, 100 °C for PLVL 71, 94 °C for PLVL 74 and 109 °C for PLVL 750025). Then, on day 14 of degradation a rapid increase in the melting enthalpy (ΔH_m) was observed as a result of the migration of L-lactide chains from the amorphous phase. The ΔH_m at this time took values of 14.3, 14.6, 19.5 and 19.9 J g^{-1} for PLVL 69, PLVL 71, PLVL 74 and PLVL 750025. During the study, the broad melting peaks of these polymers were composed of two or three different peaks, which indicates that the crystallites created may be more disordered and imperfect. Meanwhile, the corresponding melting temperature (T_m) shifted toward higher temperatures as the time submerged in PBS increased and the melting peak became narrower. PLVL 69, PLVL 71, PLVL 74 and PLVL 750025 reached a ΔH_m of 31.5, 33.5, 40.3 and 44.9 J g^{-1} at the end of the study (day 98). The larger l_{L-LA} of the latter gives it a higher crystallization capability during degradation. On the other hand, regarding their glass transition behaviour, these PLVLs exhibited a single T_g which moved toward lower temperatures and presented lower ΔC_p changes as the degradation time increased, due to the development of the aforementioned crystalline domains (and corresponding reduction in amorphous phase).

Table 3. Evolution of the thermal properties of the L-LA/ δ -VL copolymers prone to crystallization.

Sample	time (days)	1 st Scan				2 nd Scan
		T _{g1} (°C)	T _{g2} (°C)	T _m (°C)	ΔH_m (J g ⁻¹)	T _g (°C)
PLVL 69	0	26.6 (0.63)	-	-	-	26.9
	3	27.9 (0.61)	-	-	-	28.0
	7	25.9 (0.60)	-	82.0	4.51	24.9
	14	20.0 (0.50)	-	82.2	14.25	23.1
	21	19.8 (0.48)	-	84.9	15.66	24.1
	28	20.7 (0.47)	-	87.6	15.91	24.7
	35	16.0 (0.49)	-	86.6	19.00	20.2
	42	15.8 (0.47)	-	86.0	19.01	23.5
	56	13.2 (0.47)	-	94.6	21.76	20.0
	70	14.4 (0.45)	-	88.6	22.98	24.5
98	11.4 (0.42)	-	103.4	31.46	21.8	
PLVL 71	0	28.3 (0.61)	-	-	-	30.3
	3	30.4 (0.60)	-	-	-	31.7
	7	32.3 (0.54)	-	100.1	5.18	31.5
	14	26.3 (0.54)	-	88.5	14.57	31.2
	21	25.5 (0.48)	-	93.9	19.98	30.4
	28	24.3 (0.41)	-	90.3	20.79	29.3
	35	21.4 (0.49)	-	90.0	20.93	28.7
	42	20.9 (0.46)	-	102.2	21.67	27.3
	56	14.6 (0.47)	-	101.5	23.81	21.2
	70	12.8 (0.46)	-	99.5	27.01	21.5
98	17.2 (0.39)	-	108.2	33.52	30.0	
PLVL 74	0	30.3 (0.61)	-	-	-	32.3
	3	33.3 (0.61)	-	-	-	33.7
	7	31.7 (0.58)	-	93.8	5.69	32.5
	14	28.1 (0.45)	-	104.0	19.54	30.1
	21	26.5 (0.46)	-	107.3	21.38	32.6
	28	25.7 (0.44)	-	108.7	21.90	30.8
	35	19.9 (0.45)	-	109.1	23.35	25.3
	42	21.5 (0.43)	-	108.7	25.13	27.4
	56	15.5 (0.42)	-	109.3	27.24	24.5
	70	11.8 (0.41)	-	111.2	28.55	22.6
98	12.2 (0.37)	-	108.8	40.31	26.7	
PLVL 82	0	42.6 (0.59)	-	-	-	42.5
	3	42.2 (0.53)	-	-	-	41.9
	7	42.5 (0.53)	-	128.4	4.04	41.3
	14	42.3 (0.49)	65.1 (0.13)	124.3	11.95	41.5
	21	42.2 (0.43)	69.4 (0.21)	128.7	15.58	38.8
	28	39.1 (0.39)	71.3 (0.25)	127.3	18.05	40.6
	35	37.3 (0.42)	71.6 (0.26)	128.2	21.01	38.1
	42	34.6 (0.35)	69.7 (0.23)	126.3	20.78	39.9
	56	31.9 (0.35)	70.2 (0.22)	126.6	26.59	38.8
	70	25.9 (0.32)	69.8 (0.15)	129.2	30.92	36.6
98	11.2 (0.29)	-	127.0	44.05	28.8	
PLVL 70Sn	0	31.5 (0.59)	-	-	-	31.0
	3	22.1 (0.40)	68.9 (0.21)	135.4	16.21	30.7
	7	20.4 (0.40)	70.2 (0.21)	136.9	16.66	30.6
	14	18.8 (0.39)	72.8 (0.20)	139.2	17.61	29.7
	21	16.4 (0.38)	70.9 (0.20)	136.4	19.49	29.3
	28	14.9 (0.35)	68.4 (0.28)	137.4	22.90	28.2
	35	11.3 (0.39)	69.5 (0.19)	140.2	23.69	28.2
	42	10.8 (0.34)	69.8 (0.12)	135.9	27.27	27.1
	56	6.97 (0.36)	-	136.4	32.56	22.0
	70	2.11 (0.38)	-	136.3	36.84	23.0
98	2.50 (0.32)	-	135.5	44.66	28.3	

* The values of the specific heat capacity (ΔC_p) was given in brackets next to the glass transition temperatures.

The DSC curves of PLVL 82 (Figure 4c) and PLVL 70Sn (Figure 4d) were more complex than those explained above. Both copolymers displayed a double T_g behaviour which was demonstrated in a previous work of ours by DMA measurements [33] and was observable in the DSC scans from day 14 for PLVL 82 and from day 3 for PLVL 70Sn. The lower T_g is linked to the hybrid amorphous miscible LA/ δ -VL phase, whereas the higher T_g suggests the presence of phase separated amorphous lactide chains. As the time increased, the lower T_g shifted to lower temperatures (from 42 °C on day 14 to 11 °C on day 98 for PLVL 82 and from 22 °C on day 3 to 3 °C on day 98 for PLVL 70Sn) because of the incorporation of some LA from the LA/ δ -VL mixed phase to the lactide amorphous phase and to the crystalline domains. As this migration occurs, the hybrid amorphous miscible LA/ δ -VL phase became richer in δ -VL and the lactide amorphous glass transition became less defined (lower ΔC_p changes) because of the loss of lactide chains toward the crystalline phase. The higher T_g disappeared on day 98 of degradation in the case of PLVL 82 and was not appreciable on day 56 in the PLVL 70Sn thermograms. Finally, regarding the T_g behaviour, it is also worth stating that from day 3 to day 14 of the study, PLVL 82 presented a small peak of enthalpy of relaxation (δ) at the lower T_g as a result of the densification of the polymer chains.

The phase separation changes of the PLVL 82 evolve more slowly than in the other polymers (including PLVL 70Sn) due to its high initial T_g (43 °C), which is well above the *in vitro* temperature (37 °C). Therefore, on day 98 its melting enthalpy ($\Delta H_m = 44.1 \text{ J g}^{-1}$) still has not exceeded the ΔH_m values of the rest of polymers substantially, even though PLVL 82 shows the largest average sequence length of L-lactide ($l_{L-LA} = 5.55$) between the poly(lactide-co- δ -valerolactone)s employed in this work and, consequently, the higher crystallization capability. The melting temperature of PLVL 82 and PLVL 70Sn were considerably higher (~ 128 °C for PLVL 82 and ~ 136 °C for PLVL 70Sn) than those of the other L-LA-co- δ -VL copolymers (with $T_m < 110$ °C), mainly owing to the formation of more ordered and perfect crystallites of L-LA. In addition, it is also worth noting that the heat of fusion of these two copolymers had to be obtained, in some cases, from the difference between the melting enthalpy and the cold crystallization (at ~ 90 °C) enthalpy that appeared in the first few weeks of the study.

Comparing the thermal properties of the moderately blocky PLVL 70Sn ($R = 0.68$ and $l_{L-LA} = 4.94$) with those of random PLVL 71 ($R = 1.03$ and $l_{L-LA} = 3.32$), the importance of the chain microstructure distribution of sequences on the supramolecular rearrangements that took place during degradation is obvious. Both polymers have almost equal L-LA content (70.1 vs 70.8 %) and similar T_g s (at around 30-31 °C), but the blocky one is significantly more prone to suffer physical changes. Therefore, on day 3 of degradation PLVL 70Sn already exhibited a melting peak of 16.2 J g^{-1} whereas PLVL 71Sn was still amorphous, and at the end of the study, PLVL 70Sn presented a ΔH_m of 44.7 J g^{-1} while the ΔH_m of PLVL 71 reached a value of only 33.5 J g^{-1} . With regard to PLVL 70Sn, it is also worth highlighting, as a curiosity, that on day 98 the second DSC scan of PLVL 70Sn showed a cold crystallization peak accompanied by a melting peak. Therefore this copolymer on that degradation day was able to crystallize after being cooled from the melt; however, the neat heat of fusion was below 1 J g^{-1} .

Weight loss and water absorption

Figure 5 shows the remaining weight (RW) and water absorption (WA) curves obtained from the *in vitro* degradation study of the L-lactide-co- δ -valerolactone copolymers characterized in Table 1. The weight of the samples remained constant during the first few weeks of the study, and, once the molecular weight reached a critical value they started to lose mass. As can be seen in the plot of these polymeric materials, they began to lose weight from day 56, with the exception of PLVL 82, when they presented a relevant increment in water absorption. On day 70, the amorphous PLVL 53 exhibited the highest water absorption capacity (WA = 73.2 %), followed by PLVL 69 (WA = 30.8 %). PLVL 82 and PLVL 70 Sn, the two copolymers with a greater tendency to crystallize, did not take up virtually any water (6.7 % and 3.2 %, respectively) and their remaining weight did not undergo any important changes, 99.7 % and 93.5 % of RW. On the contrary, the PLVLs containing 53 to 74 % of L-lactide, with less perfect crystallites at a lower T_m , suffered a measurable loss of weight and their RW dropped to values in the range of 82 to 88 %. At the end of the study (day 98), PLVL 82 showed the first signs of weight loss (RW = 87.7 %), when its M_w took a value of 15 kg mol^{-1} . The developed highly crystalline domains and the more packed amorphous regions of PLVL 82 ($T_g = 43 \text{ °C}$) impeded the absorption of water in comparison to the other

copolymers. At this stage of degradation, PLVL 70Sn had a WA of 15.7 % and a remaining weight of 79.1 % , while PLVL 71 (with an almost equal L-LA content to PLVL 70Sn but presenting $R = 1$) and PLVL 74 presented values of WA of approximately 40 % and remaining weight of ~ 70 %. On the contrary, PLVL 53 and PLVL 69 exhibited sharp increases in water uptake (> 50 %) that led to a significant loss of mass (RW ~ 64 %).

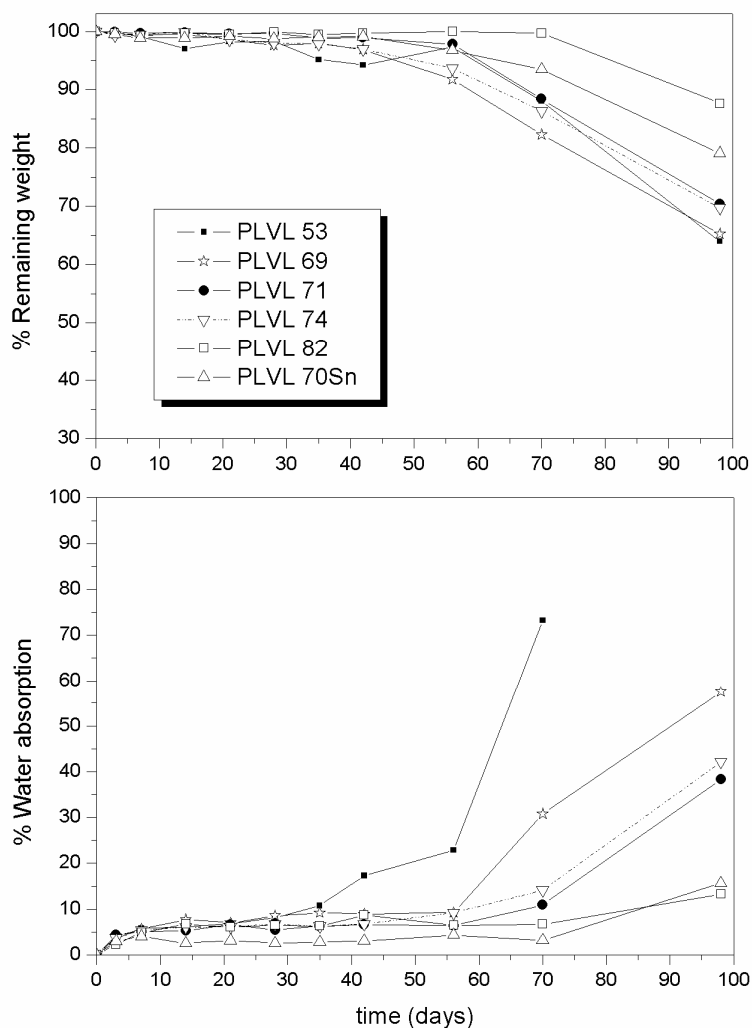


Figure 5. Evolution of the remaining weight and the water absorption of the PLVLs of the Table 1

Figure 6 shows remaining weight and water absorption curves from the *in vitro* degradation study of the terpolymers characterized in Table 2. The combination of short L-LA, D-LA and δ -VL sequences resulted in disordered polymeric structures with lower stereoregularity and, as consequently the amorphous regions were much larger

than in the case of the copolymers in Figure 5. Water has the ability to penetrate these regions easily. Therefore, PLVL 007525 started to lose weight from day 35 and PLVL 502525 and PLVL 008515 from day 42, whereas the semicrystalline PLVL 750025, together with the glassy PLVL 404515 ($T_g = 40$ °C), took longer to lose mass and did not began to take up water significantly until day 56. On day 42, the WA of the last two polymers still was less than 13 % with a RW value close to 100 %. In contrast, PLVL 502525 and PLVL 008515 showed a WA in the range of 33 to 35 % and a remaining weight of approximately 95 %. In the case of PLVL 007525, more degradation by-products were released from the sample leading to a weight loss of ~ 20 % of its initial mass. Due to its fully amorphous character and its lowest T_g (26 °C), the effect of the hydrolytic degradation is more pronounced in this material. Consequently, on day 98 its RW was only 33.5 %. On the other hand, the RW of PLVL 502525, PLVL 008515 and PLVL 404515 reached values of 40.4, 65.2 and 64.9 %. On this day of the study, the water uptake was only measurable for PLVL 750025 (WA = 36.5 %). This polymer did not contain D-LA units and is similar to the L-lactide-co- δ -valerolactone copolymers evaluated above (i.e. PLVL 74). Its RW value (71 %) was in perfect agreement with those results. This material was, at this moment of the study, in a less advanced state of degradation than the terpolymers.

As can be observed by evaluating the WA values at different times, it can be said that the order in water absorption from the highest to the lowest was: PLVL 007525, PLVL 502525 and PLVL 008515 > PLVL 404515 and PLVL 53 > PLVL 69 > PLVL 71, PLVL 74 and PLVL 750025 > PLVL 70Sn and PLVL 82. Since the mass loss and the degradation kinetics of the polyesters are dominated by water attacking to the ester bonds, water absorption capacity plays a pivotal role and is a critical parameter in the degradation mechanisms. In this section, we have seen that water uptake was favoured by the resistance of the polymers to crystallize during degradation, the presence of large amorphous domains and the decrease of the microstructural stereoregularity of the polymer chains. The absence of high glass transition temperatures (above 37 °C, body temperature, the one at which these biomaterials are usually employed) is another important factor to be taken into account. At temperatures below the glass transition, the amorphous polymers are in glassy state and behave like a rigid body which impedes

water penetration. However, if its T_g is several degrees below 37 °C, the material is softer and more viscous and, as a result, the diffusivity of water inside the polymer is easier and the water absorption of the polymer is improved.

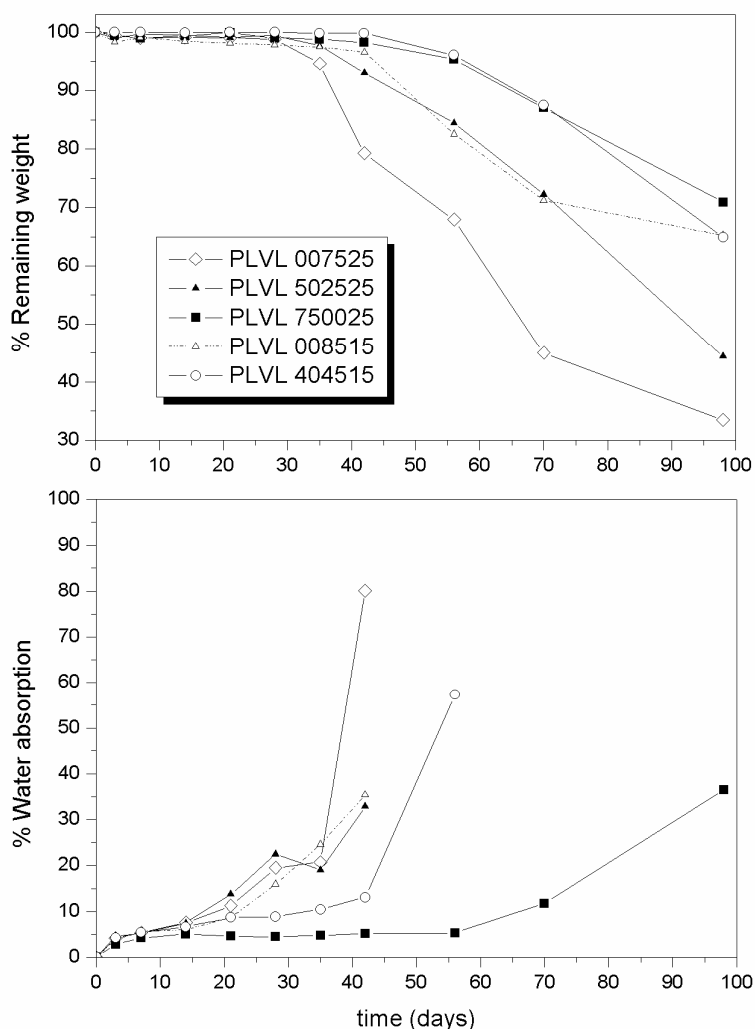


Figure 6. Evolution of the remaining weight and the water absorption of the PLVLs of the Table 2.

Molecular weights evolution and degradation kinetics

Figure 7 and Figure 8 show the progress of $\ln M_w$ versus degradation time of the lactide-co- δ -valerolactone polymers. As the degradation evolves, the M_w of the samples decreased and the dispersity increased, indicating a broader distribution of polymer chain length. The loss of M_w and the production of short polymer chains resulted in a reduction in molecular entanglement and an increase in chain mobility that directly

affected the observed glass transition temperatures in the second DSC scan. For example, T_g dropped from the initial value of 26, 30, 37, 6 and 27 °C for PLVL 007525, PLCL 502525, PLVL 008515, PLVL 53 and PLCL 69 respectively, to 14, 18, 23, -6 and 22 °C at the end of the study, when M_w were in the range of 4.5 to 9.0 kg mol⁻¹.

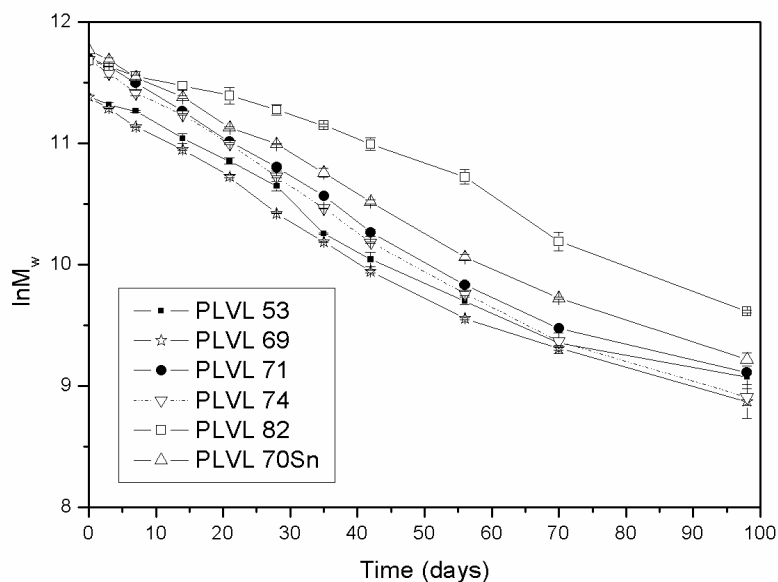


Figure 7. $\ln M_w$ versus degradation time of the PLVLs of the Table 1.

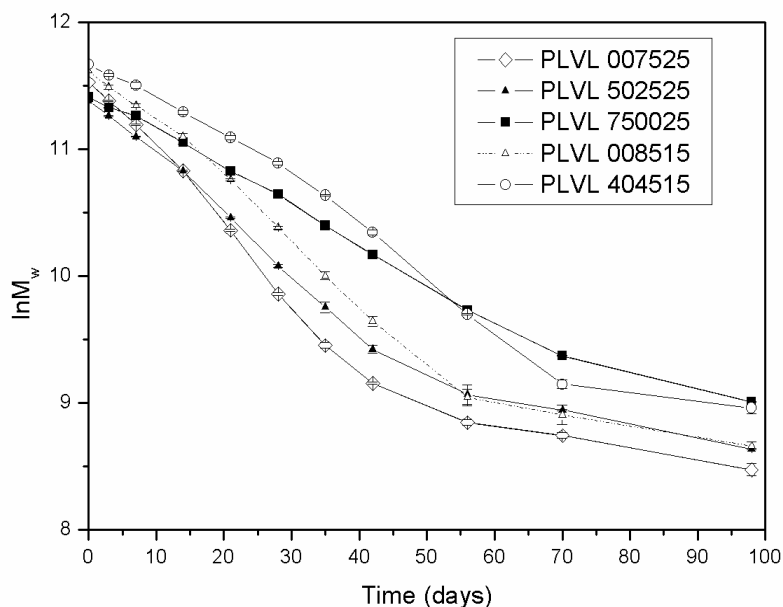


Figure 8. $\ln M_w$ versus degradation time of the PLVLs of the Table 2.

Table 4 presents the values of K_{M_w} and $t_{1/2}$ calculated from the slope of the fitting curve before the slope gradually changed and the correlation coefficient decreased. The experimental data of M_w fits the fitting curve ($R^2 > 0.98$) very well during the times at which the weight of the samples remained constant (see section 3.2.2). Then, they started to deviate. This deceleration in loss of M_w indicates that the degradation mechanism is shifting from one dominated by random scission to another controlled by chain end scission [13].

Table 4. K_{M_w} and $t_{1/2}$ of the PLVLs of this work.

Sample	K_{M_w} (day 14)	K_{M_w}	Half-molecular weight degradation time $t_{1/2}$ (days)
PLVL 53	0.0246	0.0317	21.9
PLVL 69	0.0312	0.0334	20.8
PLVL 71	0.0318	0.0339	20.5
PLVL 74	0.0322	0.0348	19.9
PLVL 82	0.0147	0.0166	41.8
PLVL 70Sn	0.0280	0.0300	23.1
PLVL 007525	0.0497	0.0601	11.5
PLVL 502525	0.0395	0.0473	14.7
PLVL 750025	0.0250	0.0302	23.0
PLVL 008515	0.0366	0.0470	14.8
PLVL 404515	0.0264	0.0340	20.4

As can be seen, the polymers that displayed higher values of water absorption also experienced the fastest degradation rates. K_{M_w} obtained for PLVL 007525, PLVL 502525 and PLVL 008515 were 0.060, 0.047 and 0.047 days⁻¹ respectively, with corresponding $t_{1/2}$ of 11.5, 14.7 and 14.8 days. On the other hand, poly(L-lactide-co- δ -valerolactone) of L-LA content ranging from 69 to 74 and PLVL 404515 exhibited values of K_{M_w} in the range of 0.033 to 0.035 days⁻¹, with a $t_{1/2}$ of approximately 20 days. Then, there is a third group of polymers, PLVL 53, PLVL 750025 and PLVL 70Sn, with K_{M_w} of 0.030 to 0.032 days⁻¹ and $t_{1/2}$ of ~ 22.5 days. Finally, the polymeric material with the slowest degradation rate (0.017 days⁻¹) and longest half-degradation time (41.8 days) was PLVL 82. In this study this PLVL is the copolymer with the largest capacity to crystallize ($I_{L-LA} = 5.55$) and the highest T_g (43 °C), which makes it the most resistant

copolymer to water uptake. However, its K_{Mw} is far above the values documented in the literature for the poly(L-lactide) homopolymer. For example, Larrañaga et al. [9] reported values of K_{Mw} and $t_{1/2}$ of 0.011 days^{-1} and 62 days for PLLA.

After evaluating the data collected for the terpolymers, it should be noted that the introduction of rigid L-lactide blocks, which increases the L-LA/D-LA ratio in the PLVL chains and raises the l_{L-LA} , leads to polymers with lower K_{Mw} and a higher resistance to hydrolytic degradation. So, the rac-lactide-co- δ -valerolactone PLVL 007525 ($K_{Mw} = 0.060 \text{ days}^{-1}$, 37.4 % of L-LA, 37.4 % of D-LA and $l_{L-LA} = 1.61$), due to its completely amorphous morphology and low stereoregularity, has a K_{Mw} value higher than that found for PLVL 502525 ($K_{Mw} = 0.047 \text{ days}^{-1}$, 62.3 % of L-LA, 12.5 % of D-LA and $l_{L-LA} = 2.80$), which is also larger than those corresponding to PLVL 750025 ($K_{Mw} = 0.030 \text{ days}^{-1}$, 73.6 % of L-LA and $l_{L-LA} = 3.82$) and the set of L-LA-co- δ -VL copolymers synthesized using PH_3Bi as catalyst. In agreement with the above, PLVL 404515 (62.9 % of L-LA, 22.7 % of D-LA and $l_{L-LA} = 2.91$), despite having similar lactide content ($\sim 86\%$) to PLVL 008515, also displayed a slower degradation rate than the rac-LA-co- δ -VL copolymer ($K_{Mw} = 0.034 \text{ days}^{-1}$ for PLVL 404515 vs. 0.047 days^{-1} for PLVL 008515). Therefore it was probed that a large structural disorder with short unit average sequence lengths improves the rate of degradation.

To provide another framework for comparison, some of the kinetic results were contrasted with those obtained in a previous work [35] that used lactide-co- ϵ -caprolactone copolymers (PLCL) with intercomparable compositions and chain microstructures ($R = 1$). The ϵ -caprolactone (ϵ -CL) unit has an identical structure to δ -VL but has one more straight methylene group sandwiched between the ester groups of the polymer chain. Therefore, ϵ -CL provides higher flexibility with respect to δ -VL [35, 36] and their lactide copolymers have lower glass transition temperatures, bringing about relevant differences in their mechanical behaviour. In accordance with the literature [33], PLVLs showed an increase in their stress related properties (secant modulus, yield strength and ultimate tensile stress) over the PLCLs, which is translated into an important improvement in their stiffness and strength. Regarding hydrolytic degradation, this paper demonstrated that PLCLs degrade at a faster rate than PLVLs. As an illustration, ϵ -CL composed PLCL 008515 (41.85 % of L-LA, 41.85 % of D-LA

and $l_{L-LA} = 1.79$) and PLCL 502525 (60.8 % of L-LA, 12.1 % of D-LA and $l_{L-LA} = 2.39$) presented values of K_{Mw} and $t_{1/2}$ of 0.066 days^{-1} and 10.5 days, and 0.056 days^{-1} and 12.4 days, respectively. Conversely, the respective polymers based on δ -VAL, PLVL 008515 and PLVL 502525, have a K_{Mw} of approximately 0.047 days^{-1} and a $t_{1/2}$ of around 14.7 days. Furthermore, it was found that a poly(L-lactide-co- ϵ -caprolactone) copolymer of 74.0 % of L-LA content (26.0 % of CL and $l_{L-LA} = 4.01$) also presents a higher K_{Mw} than PLVL 750025 (73.6 % of L-LA and $l_{L-LA} = 3.82$) ($K_{Mw} = 0.034 \text{ days}^{-1}$ vs. $K_{Mw} = 0.030 \text{ days}^{-1}$). Based on these results, it can be concluded that the T_g of the polymers has a more important role to play in the degradation than the hydrophilic character of their structural units. The fraction of hydrolytically ester bonds is richer in the case of the lactide-co- δ -valerolactone polymer chains (four straight methylenes and an ester group for δ -VAL-units and five straight methylenes together with one ester group for a unit of ϵ -CL). However, PLVLs present higher T_g s than PLCLs, which slow down the water absorption. So, PLVL 008515, PLVL 502525 and PLVL 750025 have T_g s at 37, 30 and 33 °C, respectively, while the respective LA/ ϵ -CL copolymers present initial T_g s at lower temperatures (29, 21 and 28 °C, respectively).

A series of L-lactide-co- δ -valerolactone copolymers of L-LA molar content ranging from 53.4 to 81.9 % (l_{L-LA} from 1.79 to 5.55) were also assessed in this work to study their hydrolytic degradation. The highest degradation rate belongs to the PLVL with a 74 % L-lactide content, although PLVL 69 and PLVL 71 have nearly equal values of K_{Mw} . However, if the L-LA content is increased or lowered, the degradation rate is smaller. At L-LA contents higher than 74 %, the copolymers are more prone to crystallization and the crystallites formed are more perfect. In consequence, the water uptake and the hydrolysis are clearly retarded. On the contrary, at L-LA contents lower than 69 %, the copolymers have a more amorphous morphology and show lower T_g s. Nevertheless, contrary to what was expected, its degradation rate does not rise. This is the case of the non-crystalline PLVL 53 ($l_{L-LA} = 1.79$), in which the mobility of its polymer chains is favoured due to its low T_g (6 °C) and, as we have seen previously, the water absorption begins earlier. However, PLCL 53 is rich in δ -VL units (46.6 %), and displays a higher resistance to hydrolysis than LA because of its more hydrophobic character and less proportion of ester groups. As a result, this opposite effect means that

the degradation rate obtained ($K_{Mw} = 0.030 \text{ days}^{-1}$) was slightly lower than that of some of the crystallisable copolymers.

Table 4 also collects values of K_{Mw} taken on day 14. It is worth noting that, in some cases, there were significant differences in the degradation rate (K_{Mw}) between the calculated values and those obtained over shorter periods (day 14). While the calculated values of K_{Mw} and the K_{Mw} obtained on day 14 are fairly close for the crystallisable copolymers, it was found that for the amorphous polymers (the terpolymers and PLVL 53), the degradation rate on day 14 is considerably lower than when the K_{Mw} is calculated. For example, K_{Mw} is 0.060 days^{-1} for PLVL 007525 while on day 14 it is 0.050 days^{-1} . This acceleration in the reduction of molecular weight during degradation is presumably due to autocatalytic hydrolysis [37]. The accumulation of small chains and acidic degradation products, which are not able to escape from the polymer matrix as soon as they become soluble, is reported to contribute to the acceleration of the rate of chain scission [13]. Nevertheless, in the case of the crystalline polymers, in which the state of degradation is less advanced and the changes in water uptake during the first few weeks of the study are almost negligible, this autocatalytic effect is weaker and the degradation rate is almost constant at any part of the fitting curve.

Analysis of the remnants

The changes in thermal properties, water uptake and molecular weight loss of the polymer sample were reflected in the morphological appearance of the degradation remnants. Those polymers, which do not crystallize during degradation, degraded homogeneously leaving soft and pasty residues over long degradation times. In addition, the degradation effects were macroscopically discerned in these PLVLs well before those of the crystalline polymers. Figure 9 shows three samples of PLVL 007525 after 56 days of degradation along with a square sample of the non-degraded polymer. At this stage of degradation, this PLVL had an M_w of 6.9 kg mol^{-1} and due to the high levels of water absorption, the polymer chains were partially soluble forming a whitish pasty mass at the moment when the samples were removed from the aqueous medium. Once they were air-dried and the water was eliminated, the pasty mass became an amorphous layer with no mechanical performance. In the case of the amorphous

polymers with high glass transition temperatures, as is the case of PLVL 404515, the samples became brittle before pasty. On the other hand, PLVL 53, the copolymer with the lowest T_g , was very sticky and difficult to manipulate after day 35 of the study.



Figure 9. Samples of PLVL 007525 on day 56 of degradation.

With regard to the crystalline polymers, which include the L-LA-co- δ -VL copolymers with the exception of PLVL 53, brittle crystalline residues were generated during the hydrolytic degradation study. However, their original sample shape was preserved for a long time. The type of the L-LA crystallites formed, that is, the degree of perfection and their melting temperature, also affects the physical appearance of their remnants. Hence, samples of PLVL 74 ($l_{L-LA} = 3.73$), PLVL 750025 ($l_{L-LA} = 3.82$), PLVL 70Sn ($l_{L-LA} = 4.94$) and PLVL 82 ($l_{L-LA} = 5.55$), with T_m higher than 110 °C, were highly brittle fragments from day 56 on. These remnants are undesirable in medical applications because they are very resistant to hydrolysis [38] and can cause foreign body reactions in the surrounding tissues [39-41]. On the other hand, crystallisable copolymers with shorter average sequence lengths of L-LA, such as PLVL 69 ($l_{L-LA} = 3.11$) and PLVL 71 ($l_{L-LA} = 3.32$), were not able to arrange into such highly crystalline organized structures. Due to their low T_m values, in the range of 90-100 °C, their remnants were less brittle and hydrolytically resistant than those corresponding to the other crystalline copolymers of L-LA-co- δ -VL used in this work and in particular, the polylactide

homopolymers with a T_{ms} higher than 170 °C [42]. To illustrate what is outlined above, Figure 10 shows a sample of PLVL 69 on day 98 of degradation (on the right side of the image) and also fragments of PLVL 74 (on the left) on the same day of degradation. As can be seen, PLVL 69 has suffered a visible deterioration but its sample it is not as brittle as in the case of PLVL 74. Their M_w on this day were 7.2 and 7.4 kg mol⁻¹, respectively.



Figure 10. Samples of PLVL 74 (left) and PLVL 69 (right) on day 98.

Proton nuclear magnetic resonance (¹H NMR) spectra were obtained before carrying out the hydrolytic degradation study and after 70 days submerged in PBS at 37 °C. Figure 11 shows the spectrum of the PLVL 008515 on day 70 of the study. As the degradation progresses, new signals appeared in the ¹H NMR of the PLVLs and, in addition to the lactide methine and the caprolactone methylene signals (see Figure 1 of PLVL 008515 on day 0), small peaks can be identified, these are associated to the terminal groups of degradation byproducts. In this sense, although it should be confirmed by addition of trichloroacetylisocyanate, the quadruplet at 4.35 ppm and the triplet at 3.65 ppm could be assigned to –CHOH and –CH₂OH terminal groups.

Table 5 summarizes the lactide (L-lactide + D-lactide) and δ -valerolactone molar contents of the polymeric samples before degradation and after 70 days of hydrolytic degradation. The molecular weights (M_w) on day 70, measured by GPC, are also given in the Table. As can be seen, the polymers with the slowest degradation rate have the highest molecular weights at this stage of degradation, samples of PLVL 70Sn and

PLVL 82 presented M_w of 16.7 and 26.7 kg mol^{-1} , respectively. On the other hand, the lowest values of M_w were found for PLVL 007525 (6.3 kg mol^{-1}), PLVL 502525 (7.7 kg mol^{-1}) and PLVL 008515 (7.4 kg mol^{-1}), which are amorphous polymers with low stereoregularity due to short L-LA, D-LA and δ -VL sequences in their polymer chains.

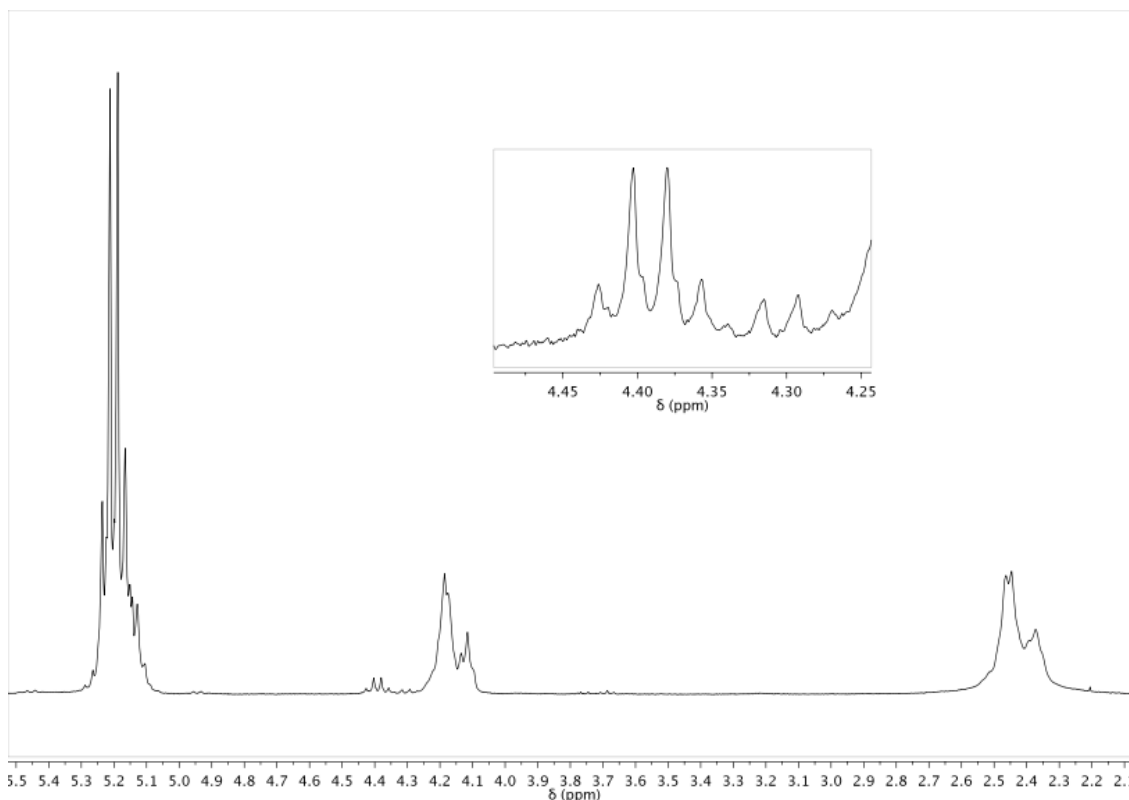


Figure 11. ^1H NMR spectrum of PLVL 008515 on day 70 of degradation.

Table 5. Copolymer molar compositions after 70 days of hydrolytic degradation.

Sample	Composition on day 0 (% molar)		R (day 0)	Composition on day 70 (% molar)		R (day 70)	M_w at day 70 (kg mol^{-1})
	% LA	% δ -VL		% LA	% δ -VL		
PLVL 53	53.4	46.6	1.20	52.1	47.9	1.23	11.6
PLVL 69	68.6	31.4	1.02	69.9	30.1	1.03	11.0
PLVL 71	70.8	29.2	1.03	73.0	27.0	1.04	13.0
PLVL 74	73.6	26.4	1.01	75.2	24.8	1.02	11.7
PLVL 82	81.9	18.1	1.00	80.5	19.5	0.99	26.7
PLVL 70Sn	70.1	29.9	0.68	72.6	27.4	0.68	16.7
PLVL 007525	74.8	25.2	0.99	70.1	29.9	1.00	6.3
PLVL 502525	74.8	25.2	0.95	72.2	27.8	0.90	7.7
PLVL 750025	73.6	26.4	0.99	75.8	24.2	0.95	11.7
PLVL 008515	85.8	14.2	0.95	82.5	17.5	0.87	7.4
PLVL 404515	86.6	14.4	0.93	84.1	15.9	0.92	9.4

With respect to the polymer composition, slight differences in the co-monomer contents measured before and after the degradation process were found. Meanwhile, the randomness parameter (R), also collected in the Table 5, stayed almost constant. For the crystalline copolymers with LA lower than 75 % it can be seen that the LA content rose as the degradation process advanced (i.e. For PLVL 74, % LA increased from 73.6 to 75.2 %). On the other hand, the LA content decreased for the amorphous polymeric materials, PLVL 53 and the terpolymers composed of L-LA, D-LA and δ -VL (i.e. For PLVL 007525, % LA lowered from 74.8 to 70.1 %). As is well known, amorphous regions are preferentially degraded because they are more easily accessible to water molecules. However, the fact is that, as degradation progresses, these amorphous regions are richer in either LA or in δ -VL depending on the polymer morphology. In the L-LA-co- δ -VL crystallizable copolymers, LA-rich segments migrate from the amorphous domains to the crystalline phase and, as a result, the amorphous phase became poorer in LA. Although the LA-units are more easily hydrolysable than those of δ -VAL, there may be a negligible content of LA in the amorphous phase (except in the case of the PLVL 82) and consequently the δ -VL blocks were degraded first and the total LA molar content in the polymer increases. On the contrary, the amorphous phases of the fully amorphous copolymers are highly heterogeneous and phase separation phenomena do not occur. Since these amorphous regions are rich in lactide, the LA blocks were preferably degraded.

2.2.4. Conclusions

In this *in vitro* degradation study repetitive square samples of different lactide-co- δ -valerolactone copolymers (PLVL) were submerged in PBS at 37 °C for a period up to 98 days. The results probe that the water absorption is a key factor in the degradation process. Therefore, the polymers that displayed higher values of water uptake also presented the fastest degradation rates, while the development of crystalline domains was probed to hinder water absorption. Large average sequence lengths of L-LA (l_{L-LA}) in the copolymer chains give them a higher crystallization capability during degradation. On the contrary, the combination of short L-lactide, D-lactide and δ -

valerolactone segments in the PLVLs resulted in a more amorphous morphology with lower stereoregularity and consequently favoured a homogeneous degradation at an accelerated rate. In addition, for these amorphous polymeric materials, their sample residues were soft and pasty, while brittle and hydrolytically resistant fragments, which are undesirable, were not generated.

Regarding the L-LA-co- δ -VL copolymers, which do not have D-LA units disrupting the microstructural arrangement of their L-LA crystallizable chains, the highest degradation rate belongs to the PLVLs with L-LA contents in the range of 69 to 74 %. If the L-LA content is increased or lowered, the degradation rate decreased. This is either because the copolymers are prone to more perfect crystallization at higher T_m s or because the δ -VL content is too large. The higher resistance to hydrolysis of δ -VL compared to LA units, is due to its more hydrophobic character and less proportion of ester groups, and seems to have a direct effect on the degradation despite the fact that water absorption begins earlier in δ -VL rich copolymers.

Finally, it is also worth mentioning the fact that although the proportion of hydrolyzable ester bonds is richer in the case of the PLVLs than in the lactide-co- ϵ -caprolactone (PLCL) polymer chains, PLVLs (with higher T_g s than PLCLs) degraded at a slower rate than the ϵ -CL based copolymers. This demonstrated that the packed amorphous regions related to high glass transition temperatures, also slow down the water absorption phenomenon.

References

- [1] Middleton, J.C, Tipton, A.J. Synthetic biodegradable polymers as orthopedic devices. *Biomaterials* 2000, 21, 2335-2346.
- [2] Vert, M.; Li, M.S.; Spenlehauer, G.; Guerin, P. Bioresorbability and Biocompatibility of Aliphatic Polyesters. *Journal of Materials Science: Materials in Medicine* 1992; 3; 432-446.
- [3] Anderson, J.M.; Rodriguez, A.; Chang, D.T. Foreign body reaction to biomaterials. *Seminars in Immunology* 2008, 20, 86-100.
- [4] Hutmacher, D.W. Scaffold Design and Fabrication Technologies for Engineering Tissues- State of the Art and Future Perspectives. *Journal of Biomaterials Science-Polymer Edition* 2001, 12, 107-124.
- [5] Hutmacher, D.W. Scaffolds in Tissue Engineering Bone and Cartilage. *Biomaterials* 2000; 21, 2529-2543.
- [6] Dorati, R.; Colonna, C.; Genta, I.; Modena, T.; Conti, B. Effect of Porogen on the Physico-Chemical Properties and Degradation Performance of PLGA Scaffolds. *Polymer Degradation and Stability* 2010, 95, 694-701.
- [7] Lu, L.; Peter, S.J.; Lyman, M.D.; Lai, H.L.; Leite, S.M.; Tamada, J.A.; Vacanti, J.P.; Langer, R.; Mikos, A.G. In Vitro Degradation of Porous Poly(L-lactic acid) Foams. *Biomaterials* 2000, 21, 1595-1605.
- [8] Pamula, E.; Menaszek, E. In Vitro and In Vivo Degradation of Poly(L-lactide-co-glycolide) Films and Scaffolds. *Journal of Materials Science: Materials in Medicine* 2008, 19, 2063-2070.
- [9] Larrañaga, A.; Martin, F.J.; Aldazabal, P.; Sarasua J.R. Hydrolytic degradation and Bioactivity of Lactide and Caprolactone based sponge-like scaffolds loaded with bioactive glass particles. *Polymer Degradation and Stability* 2014. 110, 121-128.
- [10] Göpferich, A. Mechanism of polymer degradation and erosion. *Biomaterials* 1996, 17, 103-114.
- [11] von Burkersroda, F.; Schedl, L.; Göpferich, A. Why degradable polymers undergo surface erosion or bulk erosion. *Biomaterials* 2002, 23, 4221-4231.
- [12] Kulkarni, A.; Reiche, J.; Lendlein, A. Hydrolytic degradation of poly(rac-lactide) and poly[(rac-lactide)-co-glycolide] at the air water interface. *Surface and Interface Analysis* 2007, 39, 740-746.

- [13] Gleadall, A.; Pan, J.; Kruff, M-A.; Kellomaki, M. Degradation mechanisms of bioresorbable polyesters. Part 1. Effects of random scission, end scission and autocatalysis. *Acta Biomaterialia* 2014, 10, 2223-2232.
- [14] Shih, C. Chain-end scission in acid catalyzed hydrolysis of poly (D,L-lactide) in solution. *Journal of Controlled Release* 1995, 34, 9–15.
- [15] Hofmann, D.; Entrialgo-Castaño, M.; Kratz, K.; Lendlein, A. Knowledge-Based Approach towards Hydrolytic Degradation of Polymer-Based Biomaterials. *Advanced Materials* 2009, 21, 3237-3245.
- [16] Suping, Schley, J.; Loy, B.; Lind, D.; Hobot, C.; Sparer, R.; Untereker, D. Kinetics and time-temperature equivalence of polymer degradation. *Biomacromolecules* 2007; 8, 2301–2310.
- [17] Tsuji, H. Autocatalytic hydrolysis of amorphous-made polylactides: effects of L-lactide content, tacticity, and enantiomeric polymer blending. *Polymer* 2002, 43, 1789–1796.
- [18] Siparsky, G.L.; Voorhees, K.J.; Miao, F. Hydrolysis of polylactic acid (PLA) and polycaprolactone (PCL) in aqueous acetonitrile solutions: autocatalysis. *Journal of Environmental Polymer Degradation* 1998, 6, 31–41.
- [19] Grizzi, I.; Garreau, H.; Li, S.; Vert, M. Hydrolytic degradation of devices based on poly(DL-lactic acid) size-dependence. *Biomaterials* 1995, 16, 305-311.
- [20] Dobrzynski, P.; Li, S.; Kasperczyk, J.; Bero, M.; Gasc, F.; Vert, M. Structure-property relationships of copolymers obtained by ringopening polymerization of glycolide and ϵ -caprolactone. Part 1. Synthesis and characterization. *Biomacromolecules* 2005, 6, 483-488.
- [21] Hua, J.; Gebarowska, K.; Dobrzynski, P.; Kasperczyk, J.; Wei, J.; Li, S. Influence of chain microstructure on the hydrolytic degradation of copolymers from 1,3-trimethylene carbonate and L-lactide. *Journal of Polymer Science: Part A: Polymer Chemistry* 2009, 47, 3869-3879.
- [22] Jelonek, K.; Kasperczyk, J.; Dobrzynski, P.; Jarzabek, B. Controlled poly(l-lactide-co-trimethylene carbonate) delivery system of cyclosporine A and rapamycin- the effect of copolymer chain microstructure on drug release rate. *International Journal of Pharmaceutics* 2011, 414, 203-209.
- [23] Fernández, J.; Larrañaga, A.; Etxeberria, A.; Sarasua, J.R. Effects of chain microstructures and derived crystallization capability on hydrolytic degradation of poly(L-lactide/ ϵ -caprolactone) copolymers. *Polymer Degradation and Stability* 2013, 98, 481-489.

- [24] Albertsson, A.C.; Eklund, M. Influence of molecular structure on the degradation mechanism of degradable polymers: In vitro degradation of poly(trimethylene carbonate), poly(trimethylene carbonate-co-caprolactone) and poly(adipic anhydride). *Journal of Applied Polymer Science* 1995, 57, 87-103.
- [25] Nakayama, A.; Kawasaki, N.; Maeda, Y.; Arvanitoyannis, I.; Aiba, S.; Yamamoto, N. Study of biodegradability of poly(delta-valerolactone-co-L-lactide)s. *Journal of Applied Polymer Science* 1997, 66, 741-748.
- [26] Wu, L.; Ding, J. Effects of porosity and pore size on in vitro degradation of three-dimensional porous poly(D,L-lactide-co-glycolide) scaffolds for tissue engineering. *Journal of Biomedical Materials Research* 2005, 75, 767-777.
- [27] Fernández, J.; Etxeberria, A.; Sarasua, J.R. Synthesis, structure and properties of poly(L-lactide-co-ε-caprolactone) statistical copolymers. *Journal of the Mechanical Behavior of Biomedical Materials* 2012, 9, 100-112.
- [28] Fernández, J.; Meaurio, E.; Chaos, A.; Etxeberria, A.; Alonso-Varona, A.; Sarasua J.R. Synthesis and characterization of poly(L-lactide/ ε-caprolactone) statistical copolymers with well resolved chain microstructures. *Polymer* 2013, 54, 2621-2631.
- [29] Herbert, I.R. Statistical analysis of copolymer sequence distribution. In *NMR Spectroscopy of Polymers*. Ibbet, R.N. Ed.: Blackie Academic & Professional, London, 1993:50-79. (Chapter 2).
- [30] Baimark, Y.; Molloy, R. Synthesis and Characterization of poly(l-lactide-co-ε-caprolactone) copolymers: Effects of stannous octoate initiator and diethylene glycol coinitiator concentrations. *Science Asia* 2004, 30, 327-334.
- [31] Vanhoorne, P.; Dubois, Ph.; Jerome, R.; Teyssie, Ph. Macromolecular engineering of polylactones. 7: Structural analysis of copolyesters of ε-caprolactone and L- or D,L-lactide initiated by Al(Oi-Pr)₃. *Macromolecules* 1992, 25, 37-44.
- [32] Kasperczyk, J.; Bero, M. Coordination polymerization of lactides: 2. Microstructure determination of poly[(L,L-lactide)-co-(ε-caprolactone)] with ¹³C nuclear magnetic resonance spectroscopy. *Makromolekular Chemistry* 1991, 192, 1777-17887.
- [33] Fernández, J.; Larrañaga, A.; Etxeberria, A.; Sarasua, J.R. Tensile behavior and dynamic mechanical analysis of novel poly(lactide/δ-valerolactone) statistical copolymers. *Journal of the Mechanical Behavior of Biomedical Materials* 2014, 35, 39-50.

-
- [34] Fernández, J.; Larrañaga, A.; Etxeberria, A.; Wang, W.; Sarasua, J.R. A new generation of poly(lactide/ ϵ -caprolactone) polymeric biomaterials for application in the biomedical field. *Journal of Biomedical Materials Research A* 2014, 102A, 3573–3584.
- [35] Aubin, M.; Prud'homme, R.E. Preparation and properties of poly(valerolactone). *Polymer* 1981, 22, 1223-1226.
- [36] Cao, H.; Han, H.; Li, G.; Yang, J.; Zhang, L.; Yang, Y.; Fang, X.; Li, Q. Biocatalytic Synthesis of Poly(δ -Valerolactone) Using a Thermophilic Esterase from *Archaeoglobus fulgidus* as Catalyst. *International Journal of Molecular Sciences* 2012, 13, 12232–12241.
- [37] Antheunis, H.; van der Meer, J-C., de Geus, M.; Kingma, W.; Koning C.E. Improved mathematical model for the hydrolytic degradation of aliphatic polyesters. *Macromolecules* 2009, 42, 2462–2471.
- [38] Tsuji, H.; Ikarashi, K. In vitro hydrolysis of poly(L-lactide) crystalline residues as extended-chain crystallites. Part I: long-term hydrolysis in phosphate-buffered solution at 37 °C. *Biomaterials* 2004, 25, 5449-5455.
- [39] De Jong, W.H.; Bergsma, J.E.; Robinson, J.E., Boss, R.R.M. Tissue response to partially in vitro predegraded poly-L-lactide implants. *Biomaterials* 2005, 26, 1781-1791.
- [40] Mainil-Varlet, P.; Rahn, B.; Gogolewski, S. Long term in vivo degradation and bone reaction to various polylactides. *Biomaterials* 1997, 18, 257-266.
- [41] Bergsma, J.E.; de Bruijn, W.C.; Rozema, J.R.; Boss, R.R.M.; Boering, G. Late degradation tissue response to poly(L-lactide) bone plates and screws. *Biomaterials* 1995, 16, 25-31.
- [42] Garlotta, D. A literature review of poly(lactic acid). *Journal of Polymers and the Environment* 2001, 9(2), 63-84.

Section 2- Copolymers of low glass transition temperature

Summary

Poly(ϵ -caprolactone), poly(δ -valerolactone) and some polymacrolactones, such as poly(ω -pentadecalactone) or poly(ethylene-brassylate) show an outstanding combination of properties. This group of polyesters presents high thermal stability and rapid crystallization from melt, which prevent physical aging. In addition, they also display an appealing mechanical performance, with high elongation at break values and elastic modulus below 400 MPa. However, these homopolymers biodegrade at a very slow rate owing to their high crystallinity fraction. Thus, PCL degrades at a rate (K_{Mw}) of only 0.0010 days^{-1} at $37 \text{ }^\circ\text{C}$ while PPDL is practically non-degradable in aqueous medium. Hence, the synthesis of poly(ϵ -caprolactone)-like biomaterials with an improved biodegradability is extremely interesting and could meet the requirements for a large number of potential applications in the biomedical field.

In this section several copolyesters with a glass transition temperature under $-25 \text{ }^\circ\text{C}$ and melting temperatures below $100 \text{ }^\circ\text{C}$ were synthesized by ring-opening polymerization employing triphenyl bismuth as catalyst. Then, these novel copolymers were characterized using different techniques. The mechanical behaviour of the copolymers with low T_g is heavily dependent on the crystalline phase (on their T_m and melting enthalpies), especially at temperatures close to their melting points. For this reason, the T_m of the polymers of this section should be above human body temperature ($37 \text{ }^\circ\text{C}$) in order to guarantee their mechanical performance during use.

- The copolymerization of ϵ -caprolactone with L-lactide or δ -valerolactone units was the strategy used by our research group in **Chapter 3.1**. (*Crystallization and Melting Behaviour of Poly(ϵ -Caprolactone-co- δ -Valerolactone) and Poly(ϵ -Caprolactone-co- δ -L-lactide) with Novel Chain Microstructures*) to reduce the crystallinity and so improve the biodegradability of the PCL homopolymer. NMR characterization of the copolymers showed that the poly(ϵ -caprolactone-co-L-lactide)s and the poly(ϵ -caprolactone-co- δ -valerolactone)s had semi-alternating ($R \rightarrow 2$) and random ($R \sim 1$) distribution of sequences, respectively. However, the aim of lowering the degree of crystallinity was not achieved in the case of the poly(ϵ -CL-co- δ -VAL). Non-isothermal cooling treatments at different rates and isothermal crystallizations at

different temperatures were conducted by DSC, and these demonstrated that the ϵ -CL copolymers containing δ -VAL exhibited a higher crystallization capability than those of L-LA and also arranged into crystalline structures over shorter times, regardless of their ϵ -CL average sequence length (l_{CL}). The crystallization of the ϵ -CL was easier with δ -VAL units than in the presence of rigid lactide segments, and for some compositions it was shown, via Wide Angle X-ray Scattering (WAXS), that these two lactones undergo isomorphism and co-crystallize in a single cell.

- In **Chapter 3.2**. (*In Vitro Degradation Studies and Mechanical Behaviour of Poly(ϵ -Caprolactone-co- δ -Valerolactone) and Poly(ϵ -Caprolactone-co- δ -L-lactide) with Random and Semi-alternating Chain Microstructures*), in view of their melting behaviour, only the copolymers with T_m s above body temperature (37 °C) were selected from among the materials synthesized in the previous chapter. Both ϵ -CL-co- δ -VAL copolymers, with ϵ -CL molar content ranging from 76 to 85 %, and ϵ -CL-co-L-LA copolymers, with 88 to 94 % of ϵ -CL, exhibited faster degradation rates than the polycaprolactone (PCL) homopolymer. δ -VAL copolymers degraded 3 to 5 times faster, whereas the copolymers based on lactide had K_{MW} values of between 0.0055 and 0.0105 days⁻¹. However, their mechanical behaviour was heavily dependent on the crystalline phase, especially at temperatures close to their melting point. As a result, only the poly(ϵ -CL-co-L-LA) which have a ϵ -CL molar content higher than 88 %, in addition to PCL, presented mechanical properties suitable enough at both room temperature and 37 °C.

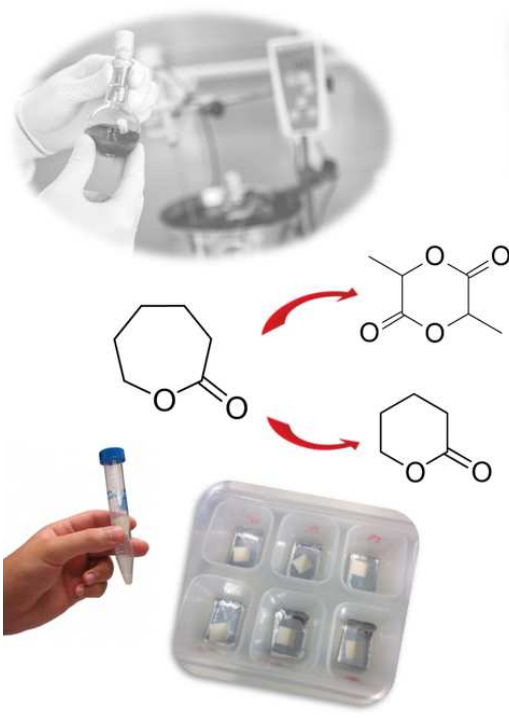
- If possible, the T_m value of this kind of copolymers of low T_g should preferably be higher than 60-65 °C (the T_m of PCL) so as to assure more stable mechanical properties. Likewise, the pair of comonomers should be chosen carefully to prevent the cocrystallization phenomenon. In **Chapter 4** (*Synthesis and Characterization of ω -Pentadecalactone-co- ϵ -Decalactone Copolymers: Evaluation of Thermal, Mechanical and Biodegradation Properties*) ω -pentadecalactone, whose homopolymer shows a T_m at ~ 100 °C, was copolymerized with ϵ -decalactone in order to reduce the high crystallization capability of PPDL. The incorporation of ϵ -

DL, a lactone identical to ϵ -CL but with a butyl side chain, decreased the crystalline fraction from 54 to 13-38 % and the T_g to around -50 °C. As a result, these copolymers with blocky chain microstructures (randomness character $R < 0.49$) and ω -PDL molar contents ranging from 30 to 78 %, displayed high elongation at break values and lower stiffness than PPDL (with secant modulus of 7 to 156 MPa) while their mechanical properties remained constant at 37 °C. However, *in vitro* degradation studies demonstrated that, despite their increased amorphous character, these materials were very resistant to hydrolysis due to the steric effect of the ϵ -DL units, and can virtually be considered as non-biodegradable polymers.

- In **Chapter 5** (*Synthesis and Properties of ω -Pentadecalactone-co- δ -Hexalactone Copolymers: A Biodegradable Thermoplastic Elastomer as an Alternative to Poly(ϵ -Caprolactone)*) δ -hexalactone, a six-membered lactone with identical structure to δ -valerolactone but possessing a methyl pendant group, was employed in place of ϵ -DL with the aim of lowering the steric effect of the ϵ -DL and at the same time increasing the hydrophilicity of the copolymers. The incorporation of 18 to 61 % molar content of δ -HL decreased the crystalline fraction of PPDL to 21-44 % and the T_g s to values below -36 °C. As a result, the degradation rates obtained for the poly(ω -PDL-co- δ -HL), which present chain microstructures that deviate slightly from a random distribution ($R > 0.74$), ranged from 0.0013 to 0.0019 days⁻¹. Owing to their lower stiffness and upgraded biodegradability in comparison to poly(ϵ -caprolactone) there are high hopes for these new thermoplastic elastomers, which also present high thermal stability and rapid crystallization from melt.
- Ethylene brassylate, a 17 member ring lactone with two ester groups (it is commercially available in large quantities and is of particular interest owing to its lower cost in comparison to other lactones and macrolactones) was copolymerized with δ -hexalactone in **Chapter 6** (*Ethylene brassylate-co- δ -hexalactone biobased polymers for application in the medical field: Synthesis, characterization and cell culture studies*). Owing to the racemic stereochemistry of the methyl side chain of the δ -HL unit, only the EB sequences were able to crystallize and as a result the

crystallinity fraction decreased from a 47 % (PEB homopolymer) to ~ 23-39 % (when 10 to 51 % of δ -HL units were incorporated). The poly(EB-co- δ -HL)s showed a slightly deviated from random distribution of sequences ($R > 0.71$) and thermal properties ($T_{gs} < -27$ °C and T_{ms} from 50 to 65 °C) which led to to a mechanical behaviour with improved flexibility in comparison to poly(ϵ -caprolactone) or poly(ω -pentadecalactone) (elastic modulus from 57 to 274 MPa with high elongation at break values) at both 21 °C and 37 °C. In addition, the incorporation of δ -HL allowed a degradation rate almost 4 times higher than that of Poly(ϵ -caprolactone) (K_{Mw} values in the range of 0.0028 to 0.0041 days⁻¹). Finally, cell culture studies of metabolic activity and cell morphology with Human Dermal Fibroblasts demonstrated that these materials are not cytotoxic and provide a valid substrate for cells to attach and proliferate. This opens the door to the use of these polymers in the biomedical field, particularly, for the regeneration of soft tissues and for various clinical implants and devices.

Chapter 3. ϵ -Caprolactone Copolymers with L-Lactide and δ -Valerolactone



**Chapter 3.1 Crystallization and Melting
Behaviour of Poly(ϵ -Caprolactone-co- δ -
Valerolactone) and Poly(ϵ -Caprolactone-
co-L-Lactide) with Novel Chain
Microstructures**

Journal of Applied Polymer Science 2015, 132, 45534.

Abstract

NMR characterization of the statistical copolymers of this study showed that the poly(ϵ -caprolactone-co-L-lactide)s, with ϵ -CL molar contents ranging from 70 to 94 % and l_{CL} (ϵ -CL average sequence length) between 2.20-9.52, and the poly(ϵ -caprolactone-co- δ -valerolactone)s, with 60 to 85 % of ϵ -CL and l_{CL} between 2.65-6.08, present semi-alternating ($R \rightarrow 2$) and random ($R \sim 1$) distribution of sequences, respectively. These syntheses were carried out with the aim of reducing the crystallinity of poly(ϵ -caprolactone), needed to provide mechanical strength to the material but also responsible for its slow degradation rate. However, this was not achieved in the case of the ϵ -CL-co- δ -VAL. Non-isothermal cooling treatments at different rates and isothermal crystallizations (at 5, 10, 21 and 37 °C) were conducted by DSC, and demonstrated that ϵ -CL copolymers containing δ -VL exhibited a larger crystallization capability than those of L-LA and also arranged into crystalline structures over shorter times. The crystallization enthalpies of the ϵ -CL-co- δ -VL copolymers during the cooling treatments and their heat of fusion at the different isothermal temperatures were very large (i.e. $\Delta H_c > 53 \text{ J g}^{-1}$) and in some cases, unrelated to the copolymer composition. In some compositions, such as the 60:40, WAXS proved that that these two lactones undergo isomorphism and co-crystallize in a single cell.

3.1.1. Introduction

Lactones and macrolactones are used in the chemical industry as flavors and fragrances but are also being employed in the manufacture of highly specialized biopolymers. Cyclic esters larger than five-membered rings lead to homopolymers that show a similar mechanical behaviour, with good ductility and strength which resemble the properties of low density polyethylene (LDPE). δ -valerolactone [1-4], ϵ -caprolactone [5-6], ethylene brassylate [7], ω -pentadecalactone [8-11] or hexadecalactone [12], containing respectively four, five, thirteen, fourteen or fifteen straight methylenes, together with an ester group (two in the case of ethylene brassylate), allow the formation of flexible semi-crystalline polymers with low melting points (< 100 °C) and glass transition temperatures (< -27 °C) that make them easy to manipulate with thermoplastic processing techniques. Nevertheless, these polylactones degrade at a very slow rate under hydrolytic conditions, over several years, which restricts their potential applications in the biomedical field.

Poly(ϵ -caprolactone) (PCL) was one of the earliest polymers synthesized by the Carothers' group in the early 1930s [13] and was used extensively in the biomaterials field during the resorbable-polymer-boom of the 1970s and 1980s. Nowadays it is still popular due to its outstanding rheological and viscoelastic properties [6] and is employed in medical devices and for tissue engineering, including among others, sutures for wound dressings, artificial blood vessels, nerve regeneration, drug-delivery devices and bone engineering applications [14]. PCL is a semi-crystalline polymer having a glass transition (T_g) at (-60) - (-65) °C and a melting point between 56 and 65 °C [5]; the crystalline nature of PCL makes it easily formable at relatively low temperatures. Likewise, this polyester presents exceptional blend-compatibility, efficient processing with thermoplastic techniques, high thermal stability [15-17] and very attractive mechanical properties, with high elongation at break values (750-1000 %) and Young's Modulus from 210 to 440 MPa [18]. However, among its disadvantages are its resistance to hydrolytic degradation. PCL homopolymer biodegrades slowly and shows complete degradation after 2-4 years depending on the

initial molecular weight of the device or implant [19-22]. In the hydrolytic degradation of polyesters, amorphous regions are preferentially degraded over the crystalline lamellae [23-25]. Therefore, the rate of biodegradation is highly influenced by the crystallization capability and the degree of crystallinity [26], reaching 69 % in the case of PCL [27].

In this study the copolymerization of ϵ -caprolactone with L-lactide [28-29] or δ -valerolactone [30-33] units was the strategy used to reduce the crystallinity and so improve the biodegradability of the PCL homopolymer. For this purpose, several poly(ϵ -caprolactone-co- L-lactide) and poly(ϵ -caprolactone-co- δ -valerolactone) copolymers were synthesized using triphenyl bismuth (Ph_3Bi), a catalyst that is known to favour random sequences [34]. Above their glass transition, the crystalline phase is the responsible of the mechanical properties of these low glass transition temperature's polymers and, therefore, ϵ -CL rich compositions were used. On the other hand, it should also be taken into consideration that their melting temperatures should be above the body temperature (37 °C), the one at which they would be employed, in order to ensure their mechanical performance during the application.

The polymers were characterized by proton and carbon nuclear magnetic resonance spectroscopy (^1H NMR and ^{13}C NMR) and gel permeation chromatography (GPC) measurements. In this first paper crystallization studies were carried out by means of non-isothermal cooling and isothermal experiments made on a differential scanning calorimetry (DSC) device, while wide angle X-ray diffraction (WAXRD) and Polarized Light Optical Microscopy (PLOM) techniques were also employed to complement the study. In the future, the analysis of these biomaterials will be completed after conducting mechanical characterization and *in vitro* hydrolytic degradation studies on the copolymers with high melting temperatures.

3.1.2. Materials and methods

Materials

ϵ -caprolactone monomer (assay > 98 %) was provided by Merck. L-lactide monomer (assay > 99.5 %) was supplied by Purac Biochem (The Netherlands) while δ -valerolactone monomer (assay > 98 %) was provided by Tokyo Chemical Industry (Cymit Quimica). The triphenyl bismuth (Ph_3Bi) catalyst was obtained from Gelest. 1-hexanol was supplied by Sigma Aldrich.

Synthesis procedure

Statistical copolymers from ϵ -caprolactone, L-lactide and δ -valerolactone were synthesized in bulk by one pot-one-step ring-opening polymerizations (ROP). The synthesis reactions were carried out in a flask immersed in a controlled temperature oil bath. In each polymerization, predetermined amounts of the different comonomers at the chosen mass feed ratio were simultaneously added and melted into the flask. 1-hexanol was also added to provide ROH groups in order to control the molecular weight. The flask was purged for 30 minutes with a nitrogen stream under the surface of the melt. The catalyst (Ph_3Bi) was then added (at 500:1 comonomers/catalyst molar ratio) and the magnetic stirrer maintained at 100 rpm. The ϵ -caprolactone-co- L-lactide polymerizations were carried out for 48 hours at 130 °C whereas the synthesis reactions of the ϵ -caprolactone-co- δ -valerolactone copolymers were conducted for 48 hours at 120 °C. The ϵ -caprolactone homopolymer was synthesized at 130 °C after 24 hours of reaction.

After the corresponding reaction time the products were dissolved in chloroform and precipitated, pouring the polymer solution into an excess of methanol in order to remove the catalyst impurities and those monomers that had not reacted. Finally the product was dried at room temperature and then subjected to a heat treatment at 140 °C for 1 hour to ensure the complete elimination of any remaining solvent.

Methods

Proton and carbon nuclear magnetic resonance (^1H NMR and ^{13}C NMR) spectra were recorded in a Bruker Avance DPX 300 at 300.16 MHz and at 75.5 MHz of resonance frequency respectively, using 5 mm O.D. sample tubes. All spectra were obtained at room temperature from solutions of 0.7 mL of deuterated chloroform (CDCl_3). Experimental conditions were as follows: a) for ^1H NMR: 10 mg of sample; 3 s acquisition time; 1 s delay time; 8.5 μs pulse; spectral width 5000 Hz and 32 scans; b) for ^{13}C NMR: 40 mg, inverse gated decoupled sequence; 3 s acquisition time; 4 s delay time; 5.5 μs pulse; spectral width 18800 Hz and more than 10000 scans.

The molecular weights of the polymers were determined by GPC using a Waters 1515 GPC device equipped with two Styragel columns ($10^2 - 10^4 \text{ \AA}$). Chloroform was used as eluent at a flow rate of 1 mL min^{-1} and polystyrene standards (Shodex Standards, SM-105) were used to obtain a primary calibration curve. The samples were prepared at a concentration of 10 mg in 2 mL.

The crystallization behaviour and the thermal properties of the polymers were studied on a DSC 2920 (TA Instruments). Samples of 6-9 mg were melted at $100 \text{ }^\circ\text{C}$ and then quenched to $-50 \text{ }^\circ\text{C}$ at different cooling rates (5, 10 and $20 \text{ }^\circ\text{C min}^{-1}$) to study the crystallization process during the cooling. On the other hand, the isothermal treatments were conducted at 5, 10, 21 and $37 \text{ }^\circ\text{C}$ for 1, 10, 30, 60, 180, 300, 600 and 1440 min. The melting temperature (T_m) and the heat of fusion (ΔH_m) were obtained from the scans completed from the corresponding isothermal temperature to $100 \text{ }^\circ\text{C}$ at $20 \text{ }^\circ\text{C min}^{-1}$. The values determined from the scans which were made immediately after cooling at $40 \text{ }^\circ\text{C min}^{-1}$ to the isothermal temperature were used as initial time values (time zero). Finally, a scan was also made at $20 \text{ }^\circ\text{C min}^{-1}$ from -85 to $100 \text{ }^\circ\text{C}$ to determine the glass transition temperatures (T_g) of the samples.

Polarized light optical microscopy (PLOM) was used to study the nucleation and growth of spherulites in some of the (co)polymers: the PCL homopolymer and two ϵ -CL-co-LA and ϵ -CL-co- δ -VL copolymers with similar average sequence length of ϵ -caprolactone unit. The samples were melted at $180 \text{ }^\circ\text{C}$ in an oven and then immediately

put under a polarizing microscope (Leica DMLM). The evolution of spherulites was followed during 20 min with images recorded at different times.

Wide angle X-ray diffraction (WAXRD) data were collected on a Bruker D8 Advance diffractometer operating at 30 kV and 20 mA. This device is equipped with a Cu tube ($\lambda = 1.5418 \text{ \AA}$), a Vantec-1 PSD detector, an Anton Parr HTK2000 high-temperature furnace and an Anton Parr MRI-wide low-temperature chamber. The powder patterns of the high-temperature furnace were recorded in 2θ steps of 0.033° in the $10 \leq 2\theta \leq 38$ range, counting for 0.2 s per step, from 30 to 122 °C every 2 °C using a heating rate of $0.17 \text{ }^\circ\text{C s}^{-1}$. The powder patterns of the low-temperature chamber were recorded in 2θ steps of 0.033° in the $10 \leq 2\theta \leq 38$ range, counting for 0.2 s per step, from 2 to 62 °C every 2 °C using a heating rate of $0.2 \text{ }^\circ\text{C s}^{-1}$.

3.1.3. Results and discussion

Characterization

Tables 1 and 2 summarize the characterization data of the copolymers studied. As can be observed, the initial molecular weights (M_w) of each polymer are large, ranging from 91 to 173 kg mol^{-1} with dispersities (D) between 1.70 - 1.92. For proper evaluation of the behaviour of the ϵ -caprolactone based copolymers, a polycaprolactone (PCL) homopolymer was also synthesized. This material has a M_w of 135 kg mol^{-1} with a dispersity of 1.74, and a glass transition temperature (T_g) at $-60.4 \text{ }^\circ\text{C}$.

ϵ -Caprolactone-co-L-Lactide copolymers

The characterization data of the poly(ϵ -caprolactone-co-L-lactide) are gathered in Table 1. This set of copolymers show glass transition temperatures (T_g s) that range from -57 to $-33 \text{ }^\circ\text{C}$, in ascending order as the ϵ -CL content decreases. Their lactide molar content ranges from $\sim 6 \%$ (CL-LA 94) to 30% (CL-LA 70) with average sequence lengths of ϵ -CL (l_{CL}) from 9.52 to 2.20, and possess a semi-alternating distribution of sequences.

The randomness character (R) value in all cases is higher than 1.50 and tends toward 2 as the ϵ -CL content increases.

Table 1. Characterization data of the different poly(ϵ -caprolactone-co-L-lactide).

Sample	Composition ¹ (% molar)		M_w kg mol ⁻¹	D	Microstructural Magnitudes ²			T_g ³ °C
	% ϵ -CL	% L-LA			l_{CL}	l_{LA}	R	
CL-LA 94	94.3	5.7	143.1	1.70	9.52	0.58	1.84	-57.4
CL-LA 92	91.6	8.4	131.6	1.77	6.65	0.61	1.80	-54.0
CL-LA 88	88.3	11.7	132.6	1.84	4.91	0.65	1.74	-54.6
CL-LA 83	83.3	16.7	172.9	1.92	3.54	0.71	1.69	-48.2
CL-LA 70	70.0	30.0	123.1	1.86	2.20	0.94	1.51	-32.9

¹ Calculated from ¹H NMR spectra.

² l_{CL} and l_{LA} are the CL and LA number average sequence lengths obtained from ¹H NMR. These values are compared to the Bernoullian random number-average sequence lengths ($l_{CL}=1/LA$ and $l_{LA}=1/CL$), obtaining the randomness character value (R).

³ Obtained from a DSC scan made at 20 °C min⁻¹ from -85 to 100 °C

The ϵ -caprolactone and L-lactide molar content and the microstructural magnitudes of the copolymers were obtained from the average dyad relative molar fractions. The lactide methine signals, centered at 5.15 ppm, and those of the α and ϵ methylenes of the ϵ -caprolactone, around 2.35 and 4.10 ppm, seen in the ¹H NMR spectrum (see Figure 1) were assigned to the different dyads [28]. Then, equations 1-3 [35] were employed to obtain the number-average sequence lengths (l_i), the Bernoullian random number-average sequence lengths (l_i) and the randomness character (R):

$$l_{LA} = \frac{(LA - LA) + \frac{1}{2}(LA - CL)}{\frac{1}{2}(LA - CL)} = \frac{2(LA)}{(LA - CL)} ; \quad (1)$$

$$l_{CL} = \frac{(CL - CL) + \frac{1}{2}(LA - CL)}{\frac{1}{2}(LA - CL)} = \frac{2(CL)}{(LA - CL)}$$

$$(l_{CL})_{random} = \frac{1}{(LA)} ; \quad (l_{LA})_{random} = \frac{1}{(CL)} \quad (2)$$

$$R = \frac{(I_{\text{CL}})_{\text{random}}}{I_{\text{CL}}} = \frac{(I_{\text{LA}})_{\text{random}}}{I_{\text{LA}}} \quad (3)$$

where (CL) and (LA) are the ϵ -caprolactone and L-lactide molar fractions and (CL-LA) is the CL-LA average dyad relative molar fraction.

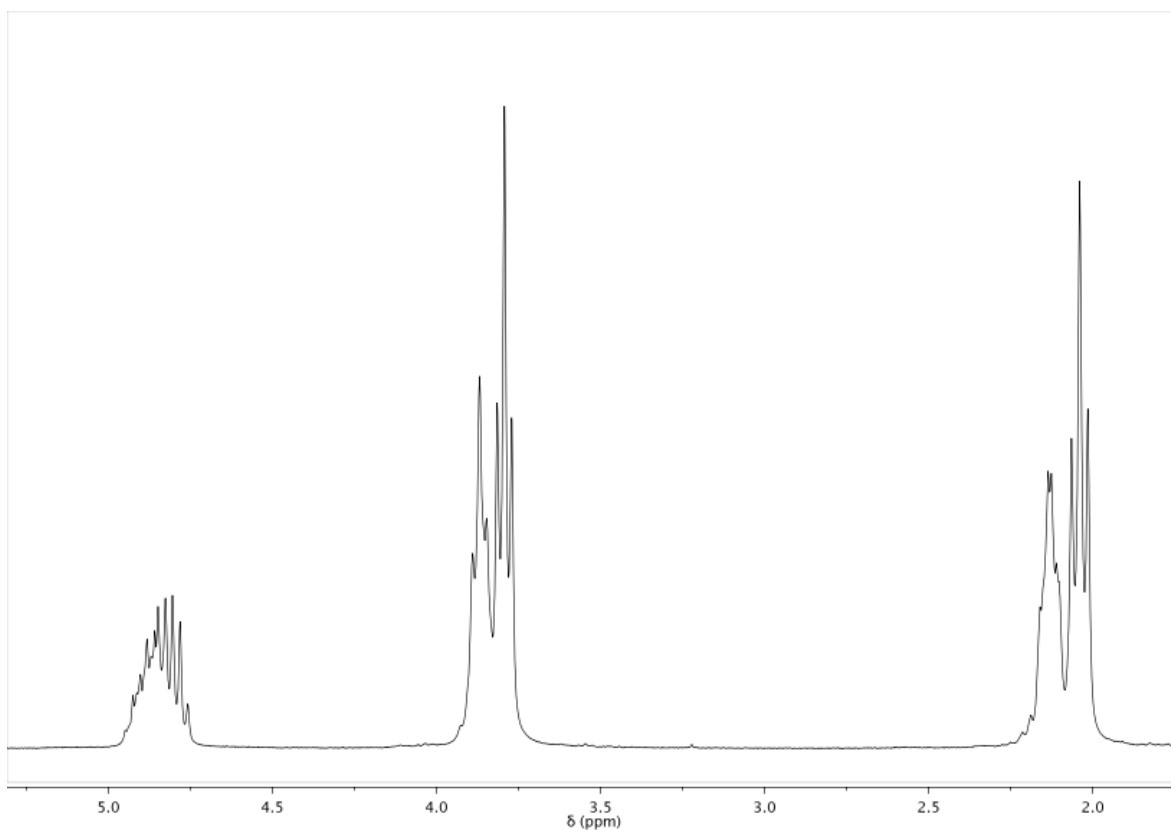


Figure 1. ^1H NMR spectrum of CL-LA 70.

To confirm the semi-alternating character ($R \rightarrow 2$) of this group of copolymers, the ^{13}C NMR spectrum was recorded for CL-LA 88, a copolymer showing an R value of 1.74 in the proton nuclear magnetic resonance. The region of β and γ methylene carbon atoms, located between 24 - 26 ppm, [29, 36-37] was employed for obtaining the randomness character from eq. (4).

$$R = \frac{(I_{\text{CL}})_{\text{random}}}{I_{\text{CL}}} \quad \text{where} \quad I_{\text{CL}} = \frac{I_{\text{CL-CL-CL}} + I_{\text{LA-CL-CL}}}{I_{\text{CL-CL-LA}} + I_{\text{LA-CL-LA}}} + 1 \quad (4)$$

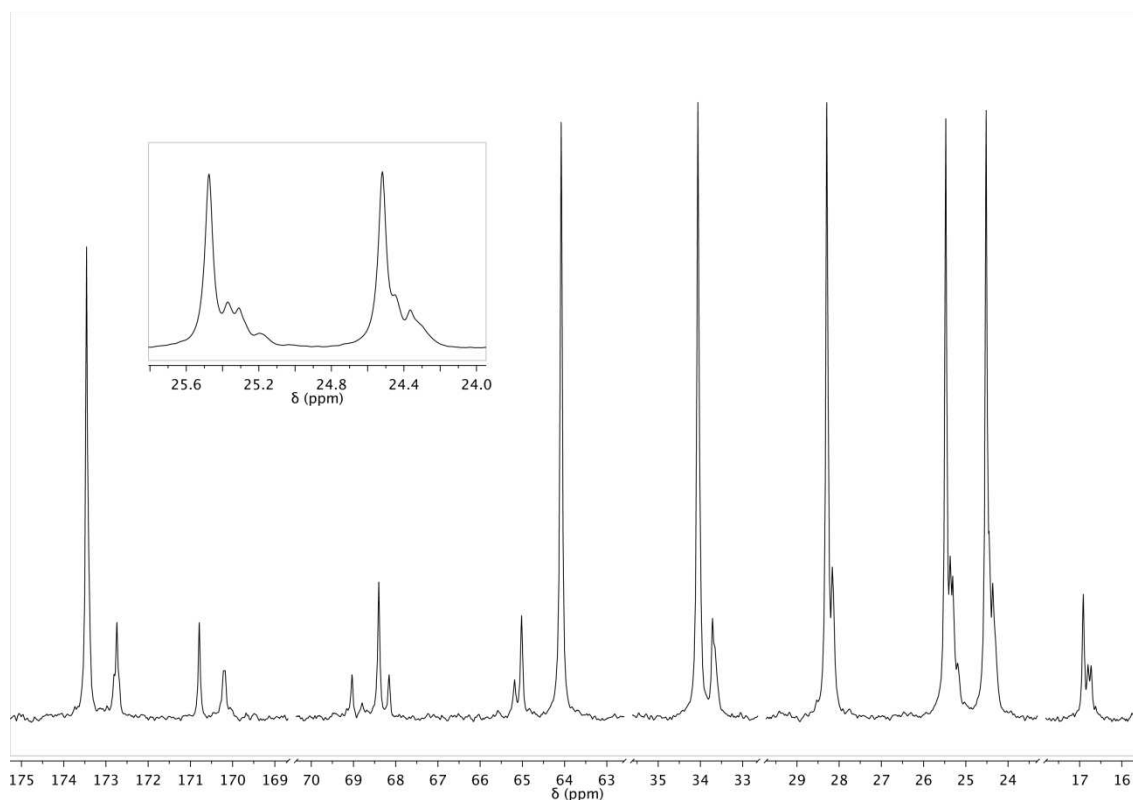


Figure 2. ^{13}C NMR spectrum of CL-LA 88; region of β and γ -methylene carbon atoms is enlarged.

Figure 2 shows the ^{13}C NMR spectrum of CL-LA 88 with the region of β and γ -methylene carbon atoms enlarged. CL-CL-CL, LA-CL-CL, CL-CL-LA and LA-CL-LA triads can be assigned from left to right in both methylene signals [37]. It can be observed that the CL-CL-CL triad signals are significantly more intense than in the rest of the triads. However, for a random ($R \sim 1$) or blocky ($R \rightarrow 0$) distribution of sequences, the peaks corresponding to the other triads should be lower, primarily in the case of the LA-CL-LA signal, a peak which is distinguishable in the β carbon atom signal at 25.2 ppm. The calculated value of R for this copolymer was 1.85, proving again the semi-alternating chain microstructure of these poly(ϵ -caprolactone-co-L-lactide) polymeric materials synthesized with Ph_3Bi .

ϵ -Caprolactone-co- δ -Valerolactone copolymers

In the case of the ϵ -caprolactone-co- δ -valerolactone copolymers the resonances for the protons of either repeat unit overlap sufficiently to prevent accurate integration of the

peak areas [31, 38-39]. For this reason, the molar composition and the microstructural parameters were calculated through the integration of the ^{13}C NMR spectra.

Table 2. Characterization data of the different poly(ϵ -caprolactone-co- δ -valerolactone).

Sample	Composition ¹ (% molar)		M_w kg mol ⁻¹	D	Microstructural Magnitudes ²			T_g ³ °C
	% ϵ -CL	% δ -VL			l_{CL}	l_{VL}	R	
CL-VAL 85	85.3	14.7	90.9	1.75	6.08	1.05	1.12	-64.3
CL-VAL 76	76.1	23.9	109.7	1.76	3.94	1.24	1.06	-63.7
CL-VAL 70	70.2	29.8	94.2	1.75	3.30	1.40	1.01	-63.6
CL-VAL 60	60.0	40.0	123.6	1.77	2.65	1.77	0.94	-65.3

¹ Calculated from ^{13}C NMR spectra.

² l_{CL} and l_{VL} are the CL and VL number average sequence lengths obtained from ^{13}C NMR. These values are compared to the Bernoullian random number-average sequence lengths ($l_{CL}=1/VL$ and $l_{VL}=1/CL$), obtaining the randomness character value (R).

³ Obtained from a DSC scan made at $20\text{ }^\circ\text{C min}^{-1}$ from -85 to $100\text{ }^\circ\text{C}$.

Table 2 summarizes the data obtained from the ^{13}C NMR, molecular weights and glass transition temperatures of the different poly(ϵ -caprolactone-co- δ -valerolactone) synthesized. These copolymers present ϵ -CL molar contents ranging from 85.3 to 60.0 % (l_{CL} from 6.08 to 2.65) and show a random distribution of sequences ($R \sim 1$). Owing to the similarities between the glass transition temperatures of both homopolymers (at $-65\text{ }^\circ\text{C}$ for PCL and at $-57\text{ }^\circ\text{C}$ for PVL [40]), the T_g values of this series of copolymers are almost equal, around $-64\text{ }^\circ\text{C}$.

Figure 3 shows the ^{13}C NMR spectrum of CL-VAL 70, a ϵ -caprolactone-co- δ -valerolactone copolymer with a ϵ -CL molar content of 70 %. The signals appearing between 21 and 174 ppm of chemical shift (δ) can be assigned to the different carbons of the repeat units as follows. The signals centered at 173.5 ppm belong to the carbonyl carbon of the ϵ -CL and δ -VL units, the peaks at 64.0, 34.0 and 28.3 ppm are respectively assigned to ϵ -, α - and δ - methylenes and the region 20-26 ppm contain the remaining methylene carbons. The peaks at 25.5 ppm and 24.6 correspond to the β - and γ -methylenes of the ϵ -CL repeat unit (δ -VL unit does not have γ -CH₂ in its structure, see Figure 4) whereas the β -methylene of the δ -VL repeat unit give a signal at 21.4 ppm of

chemical shift. The molar composition of the copolymers can be easily determined by comparing the area under the peak due to the β -carbon in the δ -VL unit to either the area of the β -CH₂ or the γ -CH₂ of the ϵ -CL. The area calculated from the β -carbon of the ϵ -CL was reported by Storey et al. [31] to always be larger than that of the γ -carbon because of an added contribution from the initiator fragment. So, in this paper the calculus was made based on the ratio of the integrated areas of the γ -methylene group from the ϵ -CL to that of the β -CH₂ of the δ -VL repeat unit.

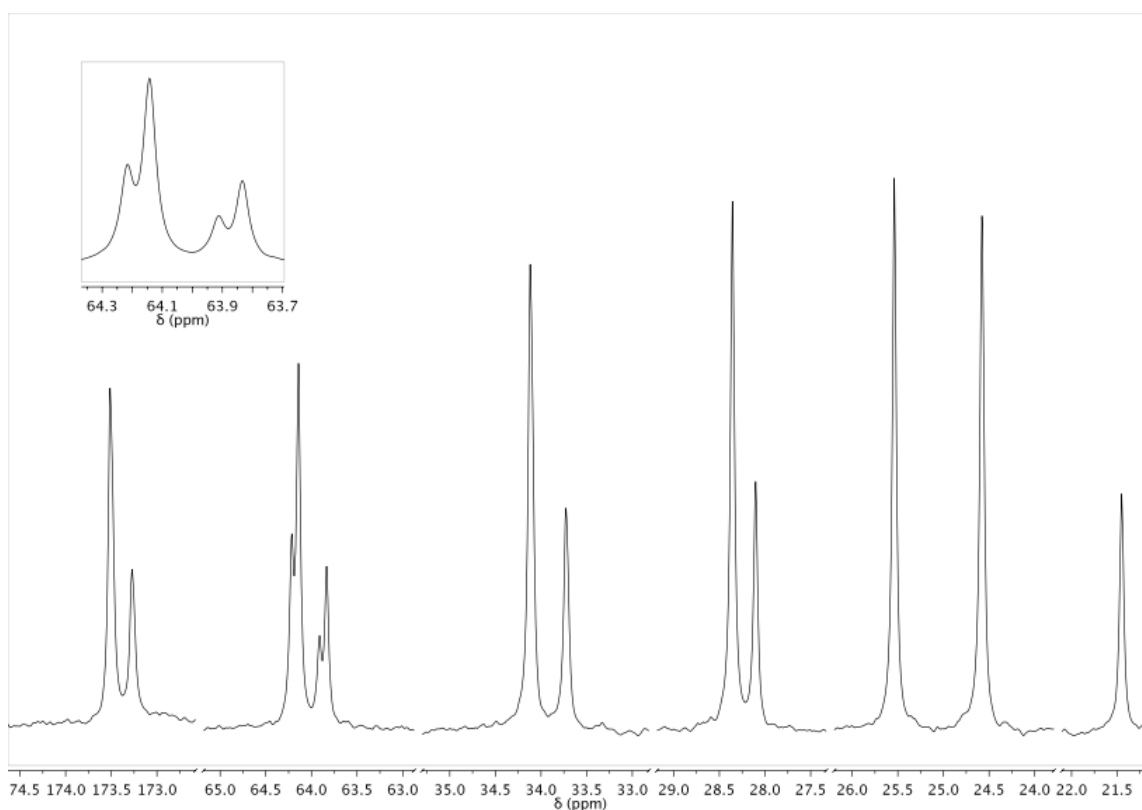


Figure 3. ¹³C NMR spectrum of CL-VAL 70; region of ϵ -methylene carbon atoms is enlarged.

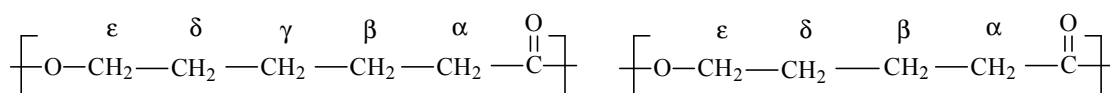


Figure 4. Scheme of the units of ϵ -caprolactone (left) and δ -valerolactone (right).

In Figure 3, the ϵ -CH₂ region at 63.5 to 64.5 ppm is also expanded. As can be seen these signals present dyad sensitivity. Hence, the peaks at 64.22, 64.14, 63.91 and 63.83 ppm can be assigned to CL-VL, CL-CL, VL-VL and VL-CL dyads, respectively, and the

average dyad relative molar fractions calculated. This allowed the number-average sequence lengths (l_i), the Bernoullian random number-average sequence lengths (l_i) and the randomness character (R) to be obtained, using the equations 5-7.

$$l_{CL} = \frac{(CL - CL) + \frac{1}{2}(CL - VL)}{\frac{1}{2}(CL - VL)} = \frac{2(CL)}{(CL - VL)} ; \quad (5)$$

$$l_{VL} = \frac{(VL - VL) + \frac{1}{2}(CL - VL)}{\frac{1}{2}(CL - VL)} = \frac{2(VL)}{(CL - VL)}$$

$$(l_{CL})_{random} = \frac{1}{(VL)} ; \quad (l_{VL})_{random} = \frac{1}{(CL)} \quad (6)$$

$$R = \frac{(l_{CL})_{random}}{l_{CL}} = \frac{(l_{VL})_{random}}{l_{VL}} \quad (7)$$

Crystallization studies

Non-isothermal crystallization during the cooling

Several DSC cooling treatments from 100 to -50 °C at rates of 5, 10 and 20 °C min⁻¹ were conducted successively on the polymer samples. As an illustration, Figure 5 shows the different scans of CL-LA 92.

The crystallization temperature (T_c) and the enthalpy of crystallization (ΔH_c) of each material were obtained from these scans and gathered in Table 3. As can be observed not all the polymers were able to crystallize during the cooling treatments. CL-LA 83 and CL-LA 70 copolymers, with average sequence lengths of ϵ -CL (l_{CL}) of 3.54 and 2.20, did not exhibit a crystallization peak at any cooling rate despite the fact that, as will be seen below, crystalline domains were formed during isothermal studies. Conversely, the ϵ -CL sequences of the rest of poly(ϵ -caprolactone-co-L-lactide), within the length range of 4.91 to 9.52, were large enough to crystallize during the cooling process. Likewise, the four poly(ϵ -caprolactone-co- δ -valerolactone) copolymers, with l_{CL} ranging from 2.65 to 6.08, arranged into crystalline structures presenting high

enthalpy of crystallization values ($\Delta H > 53 \text{ J g}^{-1}$ in all cases) with slight differences between them.

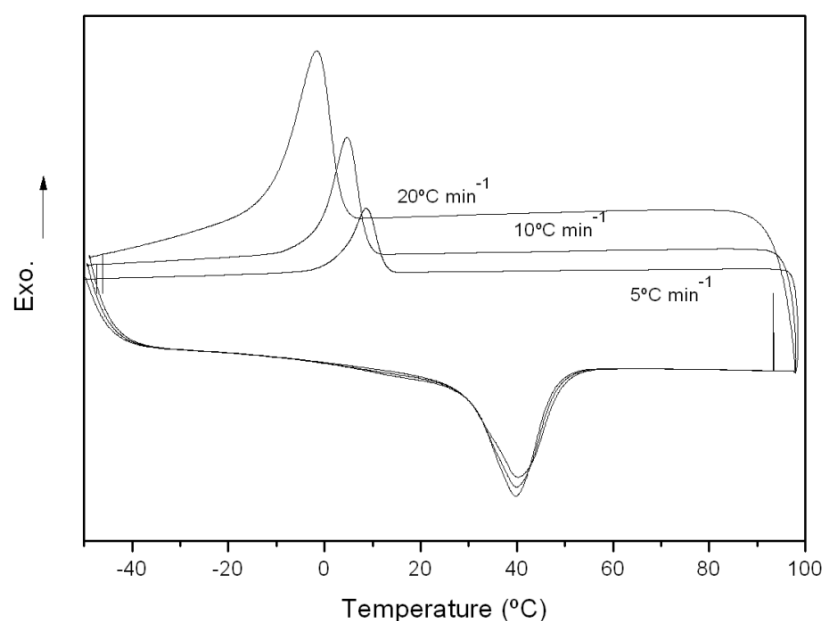


Figure 5. Crystallization process during the cooling at different cooling rates (5, 10 and 20 °C min⁻¹) of CL-LA 92.

Table 3. Characterization data obtained from the cooling treatments on the different poly(ϵ -caprolactone-co-L-lactide) and poly(ϵ -caprolactone-co- δ -valerolactone).

Sample	Cooling rate at 5 °C min ⁻¹		Cooling rate at 10 °C min ⁻¹		Cooling rate at 20 °C min ⁻¹	
	ΔH (J g ⁻¹)	T_c (°C)	ΔH (J g ⁻¹)	T_c (°C)	ΔH (J g ⁻¹)	T_c (°C)
PCL	68.6	32.8	65.7	30.8	65.4	28.2
CL-LA 94	49.6	23.0	47.9	19.5	47.2	14.8
CL-LA 92	42.8	8.6	41.4	4.7	41.1	-1.6
CL-LA 88	34.0	-7.9	30.9	-16.2	16.4	-25.7
CL-LA 83	-	-	-	-	-	-
CL-LA 70	-	-	-	-	-	-
CL-VAL 85	59.8	12.9	58.2	11.6	57.8	9.6
CL-VAL 76	59.4	8.9	58.3	7.5	57.7	4.8
CL-VAL 70	56.7	8.5	55.0	6.3	54.0	3.0
CL-VAL 60	55.4	1.4	53.7	-1.0	53.0	-4.3

As expected, a decrease in the cooling rate meant that the crystallites appeared at a higher temperature, presenting a narrower crystallization peak. At lower cooling rates there is more time for the crystal nucleus to develop, leading to higher crystallization temperatures [41]. The differences between the respective enthalpies from the same

copolymer were small, although it was noted that at $5\text{ }^{\circ}\text{C min}^{-1}$ (the slowest cooling rate) the ΔH associated to the crystallization peak was larger than those corresponding to the other cooling treatments. As an illustration, at a rate of $20\text{ }^{\circ}\text{C min}^{-1}$ the ΔH_{c} s of PCL homopolymer, CL-LA 92 and CL-VAL 85 were 65.4, 41.1 and 57.8 J g^{-1} respectively, while at a rate of $5\text{ }^{\circ}\text{C min}^{-1}$ they presented slightly higher values of 68.6, 49.6 and 59.8 J g^{-1} . On the other hand, it was also observed that the changes in the crystallization temperatures were more important in the ϵ -CL-co-LA copolymers than in the δ -VL based ones. For example, the T_{c} s at a cooling rate of $20\text{ }^{\circ}\text{C min}^{-1}$ for CL-LA 92 and CL-VAL 85 (both copolymers have a l_{CL} in the range of 6.0 to 6.7) were -1.6 and $9.8\text{ }^{\circ}\text{C}$ respectively, whereas at $5\text{ }^{\circ}\text{C min}^{-1}$ their T_{c} s were 8.6 and $12.9\text{ }^{\circ}\text{C}$.

Another aspect to take into account is that the CL-co-LA copolymers show a lower crystallization capability than the CL-co-VAL, regardless of their l_{CL} (a parameter that depends on both the composition and the randomness character). This fact can be explained by the higher T_{g} values of those materials containing lactide (supramolecular arrangements occur quickly if the polymer presents lower glass transition temperature, perhaps because the small rigid chains of L-lactide disrupt the crystal structure of the ϵ -CL domains or it could even be due to an isomorphism phenomenon between the ϵ -CL and δ -VL crystal lattice. Therefore, it is worth mentioning the fact that the enthalpies associated with the crystallization of some of the poly(ϵ -caprolactone-co- δ -valerolactone), such as CL-VAL 60, were surprisingly very large and unrelated to the copolymer composition. In depth analysis of these findings is discussed in the following sections.

Crystallization during isothermal treatments

Isothermal treatments were carried out at 5, 10, 21 and $37\text{ }^{\circ}\text{C}$ for 1, 10, 30 and 60 min and 3, 5, 10 and 24 hours. These temperatures were selected because the biomaterials are usually stored or used at this range of temperatures. The melting temperature (T_{m}) and the heat of fusion (ΔH_{m}) with respect to the time were obtained from the DSC scans, made from the selected isothermal temperature to $100\text{ }^{\circ}\text{C}$.

Some of the polymers (PCL, CL-LA 94, CL-LA 92, CL-VAL 85, CL-VAL 76 and CL-VAL 70) were able to crystallize during the cooling process at $40\text{ }^{\circ}\text{C min}^{-1}$ to the isothermal temperature. Those which presented a crystallization temperature above $-2\text{ }^{\circ}\text{C}$ at a cooling rate of $20\text{ }^{\circ}\text{C min}^{-1}$, exhibited a melting peak during the scan made after the cooling to $5\text{ }^{\circ}\text{C}$ despite the fact that at higher cooling rates the crystallization temperatures are lower. From now on, the enthalpies obtained immediately after this cooling process, summarized in Table 4, will be used as initial time values of heat of fusion (time zero) in the isothermal study.

Table 4. Melting enthalpies of the polymers studied after cooling at $40\text{ }^{\circ}\text{C min}^{-1}$ to the isothermal temperature.

Sample	ΔH_m (J g^{-1}) after cooling at $40\text{ }^{\circ}\text{C min}^{-1}$ to Isothermal Temperature ¹			
	$T_c = 5\text{ }^{\circ}\text{C}$	$T_c = 10\text{ }^{\circ}\text{C}$	$T_c = 21\text{ }^{\circ}\text{C}$	$T_c = 37\text{ }^{\circ}\text{C}$
PCL	66.2	64.3	55.1	-
CL-LA 94	45.5	47.0	10.0	-
CL-LA 92	30.4	1.6	-	-
CL-LA 88	-	-	-	-
CL-LA 83	-	-	-	-
CL-LA 70	-	-	-	-
CL-VAL 85	61.9	56.8	-	-
CL-VAL 76	52.7	-	-	-
CL-VAL 70	40.3	-	-	-
CL-VAL 60	-	-	-	-

¹ Obtained from a DSC scan made at $20\text{ }^{\circ}\text{C min}^{-1}$ from the isothermal crystallization temperature up to $100\text{ }^{\circ}\text{C}$ immediately after cooling at $40\text{ }^{\circ}\text{C min}^{-1}$.

Table 5 summarizes the melting temperatures (T_m) of the polymers studied, which were determined at the different isothermal temperatures. As the isothermal temperature decreased, it was found that the T_m also dropped towards lower values. The growth of the crystal nucleus was less pronounced and the crystallites formed were thinner and less perfect. As can be seen, only PCL, CL-LA 94, CL-LA 92 and CL-VAL 85 were capable to form a crystalline phase at $37\text{ }^{\circ}\text{C}$. The rest of copolymers presented T_m values around this temperature or even at lower values, which will restrict its potential application in the biomedical field.

Table 5. Melting temperatures of the polymers studied with respect to the isothermal temperature.

Sample	T_m (°C) with respect to Isothermal Temperature ¹			
	$T_c = 5$ °C	$T_c = 10$ °C	$T_c = 21$ °C	$T_c = 37$ °C
PCL	57.8	59.4	59.0	63.2
CL-LA 94	45.8	45.9	47.5	54.3
CL-LA 92	39.2	40.1	42.9	50.3
CL-LA 88	32.2	33.5	38.7	-
CL-LA 83	24.7	25.8	-	-
CL-LA 70	-	-	-	-
CL-VAL 85	43.6	44.0	46.8	51.1
CL-VAL 76	33.6	35.9	39.5	-
CL-VAL 70	30.9	33.3	35.5	-
CL-VAL 60	26.9	28.1	-	-

¹ Obtained from a DSC scan made at 20 °C min^{-1} from the isothermal crystallization temperature up to 100 °C. The values given correspond to the isothermal treatments during 24 hours.

- *Poly(ϵ -caprolactone) homopolymer*

Figure 6 shows the evolution of the melting enthalpy of the poly(ϵ -caprolactone) homopolymer at the four isothermal temperatures. The highest values of heat of fusion were achieved at 37 °C (84.3 J g^{-1} after 24 hours), with a melting peak appearing at ~ 63 °C. Using Crescenzi's [42] value of 139.5 J g^{-1} for the heat of fusion for 100 % crystalline material (ΔH_m^0), the calculated crystalline fraction was 60.4 %, which is in agreement with the PCL values found in literature [27]. The T_m moved towards lower values as the isothermal temperature decreased, just as in the case of the rest of copolymers in this study (see Table 5). Hence, following the isothermal experiment conducted at 5 °C, the T_m was located at around 58 °C (5 degrees less than at 37 °C) and after 24 hours at this temperature the ΔH reached a final value of 77.9 J g^{-1} with an associated crystallinity of 55.8 %.

At a lower isothermal temperature, that is further from the melting point of the ϵ -CL crystallites, the undercooling is larger and the changes in the polymer structure also occurred much more quickly owing to the more efficient nucleating abilities under those conditions. However, in the case of PCL, noteworthy differences were only observed at the initial state (time zero) and after the isothermal treatment of 1 min, that is at very short times. PCL homopolymer crystallizes very fast and at 5 , 10 or 21 °C the heat of fusion after "1 min" was in the range of 68 to 70 J g^{-1} while in all cases the DSC

thermograms made immediately after cooling to the isothermal temperature presented a large melting peak, over 55 J g^{-1} . On the other hand the sample cooled to $37 \text{ }^\circ\text{C}$ at $40 \text{ }^\circ\text{C min}^{-1}$ was not capable of crystallizing during the cooling process while a melting peak of 41 J g^{-1} was found after 1 min at this temperature.

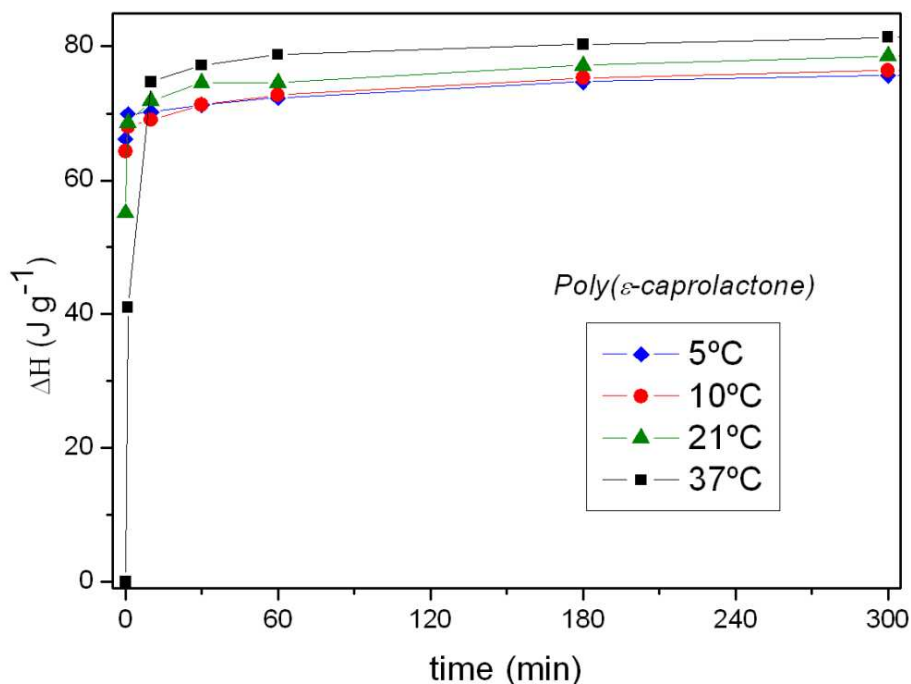


Figure 6. Melting enthalpies obtained from the isothermal treatments on poly(ϵ -caprolactone) at $5 \text{ }^\circ\text{C}$ ($-\diamond-$), $10 \text{ }^\circ\text{C}$ ($-\bullet-$), $21 \text{ }^\circ\text{C}$ ($-\blacktriangle-$) and $37 \text{ }^\circ\text{C}$ ($-\blacksquare-$). The values obtained after 10 and 24 hours at those temperatures are not shown.

- ϵ -Caprolactone-co-L-Lactide copolymers

The same isothermal treatments at 5 , 10 , 21 and $37 \text{ }^\circ\text{C}$ were carried out for the poly(ϵ -caprolactone-co-L-lactide) samples. The evolution of ΔH_m against time is plotted in Figure 7. As was expected, at a larger average sequence length of ϵ -CL (l_{CL}) the crystallization capability of the copolymers was greater. CL-LA 94 ($l_{CL} = 9.52$) was the copolymer that exhibited the highest value of melting enthalpy (62.1 J g^{-1} after 24 hours at $21 \text{ }^\circ\text{C}$ with a T_m at $48 \text{ }^\circ\text{C}$). This ΔH_m value was several J g^{-1} below than that of the PCL following the same treatment (81.9 J g^{-1} with a T_m at $59 \text{ }^\circ\text{C}$), proving that a 6% L-lactide content was enough to significantly alter the thermal properties of the

homopolymer. On the other hand, and in general, the crystallization process of these polymeric materials was more important and progressed faster at the lowest isothermal temperature of the study (5 °C), at which crystal nucleation was favored. CL-LA 83 ($l_{CL} = 3.54$), despite not being capable of crystallizing during the cooling studies outlined in the previous section, arranged into crystalline structures under isothermal conditions at 5 and 10 °C. A melting peak, at around 25 °C, was found after 3 hours at 5 °C and after 5 hours at 10 °C, and reached a final value of ΔH_m of 25.5 and 17.5 J g⁻¹, respectively. On the contrary, CL-LA 70 ($l_{CL} = 2.20$) did not exhibit a crystalline phase after any of the isothermal conditions employed in this study.

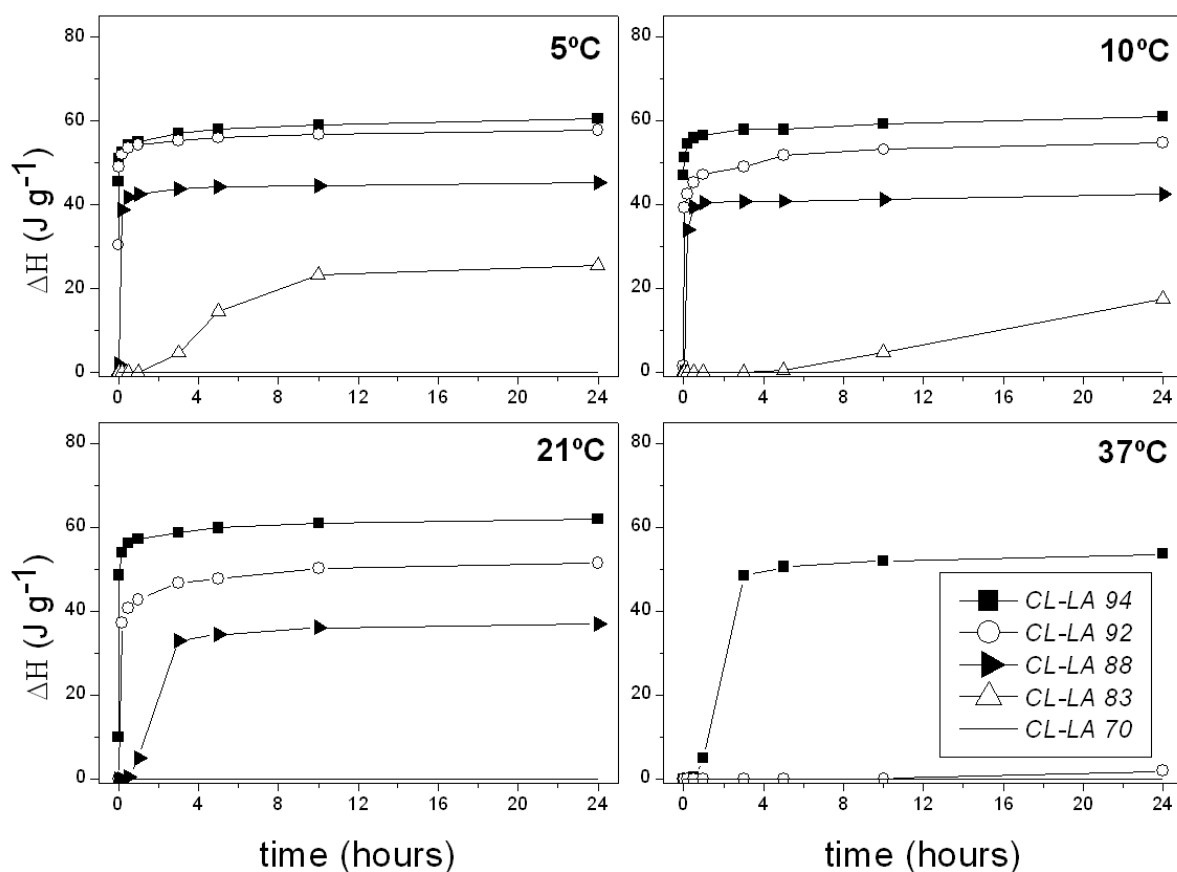


Figure 7. Melting enthalpies of the poly(ϵ -caprolactone-co-L-lactide) obtained after different isothermal treatments. CL-LA 94 (-■-), CL-LA 92 (-○-), CL-LA 88 (-▶-), CL-LA 83 (-Δ-) and CL-LA 70 (—).

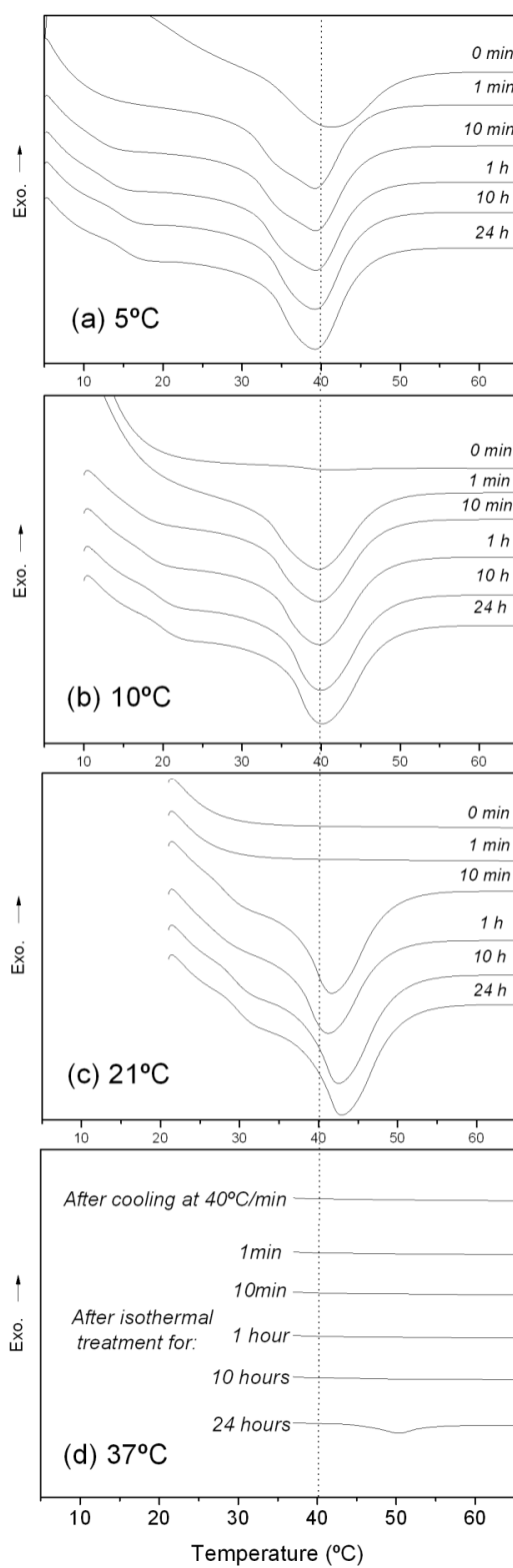


Figure 8. DSC thermograms of CL-LA 92 after different isothermal treatments at 5 °C (a), 10 °C (b), 21 °C (c) and 37 °C (d).

The behaviour of CL-LA 94, CL-LA 92 and CL-LA 88 was quite similar at 5, 10 or 21 °C: ΔH_m was almost stabilized after the first hour of the experiment and the differences between their ΔH_m values with respect to the isothermal temperature were not very large. As viewed above, higher T_m values were achieved at the highest isothermal temperatures for each of the polymers (see Table 5). Figure 8 shows the evolution of the DSC thermograms of CL-LA 92 after the different isothermal treatments at 5, 10, 21 and 37 °C. As can be seen, this copolymer has its T_m between 39 - 50 °C and the final melting peak values ΔH_m , with the exception of that from the isothermal treatment at 37 °C, are between 51.6 and 57.7 J g⁻¹ (of these the highest value corresponds to the isotherm at 5 °C). At 37 °C a small melting peak does not appear until at least 10 hours have passed and after 24 hours at this temperature, the associated ΔH_m was only 1.9 J g⁻¹. This copolymer, with an l_{CL} of 6.65, along with CL-LA 94, was the only one that crystallized at 37 °C and also had a melting peak at time zero (immediately after cooling) in the experiments at 5 or 10 °C. With regard to CL-LA 94 at 37 °C, it is worth mentioning that it started to crystallize after 30 minutes and from hour 3 to hour 24 the melting peak was almost stable and did not undergo virtually any change (ΔH_m rose from 48.4 to 53.7 J g⁻¹).

- ϵ -Caprolactone-co- δ -Valerolactone copolymers

Figure 9 shows the evolution of the melting enthalpies of the poly(ϵ -caprolactone-co- δ -valerolactone) obtained at isothermal temperatures of 5, 10, 21 and 37 °C. At the latter temperature the only copolymer that presented a melting peak during the experiment was that containing an 85 % molar content of ϵ -CL, CL-VAL 85. Its T_m was centred at 51 °C, which is well above the isothermal temperature (37 °C), and its ΔH_m was 21.5 J g⁻¹ after 24 hours of treatment. This value was considerably lower than those measured after 24 hours at 5, 10 or 21 °C (ΔH_m was 80.5, 74.8 and 72.5 J g⁻¹, respectively). The melting of the crystal phase usually occurs over a wide range of temperatures. Therefore, at 37 °C it is possible that imperfect crystallites of low T_m may not be able to form, reducing the crystallization capability of the polymer or it is possible that the time required at these conditions for the activation of the nuclei was too short (more than 24 hours would be needed).

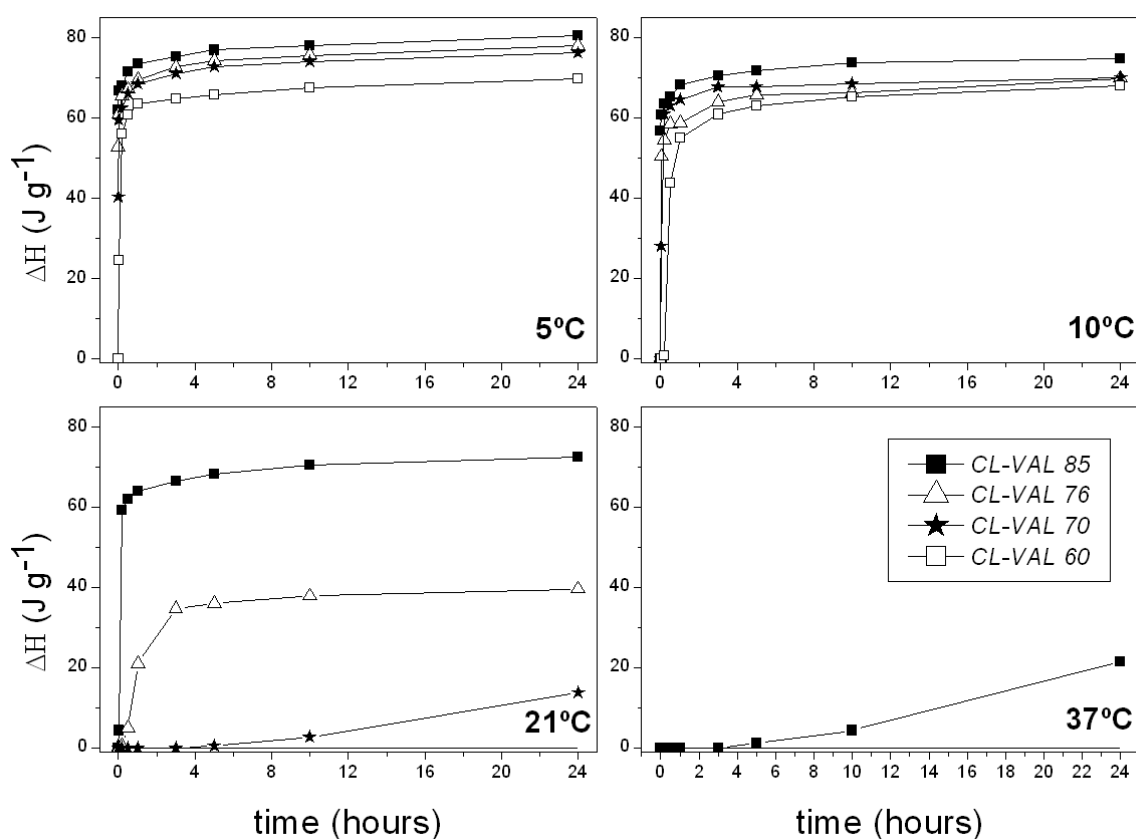


Figure 9. Melting enthalpies of the poly(ϵ -caprolactone-co- δ -valerolactone) obtained after different isothermal treatments. CL-VAL 85 (-■-), CL-VAL 76 (-△-), CL-VAL 70 (-*-) and CL-LA 60 (-□-).

In the case of the copolymers with lower ϵ -CL contents, those ranging from 60 to 76 %, no crystalline peaks were found at the DSC during the 24 hours at 37 °C. However, at an isothermal temperature of 21 °C, CL-VAL 76 showed a melting peak with a final ΔH_m value of 39.6 J g^{-1} ($T_m = 39.5$ °C), whereas CL-VAL 70 had a ΔH_m of 13.8 J g^{-1} ($T_m = 35.5$ °C). On the other hand CL-VAL 60 did not crystallize at all. Referring to CL-VAL 76, its ΔH_m was practically constant from the third hour of the experiment proving that the growth of the melting peak is limited by the fraction of crystals that have a melting temperature higher than 21 °C. With respect to CL-VAL 70, the crystallization process began after 5 hours and after 24 hours the ΔH_m values did not attain stability yet. The nucleation occurred at a slow rate. Therefore, for this poly(ϵ -caprolactone-co- δ -valerolactone) copolymer, the enthalpy associated with its melting peak might be larger if the treatment had been extended for more than 24 hours.

At 5 and 10 °C, the four ϵ -CL-co- δ -VL studied had high values of ΔH_m after 24 hours, ranging from 69.8 to 80.5 J g⁻¹ at 5 °C and from 68.0 to 74.8 J g⁻¹ at 10 °C. Those copolymers with a lower average sequence length of ϵ -CL, such as CL-VAL 60, took longer to develop a crystalline phase and had a slightly lower final ΔH_m . However, contrary to what was expected, the differences in the ΔH_m between CL-VAL 85 ($l_{CL} = 6.08$), CL-VAL 76 ($l_{CL} = 3.94$), CL-VAL 70 ($l_{CL} = 3.30$) and CL-VAL 60 ($l_{CL} = 2.65$) were not really noteworthy despite their different copolymer composition. The melting enthalpy was in some cases very large and did not change gradually with composition. This suggests that ϵ -CL and δ -VL units co-crystallize, giving rise to a conspicuous crystal phase [43].

Wide Angle X-Ray Scattering (WAXS)

WAXS was employed to study those ϵ -caprolactone-co- δ -valerolactone copolymers that exhibited an uncommon crystallization behaviour in the DSC. The WAXS profiles of the poly(ϵ -caprolactone-co-l-lactide) will be similar to those of the PCL and it was not considered necessary their discussion.

Figure 10, three-dimensional, shows the diffraction profiles of CL-VAL 85 and CL-VAL 60, in the range of diffraction angles 2θ between 10 and 38°, in which the “z” axis represents the number of scans. These scans were made every 2 °C from 30 to 122 °C in the case of CL-VAL 85 and from 2 to 62 °C for the ϵ -CL-co- δ -VL copolymer containing 60 % of ϵ -CL units. As can be observed, as the temperature increased the reflection intensity of the crystal bands decreases and eventually vanishes. This is the consequence of the transition from a crystalline phase to an amorphous one. These two copolymers, CL-VAL 85 and CL-VAL 60, presented a stable crystalline phase respectively until 50 and 28 °C, values that are consistent with their corresponding melting temperatures (from 44 to 51 °C for CL-VAL 85 and ~ 28 °C for CL-VAL 60). On the other hand, the PCL homopolymer, whose profile is not shown, displayed a stable crystalline phase up to a higher temperature, 61 °C.

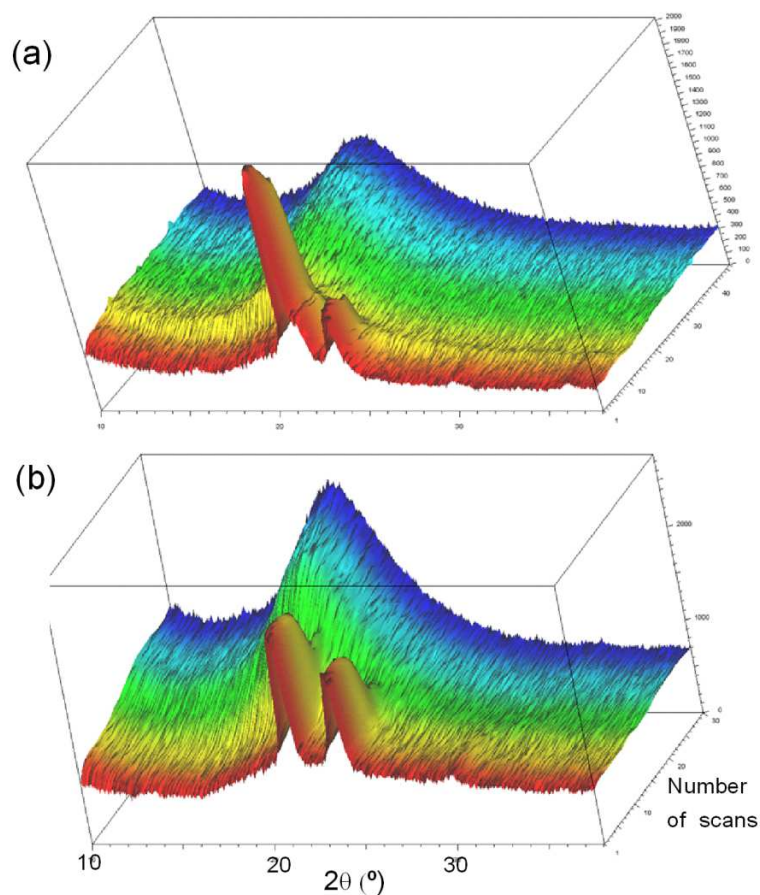


Figure 10. Three dimensional WAXS profiles of CLVAL 85 (a) and CLVAL 60 (b). “X” axis represents the diffraction angle (2θ), Y” axis the intensity and “Z” axis the number of scans. The scans were made every 2 °C from 30 to 122 °C in the case of CL-VAL 85 and from 2 to 62 °C for CL-VAL 60.

Figure 11 shows the diffraction profiles of CL-VAL 85 and CL-VAL 60 together with the diffractogram of the reference homopolymer (PCL). CL-VAL 85 presented exactly the same signals as PCL at 15.0, 21.6, 22.2, 23.8, 30.0 and 36.4 °, while the peaks in the $21 \leq 2\theta \leq 24^\circ$ range were the most intense. Therefore, it can be stated that both polymers present the same crystal structure. However, this cannot be said for CL-VAL 60. Conversely, this copolymer did not exhibit the shoulder-shaped signal at 22.2° whereas the peak at 23.8 shifted to 24.2° (see the magnification in the figure). The latter peak was broader and encompassed the signals of PCL at 23.8° and that of the poly(δ -valerolactone) (PVL), centered at 24.4° [44]. Hence, it can be concluded that CL-VAL 60 presents a different crystalline phase. Moreover, the fact that the WAXRD patterns of PCL and PVL are very similar proves that the lattice parameters of both lactones are

analogous and confirms that ϵ -CL and δ -VL units are co-crystallizing in this copolymer composition.

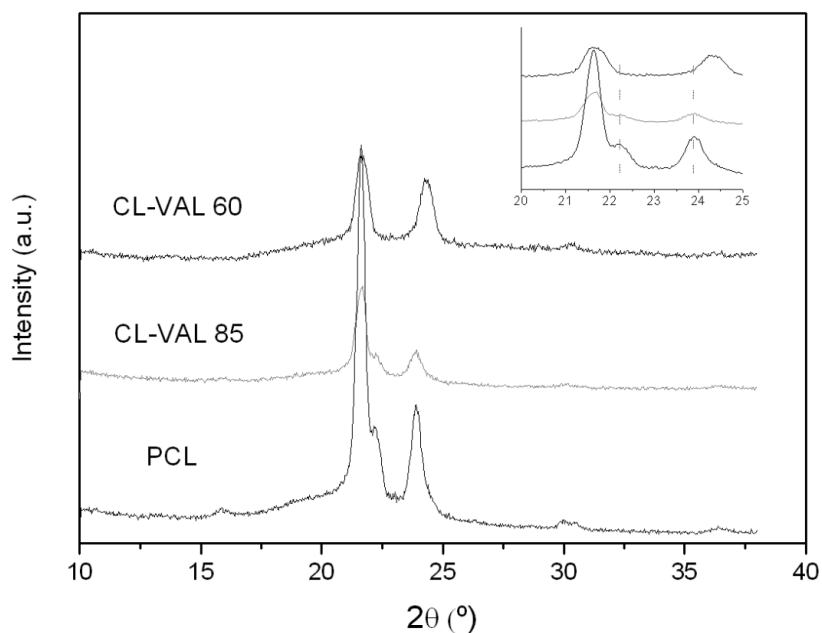


Figure 11. Initial WAXS profiles of PCL, CL-VAL 85 and CL-VAL 60 in the $10 \leq 2\theta \leq 38$ range.

The term isomorphism refers to two or more distinct substances with similar crystalline structure that crystallize together in a single crystal unit cell [45-48]. The different types of isomorphism have been classified by Natta [49] and co-workers, the subject was later reviewed by Wunderlich [50] and by Allegra et al. [51-52]. Macromolecular isomorphism represents the statistical co-crystallization of different constitutional repeating units in a single isomorphous crystalline lattice. In a strict sense, isomorphism means that only one crystalline phase is observed, and the crystal structure is essentially the same, irrespective of the composition. On the contrary, when the reference homopolymers have different crystal structures, copolymers crystallize in either of the crystal lattices depending on composition (isodimorphism), and often both crystals coexist at some intermediate composition. As stated by Allegra and Bassi [51], macromolecular isomorphism should meet several requirements: (i) the different types of monomer units must have approximately the same shape and occupy the same volume, (ii) the chain conformation of the parent homopolymers must be compatible with either crystal lattice, and (iii) the crystalline structures of parent homopolymers

should be analogous in the chain conformation, as well as in lattice symmetry and dimensions. In agreement with early observations by Wunderlich [50], PCL and other polylactones adopt polyethylene-like crystal structures, in which the length of the methylene sequences determines the packing of polyethylene.

ϵ -caprolactone is known to crystallize in an extended zigzag conformation and its units cells are orthorhombic [53], with $a = 7.496 \text{ \AA}$, $b = 4.974 \text{ \AA}$ and c (fiber axis) = 17.297 \AA . δ -valerolactone, with one less methylene in its chemical structure, was also found to arrange itself into orthorhombic lattices with parameters $a = 7.47 \text{ \AA}$, $b = 5.02 \text{ \AA}$ and c (fiber axis) = 7.42 \AA [54]. The identity of the chain conformation and the close similarity of unit-cell lateral dimensions allow both units to co-crystallize, as was seen in the 60:40 ϵ -CL-co- δ -VL copolymer. Several other co-crystallizing copolymer systems containing ϵ -CL repeat units have been documented in literature. Shalaby and Kafrawy [55] prepared random poly(ϵ -caprolactone-co-1,5-dioxepan-2-one), suggesting that isomorphic crystallization of these copolyesters took place. Jérôme and coworkers [56] reported co-crystallization of poly(ϵ -caprolactone-co-2-oxepane-1,5-dione) random copolymers. Bikiaris et al. [57] studied the crystalline structure and crystallization kinetics of poly(ϵ -caprolactone-co-propylene succinate) stating that co-crystallization occurs in these copolymers to some extent. Finally, Scandola and Ceccorulli [43] investigated the co-crystallization behaviour of poly(ϵ -caprolactone-co- ω -pentadecalactone) while Gross and co-workers with Scandola [58-60] also studied other isomorphic copolymers containing pentadecalactone units.

Polarized Light Optical Microscopy (PLOM)

In the previous sections it has been demonstrated that at certain compositions of ϵ -CL and δ -VAL, ϵ -caprolactone-co- δ -valerolactone copolymers undergo isomorphic crystallization. As a result they are highly crystalline over the whole composition range studied. Nevertheless, ϵ -CL-co- δ -VL copolymers also exhibited a higher crystallization capability than some poly(ϵ -caprolactone-co-L-lactide) with higher average sequence lengths of ϵ -CL. This cannot be explained by the co-crystallization phenomenon. As has been proved, CL-VAL 85, with an 85.3 % of ϵ -CL and a l_{CL} of 6.08, is not a co-crystallizing polymer system, however it displayed a large crystallizing ability in

comparison to CL-LA 92, a L-lactide based copolymer that has a higher content of ϵ -CL (91.6 %) and a larger l_{CL} (6.65). CL-VAL 85 reached a maximum of crystallization after 24 hours at 5 °C, with a ΔH_m of 80.5 J g⁻¹, while it presented a crystallization peak of 59.8 J g⁻¹ following a cooling treatment at 5 °C min⁻¹ from 100 °C. Conversely, CL-LA 92 showed lower values of 57.7 J g⁻¹ of ΔH_m and 49.6 J g⁻¹ of ΔH_c after the same experiments in the DSC. In addition, during the isothermal process at 21 °C it was noted that after 1 min only CL-VAL 85 showed a melting peak, demonstrating that the supramolecular arrangements take place faster in this copolymer. In order to complete the study of crystallization of those two copolymers that have a very low T_g (-64.3 °C for CL-VAL 85 vs. -54.0 °C for CL-LA 92) and similar T_m (from 43 to 51 °C for CL-VAL 85 vs. from 39 to 50 °C for CL-LA 92), Polarized Light Optical Microscopy (PLOM) measurements were carried out

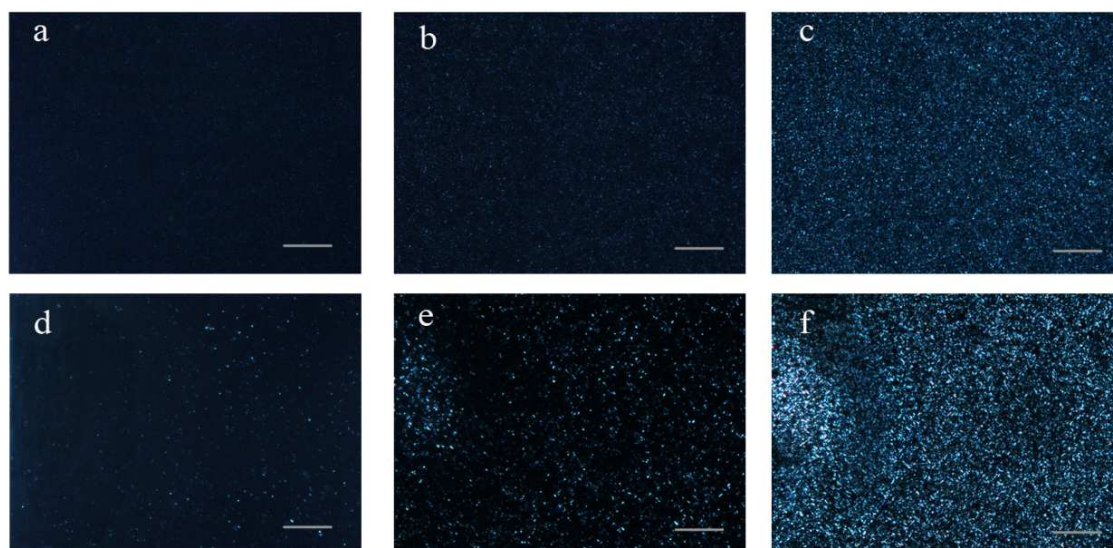


Figure 12. PLOM images of CL-VAL 85 after: a) 6min, b) 7min and c) 10min; and CL-LA 92: d) 9 min, e) 10min and f) 15min.

PCL, CL-LA 92 and CL-VAL 85 samples were melted in an oven and then immediately brought to the polarizing microscope, simulating the cooling to room temperature (21 °C) during a thermoplastic processing. Then, images were taken at different times. Figure 12 shows PLOM micrographs of CL-VAL 85 after 6, 7 and 10 min (above) and CL-LA 92 after 9, 10 and 15 min (below) after the start of the cooling to room temperature. It was found that the nucleation and the spherulite growth began earlier in

the case of CL-VAL 85, at minute 6, while the first crystal spherulites of ϵ -CL from CL-LA 92 were observed at 9 min. The crystalline structures of CL-VAL 85 and CL-LA 92 were stable after 10 and 15 min, respectively, while the PCL homopolymer (whose images are not shown) was already highly crystalline after 2 minutes.

On the basis of the DSC, WAXS and these PLOM studies, it can be said that the crystallization of the ϵ -CL units was easier in the presence of δ -VL units; both lactones have a similar structure (five straight methylenes and an ester group for ϵ -CL-units and four straight methylenes together with one ester group for a unit of δ -VAL). However, rigid L-lactide segments disrupt the structure of the crystal lattice of ϵ -CL, which decrease its crystallization capability.

3.1.4. Conclusions

In this work, ϵ -caprolactone was co-polymerized with L-lactide or δ -valerolactone monomers with the aim of reducing the crystallinity of the poly(ϵ -caprolactone) homopolymer, so as to improve its biodegradability properties. The poly(ϵ -caprolactone-co- L-lactide) and poly(ϵ -caprolactone-co- δ -valerolactone) copolymers were synthesized using triphenyl bismuth (Ph_3Bi) as catalyst and were characterized by nuclear magnetic resonance spectroscopy (NMR), showing respectively semi-alternating ($R \rightarrow 2$) or random ($R \sim 1$) distribution of sequences.

By means of differential scanning calorimetry (DSC), non-isothermal crystallizations were conducted at different cooling rates (at 5, 10 and 20 $^{\circ}\text{C min}^{-1}$) and several isothermal experiments (at 5, 10, 21 and 37 $^{\circ}\text{C}$) were also carried out over 24 hours. ϵ -CL-co-LA copolymers (with ϵ -CL molar contents ranging from 70 to 94 %) exhibited a lower crystallization capability than the ϵ -CL-co- δ -VL (with ϵ -CL content in the range of 60 to 85 %). This was observed regardless of their ϵ -CL average sequence length (l_{CL}), a parameter that depends on both the composition and the randomness character. In addition, supramolecular arrangements occurred slower in those copolymers containing lactide owing to their higher T_g values ($\sim (-64)$ $^{\circ}\text{C}$ for the ϵ -CL-co- δ -VL and from (-57) to (-33) $^{\circ}\text{C}$ for the ϵ -CL-co-LA).

Likewise, it was demonstrated that rigid L-lactide segments interfered with the structure of the crystal lattice of ϵ -CL, limiting the crystallization capability in CL-co-LA structures. On the other hand, crystallization of the ϵ -CL was easier in the presence of δ -VL units. Furthermore, for some compositions, such as the 60:40 ϵ -CL-co- δ -VL copolymer, it was found that ϵ -CL and δ -VL undergo isomorphic crystallization. The WAXS pattern of this copolymer differed from the diffraction profiles of the PCL homopolymer and the 85:15 copolymer, proving that the crystal phase of the CL-VAL 60 was different. As a result, the ϵ -CL-co- δ -VL copolymers were highly crystalline over a broad composition range, at the same time their crystallization and melting enthalpies were very large, unrelated to the copolymer composition. To the best of the authors' knowledge this is the first time that this co-crystallizing system has been reported in literature.

In further studies the mechanical performance of these polymeric materials will be studied by testing their mechanical properties at room temperature (21 °C) and at 37 °C, human body temperature, at which these biomaterials are intended to be employed. Moreover, an *in vitro* hydrolytic degradation study, in phosphate buffered solution (PBS) at 37 °C for a period up to 26 weeks, will be carried out so as to evaluate in depth their biodegradation mechanisms. These studies have started and will be reported on in due course.

References

- [1] Na, Y.-H.; He, Y.; Asakawa, N.; Yoshie, N.; Inoue, Y. Miscibility and phase structure of blends of poly(ethylene oxide) with poly(3-hydroxybutyrate), poly(3-hydroxypropionate), and their copolymers. *Macromolecules* 2002, 35(3), 727–735.
- [2] Aubin, M.; Prud'homme, R.E. Preparation and properties of poly(valerolactone). *Polymer* 1981, 22, 1223-1226.
- [3] Cao, H.; Han, H.; Li, G.; Yang, J.; Zhang, L.; Yang, Y.; Fang, X.; Li, Q. Biocatalytic Synthesis of Poly(δ -Valerolactone) Using a Thermophilic Esterase from *Archaeoglobus fulgidus* as Catalyst. *International Journal of Molecular Sciences* 2012, 13, 12232–12241.
- [4] Nakayama, A.; Kawasaki, N.; Maeda, Y.; Arvanitoyannis, I.; Aiba, S.; Yamamoto, N. Study of biodegradability of poly(δ -valerolactone-co-L-lactide)s. *Journal of Applied Polymer Science* 1997, 66, 741-748.
- [5] Labet, M.; Thielemans, W. Synthesis of polycaprolactone: a review. *The Royal Society of Chemistry* 2009, 38, 3484-3504.
- [6] Woodruff, M.A.; Hutmacher, D.W. The Return of a forgotten polymer: Polycaprolactone in the 21st century. *Progress in polymer Science* 2010, 35, 1217-1256.
- [7] Pascual, A.; Sardon, H.; Veloso, A.; Ruipérez, F.; Mecerreyes, D. Organocatalyzed synthesis of aliphatic polyesters from ethylene brassylate: a cheap and renewable macrolactone. *ACS Macro Letter* 2014, 3, 849-853.
- [8] de Geus, M.; van der Meulen, I.; Goderis, B.; van Hecke, K.; Doschu, M.; van der Werff, H.; Koning, C.E.; Heise, A. Performance polymers from renewable monomers: high molecular weight poly(pentadecalactone) for fiber applications. *Polymer Chemistry* 2010, 1, 525-533.
- [9] Bouyahyi, M.; Pepels, M.P.F.; Heise, A.; Duchateau, R. ω -Pentadecalactone polymerization and ω -pentadecalactone/ ϵ -caprolactone copolymerization reactions using organic catalysts. *Macromolecules* 2012, 45, 3356-3366.
- [10] Bouyahyi, M.; Duchateau, R. Metal-Based catalysts for Controlled Ring-Opening Polymerization of Macrolactones: High Molecular Weight and Well-Defined Copolymer Architectures. *Macromolecules* 2014, 47, 517-524.

- [11] Focarete, M.L.; Scandola, M.; Kumar, A.; Gross, R.A. Physical characterization of poly(ω -pentadecalactone) synthesized by lipase-catalyzed ring opening polymerization. *Journal of Polymer Science Part B: Polymer Physics* 2001, 39, 1721-1729.
- [12] van der Meulen, I.; de Geus, M.; Antheunis, H.; Deumens, R.; Joosten, E.A.J.; Koning, C.E.; Heise, A. Polymers from functional macrolactones as potential biomaterials: Enzymatic ring opening polymerization, biodegradation and biocompatibility. *Biomacromolecules* 2008, 9, 3404-3410.
- [13] Van Natta, F.J.; Hill, J.W.; Carruthers, W.H. Polymerization and ring formation, ϵ -caprolactone and its polymers. *Journal of American Chemistry Society* 1934, 56, 455-459.
- [14] Salerno, A.; Guarnieri, D.; Iannone, M.; Zeppetelli, S.; Netti, P.A. Effect of Micro- and Macroporosity of Bone Tissue Three-Dimensional-Poly(ϵ -Caprolactone) Scaffold on Human Mesenchymal Stem Cells Invasion, Proliferation, and Differentiation *In Vitro*. *Tissue Engineering Part A* 2010, 16, 2661-2673.
- [15] Fernández, J.; Etxeberria, A.; Sarasua, J.R. Effects of repeat unit sequence distribution and residual catalyst on thermal degradation of poly(L-lactide/ ϵ -caprolactone) statistical copolymers. *Polymer Degradation and Stability* 2013, 98, 1293-1299.
- [16] Larrañaga, A.; Sarasua, J.R. Effect bioactive glass particles on the thermal degradation behavior of medical polyesters. *Polymer Degradation and Stability* 2013, 98, 751-758.
- [17] Persenaire, O.; Alexandre, M.; Degée, P.; Dubois, P. Mechanisms and kinetics of thermal degradation of poly(epsilon-caprolactone). *Biomacromolecules* 2001, 2(1), 288-294.
- [18] Van de Velde, K.; Kienkens, P. Biopolymers: overview of several properties and consequences on their applications. *Polymer Testing* 2002, 21, 433-442.
- [19] Holland, S.J.; Tighe, B.J. Biodegradable polymers. In: Ganderton D, Jones TJ, editors. *Advances in pharmaceutical science*, vol 6. London: Academic Press Inc., 1992. 101-164.
- [20] Middleton, J.C.; Tipton, A.J. Synthetic biodegradable polymers as orthopedic devices. *Biomaterials* 2000, 21, 2335-2346.
- [21] Gunatillake, P.A.; Adhikari, R. Biodegradable synthetic polymers for tissue engineering. *European Cells and Materials* 2003, 5, 1-16.
- [22] Nair, L.S.; Laurencin, C.T. Biodegradable polymers as biomaterials. *Progress in Polymer Science* 2007, 32, 762-798.

- [23] Albertsson, A.C.; Eklund, M. Influence of molecular structure on the degradation mechanism of degradable polymers: In vitro degradation of poly(trimethylene carbonate), poly(trimethylene carbonate-co-caprolactone) and poly(adipic anhydride). *Journal of Applied Polymer Science* 1995, 57, 87-103.
- [24] Fernández, J.; Larrañaga, A.; Etxeberria, A.; Sarasua, J.R. Effects of chain microstructures and derived crystallization capability on hydrolytic degradation of poly(L-lactide/ ϵ -caprolactone) copolymers. *Polymer Degradation and Stability* 2013, 98, 481-489.
- [25] Fernández, J.; Etxeberria, A.; Sarasua, J.R. In vitro degradation study of biopolyesters using poly(lactide/ δ -valerolactone) copolymers. *Polymer Degradation and Stability* 2015, 112, 104-116.
- [26] Jenkins, M.J.; Harrison, K.L. The effect of molecular weight on the crystallization kinetics of polycaprolactone. *Polymers for Advanced Technologies* 2006, 17, 474-478.
- [27] Iroh, J.O. In *Polymer Data Handbook*, ed. Mark JE. Oxford University Press, New York 1999, 361-362.
- [28] Fernández, J.; Etxeberria, A.; Sarasua, J.R. Synthesis, structure and properties of poly(L-lactide-co- ϵ -caprolactone) statistical copolymers. *Journal of the Mechanical Behavior of Biomedical Materials* 2012, 9, 100-112.
- [29] Fernández, J.; Meaurio, E.; Chaos, A.; Etxeberria, A.; Alonso-Varona, A.; Sarasua, J.R. Synthesis and characterization of poly(L-lactide/ ϵ -caprolactone) statistical copolymers with well resolved chain microstructures. *Polymer* 2013, 54, 2621-2631.
- [30] Lin, W-J. Comparison of thermal characteristics and degradation properties of ϵ -caprolactone copolymers. *Journal of Biomedical Materials Research* 1999, 47, 420-423.
- [31] Storey, R.F.; Douglas, C.; Hoffman, D.C. Copolymerization of ϵ -caprolactone and δ -valerolactone. *Makromolekulare Chemie, Macromolecular Symposia* 1991, 42/42, 185-193
- [32] Toncheva, N.; Jerome, R.; Mateva, R. Anionically prepared poly(ϵ -caprolactam-co- ϵ -caprolactone) and poly(ϵ -caprolactam-co- δ -valerolactone) copolymers: Thermal and mechanical properties. *European Polymer Journal* 2011, 47, 238-247.
- [33] Fay, F.; Renard, E.; Langlois, V.; Linossier, I.; Vallée-Rehel, K. Development of poly(ϵ -caprolactone-co-L-lactide) and poly(ϵ -caprolactone-co- δ -valerolactone) as new degradable binder used for antifouling paint. *European Polymer Journal* 2007, 43, 4800-4813.

- [34] Fernández, J.; Larrañaga, A.; Etxeberria, A.; Sarasua, J.R. Tensile behavior and dynamic mechanical analysis of novel poly(lactide/ δ -valerolactone) statistical copolymers. *Journal of the Mechanical Behavior of Biomedical Materials* 2014, 35, 39-50.
- [35] Herbert, I.R. Statistical analysis of copolymer sequence distribution. In *NMR Spectroscopy of Polymers*. Ibbet, R.N. Ed.: Blackie Academic & Professional, London, 1993, 50-79. (Chapter 2).
- [36] Kasperczyk, J.; Bero, M. Coordination polymerization of lactides, 2. Microstructure determination of poly[(L,L-lactide)-co-(ϵ -caprolactone)] with ^{13}C nuclear magnetic resonance spectroscopy. *Makromol Chem.* 1991, 192, 1777-1787.
- [37] Fernández, J.; Etxeberria, A.; Ugartemendia, J.M.; Petisco, S.; Sarasua, J.R. Effects of chain microstructures on mechanical behaviour and aging of poly(L-lactide-co- ϵ -caprolactone) biomedical thermoplastic elastomer. *Journal of the Mechanical Behavior of Biomedical Materials* 2012, 12, 29–38.
- [38] Storey, R.F.; Herring, K.R.; Hoffman, D.C. *Journal of Polymer Science Polymer Chemistry Ed* 1991, 29, 1759–1777.
- [39] Zeng, Y.; Zhang, Y.; Lang, M. Synthesis and Characterization of Poly(ϵ -caprolactone-co- δ -valerolactone) with Pendant Carboxylic Functional Groups. *Chinese Journal of Chemistry* 2011, 29, 343-350.
- [40] Moore, T.; Adhikari, R.; Gunatillake, P. Chemosynthesis of bioresorbable poly(γ -butyrolactone) by ring-opening polymerization: a review. *Biomaterials* 2005, 26, 3771-3782.
- [41] Skoglund, P.; Fransson, A. Continuous cooling and isothermal crystallization of polycaprolactone. *Journal of Applied Polymer Science* 1996, 61, 2455-2465.
- [42] Crescenzi, V.; Manzini, G.; Galzolari, G.; Borri, C. Thermodynamics of fusion of poly- β -propiolactone and poly- ϵ -caprolactone. Comparative analysis of the melting of aliphatic polylactone and polyester chains. *European Polymer Journal* 1972, 8, 449-463.
- [43] Ceccorulli, G.; Scandola, M.; Kumar, A.; Kalra, B.; Gross, R.A. Cocrystallization of random copolymers of ω -pentadecalactone and ϵ -caprolactone synthesized by lipase catalysis. *Biomacromolecules* 2005, 6, 902-907.
- [44] Kasyapi, N.; Bhowmick, A.K. Nanolamellar triblock of poly-D,L-lactide- δ -valerolactone-D,L-lactide with tuneable glass transition temperature and crystallinity for use as a drug-delivery vesicle. *RSC Advances* 2014, 4, 27439-27451.

- [45] Pan, P.; Inoue, Y. Polymorphism and isomorphism in biodegradable polyesters. *Progress in Polymer Science* 2009, 34, 605-640.
- [46] Liang, Z.; Pan, P.; Zhu, B.; Dong, T.; Hua, L.; Inoue, Y. Crystalline Phase of Isomorphic Poly(hexamethylene-co-hexamethylene adipate) Copolyester: Effects of Comonomer Composition and Crystallization Temperature. *Macromolecules* 2010, 43, 2925-2932.
- [47] Liang, Z.; Pan, P.; Zhu, B.; Inoue, Y. Isomorphic crystallization of aliphatic copolyesters derived from 1,6-hexanediol: Effect of the chemical structure of comonomer units on the extent of cocrystallization. *Polymer* 2011, 52, 2667-2676.
- [48] Liang, Z.; Pan, P.; Zhu, B.; Yang, J.; Inoue, Y. Critical role of the conformation of comonomer units in isomorphic crystallization of poly(hexamethylene adipate-co-butylene adipate) forming Poly(hexamethylene adipate) type crystal. *Polymer* 2011, 52, 5204-52011
- [49] Natta, G.; Corradini, P.; Sianesi, D.; Morero, D. Isomorphism phenomena in macromolecules. *Journal of Polymer Science* 1961, 51, 527-539.
- [50] Wunderlich, B. Crystal Structure, Morphology, Defects. In *Macromolecular Physics*; Ed: Academic Press, New York 1973, Vol. 1 (Chapter 2).
- [51] Allegra, G.; Bassi, I.W. Isomorphism in synthetic macromolecular systems. *Advanced Polymer Science* 1969, 6, 549-574.
- [52] Allegra, G.; Meille, S.V. In *Polymer Handbook*, 4th ed.; Bandrup J, Immergut EH, Grulke EA. Eds.; Wiley, New York 1999.
- [53] Bittiger, H.; Marchessault, R.H.; Niegisch, W.D. *Acta Crystallographica Sect B* 1970, 26, 1923-1927.
- [54] Furuhashi, Y.; Sikorski, P.; Atkins, E.; Iwata, T.; Doi, Y. Structure and Morphology of the Aliphatic Polyester Poly(δ -valerolactone) in Solution Grown, Chain Folded Lamellar Crystals. *Journal of Polymer Science Part B: Polymer Physics* 2001, 39, 2622-2634.
- [55] Shalaby, S.W.; Kafrawy, A. Synthesis and some properties of isomorphic copolymers of ϵ -caprolactone and 1,5-dioxepan-2-one. *Journal of Polymer Science Polymer Chemistry Ed* 1989, 27, 4423-4426.
- [56] Dwan'Isa, J.P.L.; Lecomte, P.; Dubois, P.; Jérôme, R. Synthesis and characterization of random copolyesters of ϵ -caprolactone and 2-oxepane-1,5-dione. *Macromolecules* 2003, 36, 2609-15.

[57] Papadimitriou, S.A.; Papageorgiou, G.Z.; Bikiaris, D.N. Crystallization and enzymatic degradation of novel poly(ϵ -caprolactone-co-propylene succinate) copolymers. *European Polymer Journal* 2008, 44, 2356–2366.

[58] Focarete, M.L.; Gazzano, M.; Scandola, M.; Kumar, A.; Gross, R.A. Copolymers of ω -pentadecalactone and trimethylene carbonate from lipase catalysis: influence of microstructure on solid-state properties. *Macromolecules* 2002, 35, 8066–8071.

[59] Kalra, B.; Kumar, A.; Gross, R.A.; Baiardo, M.; Scandola, M. Chemoenzymatic synthesis of new brush copolymers comprising poly(ω -pentadecalactone) with unusual thermal and crystalline properties. *Macromolecules* 2004, 37, 1243–1250.

[60] Focarete, M.L.; Gazzano, M.; Scandola, M.; Gross, R.A. Polymers from Biocatalysis: Materials with a Broad Spectrum of Physical Properties. *Macromolecules* 2002, 35, 8066-8071.

**Chapter 3.2 In Vitro Degradation Studies
and Mechanical Behaviour of Poly(ϵ -
Caprolactone-co- δ -Valerolactone) and
Poly(ϵ -Caprolactone-co-L-Lactide) with
Random and Semi-alternating Chain
Microstructures**

European Polymer 2015, 71, 585-595.

Abstract

Poly(ϵ -caprolactone) (PCL) is one of the most common polymers employed in the biomedical field owing to its outstanding properties, however, it degrades slowly, at a degradation rate (K_{Mw}) of 0.0010 days^{-1} at $37 \text{ }^\circ\text{C}$. The incorporation of a second comonomer and the tailoring of more disordered chain microstructures were tested to accelerate hydrolysis. Both ϵ -caprolactone-co- δ -valerolactone and ϵ -caprolactone-co-L-lactide copolymers, synthesized with random ($R \sim 1$) and semi-alternating ($R \rightarrow 2$) distribution of sequences, exhibited faster degradation rates than PCL. ϵ -CL-co- δ -VAL, with ϵ -CL molar contents ranging from 76 to 85 %, possessed K_{Mw} values of between 0.0052 and 0.0033 days^{-1} , whereas the copolymers based on lactide, with 88 to 94 % of ϵ -CL, had a K_{Mw} 6 to 10 times higher than that of the homopolymer. The crystalline phase played a pivotal role in water absorption and degradation process, but was also responsible for the mechanical behaviour of these low glass transition temperature polymers. At $21 \text{ }^\circ\text{C}$ all the copolymers showed excellent ductility (strain at break > 1000 %) and improved flexibility compared to PCL (with secant modulus between 56 to 185 MPa). At body temperature ($37 \text{ }^\circ\text{C}$) it was only possible to measure the properties of the copolymers which had a T_m above $52 \text{ }^\circ\text{C}$ or a high enough melting enthalpy ($> 33 \text{ J g}^{-1}$). Moreover, at this temperature, PCL and the ϵ -CL-co-L-LA with a ϵ -CL content higher than 88 % exhibited lower stress related properties. Nevertheless, the mechanical performance at both temperatures of these poly(ϵ -CL-co-L-LA), in addition to their upgraded biodegradability, make them potential substitutes for PCL.

3.2.1. Introduction

Poly(ϵ -caprolactone) (PCL) is a well-known biopolyester, much appreciated in the biomedical and tissue engineering fields. This polymer presents very good biocompatibility, exceptional blend-compatibility, efficient processing with thermoplastic techniques, high thermal stability and very attractive mechanical properties with high elongation at break values [1-8]. In addition, its great permeability to various molecules [9-10] facilitates its use as a matrix for drug delivery. However, PCL, due to its high crystallinity, biodegrades slowly and is completely degraded after 2-4 years depending on the geometry and the initial molecular weight of the device or implant [11-15]. Amorphous regions are preferentially degraded, since water absorption is impeded in the crystalline zones [16-22]. In consequence, the rate of biodegradation of the polyesters is significantly influenced by their crystallization capability [23-24]

The copolymerization of ϵ -caprolactone with L-lactide [25-26] or δ -valerolactone [27-30] units was the strategy used by our research group to reduce crystallinity and so improve the biodegradability of the PCL homopolymer [31]. For this purpose, several ϵ -caprolactone-co-L-lactide and ϵ -caprolactone-co- δ -valerolactone copolymers were synthesized in a previous study of ours [32] using triphenyl bismuth (Ph_3Bi), a catalyst that is known to favour random sequences [33]. NMR characterization of the copolymers showed that the poly(ϵ -caprolactone-co-L-lactide)s and the poly(ϵ -caprolactone-co- δ -valerolactone)s had semi-alternating ($R \rightarrow 2$) and random ($R \sim 1$) distribution of sequences, respectively. However, the aim of lowering the degree of crystallinity was not achieved in the case of the ϵ -CL-co- δ -VAL. Non-isothermal cooling treatments at different rates and isothermal crystallizations at different temperatures were conducted by DSC, and these demonstrated that the ϵ -CL copolymers containing δ -VL exhibited a higher crystallization capability than those of L-LA and also arranged into crystalline structures over shorter times, regardless of their ϵ -CL average sequence length (l_{CL}). The crystallization of the ϵ -CL was easier with δ -VL units than in the presence of rigid lactide segments, and for some compositions it

was shown, via Wide Angle X-ray Scattering (WAXS), that these two lactones undergo isomorphism and co-crystallize in a single cell [32].

At temperatures well above their glass transition, the crystalline phase is responsible for the mechanical properties of these low glass transition temperature polymers. Therefore, only those whose melting temperatures (T_m) are higher than 37 °C are of interest, as this ensures their mechanical performance during the biomedical application. In this work, in view of their melting behaviour, only the polymers with T_m s above body temperature (37 °C) were selected from among the materials synthesized in our previous study [32]. The mechanical behaviour of the ϵ -CL-co- δ -VL and ϵ -CL-co-L-LA copolymers was studied by testing their mechanical properties at room temperature (21 °C) and at 37 °C, the temperature at which these biomaterials are intended to be employed. Moreover, an *in vitro* hydrolytic degradation study, in phosphate buffered solution (PBS) at 37 °C for a period up to 26 weeks, was carried out so as to evaluate in depth their biodegradation factors and mechanisms. As a result, the changes in water absorption, weight loss, macroscopic morphology, crystallinity, phase structure and molecular weight of the copolymers were monitored.

3.2.2. Materials and methods

Materials

ϵ -caprolactone monomer (assay > 98 %) was provided by Merck. L-lactide monomer (assay > 99.5 %) was supplied by Purac Biochem (The Netherlands) while δ -valerolactone monomer (assay > 98 %) was provided by Tokyo Chemical Industry (Cymit Quimica). The triphenyl bismuth (Ph_3Bi) catalyst was obtained from Gelest. 1-hexanol was supplied by Sigma Aldrich. Phosphate buffer saline (PBS) (pH 7.2) was obtained from Fluka Analytical (Sigma Aldrich).

Synthesis procedure

Statistical copolymers from ϵ -caprolactone, L-lactide and δ -valerolactone were synthesized in bulk by one pot-one-step ring-opening polymerizations (ROP). The synthesis reactions were carried out in a flask immersed in a controlled temperature oil bath. In each polymerization, predetermined amounts of the different comonomers at the chosen mass feed ratio were simultaneously added and melted into the flask. 1-hexanol was also added to provide ROH groups in order to control the molecular weight. The flask was purged for 30 minutes with a nitrogen stream under the surface of the melt. The catalyst (Ph_3Bi) was then added (at 500:1 comonomers/catalyst molar ratio) and the magnetic stirrer maintained at 100 rpm. The ϵ -caprolactone-co-L-lactide polymerizations were carried out for 48 hours at 130 °C whereas the synthesis reactions of the ϵ -caprolactone-co- δ -valerolactone copolymers were conducted for 48 hours at 120 °C. The ϵ -caprolactone homopolymer was synthesized at 130 °C after 24 hours of reaction time. After the corresponding period of reaction time the products were dissolved in chloroform and precipitated, pouring the polymer solution into an excess of methanol in order to remove the catalyst impurities and those monomers that had not reacted. Finally the product was dried at room temperature and then subjected to a heat treatment at 140 °C for 1 hour to ensure the complete elimination of any remaining solvent.

Methods

Proton and carbon nuclear magnetic resonance (^1H NMR and ^{13}C NMR) spectra were recorded in a Bruker Avance DPX 300 at 300.16 MHz and at 75.5 MHz of resonance frequency respectively, using 5 mm O.D. sample tubes. All spectra were obtained at room temperature from solutions of 0.7 mL of deuterated chloroform (CDCl_3). Experimental conditions were as follows: a) for ^1H NMR: 10 mg of sample; 3 s acquisition time; 1 s delay time; 8.5 μs pulse; spectral width 5000 Hz and 32 scans; b) for ^{13}C NMR: 40 mg, inverse gated decoupled sequence; 3 s acquisition time; 4 s delay time; 5.5 μs pulse; spectral width 18800 Hz and more than 10000 scans.

The lactide methine signals, centered at 5.15 ppm, and those of the α and ϵ methylenes of the ϵ -caprolactone, around 2.35 and 4.10 ppm, seen in the ^1H NMR spectrum [32] can be assigned to the different dyads [25]. This allowed the ϵ -caprolactone and L-lactide molar content and the microstructural magnitudes of these copolymers to be obtained from the average dyad relative molar fractions. In the case of the poly(ϵ -caprolactone-co- δ -valerolactone) the molar composition and the microstructural parameters were calculated via the integration of the ^{13}C NMR spectra [32] because the resonances for the protons of both repeat units overlapped preventing an accurate integration of the peak areas [28, 34-35].

200-300 μm films were prepared by pressure melting at 175 $^\circ\text{C}$, followed by water quenching so as to achieve an amorphous state. They were then stored for 24 hours in a fridge (at 0-5 $^\circ\text{C}$), the temperature at which biomaterials are usually stored. From these films repetitive square samples for the *in vitro* degradation study (1x1 cm^2) and repetitive samples for mechanical characterization (10x1 cm^2) were obtained. The specimens for mechanical testing at 37 $^\circ\text{C}$ were stored for another 24 hours at 37 $^\circ\text{C}$ before tests at this temperature were performed. DSC scans were made at 20 $^\circ\text{C min}^{-1}$ for each polymer sample before the mechanical testing in order to monitor the thermal properties of the specimens.

The mechanical properties were determined by tensile tests with an Instron 5565 testing machine at a crosshead displacement rate of 10 mm min^{-1} . These tests were performed at room temperature (21 \pm 2 $^\circ\text{C}$) and at human body temperature (37 $^\circ\text{C}$) following ISO 527-3/1995. The specimens had the following dimensions: overall length = 100 mm, distance between marks = 50 mm, width = 10 mm; and were cut out from films of 200-300 μm thickness. The mechanical properties reported (secant modulus at 2 %, yield strength, ultimate tensile strength and elongation at break) correspond to average values of at least 5 determinations. Mechanical testing at 37 $^\circ\text{C}$ was conducted in an Instron controlled temperature chamber. The tests were stopped at 300 % of strain due to the size limitations of the temperature chamber. The start of the tensile curves of the polymers of this work at 21 and at 37 $^\circ\text{C}$ was lineal so the values of secant modulus at 2 % can be compared to the Young's Modulus values reported in the bibliography for other polymers.

For the *in vitro* degradation study, square samples (25-35 mg of initial weight (W_0) and $n = 3$) of the different copolymers were placed in Falcon tubes containing phosphate buffered saline (PBS) (pH = 7.2) maintaining a surface area to volume ratio equal to 0.1 cm^{-1} . The samples were stored in an oven at $37 \text{ }^\circ\text{C}$. Three samples of each polymer were removed at different times from the PBS and weighed wet (W_w) immediately after wiping the surface with filter paper to absorb the surface water. These samples were air-dried overnight at $37 \text{ }^\circ\text{C}$. Then they were weighed again to obtain the dry weight (W_d). Water absorption (% WA) and remaining weight (% RW) were calculated according to Eqs. (1) and (2):

$$\% \text{WA} = \frac{W_w - W_d}{W_d} \cdot 100 \quad (1)$$

$$\% \text{RW} = \frac{W_d}{W_0} \cdot 100 \quad (2)$$

In order to compare the degradation rate of the studied PLVLs, the exponential relationship between molecular weight and degradation time for biodegradable polyesters degrading under bulk degradation was used [23-24]:

$$\ln M_w = \ln M_{w0} - K_{Mw} \cdot t \quad (3)$$

$$t_{1/2} = 1/K_{Mw} * \ln 2 \quad (4)$$

where M_w is the weight-averaged molecular weight, M_{w0} is the initial weight-averaged molecular weight, K_{Mw} is the apparent degradation rate and $t_{1/2}$ is the half degradation time (the amount of time required to fall to half the initial value of molecular weight).

The molecular weights of the polymers were determined by GPC using a Waters 1515 GPC device equipped with two Styragel columns ($10^2 - 10^4 \text{ \AA}$). Chloroform was used as eluent at a flow rate of 1 mL min^{-1} and polystyrene standards (Shodex Standards, SM-105) were used to obtain a primary calibration curve. The samples were prepared at a concentration of 10 mg in 2 mL .

The thermal properties were determined on a DSC 2920 (TA Instruments) immediately after the drying at 37 °C of the polymer samples removed from the degradation medium. Samples of 5-9 mg were heated from 21 °C to 100 °C at 20 °C min⁻¹. This first scan was used to determine the melting temperature (T_m) and the heat of fusion (ΔH_m). After this first scan, the samples were quenched in the DSC and a second scan was made from -85 °C to 100 °C at 20 °C min⁻¹. In this second scan the glass transition temperatures (T_g) of the samples were determined.

3.2.3. Results and discussion

Characterization

As mentioned in the introduction, the polymers employed in this study, with the exception of CL-VAL 80, were synthesized and thoroughly characterized in a previous study [32]. Table 1 summarizes the characterization data of the different biomaterials. As can be observed, the initial molecular weights (M_w) of each polymer are large, ranging from 91 to 170 kg mol⁻¹ with dispersities (D) between 1.70 - 1.84.

Table 1. Characterization data of the PCL and the different ϵ -caprolactone-co-L-lactide and ϵ -caprolactone-co- δ -valerolactone copolymers.

Sample	Composition ¹ (% molar)		M_w kg mol ⁻¹	D	Microstructural Magnitudes ²			T_g^3 °C
	% ϵ -CL	% L-LA or % δ -VL			l_{CL}	l_{LA} or l_{VL}	R	
PCL	100	0	135.0	1.74	-	-	-	-60.4
CL-LA 94	94.3	5.7	143.1	1.70	9.52	0.58	1.84	-57.4
CL-LA 92	91.6	8.4	131.6	1.77	6.65	0.61	1.80	-54.0
CL-LA 88	88.3	11.7	132.6	1.84	4.91	0.65	1.74	-54.6
CL-VAL 85	85.3	14.7	90.9	1.75	6.08	1.05	1.12	-64.3
CL-VAL 80	79.6	20.4	170.0	1.72	4.67	1.20	1.05	-63.7
CL-VAL 76	76.1	23.9	109.7	1.76	3.94	1.24	1.06	-63.7

¹ Calculated from ¹H NMR spectra for the ϵ -CL-co-L-LA copolymers and calculated from ¹³C NMR spectra in the case of the ϵ -CL-co- δ -VL copolymers.

² l_{CL} and l_{LA} are the CL and LA number average sequence lengths of the ϵ -CL-co-L-LA copolymers obtained from ¹H NMR, while l_{CL} and l_{VL} are the CL and VL number average sequence lengths of the ϵ -CL-co- δ -VL copolymers obtained from ¹³C NMR. These values are compared to the Bernoullian random number-average sequence lengths obtaining the randomness character value (R) of the different copolymers.

³ Obtained from a DSC scan made at 20 °C min⁻¹ from -85 to 100 °C.

Polycaprolactone homopolymer (PCL) shows a glass transition temperature (T_g) at -60 °C, while the ϵ -caprolactone-co-L-lactide copolymers, as a result of the incorporation of the comonomer, present higher T_g s. Therefore, the latter have T_g s that range from -57 to -55 °C and possess a semi-alternating distribution of sequences. Their lactide molar content ranges from ~ 6 % (CL-LA 94) to 12 % (CL-LA 88) with average sequence lengths of ϵ -CL (l_{CL}) from 9.52 to 4.91 whereas their randomness character (R) value is in all cases higher than 1.70 and tends toward 2 as the ϵ -CL content increases. Regarding the set of ϵ -caprolactone-co- δ -valerolactone copolymers, they present ϵ -CL molar contents that range from 85 to 76 % (l_{CL} from 6.08 to 3.94) and show a random distribution of sequences ($R \sim 1$). Owing to the similarities between the glass transition temperatures of both homopolymers (at -60 to -65 °C for PCL and at -57 °C for PVL [36]), the T_g values of this series of copolymers are almost equal, around -64 °C.

Hydrolytic degradation study

Evolution of thermal properties

DSC scans were made from 21 to 100 °C: at room temperature before submerging the samples in PBS, after storage for 24 hours at 37 °C and at different times of degradation. The data relating to melting enthalpies (ΔH_m) and temperatures (T_m) at the start and at the end of the study for all the polymer films are gathered in Table 2.

Table 2. Melting enthalpies and temperatures of all the polymer films at the start and at the end of the degradation study.

Sample	21 °C		37 °C		On day 182 of degradation at 37 °C	
	ΔH (J g ⁻¹)	T_m (°C)	ΔH (J g ⁻¹)	T_m (°C)	ΔH (J g ⁻¹)	T_m (°C)
PCL	77.2	66.3	85.0	68.3	94.0	75.1
CL-LA 94	56.6	51.7	57.0	56.2	75.2	58.8
CL-LA 92	39.8	48.1	46.0	51.7	58.8	57.4
CL-LA 88	21.1	41.3	22.2	49.6	37.2	53.7
CL-VAL 85	58.7	52.1	61.9	56.9	72.8	59.7
CL-VAL 80	56.6	45.7	32.4	52.0	39.0	54.8
CL-VAL 76	50.5	40.9	-	-	-	-

It can be observed that there are some differences between the melting behaviour of the polymers at room temperature (21 °C) and after storage at 37 °C for 24 hours. Hence,

with the exception of CL-VAL 76 and CL-VAL 80, PCL and the rest of copolymers presented slightly higher melting peaks after being stored for 24h at 37 °C. Likewise, the T_m values shifted to higher temperatures (2 to 7 °C higher), a tendency that is observed for all the materials. The rearrangements of the crystalline phase occurring at 37 °C were the result of the appearance of new crystallites that melt at higher temperatures, and also the disappearance of other crystalline structures with a melting point between 21 °C to ~ 37 °C. Therefore, it was found that the ΔH_m of CL-VAL 80 (with a T_m at 45.7 °C at room temperature) decreased from almost 57 to 32 J g⁻¹, while CL-VAL 76 (T_m = 40.9), which had a ΔH_m of 51 J g⁻¹, was not able to crystallize and was totally amorphous after storage at 37 °C.

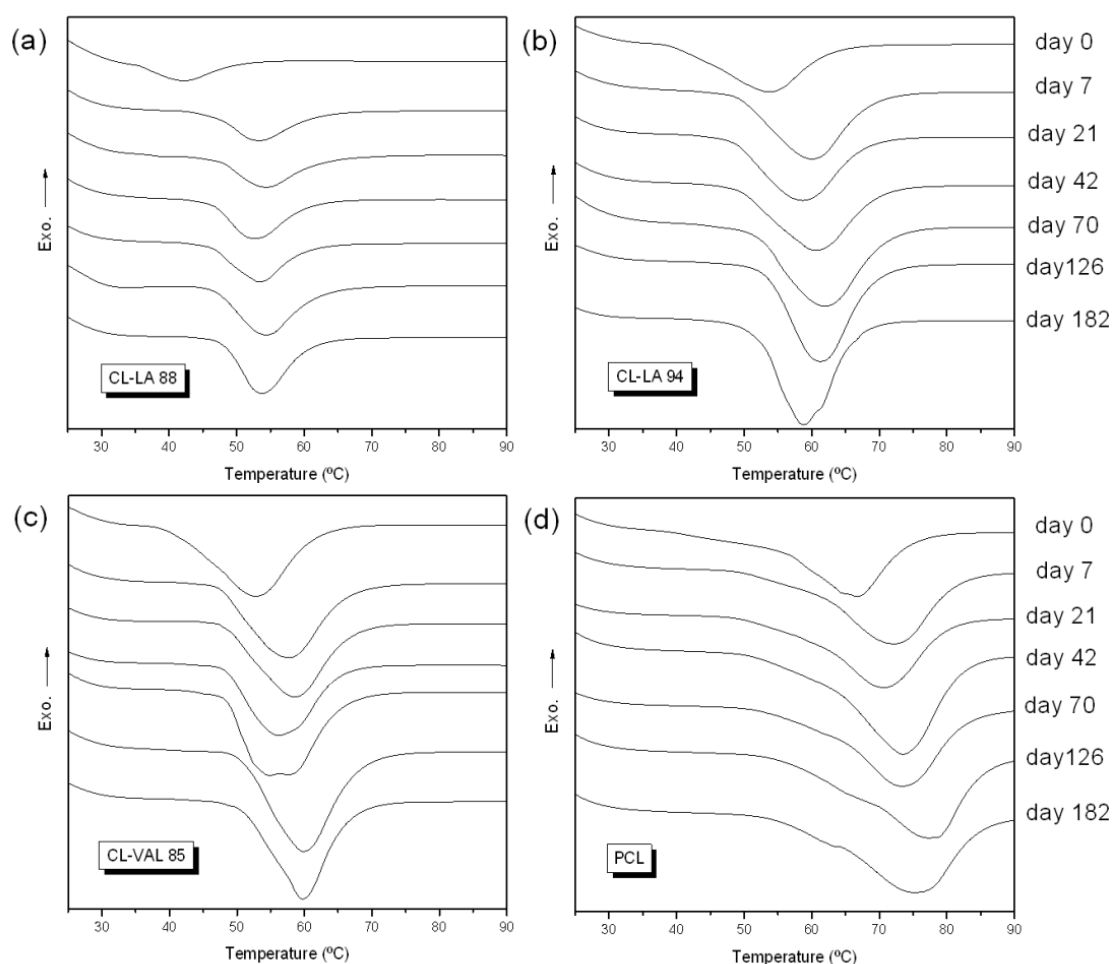


Figure 1. DSC evolution during degradation of CL-LA 88 (a), CL-LA 94 (b), CL-VAL 85 (c) and PCL (d). “Day 0” curves belongs to scans made on day 0 at room temperature, whereas the other curves correspond to scans made immediately after drying the samples for 24 hours at 37 °C.

Figure 1 shows the typical DSC thermograms of CL-LA 88, CL-LA 94, CL-VAL 85 and PCL submerged in PBS for different days. The evolution of the curves of CL-LA 92 and CL-VAL 80 followed the trends shown for CL-LA 94 and CL-VAL 85, respectively. On the contrary, the DSC curves of CL-VAL 76 did not present any melting peaks during the hydrolytic degradation process at 37 °C. After these first scans, the samples were quenched in the DSC to -85 °C for second scans (not shown). Anyway, the polymer chains were enough large and the glass transition temperatures of the PCL and its copolymers did not move towards lower temperatures and remained constant during the entire study.

The experimental data show a progressive increase in the melting peaks (ΔH_m) and the T_m values (see Figure 1). This is more noticeable in the copolymers with lower T_m and may be explained by the growth of crystalline regions by hydration, enlarging the space available for movement between chains. While the melting enthalpy of PCL only increased from 85 to 94 J g⁻¹, some copolymers such as CL-LA 88 experienced on day 182, the final day of the study, an increase of ~ 68 % over the initial value of ΔH_m at 37 °C. As will be seen below, those polymers which were more prone to crystallization changes also displayed higher values of water uptake during the degradation period.

Weight loss and water absorption

Figure 2 shows the remaining weight (RW) and water absorption (WA) curves obtained from the *in vitro* degradation study of the polymers in Table 1. As can be observed in the plot, the weight of the samples remained constant during the entire study. The molecular weight has to be reduced substantially to permit mass loss through solubilization of the oligomers and in this study, only CL-LA 88 showed signs of weight loss, (RW ~ 92 %) on day 154, when it presented a relevant increase in the water uptake (WA > 20 %) and a molecular weight of 24 kg mol⁻¹. Weight loss is dominated by water attacking the ester bonds [24] so water absorption capacity is a key factor in the degradation process. However, the highly crystalline domains of these ϵ -CL rich copolymers impeded the absorption of water and what is more, their low proportion of hydrolysable ester bonds slowed hydrolysis down. Consequently, with the exception of CL-LA 88 and CL-VAL 76 (which is fully amorphous at 37 °C), water absorption was

negligible. As it will be shown later, this will be reflected on the degradation rates (K_{M_w}) of this family of copolymers.

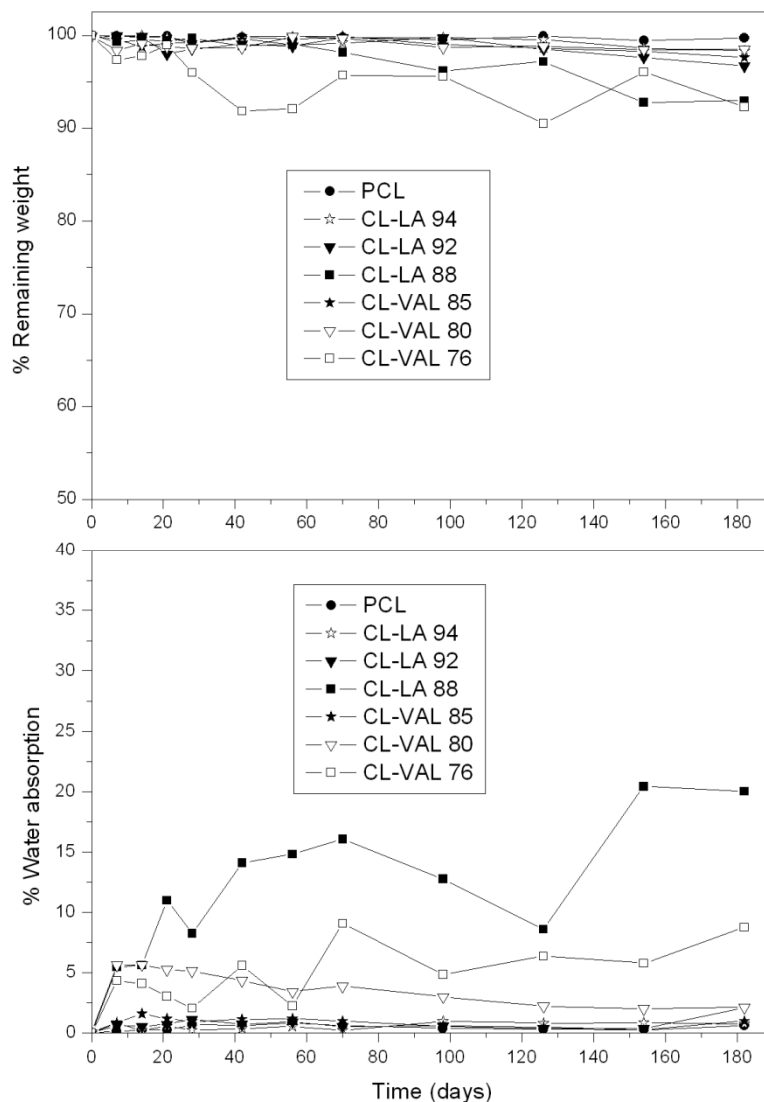


Figure 2. Evolution of the remaining weight and the water absorption of the PCL and copolymers.

Molecular weight evolution and degradation kinetics

Figure 3 shows the progress of $\ln M_w$ against degradation time of the PCL and copolymers. As the degradation evolves, the M_w of the samples decreased while the dispersity rose, indicating a broader distribution of polymer chain length. ϵ -caprolactone-co-L-lactide copolymers (on the left) showed higher falls, that is, faster

degradation rates, than PCL and poly(ϵ -caprolactone-co- δ -valerolactone)s (shown in the graph on the right).

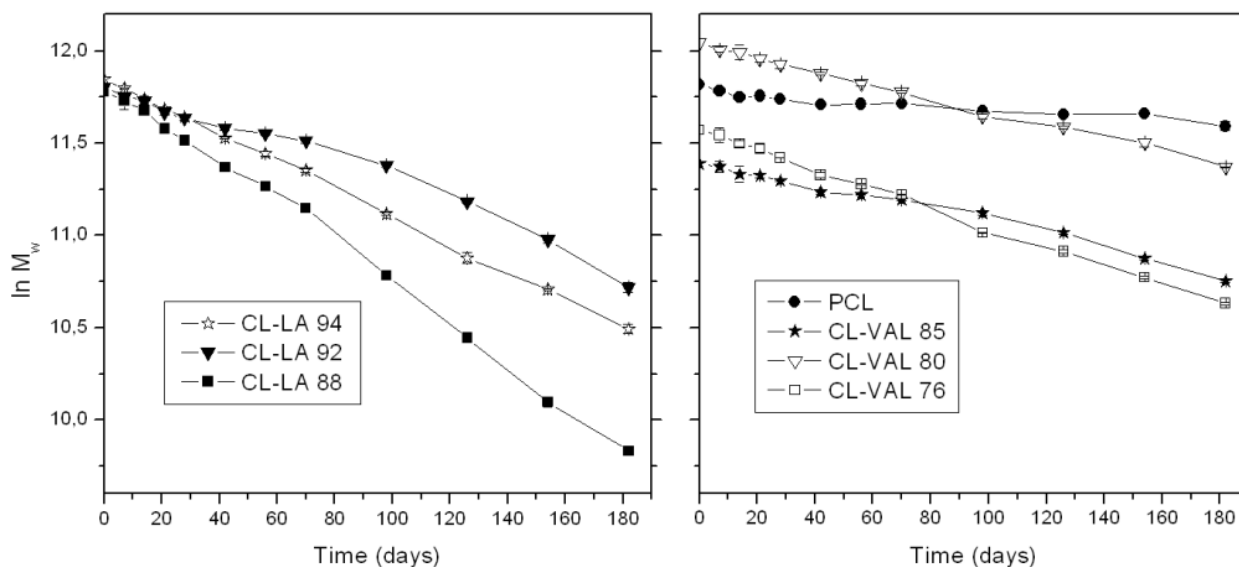


Figure 3. $\ln M_w$ against degradation time of PCL and its copolymers.

Table 3. K_{Mw} and $t_{1/2}$ of PCL and its copolymers.

Sample ¹	K_{Mw} (days ⁻¹)	Half-molecular weight degradation time $t^{1/2}$ (days)
PCL	0.0010	693
CL-LA 94	0.0075	92
CL-LA 92	0.0055	126
CL-LA 88	0.0105	66
CL-VAL 85	0.0033	210
CL-VAL 80	0.0036	193
CL-VAL 76	0.0052	133

¹ Calculated on day 182, the final day of the study, with the exception of CL-LA 88. For this polymer the calculus was made on day 126.

Table 3 shows the degradation rate values (K_{Mw}) and half degradation times ($t_{1/2}$) calculated from the slope of the fitting curve. The M_w experimental data adapts to the fitting curve ($R^2 > 0.9$ for PCL and $R^2 > 0.98$ for the copolymers) very well over the 182 days. Only the curve of CL-LA 88 began to deviate, from day 126 on. This change in the slope indicates that the degradation mechanism is shifting from one dominated by random scission to another controlled by chain end scission [37].

The copolymers containing lactide presented the fastest degradation rates. K_{Mw} obtained for CL-LA 94, CL-LA 92 and CL-LA 88 were 0.0075, 0.0055 and 0.0105 days⁻¹ respectively, with corresponding $t_{1/2}$ of 92, 126 and 66 days. These K_{Mw} values were 6 to 10 times higher than that of the PCL homopolymer (0.0010 days⁻¹), whose molecular mass and distribution were quite stable during the degradation period. The reduction in the crystallization capacity and the large structural disorder (randomness character, R , > 1.70) of this kind of ϵ -CL-co-L-LA copolymers of short unit average sequence lengths of ϵ -CL (l_{CL} from 4.91 to 9.52), substantially accelerated their hydrolytic degradation. However, their low water absorption levels make them more resistant to degradation than the set of L-LA rich ϵ -CL-co-L-LA copolymers used in a previous study [23, 38].

In accordance with the degradation studies at 20 °C of Faÿ et al. [31], poly(ϵ -CL-co- δ -VAL) degrades more slowly than the lactide copolymers due to the higher hydrolyzability of lactic acid unit sequences. K_{Mw} values of CL-VAL 85, CL-VAL 80 and CL-VAL 76 were 0.0033, 0.0035 and 0.0052 days⁻¹, with $t_{1/2}$ ranging from 210 to 133 days. The degradation of the copolymer with an increased amount of valerolactone (CL-VAL 76) was the fastest, in good agreement with the published results of Faÿ and Lin [27, 31]. These ϵ -CL-co- δ -VL copolymers were found to be highly crystalline over a broad composition range (from 85 to 60 % of ϵ -CL) with a high level of crystallization and melting enthalpies unrelated to the copolymer composition [32]. Nevertheless, as a result of the increasing amount of comonomer (δ -VAL) in PCL, their crystal structure differs from that of the homopolymer and presents lower melting temperatures. The melting of the crystal phase occurs over a wide range of temperatures and at 37 °C some imperfect crystallites of low T_m were unable to form, reducing the crystallization capability of the copolymers. CL-VAL 85, which presents a T_m of ~ 60 °C, close to that of PCL (T_m of ~ 70 °C), exhibited a high melting peak (ΔH_m of 75 J g⁻¹) on day 182. On the contrary, CL-VAL 80 had a ΔH_m of 39 J g⁻¹ at the end of the study, while CL-VAL 76 was fully amorphous at 37 °C. Due to its amorphous character, the latter copolymer presented higher values of water uptake (around 7 %), even greater than those of some ϵ -CL-LA copolymers in this work, which enhances its hydrolysis process.

Analysis of the remnants

The changes in thermal properties, water uptake and molecular weight loss of the polymer samples were reflected in the morphological appearance of some of the degradation remnants.

Figure 4 shows samples of CL-VAL 76 and CL-VAL 80 after 182 days submerged in PBS (above) along with square samples of the non-degraded polymers (below). At this stage of degradation CL-VAL 76 had an M_w of 41 kg mol^{-1} and, as can be seen, the sample is transparent and has lost its original shape. In the case of CL-VAL 80, with a higher melting temperature, the square sample has suffered a slight deformation. This sample, as well as those corresponding to PCL and the rest of copolymers, was crystalline and had a whitish colour.



Figure 4. Samples of CL-VAL 76 on day 0 and on day 182 (left) and CL-VAL 80 on day 0 and on day 182 (right).

Figure 5 shows a sample of CL-LA 88 on day 0 (below) and on day 182 (above), when it had an M_w of approximately 19 Kg mol^{-1} . This copolymer is the one that displayed the highest degradation rate, and as a result suffered an obvious surface deterioration. On day 182, all the polymers (with the exception of CL-VAL 76) continued to exhibit a

flexible mechanical behaviour and since they had low melting points ($> 100\text{ }^{\circ}\text{C}$) did not generate hard and rigid remnants. However, some of them became brittle after a specific day, a result of the degradation process. Thus, the samples of CL-LA 92 and CL-LA 88 became brittle from day 98, those of CL-VAL 85 from day 126 and the remnants of CL-LA 94 and CL-VAL 80 (presented the highest initial M_w) were found to be more fragile on the final day of the study. Conversely, no morphological change on the PCL samples were appreciated, its M_w only dropped from 135 to 108 kg mol^{-1} over the whole period of the study.



Figure 5. Samples of CL-LA 88 on day 0 (below) and on day 182 (above).

Mechanical properties

Tables 4 and 5 summarize the mechanical testing data of PCL and its copolymers at $21\text{ }^{\circ}\text{C}$ and at $37\text{ }^{\circ}\text{C}$. The mechanical performance of these low T_g polymers was heavily dependent on the crystalline phase, especially at temperatures close to their melting point. In the cases of CL-VAL 80, CL-VAL 76 and CL-LA 88, it proved impossible to measure their mechanical properties at $37\text{ }^{\circ}\text{C}$ because they were too soft and sticky at this temperature. All of them had a T_m under $52\text{ }^{\circ}\text{C}$ and the enthalpy associated with their melting peak was not very high enough ($\Delta H_m < 33\text{ J g}^{-1}$) to provide mechanical support. As mentioned above, CL-VAL 76 was amorphous at this temperature. On the

other hand, these three copolymers exhibited an interesting mechanical response with excellent flexibility and ductility at room temperature. Hence, CL-LA 88, which had a degradation rate similar to that of PLLA, showed a secant modulus value of 56.2 MPa, 8.5 MPa of ultimate tensile strength and an elongation at break of 1227 %. CL-VAL 76 and CL-VAL 80 presented secant modulus in the range of 105 to 132 MPa, tensile strengths of 8.5 and 19.1 MPa and strain at break values higher than 1100 %. It should be noted that as a result of its higher molecular weight (with a greater number of entanglements in its polymer chains), CL-VAL 80 show a much larger ultimate tensile strength than the other CL-VAL copolymers and had an elongation at break value of ~ 1300 %.

As can be seen in Figure 6, which presents the typical stress-strain curves of the materials studied, the copolymers of ϵ -caprolactone with L-lactide or δ -valerolactone showed a marked improvement in their flexibility compared to PCL. The homopolymer exhibited a secant modulus value of 311.7 MPa, yield strength of 13.7 MPa, ultimate tensile strength of 30.5 MPa and strain at break values of 937 %; mechanical data that are in agreement with other values obtained for PCL [1,2,4]. However, at 37 °C its stress related properties were found to be higher than those of the copolymers at 21 °C. CL-LA 94 ($l_{CL} = 9.52$, $T_m \sim 52$ °C and $\Delta H_m \sim 57$ J g⁻¹) and CL-LA 92 ($l_{CL} = 6.65$, $T_m \sim 48$ °C and $\Delta H_m \sim 40$ J g⁻¹) showed increased values for elongation at break (> 1110 %) and strain recovery rates (45 and 65 % for CL-LA 94 and CL-LA 92 vs. 31 % for PCL) compared to PCL. Their appearance is very similar to that of the silicone rubber with secant modulus of 159.3 and 89.5 MPa yield strengths of 6.7 and 3.9 MPa and final strength values of 18.4 and 11.3 MPa. Regarding CL-VAL 85, the ϵ -caprolactone-co- δ -valerolactone copolymer with a higher melting temperature, this exhibited a more glassy semicrystalline behaviour than the ϵ -CL-co-L-LA copolymers with a higher ϵ -CL content (such as CL-LA 94 or CL-LA 92). Owing to its different crystal structure and its large ΔH_m (57 J g⁻¹), it presented values of secant modulus of 185.2 MPa, 7.3 MPa of yield strength and a strain recovery of 29 %. However, the stress-strain curves of this copolymer did not show a cold-drawing profile and its tensile strength at break was lower (8.9 MPa) than the σ_u of the ϵ -CL-co-L-LA.

Table 4. Mechanical properties of PCL and ϵ -caprolactone-co- δ -valerolactone copolymers.

Sample	Testing Temperature ¹	Secant Modulus at 2 %	Yield Strength (Yield Point)	Tensile Strength at 300 %	Ultimate Tensile Strength ²	Elongation at break	Strain Recovery after break ³
		(MPa)	(MPa)	(MPa)	(MPa)	(%)	(%)
PCL	21 °C	311.7 ± 16.2	13.7 ± 1.2 (9.0 %)	13.8 ± 0.3	30.5 ± 3.6	937	30.8 ± 3.2
	37 °C	276.3 ± 11.4	9.8 ± 0.9 (5.3 %)	13.7 ± 0.9	-	-	-
CL-VAL 85	21 °C	185.2 ± 20.4	7.3 ± 1.0 (7.7 %)	6.5 ± 0.5	8.9 ± 1.1	1079	29.0 ± 4.6
	37 °C	125.2 ± 11.7	3.8 ± 0.4 (3.9 %)	-	2.3 ± 0.4	5.0	-
CL-VAL 80	21 °C	132.0 ± 11.5	5.3 ± 0.5 (10.8 %)	5.5 ± 0.2	19.1 ± 2.6	1300	31.2 ± 0.8
	37 °C ⁴	*	*	*	*	*	*
CL-VAL 76	21 °C	105.1 ± 7.3	3.3 ± 0.3 (7.1 %)	4.4 ± 0.3	8.5 ± 1.6	1104	27.1 ± 1.3
	37 °C ⁴	*	*	*	*	*	*

¹ At 37°, the tests were stopped at 300 % of strain due to the size limitations of the temperature chamber.

² The tensile strength was determined as ultimate stress value (σ_u).

³ Measured 24 hours after break.

⁴ No measurable mechanical properties at 37 °C

Table 5. Mechanical properties of ϵ -caprolactone-co-L-lactide copolymers.

Sample	Testing Temperature ¹	Secant Modulus at 2 %	Yield Strength (Yield Point)	Tensile Strength at 300 %	Ultimate Tensile Strength ²	Elongation at break	Strain Recovery after break ³
		(MPa)	(MPa)	(MPa)	(MPa)	(%)	(%)
CL-LA 94	21 °C	159.3 ± 12.5	6.7 ± 0.5 (8.8 %)	7.6 ± 0.2	18.4 ± 0.9	1142	45.0 ± 2.3
	37 °C	115.8 ± 6.3	3.9 ± 0.5 (5.5 %)	4.9 ± 0.1	-	-	-
CL-LA 92	21 °C	89.5 ± 16.8	3.9 ± 0.5 (9.3 %)	4.2 ± 0.2	11.3 ± 1.6	1110	65.1 ± 9.3
	37 °C	40.9 ± 9.8	1.8 ± 0.2 (12.8 %)	2.7 ± 0.2	-	-	-
CL-LA 88	21 °C	56.2 ± 8.1	2.2 ± 0.4 (9.4 %)	2.9 ± 0.1	8.5 ± 0.4	1227	76.6 ± 3.0
	37 °C ³	*	*	*	*	*	*

¹ At 37°, the tests were stopped at 300 % of strain due to the size limitations of the temperature chamber.

² The tensile strength was determined as ultimate stress value (σ_u).

³ Measured 24 hours after break.

⁴ No measurable mechanical properties at 37 °C

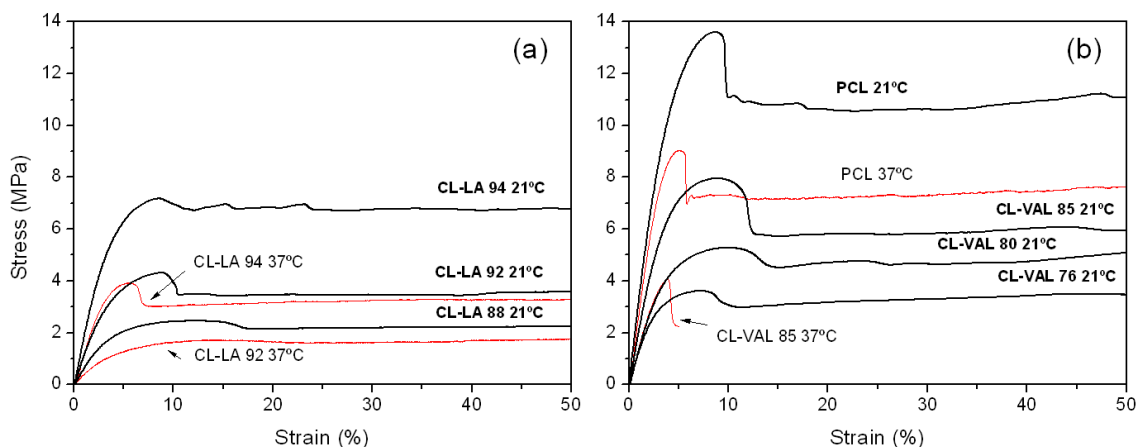


Figure 6. Tensile stress-strain curves of PCL and their L-lactide and δ -valerolactone copolymers at 21 °C and at 37 °C.

The mechanical behaviour at 37 °C of the materials studied, for those that allowed mechanical testing to be carried out, was more elastomeric. At this temperature, the polymers are closer to their melting temperature and after 24 hours of storage have undergone supramolecular arrangements in their crystal structure. Consequently, PCL and the copolymers present lower stress related properties (secant modulus and tensile strength values at 300 %) than at room temperature. PCL homopolymer, with a T_m of 68 °C after storage at 37 °C, exhibited the smallest differences: its secant modulus dropped from ~ 312 to 276 MPa while its yield strength shifted from almost 14 MPa to 9.8 MPa. In the case of CL-VAL 85 it was just the opposite, the secant modulus decreased a 32 % and the copolymer became brittle and broke at 5 % of strain just after the yield point. With regard to CL-LA 94 and CL-92, their secant modulus values at 37 °C were 115.8 and 40.9 MPa, respectively, representing a drop of 27 % and 54 % in their initial values. The changes in yield strength and tensile strength at 300 % were also significant. As an illustration, the yield strength of CL-LA 94 went down to 3.9 MPa while its $\sigma_{300\%}$ decreased from 7.6 to 4.9 MPa. Nonetheless, the mechanical properties of CL-LA 94 and CL-LA 92 are suitable enough to make them useful for medical applications that

require a flexible mechanical performance at both room temperature and at human body temperature.

3.2.4. Conclusions

In this work an in vitro degradation study at 37 °C was carried out in phosphate buffered saline (PBS) with poly(ϵ -caprolactone-co- δ -valerolactone) and poly(ϵ -caprolactone-co-L-lactide), which have melting temperatures (T_m) above body temperature (37 °C). Moreover, the mechanical performance of the different copolymers was assessed by testing their mechanical properties at room temperature (21 °C) and at 37 °C with an Instron testing machine.

Both ϵ -CL-co- δ -VL copolymers, with ϵ -CL molar content ranging from 76 to 85 % and random ($R \sim 1$) chain microstructures, and ϵ -CL-co-L-LA copolymers, with 88 to 94 % of ϵ -CL and semi-alternating ($R \rightarrow 2$) distribution of sequences, exhibited faster degradation rates than a polycaprolactone (PCL) homopolymer. The latter, whose M_w only dropped from 135 to 108 kg mol⁻¹ during the entire study (182 days), had a degradation rate (K_{Mw}) of 0.0010 days⁻¹. On the contrary, the δ -VL copolymers degraded 3 to 5 times faster, whereas the copolymers based on lactide had K_{Mw} values of between 0.0055 and 0.0105 days⁻¹.

However, their mechanical behaviour was heavily dependent on the crystalline phase (on their T_m and melting enthalpies), especially at temperatures close to their melting point. As a result, only the ϵ -CL-co-L-LA copolymers which have a ϵ -CL molar content higher than 88 %, in addition to PCL, presented mechanical properties suitable enough at both room temperature and 37 °C (less flexible and very resistant to hydrolytic degradation). Their secant modulus values between 56 and 159 MPa and excellent ductility (strain at break > 1100 %) make them very useful for medical applications that require a flexible mechanical performance and at the same time provide improved biodegradability.

References

- [1] Labet, M.; Thielemans, W. Synthesis of polycaprolactone: a review. *The Royal Society of Chemistry* 2009, 38, 3484-3504.
- [2] Woodruff, M.A.; Hutmacher, D.W. The Return of a forgotten polymer: Polycaprolactone in the 21st century. *Progress in polymer Science* 2010, 35, 1217-1256.
- [3] Fernández, J.; Etxeberria, A.; Sarasua, J.R. Effects of repeat unit sequence distribution and residual catalyst on thermal degradation of poly(L-lactide/ ϵ -caprolactone) statistical copolymers. *Polymer Degradation and Stability* 2013, 98, 1293-1299.
- [4] Van de Velde, K.; Kienkens, P. Biopolymers: overview of several properties and consequences on their applications. *Polymer Testing* 2002, 21, 433-442.
- [5] Larrañaga, A.; Sarasua, J.R. Effect bioactive glass particles on the thermal degradation behavior of medical polyesters. *Polymer Degradation and Stability* 2013, 98, 751-758.
- [6] Larrañaga, A.; Diamanti, E.; Rubio E.; Palomares T.; Alonso-Varona A.; Aldazabal, P.; Martin F.J.; Sarasua, J.R. A study of the mechanical properties and cytocompatibility of lactide and caprolactone based scaffolds filled with inorganic bioactive particles. *Materials Science and Engineering C* 2014, 42, 451-460.
- [7] Larrañaga, A.; Martin, F.J.; Aldazabal, P.; Sarasua, J.R. Hydrolytic degradation and Bioactivity of Lactide and Caprolactone based sponge-like scaffolds loaded with bioactive glass particles. *Polymer Degradation and Stability* 2014, 110, 121-128.
- [8] Larrañaga, A.; Alonso-Varona A.; Palomares T.; Rubio-Azpeitia, E.; Aldazabal, P.; Martin F.J.; Sarasua, J.R. Effect of bioactive glass particles on osteogenic differentiation of adipose-derived mesenchymal stem cells seeded on lactide and caprolactone based scaffolds. *Journal of Biomedical Materials Research Part A* 2015, 103, 3815-3824.
- [9] Murphy, RSR. *Biodegradable Polymers*; Jain, NK, Ed; CBS Publisher: New Dehli 1997; pp 27-51.
- [10] Coombes, A.; Rizzi, S.; Williamson, M.; Barralet, J.; Downes, S.; Wallace, W. Precipitation casting of polycaprolactone for applications in tissue engineering and drug delivery. *Biomaterials* 2004, 25, 315.
- [11] Holland, S.J.; Tighe, B.J. Biodegradable polymers. In: Ganderton D, Jones TJ, editors. *Advances in pharmaceutical science*, vol 6. London: Academic Press Inc.; 1992, 101-164.

- [12] Middleton, J.C.; Tipton, A.J. Synthetic biodegradable polymers as orthopedic devices. *Biomaterials* 2000, 21, 2335–2346.
- [13] Gunatillake, P.A.; Adhikari, R. Biodegradable synthetic polymers for tissue engineering. *European Cells and Materials* 2003, 5, 1–16.
- [14] Nair, L.S.; Laurencin, C.T. Biodegradable polymers as biomaterials. *Progress in Polymer Science* 2007, 32, 762–798.
- [15] Ali, S.A.M.; Zhong, S.-P.; Doherty, P.J.; Williams, D.F. Mechanisms of polymer degradation in implantable devices: I. Poly(ϵ -caprolactone). *Biomaterials* 1993, 14, 648–656.
- [16] Albertsson, A.C.; Eklund, M. Influence of molecular structure on the degradation mechanism of degradable polymers: In vitro degradation of poly(trimethylene carbonate), poly(trimethylene carbonate-co-caprolactone) and poly(adipic anhydride). *Journal of Applied Polymer Science* 1995, 57, 87–103.
- [17] Jenkins, M.J.; Harrison, K.L. The effect of molecular weight on the crystallization kinetics of polycaprolactone. *Polymers for Advanced Technologies* 2006, 17, 474–478.
- [18] Li, S.; Garreau, H.; Vert, M. Structure-property relationships in the case of degradation of massive aliphatic poly(α -hydroxy acids) in aqueous media. Part 3. Influence of the morphology of poly(L-lactic acid). *Journal of Materials Science: Materials in Medicine* 1990, 1, 198–206.
- [19] Vert, M.; Li, S.; Garreau, H. More about the degradation of LA/GA-derived matrices in aqueous media. *Journal of Controlled Release* 1991, 16, 15–26.
- [20] Malin, M.; Hiljanen-Vainio, M.; Karjalainen, T.; Seppälä, J. Biodegradable lactone copolymers. II. Hydrolytic study of ϵ -caprolactone and lactide copolymers. *Journal of Applied Polymer Science* 1998, 59, 1289–1298.
- [21] Tsuji, H.; Ono, T.; Saeki, T.; Daimon, H.; Fujie, K. Hydrolytic degradation of poly(ϵ -caprolactone) in the melt. *Polymer Degradation and Stability* 2005, 89, 336–343.
- [22] Sinha, V.; Bansal, K.; Kaushik, R.; Kumria, R.; Trehan, A. *International Journal of Pharmaceutics* 2004, 278, 1–23.
- [23] Fernández, J.; Larrañaga, A.; Etxeberria, A.; Sarasua, J.R. Effects of chain microstructures and derived crystallization capability on hydrolytic degradation of poly(L-lactide/ ϵ -caprolactone) copolymers. *Polymer Degradation and Stability* 2013, 98, 481–489.
- [24] Fernández, J.; Etxeberria, A.; Sarasua, J.R. In vitro degradation study of biopolyesters using poly(lactide/ δ -valerolactone) copolymers. *Polymer Degradation and Stability* 2015, 112, 104–116.

- [25] Fernández, J.; Etxeberria, A.; Sarasua, J.R. Synthesis, structure and properties of poly(L-lactide-co- ϵ -caprolactone) statistical copolymers. *Journal of the Mechanical Behavior of Biomedical Materials* 2012, 9, 100-112.
- [26] Fernández, J.; Meaurio, E.; Chaos, A.; Etxeberria, A.; Alonso-Varona, A.; Sarasua, J.R. Synthesis and characterization of poly(L-lactide/ ϵ -caprolactone) statistical copolymers with well resolved chain microstructures. *Polymer* 2013, 54, 2621-2631.
- [27] Lin, W-J. Comparison of thermal characteristics and degradation properties of ϵ -caprolactone copolymers. *Journal of Biomedical Materials Research* 1999, 47, 420-423.
- [28] Storey, R.F.; Douglas, C.; Hoffman, D.C. Copolymerization of ϵ -caprolactone and δ -valerolactone. *Makromolekulare Chemie, Macromolecular Symposia* 1991, 42/42, 185-193
- [29] Toncheva, N.; Jerome, R.; Mateva, R. Anionically prepared poly(ϵ -caprolactam-co- ϵ -caprolactone) and poly(ϵ -caprolactam-co- δ -valerolactone) copolymers: Thermal and mechanical properties. *European Polymer Journal* 2011, 47, 238-247.
- [30] Fay, F.; Renard, E.; Langlois, V.; Linossier, I.; Vallée-Rehel, K. Development of poly(ϵ -caprolactone-co-L-lactide) and poly(ϵ -caprolactone-co- δ -valerolactone) as new degradable binder used for antifouling paint. *European Polymer Journal* 2007, 43, 4800-4813.
- [31] Faÿ, F.; Linossier I.; Langlois, V.; Renard, E.; Vallée-Rehel, K. Degradation and Controlled Release Behavior of ϵ -Caprolactone Copolymers in Biodegradable Antifouling Coatings. *Biomacromolecules* 2006, 7, 851-857.
- [32] Fernández, J.; Etxeberria, A.; Sarasua, J.R. Crystallization and melting behavior of poly(ϵ -caprolactone-co- δ -valerolactone) and poly(ϵ -caprolactone-co-L-lactide) copolymers with novel chain microstructures. *Journal of Applied Polymer Science* 2015, 132, 42534.
- [33] Fernández, J.; Larrañaga, A.; Etxeberria, A.; Sarasua, J.R. Tensile behavior and dynamic mechanical analysis of novel poly(lactide/ δ -valerolactone) statistical copolymers. *Journal of the Mechanical Behavior of Biomedical Materials* 2014, 35, 39-50.
- [34] Storey, R.F.; Herring, K.R.; Hoffman, D.C. Hydroxy-terminated poly(ϵ -caprolactone-co- δ -valerolactone) oligomers: Synthesis, characterization, and polyurethane network formation. *Journal of Polymer Science Polymer Chemistry Ed* 1991, 29, 1759-1777.
- [35] Zeng, Y.; Zhang, Y.; Lang, M. Synthesis and Characterization of Poly(ϵ -caprolactone-co- δ -valerolactone) with Pendant Carboxylic Functional Groups. *Chinese Journal of Chemistry* 2011, 29, 343-350.

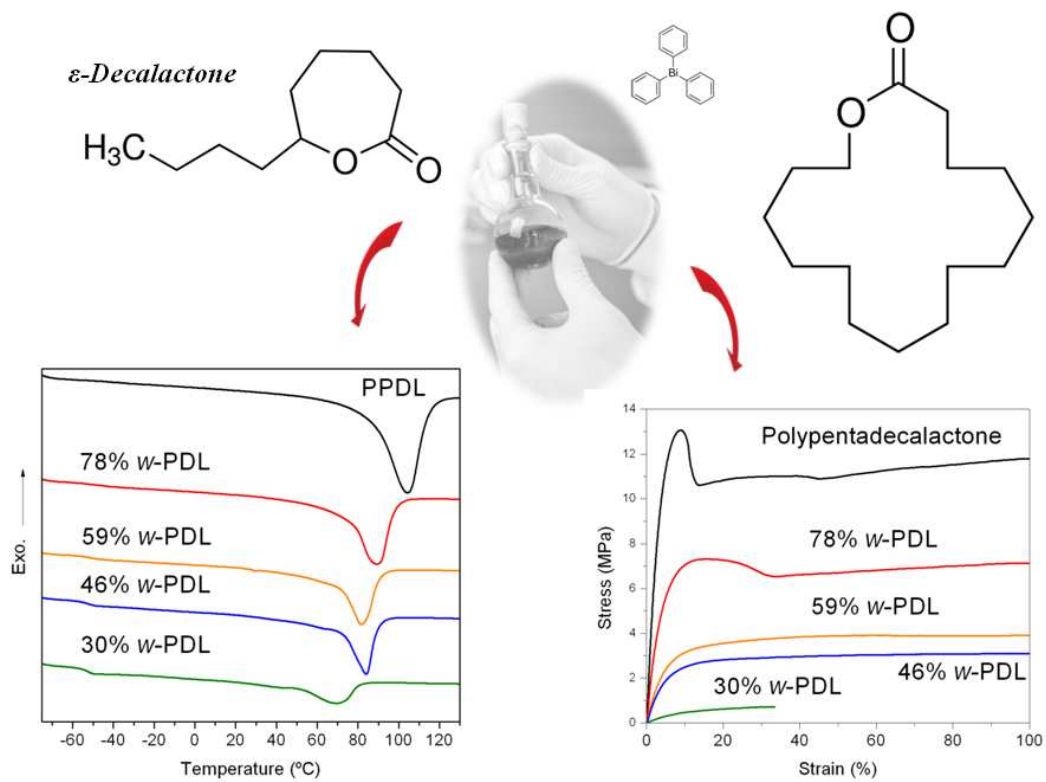
[36] Moore, T.; Adhikari, R.; Gunatillake, P. Chemosynthesis of bioresorbable poly(γ -butyrolactone) by ring-opening polymerization: a review. *Biomaterials* 2005, 26, 3771-3782.

[37] Gleadall, A.; Pan, J.; Kruff, M-A.; Kellomaki, M. Degradation mechanisms of bioresorbable polyesters. Part 1. Effects of random scission, end scission and autocatalysis. *Acta Biomaterialia* 2014, 10, 2223-2232.

[38] Fernández, J.; Larrañaga, A.; Etxeberria, A.; Wang, W.; Sarasua, JR. A new generation of poly(lactide/ ϵ -caprolactone) polymeric biomaterials for application in the biomedical field. *Journal of Biomedical Materials Research A* 2014, 102A, 3573–3584.

**Chapter 4. Synthesis and Characterization of
 ω -Pentadecalactone-co- ϵ -Decalactone
Copolymers: Evaluation of Thermal,
Mechanical and Biodegradation Properties**

Polymer 2015, 81, 12-22.



Abstract

ϵ -Decalactone (ϵ -DL), whose homopolymer is completely amorphous owing to the racemic stereochemistry of its butyl side chain, was copolymerized with ω -pentadecalactone (ω -PDL) in order to reduce the high crystallization capability of the latter. NMR characterization showed that the poly(ω -PDL-co- ϵ -DL), with ω -PDL molar contents ranging from 30 to 78 %, presented a blocky chain microstructure (randomness character $R < 0.49$). ω -PDL homopolymer (PPDL), with a T_m at 104 °C and a T_g at ~ -36 °C, exhibited a degree of crystallinity of 54 % and the incorporation of ϵ -DL decreased its crystalline fraction to 13-38 % and the T_g to around -50 °C. As a result, these copolymers displayed high elongation at break values and lower stiffness than PPDL (with secant modulus of 7 to 156 MPa) while their mechanical properties remained constant at 37 °C. The poly(ω -PDL-co- ϵ -DL), with a melting enthalpy in the range of between 36-106 J g⁻¹, presented a melting temperature higher than 69 °C and showed great thermal stability, degrading at temperatures higher than 400 °C. However, *in vitro* degradation studies during 182 days demonstrated that, despite their increased amorphous character, these materials were very resistant to hydrolysis due to the steric effect of the ϵ -DL units, and can virtually be considered as non-biodegradable polymers.

4.1. Introduction

Poly(ω -pentadecalactone) (PPDL) is a semicrystalline polymer obtained from a readily available resource, pentadecanolide or ω -pentadecalactone (ω -PDL), which is a macrolactone commercially available in large quantities and used in the fragrance industry [1,2]. The crystallization behaviour and the crystal structure of this polymer shared many similarities with polyethylene (PE) [3-5] so PPDL is often referred to as a degradable PE because of the presence of hydrolysable ester bonds in its polymer main chain. Nevertheless, although upon hydrolysis, the ω -pentadecalactone sequences would be converted into ω -hydroxypentadecanoic acid [6] (a typical hydroxyl-substituted fatty acid), some studies have shown that PPDL was neither enzymatically nor hydrolytically degradable in buffer solutions [7]. Its PE-like properties are mainly due to the long alkyl chain backbone [8] which induces a melting point around 100 °C and a glass transition temperature (T_g) far below room temperature (-27 °C) [9-10]. As a result, PPDL exhibits good ductility and a tensile strength comparable to that of low-density polyethylene (LDPE) [1], a thermoplastic with a melting temperature between 97 to 117 °C and a T_g at -25 °C.

Ring-opening polymerization (ROP) has proved to be a very efficient method to produce high molecular weight polyesters containing long methylene sequences [11]. However, the ROP mechanism of the macrolactones differs from the behaviour of small or medium size cyclic lactones, such as ϵ -caprolactone (ϵ -CL), that have a large and negative enthalpy of ring-opening as a result of ring-strain. On the contrary, the polymerization reactions of macrolactones are driven mainly by entropy as a consequence of the low ring strain associated to their larger ring size [12-15]. Hence, macrolactones are difficult to polymerize by traditional chemical methods and a limited number of catalysts have been found to be effective in contrast to the numerous routes of synthesis published to date related to small lactones. Duchateau et al. [16] have reported on the polymerization of ω -PDL using organic catalysts while a few examples of metal catalyzed ROP have also been published in literature employing tin, zinc,

yttrium and aluminium complexes [11, 14, 17-23]. However, in general, long polymerization times were necessary to reach high conversions and only moderate molecular weight products have been obtained. The most successful approach are those based on the use of enzymes [1, 7, 12, 24-26] (i.e. *Candida Antarctica* Lipase B), but the enzymatic polymerization also has some limitations such as poor level of control of the polymer microstructure as a result of transesterification.

In order to produce improved biomaterials with tailored properties, ω -PDL has been copolymerized with several monomers using different catalysts. The reactions proceeded at different rates of consumption for each monomer and, in some cases, only rather low molecular weight polymers were obtained. Thus, various ω -PDL-containing copolyesters including poly(ω -pentadecalactone-co- ϵ -caprolactone), poly(ω -pentadecalactone-co-p-dioxanone), poly(ω -pentadecalactone-co- δ -valerolactone) or poly(ω -pentadecalactone-co-trimethylene carbonate) have been proposed as alternative bioresorbable materials [15, 27-35]. However, in most of these cases both comonomers cocrystallize and the crystalline fraction was not reduced.

ϵ -Decalactone (ϵ -DL) [36-40], a renewable monomer that belong to the decalactones, a class of lactones composed of 10 carbons that includes γ -decalactone and δ -decalactone, could be an excellent compound to copolymerize with ω -PDL and, therefore, reduce the crystallization capability of the latter. ϵ -DL is a seven-membered lactone with identical structure to ϵ -CL but possesses a butyl pendant group at the ring-closing position. For the synthesis of the ϵ -DL homopolymer, Albertsson et al. [41] employed either stannous octoate (SnOct_2) or 1,5,7-triazabicyclo [4.4.0]dec-5-ene (TBD) as catalysts, and produced an oily and viscous polymer with a T_g at approximately -53 °C. This completely amorphous nature was due to the racemic stereochemistry of the alkyl side chain and, for the same reason, it was also expected that poly(ϵ -decalactone) would be more hydrophobic than polycaprolactone (PCL). ϵ -DL was recently copolymerized with ω -PDL via catalytic ROP using a Zn complex by Jasinska-Walc and Duchateau [42-43], however the properties of these ω -pentadecalactone-co- ϵ -decalactone (ω -PDL -co- ϵ -DL) copolymers have yet to be studied in greater detail.

The objective of this paper was to focus on poly(ω -PDL -co- ϵ -DL) with the aim of carrying out a complete characterization of this kind of materials and, at the same time, to report a new successful route for its synthesis. In this work the copolymers were achieved using triphenyl bismuth (Ph_3Bi) as catalyst and were characterized by proton and carbon nuclear magnetic resonance spectroscopy (^1H and ^{13}C NMR), gel permeation chromatography (GPC) measurements and thermogravimetric analysis (TGA). Their crystallization and melting behaviour was studied by means of differential scanning calorimetry (DSC) and Wide Angle X-ray diffraction (WAXRD). In addition, films of the ω -PDL -co- ϵ -DL copolymers with ω -PDL molar contents ranging from 30 to 78 % were prepared for mechanical testing at room temperature (21 °C) and at 37 °C, body temperature, the working temperatures of these biomaterials. Finally, an *in vitro* hydrolytic degradation study was also carried out at 37 °C for a period up to 26 weeks in phosphate buffer solution (PBS). Thus, the changes in water absorption, weight loss, macroscopic morphology, crystallinity, phase structure and molecular weight of the copolymers were monitored.

4.2. Materials and Methods

Materials

ϵ -decalactone monomer (assay > 99 %) was provided by Sigma Aldrich (W361305). ω -pentadecalactone monomer (assay > 98 %) was also supplied by Sigma Aldrich (W284009). The triphenyl bismuth (Ph_3Bi) catalyst was obtained from Gelest. Phosphate buffer solution (PBS) (pH 7.2) was obtained from Fluka Analytical (Sigma Aldrich).

Synthesis procedure

Statistical copolymers from ω -pentadecalactone and ϵ -decalactone (see Figure 1) were synthesized in bulk by one pot-one-step ring-opening polymerizations (ROP). The synthesis reactions were conducted in a flask immersed in a controlled temperature oil bath. In each polymerization, predetermined amounts of the different comonomers at

the chosen mass feed ratio were simultaneously added and melted into the flask. The flask was purged for 30 minutes with a nitrogen stream under the surface of the melt. The catalyst (Ph_3Bi) was then added (at 250:1 to 500:1 comonomers/catalyst molar ratio) and the magnetic stirrer maintained at 100 rpm. No initiator compound was added to the reaction mix so the catalyst was activated by the ROH provided by the monomers (H_2O and impurities). The ω -pentadecalactone-co- ϵ -decalactone polymerizations were carried out over 6 days. After the corresponding period of reaction time the products were dissolved in chloroform and precipitated, pouring the polymer solution into an excess of methanol in order to remove the catalyst impurities and those monomers that had not reacted. Finally the product was dried at room temperature and then subjected to a heat treatment at 140 °C for 1 hour to ensure the complete elimination of any remaining solvent. Then, the polymer was weighed obtaining the yield of the synthesis process, given in Tables 1 and 2.

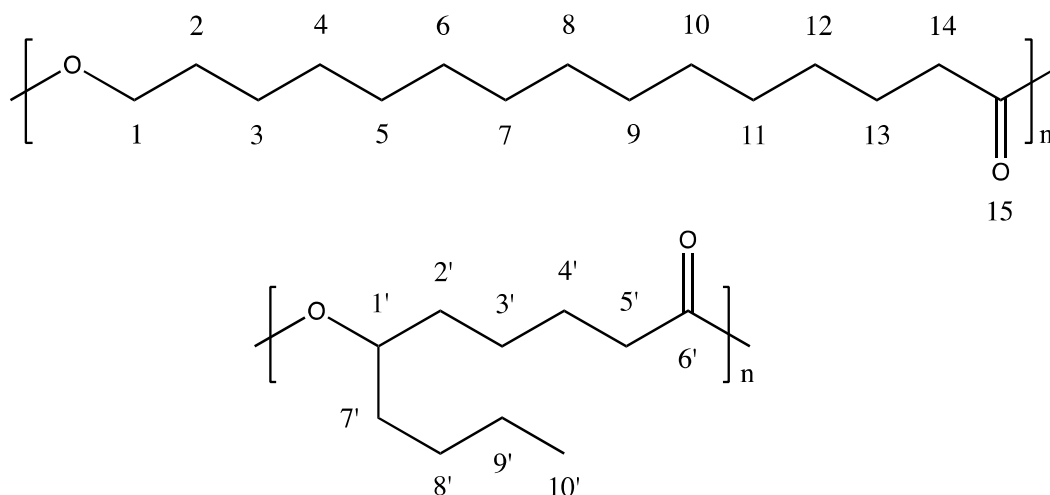


Figure 1. Scheme of the units of ω -pentadecalactone (above) and ϵ -decalactone (below).

Methods

Proton and carbon nuclear magnetic resonance (^1H and ^{13}C NMR) spectra were recorded in a Bruker Avance DPX 300 at 300.16 MHz and at 75.5 MHz of resonance frequency respectively, using 5 mm O.D. sample tubes. All spectra were obtained at room temperature from solutions of 0.7 mL of deuterated chloroform (CDCl_3).

Experimental conditions were as follows: a) for ^1H NMR: 10 mg of sample; 3 s acquisition time; 1 s delay time; 8.5 μs pulse; spectral width 5000 Hz and 32 scans; b) for ^{13}C NMR: 40 mg, inverse gated decoupled sequence; 3 s acquisition time; 4 s delay time; 5.5 μs pulse; spectral width 18800 Hz and more than 10000 scans. The assignment of the different signals were made employing the tables of structural determination from Prestch et al. [44]. The data of copolymer composition, average sequence lengths and randomness character from Tables 1 and 2 were calculated averaging the values of molar contents and the PDL-DL dyad relative molar fractions that were obtained by means of ^1H and ^{13}C NMR spectroscopy. Equations 1-3 [45] were employed to obtain the number-average sequence lengths (l_i), the Bernoullian random number-average sequence lengths (l_i) and the randomness character (R):

$$l_{\text{PDL}} = \frac{(\text{PDL} - \text{PDL}) + \frac{1}{2}(\text{PDL} - \text{DL})}{\frac{1}{2}(\text{PDL} - \text{DL})} = \frac{2(\text{PDL})}{(\text{PDL} - \text{DL})} ; \quad (1)$$

$$l_{\text{DL}} = \frac{(\text{DL} - \text{DL}) + \frac{1}{2}(\text{PDL} - \text{DL})}{\frac{1}{2}(\text{PDL} - \text{DL})} = \frac{2(\text{DL})}{(\text{PDL} - \text{DL})}$$

$$(l_{\text{DL}})_{\text{random}} = \frac{1}{(\text{PDL})} ; \quad (l_{\text{PDL}})_{\text{random}} = \frac{1}{(\text{DL})} \quad (2)$$

$$R = \frac{(l_{\text{DL}})_{\text{random}}}{l_{\text{DL}}} = \frac{(l_{\text{PDL}})_{\text{random}}}{l_{\text{PDL}}} \quad (3)$$

where (DL) and (PDL) are the ϵ -decalactone and ω -pentadecalactone molar fractions and (PDL-DL) is the PDL-DL average dyad relative molar fraction.

200-300 μm films were prepared by pressure melting at 200 $^{\circ}\text{C}$ followed by water quenching. They were then stored for 24 hours in a fridge (at 0-5 $^{\circ}\text{C}$), the typical storage temperature for biopolymers. From these films repetitive square samples for the *in vitro* degradation study (1x1 cm^2) and repetitive samples for mechanical characterization (10x1 cm^2) were obtained. The specimens for mechanical testing at 37 $^{\circ}\text{C}$ were stored for another 24 hours at 37 $^{\circ}\text{C}$ before tests were conducted at this temperature. DSC

scans were made at 20 °C min⁻¹ for each polymer sample before the mechanical testing in order to monitor the thermal properties of the specimens.

The mechanical properties were determined by tensile tests with an Instron 5565 testing machine at a crosshead displacement rate of 10 mm min⁻¹. These tests were performed at room temperature (21 ± 2 °C) and at human body temperature (37 °C) following ISO 527-3/1995. The specimens had the following dimensions: overall length = 100 mm, distance between marks = 50 mm, width = 10 mm; and were cut out from films of 200-300 µm in thickness. The mechanical properties reported (secant modulus at 2 %, yield strength, ultimate tensile strength and elongation at break) correspond to average values of at least 5 determinations. Mechanical testing at 37 °C was conducted in an Instron controlled temperature chamber. The tests were stopped at 300 % of strain due to the size limitations of the temperature chamber.

For the *in vitro* degradation study, square samples (25-35 mg (W_0) ($n = 3$)) of the different copolymers were placed in Falcon tubes containing phosphate buffer solution (PBS) (pH = 7.2) maintaining a surface area to volume ratio equal to 0.1 cm⁻¹. The samples were stored in an oven at 37 °C. Three samples of each polymer were removed at different times from the PBS and weighed wet (W_w) immediately after wiping the surface with filter paper to absorb the surface water. These samples were air-dried overnight at 37 °C. Then they were weighed again to obtain the dry weight (W_d). Water absorption (% WA) and remaining weight (% RW) were calculated according to Eqs. (4) and (5):

$$\% \text{WA} = \frac{W_w - W_d}{W_d} \cdot 100 \quad (4)$$

$$\% \text{RW} = \frac{W_d}{W_0} \cdot 100 \quad (5)$$

In order to compare the degradation rate of the studied copolymers, the exponential relationship between molecular weight and degradation time for biodegradable polyesters degrading under bulk degradation was used [46-47]:

$$\ln M_w = \ln M_{w0} - K_{Mw} \cdot t \quad (6)$$

$$t_{1/2} = 1/K_{Mw} * \ln 2 \quad (7)$$

where M_w is the weight-averaged molecular weight, M_{w0} is the initial weight-averaged molecular weight, K_{Mw} is the apparent degradation rate and $t_{1/2}$ is the half degradation time (the amount of time required to fall to half the initial value of molecular weight).

The molecular weights of the polymers were determined by GPC using a Waters 1515 GPC device equipped with two Styragel columns ($10^2 - 10^4 \text{ \AA}$). Chloroform was used as eluent at a flow rate of 1 mL min^{-1} and polystyrene standards (Shodex Standards, SM-105) were used to obtain a primary calibration curve at 50 mV of signal. The samples were prepared at a concentration of 10 mg in 1.5 mL. While the ω -PDL-co- ϵ -DL copolymers dissolved easily in chloroform, it was needed to store the solutions of the PPDL homopolymer at $37 \text{ }^\circ\text{C}$ for $\sim 30 \text{ min}$ in order to accelerate the solution of the latter. Since polystyrene standards were used, the reported values measured are likely to be higher than the actual molecular weights owing to the differences in hydrodynamic volume of the copolymers and polystyrene.

The thermal properties of the polymers were studied on a DSC 2920 (TA Instruments). Samples of 6-9 mg were melted at $140 \text{ }^\circ\text{C}$ and then quenched to $5 \text{ }^\circ\text{C}$ at different cooling rates ($5, 10, 20$ and $40 \text{ }^\circ\text{C min}^{-1}$) to study the crystallization process during the cooling. Finally, a scan was also made at $20 \text{ }^\circ\text{C min}^{-1}$ from -85 to $140 \text{ }^\circ\text{C}$ to determine the glass transition temperature (T_g), the melting temperature (T_m) and the heat of fusion or melting enthalpy per gram (ΔH_m) of the samples. During the *in vitro* degradation study, the DSC samples were heated from $21 \text{ }^\circ\text{C}$ to $140 \text{ }^\circ\text{C}$ at $20 \text{ }^\circ\text{C min}^{-1}$, immediately after the drying at $37 \text{ }^\circ\text{C}$ of the polymer samples removed from the degradation medium. After this first scan, the samples were quenched in the DSC and a second scan was made from $-85 \text{ }^\circ\text{C}$ to $140 \text{ }^\circ\text{C}$ at $20 \text{ }^\circ\text{C min}^{-1}$.

Wide angle X-ray diffraction (WAXRD) data were collected on a Bruker D8 Advance diffractometer operating at 30 kV and 20 mA. This device is equipped with a Cu tube ($\lambda = 1.5418 \text{ \AA}$), a Vantec-1 PSD detector and an Anton Parr HTK2000 high-temperature furnace. The powder patterns were recorded in 2θ steps of 0.033° in the $10 \leq 2\theta \leq 38$

range, counting for 0.2 s per step, from 50 to 122 °C every 2 °C using a heating rate of 0.2 °C s⁻¹.

Thermal degradation was studied under nitrogen by means of thermogravimetric analysis (TGA) into a TGA model Q50-0545 (TA Instruments). Samples of 10-15 mg were heated from room temperature to 500 °C at a heating rate (β) of 5 °C min⁻¹, recording continuously the heat flow, sample temperature, residual sample weight and its time derivative. In this temperature range, the polymers degraded completely.

4.3. Results and Discussion

Synthesis conditions

Firstly, several copolymerizations were carried out at a 75/25 mass feed ratio of ω -PDL/ ϵ -DL (that is, a 62/38 molar ratio) in order to evaluate the influence of the temperature and the monomers/catalyst molar ratio (M/C). Long reaction times, 6 days, were necessary to obtain substantial yields due to the low reactivity of the mixture of monomers. The synthesis results are summarized in Table 1.

As can be seen in the Table 1, the conversion of ϵ -DL was in all cases higher than that of ω -PDL. The highest weight average molecular weights ($M_w = 150.2 \text{ kg mol}^{-1}$), yield of reactions ($\sim 75 \%$) and ω -PDL conversions ($\sim 71 \%$) were obtained at 130 °C with a M/C of 250. When less PH_3Bi was added (at 500 of M/C), the copolymer composition (46.1 % of ω -PDL) differed more from the feed composition, the overall conversion of ω -PDL was much lower (46 %) and the final molecular weight decreased substantially ($M_w < 85 \text{ kg mol}^{-1}$). That means that the reaction evolved more slowly and that the catalyst firstly favored the formation of ϵ -DL-rich domains. The same was true for the copolymerization made at a lower temperature of reaction, 110 °C (PDL-DL 1), in which the yield was approximately 75 % but the M_w had a value of 113.8 kg mol⁻¹ and the molar content of ω -PDL failed to reach to 46 % (when the feed composition had a 62.3 % molar content of this monomer). In this case, the conversion of ϵ -DL reached a 100 % while only a 59 % of ω -PDL became a part of the copolymer after the synthesis.

Therefore, it can be concluded that the reactivity of ϵ -DL was higher than the observed for ω -PDL. The initiating species formed by means of the activation of the catalyst with ROH (H_2O or impurities provided by the monomers or the catalyst) may prefer the incorporation of ϵ -DL rather than the large and unstrained ω -PDL units so the consumption of ϵ -DL was faster. This is in accordance with the reports of Jasinska-Walc, Duchateau et al. [43] despite the assumed higher steric hindrance of ϵ -DL during the coordination and insertion mechanism.

Table 1. Characterization of the ω -PDL-co- ϵ -DL copolymers synthesized at the same feed composition (62.3/37.7 ω -PDL/ ϵ -DL).

Sample	M/C	T	Composition ¹ (% mol)		Yield (%)	Conversion (%)		M_w kg mol ⁻¹	D	Microstructural Magnitudes ²		
			%PDL	%DL		PDL	DL			l_{PDL}	l_{DL}	R
PDL-DL 1	250	110	45.9	54.1	75.9	59.1	100	113.8	1.78	4.83	5.70	0.38
PDL-DL 2	250	130	59.1	40.9	74.3	71.2	81.5	150.2	1.73	6.26	4.32	0.39
PDL-DL 3	500	130	46.1	53.9	59.0	46.1	89.1	84.5	1.79	4.09	4.79	0.45
PDL-DL 4	250	150	58.2	41.8	57.1	54.1	64.1	106.2	1.74	5.78	4.16	0.41

¹ Calculated averaging the copolymer compositions obtained by ¹H and ¹³C NMR

² l_{PDL} and l_{DL} are the PDL and DL number average sequence lengths of the ω -PDL-co- ϵ -DL copolymers obtained from the average dyad relative molar fraction (PDL-DL) in ¹³C NMR. These values are compared to the Bernoullian random number-average sequence lengths obtaining the randomness character value (R) of the different copolymers.

With regard to the chain microstructures parameters, as a consequence of the different reactivity of the comonomers, the synthesis reactions led to blocky ($R \rightarrow 0$) rather than random copolymers ($R \rightarrow 1$), which will not allow us to suppress the crystallization of the ω -PDL segments as much as we would like. ϵ -DL monomers polymerized first whereas the ω -PDL units reacted later favoring the formation of large sequences of ω -PDL and ϵ -DL. PDL-DL 3, with the lowest content of catalyst, showed the highest randomness character ($R = 0.45$), with ω -PDL and ϵ -DL-unit average sequence lengths of 4.09 and 4.79, respectively.

A second series of copolymerizations of poly(ω -PDL-co- ϵ -DL) were also conducted with a variation in the feed composition and will be thoroughly analyzed in the following sections. Table 2 summarized the characterization data of these copolymers

synthesized at 130 °C for 6 days with a M/C of 250 (the synthesis conditions at which the conversion of ω -PDL was higher). As can be observed, the molecular weights of the copolymers increase proportionally with the ω -PDL content and range from 99 to 230 kg mol⁻¹, while their dispersity values are in the range of 1.73 to 1.79. The ω -PDL molar content of this set of copolymers ranges from ~ 30 % (PDL-DL 30) to 78 % (PDL-DL 78) with average sequence lengths of ω -PDL (l_{PDL}) from 3.29 to 9.22. The randomness character (R) value is in all cases lower than 0.49 while the copolymers richer in ϵ -DL showed a slightly blockier distribution of sequences ($R < 0.43$). For proper evaluation of the behaviour of the ω -PDL-co- ϵ -DL copolymers, a poly(ω -pentadecalactone) (PPDL) homopolymer was also synthesized. This material had a M_w of 365 kg mol⁻¹ with a dispersity of 1.98.

Table 2. Characterization data of the ω -PDL-co- ϵ -DL copolymers of different compositions synthesized at 130 °C with a monomers/catalyst molar ratio of 250.

Sample	Feed Molar Composition		Composition ¹ (% mol)		Yield (%)	Conversion (%)		M_w kg mol ⁻¹	D	Microstructural Magnitudes ²		
	%PDL	%DL	%PDL	%DL		PDL	DL			l_{PDL}	l_{DL}	R
PPDL	100	0	100	0	64.3	64.3	-	365.1	1.98	-	-	-
PDL-DL 78	80.1	19.9	77.8	22.2	74.2	72.6	83.2	230.0	1.78	9.22	2.64	0.49
PDL-DL 59	62.3	37.7	59.1	40.9	74.3	71.2	81.5	150.2	1.73	6.26	4.32	0.39
PDL-DL 46	44.4	50.6	45.5	54.5	87.2	85.8	88.9	118.5	1.73	4.88	5.84	0.38
PDL-DL 30	36.7	63.3	29.8	70.2	76.2	63.5	86.6	99.4	1.79	3.29	7.74	0.43

¹ Calculated averaging the copolymer molar compositions obtained by ¹H and ¹³C NMR

² l_{PDL} and l_{DL} are the PDL and DL number average sequence lengths of the ω -PDL-co- ϵ -DL copolymers obtained from the average dyad relative molar fraction (PDL-DL) in ¹³C NMR. These values are compared to the Bernoullian random number-average sequence lengths obtaining the randomness character value (R) of the different copolymers.

NMR Characterization

Figure 2 and 3 present the ¹H and ¹³C NMR spectra of the ω -pentadecalactone-co- ϵ -decalactone copolymer with a 46 % of ω -PDL (PDL-DL 46). In the ¹H NMR spectrum, the calculus of the molar composition was made based on the signals of the ω -PDL methylene bonded to the ester group, which appears centered at 4.09 ppm, with regard

to the ϵ -DL methine at around 4.89 ppm. The rest of peaks (see scheme in Figure 1) are assigned in Table 3 to the other hydrogens of the copolymer.

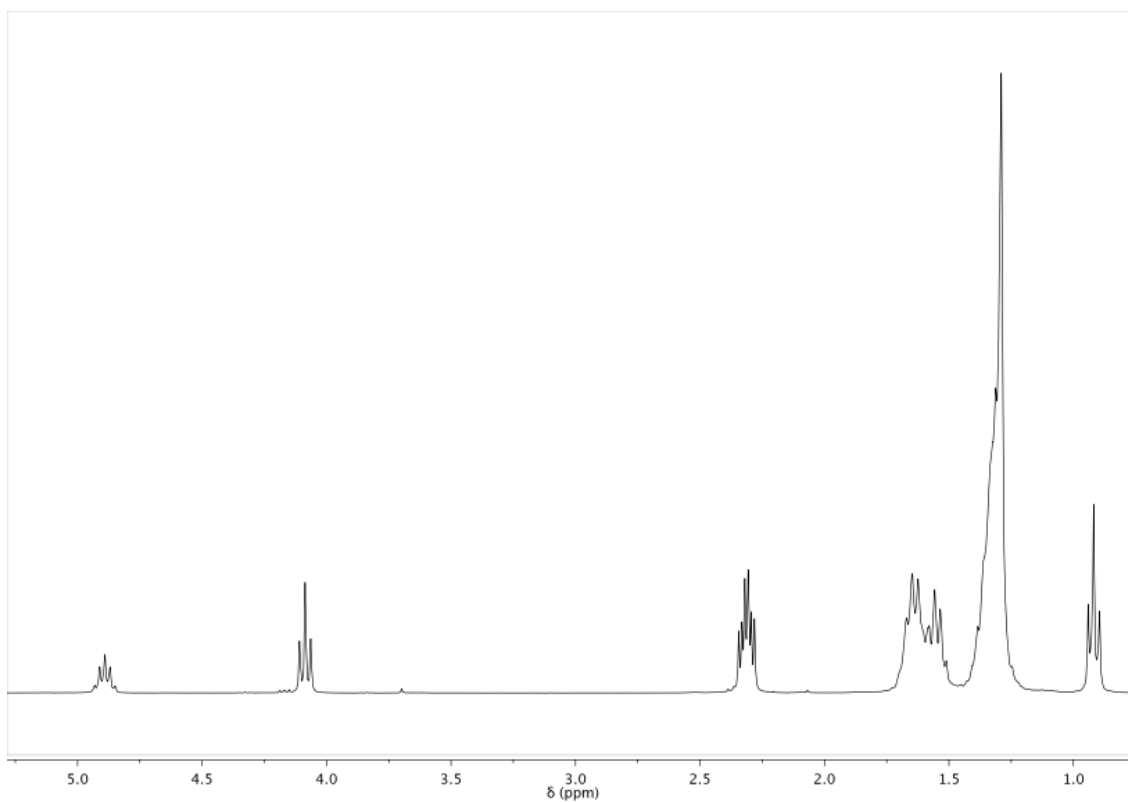


Figure 2. ^1H NMR spectrum of PDL-DL 46.

Table 3. Assignment of the different signals to the hydrogens of the ω -PDL-co- ϵ -DL.

Number of C	H ω -PDL	H ϵ -DL	
	δ (ppm)	δ (ppm)	
1	4.09	4.89	
2	1.65	1.56	
3	1.29	1.29	
4		1.65	
5		2.32	
6		-	
7		1.65	
8		1.29	
9		1.29	
10		0.92	
11			
12			
13	1.65		
14	2.32		
15	-		

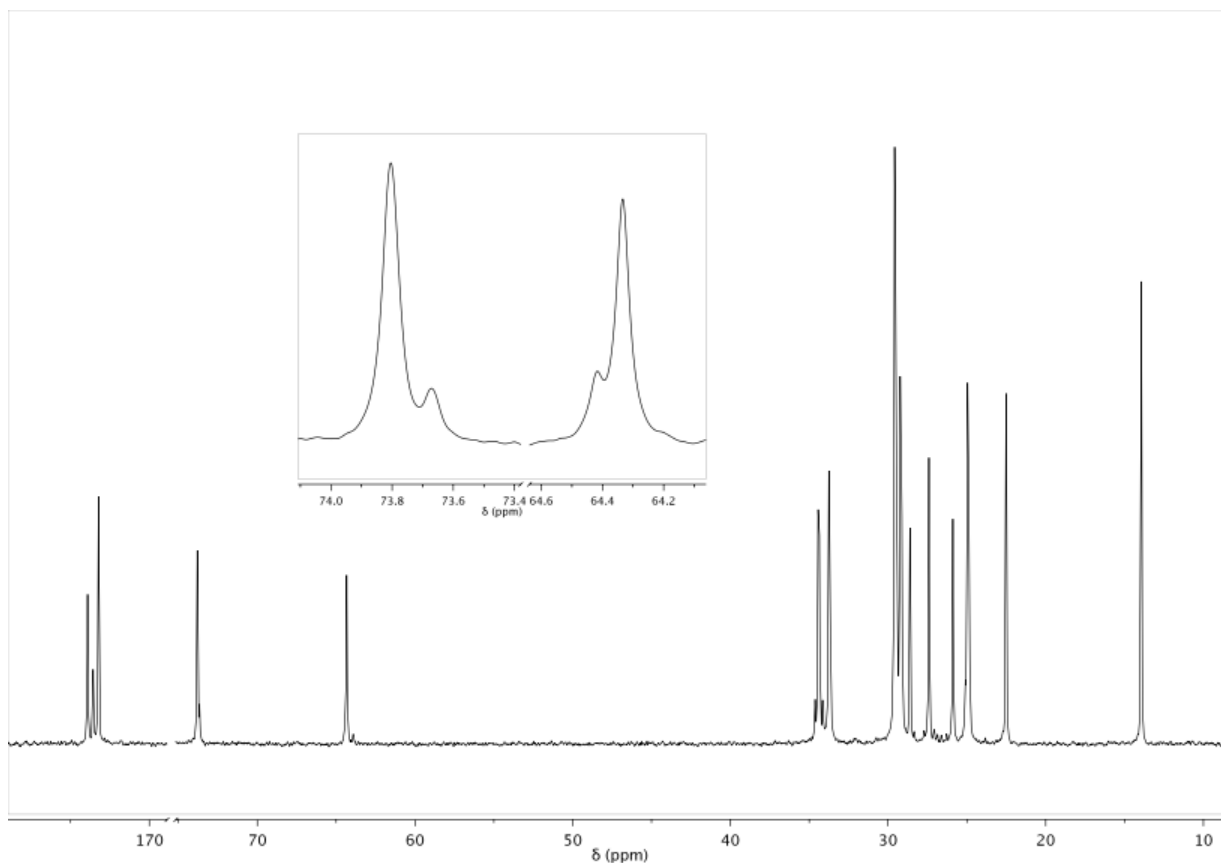


Figure 3. ^{13}C NMR spectrum of PDL-DL 46.

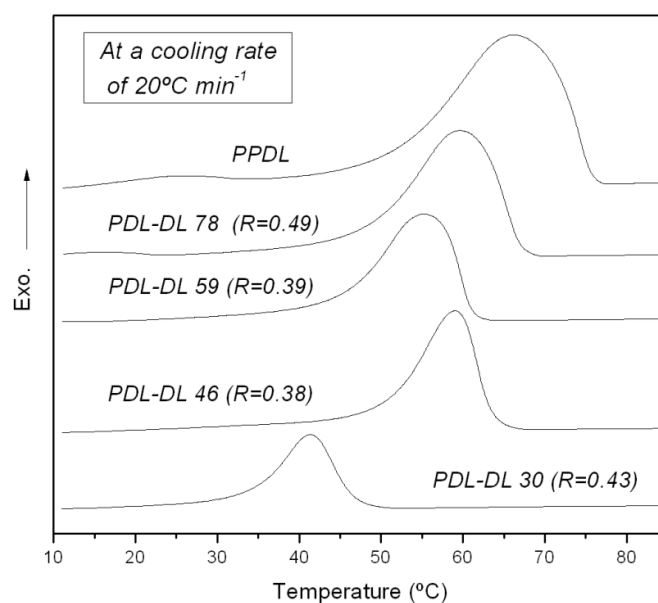
Figure 3 shows the ^{13}C NMR spectrum of the ω -PDL-co- ϵ -DL copolymer with some regions of interest enlarged. The different signals appearing between 13 and 175 ppm of chemical shift (δ) are assigned in Table 4 to the different carbons numbered in Figure 1. The signals at 173.23 and 173.75 ppm belong to the carbonyl carbons of the ϵ -decalactone and ω -pentadecalactone units, whereas the peaks at 64.39 and 73.80 ppm can be respectively assigned to the ω -PDL methylene bonded to the ester group (carbon **1**) and the ϵ -DL methine (carbon **1'**). Therefore, the molar composition of these copolymers can be easily determined in these two regions by comparing the areas under the peaks due to the ω -PDL and ϵ -DL units. On the other hand, since these two signals present dyad sensitivity (see the enlargement in Figure 3), the PDL-DL dyad relative molar fraction can also be calculated. Hence, the signals at 73.69 and 73.83 ppm can be respectively assigned to the PDL-DL and DL-DL dyads (underlining is used to emphasize that the analysed nuclei belongs to that unit), while the PDL-DL and PDL-PDL dyads appears, from left to right, at the peak at 64.39 ppm [43].

Table 4. Assignment of the different signals to the carbons of the ω -PDL-co- ϵ -DL.

Number of C	C ω -PDL	C ϵ -DL
	δ (ppm)	δ (ppm)
1	64.39	73.80
2	28.6-29.6	33.76
3	25.90	24.98
4	28.6-29.6	24.98
5		33.76
6		173.23
7		34.36
8		27.42
9		22.52
10		13.95
11		
12		
13	24.98	
14	34.36	
15	173.6-173.9	

Thermal Properties

In this section the crystallization and melting behaviour of the copolymers from Table 2 were studied. Firstly, several cooling treatments at different rates (5, 10, 20 and 40 °C min⁻¹) were conducted in the DSC. The crystallization temperatures (T_c) and the enthalpy of crystallization (ΔH_c) of each material are shown in Table 5, whereas the DSC traces at a cooling rate of 20 °C min⁻¹ are shown in Figure 4.

**Figure 4.** DSC cooling scans at 20 °C min⁻¹ of the ω -PDL-co- ϵ -DL copolymers.

As can be seen in Table 5, the crystallization peaks of each polymer appeared at a higher temperature as the cooling rate decreased. This is due to the fact that at lower cooling rates, crystal nuclei have more time to develop [48-49]. As an illustration, the T_c of PDL-DL 78 at a rate of $5\text{ }^\circ\text{C min}^{-1}$ was $71\text{ }^\circ\text{C}$, while at $40\text{ }^\circ\text{C min}^{-1}$ its crystallization peak was located at $\sim 52\text{ }^\circ\text{C}$. ω -PDL chains crystallized very fast and the ΔH_c of the PPDL homopolymer and their copolymers was almost independent of cooling rate. The differences between the respective enthalpies from the same polymer were small (particularly for those with higher contents of ε -DL), although it was noted that at the slowest cooling rate, the ΔH_c was slightly larger than those corresponding to the other cooling treatments.

Table 5. Crystallization enthalpies and temperatures obtained for the ω -PDL-co- ε -DL copolymers at cooling rates in the $5 - 40\text{ }^\circ\text{C min}^{-1}$ range.

Sample	$5\text{ }^\circ\text{C min}^{-1}$		$10\text{ }^\circ\text{C min}^{-1}$		$20\text{ }^\circ\text{C min}^{-1}$		$40\text{ }^\circ\text{C min}^{-1}$	
	$\Delta H\text{ (J g}^{-1}\text{)}$	$T_c\text{ (}^\circ\text{C)}$	$\Delta H\text{ (J g}^{-1}\text{)}$	$T_c\text{ (}^\circ\text{C)}$	$\Delta H\text{ (J g}^{-1}\text{)}$	$T_c\text{ (}^\circ\text{C)}$	$\Delta H\text{ (J g}^{-1}\text{)}$	$T_c\text{ (}^\circ\text{C)}$
PPDL	129.2	76.0	127.5	72.2	123.8	63.2	117.1	56.7
PDL-DL 78	97.6	71.0	93.3	65.1	85.5	59.7	84.7	52.2
PDL-DL 59	69.2	64.0	68.0	60.8	66.5	55.3	64.6	46.9
PDL-DL 46	58.2	66.4	56.3	63.4	55.4	59.0	55.1	50.4
PDL-DL 30	30.3	50.1	30.0	46.4	29.6	41.3	28.4	36.6

As expected, PPDL and the ω -PDL rich copolymers presented broader crystallization peaks and higher crystallization capability in comparison to other copolymers as PDL-DL 30 (see Figure 4). Nevertheless, it is worth mentioning the fact that PDL-DL 78, PDL-DL 59 and PDL-DL 46 presented similar T_c s (at around $55\text{-}60\text{ }^\circ\text{C}$ at a cooling rate of $20\text{ }^\circ\text{C min}^{-1}$) despite their different compositions. This could be explained by their different chain microstructures. PDL 78 show a more random distribution of sequences ($R \sim 0.49$) and, as a result, its ω -PDL average sequence length was lower than the expected ($l_{\text{PDL}} = 9.22$).

The DSC heating curves obtained after the cooling treatments were virtually identical for each polymer, both having practically the same melting temperatures and enthalpies (T_m and ΔH_m) after the cooling process. Figure 5 shows the DSC curves of scans made

from -85 to 140 °C at 20 °C min⁻¹, with the glass transition temperatures (T_g s) marked by an arrow.

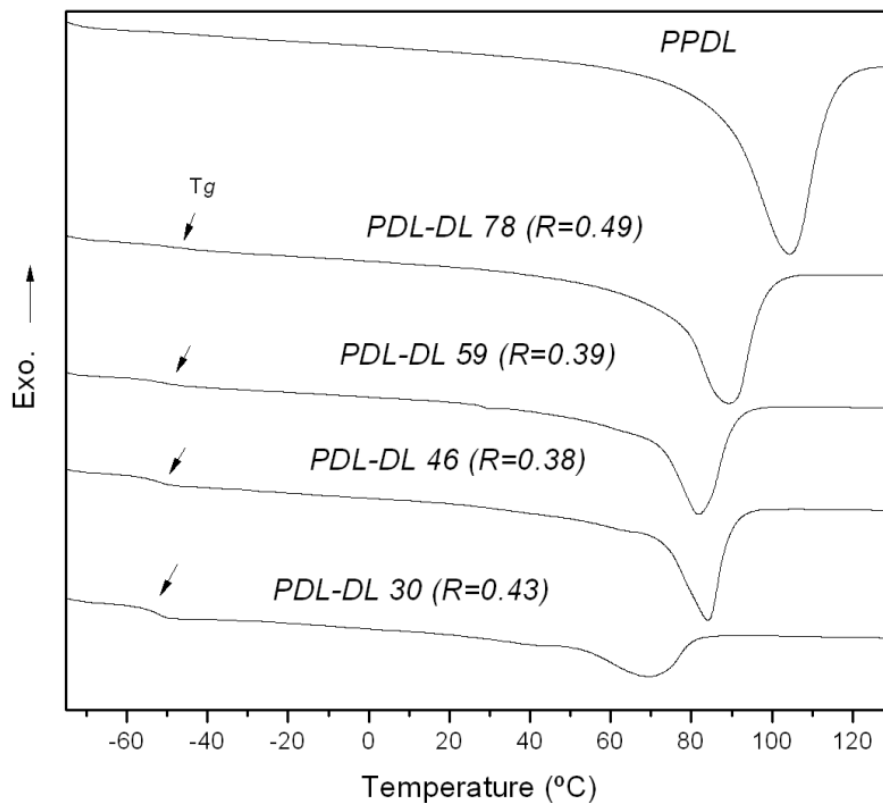


Figure 5. DSC heating curves at 20 °C min⁻¹ from -85 to 140 °C of the different ω -PDL-co- ϵ -DL copolymers.

PPDL homopolymer exhibited a large melting peak, over 136 J g⁻¹, with a T_m at 104 °C, results that are in agreement with other reports [1, 9]. As can be observed in Figure 5, as the ω -PDL content decreased the melting peaks became smaller. The associated ΔH_m s values were slightly higher than those of the crystallization peaks and, as well as in the case of their T_{cs} , the T_m s of the copolymers with a ω -PDL content of 78, 59 and 46 % were within a similar range of values (82 °C < T_m < 90 °C). However, the ΔH_m values of these poly(ω -PDL-co- ϵ -DL) were between ~ 70 to 106 J g⁻¹. With regard to PDL-DL 30, with only a 30 % molar content of ω -PDL, it was able to crystallize and presented the smallest melting peak (ΔH_m of 35.8 J g⁻¹) at around 69 °C. Its T_g , at -52 °C, was easily distinguished because of its lower crystallization capability and increased amorphous character, while its heat capacity (ΔC_p) had a value of 0.34 J g⁻¹ °C⁻¹, which

shifted to lower values in the other polymers when the ω -PDL content was raised. The glass transition became more difficult to discern in the ω -PDL homopolymer, and was located at around $-36\text{ }^{\circ}\text{C}$ with a ΔC_p of $0.16\text{ J g}^{-1}\text{ }^{\circ}\text{C}^{-1}$. The T_g s of the copolymers did not change significantly with the polymer composition and the T_g of PDL-DL 78 was only $3\text{ }^{\circ}\text{C}$ higher than those of PDL-DL 30. Therefore, the glass transition temperatures were in the -52 to $-49\text{ }^{\circ}\text{C}$ range for the four copolymers.

The DSC heating results discussed above are summarized in Table 6 along with the melting temperature, the crystal fraction (X_c) and the average crystal size (c.s.) from Wide Angle X-ray Scattering (WAXS). The latter data were calculated from the two most intense peaks in the diffraction pattern: at $2\theta = 21.7^{\circ}$ and at $2\theta = 24.1^{\circ}$. The T_{ms} given are the temperatures until the crystalline phase became stable, values that are consistent with their corresponding melting temperatures obtained by DSC.

Table 6. Calorimetric and X-ray Diffraction data of the ω -PDL-co- ϵ -DL copolymers.

Sample	I_{PDL}	T_m^1	X_c	c.s	ΔH_m	T_m^2	T_g	ΔC_p
		$^{\circ}\text{C}$	(%)	nm	J g^{-1}	$^{\circ}\text{C}$	$^{\circ}\text{C}$	$\text{J g}^{-1}\text{ }^{\circ}\text{C}^{-1}$
PPDL	-	104.0	53.8	27	136.1	104.3	-35.6	0.16
PDL-DL 78	9.22	96.0	38.4	20	106.3	89.4	-49.1	0.22
PDL-DL 59	6.26	88.0	29.6	23	77.6	81.8	-50.7	0.25
PDL-DL 46	4.88	88.0	29.4	22	69.8	84.0	-52.2	0.29
PDL-DL 30	3.29	74.0	12.7	20	35.8	69.0	-52.1	0.34

¹ Obtained by WAXS. This is the crystalline phase-stable temperature.

² Obtained from a DSC at $20\text{ }^{\circ}\text{C min}^{-1}$ from -85 to $140\text{ }^{\circ}\text{C}$.

Figure 6 shows the diffraction profiles of the poly(ω -PDL-co- ϵ -DL) together with the diffractogram of the reference homopolymer (PPDL). As can be seen, at higher contents of ϵ -DL in the copolymers the reflection intensity decreases. However, the poly(ω -PDL-co- ϵ -DL) presented exactly the same signals as PPDL at a 2θ of 21.7 , 24.1 , 30.1 and 36.3° (the peak at 27.3° may be due to the bismuth compounds because it also appeared at high temperatures when the polymers were fully amorphous). Hence, it can be stated

that the ω -PDL-co- ϵ -DL copolymers and the PPDL present the same crystal structure and confirms that only the ω -PDL units were able to crystallize.

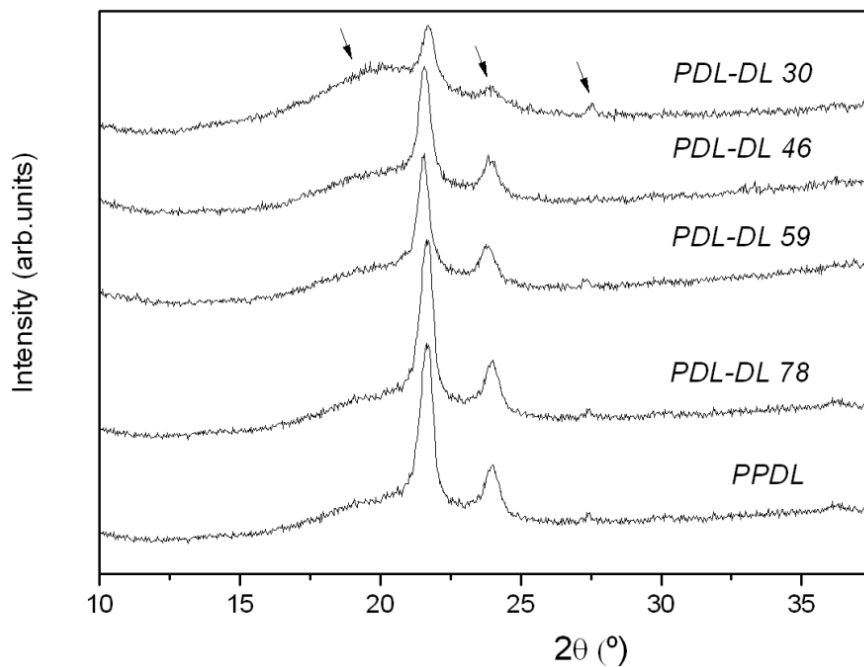


Figure 6. WAXS profiles of PPDL and the ω -PDL-co- ϵ -DL copolymers in the $10 \leq 2\theta \leq 38$ range.

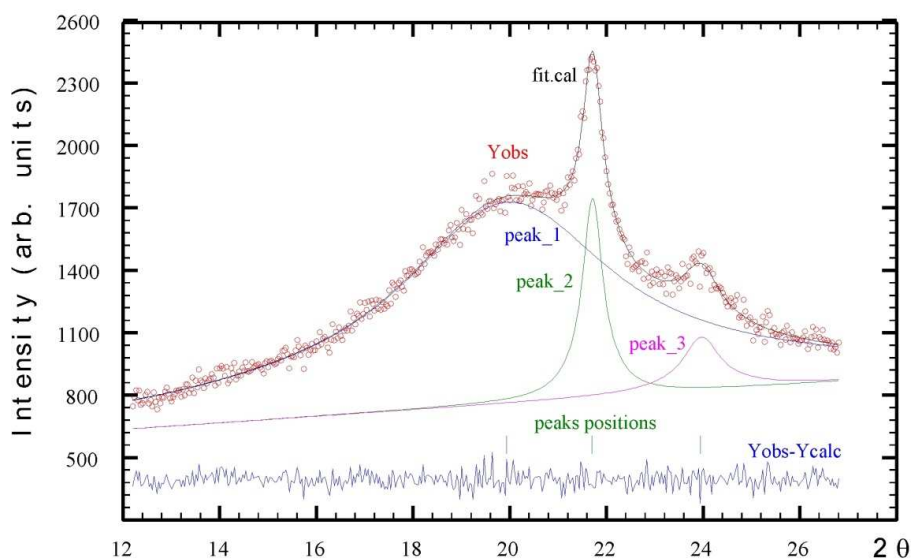


Figure 7. Deconvolution of the signal in the $12 \leq 2\theta \leq 27$ range.

The peaks in the $20 \leq 2\theta \leq 25$ range were the most intense of the WAXS profiles. Figure 7 shows this region for one of the copolymers, PDL-DL 30, with the amorphous

area and the crystalline peaks isolated. The degree of crystallinity (χ_c) was determined as the ratio of the crystalline peak areas to the total area under the scattering curve, while the average crystal size was obtained employing the Scherrer equation [50] with a shape factor “k” of 0.90.

The calculated crystalline fraction for PPDL was 53.8 % and, using its ΔH_m of 136.1 J g⁻¹ from the DSC measurements, a value of heat of fusion for 100 % crystalline material (ΔH_m^0) of 253.0 J g⁻¹ was estimated. As the ϵ -DL content increased, the degree of crystallinity of the copolymers fell, as expected. Therefore, PDL-DL 78 and PDL-DL 30, presented χ_c of 38.4 and 12.7 %, respectively. With regard to PDL-DL 59 and PDL 46, both showed a similar crystalline fraction (~ 29 %), which is in accordance with the melting behaviour seen in the DSC (ΔH_m of PDL-DL 59 was slightly larger than that of PDL-DL 46). Finally, the fact that the calculated average crystal size of the copolymers was in the 20 to 23 nm range should also be mentioned, all values lower than those obtained for the homopolymer which had an average crystal size near 27 nm.

Hydrolytic degradation study

DSC scans were made from 21 to 140 °C: at room temperature before submerging the samples in PBS, after storage for 24 hours at 37 °C and at different degradation times. The data relating to melting enthalpies and temperatures at the start and at the end of the study for all the polymer films are gathered in Table 7.

Table 7. Melting enthalpies and temperatures of all the polymer films at the start and at the end of the degradation study.

Sample	21 °C		37 °C		On day 182 of degradation at 37 °C	
	ΔH (J g ⁻¹)	T _m (°C)	ΔH (J g ⁻¹)	T _m (°C)	ΔH (J g ⁻¹)	T _m (°C)
PPDL	133.3	102.2	133.8	102.8	147.4	106.1
PDL-DL 78	102.5	92.4	104.4	90.8	112.1	92.0
PDL-DL 59	80.5	83.9	77.8	84.9	77.6	90.0
PDL-DL 46	67.6	85.4	62.9	88.0	71.5	90.4
PDL-DL 30	33.8	72.6	30.9	73.1	39.3	72.7

The thermal properties of the polymers at 21 °C and at 37 °C can be considered as very similar (the small differences may be due to the precision of the measurements). However, it can be observed that on day 182 of degradation, the samples were slightly more crystalline with higher ΔH_m values. This is particularly true in the case of PDL-DL 30, in which the melting enthalpy rose from 30.9 to 39.3 J g⁻¹ because of the rearrangements of its crystalline phase. However, as a consequence of the highly crystalline domains of ω -PDL, water absorption was negligible and did not exceed a value of 1 % in any case. Consequently, the polymers did not lose mass and the weight of the samples remained constant during the entire study.

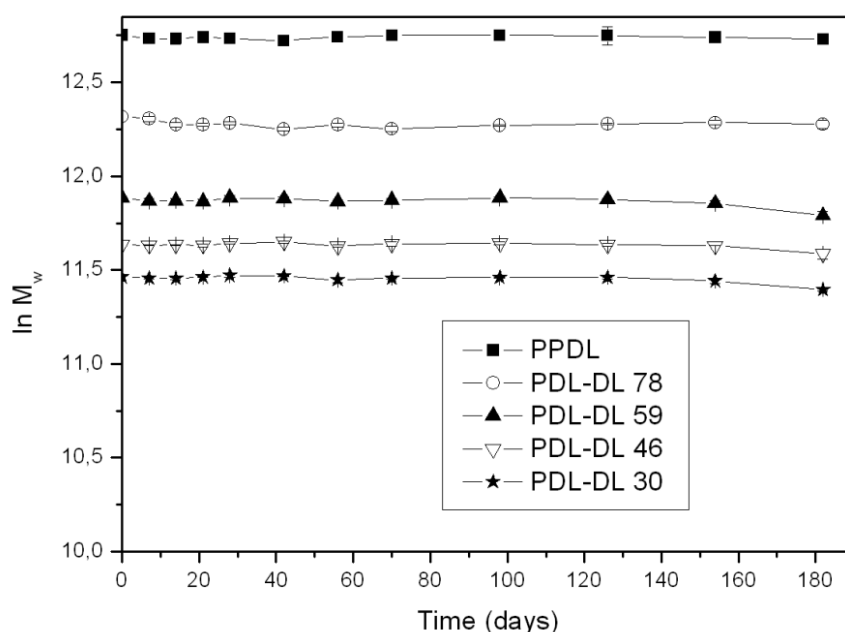


Figure 8. $\ln M_w$ against degradation time of PPDL and its ϵ -DL copolymers.

Figure 8 shows the progress of $\ln M_w$ against degradation time of the PPDL homopolymer and the ϵ -DL copolymers. As can be seen, M_w remained practically constant during the 182 days, regardless of the polymer composition. The higher melting temperature of the ω -PDL crystals and the lower proportion of hydrolysable ester bonds of ω -PDL in comparison to ϵ -CL, make PPDL more resistant to hydrolytic degradation than the well-studied poly(ϵ -caprolactone) (PCL). With the incorporation of ϵ -DL units, the crystal structure of ω -PDL (54 % crystalline fraction) is disrupted and the copolymers became significantly more amorphous (13-38 % crystalline fraction).

However, the steric effect of the butyl pendant group of the ϵ -DL may slow the hydrolysis process down. The same applies to some polyhydroxyalkanoates (PHAs), in which the degradation rate is greatly affected by the length of the pendant groups and the distance between their ester linkages [51-52].

No morphological changes were appreciated on the PPDL and poly(ω -PDL-co- ϵ -DL) samples and their M_w at the end of the study was approximately the same as at the start. Only the M_w of PDL-DL 46 and PDL-DL 30 slightly decreased to final values of 107 and 89 kg mol⁻¹, which allows the calculus of an approximated degradation rate (K_{M_w}) of 0.0002 days⁻¹ (and a half degradation time of \sim 9.5 years). This K_{M_w} value is well below the obtained for PCL (0.0010 days⁻¹) in a previous study by this group [53] but it would be necessary to carry out a longer degradation study to get more exact results.

Mechanical Properties

Table 8 summarizes the mechanical testing results at 21 °C and at 37 °C for the PPDL and poly(ω -PDL-co- ϵ -DL)s films, whose DSC data, before performing the mechanical tests, were already shown in Table 7. Figure 9 shows the typical stress-strain curves of the polymers at 21 °C while Figure 10 displays the start of the curves at 21 and 37 °C. As can be seen in Figure 10, the behaviour at both temperatures was very similar and these materials maintain their properties at body temperature, in contrast to other polyesters of high T_g (i.e. Polylactide, polyglycolide and their copolymers [54]) or biopolymers of low T_m ($<$ 65 °C) such as PCL and its copolymers [53]. Nevertheless, it is worth noting that at 37 °C the yield points were broader and their stress related properties (secant modulus, yield strength and tensile strength at 300 %) were found to be slightly lower than at 21 °C.

PPDL homopolymer exhibited a secant modulus value of 327.1 MPa, ultimate tensile strength of 28.8 MPa and strain at break values of 847 %; mechanical data that are in agreement with the results obtained by our group for another polyester in the same family, poly(ϵ -caprolactone) (PCL) [53]. At 37 °C the secant modulus of PPDL decreased to 307.3 MPa, representing a drop of 6 %, while its yield strength shifted from 13.1 MPa to 11.6 MPa. In the case of PCL, the loss of strength was more

important and the secant modulus dropped from ~ 312 to 276 MPa and its yield strength shifted from almost 14 MPa to 9.8 MPa. These changes were even more relevant on the PCL copolymers studied in a previous work by this group, due to their lower melting temperatures [49, 53].

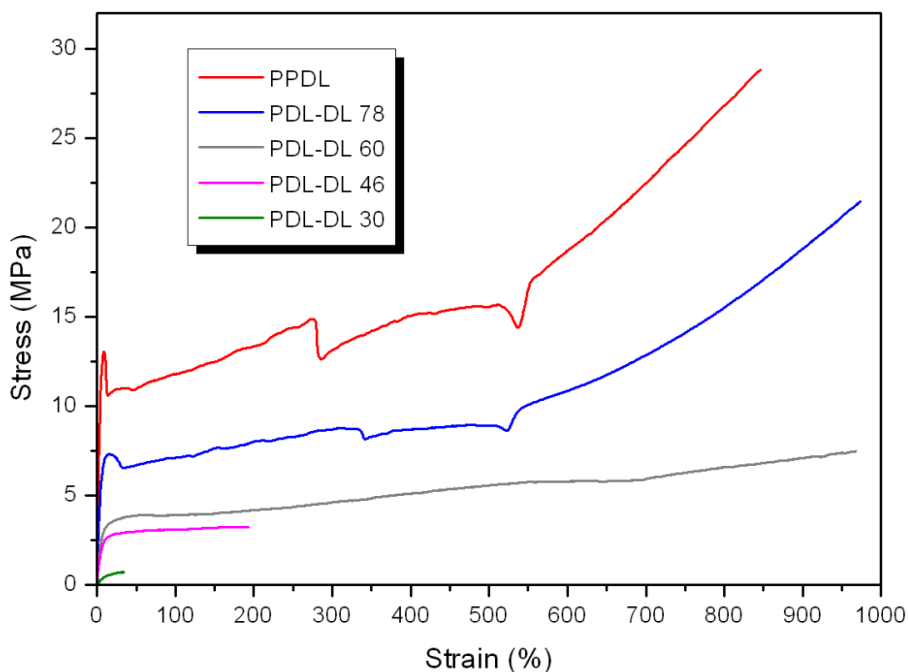


Figure 9. Typical tensile stress-strain curves of PPDL and the ω -PDL-co- ϵ -DL copolymers at 21 °C.

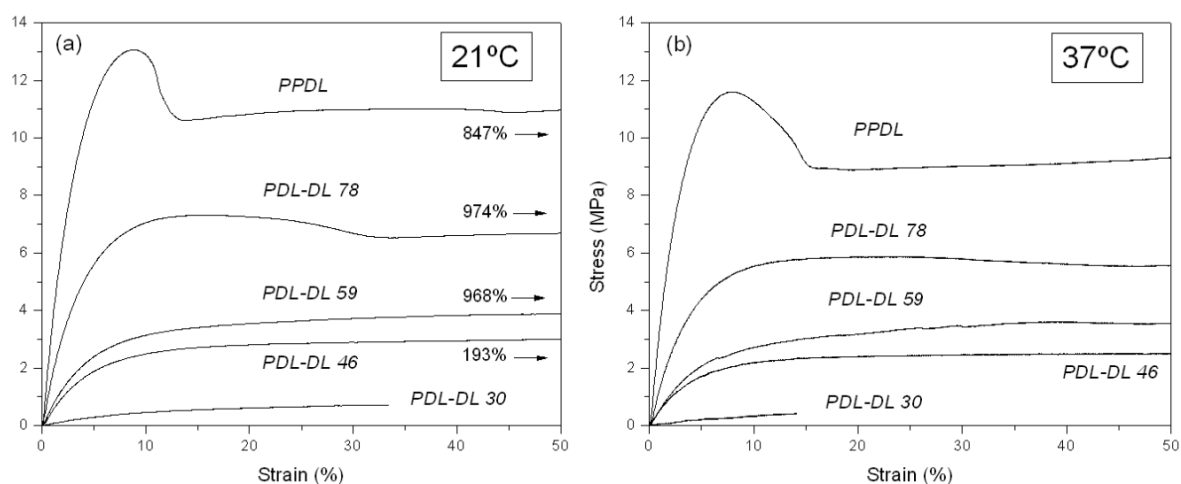


Figure 10. Tensile stress-strain curves until 50 % of strain of PPDL and the ω -PDL-co- ϵ -DL copolymers at 21 °C and at 37 °C.

Table 8. Mechanical properties of the PDDL and the ω -PDL-co- ϵ -DL copolymers.

Sample	Testing Temperature ¹	Secant Modulus at 2 %	Yield Strength (Yield Point) or Offset Yield Strength at 10 % ²	Tensile Strength at 300 %	Ultimate Tensile Strength ³	Elongation at break	Strain Recovery after break ⁴
		(MPa)	(MPa)	(MPa)	(MPa)	(%)	(%)
PDDL	21 °C	327.1 ± 16.8	13.1 ± 0.8 (8.3 %)	14.5 ± 1.4	28.8 ± 2.5	847	37.6 ± 2.2
	37 °C	307.3 ± 6.5	11.6 ± 0.8 (8.3 %)	12.4 ± 0.9	-	> 300	-
PDL-DL 78	21 °C	156.2 ± 3.2	7.2 ± 0.4 (15.3 %)	8.3 ± 0.3	21.5 ± 1.1	974	43.3 ± 2.4
	37 °C	124.0 ± 4.4	5.9 ± 0.3 (22.1 %)	6.9 ± 0.2	-	> 300	-
PDL-DL 59	21 °C	65.9 ± 2.6	3.4 ± 0.4	4.7 ± 0.1	7.5 ± 0.3	968	51.7 ± 1.7
	37 °C	53.6 ± 2.3	3.0 ± 0.2	4.6 ± 0.3	-	> 300	-
PDL-DL 46	21 °C	50.1 ± 2.1	2.7 ± 0.1	-	3.1 ± 0.2	193	77.8 ± 2.4
	37 °C ⁴	46.7 ± 1.6	2.3 ± 0.1	-	2.5 ± 0.1	86	-
PDL-DL 30	21 °C	6.7 ± 0.3	0.57 ± 0.03	-	0.67 ± 0.09	34	93.3 ± 1.1
	37 °C ⁴	4.3 ± 0.7	-	-	0.39 ± 0.09	14	-

¹At 37 °C, the tests were stopped at 300 % of strain due to the size limitations of the temperature chamber.

² Offset Yield Strength at 10 % was calculated for PDL-DL 59, PDL-DL 46 and PDL-DL 30.

³ The tensile strength was determined as ultimate stress value (σ_u).

⁴ Measured 24 hours after break.

The ω -PDL-co- ϵ -DL copolymers showed a marked improvement in flexibility compared to PDDL (and PCL) with lower secant modulus and increased strain recovery rates (from 43 to 93 %). PDL-DL 78 ($T_m \sim 92$ °C and $\Delta H_m \sim 103$ J g⁻¹) and PDL-DL 59 ($T_m \sim 84$ °C and $\Delta H_m \sim 81$ J g⁻¹) presented high values for elongation at break (~ 970 %), secant modulus of 156.2 and 65.9 MPa yield strengths of 7.2 and 3.4 MPa and final strength values of 21.5 and 7.5 MPa. Regarding PDL-DL 46, it had secant modulus values of 50.1 MPa, 2.7 MPa of yield strength and only 3.1 MPa of ultimate tensile strength. Owing to its lower ΔH_m (68 J g⁻¹) its testing samples broke at only 193 % of strain but exhibited a strain recovery rate of almost 78 %. The mechanical performance

of PDL-DL 30 ($T_m \sim 73$ °C and $\Delta H_m \sim 34$ J g⁻¹), the copolymer with highest content of ϵ -DL, was the most elastomeric material. However, its performance was heavily dependent on its crystalline phase. Hence, this material presented an elongation at break value of only 34 % and its secant modulus decreased approximately a 36 % (from 6.7 MPa at 21 °C to 4.3 MPa) when the mechanical tests were conducted at 37 °C. In the case of the other copolymers the changes in secant modulus, yield strength and tensile strength at 300 % were not so relevant and it can be said that their mechanical properties were stable at 21 °C, the temperature at which these biomaterials will be implanted, and at 37 °C, body temperature, at which they would be employed.

Thermogravimetric analysis

Figure 11 shows the curves of percent weight loss and first derivative of weight loss against temperature (TG and DTG curves) belonging to the PPDL homopolymer and the ω -PDL-co- ϵ -DL copolymers. As can be seen, three well-defined peaks can be distinguished in the DTG curves, which support the blocky structure found for the copolymers. The first stage of thermal degradation at around 325 °C was attributed to the decomposition of ϵ -DL-rich sequences. This peak did not appear in the curve of the PPDL and was more pronounced in the case of PDL-DL 30, the copolymer with the highest ϵ -DL content. As the ω -PDL content increased, the intensity of this peak decreased and it eventually vanished in PPDL. Two stages of degradation of ω -PDL were found in the DTG curve of PPDL that also appeared in the poly(ω -PDL-co- ϵ -DL) curves. The first peak, the more intense, appeared at ~ 400 °C whereas the thermal degradation of the (assumed) ω -PDL catalyst free chains was delayed to around 440 °C. This second peak was weaker due to the high residual catalyst content of this kind of polymers (a low monomer/catalyst molar ratio was used in their synthesis). As a result of the accelerating effect of the metal compounds on the pyrolysis of the polyesters [55], the peak of thermal degradation of ϵ -DL (with an identical structure to ϵ -CL but having a butyl pendant group) shifted to a lower temperature than that of PCL, which had a degradation peak in the range of 350 to 400 °C [55]. Conversely, the ω -PDL blocks, with a lower proportion of ester groups, were more stable to thermal degradation than PCL and resisted higher temperatures.

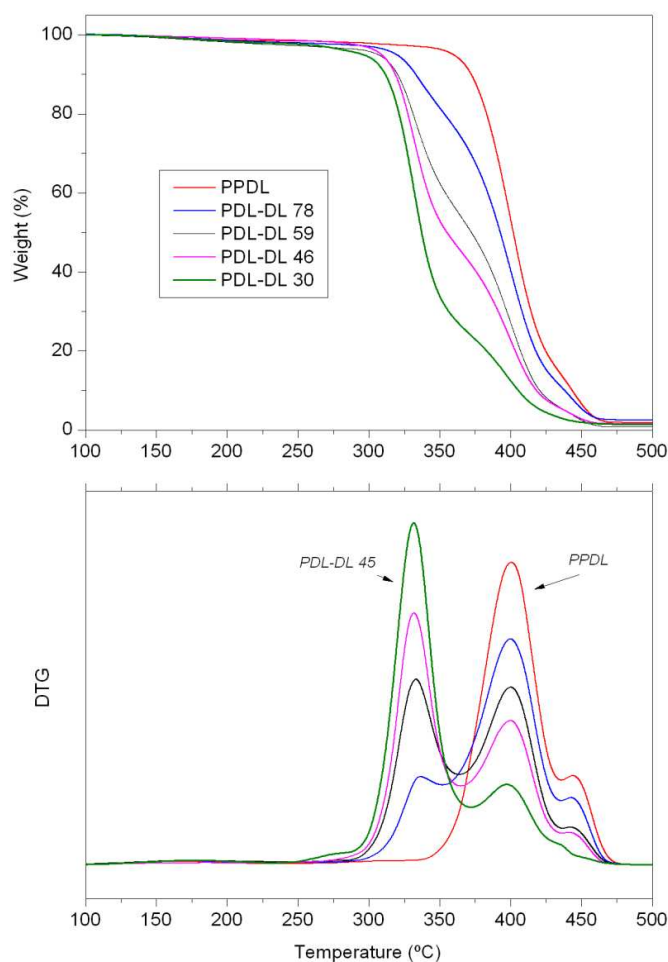


Figure 11. Thermogravimetric (TG) and differential thermogravimetric (DTG) curves of PPDL and the ω -PDL-co- ϵ -DL copolymers.

4.4. Conclusions

In this work several statistical copolymers based on ω -pentadecalactone and ϵ -decalactone were synthesized with triphenyl bismuth. Due to the low reactivity of the mix of monomers, long reactions times were necessary to obtain high molecular weights ($M_w > 99 \text{ kg mol}^{-1}$) and efficient overall yields ($> 74 \%$). The poly(ω -PDL-co- ϵ -DL)s showed a blocky distribution of sequences ($R < 0.49$) and were carefully characterized by NMR, GPC, DSC, WAXS and TGA measurements. In addition, their mechanical properties were tested at room temperature (21 °C) and at body temperature (37 °C),

whereas an *in vitro* degradation study was also carried out at 37 °C for 182 days. Despite their increased amorphous character (with a crystalline fraction of 13-38 % vs. 54 % for ω -pentadecalactone homopolymer), these biomaterials were found to be very resistant to hydrolytic degradation due to the steric effect of the ϵ -DL units. However, their (assumed) biocompatibility, upgraded thermal stability, rapid crystallization from melt, proper processing with thermoplastic techniques of these copolyesters and their attractive mechanical properties (are stable at 21 °C and at 37 °C in contrast to other polyesters of high T_g (i.e. polylactide) or of low T_m (< 65 °C) such as poly(ϵ -caprolactone), present lower values of secant modulus than poly(ϵ -caprolactone) and, therefore, a lower stiffness), make them very interesting substitutes for silicone or low density polyethylene.

References

- [1] de Geus, M., van der Meulen, I., Goderis, B., van Hecke, K., Doschu, M., van der Werff, H., Koning, C.E., Heise, A. Performance polymers from renewable monomers: high molecular weight poly(pentadecalactone) for fiber applications. *Polymer Chemistry* 2010, 1, 525-533.
- [2] Panten, J., Surburg, H., Hölscher. New Oxa-Bridged Macrocycles. *Chemical Biodiversity* 2008, 5, 1011-1022.
- [3] Skoglund, P., Fransson, A. Crystallization kinetics polytridecanolactone and polypentadecalactone. *Polymer* 1998, 39, 3143-3146.
- [4] Skoglund, P., Fransson, A. Thermophysical properties of polypentadecalactone. *Polymer* 1998, 39, 1899-1906.
- [5] Cai, J., Hsiao, B.S., Gross, R.A. Polypentadecalactone prepared by lipase catalysis: crystallization kinetics and morphology. *Polymer International* 2009, 58, 944-953.
- [6] Jiang, Z., Azim, H., Gross, R.A. Lipase-Catalyzed Copolymerization of ω -Pentadecalactone with p-dioxanone and Characterization of Copolymer Thermal and Crystalline Properties. *Biomacromolecules* 2007, 8, 2262-2269.
- [7] van der Meulen, I., de Geus, M., Antheunis, H., Deumens, R., Joosten, E.A.J., Koning, C.E., Heise, A. Polymers from Functional Macrolactones as Potential Biomaterials: Enzymatic Ring Opening Polymerization, Biodegradation and Biocompatibility. *Biomacromolecules* 2008, 9, 3404-3410.
- [8] Pepels, M.P.F.; Hanse, M.R.; Goossens, H.; Duchateau, R. From Polyethylene to Polyester: Influence of Ester Groups on the Physical Properties. *Macromolecules* 2013, 46, 7668-7677.
- [9] Focarete, M.L., Scandola, M., Kumar, A., Gross, R.A. Physical characterization of poly(ω -pentadecalactone) synthesized by lipase-catalyzed ring opening polymerization. *Journal of Polymer Science Part B: Polymer Physics* 2001, 39, 1721-1729.
- [10] Gazzano, M., Malta, V., Focarete, M.L., Scandola, M., Gross, R.A. Crystal structure of poly(ω -pentadecalactone). *Journal of Polymer Science Part B: Polymer Physics* 2003, 41, 1009-1013.
- [11] Bouyahyi, M., Duchateau, R. Metal-Based catalysts for Controlled Ring-Opening Polymerization of Macrolactones: High Molecular Weight and Well-Defined Copolymer Architectures. *Macromolecules* 2014, 47, 517-524.
- [12] Van der Mee, L., Helmich, F., de Bruijn, R., Vekemans, J.A.J.M., Palmans A.R.A., Meijer, E.W. Investigation of Lipase-Catalyzed Ring-Opening Polymerizations of Lactones with Various Ring Sizes: Kinetic Evaluation. *Macromolecules* 2006, 39, 5021-
- [13] Pascual, A., Leiza, J.R., Mecerreyes, D. Acid catalyzed polymerization of macrolactones in bulk and aqueous miniemulsion: Ring opening vs. condensation. *European Polymer Journal* 2013, 49, 1601-1609.
- [14] Pepels, M.P.F., Bouyahyi, M., Heise, A., Duchateau, R. Kinetic Investigation on the Catalytic Ring-Opening (Co)Polymerization of (Macro)Lactones Using Aluminium Salen Catalysts. *Macromolecules* 2013, 46, 4324-4334.
- [15] Wilson, J.A., Hopkins S.A., Wright, P.M., Dove, A.P. Synthesis of ω -Pentadecalactone Copolymers with Independently Tunable Thermal and Degradation Behavior. *Macromolecules* 2015, 48, 950-958.

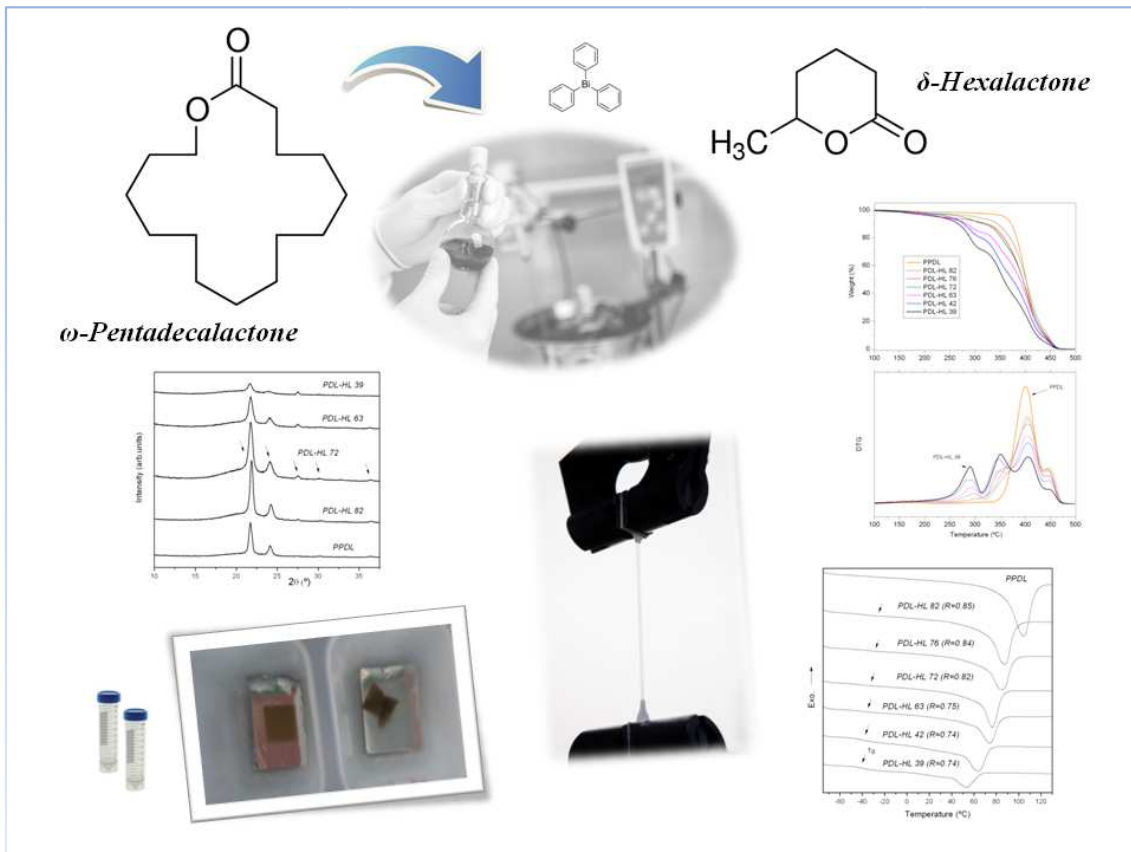
- [16] Bouyahyi, M., Pepels, M.P.F., Heise, A., Duchateau, R. ω -Pentadecalactone polymerization and ω -pentadecalactone/ ϵ -caprolactone copolymerization reactions using organic catalysts. *Macromolecules* 2012, 45, 3356-3366.
- [17] Lebedev, B., Yevstropov, A. Thermodynamic properties of polylactones. *Macromolecular Chemistry and Physics* 1984, 185, 1235-1253.
- [18] Zhong, Z., Dijkstra, P. J., Feijen, J. Controlled ring-opening polymerization of ω -pentadecalactone with yttrium isopropoxide as initiator. *Macromolecular Chemistry and Physics* 2000, 201, 1329-1333.
- [19] Nakayama, Y., Watanabe, N., Kusaba, K., Sasaki, K., Cai, Z., Shiono, T., Tsutsumi, C. High activity of rare earth tetrahydroborates for ring-opening polymerization of ω -pentadecalactone. *Journal of Applied Polymer Science* 2011, 121, 2098-2103.
- [20] Hori, Y., Hongo, H., Hagiwara, T. Ring-Opening Copolymerization of (R)- β -Butyrolactone with Macrolide: A New Series of Poly(Hydroxyalkanoate)s. *Macromolecules* 1999, 32, 3537-3539.
- [21] Slivniak, R., Domb, J. A. Macrolactones and polyesters from ricinoleic acid. *Biomacromolecules* 2005, 6, 1679-1688.
- [22] Duda, A., Kowalski, A., Penczek, S., Uyama, H., Kobayashi, S. Kinetics of the Ring-Opening Polymerization of 6-, 7-, 9-, 12-, 13-, 16-, and 17-Membered Lactones. Comparison of Chemical and Enzymatic Polymerizations. *Macromolecules* 2002, 35, 4266-4270.
- [23] Van der Meulen, I., Gubbels, E., Huijser, S., Sablong, R., Koning, C. E., Heise, A., Duchateau, R. Catalytic Ring-Opening Polymerization of Renewable Macrolactones to High Molecular Weight Polyethylene-like Polymers. *Macromolecules* 2011, 44, 4301-4305.
- [24] van der Meulen, I., Li, Y., Deumens, R., Joosten, E.A., Koning, C.E., Heise, A. Copolymers from unsaturated macrolactones: toward the design of cross-linked biodegradable polyesters. *Biomacromolecules* 2011, 12, 837-843.
- [25] Takwa, M., Simpson, N., Malmström, E., Hult, K., Martinelle, M. One-Pot Difunctionalization of Poly(ω -pentadecalactone) with Thiol-Thiol or Thiol-Acrylate Groups, Catalyzed by *Candida antarctica* Lipase B. *Macromolecular Rapid Communications* 2006, 27, 1932-1936.
- [26] Bisht, K. S., Henderson, L. A., Gross, R. A., Kaplan, D. L., Swift, G. Enzyme catalyzed ring-opening polymerization of ω -pentadecalactone. *Macromolecules* 1997, 30, 2705-2711.
- [27] Kumar, A., Kalra, B., Dekhterman, A., Gross, R.A. Efficient Ring-Opening Polymerization and Copolymerization of ϵ -Caprolactone and ω -Pentadecalactone Catalyzed by *Candida antartica* Lipase B. *Macromolecules* 2000, 33, 6303-6309.
- [28] Ceccorulli, G., Scandola, M., Kumar, A., Kalra, B., Gross, R.A. Cocrystallization of random copolymers of ω -pentadecalactone and ϵ -caprolactone synthesized by lipase catalysis. *Biomacromolecules* 2005, 6, 902-907.
- [29] Liu, J., Jiang, Z., Zhang, S., Liu, C., Gross, R.A., Kyriakides, T.R., Saltzman, W.M. Biodegradation, biocompatibility and drug delivery in poly(ω -pentadecalactone-co-p-dioxanone) copolyesters. *Biomaterials* 2011, 32, 6646-6654.
- [30] Focarete, M.L., Gazzano, M., Scandola, M., Kumar, A., Gross, R.A. Copolymers of ω -pentadecalactone and trimethylene carbonate from lipase catalysis: influence of microstructure on solid-state properties. *Macromolecules* 2002, 35, 8066-8071.

- [31] Kumar, A., Garg, K., Gross, R. A. Copolymerizations of ω -Pentadecalactone and Trimethylene Carbonate by Chemical and Lipase Catalysis. *Macromolecules* 2001, 34, 3527–3533.
- [32] Kalra, B., Kumar, A., Gross, R.A., Baiardo, M., Scandola, M. Chemoenzymatic synthesis of new brush copolymers comprising poly(ω -pentadecalactone) with unusual thermal and crystalline properties. *Macromolecules* 2004, 37,1243–50.
- [33] Focarete, M.L., Gazzano, M., Scandola, M., Gross, R.A. Polymers from Biocatalysis: Materials with a Broad Spectrum of Physical Properties. *Macromolecules* 2002, 35, 8066.
- [34] Mazzocchetti, L., Scandola, M., Jiang, Z. Enzymatic Synthesis and Structural and Thermal Properties of Poly(ω -pentadecalactone-co-butylene-co-succinate). *Macromolecules* 2009, 42, 7811–7819.
- [35] Mazzocchetti, L., Scandola, M., Jiang, Z. Random copolymerization with a large lactone enhances aliphatic polycarbonate crystallinity. *European Polymer Journal* 2012, 48, 1883–1891.
- [36] Pitt, C.G.; Graetzl, M.M.; Kimmel G.L.; Surles, J.; Schidler, A. Aliphatic polyesters II. The degradation of poly(DL-lactide), poly(epsilon-caprolactone), and their copolymers in vivo. *Biomaterials* 1981, 2, 215-220.
- [37] Glavas, L.; Olsén, P.; Odelius, K.; Albertsson A-C. Achieving Micelle Control through Core Crystallinity. *Biomacromolecules* 2013, 14, 4150-4156.
- [38] Schneiderman D.K.; Hill, E.M.; Martello, M.T.; Hillmyer, M.A. Poly(lactide)-block-poly(ϵ -decalactone)-block-poly(lactide) copolymer elastomers. *Polymer Chemistry* 2015, 6, 3641-3651.
- [39] Lin, J.O.; Chen, W.; Shen, Z.; Ling, J. Homo- and Block Copolymerization of ϵ -decalactone with L-lactide catalyzed by Lanthanum compounds. *Macromolecules* 2013, 46, 7769-7776.
- [40] Chuang, H. J.; Chen, H. L.; Huang, B. H.; Tsai, T. E.; Huang, P. L.; Liao, T. T.; Lin, C. C. Efficient zinc initiators supported by NNO-tridentate ketiminate ligands for cyclic esters polymerization. *Journal of Polymer Science, Part A: Polymer Chemistry* 2013, 51, 1185–1196.
- [41] Olsén, P., Borke, T., Odelius, K., Albertsson, A.C. ϵ -Decalactone: A Thermoresilient and Toughening Comonomer to Poly(L-lactide). *Biomacromolecules* 2013, 14, 2883-2890.
- [42] Jasinska-Walc, L., Hansen, M.R., Dudenko, D., Rozanski, A., Bouyahyi, M., Wagner, M., Graf, R., Duchateau, R. Topological behaviour mimicking ethylene-hexene copolymers using branched lactones and macrolactones. *Polymer Chemistry* 2014, 5, 3306-3310.
- [43] Jasinska-Walc, L.; Bouyahyi M.; Rozanski A.; Graf, R.; Hansen, M.R.; Duchateau, R. Synthetic Principles Determining Local Organization of Copolyesters Prepared from Lactones and Macrolactones. *Macromolecules* 2015, 48, 502-510.
- [44] Prestch, E., Clerc, T., Seibl, J., Simon, W. Tables of Spectral Data for Structure Determination of Organic Compounds. Chemical Laboratory Practice. Ed. Springer Science & Business Media 2013. Springer-Verlag Berlin Heidelberg GmbH.
- [45] Herbert, I.R. Statistical analysis of copolymer sequence distribution. In *NMR Spectroscopy of Polymers*. Ibbet, R.N. Ed.: Blackie Academic & Professional, London, 1993,50-79. (Chapter 2).
- [46] Fernández, J.; Larrañaga, A.; Etxeberria, A.; Sarasua, J.R. Effects of chain microstructures and derived crystallization capability on hydrolytic degradation of poly(L-lactide/ ϵ -caprolactone) copolymers. *Polymer Degradation and Stability* 2013, 98, 481-489.

- [47] Fernández, J.; Etxeberria, A.; Sarasua, J.R. In vitro degradation study of biopolyesters using poly(lactide/ δ -valerolactone) copolymers. *Polymer Degradation and Stability* 2015, 112, 104-116.
- [48] Skoglund, P., Fransson, A. Continuous cooling and isothermal crystallization of polycaprolactone. *Journal of Applied Polymer Science* 1996, 61, 2455-2465.
- [49] Fernández, J.; Etxeberria, A.; Sarasua, J.R. Crystallization and melting behavior of poly(ϵ -caprolactone-co- δ -valerolactone) and poly(ϵ -caprolactone-co-L-lactide) copolymers with novel chain microstructures. *Journal of Applied Polymer Science* 2015, 132, 42534.
- [50] Scherrer, P. Bestimmung der Grosse und der inneren Struktur von Kolloidteilchen mittels Röntgenstrahlen. *Nachr Ges Wiss Gottingen*, 26, pp. 98-100, 1918.
- [51] Williams, S.F., Martin, D.P. Application of PHAs in medicine and pharmacy. *Biopolymers* 2002, 4, 91-127.
- [52] Larrañaga, A., Fernandez, J., Vega, A., Etxeberria, A., Ronchel, C., Adrio, J.L., Sarasua, J.R. Crystallization and its effect on the mechanical properties of a medium chain length polyhydroxyalkanoate. *Journal of the Mechanical Behaviour of Biomedical Materials* 2014, 39, 87-94.
- [53] Fernandez, J., Etxeberria A., Sarasua, J.R. In vitro degradation studies and mechanical behavior of poly(ϵ -caprolactone-co- δ -valerolactone) and poly(ϵ -caprolactone-co-L-lactide) with random and semi-alternating chain microstructures. *European Polymer Journal* 2015, 71, 585-595.
- [54] Fernández, J.; Larrañaga, A.; Etxeberria, A.; Sarasua, J.R. Tensile behavior and dynamic mechanical analysis of novel poly(lactide/ δ -valerolactone) statistical copolymers. *Journal of the Mechanical Behaviour of Biomedical Materials* 2014, 35, 39-50.
- [55] Fernandez, J.; Etxeberria, A.; Sarasua, J.R. Effects of repeat unit sequence distribution and residual catalyst on thermal degradation of poly(L-lactide/ ϵ -caprolactone) statistical copolymers. *Polymer Degradation and Stability* 2013, 98, 1293-1299

**Chapter 5. Synthesis and Properties of ω -
Pentadecalactone-co- δ -Hexalactone
copolymers: A Biodegradable thermoplastic
elastomer as an Alternative to Poly(ϵ -
Caprolactone)**

RSC Advances 2016, 6, 3137-3149.



Abstract

The copolymerization of ω -pentadecalactone with the little-known δ -hexalactone, a cyclic ester with identical structure to δ -valerolactone but possessing a methyl pendant group, creates a new kind of low glass transition polyester that shows improved biodegradability in comparison to poly(ϵ -caprolactone) (PCL). The poly(ω -PDL-co- δ -HL), with ω -PDL molar contents ranging from 39 to 82 %, were synthesized using triphenyl bismuth as catalyst and presented a chain microstructure that deviated slightly from a random distribution ($R > 0.74$) while WAXS measurements proved that only the ω -PDL blocks were able to crystallize. Therefore, the incorporation of δ -HL decreased the crystalline fraction of the poly(ω -pentadecalactone) to 21-44 % and the T_m s of the copolymers shifted from 104 °C to temperatures between 53 and 88 °C. On the other hand, the low glass transition temperatures (< -36 °C) of these thermoplastic elastomers allow a rapid crystallization from melt, which prevents physical aging during their storage or application. The degradation rates obtained for the poly(ω -PDL-co- δ -HL), after carrying out *in vitro* degradation studies in phosphate buffer solution (at 37 °C for 182 days), ranged from 0.0013 to 0.0019 days⁻¹. Thermogravimetric analysis also demonstrated their great thermal stability, since they were completely degraded at temperatures close to 500 °C. These ω -PDL-co- δ -HL copolymers displayed tunable mechanical properties, adjusted according to their composition, with lower elastic modulus values than PCL and a mechanical performance that was quite steady at both room temperature (21 °C) and body temperature (37 °C).

5.1. Introduction

Nowadays, one of the challenges of polymer chemistry is synthesizing biodegradable materials with the same properties as petroleum based polymers. Since the 1980s, an important research work has been focused on aliphatic polyesters while the ring-opening polymerization (ROP) of lactones and macrolactones [1-10] has been proven as a useful approach in obtaining copolyesters with tuned topology and microstructure. However, the polyesters most often employed in medical science either display a glassy mechanical behaviour with high elastic modulus and rather low elongation at break values, owing to their high glass transition (T_g) and melting temperatures (T_m) (i.e. polylactide (PLA) or polyglycolide (PGA) [11]), or show an optimal combination of properties but biodegrade at a very slow rate, as is the case of poly(ϵ -caprolactone) (PCL) [12-13] and the polyethylene-like polymacrolactones [14-15]. These materials are, therefore, clearly inappropriate for numerous clinical uses, where highly elastomeric biodegradable materials are required.

The copolymerization of lactide or glycolide with a complementing monomer that reduces the crystallinity and the melting point is a good strategy to enhance the flexibility and ductility of PLA and PGA, as long as the glass transition of these new materials is kept above room temperature. However, some of the ϵ -caprolactone, δ -valerolactone, ϵ -decalactone, trimethylene carbonate or p-dioxanone [16-33] based copolymers frequently suffer from supramolecular rearrangements in their chains, associated with the development of lactide/glycolide crystalline domains, which cause undesirable changes in their properties during storage or biodegradation. Moreover, these lactide or glycolide-rich copolymers usually do not exhibit a suitable mechanical performance at both room temperature (21 °C) and at human body temperature (37 °C) because their mechanical properties are not stable at temperatures above T_g .

On the contrary, linear copolymers with a relatively low concentration of ester groups show low glass transition ($< - 25$ °C) and melting temperatures (< 100 °C), thereby ensuring a very efficient processing with thermoplastic techniques. Likewise, these

polyesters present high thermal stability and a rapid crystallization from melt, which prevent physical aging. Another important feature of these low T_g copolymers is their attractive mechanical behaviour, with high elongation at break values and elastic modulus below 400 MPa. Hence, the synthesis of poly(ϵ -caprolactone)-like biomaterials with an improved biodegradability is extremely interesting and could meet the requirements for a large number of potential applications in the biomedical field. However, it should also be taken into consideration that the T_m of these polymers should be above human body temperature in order to guarantee their mechanical performance during use. In addition, if possible, this T_m value should preferably be higher than 60-65 °C, the T_m of PCL, so as to assure more stable mechanical properties. The mechanical behaviour of the copolymers with low T_g is heavily dependent on the crystalline phase (on their T_m and melting enthalpies), especially at temperatures close to their melting points. Therefore, with the incorporation of another monomer, the ϵ -caprolactone-rich copolymers [34-35] present lower T_m and melting enthalpies and as a result exhibit lower stress related properties at 37 °C than at 21 °C [34].

ω -Pentadecalactone, whose homopolymer is highly crystalline and melts at around 100 °C [36], has been copolymerized with numerous monomers. Thus, several ω -PDL-containing copolyesters including poly(ω -pentadecalactone-co- ϵ -caprolactone), poly(ω -pentadecalactone-co-p-dioxanone), poly(ω -pentadecalactone-co- δ -valerolactone) and poly(ω -pentadecalactone-co-trimethylene carbonate) have been proposed as alternative bioresorbable materials [37-47]. However, in most of these cases both comonomers cocrystallize. Only, in the case of poly(ω -pentadecalactone-co- ϵ -decalactone) [48-50] was the crystalline fraction reduced, owing to the racemic stereochemistry of the butyl side chain of this decalactone. Nevertheless, the latter materials were found to be very resistant to hydrolytic degradation because of their blocky distribution of sequences and the steric effect of the ϵ -DL units [50]. Therefore, in this paper δ -hexalactone [51-54], a six-membered lactone with identical structure to δ -valerolactone but possessing a methyl pendant group (also known as δ -caprolactone and found in heated milk fat), was employed in place of ϵ -DL with the aim of lowering the steric effect of the ϵ -DL and at the same time increasing the hydrophilicity of the copolymers.

The poly(ω -pentadecalactone-co- δ -hexalactone) of this study were synthesized using triphenyl bismuth (Ph_3Bi) [55] as catalyst and characterized using proton and carbon nuclear magnetic resonance spectroscopy (^1H and ^{13}C NMR), gel permeation chromatography (GPC) measurements and thermogravimetric analysis (TGA). Their crystallization and melting behaviour was studied by means of differential scanning calorimetry (DSC) and Wide Angle X-ray diffraction (WAXRD). In addition, films of the ω -PDL-co- δ -HL copolymers with ω -PDL molar contents ranging from 39 to 82 % were prepared for mechanical testing at room temperature (21 °C) and at 37 °C, the working temperatures of these biomaterials. Finally, an *in vitro* hydrolytic degradation study was also carried out at 37 °C for a period up to 26 weeks in phosphate buffer solution (PBS). Thus, the changes in water absorption, weight loss, macroscopic morphology, crystallinity, phase structure, molecular weight and mechanical properties of the copolymers were monitored.

5.2. Materials and Methods

Materials

δ -hexalactone monomer (assay > 98 %) was provided by Sigma Aldrich (W316709). ω -pentadecalactone monomer (assay > 98 %) was also supplied by Sigma Aldrich (W284009). The triphenyl bismuth (Ph_3Bi) catalyst was obtained from Gelest. Phosphate buffer solution (PBS) (pH 7.2) was obtained from Fluka Analytical (Sigma Aldrich). For proper evaluation of the behaviour of the ω -PDL-co- δ -HL copolymers, a poly(ω -pentadecalactone) (PPDL) homopolymer, synthesized in a previous work [50], was also employed. This material had a M_w of 365 kg mol⁻¹ with a dispersity of 1.98.

Synthesis procedure

Statistical copolymers from ω -pentadecalactone and δ -hexalactone at different compositions were synthesized in bulk by one pot-one-step ring-opening polymerizations (ROP). The synthesis reactions were conducted in a flask immersed in a controlled temperature oil bath. In each polymerization, predetermined amounts of the

different comonomers at the chosen mass feed ratio were simultaneously added and melted into the flask. The flask was purged for 30 minutes with a nitrogen stream under the surface of the melt. The catalyst (Ph_3Bi) was then added (at 100:1 comonomers/catalyst molar ratio) and the magnetic stirrer maintained at 100 rpm. No initiator compound was added to the reaction mix so the catalyst was activated by the ROH provided by the monomers (H_2O and impurities). The ω -pentadecalactone-co- δ -hexalactone polymerizations were carried out at 130 °C over 6 days. Long reaction times were necessary to obtain substantial yields due to the low reactivity of the mixture of monomers. Moreover, at lower reaction temperatures or when less PH_3Bi was added the efficiency of the process decreased and products with low molecular mass were obtained.

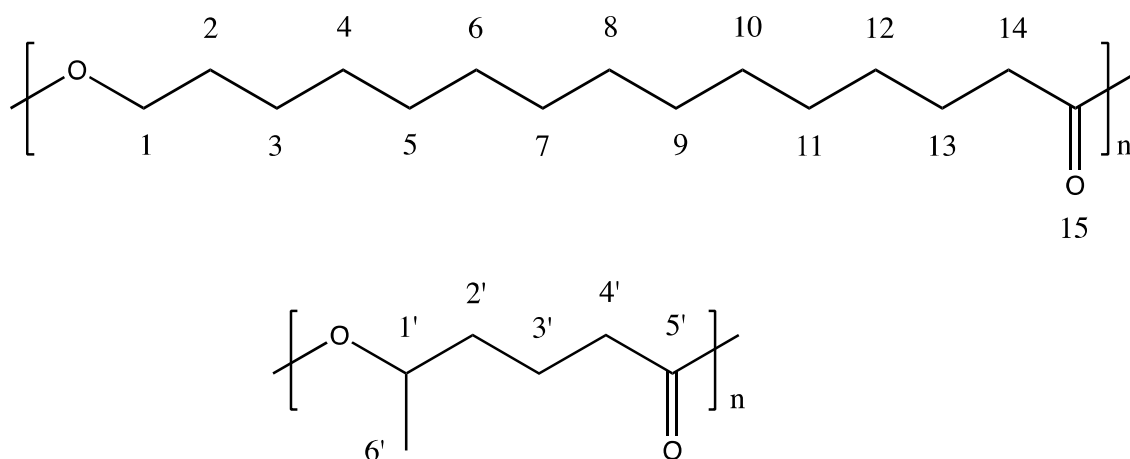


Figure 1. Scheme of the units of ω -pentadecalactone (above) and δ -hexalactone (below).

After the corresponding period of reaction time the product was dissolved in chloroform and precipitated, pouring the polymer solution into an excess of methanol in order to remove the catalyst impurities and those monomers that had not reacted. Finally the product was dried at room temperature and then subjected to a heat treatment at 140 °C for 1 hour to ensure the complete elimination of any remaining solvent. The polymer sample then weighed, obtaining the yield of the synthesis process which is shown in Table 1.

Methods

Proton and carbon nuclear magnetic resonance (^1H and ^{13}C NMR) spectra were recorded in a Bruker Avance DPX 300 at 300.16 MHz and at 75.5 MHz of resonance frequency respectively, using 5 mm O.D. sample tubes. All spectra were obtained at room temperature from solutions of 0.7 mL of deuterated chloroform (CDCl_3). Experimental conditions were as follows: a) for ^1H NMR: 10 mg of sample; 3 s acquisition time; 1 s delay time; 8.5 μs pulse; spectral width 5000 Hz and 32 scans; b) for ^{13}C NMR: 40 mg, inverse gated decoupled sequence; 3 s acquisition time; 4 s delay time; 5.5 μs pulse; spectral width 18800 Hz and more than 10000 scans. The assignment of the different signals was made employing the tables of structural determination devised by Prestch et al. [56]. The copolymer composition data, average sequence lengths and randomness character in Table 1 were calculated by averaging the values of molar contents and the PDL-HL dyad relative molar fractions that were obtained by means of ^1H and ^{13}C NMR spectroscopy. Equations 1-3 [57] were employed to obtain the number-average sequence lengths (l_i), the Bernoullian random number-average sequence lengths (l_i) and the randomness character (R):

$$l_{\text{PDL}} = \frac{(\text{PDL} - \text{PDL}) + \frac{1}{2}(\text{PDL} - \text{HL})}{\frac{1}{2}(\text{PDL} - \text{HL})} = \frac{2(\text{PDL})}{(\text{PDL} - \text{HL})} ; \quad (1)$$

$$l_{\text{HL}} = \frac{(\text{HL} - \text{HL}) + \frac{1}{2}(\text{PDL} - \text{HL})}{\frac{1}{2}(\text{PDL} - \text{HL})} = \frac{2(\text{HL})}{(\text{PDL} - \text{HL})}$$

$$(l_{\text{HL}})_{\text{random}} = \frac{1}{(\text{PDL})} ; \quad (l_{\text{PDL}})_{\text{random}} = \frac{1}{(\text{HL})} \quad (2)$$

$$R = \frac{(l_{\text{HL}})_{\text{random}}}{l_{\text{HL}}} = \frac{(l_{\text{PDL}})_{\text{random}}}{l_{\text{PDL}}} \quad (3)$$

where (HL) and (PDL) are the δ -hexalactone and ω -pentadecalactone molar fractions and (PDL-HL) is the PDL-HL average dyad relative molar fraction.

200-300 μm films were prepared by pressure melting at 200 $^{\circ}\text{C}$ followed by water quenching. These were then stored for 24 hours in a fridge (at 0-5 $^{\circ}\text{C}$), the typical storage temperature for biopolymers. From these films repetitive square samples for the *in vitro* degradation study (1x1 cm^2) and repetitive samples for mechanical characterization (10x1 cm^2) were obtained. The specimens for mechanical testing at 37 $^{\circ}\text{C}$ were stored for another 24 hours at 37 $^{\circ}\text{C}$ before tests were conducted at this temperature. In addition, DSC scans were made at 20 $^{\circ}\text{C min}^{-1}$ for each polymer sample before mechanical testing, in order to monitor the thermal properties of the specimens.

The mechanical properties were determined by tensile tests with an Instron 5565 testing machine at a crosshead displacement rate of 10 mm min^{-1} . These tests were performed at room temperature (21 \pm 2 $^{\circ}\text{C}$) and at human body temperature (37 $^{\circ}\text{C}$) following ISO 527-3/1995. The specimens had the following dimensions: overall length = 100 mm, distance between marks = 50 mm, width = 10 mm; and were cut from 200-300 μm thick films. The mechanical properties reported (secant modulus at 2 %, yield strength, ultimate tensile strength and elongation at break) correspond to average values of at least 5 determinations. Mechanical testing at 37 $^{\circ}\text{C}$ was conducted in an Instron controlled temperature chamber. The tests were stopped at 300 % of strain due to the size limitations of the temperature chamber.

For the *in vitro* degradation study, square samples (25-35 mg (W_0) ($n = 3$)) of the different copolymers were placed in Falcon tubes containing phosphate buffer solution (PBS) (pH = 7.2) maintaining a surface area to volume ratio equal to 0.1 cm^{-1} . The samples were stored in an oven at 37 $^{\circ}\text{C}$. Three samples of each polymer were removed at different times from the PBS and weighed wet (W_w) immediately after wiping the surface with filter paper to absorb the surface water. These samples were air-dried overnight at 37 $^{\circ}\text{C}$. Then they were weighed again to obtain the dry weight (W_d). Water absorption (% WA) and remaining weight (% RW) were calculated according to Eqs. (4) and (5). At the end of the degradation study (182 days) the mechanical properties of the poly(ω -pentadecalactone-co- δ -hexalactone) were also measured at 37 $^{\circ}\text{C}$.

$$\% \text{WA} = \frac{W_w - W_d}{W_d} \cdot 100 \quad (4)$$

$$\%RW = \frac{W_d}{W_0} \cdot 100 \quad (5)$$

In order to compare the degradation rate of the studied copolymers, the exponential relationship between molecular weight and degradation time for biodegradable polyesters degrading under bulk degradation was used [58-59]:

$$\ln M_w = \ln M_{w0} - K_{Mw} \cdot t \quad (6)$$

$$t_{1/2} = 1/K_{Mw} * \ln 2 \quad (7)$$

where M_w is the weight-averaged molecular weight, M_{w0} is the initial weight-averaged molecular weight, K_{Mw} is the apparent degradation rate and $t_{1/2}$ is the half degradation time (the amount of time required to fall to half the initial value of molecular weight).

The molecular weights of the polymers were determined by GPC using a Waters 1515 GPC device equipped with two Styragel columns ($10^2 - 10^4 \text{ \AA}$). Chloroform was used as eluent at a flow rate of 1 mL min^{-1} and polystyrene standards (Shodex Standards, SM-105) were used to obtain a primary calibration curve. The samples were prepared at a concentration of 10 mg in 1.5 mL. The reported values are likely to be higher than the actual molecular weights owing to the differences in hydrodynamic volume of the copolymers and polystyrene.

The thermal properties of the polymers were studied on a DSC 2920 (TA Instruments). Samples of 6-9 mg were melted at $140 \text{ }^\circ\text{C}$ and then quenched to $5 \text{ }^\circ\text{C}$ at different cooling rates ($5, 10$ and $20 \text{ }^\circ\text{C min}^{-1}$) to study the crystallization process during the cooling. Finally, a scan was also made at $20 \text{ }^\circ\text{C min}^{-1}$ from -85 to $140 \text{ }^\circ\text{C}$ to determine the glass transition temperature (T_g), the melting temperature (T_m) and the heat of fusion or melting enthalpy per gram (ΔH_m) of the samples. During the *in vitro* degradation study, the DSC samples were heated from $21 \text{ }^\circ\text{C}$ to $140 \text{ }^\circ\text{C}$ at $20 \text{ }^\circ\text{C min}^{-1}$, immediately after the drying at $37 \text{ }^\circ\text{C}$ of the polymer samples removed from the degradation medium. After this first scan, the samples were quenched in the DSC and a second scan was made from $-85 \text{ }^\circ\text{C}$ to $140 \text{ }^\circ\text{C}$ at $20 \text{ }^\circ\text{C min}^{-1}$.

Wide angle X-ray diffraction (WAXRD) data were collected on a Bruker D8 Advance diffractometer operating at 30 kV and 20 mA. This device is equipped with a Cu tube ($\lambda = 1.5418 \text{ \AA}$), a Vantec-1 PSD detector and an Anton Parr HTK2000 high-temperature furnace. The powder patterns were recorded in 2θ steps of 0.033° in the $10 \leq 2\theta \leq 38$ range, counting for 0.2 s per step, from 30 to 120 °C every 2 °C using a heating rate of $0.16 \text{ }^\circ\text{C s}^{-1}$. The degree of crystallinity (X_c) was determined as the ratio of the crystalline peak areas to the total area under the scattering curve, while the average crystal size was obtained employing the Scherrer equation [60] with a shape factor “k” of 0.90. The latter data were calculated from the two most intense peaks in the diffraction pattern: at $2\theta = 21.7^\circ$ and at $2\theta = 24.1^\circ$. On the other hand, the melting temperatures (T_m s) estimated are the temperatures until the crystalline phase became stable.

Thermal degradation was studied under nitrogen by means of thermogravimetric analysis (TGA) into a TGA model Q50-0545 (TA Instruments). Samples of 10-15 mg were heated from room temperature to 500 °C at a heating rate (β) of $5 \text{ }^\circ\text{C min}^{-1}$, with the heat flow, sample temperature, residual sample weight and its time derivative being continuously recorded. In this temperature range, the polymers degraded completely.

5.3. Results and Discussion

Synthesis characterization

Table 1 summarizes the characterization data of several poly(ω -PDL-co- δ -HL) with different composition synthesized at 130 °C for 6 days with a monomers/catalyst molar ratio (M/C) of 100. As can be observed, the molecular weights of the copolymers increase proportionally with the ω -PDL content, ranging from 62 to 249 kg mol^{-1} , while their dispersity values (D) are in the range of 1.77 to 2.03. The ω -PDL molar content in this set of copolymers ranges from $\sim 39 \%$ (PDL-HL 39) to 82 % (PDL-HL 82) with average sequence lengths of ω -PDL (l_{PDL}) from 2.22 to 6.67. The consequence of the different reactivity of the comonomers is that the synthesis reactions led to gradient

copolymers with a slightly random distribution of sequences ($R \rightarrow 1$). The randomness character (R) value is, in all cases, higher than 0.74 while the copolymers richer in ω -PDL showed a more random distribution of sequences ($R > 0.82$).

Table 1. Characterization data of the ω -PDL-co- δ -HL copolymers of different compositions synthesized at 130 °C with a monomers/catalyst molar ratio of 100.

Sample	Feed Molar Composition		Composition ¹ (% molar)		Yield (%)	Conversion (%)		M _w (kg mol ⁻¹)	D	Microstructural Magnitudes ²		
	%PDL	%HL	%PDL	%HL		PDL	HL			<i>I</i> _{PDL}	<i>I</i> _{HL}	<i>R</i>
PDL-HL 82	72.9	27.1	82.4	17.6	74.9	80.0	46.0	249.2	2.03	6.67	1.42	0.85
PDL-HL 76	65.5	34.5	75.8	24.2	65.4	71.0	43.0	180.1	1.91	4.91	1.57	0.84
PDL-HL 72	58.8	41.2	71.6	28.4	76.0	85.3	48.2	156.7	1.82	4.30	1.71	0.82
PDL-HL 63	50.2	49.8	62.6	37.4	67.4	77.2	46.5	103.9	1.79	3.58	2.14	0.75
PDL-HL 42	36.7	63.3	42.2	57.8	57.0	62.8	49.9	83.5	1.77	2.36	3.22	0.74
PDL-HL 39	28.0	72.0	38.7	61.3	48.9	62.0	38.2	62.0	1.81	2.22	3.51	0.74

¹ Calculated averaging the copolymer molar compositions obtained by ¹H and ¹³C NMR

² *I*_{PDL} and *I*_{HL} are the PDL and HL number average sequence lengths of the ω -PDL-co- δ -HL copolymers obtained from the average dyad relative molar fraction (PDL-HL) in ¹³C NMR. These values are compared to the Bernoullian random number-average sequence lengths obtaining the randomness character value (*R*) of the different copolymers.

As can be seen in Table 1, the conversion of ω -PDL was higher than that of δ -HL in all polymerizations. Therefore, higher yield of reactions and molecular weights were obtained when the feed was richer in ω -PDL. For example, PDL-HL 39, the copolymer with the lowest content of ω -PDL, only 38 % of δ -HL became a part of the copolymer after the synthesis reaction and the molar content of this unit failed to reach to 61 % (when the feed composition had a 72 % molar content of this monomer). The initiating species formed by means of the activation of the catalyst with ROH (H₂O or impurities provided by the monomers or the catalyst) may prefer the incorporation of ω -PDL rather than δ -HL units. Thus, the consumption of ω -PDL was faster than that of δ -HL owing to the low reactivity of the latter. This is different from what was observed in the study of the ω -pentadecalactone-co- ϵ -decalactone copolymers. In accordance with our own results [50] and the reports of Jasinska-Walc and Duchateau [48-49], the reactivity of ϵ -DL was higher than that of ω -PDL leading to a blockier distribution of sequences ($R < 0.49$). Thermodynamic polymerizability has been shown to increase along with the

ring size in the cyclic small-medium lactones [61]. So, it may be possible that the smaller ring strain of δ -HL (six-membered ring) when compared to ϵ -DL (seven-membered ring) explains the contrasting reactivity of these two lactones in presence of ω -PDL, whose polymerization route is, in contrast, mainly entropically driven [62].

NMR Characterization

Figures 2 and 3 present the ^1H and ^{13}C NMR spectra of the ω -pentadecalactone-co- δ -hexalactone copolymer with 63 % of ω -PDL (PDL-HL 63).

In the ^1H NMR spectrum, the calculus of the molar composition was made based on the signals of the ω -PDL methylene bonded to the ester group, which appears centered at 4.09 ppm, with regard to the δ -HL methine at around 4.95 ppm. The rest of the peaks (see scheme in Figure 1) are assigned to the other hydrogens of the copolymer in Table 2, although some signals appear overlapped.

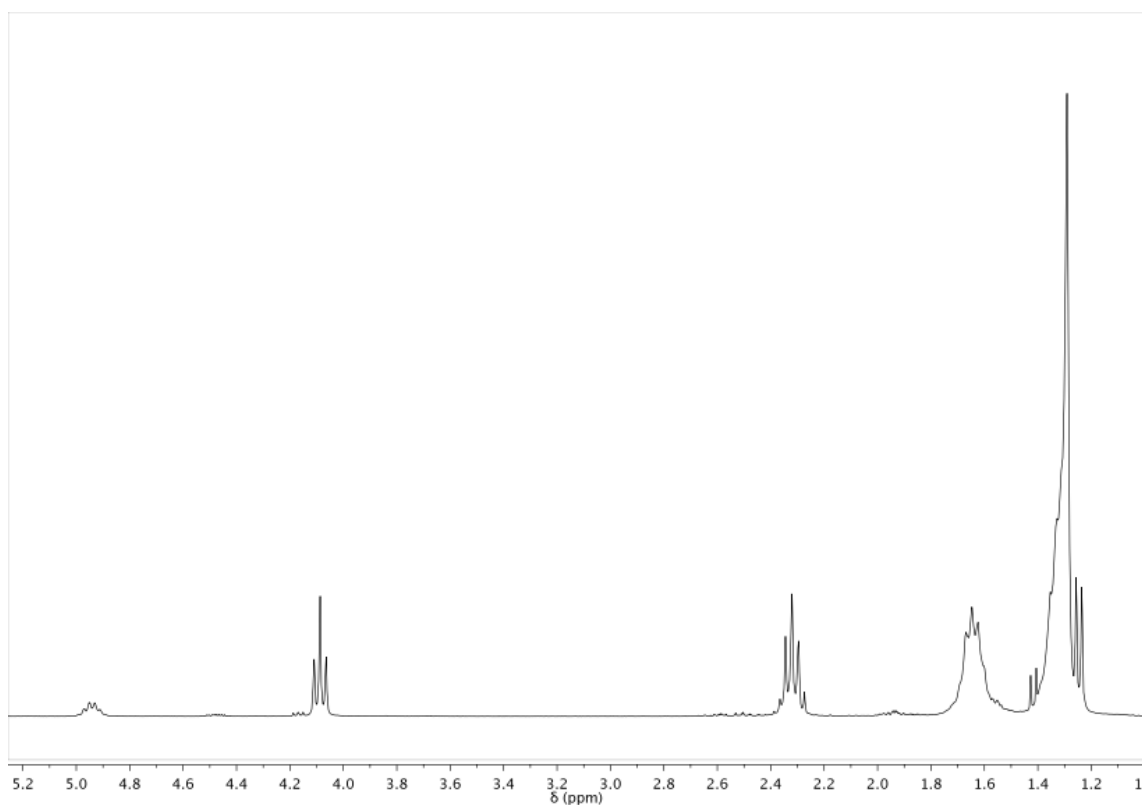


Figure 2. ^1H NMR spectrum of PDL-HL 63.

Table 2. Assignment of the different signals to the hydrogens of the ω -PDL-co- δ -HL.

Number of C	H	H
	ω -PDL	δ -HL
	δ (ppm)	δ (ppm)
1	4.09	4.95
2	1.65	1.65
3	1.29	1.29
4		2.32
5		-
6		1.22
7		
8		
9		
10		
11		
12		
13	1.65	
14	2.32	
15	-	

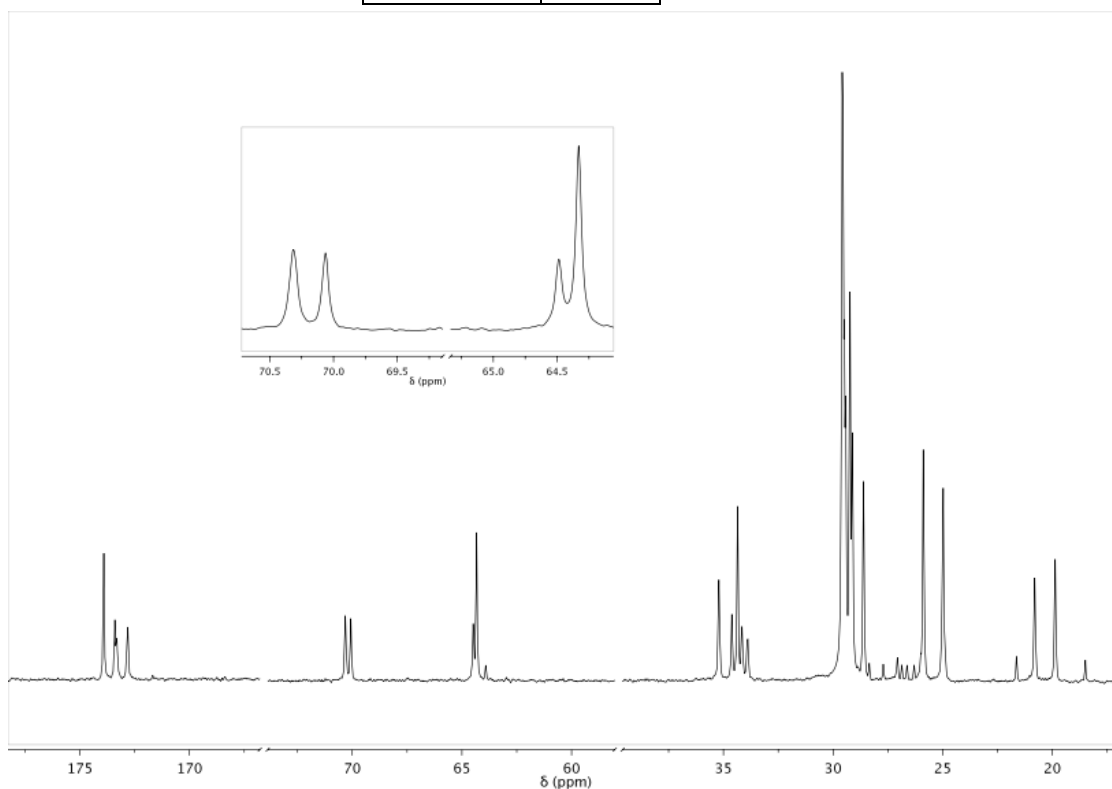
**Figure 3.** ^{13}C NMR spectrum of PDL-HL 63. The region enlarged shows the signals of the ω -PDL methylene bonded to the ester group (carbon 1) and the δ -HL methine (carbon 1'), respectively.

Table 3. Assignment of the different signals to the carbons of the ω -PDL-co- δ -HL.

Number of C	C ω -PDL	C δ -HL
	δ (ppm)	δ (ppm)
1	64.34 PDL-PDL 64.50 <u>PDL</u> -HL	70.07 <u>HL</u> -PDL 70.31 HL-HL
2	28.6-29.6	35.19
3	25.90	20.79
4	28.6-29.6	33.90-34.62
5		172.82 HL-HL 172.85 <u>HL</u> -PDL
6		19.86
7		
8		
9		
10		
11		
12		
13	24.98	
14	34.36	
15	173.32 <u>PDL</u> -HL 173.36 <u>PDL</u> -HL 173.42 <u>PDL</u> -HL 173.93 PDL-PDL	

Figure 3 shows the ^{13}C NMR spectrum of the ω -PDL-co- δ -HL copolymer. The different signals appearing between 19 and 175 ppm of chemical shift (δ) are assigned in Table 3 to the different carbons numbered in Figure 1. Hence, the molar composition of these copolymers can be easily determined by comparing the areas under the peaks due to the ω -PDL and δ -HL carbons. On the other hand, the signals of the ^{13}C NMR spectrum at 172.8 and at 173.5 ppm, which belong to the carbonyl carbons of the δ -hexalactone and ω -pentadecalactone units respectively, show sequence sensitivity. The peak at 172.83 split into two shoulders that can be assigned to the HL-HL and HL-PDL dyads (underlining is used to emphasize that the analysed nuclei belong to that unit). Furthermore, the PDL-PDL dyad appears at 173.93 ppm whereas the signals found at 173.36 ppm are related to the PDL-HL dyad. However, the carbonyl peaks were not well-resolved and it is a better idea to calculate the dyad relative molar fractions from

another region, in which the four PDL-HL dyads are clearly distinguishable. The signals from the region enlarged in Figure 3 and centered at 64.40 and 70.25 ppm, can be assigned to the ω -PDL methylene bonded to the ester group (carbon **1**) and the δ -HL methine (carbon **1'**), respectively. The HL-HL and HL-PDL dyads, along with the PDL-HL and PDL-PDL dyads, appear from left to right at 70.31 and 70.07 ppm, and at the peak at 64.40 ppm, at around 64.50 and 64.34 ppm.

Thermal properties

In this section the crystallization and melting behaviour of the copolymers in Table 1 were studied. First of all, several cooling treatments at different rates (5, 10 and 20 °C min⁻¹) were conducted in the DSC. The crystallization temperatures (T_c) and the enthalpy of crystallization (ΔH_c) of each material are shown in Table 4.

Table 4. Crystallization enthalpies and temperatures obtained for the ω -PDL-co-HL copolymers at cooling rates in the 5 - 20 °C min⁻¹ range.

Sample	5 °C min ⁻¹		10 °C min ⁻¹		20 °C min ⁻¹	
	ΔH (J g ⁻¹)	T_c (°C)	ΔH (J g ⁻¹)	T_c (°C)	ΔH (J g ⁻¹)	T_c (°C)
PPDL	129.2	76.0	127.5	72.2	123.8	63.2
PDL-HL 82	100.3	64.6	95.5	61.1	86.3	55.7
PDL-HL 76	87.0	62.7	85.5	58.8	76.9	52.7
PDL-HL 72	81.0	56.4	77.9	53.6	71.4	49.1
PDL-HL 63	67.3	52.7	66.4	49.6	64.8	45.0
PDL-HL 42	55.0	47.0	53.6	43.3	51.1	38.3
PDL-HL 39	39.5	34.7	38.4	31.3	35.8	28.3

As can be seen in Table 4, the differences between the respective ΔH_c from the same polymer were small (particularly for those with higher contents of δ -HL), although it was noted that at the slowest cooling rate, the ΔH_c was slightly larger than those corresponding to the other cooling treatments. Therefore, it can be stated that the ω -PDL chains crystallized from the melt very fast and the ΔH_c of the PPDL homopolymer and their copolymers were almost independent of the cooling rate. Likewise, the crystallization peaks of each polymer appeared at a higher temperature as the cooling

rate decreased. This is due to the fact that at lower cooling rates the crystal nuclei have more time to develop.

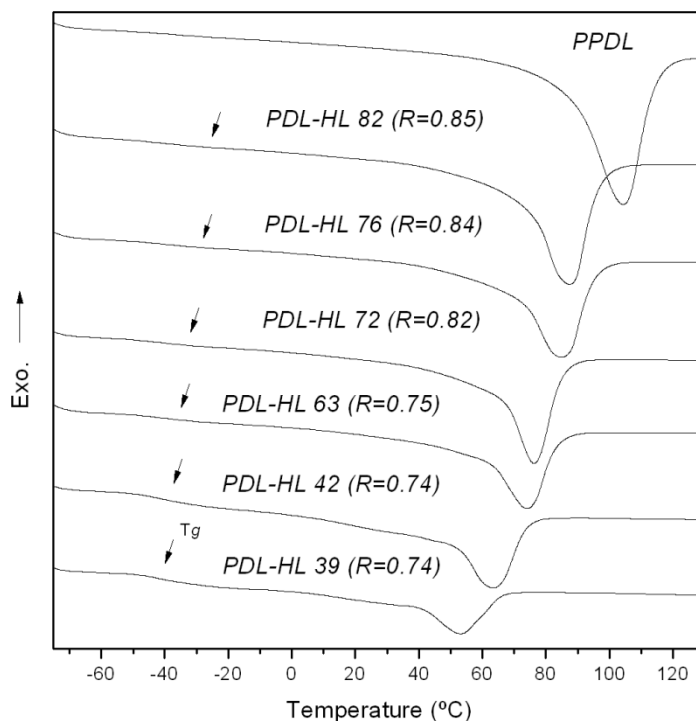


Figure 4. DSC heating curves at 20 °C min⁻¹ from -85 to 140 °C of the different ω-PDL-co-δ-HL copolymers.

Table 5. Calorimetric and X-ray Diffraction data of the ω-PDL-co-δ-HL copolymers.

Sample	l_{PDL}	T_m^1	X_c	$c.s$	ΔH_m	T_m^2	T_g	ΔC_p
		°C	(%)	nm	J g ⁻¹	°C	°C	J g ⁻¹ °C ⁻¹
PPDL	-	104.0	53.8	27	136.1	104.3	-35.6	0.16
PDL-HL 82	6.67	78.0	41.1	24	107.1	87.5	-38.6	0.19
PDL-HL 76	4.91	76.0	44.1	19	101.2	85.0	-37.4	0.21
PDL-HL 72	4.30	70.0	38.4	17	94.8	76.3	-40.2	0.27
PDL-HL 63	3.58	65.0	35.7	17	84.5	74.1	-42.5	0.28
PDL-HL 42	2.36	59.0	27.6	12	68.9	63.2	-41.8	0.45
PDL-HL 39	2.22	50.0	21.1	17	51.2	53.1	-42.5	0.48

¹ Obtained by WAXS. This is the crystalline phase-stable temperature..

² Obtained from a DSC at 20 °C min⁻¹ from -85 to 140 °C.

The DSC heating curves obtained after the cooling treatments were virtually identical for each polymer, all of them having practically the same melting temperatures and enthalpies (T_m and ΔH_m) after the cooling process. Figure 4 shows the DSC curves of scans made from -85 to 140 °C at 20 °C min⁻¹ while the data obtained from them (the glass transition temperature (T_g) with its associated heat capacity (ΔC_p) and the melting enthalpies and temperatures) are summarized in Table 5 along with the T_m , the crystal fraction (χ_c) and the average crystal size (c.s.) from Wide Angle X-ray Scattering (WAXS).

As can be noted, the PPDL homopolymer and the ω -PDL rich copolymers showed broader melting peaks and higher crystallization capability in comparison to other copolymers such as PDL-HL 39, the poly(ω -PDL-co- δ -HL) that presented the lowest melting peak. The associated ΔH_m s values of these δ -HL copolymers, with ω -PDL contents from 39 to 82 % and average sequence lengths of ω -PDL in the range of 2.22 - 6.67, were slightly larger than those of the crystallization peaks (from Table 4) and were between ~ 51 to 107 J g⁻¹. Their calculated crystalline fraction ranged from 21.1 to 44.1 %, values lower than those of PPDL (with a χ_c of 53.8 %, a ΔH_m of 136.1 J g⁻¹ and a T_m at 104 °C). On the other hand, the melting temperature values obtained by WAXS for the poly (ω -PDL-co- δ -HL) (from 50 to 78 °C) were consistent with their corresponding T_m s obtained by DSC (from 53 to 88 °C), although they are somewhat lower. With regard to their glass transition behaviour, the T_g s shifted to lower values when the δ -HL content was raised and were more easily distinguished (with higher ΔC_p values) as the amorphous phase increased. The measured values were between -37 and -43 °C, temperatures higher than those of the ω -pentadecalactone-co- ϵ -decalactone copolymers.

To provide another framework for comparison, some of the melting results were contrasted with those obtained for the ω -pentadecalactone-co- ϵ -decalactone copolymers, in which ϵ -DL, with an identical structure to ϵ -caprolactone but with a butyl pendant group, also lowered the crystallization capability of ω -PDL. Figure 5 shows the melting enthalpies and temperatures of the copolymers in this work (in bold squares) along with those of the poly(ω -PDL-co- ϵ -DL) [50]. As can be seen the ΔH_m values and the crystallinity degree (not shown) of both kinds of copolymers are related

to the ω -PDL content. This is quite unexpected because the poly(ω -PDL-co- ε -DL) have a blockier character ($0.38 < R < 0.49$), and consequently should exhibit an increased crystalline fraction with the same composition. Nevertheless, the T_m s of the δ -HL based copolymers were certainly lower than those measured for the ω -PDL-co- ε -DL copolymers. This makes more sense, because it has been reported that random copolymers possess lower T_m s than the blocky copolymers [21]. One possible explanation for this fact may be that the butyl pendant chain of the ε -DL, could, to a certain extent, hinder the crystallization of ω -PDL. During the crystallization, few crystal nuclei would be formed facilitating the growth of the crystals. Thus, the ω -PDL crystals of the poly(ω -PDL-co- ε -DL) would be more stable, more perfect and consequently melt at higher temperatures. Indeed, the average crystal size measurements, determined by WAXS, support this theory. While the crystal size of the poly(ω -PDL-co- δ -HL) ranged from 12 to 19 nm (with the exception of PDL-HL 82), it was in the 20 to 23 nm range for the ε -DL based copolymers, so it can be stated that the latter are bigger.

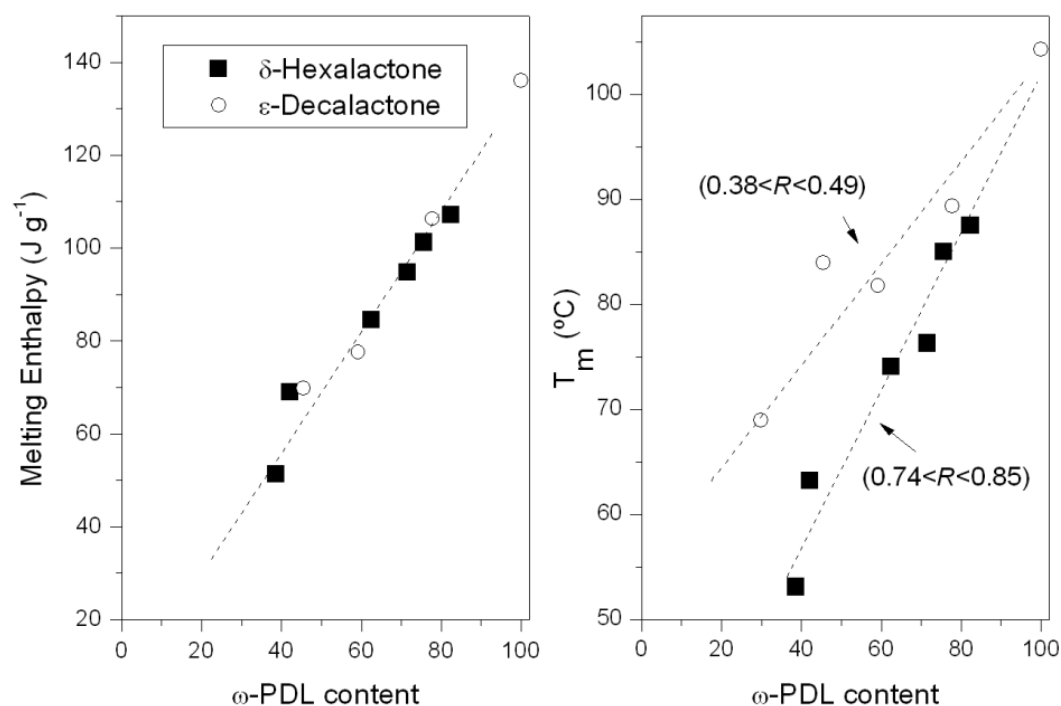


Figure 5. Melting enthalpies and temperatures of poly(ω -pentadecalactone-co- δ -hexalactone) and poly(ω -pentadecalactone-co- ε -decalactone) with different chain microstructures at different compositions.

Figure 6 shows the diffraction profiles of some poly(ω -PDL-co- δ -HL) together with the diffractogram of the reference homopolymer (PPDL). As can be seen, at higher contents of δ -HL in the copolymers the reflection intensity decreases. However, the poly(ω -PDL-co- δ -HL) presented exactly the same signals as PPDL at 2θ of 21.7, 24.1, 30.1 and 36.3° (the peak at 27.3° may be due to the bismuth compounds because it also appeared at high temperatures when the polymers were fully amorphous). Hence, it was demonstrated that the ω -PDL-co- δ -HL copolymers and the PPDL present the same crystal structure, confirming the fact that only the ω -PDL units were able to crystallize.

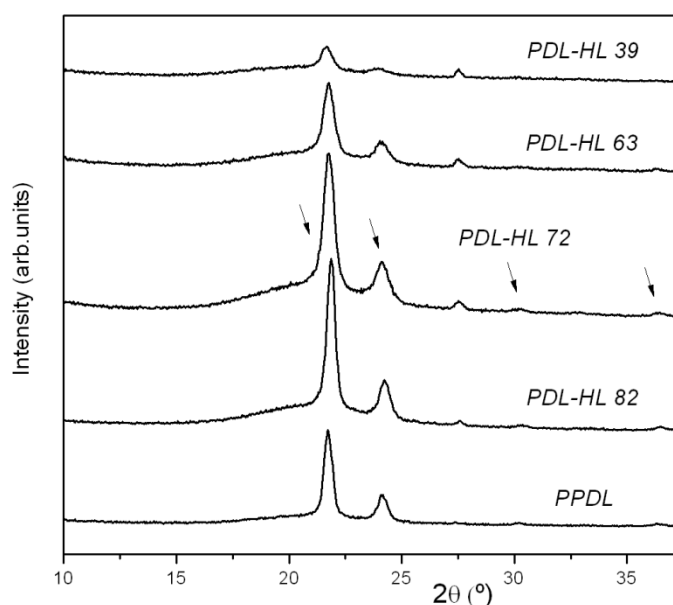


Figure 6. WAXS profiles of PPDL and the ω -PDL-co- δ -HL copolymers in the $10 \leq 2\theta \leq 38$ range.

Thermogravimetric analysis

Figure 7 shows the curves of percent weight loss and first derivative of weight loss against temperature (TG and DTG curves) belonging to the PPDL homopolymer and the ω -PDL-co- δ -HL copolymers. As can be seen, four well-defined peaks (especially true in the case of PDL-HL 39) can be distinguished in the DTG curves, which were generated because of the high residual catalyst content of these polymers (a monomer/catalyst molar ratio of 100 was used in their synthesis). With increased metal catalyst content there are more units bonded to the metal atoms so metal-accelerated

depolymerization is a more significant phenomenon in the pyrolysis of the polyesters [63]. As a result of this effect, the peaks of thermal degradation of δ -HL and ω -PDL split into two stages: the decomposition of the bismuth accelerated sequences and the degradation of the catalyst free chains.

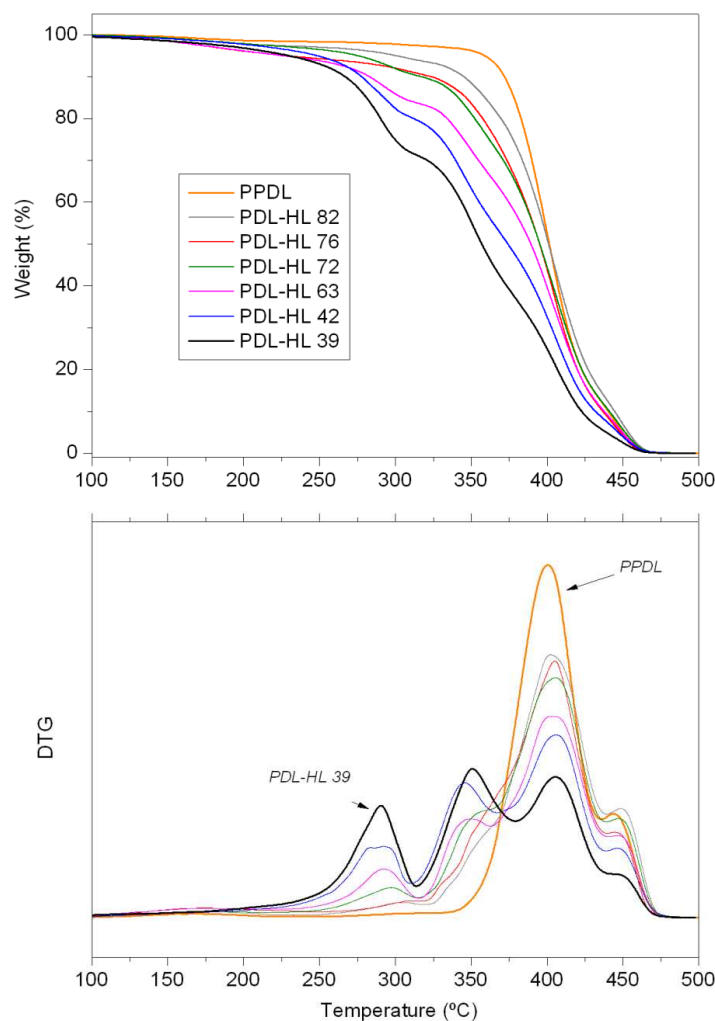


Figure 7. Thermogravimetric (TG) and differential thermogravimetric (DTG) curves of PPDL and the ω -PDL-co- δ -HL copolymers.

The first two peaks of thermal degradation at around 275 °C and 350 °C were attributed to the decomposition of δ -HL-rich sequences. These two peaks did not appear in the curve of the PPDL and were more pronounced in the case of PDL-HL 39, the copolymer with the highest δ -HL content. As the ω -PDL content rose, the intensity of these peaks decreased and they eventually vanished in PPDL. Conversely, two stages of

degradation of ω -PDL were also found in the DTG curve of PPDL that also appeared in the poly(ω -PDL-co- δ -HL) curves. The first peak, the more intense, appeared at ~ 400 °C whereas the thermal degradation of the ω -PDL sequences that are less exposed to the residual metal was delayed to around 440 °C. These two peaks of degradation of the ω -PDL blocks were more stable under thermal degradation than PCL (which degrades in the range of 350 to 400 °C), owing to the lower proportion of ester groups in the macrolactone.

On the other hand, it is also worth mentioning that these kind of copolymers show a more random distribution of sequences than the poly(ω -pentadecalactone- ϵ -decalactone) studied previously by our group ($0.38 < R < 0.49$) [50]. This is reflected in the DTG curves of the ω -PDL-co- δ -HL copolymers with a higher content of ω -PDL (from 72 to 82 %). Due to their random tendency ($0.82 < R < 0.85$) the peaks assigned to the thermal degradation of δ -HL blocks were difficult to distinguish and appear almost overlapped with the peak at 400 °C.

Hydrolytic degradation study

Table 6. Melting enthalpies and temperatures of all the polymer films at the start and at the end of the degradation study.

Sample	21 °C		37 °C		On day 98 of degradation at 37 °C		On day 182 of degradation at 37 °C	
	ΔH (J g ⁻¹)	T _m (°C)	ΔH (J g ⁻¹)	T _m (°C)	ΔH (J g ⁻¹)	T _m (°C)	ΔH (J g ⁻¹)	T _m (°C)
PPDL	133.3	102.2	133.8	102.8	149.2	102.9	147.4	106.1
PDL-HL 82	106.8	91.0	111.1	88.9	118.4	88.1	115.5	90.2
PDL-HL 76	102.1	88.2	105.9	84.9	109.6	87.5	111.9	87.9
PDL-HL 72	95.2	79.6	96.5	79.8	103.7	79.8	101.2	84.4
PDL-HL 63	77.1	74.4	80.7	76.2	84.3	79.1	90.4	80.2
PDL-HL 42	58.4	69.2	60.6	65.3	66.6	63.4	65.2	72.3
PDL-HL 39	48.3	55.4	44.0	59.0	49.7	58.7	52.7	61.4

DSC scans were made from 21 to 140 °C: at room temperature (before submerging the samples in PBS), after storage for 24 hours at 37 °C and at different degradation times

(after drying). The data relating to melting enthalpies and temperatures at the start, on day 98 and at the end of the study for all the polymer films are gathered in Table 6.

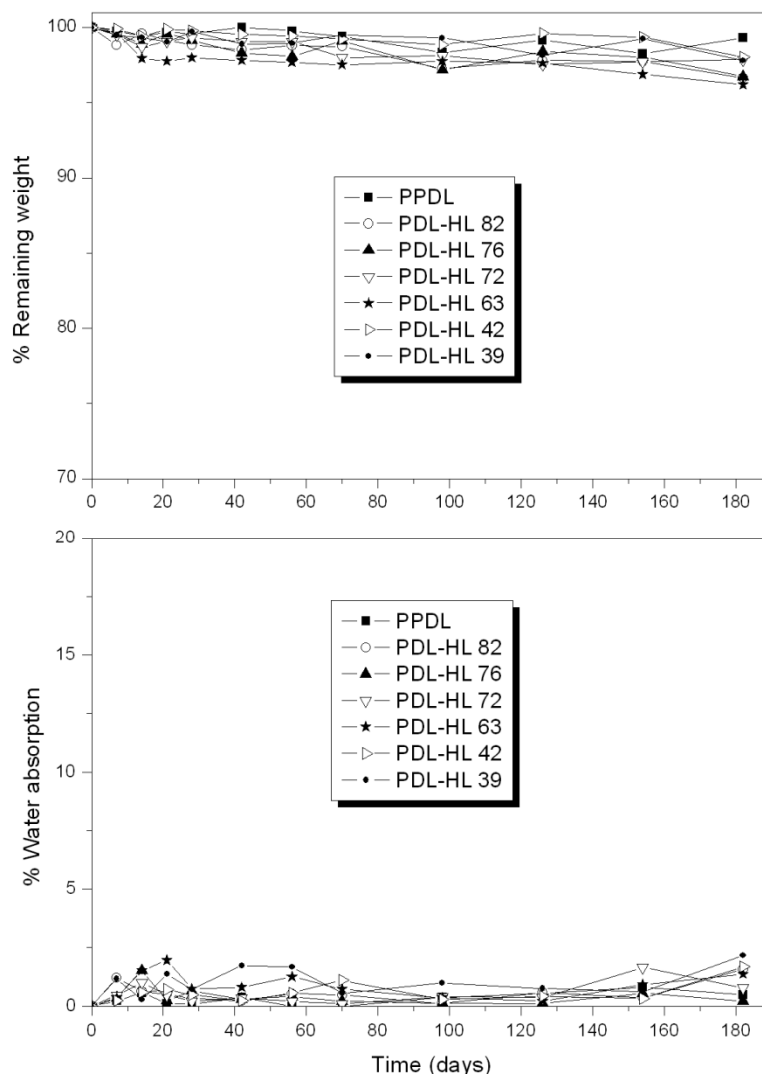


Figure 8. Evolution of the remaining weight and the water absorption of the poly(ω -pentadecalactone-co- δ -hexalactone).

The thermal properties of the poly(ω -PDL-co- δ -HL) films at 21 °C and at 37 °C can be considered as very similar (the small differences may be due to the precision of the measurements). However, it can be observed that on days 98 and 182 of degradation, the samples were slightly more crystalline with higher ΔH_m values. Moreover, the T_m values shifted to higher temperatures (2–7 °C higher), a tendency that is observed for all the materials owing to rearrangements of the crystalline phase. This is particularly

true in the case of the copolymers with lower contents of ω -PDL. However, as a consequence of the highly crystalline domains of all the polymers ($> 44 \text{ J g}^{-1}$), water absorption was negligible and did not exceed a value of 2.5 % in any case. Consequently, the polymers did not lose mass and the weight of the samples remained almost constant during the entire study (see Figure 8).

Figure 9 shows the progress of $\ln M_w$ against degradation time of the PPDL homopolymer and the δ -HL copolymers. As the degradation evolves, the weight average molecular weight (M_w) of the samples decreased while the dispersity rose, indicating a broader distribution of polymer chain length. As can be seen, the ω -PDL-co- δ -HL copolymers curves displayed similar slight drops, while the M_w of PPDL homopolymer remained practically constant during the 182 days.

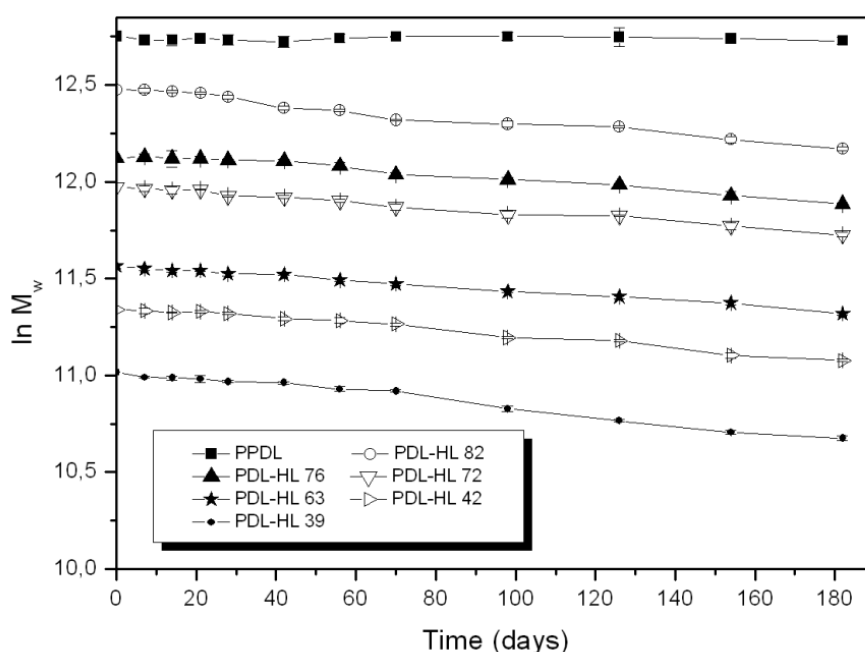


Figure 9. $\ln M_w$ against degradation time of PPDL and its δ -HL copolymers.

Table 7 presents the degradation rate values (K_{M_w}) and half degradation times ($t_{1/2}$) calculated from the slope of the fitting curve. The M_w experimental data adapts to the fitting curve ($R^2 > 0.98$) very well over the 182 days and the K_{M_w} estimated for the copolymers were in the $0.0013\text{-}0.0019 \text{ days}^{-1}$ range with corresponding $t_{1/2}$ of 365 to 533 days. All the values of degradation rate were above the obtained for PCL (0.0010

days⁻¹) in a previous study by this group [34] and also higher than those of the poly(ω -PDL-co- ϵ -DL) [50], which are almost non-biodegradable polymers.

Table 7. K_{Mw} , calculated on the final day of the study (day 182), and $t_{1/2}$ of the poly(ω -PDL-co- δ -HL).

Sample	K_{Mw} (days ⁻¹)	Half-molecular weight degradation time $t_{1/2}$
PPDL	< 0.0002	> 9.5 years
PDL-HL 82	0.0017	408 days
PDL-HL 76	0.0014	495 days
PDL-HL 72	0.0013	533 days
PDL-HL 63	0.0013	533 days
PDL-HL 42	0.0015	462 days
PDL-HL 39	0.0019	365 days

With the incorporation of δ -HL units, the crystal structure of ω -PDL (54 % crystalline fraction) was disrupted and the copolymers became significantly more amorphous (21-44 % crystalline fraction). Likewise, the proportion of ester bonds increased, which should help to promote the hydrolysis process. However, despite the fact that PDL-HL 39 (the copolymer with the highest δ -HL content) which showed the highest degradation rate (0.0019 days⁻¹), the differences between the respective K_{Mw} of the poly(ω -PDL-co- δ -HL) were small. This may be due to the more random chain microstructure of the copolymers of increased ω -PDL content. On the other hand, it is important to mention that no morphological changes were appreciated on the PPDL and poly(ω -PDL-co- δ -HL) samples, and the M_w of PDL-HL 82, PDL-HL 76, PDL-HL 72, PDL-HL 63, PDL-HL 42 and PDL-HL 39 decreased slightly to final values of 193, 145, 124, 82, 65 and 43 kg mol⁻¹. In the latter case, the film of this material became brittle after day 126 but it was studied on day 182 by polarized light optical microscopy and no sign of deterioration was found with respect to the initial sample.

Mechanical properties

Table 8 summarizes the mechanical testing results at 21° and at 37 °C (at the start and on day 182 of degradation) for the poly(ω -PDL-co- δ -HL) films, whose DSC data, before performing the mechanical tests, are already shown in Table 6.

Table 8. Mechanical properties of the PDDL and the ω -PDL-co- δ -HL copolymers.

Sample	Testing Temperature ¹	Secant Modulus at 2 %	Yield Strength (Yield Point) or Offset Yield Strength at 10 % ²	Tensile Strength at 300 % ³	Ultimate Tensile Strength ⁴	Elongation at break	Strain Recovery after break ⁵
		(MPa)	(MPa)	(MPa)	(MPa)	(%)	(%)
PDL-HL 82	21 °C	179.0 ± 13.5	7.9 ± 0.4 (18.2 %)	8.8 ± 0.2	20.2 ± 2.2	1145 ± 100	43.3 ± 6.0
	37 °C	154.3 ± 2.8	6.9 ± 0.2 (28.4 %)	7.6 ± 0.1	-	> 300	-
	On day 182 (37 °C)	185.3 ± 9.2	7.5 ± 0.5 (14.6 %)	7.4 ± 0.6	-	> 300	-
PDL-HL 76	21 °C	155.8 ± 6.3	7.0 ± 0.5 (18.6 %)	7.3 ± 0.2	12.6 ± 1.3	961 ± 80	37.7 ± 4.7
	37 °C	118.3 ± 4.4	5.4 ± 0.2 (22.1 %)	6.2 ± 0.3	-	> 300	-
	On day 182 (37 °C)	161.3 ± 1.6	6.4 ± 0.2 (13.1 %)	6.8 ± 0.2	-	> 300	-
PDL-HL 72	21 °C	115.8 ± 2.3	6.3 ± 0.4 (36.8 %)	7.2 ± 0.2	9.9 ± 1.1	765 ± 87	41.1 ± 2.7
	37 °C	81.2 ± 3.1	5.1 ± 0.2 (46.5 %)	5.6 ± 0.1	-	> 300	-
	On day 182 (37 °C)	111.2 ± 4.1	5.4 ± 0.4 (25.7 %)	-	4.8 ± 0.4	102 ± 13	-
PDL-HL 63	21 °C	82.9 ± 1.4	4.7 ± 0.2 (38.9 %)	-	4.4 ± 0.3	82 ± 10	80.0 ± 5.9
	37 °C	58.9 ± 1.3	3.1 ± 0.1	-	3.3 ± 0.1	25 ± 7	-
	On day 182 (37 °C)	80.0 ± 4.8	-	-	3.7 ± 0.2	13 ± 2	-
PDL-HL 42	21 °C	50.9 ± 4.7	3.1 ± 0.1	-	4.0 ± 0.1	64 ± 8	92.2 ± 1.9
	37 °C	34.7 ± 2.3	2.1 ± 0.1	-	2.4 ± 0.2	25 ± 5	-
	On day 182 (37 °C)	38.4 ± 2.5	-	-	1.9 ± 0.1	8.3 ± 0.7	-
PDL-HL 39	21 °C	25.7 ± 1.1	1.8 ± 0.1	-	2.0 ± 0.2	28 ± 6	95.1 ± 1.3
	37 °C	15.8 ± 0.3	-	-	0.81 ± 0.06	8.7 ± 0.5	-
	On day 182 (37 °C)	14.4 ± 1.9	-	-	0.31 ± 0.08	2.3 ± 0.3	-

¹ At 37 °C, the tests were stopped at 300 % of strain due to the size limitations of the temperature chamber.

² Offset Yield Strength at 10 % was calculated for PDL-HL 42 and PDL-HL 39.

³ Some specimens broke before 300 % of strain.

⁴ The tensile strength was determined as ultimate stress value (σ_u).

⁵ Measured 24 hours after break.

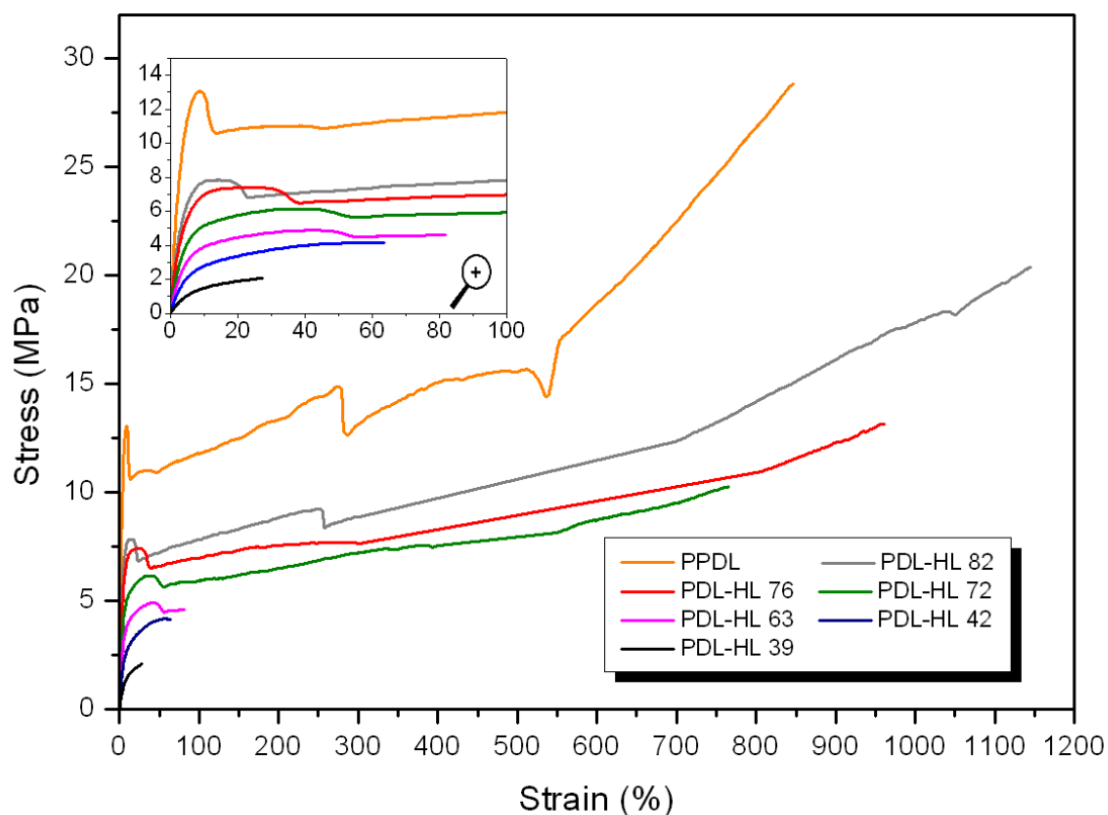


Figure 10. Tensile stress-strain curves of PPDL and the ω -PDL-co- δ -HL copolymers at 21 °C.

As can be seen in Figure 10, which displays typical stress-strain curves of the polymers studied, the ω -PDL-co- δ -HL copolymers showed a marked improvement in flexibility (with lower secant modulus and increased strain recovery rates) compared to PPDL and poly(ϵ -Caprolactone) homopolymers (secant modulus from 300 to 400 MPa, ultimate tensile strength of 28-32 MPa and deformation at break values > 750 %) [34,50]. Nevertheless, the tensile samples of the copolymers having a ω -PDL content below 63 % (with a crystalline fraction under 36 % and $T_{ms} < 74$ °C) broke early at strains lower than 100 % and their performance was greatly influenced by their crystalline phase. Owing to their rather random distribution of sequences ($0.74 < R < 0.85$), the ω -PDL average sequence lengths of PDL-HL 63, PDL HL 42 and PDL-HL 39 were only in the range of 2.22-3.58 and that was not enough to induce a process of crystallization by orientation during the tensile test, that could increase the ductility. Conversely, in the

case of the poly(ω -PDL-co- ϵ -DL) with ω -PDL content of 59 and 46 %, the alignment of the polymer chains allowed elongation at breaks of 968 and 193 % to be reached, respectively. These two copolymers, with a more perfect crystalline structure (with higher average crystal sizes and T_m s), were blockier ($R \sim 0.38$) and had larger ω -PDL-blocks, l_{PDL} of 6.26 and 4.88, in their chain microstructure [50].

Despite the low strain at break of the three poly(ω -PDL-co- δ -HL) mentioned above, which is even more remarkable at 37 °C, they all presented strain recoveries higher than 80 % with secant modulus values between 25.7 and 82.9 MPa and final strength values in the range of 2.0 and 4.4 MPa. On the contrary, the rest of the copolymers with ω -PDL contents over 72 % exhibited lower strain recoveries but elongation at break values well-above 765 %. The secant modulus values obtained for PDL-HL 82 and PDL-HL 72 were 179 and 115.8 MPa and presented yield strengths of 7.9 and 6.3 MPa and tensile strengths at break of 20.2 and 9.9 MPa.

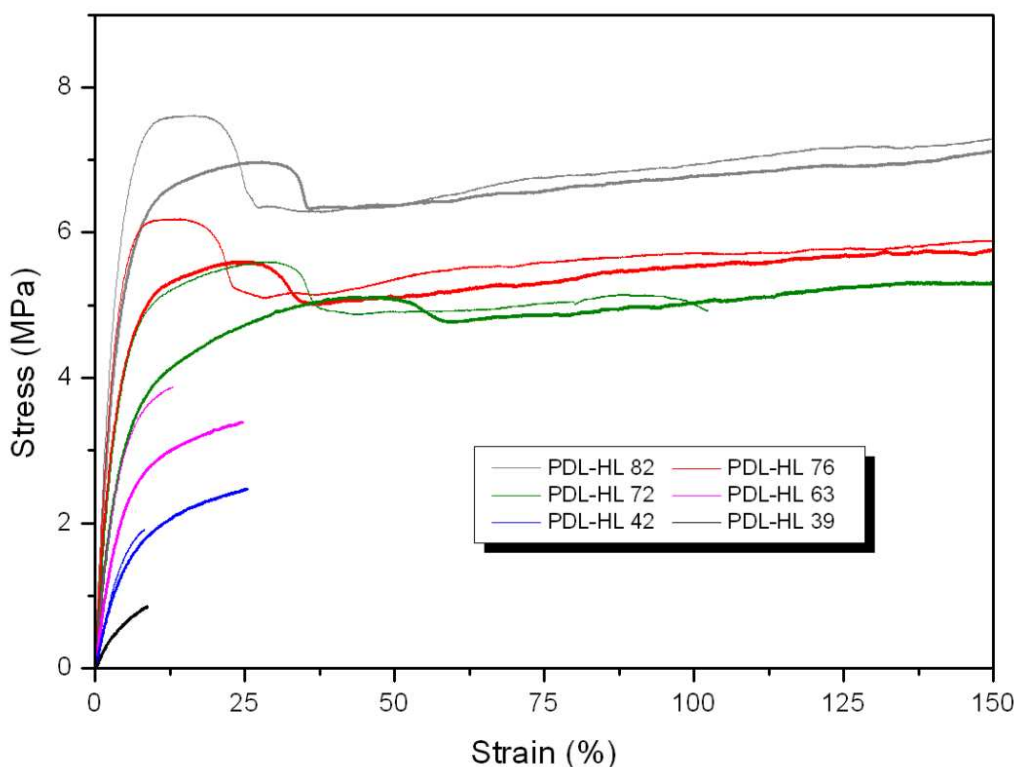


Figure 11. Tensile stress-strain curves up to 150 % of strain of PPDL and the ω -PDL-co- δ -HL copolymers at 37 °C. The curves of the non-degraded samples are in bold type.

Figure 11 show the tensile stress-strain curves up to 150 % of strain of the tensile tests conducted at 37 °C with non-degraded (curves in bold type) and degraded specimens. As a result of the crystallization during the hydrolytic degradation process, the stress related properties were found slightly higher than at the start of the study. As can be noted, the elastic modulus of the samples submerged for 182 days in PBS (see also Table 8) increased with respect to that of the non-degraded films, reaching secant modulus values similar to those obtained at 21 °C. In addition, the stress also took greater values at the same strain and the yield points were narrower (with higher yield strengths), and shifted to lower values. However, owing to the changes in molecular weight and the mechanical deterioration experienced in an aqueous medium, the poly(ω -PDL-co- δ -HL) with ω -PDL contents lower than 76 % lost their deformation capability. For example, PDL-HL 72 exhibited elongation at break values above 300 % but at the end of the degradation study broke at only 102 %.

With the exception of PDL-HL 39, the ω -PDL-co- δ -HL copolymers displayed good mechanical stability between 21 and 37 °C, although the poly(ω -PDL-co- ϵ -DL) (with higher l_{PDL} and melting temperatures) showed steadier mechanical properties [50]. Thus, at 37 °C the loss in secant modulus and strength of PDL-HL 82 was about 14 % compared to its performance at room temperature, when the PCL homopolymer suffered a drop of around 12 %. These changes were even more relevant (> 27 %) on the PCL copolymers studied previously by this group [34].

5.4. Conclusions

In this work several statistical copolymers based on ω -pentadecalactone and δ -hexalactone were synthesized with triphenyl bismuth as catalyst. The poly(ω -PDL-co- δ -HL)s showed a slightly deviated from random distribution of sequences ($0.74 < R < 0.85$) and were carefully characterized by NMR, GPC, DSC, WAXS and TGA measurements. In addition, their mechanical properties were tested at room temperature (21 °C) and at body temperature (37 °C), whereas an *in vitro* degradation study was also carried out at 37 °C for 182 days in phosphate buffer solution. Owing to their lower

stiffness and upgraded biodegradability in comparison to poly(ϵ -caprolactone) there are high hopes for these new thermoplastic elastomers, which also present high thermal stability and rapid crystallization from melt. However, significant improvements are necessary in the methodology of synthesis in order to shorten the reaction times and make the process better adapted to industry.

References

- [1] Albertsson, A-C.; Varma, I. *Degradable Aliphatic Polyesters*; Springer: Berlin, Heidelberg 2002, 157.
- [2] Jerome, C.; Lecomte, P. Recent advances in the synthesis of aliphatic polyesters by ring-opening polymerization. *Adv. Drug Delivery Rev.* 2008, 60, 1056-1076.
- [3] Albertsson, A-C.; Varma, I-K. Recent developments in ring opening polymerization of lactones for biomedical applications. *Biomacromolecules* 2003, 4, 1466-1486.
- [4] Van der Meulen, I., Gubbels, E., Huijser, S., Sablong, R., Koning, C. E., Heise, A., Duchateau, R. Catalytic Ring-Opening Polymerization of Renewable Macrolactones to High Molecular Weight Polyethylene-like Polymers. *Macromolecules* 2011, 44, 4301-4305.
- [5] Bouyahyi, M., Pepels, M.P.F., Heise, A., Duchateau, R. ω -Pentadecalactone polymerization and ω -pentadecalactone/ ϵ -caprolactone copolymerization reactions using organic catalysts. *Macromolecules* 2012, 45, 3356-3366.
- [6] Martin, E.; Dubois, P.; Jerome, R. "In Situ" Formation of Yttrium Alkoxides: A Versatile and Efficient Catalyst for the ROP of ϵ -Caprolactone. *Macromolecules* 2003, 36, 5934-5941.
- [7] Dove, A.P. Controlled ring-opening polymerisation of cyclic esters: polymer blocks in self-assembled nanostructures. *Chemical Communications* 2008, 48, 6446-6470.
- [8] Bouyahyi, M., Duchateau, R. Metal-Based catalysts for Controlled Ring-Opening Polymerization of Macrolactones: High Molecular Weight and Well-Defined Copolymer Architectures. *Macromolecules* 2014, 47, 517-524.
- [9] Pepels, M.P.F.; Souljé, P.; Peters, R.; Duchateau, R. Theoretical and Experimental Approach to Accurately Predict the Complex Molecular Weight Distribution in the Polymerization of Strainless Cyclic Esters. *Macromolecules* 2014, 47, 5542-5550.
- [10] Duda, A., Kowalski, A., Penczek, S., Uyama, H., Kobayashi, S. Kinetics of the Ring-Opening Polymerization of 6-, 7-, 9-, 12-, 13-, 16-, and 17-Membered Lactones. Comparison of Chemical and Enzymatic Polymerizations. *Macromolecules* 2002, 35, 4266-4270.
- [11] Middleton, J.C.; Tipton, A.J.; Synthetic biodegradable polymers as orthopedic devices. *Biomaterials* 2000, 21, 2335-2346.
- [12] Labet, M.; Thielemans, W. Synthesis of polycaprolactone: a review. *The Royal Society of Chemistry* 2009, 38, 3484-3504.

- [13] Woodruff, M.A.; Hutmacher, D.W. The Return of a forgotten polymer: Polycaprolactone in the 21st century. *Progress in Polymer Science* 2010, 35, 1217-1256.
- [14] van der Meulen, I., de Geus, M., Antheunis, H., Deumens, R., Joosten, E.A.J., Koning, C.E., Heise, A. Polymers from Functional Macrolactones as Potential Biomaterials: Enzymatic Ring Opening Polymerization, Biodegradation and Biocompatibility. *Biomacromolecules* 2008, 9, 3404-3410.
- [15] Pepels, M.P.F.; Hanse, M.R.; Goossens, H.; Duchateau, R. From Polyethylene to Polyester: Influence of Ester Groups on the Physical Properties. *Macromolecules* 2013, 46, 7668-7677.
- [16] Dobrzynski, P.; Li, S.; Kasperczyk, J.; Bero, M.; Gasc, F.; Vert, M. Structure property relationships of copolymers obtained by ring-opening polymerization of glycolide and ϵ -caprolactone. Part 1. Synthesis and characterization. *Biomacromolecules* 2005, 6, 483-488.
- [17] Li, S.; Dobrzynski, P.; Kasperczyk, J.; Bero, M.; Braud, C.; Vert, M. Structure property relationships of copolymers obtained by ring-opening polymerization of glycolide and ϵ -caprolactone. Part 2. Influence of composition and chain microstructure on the hydrolytic degradation. *Biomacromolecules* 2005, 6, 489-497.
- [18] Kasperczyk, J.; Li, S.; Jaworska, J.; Dobrzyński, P.; Vert, M. Degradation of copolymers obtained by ring-opening polymerization of glycolide and ϵ -caprolactone: A high resolution NMR and ESI-MS study. *Polymer Degradation and Stability* 2008, 93, 990-999.
- [19] Vanhoorne, P.; Dubois, P.; Jerome, R.; Teyssie, P. Macromolecular engineering of polylactones and polylactides. 7. Structural analysis of copolyesters of epsilon-caprolactone, L-lactide or D,L-lactide initiated by AL(OIPR)₃. *Macromolecules* 1992, 25, 37-44
- [20] Hiljanen Vainio, M.; Karjalainen, T.; Seppala, J. Biodegradable lactone copolymers .1. Characterization and mechanical behavior of epsilon-caprolactone and lactide copolymers. *Journal of Applied Polymer Science* 1996, 59, 1281-1288.
- [21] Fernández, J.; Meaurio, E.; Chaos, A.; Etxeberria, A.; Alonso-Varona, A.; Sarasua J.R. Synthesis and characterization of poly(L-lactide/ ϵ -caprolactone) statistical copolymers with well resolved chain microstructures. *Polymer* 2013, 54, 2621-2631.
- [22] Fernández, J.; Larrañaga, A.; Etxeberria, A.; Wang, W.; Sarasua, J.R. A new generation of poly(lactide/ ϵ -caprolactone) polymeric biomaterials for application in the biomedical field. *Journal of Biomedical Materials Research A*. 2014, 102A, 3573-3584.

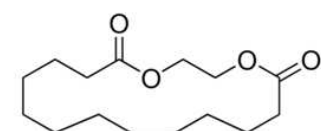
- [23] Fernández, J.; Larrañaga, A.; Etxeberria, A.; Sarasua, J.R. Tensile behavior and dynamic mechanical analysis of novel poly(lactide/δ-valerolactone) statistical copolymers. *Journal of the Mechanical Behaviour of Biomedical Materials* 2014, 35, 39-50.
- [24] Pitt, C.G.; Graetzl, M.M.; Kimmel G.L.; Surles, J.; Schidler, A. Aliphatic polyesters II. The degradation of poly(DL-lactide), poly(epsilon-caprolactone), and their copolymers in vivo. *Biomaterials* 1981, 2, 215-220.
- [25] Olsén, P., Borke, T., Odelius, K., Albertsson, A.C. ε-Decalactone: A Thermoresilient and Toughening Comonomer to Poly(L-lactide). *Biomacromolecules* 2013, 14, 2883-2890.
- [26] Zurita, R.; Puiggali, J.; Franco, L.; Rodriguez-Galán, A. Copolymerization of glycolide and trimethylene carbonate. *Journal of Applied Polymer Science Part A: Polymer Chemistry* 2006, 44, 993-1013.
- [27] Smola, A.; Dobrzynski, P.; Cristea, M.; Kasperczyk, J.; Sobota, M.; Gebarowska, K.; Janeczek, H. Bioresorbable terpolymers based on L-lactide, glycolide and trimethylene carbonate with shape memory behaviour. *Polymer Chemistry* 2014, 5, 2442-2452.
- [28] Pégo, A.P.; Poot, A.A.; Grijpma, D.W.; Feijen, J. Physical properties of high molecular weight 1,3-trimethylene carbonate and D,L-lactide copolymers. *Journal of Materials Science: Materials in Medicine* 2003, 14, 767-773.
- [29] Darensbourg, D.J.; Choi, W.; Karroonnirun, O.; Bhuvanesh, N. Ring-Opening Polymerization of Cyclic Monomers by Complexes Derived from Biocompatible Metals. Production of Poly(lactide), Poly(trimethylene carbonate), and Their Copolymers. *Macromolecules* 2008, 41, 3494-3502.
- [30] Guerin, W.; Helou, M.; Carpentier, J.F.; Slawinski, M.; Brusson, J.M.; Guillaume, S.M. Macromolecular engineering *via* ring-opening polymerization (1): L-lactide/trimethylene carbonate block copolymers as thermoplastic elastomers. *Polymer Chemistry* 2013, 4, 1095-1106.
- [31] Ji, L.J.; Lai, K-L.; He, B.; Wang, G.; Song, L-Q.; Wu, Y.; Gu, Z-W. Study on poly(l-lactide-co-trimethylene carbonate): synthesis and cell compatibility of electrospun film. *Biomedical Materials* 2010, 5, 045009.
- [32] Bhattarai, N.; Jiang, W.Y.; Kim, H.Y.; Lee, D.R.; Park, S.J. Synthesis and Hydrolytic Degradation of a Random Copolymer Derived from 1,4-Dioxan-2-one and Glycolide. *Journal of Polymer Science: Part B: Polymer Physics* 2004, 42, 2558-2566.

- [33] Zhao, H.Z.; Hao, J.Y.; Xiong, C.D.; Deng, X.M. Different crystallinity of poly(d,l-lactide-co-p-dioxanone) copolymers acquired by control of chain microstructure. *Chinese Chemical Letters* 2009, 20, 1506–1509.
- [34] Fernandez, J., Etxeberria A., Sarasua, J.R. In vitro degradation studies and mechanical behavior of poly(ϵ -caprolactone-co- δ -valerolactone) and poly(ϵ -caprolactone-co-L-lactide) with random and semi-alternating chain microstructures. *European Polymer Journal* 2015, 71, 585-595.
- [35] Fernández, J.; Etxeberria, A.; Sarasua, J.R. Crystallization and melting behavior of poly(ϵ -caprolactone-co- δ -valerolactone) and poly(ϵ -caprolactone-co-L-lactide) copolymers with novel chain microstructures. *Journal of Applied Polymer Science* 2015, 132, 42534.
- [36] de Geus, M., van der Meulen, I., Goderis, B., van Hecke, K., Doschu, M., van der Werff, H., Koning, C.E., Heise, A. Performance polymers from renewable monomers: high molecular weight poly(pentadecalactone) for fiber applications. *Polymer Chemistry* 2010, 1, 525-533.
- [37] Wilson, J.A., Hopkins S.A., Wright, P.M., Dove, A.P. Synthesis of ω -Pentadecalactone Copolymers with Independently Tunable Thermal and Degradation Behavior. *Macromolecules* 2015, 48, 950-958.
- [38] Kumar, A., Kalra, B., Dekhterman, A., Gross, R.A. Efficient Ring-Opening Polymerization and Copolymerization of ϵ -Caprolactone and ω -Pentadecalactone Catalyzed by *Candida antartica* Lipase B. *Macromolecules* 2000, 33, 6303-6309.
- [39] Ceccorulli, G., Scandola, M., Kumar, A., Kalra, B., Gross, R.A. Cocrystallization of random copolymers of ω -pentadecalactone and ϵ -caprolactone synthesized by lipase catalysis. *Biomacromolecules* 2005, 6, 902-907.
- [40] Liu, J., Jiang, Z., Zhang, S., Liu, C., Gross, R.A., Kyriakides, T.R., Saltzman, W.M. Biodegradation, biocompatibility and drug delivery in poly(ω -pentadecalactone-co-p-dioxanone) copolyesters. *Biomaterials* 2011, 32, 6646-6654.
- [41] Jiang, Z., Azim, H., Gross, R.A. Lipase-Catalyzed Copolymerization of ω -Pentadecalactone with p-dioxanone and Characterization of Copolymer Thermal and Crystalline Properties. *Biomacromolecules* 2007, 8, 2262-2269.
- [42] Focarete, M.L., Gazzano, M., Scandola, M., Kumar, A., Gross, R.A. Copolymers of ω -pentadecalactone and trimethylene carbonate from lipase catalysis: influence of microstructure on solid-state properties. *Macromolecules* 2002, 35, 8066–8071.
- [43] Kumar, A., Garg, K., Gross, R. A. Copolymerizations of ω -Pentadecalactone and Trimethylene Carbonate by Chemical and Lipase Catalysis. *Macromolecules* 2001, 34, 3527–3533.

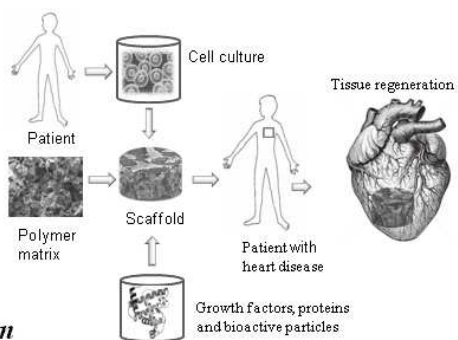
- [44] Kalra, B., Kumar, A., Gross, R.A., Baiardo, M., Scandola, M. Chemoenzymatic synthesis of new brush copolymers comprising poly(ω -pentadecalactone) with unusual thermal and crystalline properties. *Macromolecules* 2004, 37, 1243–50.
- [45] Focarete, M.L., Gazzano, M., Scandola, M., Gross, R.A. Polymers from Biocatalysis: Materials with a Broad Spectrum of Physical Properties. *Macromolecules* 2002, 35, 8066.
- [46] Mazzocchetti, L., Scandola, M., Jiang, Z. Enzymatic Synthesis and Structural and Thermal Properties of Poly(ω -pentadecalactone-co-butylene-co-succinate). *Macromolecules* 2009, 42, 7811–7819.
- [47] Mazzocchetti, L., Scandola, M., Jiang, Z. Random copolymerization with a large lactone enhances aliphatic polycarbonate crystallinity. *European Polymer Journal* 2012, 48, 1883–1891.
- [48] Jasinska-Walc, L., Hansen, M.R., Dudenko, D., Rozanski, A., Bouyahyi, M., Wagner, M., Graf, R., Duchateau, R. Topological behaviour mimicking ethylene-hexene copolymers using branched lactones and macrolactones. *Polymer Chemistry* 2014, 5, 3306-3310.
- [49] Jasinska-Walc, L.; Bouyahyi M.; Rozanski A.; Graf, R.; Hansen, M.R.; Duchateau, R. Synthetic Principles Determining Local Organization of Copolyesters Prepared from Lactones and Macrolactones. *Macromolecules* 2015, 48, 502-510.
- [50] Fernández, J.; Etxeberria, A., Larrañaga Varga A.; Sarasua, J.R.; Synthesis and characterization of ω -pentadecalactone-co- ϵ -decalactone copolymers: Evaluation of thermal, mechanical and biodegradatin properties. *Polymer* 2015, 81, 12-22.
- [51] Biazus, T.F.; Cezaro, A.M.; Borges, G.R.; Bender, J.P.; Franceschi, E.; Corazza, M.L.; Oliveira, J.V. Vapour pressure data of ϵ -caprolactone, δ -hexalactone, and γ -caprolactone. *Journal of Chemical Thermodynamics* 2008, 40, 437–441.
- [52] Parliament, T.H.; Nawar, W.W.; Fagerson, I.S. Delta-caprolactone in heated milk fat. *Journal of Dairy Science* 1965, 48, 615-616.
- [53] Kikuchi, H.; Uyama, H; Kobayashi, S. Lipase-catalyzed enantioselective copolymerization of substituted lactones to optically active polyesters. *Macromolecules* 2000, 33, 8971-8975.
- [54] Kobayashi, S. Enzymatic ring-opening polymerization of lactones by lipase catalyst: Mechanistic aspects. *Macromolecular Symposia* 2006, 240, 178-185.
- [55] Kricheldorf, H.R.; Behnken, G.; Schwarz, G.; Brockaert, J.A. High molecular weight Poly(ϵ -caprolactone) by initiation with triphenyl bismuth. *Macromolecular Chemistry and Physics* 2008, 209, 1586-1592.

-
- [56] Prestch, E., Clerc, T., Seibl, J., Simon, W. Tables of Spectral Data for Structure Determination of Organic Compounds. Chemical Laboratory Practice. Ed. Springer Science & Business Media. Springer-Verlag Berlin Heidelberg GmbH 2013.
- [57] Herbert, I.R. Statistical analysis of copolymer sequence distribution. In *NMR Spectroscopy of Polymers*. Ibbet, R.N. Ed.: Blackie Academic & Professional, London, 1993,50-79. (Chapter 2).
- [58] Fernández, J.; Larrañaga, A.; Etxeberria, A.; Sarasua, J.R. Effects of chain microstructures and derived crystallization capability on hydrolytic degradation of poly(L-lactide/ ϵ -caprolactone) copolymers. *Polymer Degradation and Stability* 2013, 98, 481-489.
- [59] Fernández, J.; Etxeberria, A.; Sarasua, J.R. In vitro degradation study of biopolyesters using poly(lactide/ δ -valerolactone) copolymers. *Polymer Degradation and Stability* 2015, 112, 104-116.
- [60] Scherrer, P. Bestimmung der Grosse und der inneren Struktur von Kolloidteilchen mittels Rontgenstrahlen. *Nachr Ges Wiss Gottingen*, 26, pp. 98-100, 1918.
- [61] Moore, T.; Adhikari, R.; Gunatillake, P. Chemosynthesis of bioresorbable poly(γ -butyrolactone) by ring-opening polymerization: a review. *Biomaterials* 2005, 26, 3771-3782.
- [62] Dubois, P.; Coulembier, O.; Raquez, J.M. *Handbook of Ring Opening Polymerization*; Wiley-VCH Verlag GmbH & Co. KGaA: Weinheim 2009.
- [63] Fernandez, J.; Etxeberria, A.; Sarasua, J.R. Effects of repeat unit sequence distribution and residual catalyst on thermal degradation of poly(L-lactide/ ϵ -caprolactone) statistical copolymers. *Polymer Degradation and Stability* 2013, 98, 1293-1299.

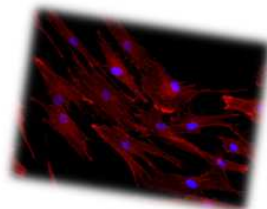
**Chapter 6. Ethylene brassylate-co- δ -
Hexalactone Biobased Polymers for
Application in the Medical Field: Synthesis,
Characterization and Cell Culture Studies**



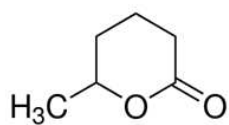
Ethylene brassylate



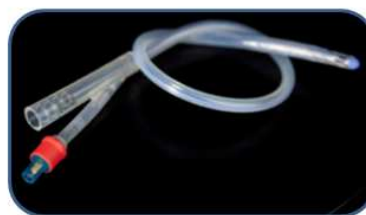
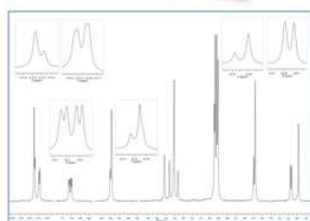
Synthesis & Characterization



Medical applications



δ-Hexalactone



Abstract

In this work novel copolymers based on ethylene brassylate (EB) and δ -hexalactone (δ -HL), two monomers obtained from renewable sources, were synthesized with triphenyl bismuth (Ph_3Bi) by ring-opening polymerization and then thoroughly characterized. The poly(EB-co- δ -HL), with EB molar contents ranging from 49 to 90 %, presented a slightly deviated from random distribution of sequences ($R > 0.71$) while WAXS measurements proved that only the EB blocks were able to crystallize (with crystallinity degrees of ~ 23 -39 %). The low T_g s (< -27 °C), their reduced crystallization capability and melting temperatures from 50 to 65 °C (with the exception of the copolymer with an EB of 49 %) make these thermoplastic elastomers (of good thermal stability) very easy to process. Likewise, their thermal properties led to mechanical behaviour with improved flexibility in comparison to poly(ϵ -caprolactone) or poly(ω -pentadecalactone) (elastic modulus from 57 to 274 MPa with high elongation at break values) at both 21 °C and 37 °C. On the other hand, the incorporation of δ -HL in addition to increase the amorphous character, brought a more disordered chain microstructure distribution, resulting in higher degradation rates in the range of 0.0028 to 0.0041 days⁻¹. Finally, metabolic activity and cell morphology studies using human dermal fibroblasts (HDFs) demonstrated that these materials are not cytotoxic and provide a valid substrate for cells to attach and proliferate, meaning that they are suitable for use in the biomedical field.

6.1. Introduction

For conformation of reliable medical devices absolute confidence in the material is essential, its properties must include stability, durability and predictability and at the same time, meet the requirements of a specific application. Since the 1980s, most research work to obtain suitable materials for biomedical uses has been focused on aliphatic polyesters. However, there are still a large number of cyclic esters that have received hardly any attention. This paper presents the properties of statistical copolymers based on ethylene brassylate macrolactone and δ -hexalactone, which were synthesized for the first time by our group.

Ethylene brassylate is a 17 member ring lactone with two ester groups, it is commercially available in large quantities and is of particular interest owing to its lower cost in comparison to other lactones and macrolactones, such as lactide, ϵ -caprolactone or ω -pentadecalactone. This compound can be obtained from tridecanoic acid which is itself synthesized from 10-undecanoic acid [1], an unsaturated fatty acid derived from castor oil, a renewable source. Ethylene brassylate is a colorless to very pale yellow viscous liquid with a sweet musk-like odor [2], for this reason it is widely used in many fragrances (cosmetics, fine perfumes, shampoos, toilet soaps and other toiletries), and non-cosmetic products such as household cleaners and detergents [3]. The volume of ethylene brassylate used worldwide in 2008 was over than 1000 metric tonnes (International Fragrance Association).

The ring-opening polymerization of ethylene brassylate was first reported by Kobayashi in 1999 [4] but low molecular weights were obtained using lipase enzymes. More recently, Mecerreyes et al. [5] employed acidic and basic organic compounds as catalysts. TBD-guanidine super base (1,5,7-triazabicyclo[4-4-0]dec-5-ene) was the most efficient catalyst in the process of synthesis, producing the fastest polymerization rates. The poly(ethylene brassylate) homopolymers, with molecular weights ranging between 2 and 14 kg mol⁻¹, presented similar properties to poly(ϵ -caprolactone) [6-8] but with a slightly higher melting temperature ($T_m = 69$ °C), a glass transition temperature at -33

°C and good thermal stability [5]. In more recent works, ethylene brassylate has been also copolymerized with other monomers such as ethylene glycol [9] or ϵ -caprolactone [10]. The poly(ethylene brassylate-co- ϵ -caprolactone)s synthesized by the Mecerreyes' group were highly crystalline and showed a range of melting temperatures between 39 and 69 °C, depending on the comonomer content,. However, the large melting enthalpy values ($\sim 85 \text{ J g}^{-1}$) and the close similarity of unit-cell lateral dimensions of ethylene brassylate and ϵ -caprolactone suggest a cocrystallization of both units, similar to other isomorphous copolymers containing ϵ -caprolactone [11-16].

With the aim of preventing the isomorphous cocrystallization phenomenon, ethylene brassylate was copolymerized in this study with δ -hexalactone (δ -caprolactone) [17-19], a six-membered lactone with identical structure to δ -valerolactone but possessing a methyl pendant group. This little known lactone, found in heated milk fat [20], was successfully copolymerized in a previous work by our group with ω -pentadecalactone [21]. The incorporation of δ -HL allowed the reduction of the crystalline fraction of the poly(ω -pentadecalactone) homopolymer owing to the racemic stereochemistry of the methyl side chain of the δ -HL unit. As a result, copolymers with a lower level of stiffness and upgraded biodegradability were achieved.

The poly(ethylene brassylate-co- δ -hexalactone)s in this paper were synthesized using triphenyl bismuth (Ph_3Bi) [22] as a catalyst and characterized using proton and carbon nuclear magnetic resonance spectroscopy (^1H and ^{13}C NMR), gel permeation chromatography (GPC) measurements and thermogravimetric analysis (TGA). Their crystallization and melting behaviour was studied by means of differential scanning calorimetry (DSC) and Wide Angle X-ray diffraction (WAXRD). In addition, films of EB-co- δ -HL copolymers with EB molar contents ranging from 49 to 90 % were prepared for mechanical testing at room temperature (21 °C) and at human body temperature (37 °C), the typical working temperatures of biomaterials. Finally, an *in vitro* hydrolytic degradation study was also carried out at 37 °C for a period up to 26 weeks in phosphate buffer solution (PBS). Thus, any changes in water absorption, weight loss, macroscopic morphology, crystallinity, phase structure, molecular weight and mechanical properties of the copolymers were monitored.

Of the metal catalysts available, bismuth salts or complexes, such as Ph_3Bi , are notable for their low toxicity [23]. In this context, several studies [24-27] have demonstrated that bismuth compounds belong to the group of least toxic heavy metal compounds, while Bi^{3+} performed even better than Zn^{2+} , although small amounts of zinc are needed by the human metabolism. However, cell viability studies with some of the materials of this work were deemed necessary in order to rule out the possible cytotoxicity of these Bi-containing polymers and confirm their safe use in medical and tissue engineering applications. Therefore, human dermal fibroblasts (HDFs) were cultured on samples obtained from films of the poly(EB-co- δ -HL) and the metabolic activity and morphology were investigated by means of AlamarBlue[®] assay and using an inverted fluorescent microscope.

6.2. Materials and methods

Materials

δ -hexalactone monomer (assay > 98 %) was provided by Sigma Aldrich (W316709). Ethylene brassylate monomer (assay > 95 %) was also supplied by Sigma Aldrich (W354309). The triphenyl bismuth (Ph_3Bi) catalyst was obtained from Gelest. Phosphate buffer solution (PBS) (pH 7.2) was obtained from Fluka Analytical (Sigma Aldrich). Dulbecco's modified Eagle's medium (DMEM), fetal bovine serum (FBS), Hank's balanced salt solution (HBSS) and penicillin-streptomycin (PS) solution were purchased from Sigma-Aldrich (Ireland). AlamarBlue[®] and rhodamine phalloidin were obtained from ThermoFisher Scientific (Ireland); Hoechst staining solution was from Sigma-Aldrich (Ireland). Human dermal fibroblasts (HDFs) were obtained from Sigma-Aldrich (Ireland).

Synthesis procedure

Statistical copolymers from ethylene brassylate and δ -hexalactone (see Figure 1 for structure) at differing compositions were synthesized in bulk by one pot-one-step ring-opening polymerizations (ROP). For the correct evaluation of the EB-co- δ -HL

copolymer behaviour, a poly(ethylene brassylate) (PEB) homopolymer was also synthesized. The reactions were conducted in a flask immersed in a controlled temperature oil bath. In each polymerization, predetermined amounts of the different comonomers at the chosen mass feed ratio were simultaneously added and melted into the flask. The flask was purged for 30 minutes with a nitrogen stream under the surface of the melt. Then the catalyst (Ph_3Bi) was added (at 100:1 comonomers/catalyst molar ratio) and the magnetic stirrer maintained at 100 rpm. No initiator compound was added to the reaction mix so the catalyst was activated by the ROH provided by the monomers (H_2O and impurities), with the exception of the PEB homopolymer and the copolymers with higher contents of EB. In those cases 1-hexanol was added in order to control the molecular weight. The ethylene brassylate-co- δ -hexalactone polymerizations were carried out at 130 °C over 3 or 6 days.

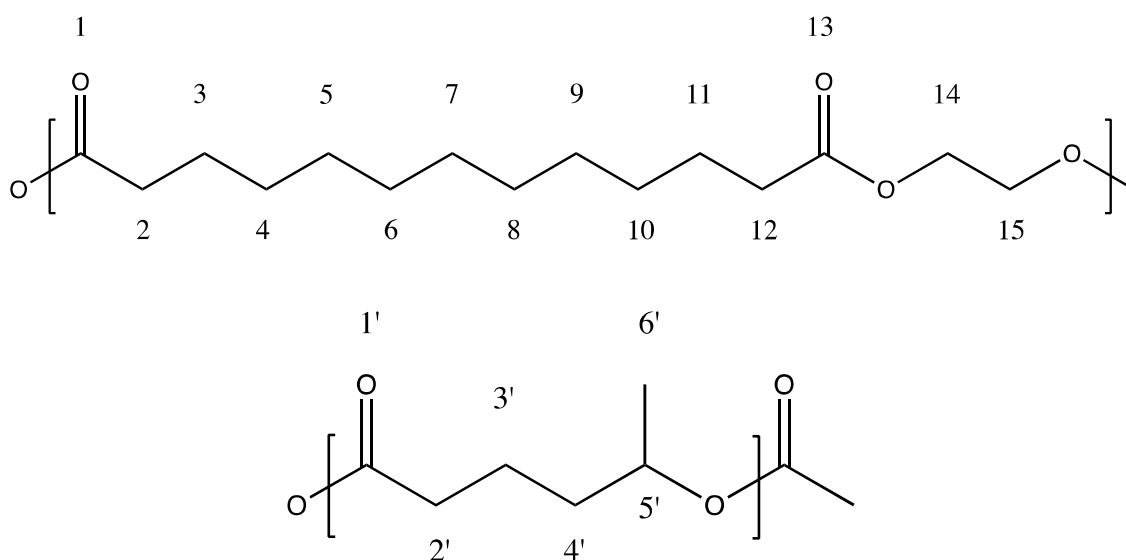


Figure 1. Scheme of the units of ethylene brassylate (above) and δ -hexalactone (below).

After the corresponding period of reaction time the product was dissolved in chloroform and precipitated, pouring the polymer solution into an excess of methanol in order to remove the catalyst impurities and those monomers that had not reacted. Finally the product was dried at room temperature and then subjected to a heat treatment at 140 °C for 1 hour to ensure the complete elimination of any remaining solvent. Then, the polymer sample was weighed obtaining the yield of the synthesis process.

Methods

Proton and carbon nuclear magnetic resonance (^1H and ^{13}C NMR) spectra were recorded in a Bruker Avance DPX 300 at 300.16 MHz and at 75.5 MHz of resonance frequency respectively, using 5 mm O.D. sample tubes. All spectra were obtained at room temperature from solutions of 0.7 mL of deuterated chloroform (CDCl_3). Experimental conditions were as follows: a) for ^1H NMR: 10 mg sample; 3 s acquisition time; 1 s delay time; 8.5 μs pulse; spectral width 5000 Hz and 32 scans; b) for ^{13}C NMR: 40 mg, inverse gated decoupled sequence; 3 s acquisition time; 4 s delay time; 5.5 μs pulse; spectral width 18800 Hz and more than 10000 scans.

The assignment of the different signals was made employing the tables of structural determination from Prestch et al. [28]. The copolymer composition data, average sequence lengths and randomness character from Table 1 were calculated by averaging the values of molar contents and the EB-HL dyad relative molar fractions that were obtained by means of ^1H and ^{13}C NMR spectroscopy. Equations 1-3 [29] were employed to obtain the number-average sequence lengths (l_i), the Bernoullian random number-average sequence lengths (l_i) and the randomness character (R):

$$l_{\text{EB}} = \frac{(\text{EB} - \text{EB}) + \frac{1}{2}(\text{EB} - \text{HL})}{\frac{1}{2}(\text{EB} - \text{HL})} = \frac{2(\text{EB})}{(\text{EB} - \text{HL})} ; \quad (1)$$

$$l_{\text{HL}} = \frac{(\text{HL} - \text{HL}) + \frac{1}{2}(\text{EB} - \text{HL})}{\frac{1}{2}(\text{EB} - \text{HL})} = \frac{2(\text{HL})}{(\text{EB} - \text{HL})}$$

$$(l_{\text{HL}})_{\text{random}} = \frac{1}{(\text{EB})} ; \quad (l_{\text{EB}})_{\text{random}} = \frac{1}{(\text{HL})} \quad (2)$$

$$R = \frac{(l_{\text{HL}})_{\text{random}}}{l_{\text{HL}}} = \frac{(l_{\text{EB}})_{\text{random}}}{l_{\text{EB}}} \quad (3)$$

where (HL) and (EB) are the δ -hexalactone and ethylene brassylate molar fractions and (EB-HL) is the EB-HL average dyad relative molar fraction.

200-300 μm films were prepared by pressure melting at 175 $^{\circ}\text{C}$ followed by water quenching. The films were then stored for 24 hours in a fridge (at 0-5 $^{\circ}\text{C}$), the typical storage temperature for biopolymers. From these films repetitive square samples for the *in vitro* degradation study (1x1 cm^2) and repetitive samples for mechanical characterization (10x1 cm^2) were obtained. The specimens for mechanical testing at 37 $^{\circ}\text{C}$ were stored for another 24 hours at 37 $^{\circ}\text{C}$ before tests were conducted at the same temperature. In addition, DSC scans were made at 20 $^{\circ}\text{C min}^{-1}$ for each polymer sample before the mechanical testing, in order to monitor the thermal properties of the specimens.

The mechanical properties were determined by tensile tests with an Instron 5565 testing machine at a crosshead displacement rate of 10 mm min^{-1} . These tests were performed at room temperature (21 \pm 2 $^{\circ}\text{C}$) and at human body temperature (37 $^{\circ}\text{C}$) following ISO 527-3/1995. The specimens had the following dimensions: overall length = 100 mm, distance between marks = 50 mm, width = 10 mm; and were cut from 200-300 μm thick films. The mechanical properties reported (secant modulus at 2 %, yield strength, ultimate tensile strength and elongation at break) correspond to average values of at least 5 determinations. Mechanical testing at 37 $^{\circ}\text{C}$ was conducted in an Instron controlled temperature chamber. The tests were stopped at 300 % of strain due to the size limitations of the temperature chamber.

For the *in vitro* degradation study, square samples (25-35 mg (W_0) ($n = 3$)) of the different copolymers were placed in Falcon tubes containing phosphate buffer solution (PBS) (pH = 7.2) maintaining a surface area to volume ratio equal to 0.1 cm^{-1} . The samples were stored in an oven at 37 $^{\circ}\text{C}$. Three samples of each polymer were removed at different times from the PBS and weighed wet (W_w) immediately after wiping the surface with filter paper to absorb any surface water. These samples were air-dried overnight at 37 $^{\circ}\text{C}$ and then weighed again to obtain the dry weight (W_d). Water absorption (% WA) and remaining weight (% RW) were calculated according to Eqs. (4) and (5). On day 70 and at the end of the degradation study (182 days) the mechanical properties of the poly(ethylene brassylate-co- δ -hexalactone) were also measured at 37 $^{\circ}\text{C}$.

$$\% \text{WA} = \frac{W_w - W_d}{W_d} \cdot 100 \quad (4)$$

$$\% \text{RW} = \frac{W_d}{W_0} \cdot 100 \quad (5)$$

In order to compare the degradation rate of the studied copolymers, the exponential relationship between molecular weight and degradation time for biodegradable polyesters degrading under bulk degradation was used [30-33]:

$$\ln M_w = \ln M_{w0} - K_{Mw} \cdot t \quad (6)$$

$$t_{1/2} = 1/K_{Mw} \cdot \ln 2 \quad (7)$$

where M_w is the weight-averaged molecular weight, M_{w0} is the initial weight-averaged molecular weight, K_{Mw} is the apparent degradation rate and $t_{1/2}$ is the half degradation time (the amount of time required to fall to half the initial value of molecular weight).

The molecular weights of the polymers were determined by GPC using a Waters 1515 GPC device equipped with two Styragel columns ($10^2 - 10^4 \text{ \AA}$). Chloroform was used as eluent at a flow rate of 1 mL min^{-1} and polystyrene standards (Shodex Standards, SM-105) were used to obtain a primary calibration curve. The samples were prepared at a concentration of 10 mg in 2 mL. The reported values are likely to be higher than the actual molecular weights owing to the differences in the hydrodynamic volume of the copolymers and the polystyrene.

The thermal properties of the polymers were studied on a DSC 2920 (TA Instruments). Samples of 6-9 mg were melted at $130 \text{ }^\circ\text{C}$ and then quenched to $5 \text{ }^\circ\text{C}$ at different cooling rates ($5, 10, 20$ and $30 \text{ }^\circ\text{C min}^{-1}$) to study the crystallization process during the cooling. Finally, a scan was also made at $20 \text{ }^\circ\text{C min}^{-1}$ from -85 to $130 \text{ }^\circ\text{C}$ to determine the glass transition temperature (T_g), the melting temperature (T_m) and the heat of fusion or melting enthalpy per gram (ΔH_m) of the samples. During the *in vitro* degradation study, the DSC samples were heated from $21 \text{ }^\circ\text{C}$ to $130 \text{ }^\circ\text{C}$ at $20 \text{ }^\circ\text{C min}^{-1}$, immediately after the drying at $37 \text{ }^\circ\text{C}$ of the polymer samples removed from the degradation medium.

After this first scan, the samples were quenched in the DSC and a second scan was made from -85 °C to 130 °C at 20 °C min⁻¹.

Wide angle X-ray diffraction (WAXRD) data were collected on a Bruker D8 Advance diffractometer operating at 30 kV and 20 mA. This device is equipped with a Cu tube ($\lambda = 1.5418 \text{ \AA}$), a Vantec-1 PSD detector and an Anton Parr HTK2000 high-temperature furnace. The powder patterns were recorded in 2θ steps of 0.033° in the $10 \leq 2\theta \leq 38$ range, counting for 0.2 s per step, from 30 to 120 °C every 2 °C using a heating rate of $0.16 \text{ }^\circ\text{C s}^{-1}$. The degree of crystallinity (χ_c) was determined as the ratio of the crystalline peak areas to the total area under the scattering curve, while the average crystal size was obtained employing the Scherrer equation [34] with a shape factor “k” of 0.90. The latter data were calculated from the two most intense peaks in the diffraction pattern: at $2\theta = 21.7^\circ$ and at $2\theta = 24.1^\circ$. On the other hand, the estimated melting temperatures (T_{ms}) are the temperatures until the crystalline phase became stable.

Thermal degradation was studied under nitrogen by means of thermogravimetric analysis (TGA) into a TGA model Q50-0545 (TA Instruments). Samples of 10-15 mg were heated from room temperature to 500 °C at a heating rate (β) of $5 \text{ }^\circ\text{C min}^{-1}$, with the heat flow, sample temperature, residual sample weight and its time derivative being continuously recorded. In this temperature range, the polymers degraded completely.

Cell culture studies

Human Dermal Fibroblasts (HDFs)

Human Dermal Fibroblasts (HDFs) were grown in T75 flasks using DMEM with 10 % FBS and 1 % PS. The cells were incubated at 37 °C in a 5 % CO₂ atmosphere. The culture medium was changed every 3 days. The cells were then harvested and sub-cultured when > 90 % confluence was observed.

Cell Seeding

For the metabolic activity study, HDFs were seeded on sterilized samples (circles 9 mm in diameter) at a density of 25000 cells/cm² on a 48 well tissue culture plate and

incubated in 0.5 mL of DMEM with 10 % FBS and 1 % PS (37 °C, 5 % CO₂). As a control, the cells were also seeded on a tissue culture plastic. The culture medium was replaced on the third day after seeding. With regard to the staining, HDFs were seeded on sterilized samples (circles 9 mm in diameter) at a density of 11000 cells/cm² on a 24 well tissue culture plate and incubated in 1 mL of DMEM with 10 % FBS and 1 % PS (37 °C, 5 % CO₂). As a control, the cells were also seeded on 13 mm sterile glass coverslips onto cell culture well. The culture medium was replaced on the third day after seeding.

Cell Viability Studies

AlamarBlue[®] assay was performed to quantify the metabolic activity of the HDFs seeded on two poly(ethylene brassylate-co- δ -hexalactone) (EB-HL 90 and EB-HL 63). After 1, 3 and 7 days, the cells were washed with HBSS and replaced with 0.5 ml of fresh culture media with AlamarBlue[®] (10 % v/v). After 4 hours of incubation at 37 °C in 5 % CO₂ (sheltered from the light), 100 μ l of assay media was transferred to a 96 well plate, the absorbance at 550 and 595 nm was read on a microplate reader (VarioskanFlash) and the percentage reduction of the dye was calculated.

The morphology of HDFs seeded on the copolymers was analyzed via rhodamine phalloidin and Hoechst staining. After 1, 3 and 7 days, cells were washed with HBSS and subsequently fixed with 4 % paraformaldehyde for 15 minutes at room temperature. Then, the cells were washed twice with HBSS and permeabilized with 0.5 % Triton X-100 in PBS for 10 minutes. After washing twice with PBS, cells were incubated with 1 % Bovine Serum Albumin solution in PBS for 30 minutes. Afterwards, the cells were stained with Rhodamine Phalloidin solution for 15 minutes and thoroughly washed with PBS-T (0.1 % Tween 20). Finally, the nuclei of HDFs were stained with Hoechst staining solution for 3 minutes and subsequently washed three times with PBS. Samples were observed with an inverted fluorescent microscope (Olympus IX81).

Statistics

Statistical differences were analyzed using one-way analysis of variance (ANOVA) with p-values of < 0.05 being considered significant. Experiments for metabolic activity

were performed in triplicate and each assay was repeated three times. For nuclei quantification 10 micrographs per replica were acquired resulting in the acquisition of 30 micrographs per sample.

6.3. Results and discussion

Synthesis characterization

Table 1. Characterization data of the EB-co- δ -HL copolymers of differing compositions synthesized at 130 °C with a monomers/catalyst molar ratio of 100.

Sample	Feed Molar Composition		Composition ¹ (% molar)		Yield (%)	Conversion (%)		M _w kg mol ⁻¹	D	Microstructural Magnitudes ²		
	%EB	%HL	%EB	%HL		EB	HL			<i>I</i> _{EB}	<i>I</i> _{HL}	<i>R</i>
PEB	100	0	100	0	75.0	75.0	-	270.9	2.16	-	-	-
EB-HL 90	79.2	20.8	89.8	10.2	86.9	92.1	39.8	182.4	1.86	11.69	1.32	0.84
EB-HL 83	70.5	29.5	82.6	17.4	85.2	92.0	46.4	289.8	2.29	7.50	1.58	0.77
*3 days of reaction	70.5	29.5	87.5	12.5	79.3	88.0	30.1	285.3	2.07	10.61	1.52	0.75
EB-HL 79	62.8	27.2	78.8	21.2	78.9	88.6	40.2	228.2	1.96	6.58	1.77	0.72
EB-HL 70	55.9	44.1	70.3	29.7	80.0	90.5	48.4	228.4	2.21	4.70	1.99	0.72
*3 days of reaction	55.9	44.1	77.2	28.2	74.6	86.2	39.9	152.6	1.86	6.99	2.07	0.63
EB-HL 63	47.3	52.7	63.3	36.7	76.6	90.5	47.1	156.4	1.89	3.82	2.21	0.71
EB-HL 49	34.0	66.0	49.0	51.0	71.3	90.1	48.4	148.1	2.00	2.57	2.68	0.76

¹ Calculated averaging the copolymer molar compositions obtained by ¹H and ¹³C NMR

² *I*_{EB} and *I*_{HL} are the EB and HL number average sequence lengths of the EB-co- δ -HL copolymers obtained from the average dyad relative molar fraction (EB-HL) in ¹³C NMR. These values are compared to the Bernoullian random number-average sequence lengths obtaining the randomness character value (*R*) of the different copolymers.

Table 1 summarizes the characterization data of several poly(EB-co- δ -HL) of differing compositions synthesized at 130 °C with a monomers/catalyst molar ratio (M/C) of 100. As can be seen, the yields of reaction of the PEB homopolymer (polymerized for 3 days) along with those of the two copolymers also synthesized for 3 days were under 80 %. In order to ensure a higher yield and a final composition closer to the feed composition, the remaining reactions were conducted over 6 days. Regarding the molecular weights of the copolymers, these are within the 148 to 290 kg mol⁻¹ range, while their dispersity values vary between 1.86 to 2.29. The weight average molecular

weights (M_w) increase proportionally with the EB molar content, with the exception of PEB and the copolymer with 90 % of EB. In these two cases, 0.05 to 0.1 g of 1-hexanol was added to limit the molecular weight because polymers with M_w (measured by GPC) above 400 kg mol^{-1} were obtained when 1-hexanol was not added.

The EB molar content in this set of copolymers ranges from 49 % (EB-HL 49) to ~ 90 % (EB-HL 90) with average sequence lengths of EB (l_{EB}) between 2.57 to 11.69 and l_{HL} from 1.32 to 2.68. . As can be seen in Table 1, higher reaction yields and molecular weights were obtained when the feed was richer in EB. Since the conversion of EB was higher than that of δ -HL in all the precipitated products, this suggests that the reactivity of EB is higher than that of δ -HL. Hence, under these conditions of synthesis, the consumption of EB was faster than δ -HL owing to the lower reactivity of the latter. As a result of the different reactivity of the comonomers, the synthesis reactions lead to gradient copolymers with a slightly deviated from random distribution of sequences ($R \rightarrow 1$). The randomness character (R) value was, in all cases, higher than 0.71 with the exception of one of the copolymers synthesized for 3 days.

NMR Characterization

The calculus of the molar composition of the ethylene brassylate-co- δ -hexalactone copolymers in this study was made by averaging the results obtained from ^1H and ^{13}C NMR spectroscopy. On the contrary, the data of average sequence lengths and randomness character were estimated on the basis of the EB-HL dyad relative molar fractions that were acquired only from the ^{13}C NMR spectra. Figure 2 and Figure 3 present the ^1H and ^{13}C NMR spectrum of the EB-co- δ -HL copolymer with 49 % of ethylene brassylate (EB-HL 49).

In the ^1H NMR spectrum, the analysis of the molar composition was conducted in two ways. By comparing the signals of the δ -HL methine at around 4.92 ppm (carbon **5'**) with regard to the EB methylenes bonded to the ester group (carbons **14** and **15**), which appear centered at 4.28 ppm, or using the signal of the δ -HL methylene (carbon **2'**), which is overlapped with the hydrogens of the methylenes **2** and **12** of the ethylene brassylate at approximately 2.33 ppm. The rest of the peaks (see scheme in Figure 1) are

assigned to the other hydrogens of the copolymer in Table 2, although some signals appear overlapped.

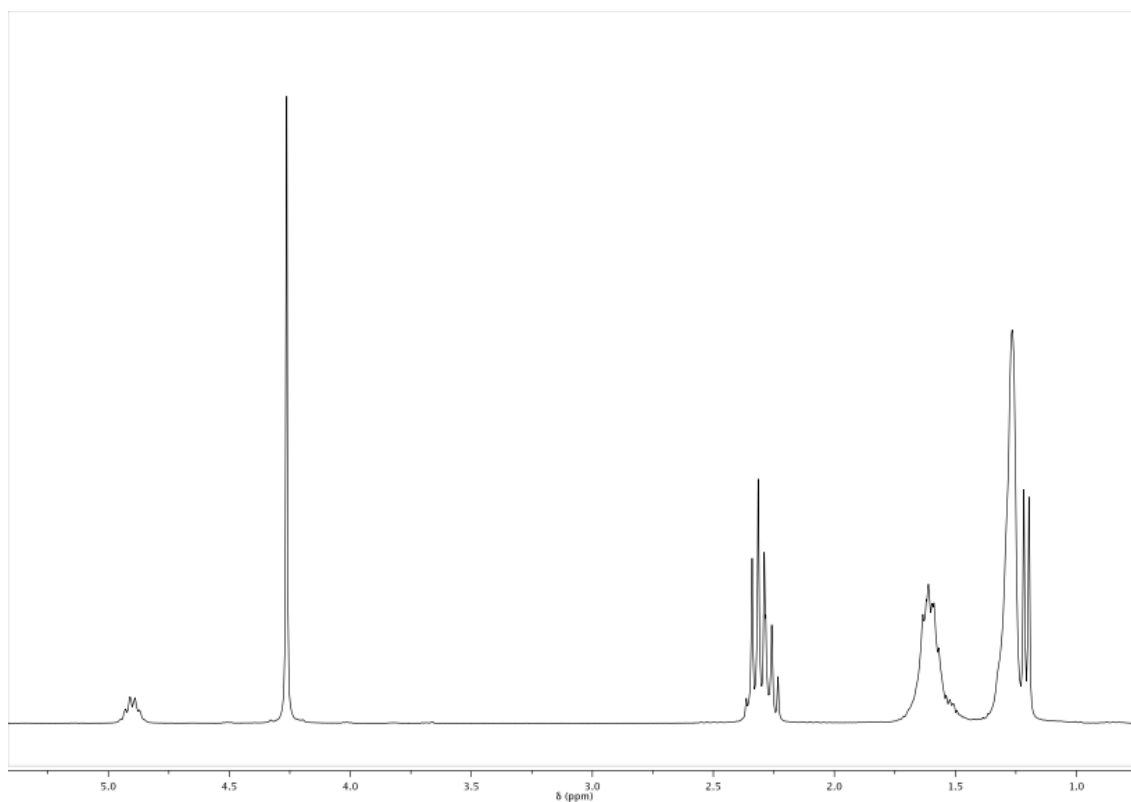


Figure 2. ^1H NMR spectrum of EB-HL 49.

Table 2. Assignment of the different signals to the hydrogens of the EB-co- δ -HL.

Number of C	H EB	H δ -HL
	δ (ppm)	δ (ppm)
1	-	-
2	2.33	2.28, 2.36
3	1.63	1.60
4	1.30	1.60
5		4.92
6		1.22
7		
8		
9		
10		
11	1.63	
12	2.33	
13	-	
14	4.28	
15	4.28	

The different signals appearing in the ^{13}C NMR spectrum between 19 and 175 ppm of chemical shift (δ) are assigned in Table 3 to the different carbons numbered in Figure 1. Hence, the molar composition of these copolymers can be easily determined by comparison of the areas under the peaks due to the δ -HL and EB carbons. In the case of the δ -hexalactone, the signals employed were those of the carbonyl carbon at 172.85 ppm (carbon **1'**), the methine centered at 70.15 ppm (carbon **5'**), the methylene **3'** at 20.70 ppm and the methyl side chain (carbon **6'**). Regarding the ethylene brassylate, an average relative value was calculated using the signals of the methylenes bonded to the ester group (carbons **14** and **15**) which appear at 61.95 ppm, and those from the methylenes **2** and **12** at 34.04 ppm, **3** and **11** at 24.90 ppm and the seven methylenes from carbons **4** to **10**, which peaks are overlapped at 29.04-29.16 ppm.

Table 3. Assignment of the different signals to the carbons of the EB-co- δ -HL.

Number of C	C EB	C δ -HL
	δ (ppm)	δ (ppm)
1	173.37 <u>EB</u> -HL 173.47 EB-EB	172.80 HL-HL 172.92 <u>HL</u> -EB
2	34.04	34.58, 34.59
3	24.80 EB-EB 24.97 <u>EB</u> -HL	20.64 <u>HL</u> -EB 20.78 HL-HL
4	29.04-29.16	35.15
5		69.96 EB-HL-EB 70.05 HL-HL-EB 70.21 EB-HL-HL 70.29 HL-HL-HL
6		19.6
7		
8		
9		
10		
11	Equal to C3	
12	Equal to C2	
13	Equal to C1	
14	61.91 EB-EB 62.07 <u>EB</u> -HL	
15	Equal to C14	

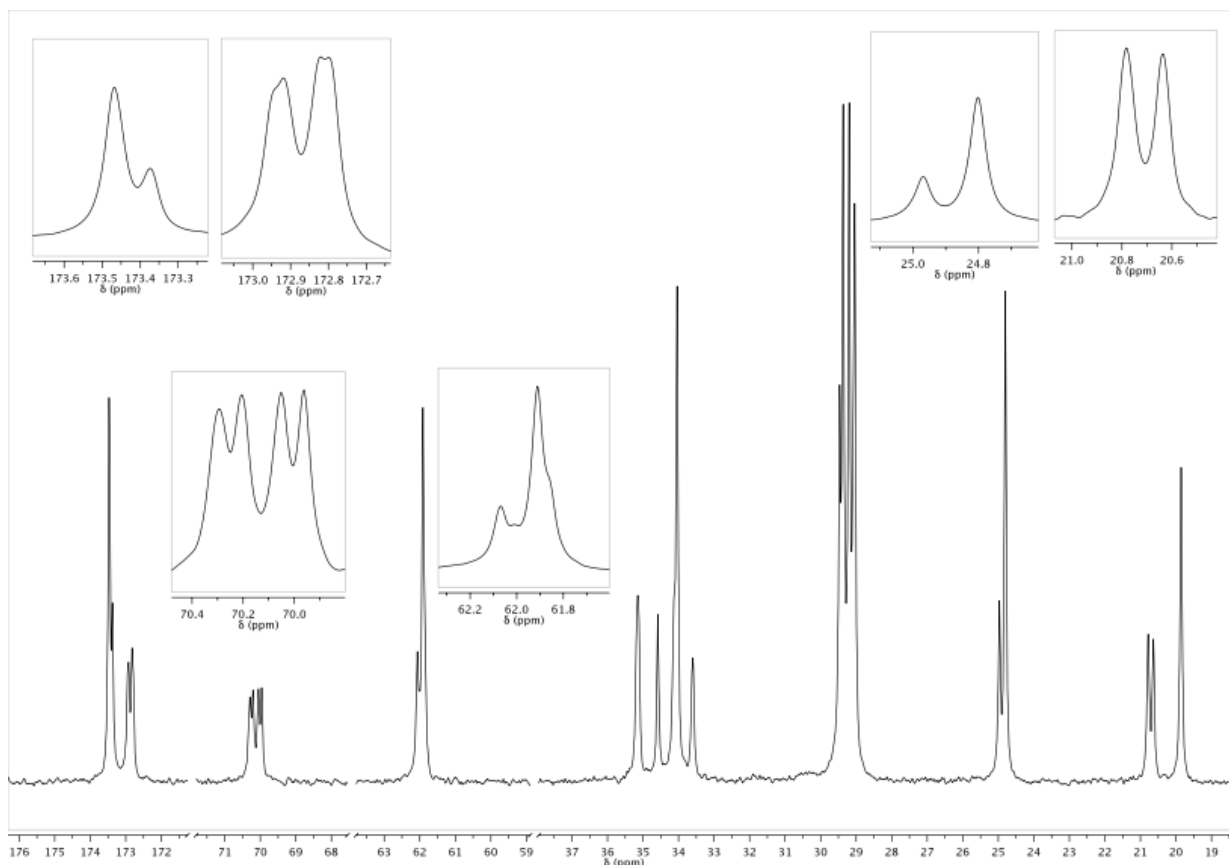


Figure 3. ^{13}C NMR spectrum of EB-HL 49 with some regions of interest enlarged.

As can be observed in the enlargement of Figure 3, some of the carbons show sequence sensitivity. The different dyads and triads found in the ^{13}C NMR spectrum are also marked in Table 3 (underlining is used to emphasize that the analysed nuclei belong to that unit). For the estimation of the chain microstructure parameters the average dyad relative molar fraction (EB-HL) was determined. This variable is the sum of the (EB-HL) and (EB-HL) average dyad relative molar fractions. The first value was obtained from the EB-HL dyads at 173.37, 62.07 and 24.97 ppm while the (EB-HL) molar fraction was estimated based on the EB-HL dyads at 172.97 and 20.78 ppm and the value provided by the triads. From the peaks of the EB-HL-EB, HL-HL-EB, EB-HL-HL and HL-HL-HL triads, which appear from left to right at around 70.15 ppm, (EB-HL) average dyad relative molar fractions can also be obtained using the equation (8) in which (HL) is the previously calculated δ -hexalactone average molar fraction.

$$(\text{EB} - \underline{\text{HL}}) = \frac{I_{\text{EB-HL-EB}} + \frac{1}{2}(I_{\text{HL-HL-EB}} + I_{\text{EB-HL-HL}})}{I_{\text{EB-HL-EB}} + I_{\text{HL-HL-EB}} + I_{\text{EB-HL-HL}} + I_{\text{HL-HL-HL}}} * (\text{HL}) \quad (8)$$

Thermal properties

In this section the crystallization and melting behaviour of the copolymers from Table 1 were studied. Firstly, several cooling treatments at different rates (5, 10, 20 and 30 °C min⁻¹) were conducted in the DSC. The crystallization temperatures (T_c) and the enthalpy of crystallization (ΔH_c) of each material are shown in Table 4. As can be seen, the differences between the respective ΔH_c from the same polymer were small (the slight exception being EB-HL 49) and the EB chains crystallized from the melt very fast. A cooling rate of 30 °C min⁻¹ was sufficient for crystallization of the polymers from the melt while slower cooling rates only result in small increases in ΔH_c . Likewise, the crystallization peaks of each polymer appeared at a higher temperature as the cooling rate decreased. This is due to the fact that at lower cooling rates the crystal nuclei have more time to develop.

Table 4. Crystallization enthalpies and temperatures obtained for the EB-co- δ -HL copolymers at cooling rates in the 5 - 30 °C min⁻¹ range.

Sample	5 °C min ⁻¹		10 °C min ⁻¹		20 °C min ⁻¹		30 °C min ⁻¹	
	ΔH (J g ⁻¹)	T_c (°C)	ΔH (J g ⁻¹)	T_c (°C)	ΔH (J g ⁻¹)	T_c (°C)	ΔH (J g ⁻¹)	T_c (°C)
PEB	91.1	52.1	86.5	49.2	84.8	44.7	83.5	40.9
EB-HL 90	89.3	47.9	86.0	47.2	85.0	40.2	84.9	35.4
EB-HL 83	76.0	41.2	75.2	36.8	71.6	29.0	69.1	21.5
EB-HL 79	74.3	36.4	67.4	34.6	68.7	24.7	64.9	20.4
EB-HL 70	63.4	28.3	62.1	25.0	60.0	19.9	60.0	16.0
EB-HL 63	58.8	25.5	58.0	22.8	55.6	18.6	54.5	14.2
EB-HL 49	40.6	16.4	35.6	13.8	35.1	9.3	33.3	6.1

The DSC heating curves obtained after the cooling treatments were virtually identical for each polymer, all of them having practically the same melting temperatures and enthalpies (T_m and ΔH_m) after the cooling process. Figure 4 shows the DSC curves of scans made from -85 to 130 °C at 20 °C min⁻¹ while the data obtained from them (the glass transition temperature (T_g) with its associated heat capacity (ΔC_p) and the melting

enthalpies and temperatures) are summarized in Table 5 along with the T_m , the crystal fraction (χ_c) and the average crystal size (c.s.) from Wide Angle X-ray Scattering.

Table 5. Calorimetric and X-ray Diffraction data of the EB-co- δ -HL copolymers.

Sample	t_{EB}	T_m^1	X_c	c.s.	ΔH_m	T_m^2	T_g	ΔC_p
		$^{\circ}C$	(%)	nm	$J g^{-1}$	$^{\circ}C$	$^{\circ}C$	$J g^{-1} ^{\circ}C^{-1}$
PEB	-	67.0	47.0	19	96.4	70.6	-27.0	0.34
EB-HL 90	11.69	64.0	34.6	30	92.4	62.7	-31.1	0.31
EB-HL 83	7.70	58.0	38.9	20	74.4	65.0	-28.3	0.31
EB-HL 79	6.58	56.0	28.1	32	64.7	61.4	-31.9	0.36
EB-HL 70	4.70	49.0	29.5	24	59.6	57.5	-33.4	0.34
EB-HL 63	3.82	47.0	22.6	41	55.5	49.6	-36.7	0.35
EB-HL 49	2.57	35.0	25.7	10	40.8	31.0	-41.2	0.36

¹ Obtained by WAXS. This is the crystalline phase-stable temperature.

² Obtained from a DSC at $20^{\circ}C min^{-1}$ from -85 to $130^{\circ}C$. The melting point of the peak that appears at the highest temperature was chosen because this is related to the most perfect crystals.

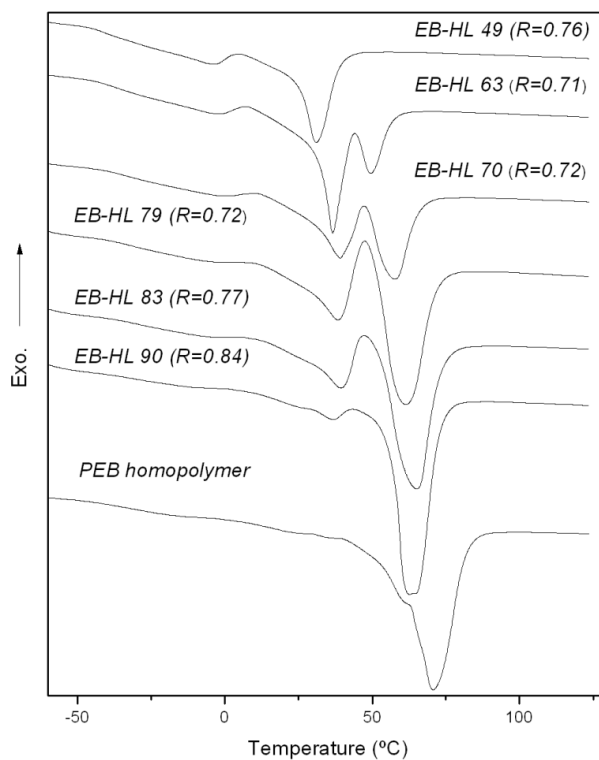


Figure 4. DSC heating curves at $20^{\circ}C min^{-1}$ from -85 to $130^{\circ}C$ of the different EB-co- δ -HL copolymers.

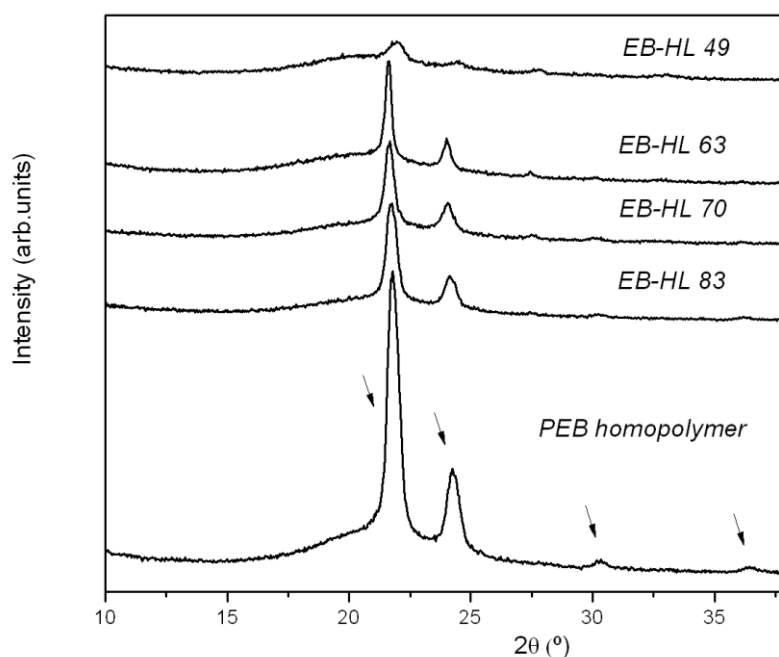


Figure 5. WAXS profiles of PEB and the EB-co- δ -HL copolymers in the $10 \leq 2\theta \leq 38$ range.

Figure 5 shows the diffraction profiles of some poly(EB-co- δ -HL) together with the diffractogram of the reference homopolymer (PEB). As can be seen, at higher contents of δ -HL in the copolymers the reflection intensity decreases. However, the poly(EB-co- δ -HL) presented exactly the same signals as PEB at 2θ of 21.7, 24.1, 30.2 and 36.4° (the small peak at 27.3° may be due to the bismuth compounds because it also appeared at high temperatures when the polymers were fully amorphous). Hence, it was demonstrated that the EB-co- δ -HL copolymers and the PEB present the same crystal structure and confirms that only the EB units were able to crystallize.

As can be observed in Figure 4, the PEB homopolymer and the EB rich copolymers showed narrower melting peaks and a higher crystallization capability in comparison to other copolymers such as EB-HL 49, the poly(EB-co- δ -HL) that presented the lowest melting peak. As the δ -hexalactone content increased, the melting peak split into two or more peaks while in the case of EB-HL 83 and EB-HL 79, a recrystallization peak also appeared between two of the melting peaks. During the heating, some imperfect crystals melt, then others form and finally the new crystallites and the more perfect crystal population melt. With regard to their glass transition behaviour, the T_g s shifted to lower

values when the δ -HL content increased and the ΔC_p values stayed almost constant as the amorphous phase increased. The measured values were between -31 and -41 °C, temperatures lower than those of the PEB homopolymer (T_g at -27 °C).

The EB-co- δ -HL copolymers, with EB content between 49 to 90 % and average sequence lengths of EB in the range of 2.57 - 11.69, presented ΔH_m s values between ~ 41 to 92 J g⁻¹ and T_m s in the range of 31 to 62 °C (the melting point of the peak that appears at the highest temperature was chosen because this is associated with the most perfect crystals), values consistent with the T_m s obtained by WAXS (from 35 to 64 °C). As expected at higher δ -HL contents, the degree of crystallinity of the copolymers fell, down to between 22.6 to 38.9 %. On the other hand, PEB homopolymer showed a melting peak of 96.4 J g⁻¹ at ~ 71 °C with an associated crystalline fraction of 47.0 %, a higher value than that of poly(ϵ -caprolactone) but lower than that of poly(ω -pentadecalactone) (with a χ_c of 53.8 %, a ΔH_m of 136.1 J g⁻¹ and a T_m at 104 °C) [35-37]. The calculated average crystal sizes of the copolymers were in the 20 to 41 nm range, all values higher than the estimate for the homopolymer which had an average crystal size of 19 nm. The crystal size distribution is very wide and this is why the DSC melting peaks were found to be so broad. It might be possible that there are large differences between the thickest and the thinnest crystallites and for this reason discordant values were obtained (such as the c.s. of EB-HL 49).

Thermogravimetric analysis

Figure 6 shows the curves of percent weight loss and first derivative of weight loss against temperature (TG and DTG curves) of the PEB homopolymer and the EB-co- δ -HL copolymers. As can be seen, the copolymers began thermal degradation at around 225 °C and were completely decomposed at 475 °C. Three well-defined peaks can be distinguished in the DTG curves. The first stage of depolymerization at around 250 °C was attributed to the decomposition of δ -HL-rich sequences, which is accelerated by the residual metal compounds from the catalyst [38]. This peak did not appear in the curve of the PEB and were more pronounced in the case of EB-HL 49, the copolymer with the highest δ -HL content. The second peak, more intense than the first, appeared at 350 °C and covers the degradation of the bismuth free blocks of δ -HL and the decomposition of

some metal accelerated sequences of EB. As the EB content rose, the intensity of this peak decreased, and at the same time it shifted to slightly higher temperatures. These first two peaks of thermal degradation, in which all the δ -HL decomposed, were also reported in the pyrolysis of poly(ω -pentadecalactone-co- δ -hexalactone) at the same temperatures [21] but were not found in the curve of the PEB homopolymer. On the other hand, the thermal degradation of most of the ethylene brassylate was delayed to ~ 425 °C, the most significant stage of depolymerization. In the case of the PEB homopolymer, a single peak appeared in the DTG curve at a temperature similar to that of the poly(ω -pentadecalactone), this only has one ester group in each structural unit instead of the two of the ethylene brassylate.

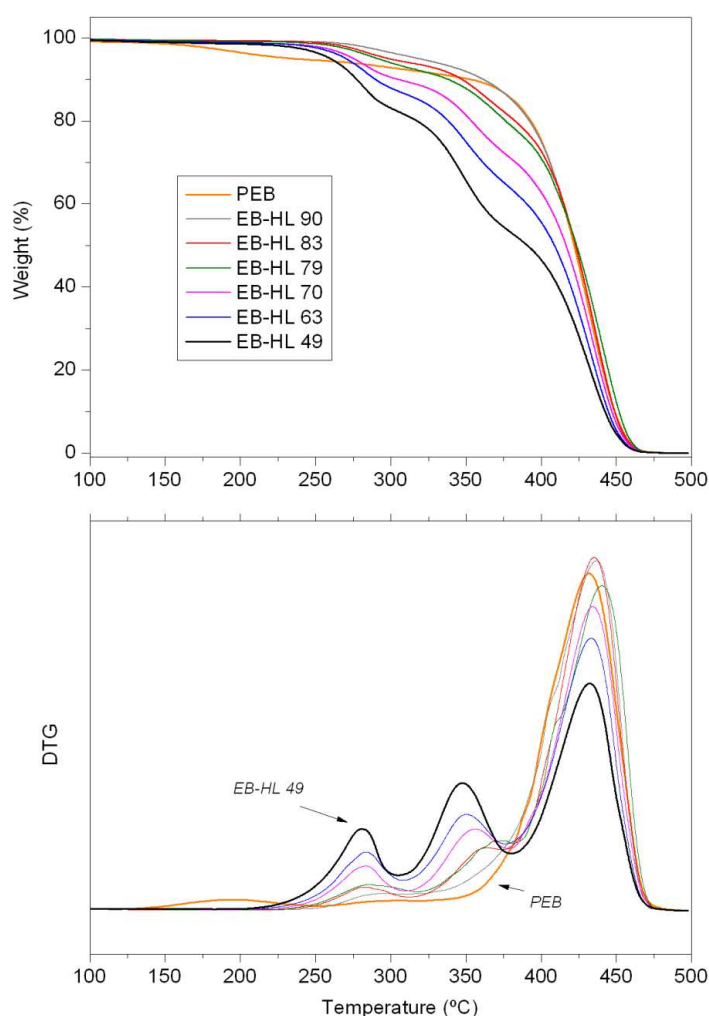


Figure 6. Thermogravimetric (TG) and differential thermogravimetric (DTG) curves of PEB and the EB-co- δ -HL copolymers.

Hydrolytic degradation study

A hydrolytic degradation study was conducted over 182 days with films of the ethylene brassylate-co- δ -hexalactone copolymers. DSC scans were made from 21 to 130 °C: at room temperature (before submerging the samples in PBS), after storage for 24 hours at 37 °C and at different degradation times (after drying). The data relating to melting enthalpies and temperatures at the start, on day 70 (when mechanical tests were performed) and at the end of the study are gathered in Table 6.

Table 6. Melting enthalpies and temperatures of all the polymer films at the start and at the end of the degradation study.

Sample	21 °C		37 °C		On day 70 of degradation at 37 °C		On day 182 of degradation at 37 °C	
	ΔH (J g ⁻¹)	T _m (°C)	ΔH (J g ⁻¹)	T _m (°C)	ΔH (J g ⁻¹)	T _m (°C)	ΔH (J g ⁻¹)	T _m (°C)
EB-HL 90	86.4	70.5	97.6	65.5	99.4	75.7	100.1	75.5
EB-HL 83	72.8	66.4	83.7	66.5	86.0	67.4	93.9	71.4
EB-HL 79	65.1	61.7	82.7	61.3	85.8	67.4	90.7	68.3
EB-HL 70	50.5	56.3	64.5	57.9	74.2	61.8	74.6	63.0
EB-HL 63	48.7	55.4	50.5	55.9	60.1	58.2	61.4	61.2
EB-HL 49	9.9	36.3	10.6	49.3	20.0	52.0	18.9	50.3

It can be noted from the DSC results that there are some differences between the melting behaviours of the poly(EB-co- δ -HL) films at 21 °C and after storage at 37 °C for 24 hours. The copolymers presented higher melting peaks after being stored for 24 hours at 37 °C while their T_m values shifted to higher temperatures, especially in the case of EB-HL 49 (from 36.3 °C to 49.3 °C). These rearrangements in the crystalline phase occurring at 37 °C were the result of the appearance of new crystallites that melt at higher temperatures, and also the disappearance of other crystalline structures with melting points between 21 °C to 37 °C or below room temperature. Hence, it was also found that the ΔH_m of EB-HL 49, which had a value of 40 J g⁻¹ after conducting a scan from -85 to 130 °C (see Table 5), crystallized only ~ 10 J g⁻¹ in the heating scans from 21 °C. The crystallization temperature of this copolymer was the lowest and, as has be

seen earlier, when it was cooled from 130 °C at a rate of 5 °C min⁻¹ it showed a T_c of approximately 16 °C.

In addition, it can be observed that on days 70 and 182 of degradation (there are no large differences in the melting behaviour within this timeframe), the samples were slightly more crystalline with higher ΔH_m values than at the start of the study. The more important changes occurred in the first week submerged in PBS and then the melting peak became almost stable. However, the T_m values shifted progressively to higher temperatures (2–7 °C higher), a tendency that is observed for all the materials owing to rearrangements of the crystalline phase. These changes in the thermal properties are more obvious in the case of the copolymers with lower EB contents. Therefore, the final ΔH_m for EB-HL 49 reached a value of around 20 J g⁻¹, twice the value recorded at the start of the study.

Figure 7 shows the remaining weight (RW) and water absorption (WA) curves obtained from the *in vitro* degradation study of the poly(ethylene brassylate-co- δ -hexalactone). As can be observed in the plot, the weight of the samples remained almost constant during the entire study. The molecular weight has to be reduced substantially ($M_w < 25$ kg mol⁻¹) to permit mass loss through solubilization of the oligomers and in this work no copolymer reached a low enough molecular weight. Moreover, water uptake was negligible and did not exceed a value of 3 % in any case. Only EB-HL 49 might be less resistant to water absorption owing to its more amorphous structure.

Figure 8 shows the progress of $\ln M_w$ against degradation time of the poly(ethylene brassylate-co- δ -hexalactone). As the degradation progressed, the weight average molecular weight (M_w) of the samples fell while the associated dispersity rose slightly. Therefore, the M_w of EB-HL 90, EB-HL 83, EB-HL 79, EB-HL 70, EB-HL 63 and EB-HL 49 decreased to final values of 108, 134, 126, 112, 87 and 77 kg mol⁻¹. In the latter case, this material displayed a macroscopic morphological deterioration after day 126 but as a result of the crystallization process became easier to handle from day 7 onward.

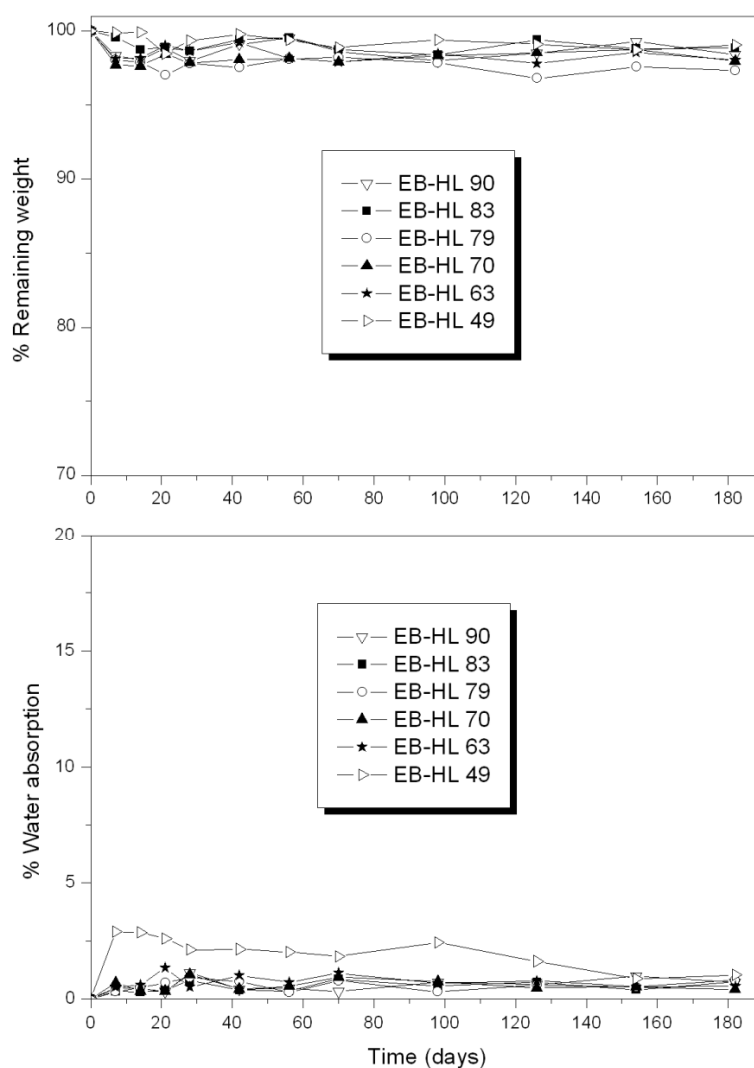


Figure 7. Evolution of the remaining weight and the water absorption of the poly(ethylene brassylate-co- δ -hexalactone).

Table 7 presents the values recorded for the degradation rate (K_{M_w}) and half degradation times ($t_{1/2}$) calculated from the slope of the fitting curve. The M_w experimental data adapts well to the fitting curve ($R^2 > 0.95$) over the 182 days. However, it seems that the drop in $\ln M_w$ is more pronounced in the first 70 days of the study, it then falls more slowly. Due to this fact, the regression line did not fit the data more perfectly. EB-HL 90, with the largest average sequence length of ethylene brassylate, exhibited the lowest degradation rate (0.0028 days^{-1}), 3 times higher than that of the PCL homopolymer (0.0010 days^{-1}) [8], while the rest of poly(EB- δ -HL) presented K_{M_w} in the range of 0.0032 - 0.0041 days^{-1} with corresponding $t_{1/2}$ of 169 to 217 days. The incorporation of δ -

HL had little effect on the degradation rate and these minor variations in K_{Mw} may be due to the differences in initial molecular weight and chain microstructure.

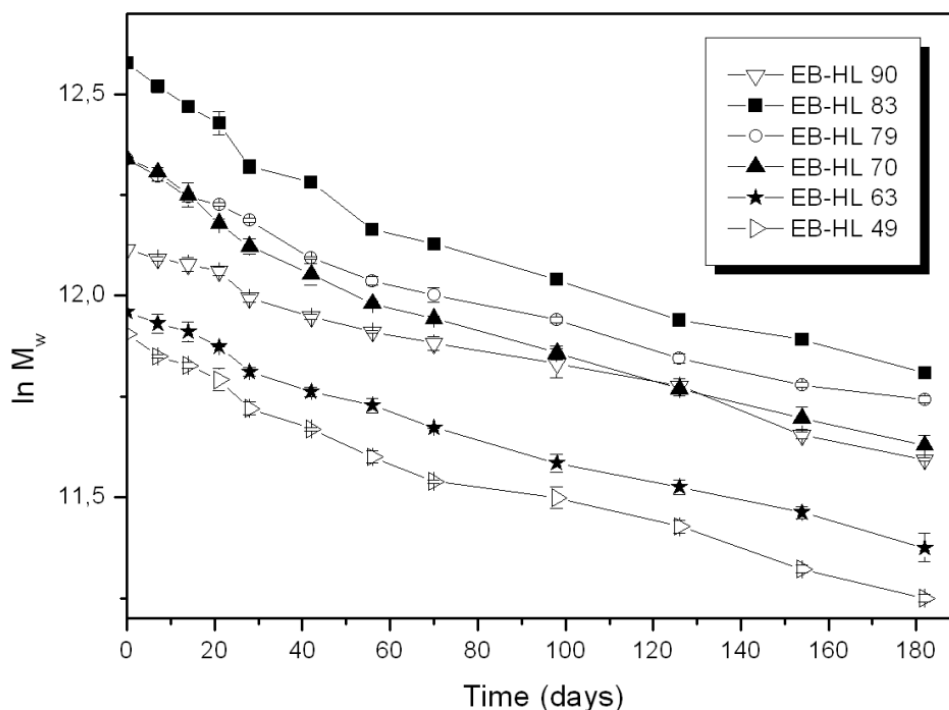


Figure 8. $\ln M_w$ against degradation time of the EB- δ -HL copolymers.

Table 7. K_{Mw} , calculated on the final day of the study (day 182), and $t_{1/2}$ of the poly(EB-co- δ -HL).

Sample	K_{Mw} (days ⁻¹)	Half-molecular weight degradation time $t^{1/2}$ (days)
EB-HL 90	0.0028	248
EB-HL 83	0.0041	169
EB-HL 79	0.0033	210
EB-HL 70	0.0038	182
EB-HL 63	0.0032	217
EB-HL 49	0.0035	198

Mechanical Properties

Table 8 summarizes the mechanical testing results at 21° and at 37 °C (at the start and on day 182 of degradation) for the poly(ω -PDL-co- δ -HL) films, whose DSC data, before performing the mechanical tests, can be seen in Table 6. As can be seen in the table and in Figure 9, which displays the typical stress-strain curves of the polymers

studied at 21 °C, the EB-co- δ -HL copolymers showed a marked improvement in flexibility (with lower secant modulus and increased strain recovery rates) compared to PEB homopolymer, without losing any ductility (deformation at break values > 918 %). Nevertheless, it proved impossible to measure the mechanical properties of EB-HL 49 because its film was too soft and sticky due to its low melting temperature (T_m at 30-35 °C). The PEB presented a secant modulus value of 308 MPa, ultimate strength of ~ 26 MPa and an elongation at break of around 937 %, results that are in accordance with those of other homopolyesters such as poly(ω -pentadecalactone) and poly(ϵ -caprolactone) (with secant modulus from 300 to 400 MPa, ultimate tensile strength of 28-32 MPa and deformation at break values > 750 %) [8,37]. On the other hand, the ethylene brassylate-co- δ -hexalactone copolymers, with EB molar content from 63 to 90 %, exhibited secant modulus in the range of 57.4-273.5 MPa at 21 °C, tensile strengths at break of 7.5-16.5 MPa and strain recoveries from 37.9 to 52.8 %. All the polymers presented yield points which were broader and less defined as the δ -HL content increased.

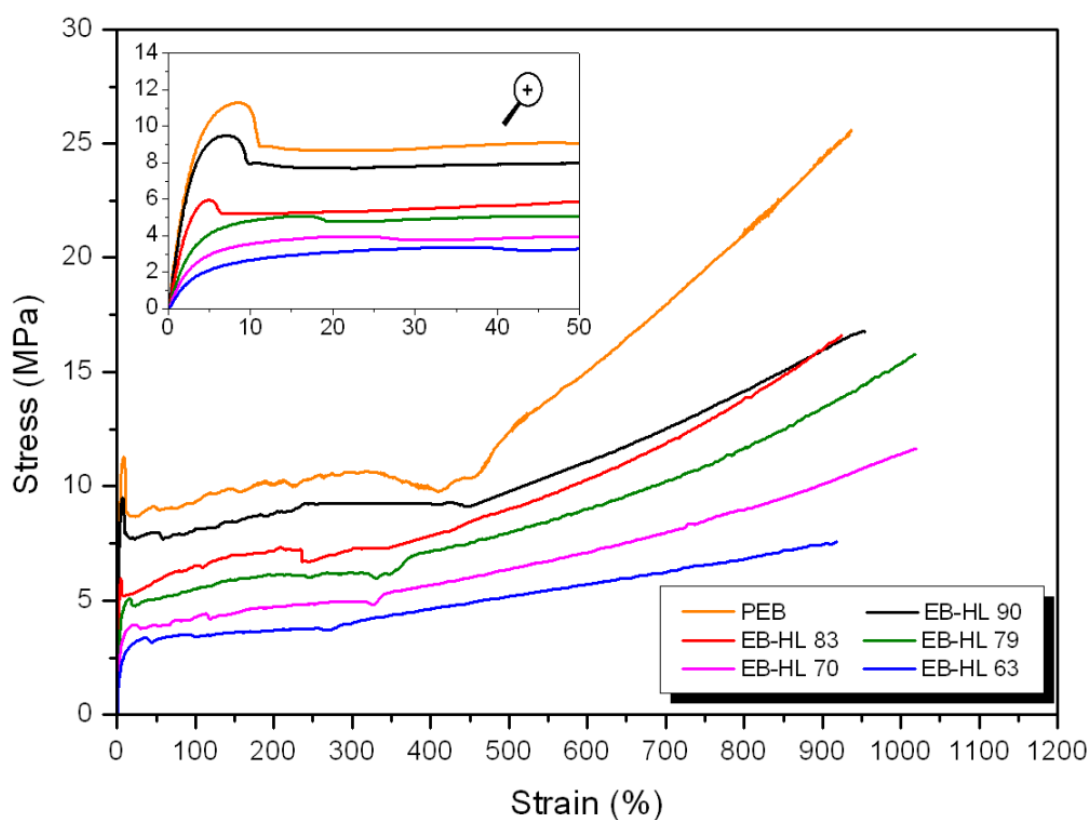


Figure 9. Tensile stress-strain curves of PEB and the EB-co- δ -HL copolymers at 21 °C.

Table 8. Mechanical properties of the PEB and the EB-co- δ -HL copolymers.

Sample	Testing Temperature ¹	Secant Modulus at 2 %	Yield Strength (Yield Point)	Tensile Strength at 300 % ²	Ultimate Tensile Strength ³	Elongation at break	Strain Recovery after break ⁴
		(MPa)	(MPa)	(MPa)	(MPa)	(%)	(%)
PEB	21 °C	307.6 ± 14.3	11.1 ± 0.5 (8.0 %)	10.5 ± 0.3	25.9 ± 7.0	937	34.1 ± 2.6
	37 °C	250.8 ± 8.5	7.3 ± 0.5 (4.4 %)	8.4 ± 0.8	-	> 300	
EB-HL 90	21 °C	273.5 ± 11.4	8.9 ± 0.6 (6.4 %)	8.5 ± 0.5	16.5 ± 2.4	954	37.9 ± 1.6
	37 °C	262.3 ± 9.6	7.8 ± 0.5 (5.1 %)	7.7 ± 0.3	-	> 300	
	On day 182 (37 °C)	303.8 ± 10.4	8.8 ± 1.1 (4.1 %)	-	6.0 ± 1.0	98	
EB-HL 83	21 °C	187.3 ± 13.8	5.6 ± 0.9 (5.3 %)	7.2 ± 0.1	16.3 ± 1.7	924	38.8 ± 3.0
	37 °C	194.8 ± 4.4	6.3 ± 0.2 (7.2 %)	6.4 ± 0.3	-	> 300	
	On day 182 (37 °C)	230.5 ± 1.8	6.5 ± 0.7 (4.4 %)	6.8 ± 1.2	-	> 300	
EB-HL 79	21 °C	137.7 ± 7.9	5.3 ± 0.3 (17.3 %)	6.3 ± 0.1	16.2 ± 2.7	1018	39.0 ± 1.6
	37 °C	155.0 ± 6.1	4.6 ± 0.5 (5.3 %)	5.8 ± 0.4	-	> 300	
	On day 182 (37 °C)	199.6 ± 3.4	5.9 ± 0.4 (5.1 %)	-	5.5 ± 0.1	233	
EB-HL 70	21 °C	92.0 ± 7.8	3.9 ± 0.3 (18.9 %)	5.0 ± 0.1	11.6 ± 1.5	1020	45.6 ± 1.2
	37 °C	94.9 ± 7.1	3.2 ± 0.5 (7.8 %)	4.1 ± 0.1	-	> 300	
	On day 182 (37 °C)	140.8 ± 16.1	4.4 ± 0.2 (5.4 %)	-	3.6 ± 0.5	144	
EB-HL 63	21 °C	57.4 ± 5.5	2.9 ± 0.4 (27.7 %)	4.0 ± 0.1	7.5 ± 1.3	918	52.8 ± 3.1
	37 °C	48.3 ± 5.0	1.9 ± 0.2 (11.4 %)	2.8 ± 0.2	-	> 300	
	On day 182 (37 °C)	88.1 ± 4.2	2.6 ± 0.2 (5.1 %)	-	1.8 ± 0.1	6.3	

¹ At 37 °C, the tests were stopped at 300 % of strain due to the size limitations of the temperature chamber.

² Some specimens broke before 300 % of strain.

³ The tensile strength was determined as ultimate stress value (σ_u).

⁴ Measured 24 hours after break.

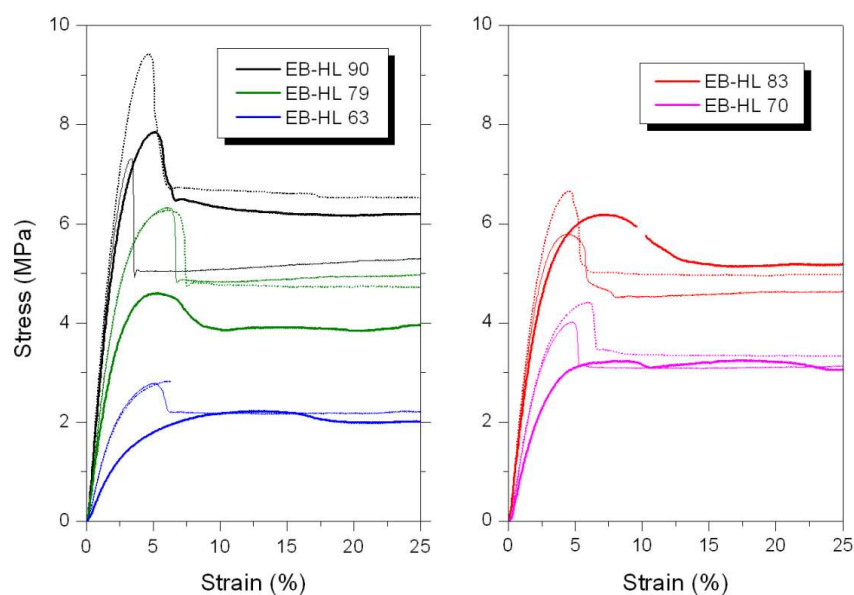


Figure 10. Tensile stress-strain curves until 25 % of strain of the EB-co- δ -HL copolymers tested at 37 °C. The curves of the non-degraded samples are in bold and those on day 182 of degradation are dotted. The curves on day 70 of degradation are also shown.

Figure 10 shows the tensile stress-strain curves up to 25 % of strain of the tensile tests conducted at 37 °C with non-degraded (curves in bold type) and degraded specimens (on days 70 and 182). The mechanical behaviour of these polymers at 37 °C were, in general, more elastomeric than at 21 °C and presented yield strengths and tensile strengths at 300 % which were in all cases lower than the values measured at room temperature. The best example is EB-HL 63, whose secant modulus shifted from 57.4 MPa to 48.3 MPa, its tensile strength at 300 % suffered a drop from 4.0 MPa to 2.8 MPa and its yield point became narrower with a yield strength that decreased from 2.9 MPa to 1.9 MPa. Nevertheless, it should be also stated that, as a result of the different melting behaviours at both temperatures, the secant modulus of these copolymers did not fall in all cases. Thus, the corresponding secant modulus of EB-HL 83, EB-HL 79 and EB-HL 70 was higher at 37 °C than at 21 °C. Mechanical performance is greatly influenced by the crystalline phase and these were the three copolymers that showed the most significant increase in melting enthalpy at 37 °C (see Table 6). However, despite the changes in their properties mentioned above, it can be said that all the EB-co- δ -HL copolymers displayed a good mechanical stability between 21 and 37 °C and their mechanical behaviour is adequate at both temperatures.

As a consequence of the hydrolytic degradation process, the stress related properties were found to be higher than at the start of the study. As can be seen in Figure 10, the yield strength of the samples submerged for 70 or 182 days rose compared to non-degraded films at 37 °C. Likewise, the elastic modulus at the end of the study reached values around 40-50 MPa higher than when measured at 37 °C on day 0. However, owing to the changes in molecular weight and the mechanical deterioration experienced in an aqueous medium, the EB-co- δ -HL copolymers (with the exception of EB-HL 83 which had on day 182 the highest M_w) lost deformation capability and their specimens broke earlier, before reaching 300 % of strain. EB-HL 90 and EB-HL 63 were the most severely affected copolymers and exhibited elongation at break values of only 98 % and 6.3 %.

Cell culture studies

In vitro compatibility studies were performed to determine the possible toxicity of the ethylene brassylate-co- δ -hexalactone copolymers, as they contain a large amount of bismuth. To achieve this, circular samples of 9 mm in diameter, obtained from 150-200 μ m films, were employed. Figure 11 shows the metabolic activity of cells seeded in EB-HL 90 and EB-HL 63 samples compared to cells seeded in tissue culture plastic (control). No significant differences were observed in the metabolic activity of HDFs with respect to the control, indicating normal metabolic activity of cells seeded on the synthesized polymers.

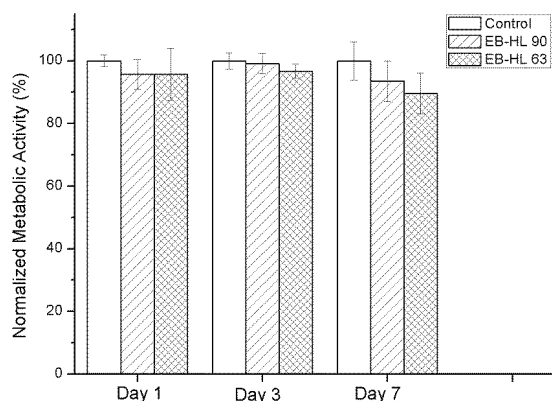


Figure 11. Metabolic activity of HDFs seeded on EB-HL 90 and EB-HL 63 with respect to the control on days 1, 3 and 7.

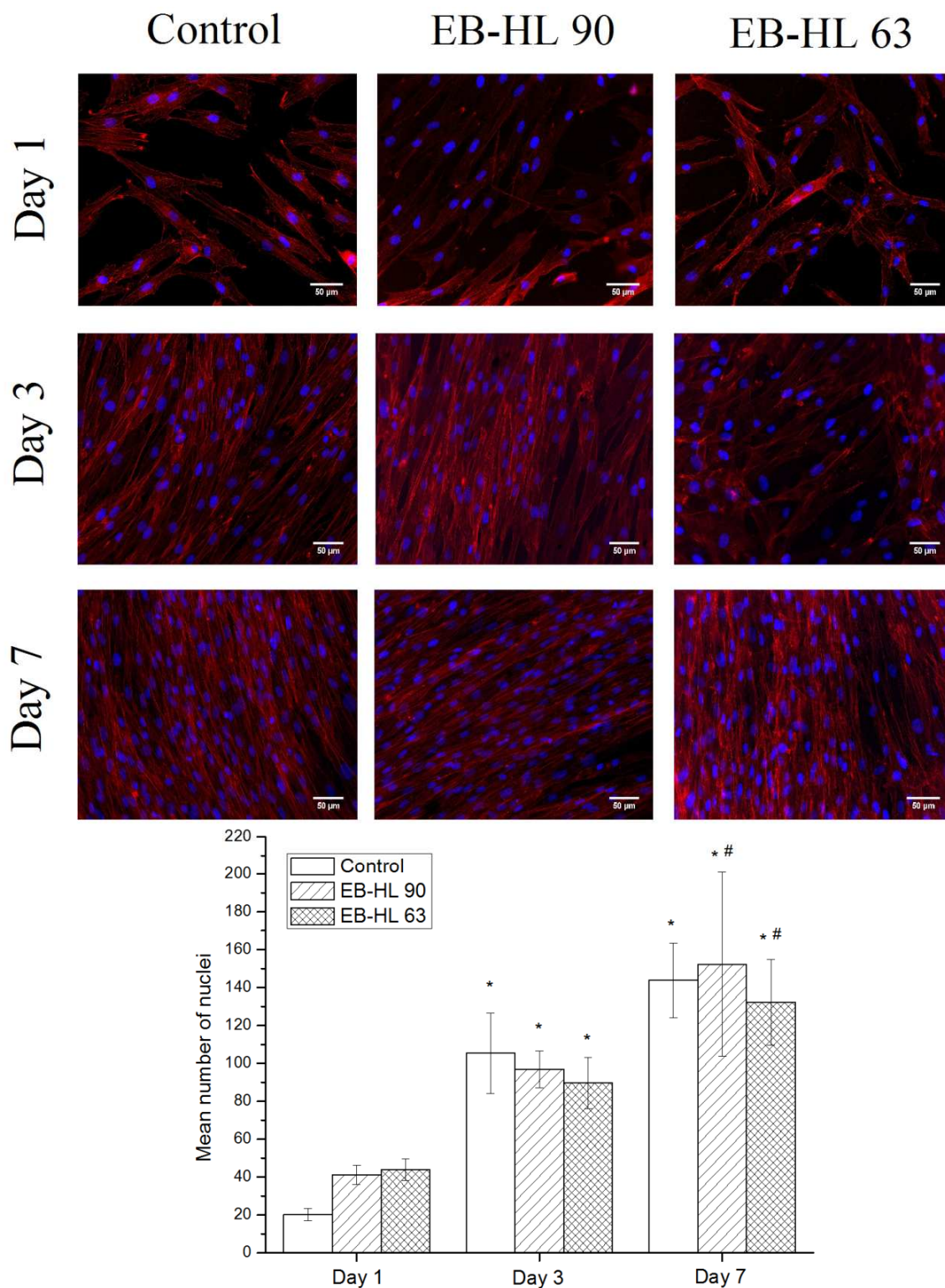


Figure 12. Fluorescent microscopy images of HDFs seeded on glass coverslips (control), EB-HL 90 and EB-HL 63 films on days 1, 3 and 7. F-actin was stained with rhodamine phalloidin (red) and nuclei with Hoechst (blue).

To observe the cytoskeleton organization and analyze the spreading and proliferation of HDFs seeded on EB-HL 90 and EB-HL 63, cells were stained with rhodamine phalloidin (red) and Hoechst (blue), see Figure 12. On day 1, individual HDFs were observed in all the samples. From these micrographs it can be observed that HDFs were able to maintain their typical fibroblastic morphology [38-39] when they were seeded on EB-HL 90 and EB-HL 63 and no differences were observed with respect to those cells seeded on glass coverslips (control). A higher number of cells were observed in all the samples on day 3, proving that there was adequate cell spreading and proliferation. This was also confirmed by nuclei quantification from these images. The symbols “*” and “#” from the graph in Figure 12 indicate significant differences ($p < 0.05$) with respect to day 1 and day 3, respectively. Therefore, it can be stated that significant differences were observed between the number of nuclei on day 3 and on day 1 in all cases. On day 7, the surface of the samples was completely covered by cells forming a monolayer of cells. The number of nuclei also increased with respect to day 3, a good sign of the proliferation of the seeded cells on the studied materials.

6.4. Conclusions

In this work several statistical copolymers based on ethylene brassylate macrolactone and δ -hexalactone were synthesized with triphenyl bismuth as catalyst. The ring-opening polymerizations were carried out for 6 days at 130 °C although after 3 days of reaction copolymers of high molecular weight were already obtained. Owing to the racemic stereochemistry of the methyl side chain of the δ -HL unit, only the ethylene brassylate sequences were able to crystallize and as a result the crystallinity fraction decreased from 47 % (PEB homopolymer) to ~ 23-39 % (when 10 to 51 % of δ -HL units were incorporated). The poly(EB-co- δ -HL)s showed a slightly deviated from random distribution of sequences ($0.71 < R < 0.84$) and were carefully characterized by NMR, GPC, DSC, WAXS and TGA measurements. In addition, their mechanical properties were tested at room temperature (21 °C) and at body temperature (37 °C), at the same time an *in vitro* degradation study was also carried out at 37 °C for 182 days in phosphate buffer solution. Moreover, cell culture studies were conducted with human

dermal fibroblasts (HDFs) seeded on samples obtained from films of some poly(EB-co- δ -HL).

These novel copolymers displayed upgraded thermal stability (they were completely degraded at high temperatures, around 475 °C), showed rapid crystallization from melt, good processing using thermoplastic techniques, very attractive mechanical properties at 21 and 37 °C (with improved flexibility and elongation at break values > 900 %) and enhanced biodegradability (with hydrolytic degradation rates almost 4 times higher than that of Poly(ϵ -caprolactone)). In addition, the cell culture studies of metabolic activity and cell morphology demonstrated that the materials employed in this work are not cytotoxic and provide a valid substrate for cells to attach to and proliferate. This set of properties makes them very interesting potential materials for use in medical applications when an elastomeric character is desirable, particularly, for the regeneration of soft tissues and for various clinical implants and devices. However, tests on animals and clinical trials should be carried out prior to their application in the biomedical field.

References

- [1] Ravi, S.; Padmanabhan, D.; Mandapur, V.R. Macrocyclic musk compounds: synthetic approaches to key intermediates for exaltolide, exaltone and dilactones. *Journal of the Indian Institute of Sciences* 2001, 81, 299-312.
- [2] Arctander, S. *Perfume and Flavor Chemicals (Aroma Chemicals)*, vol 1, 1264. S. Arctander, Montclair, New Jersey 1969.
- [3] McGinty, D.; Letizia, C.S.; Api, A.M. Fragrance material review on ethylene brassylate. *Food and Chemicals Toxicology* 2011, 49, 174-182.
- [4] Müller, S.; Uyama, H.; Kobayashi, S. Lipase-catalyzed ring-opening polymerization of cyclic diesters. *Chemical Letters* 1999, 1317-1318.
- [5] Pascual, A.; Sardón, H.; Veloso, A.; Ruipérez, F.; Mecerreyes, D. Organocatalyzed Synthesis of Aliphatic Polyesters from Ethylene Brassylate: A Cheap and Renewable Macrolactone. *ACS Macro Letters* 2014, 3, 849-853.
- [6] Labet, M.; Thielemans, W. Synthesis of polycaprolactone: a review. *The Royal Society of Chemistry* 2009, 38, 3484-3504.
- [7] Woodruff, M.A.; Hutmacher, D.W. The Return of a forgotten polymer: Polycaprolactone in the 21st century. *Progress in Polymer Science* 2010, 35, 1217-1256.
- [8] Fernandez, J.; Etxeberria A.; Sarasua, J.R. In vitro degradation studies and mechanical behavior of poly(ϵ -caprolactone-co- δ -valerolactone) and poly(ϵ -caprolactone-co-L-lactide) with random and semi-alternating chain microstructures. *European Polymer Journal* 2015, 71, 585-595.
- [9] Chen, J-C.; Li, J.H.; Liu, J-H.; Xu, L-Q. Amphiphilic poly(ethylene glycol)-b-poly(ethylene brassylate) copolymers: One-pot synthesis, self-assembly, and controlled drug release. *Chinese Chemical Letters* 2015, 26, 1319-1321.
- [10] Pascual, A.; Sardón, H.; Ruipérez, F.; Gracia, R.; Sudam, P.; Veloso, A.; Mecerreyes, D. Experimental and Computational Studies of Ring-Opening Polymerization of Ethylene Brassylate Macrolactone and Copolymerization with ϵ -Caprolactone and TBD-Guanidine Organic Catalyst. *Journal of Polymer Science, Part A: Polymer Chemistry* 2015, 53, 552-561.
- [11] Pan, P.; Inoue, Y. Polymorphism and isomorphism in biodegradable polyesters. *Progress in Polymer Science* 2009, 34, 605-640.

- [12] Fernández, J.; Etxeberria, A.; Sarasua, J.R. Crystallization and melting behavior of poly(ϵ -caprolactone-co- δ -valerolactone) and poly(ϵ -caprolactone-co-L-lactide) copolymers with novel chain microstructures. *Journal of Applied Polymer Science* 2015, 132, 42534.
- [13] Ceccorulli, G.; Scandola, M.; Kumar, A.; Kalra, B.; Gross, R.A. Cocrystallization of random copolymers of ω -pentadecalactone and ϵ -caprolactone synthesized by lipase catalysis. *Biomacromolecules* 2005, 6, 902-907.
- [14] Shalaby, S.W.; Kafrawy, A. Synthesis and some properties of isomorphic copolymers of ϵ -caprolactone and 1,5-dioxepan-2-one. *Journal of Polymer Science Polymer Chemistry Ed* 1989, 27, 4423-6.
- [15] Dwan'Isa, J.P.L.; Lecomte, P.; Dubois, P.; Jérôme, R. Synthesis and characterization of random copolyesters of ϵ -caprolactone and 2-oxepan-1,5-dione. *Macromolecules* 2003, 36, 2609-15.
- [16] Papadimitriou, S.A.; Papageorgiou, G.Z.; Bikiaris, D.N. Crystallization and enzymatic degradation of novel poly(ϵ -caprolactone-co-propylene succinate) copolymers. *European Polymer Journal* 2008, 44, 2356-66.
- [17] Biazus, T.F.; Cezaro, A.M.; Borges, G.R.; Bender, J.P.; Franceschi, E.; Corazza, M.L.; Oliveira, J.V. Vapour pressure data of ϵ -caprolactone, δ -hexalactone, and γ -caprolactone. *Journal of Chemical Thermodynamics* 2008, 40, 437-441.
- [18] Kikuchi, H.; Uyama, H.; Kobayashi, S. Lipase-catalyzed enantioselective copolymerization of substituted lactones to optically active polyesters. *Macromolecules* 2000, 33, 8971-8975.
- [19] Kobayashi, S. Enzymatic ring-opening polymerization of lactones by lipase catalyst: Mechanistic aspects. *Macromolecular Symposia* 2006, 240, 178-185.
- [20] Parliament, T.H.; Nawar, W.W.; Fagerson, I.S. Delta-caprolactone in heated milk fat. *Journal of Dairy Science* 1965, 48, 615-616.
- [21] Fernández, J.; Etxeberria, A.; Sarasua, J.R. Synthesis and Properties of ω -pentadecalactone-co- δ -hexalactone copolymers: A biodegradable thermoplastic elastomer as an alternative to poly(ϵ -caprolactone). Under revision in RSC Advances.
- [22] Kricheldorf, H.R.; Behnken, G.; Schwarz, G.; Brockaert, J.A. High molecular weight Poly(ϵ -caprolactone) by initiation with triphenyl bismuth. *Macromolecular Chemistry and Physics* 2008, 209, 1586-1592.

- [23] Kricheldorf, H.R. Syntheses of Biodegradable and Biocompatible Polymers by means of Bismuth Catalysts. *Chemical Reviews* 2009, 109, 5579-5594.
- [24] Rodilla, V.; Miles, A.T.; Jenner, W.; Harksworth, G.M. Exposure of cultured human proximal tubular cells to cadmium, mercury, zinc and bismuth: toxicity and metallothionein induction. *Chemico-Biological Interactions* 1998, 115, 71-83.
- [25] Guo, Z.; Sadler, P.J. Metalle in der Medizin. *Angewandte Chemie* 1999, 111, 1610-1630.
- [26] Briand, G.C; Burford, N. Bismuth compounds and preparations with biological or medicinal relevance. *Chemical Revisions* 1999, 99, 2601-2658.
- [27] Kricheldorf, H.R.; Behnken, G. Copolymerization of Glycolide and L-lactide initiated with Bismuth(III) n Hexanoate or Bismuth Subsalcylate. *Journal of Macromolecular Science, Part A: Pure and Applied Chemistry* 2007, 44, 795-800.
- [28] Prestch, E.; Clerc, T.; Seibl, J.; Simon, W. Tables of Spectral Data for Structure Determination of Organic Compounds. Chemical Laboratory Practice. Ed. Springer Science & Business Media. Springer-Verlag Berlin Heidelberg GmbH 2013.
- [29] Herbert, I.R. Statistical analysis of copolymer sequence distribution. In *NMR Spectroscopy of Polymers*. Ibbet, R.N. Ed.: Blackie Academic & Professional, London, 1993,50-79. (Chapter 2).
- [30] Wu, L.; Ding, J. Effects of porosity and pore size on in vitro degradation of three-dimensional porous poly(D,L-lactide-co-glycolide) scaffolds for tissue engineering. *Journal of Biomedical Materials Research* 2005, 75, 767-777.
- [31] Fernández, J.; Larrañaga, A.; Etxeberria, A.; Sarasua, J.R. Effects of chain microstructures and derived crystallization capability on hydrolytic degradation of poly(L-lactide/ ϵ -caprolactone) copolymers. *Polymer Degradation and Stability* 2013, 98, 481-489.
- [32] Fernández, J.; Etxeberria, A.; Sarasua, J.R. In vitro degradation study of biopolyesters using poly(lactide/ δ -valerolactone) copolymers. *Polymer Degradation and Stability* 2015, 112, 104-116.
- [33] Larrañaga, A.; Aldazabal, P.; Martin, F.J.; Sarasua, J.R. Hydrolytic degradation and bioactivity of lactide and caprolactone based sponge-like scaffolds loaded with bioactive glass particles. *Polymer Degradation and Stability* 2014, 110, 121-128.
- [34] Scherrer, P. Bestimmung der Grosse und der inneren Struktur von Kolloidteilchen mittels Röntgenstrahlen. *Nachr Ges Wiss Gottingen*, 26, pp. 98-100, 1918.

-
- [35] de Geus, M.; van der Meulen, I.; Goderis, B.; van Hecke, K.; Doschu, M.; van der Werff, H.; Koning, C.E.; Heise, A. Performance polymers from renewable monomers: high molecular weight poly(pentadecalactone) for fiber applications. *Polymer Chemistry* 2010, 1, 525-533.
- [36] Focarete, M.L.; Scandola, M.; Kumar, A.; Gross, R.A. Physical characterization of poly(ω -pentadecalactone) synthesized by lipase-catalyzed ring opening polymerization. *Journal of Polymer Science Part B: Polymer Physics* 2001, 39, 1721-1729.
- [37] Fernández, J.; Etxeberria, A., Larrañaga Varga A.; Sarasua, J.R.; Synthesis and characterization of ω -pentadecalactone-co- ϵ -decalactone copolymers: Evaluation of thermal, mechanical and biodegradatin properties. *Polymer* 2015, 81, 12-22.
- [38] Baxter, L.C.; Frauchiger, V.; Textor, M.; ap Gwynn, I.; Richards, R.G. Fibroblast and osteoblast adhesion and morphology on calcium phosphate surfaces. *European Cells and Materials* 2002, 4, 1-17.
- [39] Tamariz, E.; Grinnell, F. Modulation of fibroblast morphology and adhesion during collagen matrix remodeling. *Molecular Biology of the Cell* 2002, 11, 3915-3929.

General Conclusions

In the current PhD thesis an exhaustive study on several novel copolyesters has been carried out. Through the different chapters, many copolymers systems has been introduced, which include materials based on lactide (L-lactide and rac-lactide) and ϵ -caprolactone or δ -valerolactone, copolymers of ω -pentadecalactone with ϵ -decalactone or δ -hexalactone and ethylene-brassylate-co- δ -hexalactone copolymers. These biomaterials improve the performance of polylactides, poly(ϵ -caprolactone) and other polymers employed nowadays and meet most of the requirements specified in our “Scope and Objectives” section. However, although the respective conclusions are displayed at the end of each chapter, some general statements are highlighted below:

1. In regard to the copolymers of high glass transition:

- Show glass transition temperatures in the range of 20 to 45 °C.
- Are fully amorphous or present reduced capability of crystallization owing to their random chain microstructure and the addition of D-lactide to disrupt the arrangement of the L-lactide blocks.
- Exhibit high degradation rates ($K_{Mw} > 0.030 \text{ days}^{-1}$ and in some cases values higher or similar to that of poly(D,L-lactide-co-glycolide).
- Do not generate brittle and resistant remnants during the degradation process. The residues are pasty or soft crystalline remmants with a $T_m < 100 \text{ °C}$.
- Display improved mechanical properties (flexibility and ductibility) in comparison to polylactides and polyglycolides: Elastic Modulus from 5 to 1000 MPa and high elongation at break values.
- Their mechanical properties are not stable at 21 and at 37 °C. At body temperature they are more elastomeric and present lower stress-related properties (elastic modulus and tensile strength) than at room temperature.

2. In regard to the copolymers of low glass transition:

- Show glass transition temperatures in the range of -65 to -25 °C with melting temperatures below 100 °C.
- Crystallize very quickly from the melt. Do not undergo physical aging.
- Exhibit proper processing with thermoplastic techniques and upgraded thermal stability (> 300 °C).
- Present improved hydrolytic degradation rates with respect to poly(ϵ -caprolactone) as a result of their increased amorphous character. While PCL degrades at a rate of 0.0010 days⁻¹ at 37 °C, the random and semi-alternating copolymers of ϵ -caprolactone with δ -valerolactone and L-lactide shows K_{Mw} between 0.0033 to 0.0105 days⁻¹, poly(ω -pentadecalactone-co- δ -hexalactone) degrade at a rate of 0.0013 to 0.0019 days⁻¹ and the K_{Mw} of the ethylene brassylate-co- δ -hexalactone copolymers is in the range of 0.0028 to 0.0041 days⁻¹. The poly(ω -pentadecalatone-co- ϵ -decalactone) were very resistant to hydrolytic degradation and can virtually be considered as non-biodegradable polymers.
- Have appealing mechanical properties. Improvement in flexibility in comparison to poly(ϵ -caprolactone), poly(ω -pentadecalactone) or poly(ethylene brassylate) homopolymers: Elastic Modulus from 25 to 300 MPa with high elongation at break values. Moreover, these materials maintains their properties at body temperature 37 °C, in contrast to other polyesters.

Appendix

A1. Symbols and Abbreviations

β	heating rate
ΔC_p	change in heat capacity
ΔH_m	melting enthalpy
ΔH_m^0	melting enthalpy (infinite crystal thickness)
ΔH_c	crystallization enthalpy
ΔT	supercooling
δ	chemical shift / enthalpy relaxation
ε	elongation
ε_r	strain recovery
ε_u	ultimate elongation
σ	tensile strength
σ_{\max}	tensile strength
σ_u	ultimate tensile strength
σ_y	yield stress
D	dispersity index
E	elastic modulus
E'	storage modulus
E _{young}	young's modulus

H	enthalpy
K_{Mw}	apparent degradation rate
l_i	number-average sequence length of “i”
$l_{i \text{ random}}$	Bernouillian number-average sequence length of unit “i”
M_n	number average molecular weight
M_w	weight average molecular weight
M_{w0}	initial weight average molecular weight
2θ	diffraction angle
p	statistical significance value
R	randomness character
R_H	R obtained by ^1H NMR
R_C	R obtained by ^{13}C NMR
$t_{1/2}$	half-molecular weight degradation time
T_{II}	second mode transesterification
T_c	crystallization temperature
T_g	glass transition temperature
T_m	melting temperature
$\tan \delta$	tangent of the phase angle
wt. %	weight percent

X_c	crystallinity degree
ADSC	adipose derived mesenchymal stem cells
AFM	atomic force microscopy
β -BL	beta butyrolactone
γ -BL	gamma butyrolactone
Bi	bismuth
BiSS	bismuth subsalicylate
$CDCl_3$	deuterated chloroform
CL	ϵ -caprolactone
ϵ -CL	epsilon caprolactone
δ -DL	delta decalactone
ϵ -DL	epsilon decalactone
γ -DL	gamma decalactone
DMA	dynamic mechanical analysis
DMSO	dimethyl sulfoxide
DSC	differential scanning calorimetry
DTG	differential thermogravimetric
EB	ethylene brassylate
FDA	food and drug administration

FTIR	fourier transform infrared spectroscopy
GPC	gel permeation chromatography
HL	delta hexalactone
δ -HL	delta hexalactone
ICP-AES	inductively coupled plasma with atomic emission spectroscopy
M/C	monomers/catalyst molar ratio
MTT	3-(4,5-dimethylthiazol-2-yl)-2,5- diphenyltetrazolium bromide
NMR	nuclear magnetic resonance
¹ H NMR	proton NMR
¹³ C NMR	carbon NMR
LA	lactide
D-LA	D-lactide
D,L-LA or rac-LA	rac-lactide, 50:50 mix of L-lactide and D-lactide
L-LA	L-lactide
PBS	phosphate buffered saline
PCL	poly(ϵ -caprolactone)
PDL	ω -pentadecalactone

ω -PDL	omega pentadecalactone
PDLLA	poly(D,L-lactide)
PE	polyethylene
PEB	poly(ethylene brassylate)
P3HB or PHB	polyhydroxybutyrate
Ph ₃ Bi	triphenyl bismuth
PGA	polyglycolide
PLA	polylactide
PLCL	poly(lactide-co- ϵ -caprolactone)
PLGA	poly(lactide-co-glycolide)
PLLA	poly(L-lactide)
PLVL	poly(lactide-co- δ -valerolactone)
PLOM	polarized light optical microscopy
PPDL	poly(ω -pentadecalactone)
β -PL	beta propiolactone
RI	refractive index
ROP	ring-opening polymerization
ROH	alcohol radicals
RW	remaining weight
SEM	scanning electron microscope

Appendix

Sn	tin, stannous
SnOct ₂	tin (II) octoate
TGA	thermogravimetric analysis
TG	thermogravimetric
TPE	thermoplastic elastomer
VL	delta valerolactone
δ-VL	delta valerolactone
γ-VL	gamma valerolactone
WA	water absorption
W ₀	initial weight
W _w	wet weight
W _d	dry weight
WAXD	wide angle X-ray diffraction

A2. List of Publications and Congresses

As a result of this work, fifteen peer-reviewed papers have been published in international indexed scientific journals:

- Fernández, J.; Etxeberria, A.; Sarasua, J.R. Synthesis, structure and properties of poly(L-lactide-co- ϵ -caprolactone) statistical copolymers. *Journal of the Mechanical Behavior of Biomedical Materials* 2012, 9, 100-112.
- Fernández, J.; Etxeberria A.; Ugartemendia, J.M.; Petisco, S.; Sarasua, J.R. Effects of chain microstructures on mechanical behaviour and aging of a poly(L-lactide-co- ϵ -caprolactone) biomedical thermoplastic elastomer. *Journal of the Mechanical Behavior of Biomedical Materials* 2012, 12, 29-38.
- Fernández, J.; Etxeberria, A.; Sarasua, J.R. Effects of repeat unit sequence distribution and residual catalyst on thermal degradation of poly(L-lactide/ ϵ -caprolactone) statistical copolymers. *Polymer Degradation and Stability* 2013, 98, 1293-1299.
- Fernández, J.; Meaurio, E.; Chaos, A.; Etxeberria, A.; Alonso-Varona, A.; Sarasua, J.R. Synthesis and characterization of poly(L-lactide/ ϵ -caprolactone) statistical copolymers with well resolved chain microstructures. *Polymer* 2013, 54, 2621-2631.
- Fernández, J.; Larrañaga, A.; Etxeberria, A.; Sarasua, J.R. Effects of chain microstructures and derived crystallization capability on hydrolytic degradation of poly(L-lactide/ ϵ -caprolactone) copolymers. *Polymer Degradation and Stability* 2013, 98, 481-489.
- Fernández, J.; Larrañaga, A.; Etxeberria, A.; Wang, W.; Sarasua, JR. A new generation of poly(lactide/ ϵ -caprolactone) polymeric biomaterials for application in the biomedical field. *Journal of Biomedical Materials Research A* 2014, 102A, 3573–3584.

- Larrañaga, A.; Guay-Bégin, A.-A.; Chevallier, P.; Sabbatier, G.; Fernández, J.; Laroche, G.; Sarasua, J.R. Grafting of a Model Protein on Lactide and Caprolactone Based Biodegradable Films for Biomedical Applications. *Biomatter* 2014, 4, 1-11.
- Fernández, J.; Larrañaga, A.; Etxeberria, A.; Sarasua, J.R. Tensile behavior and dynamic mechanical analysis of novel poly(lactide/ δ -valerolactone) statistical copolymers. *Journal of the Mechanical Behavior of Biomedical Materials* 2014, 35, 39-50.
- Fernández, J.; Etxeberria, A.; Sarasua, J.R. In vitro degradation study of biopolyesters using poly(lactide/ δ -valerolactone) copolymers. *Polymer Degradation and Stability* 2015, 112, 104-116.
- Sabbatier, G.; Larrañaga, A.; Guay-Bégin, A.A.; Fernández, J.; Diéval, F.; Durand, B.; Sarasua, J.R.; Laroche, G. Design, degradation mechanism and long-term cytotoxicity of poly(L-lactide) and poly(lactide-co- ϵ -caprolactone) terpolymer film and air-spun nanofiber scaffold. *Macromolecular Bioscience* 2015, 15, 1392-1410.
- Fernández, J.; Etxeberria, A.; Sarasua, J.R. Crystallization and melting behavior of poly(ϵ -caprolactone-co- δ -valerolactone) and poly(ϵ -caprolactone-co-L-lactide) copolymers with novel chain microstructures. *Journal of Applied Polymer Science* 2015, 132, 45534.
- Fernandez, J., Etxeberria A., Sarasua, J.R. In vitro degradation studies and mechanical behavior of poly(ϵ -caprolactone-co- δ -valerolactone) and poly(ϵ -caprolactone-co-L-lactide) with random and semi-alternating chain microstructures. *European Polymer Journal* 2015, 71, 585-595.
- Fernández, J.; Etxeberria, A.; Larrañaga Varga A.; Sarasua, J.R. Synthesis and characterization of ω -pentadecalactone-co- ϵ -decalactone copolymers:

Evaluation of thermal, mechanical and biodegradatin properties. *Polymer* 2015, 81, 12-22.

- Fernández, J.; Etxeberria, A.; Sarasua, J.R. Synthesis and properties of ω -pentadecalactone-co- δ -hexalactone copolymers: A biodegradable thermoplastic elastomer as an alternative to poly(ϵ -caprolactone). *RSC Advances* 2016, 6, 3137-3149.
- Fernández, J.; Larrañaga, A.; Etxeberria, A.; Sarasua, J.R. Ethylene brassylate-co- δ -hexalactone biobased polymers for application in the medical field: Synthesis, characterization and cell culture studies. Submitted for publication.

We have also applied for a PCT patent, which includes the results obtained in the chapter 1.3.

- Fernández, J.; Etxeberría, A.; Sarasua, J.R. Nuevos terpolímeros aleatorios a base de d-lactida, l-lactida y ϵ -caprolactona. Número de solicitud: PCT/ES2014/070156

The results of this research, as well as other related works, have been also presented in national and international congresses as oral communication or posters. The presenting author of each work is underlined below:

- Jorge Fernández, A. Etxeberria, E. Zuza, E. Meaurio, S. Petisco, J.R. Sarasua. Synthesis and characterization of poly(L-lactide-co- ϵ -caprolactone) random copolymers. European Polymer Congress EPF/ XII GEP, 2011, Granada (Spain)
- Susana Petisco, J.M. Ugartemendia, Jorge Fernandez, J.R. Sarasua. Effect of physical aging on enthalpy relaxation and embrittlement of elastomer thermoplastic biodegradable poly(L-lactide/ ϵ -caprolactone). EUROTEC, 2011, Barcelona (Spain)
- Jorge Fernández, J.M. Ugartemendia, S. Petisco, A. Etxeberria, J.R. Sarasua. Effects of chain microstructure on physical aging, mechanical properties, and

thermal stability of a poly(L-Lactide-co- ϵ -caprolactone) elastomer thermoplastic copolymer. 9th World Biomaterials Congress, 2012, Chengdu (China).

- Aitor Larrañaga, A-A. Guay-Bégin, P. Chevallier, G. Sabbattier, Jorge Fernández, G. Laroche, J.R. Sarasua. Surface Modification and Characterization of a Lactide Caprolactone Based Biodegradable Polymer by Atmospheric Pressure Plasma. 25th European Conference on Biomaterials, 2013, Madrid (Spain).
- Aitor Larrañaga, A-A. Guay-Bégin, P. Chevallier, G. Sabbattier, Jorge Fernández, G. Laroche, J.R. Sarasua. Effect of protein grafting on the hydrolytic degradation of lactide and caprolactone based biodegradable elastomeric terpolymer. 4th International Symposium on Surface and Interface of Biomaterials ISSIB, 2013, Roma (Italy).
- Gad Sabbatier, A. Larrañaga, N.R. Ko, A. Cunningham, A.-A. Guay-Bégin, Jorge Fernandez, J. K. Oh, J.R. Sarrasua, G. Laroche. Designing Multifunctional Nanofiber Scaffold for Endothelial Cells Adhesion and Proliferation on Vascular Substitutes. Canadian Biomaterial Society, 2014, Halifax (Canada).
- Jorge Fernández, J.R. Sarasua. La degradación hidrolítica en los biopolíesteres: poli(lactida-co- δ -valerolactona). XIII GEP, 2014, Girona (Spain)

A3. Curriculum Vitae

Full name: Jorge Fernández Hernández

NIF: 78931643-J

Date of Birth: 15/02/1986

Gender: M

Contact information:

Department of Mining-Metallurgy and Materials Science, School of Engineering

University of the Basque Country (UPV-EHU), Alameda Urquijo s/n 48010 Bilbao
(España)

Email: jorge.fernandez@ehu.es

Research interests

Biodegradable polymers, copolyesters, thermoplastic elastomers, characterization techniques, ring-opening polymerization, hydrolytic degradation, tissue engineering, implants and medical devices

Graduate Studies

Chemical Engineering: 2004-2009 (E.T.S.I. Bilbao)

Master in Engineering of Advanced Materials: 2009-2010 (E.T.S.I. Bilbao)

Fellowships and Professional Experience:

Research personnel contracted by the UPV-EHU (PIC): 04/2011-12/2011

Research fellowship to carry out a PhD thesis in the University of the Basque Country:
03/2012-03/2016

Other publications unrelated to this thesis:

- Lejardi, A.; Meaurio, E.; Fernández, J.; Sarasua, JR. Miscibility of Poly(vinyl alcohol)-graft-Hydroxy Ester/Poly(vinylpyrrolidone) Blends. *Macromolecules* 2012, 44, 7351-7363.
 - Chaos, A.; Garcia, J.M.; Iriarte, M.; Fernández, J.; Sarasua, J.R. Etxeberria, A. Miscibility And Transport Properties Of Poly(Lactide)/Phenoxy System. *Macromolecular Symposia* 2012, 321-222, 20-24.
 - Larrañaga, A., Fernandez, J., Vega, A., Etxeberria, A., Ronchel, C., Adrio, J.L., Sarasua, J.R. Crystallization and its effect on the mechanical properties of a medium chain length polyhydroxyalkanoate. *Journal of the Mechanical Behaviour of Biomedical Materials* **2014**, 39, 87-94.
-

Other contributions to congresses unrelated to this thesis:

- A. Lejardi, A. Etxeberria, E. Meaurio, J. Fernández, J.R. Sarasua. Synthesis and characterization of lactide-graft-poly(vinyl alcohol) and miscibility study with poly(ethylene oxide). European Polymer Congress EPF/ XII GEP, 2011, Granada (Spain).
- J.R. Sarasua, S. Petisco, Jorge Fernandez, J.M.Ugartemendia. Aging effects, crystallinity and phase structure of polylactides. European Conference on Biomaterials, 2011, Dublin (Ireland).
- S. Petisco, Jorge Fernandez, J.J. Gonzalez, J.R. Sarasua. Viscoelastic behavior and shape memory properties of medical polylactides. European Conference on Biomaterials, 2011, Dublin (Ireland).
- S.Petisco, J. Fernández, J.R. Sarasua. Viscoelasticity and Mechanical Properties of P(L-lactide-co- ϵ -caprolactone) copolymers with well resolved chain microstructures. 25th European Conference on Biomaterials, 2013, Madrid (Spain).

“The difference between ignorant and educated people is that the latter know more facts. But that has nothing to do with whether they are stupid or intelligent”

Neal Stephenson